

AD-767 364

STOL TACTICAL AIRCRAFT INVESTIGATION.
VOLUME V. FLIGHT CONTROL TECHNOLOGY

J. Hebert, Jr., et al

General Dynamics

Prepared for:

Air Force Flight Dynamics Laboratory

May 1973

DISTRIBUTED BY:

NTIS

National Technical Information Service
U. S. DEPARTMENT OF COMMERCE
5285 Port Royal Road, Springfield Va. 22151

AFFDL-TR-73-21-Vol. V

STOL TACTICAL AIRCRAFT INVESTIGATION

VOLUME V + FLIGHT CONTROL TECHNOLOGY

J. Hebert, Jr.
G. Campbell
E. Price
L. B. White
R. Heistenberg

Convair Aerospace Division of
General Dynamics Corporation

TECHNICAL REPORT AFFDL-TR-73-21

May 1973



Approved for public release; distribution unlimited

Air Force Flight Dynamics Laboratory
Air Force Systems Command
Wright-Patterson Air Force Base, Ohio

AD 767364

NOTICE

When Government drawings, specifications, or other data are used for any purpose other than in connection with a definitely related Government procurement operation, the United States Government thereby incurs no responsibility nor any obligation whatsoever; and the fact that the government may have formulated, furnished, or in any way supplied the said drawings, specifications, or other data, is not to be regarded by implication or otherwise as in any manner licensing the holder or any other person or corporation, or conveying any rights or permission to manufacture, use, or sell any patented invention that may in any way be related thereto.

ACCESSION for	
NTIS	White Section <input checked="" type="checkbox"/>
DDC	Buff Section <input type="checkbox"/>
UNANNOUNCED	<input type="checkbox"/>
JUSTIFICATION	
BY	
DISTRIBUTION/AVAILABILITY CODES	
Dist.	A, ALL, and/or SPECIAL
A	

Copies of this report should not be returned unless return is required by security considerations, contractual obligations, or notice on a specific document.

Unclassified

Security Classification

DOCUMENT CONTROL DATA - R & D

(Security classification of title, body of abstract and indexing annotation must be entered when the overall report is classified)

1. ORIGINATING ACTIVITY (Corporate author) Convair Aerospace Division General Dynamics Corporation San Diego, California 92138		2a. REPORT SECURITY CLASSIFICATION Unclassified	
		2b. GROUP	
3. REPORT TITLE STOL Tactical Aircraft Investigation Volume V - Flight Control Technology			
4. DESCRIPTIVE NOTES (Type of report and inclusive dates) Final Report (7 June 1971 to 31 January 1973)			
5. AUTHOR(S) (First name, middle initial, last name) J. Hebert, Jr., G. Campbell, E. Price, L. B. White, R. Halstenberg			
6. REPORT DATE May 1973		7a. TOTAL NO. OF PAGES 326	7b. NO. OF REFS 6
8a. CONTRACT OR GRANT NO. F33615-71-C-1754		9a. ORIGINATOR'S REPORT NUMBER(S) GDCA-DHG73-001	
b. PROJECT NO. 643A - Task 0001		9b. OTHER REPORT NO(S) (Any other numbers that may be assigned this report) AFFDL TR-73-21-Vol V	
10. DISTRIBUTION STATEMENT Approved for Public Release Distribution Unlimited			
11. SUPPLEMENTARY NOTES ----		12. SPONSORING MILITARY ACTIVITY Air Force Flight Dynamics Laboratory (PTA) Wright Patterson AFB, Ohio 45433	
13. ABSTRACT Flight control studies conducted during the STOL Tactical Aircraft Investigation by Convair Aerospace were directed toward development of flight control systems for three versions of the Medium STOL Transport. Baseline vehicles used for flight control studies were: Externally Blown Flap (EBF), Internally Blown Flap (IBF), and Mechanical Flap/Vectored Thrust (MF/VT) configurations. Requirements of MIL-F-8785B and MIL-F-833000 for aircraft handling qualities were the guiding criteria for the control system study. The mechanization trade study concluded that fly-by-wire mechanization is preferred over the more mechanical version which requires significant fly-by-wire features to achieve the required augmentation and decoupling. Piloted flight simulations and evaluations indicated that: All three baseline configurations could be flown under normal flight conditions without augmentation. The AUTOSPEED function is an efficient speed control. The APPROACH function is helpful under turbulent conditions and of questionable value for smooth conditions. Control after failure of the critical engine in the STOL-approach mode was considerably more difficult on the EBF configuration. On the basis of Cooper/Harper ratings assigned during flight simulator evaluations, none of the STOL configurations is significantly superior to the others.			

DD FORM 1 NOV 68 1473

Unclassified

Security Classification

NATIONAL TECHNICAL
INFORMATION SERVICE

Security Classification

14. KEY WORDS	LINK A		LINK B		LINK C	
	ROLE	WT	ROLE	WT	ROLE	WT
1. Externally Blown Flaps						
2. Fixed Base Simulation						
3. Flight Controls						
4. Internally Blown Flaps						
5. Mechanical Flap/Vectored Thrust						
6. Moving Base Simulation						
7. STOL Transport Aircraft						

AFFDL-TR-73-21-Vol. V

STOL TACTICAL AIRCRAFT INVESTIGATION

VOLUME V ♦ FLIGHT CONTROL TECHNOLOGY

J. Hebert, Jr.
G. Campbell
E. Price
L. B. White
R. Halstenberg

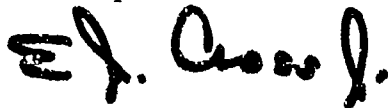
Convair Aerospace Division of
General Dynamics Corporation

FOREWORD

The Flight Control Technology studies were conducted by the Convair Aerospace Division of General Dynamics Corporation under USAF Contract F33615-71-C-1754, Project 643A, "STOL Tactical Aircraft Investigation." This contract was sponsored by the Prototype Division of the Air Force Flight Dynamics Laboratory. The USAF Project Engineer was G. Oates (PT) and the Convair Aerospace Program Manager was J. Hebert. The principal contributors were G. Campbell (Low Speed Control Methods), R. Halstenberg (Control System Mechanization Trade Studies), and E. Price and L. B. White (Flight Simulation).

The research reported was conducted during the period from 7 June 1971 through 31 January 1973. This report was submitted by the author on 31 January 1973 under contractor report number GDCA-DHG73-001.

This report has been reviewed and is approved.



E. J. CROSS, JR.
Lt. Col, USAF
Chief, Prototype Division

ABSTRACT

The flight control studies conducted during the STOL Tactical Aircraft Investigation by the Convair Aerospace Division of General Dynamics were directed toward the development of flight control systems for three versions of the Medium STOL Transport. The following baseline vehicles were used for the flight control studies: Externally Blown Flap (EBF), Internally Blown Flap (IBF), and Mechanical Flap/Vectored Thrust (MF/VT) configurations. The requirements for aircraft handling qualities in the applicable military specifications (MIL-F-8785B and MIL-F-83300) were the guiding criteria for the control system study.

The selected approach for the flight control studies was to:

1. Develop analytical models of the three baseline configurations.
2. Generate baseline control systems.
3. Analyze each configuration for compliance with the applicable MIL Specifications.
4. Determine the stability augmentation system requirements for specification compliance.
5. Conduct flight control mechanization trade studies.
6. Develop piloted flight simulations and conduct evaluations of control performance and handling qualities.

The analytical studies indicated that each baseline was deficient in some aspect of low-speed handling qualities during the STOL mode. The baseline control systems for each configuration were similar; i.e., Longitudinally -- pitch damping and an attitude-hold function were included, Laterally -- a roll rate command system was defined, and Directionally -- a yaw damper and turn coordinator were provided. The desirability to decouple aircraft responses to power adjustments and to pitch attitude changes led to the development of interconnects between throttle and flaps. Increased flight path stability was attained by adding angle-of-attack feedback into power. A speed control scheme was designed to modulate flap position in the STOL-approach configuration to regulate airspeed.

The control system was analyzed for gain and filtering requirement using root locus techniques. The interconnects to decouple aircraft responses appeared quite effective. The baselines were re-evaluated with an augmented control system for specification compliance using a non-real-time digital simulation.

The mechanization trade study concluded that fly-by-wire mechanization is preferred over the more mechanical version, primarily because the more mechanical version requires significant fly-by-wire features to achieve the required augmentation and decoupling. The maximum mechanical implementation was rated second.

The piloted flight simulations and evaluations indicated the following.

1. Initially, the IBF was found totally unacceptable in the presence of even mild disturbances at low approach speeds. Modifications were incorporated to vector engine thrust. This proved quite acceptable and was the basis for all subsequent IBF/VT simulation activities.
2. All three baseline configurations could be flown under normal flight conditions without augmentation. The addition of the augmentation features decreased pilot workload and improved pilot rating to acceptable or satisfactory levels.
3. The AUTOSPEED function, provided by modulation of flap position in the STOL-approach configuration, proved an efficient speed control. It was rated essential in the presence of turbulence and/or wind shear.
4. The APPROACH function, design to decouple aircraft response to stick and throttle inputs, was considered helpful under turbulent conditions and of questionable value for smooth conditions.
5. There was a clear preference for the STOL mode of flight control — power-lever adjustments for flight path error corrections with relatively constant pitch attitude maintained by a pitch-attitude-hold mode and airspeed regulated by the AUTOSPEED function.
6. Each baseline required configuration changes from the STOL-approach mode to minimize altitude loss to 60-70 feet after go-around initiation.
7. Control after failure of the critical engine in the STOL-approach was considerably more difficult on the EBF. The Cooper/Harper ratings assigned to the evaluations were poorest when the two-second delay preceded recovery attempts. An automatic system with an arming capability is highly desirable to enhance engine-out recovery.
8. Transition from cruise to STOL-approach using constant flap deflection rates was a challenging pilot task. It is recommended that transition be performed in two steps by using an intermediate configuration and speed to maneuver the glide path engage point to alleviate these control difficulties.
9. Cooper/Harper ratings assigned during flight simulator evaluations showed that none of the STOL configurations was significantly superior to others.

TABLE OF CONTENTS

Section		Page
1	INTRODUCTION	1-1
2	LOW SPEED CONTROL METHODS	2-1
2.1	VEHICLE DESCRIPTION	2-1
2.1.1	Externally Blown Flap	2-1
2.1.2	Internally Blown Flap, IBF-2	2-3
2.1.3	Mechanical Flap plus Vectored Thrust	2-3
2.2	ANALYTICAL MODEL	2-12
2.2.1	Wing/Body Longitudinal Aerodynamics	2-13
2.2.2	Horizontal Tail Aerodynamics	2-13
2.2.3	Lateral Directional Aerodynamics	2-13
2.2.4	Propulsion	2-13
2.2.5	Mass Properties and Dimensions	2-15
2.2.6	Landing Gear	2-15
2.3	LONGITUDINAL HANDLING QUALITIES	2-16
2.4	LONGITUDINAL STABILITY AUGMENTATION	2-28
2.5	THROTTLE/FLAP INTERCONNECT	2-33
2.6	LATERAL-DIRECTIONAL HANDLING QUALITIES	2-41
2.6.1	Engine-Out Trim Data	2-42
2.6.2	Roll Mode and Spiral Mode	2-47
2.7	LATERAL DIRECTIONAL SAS	2-56
3	CONTROL SYSTEM MECHANIZATION TRADE STUDIES	3-1
3.1	FLIGHT PATH CONTROL SYSTEM	3-1
3.2	PITCH ATTITUDE SYSTEMS	3-3
3.2.1	Original Baseline	3-4
3.2.2	Revised Baseline	3-4
3.2.3	Maximum Mechanical	3-5
3.2.4	Fly-By-Wire	3-6
3.3	LATERAL DIRECTIONAL SYSTEM	3-7
3.3.1	Original Baseline	3-7
3.3.2	Revised Lateral-Directional Baseline	3-8
3.3.3	Maximum Mechanical	3-9
3.3.4	Fly-By-Wire	3-10
3.4	SYSTEM SELECTION	3-11
3.4.1	Mechanical Versus Fly-By-Wire Comparison	3-12
3.4.2	Recommended System	3-12

TABLE OF CONTENTS, Contd

Section		Page
4	FLIGHT SIMULATION	4-1
	4.1 FLIGHT SIMULATORS	4-2
	4.1.1 Fixed-Base Simulator	4-2
	4.1.2 Moving-Base Simulator	4-13
	4.2 STAI PILOT QUALITATIVE EVALUATION	4-32
	4.2.1 Externally Blown Flap (EBF) Evaluation	4-40
	4.2.2 Internally Blown Flap (IBF) Evaluation	4-49
	4.2.3 Vectored Thrust (VT) Evaluation	4-55
	4.2.4 EBF Evaluation on the Large Amplitude Simulator (LAS)	4-60
	4.3 MOVING BASE VERSUS FIXED BASE EVALUATION	4-64
5	CONCLUSIONS AND RECOMMENDATIONS	5-1
6	REFERENCES	6-1
Appendix		
I	CONVAIR AEROSPACE TRIM-STAB DIGITAL COMPUTER PROGRAM	I-1
II	MODIFICATIONS TO MIL-F-8785B TURBULENCE MODEL FOR STAI SIMULATION TASKS	II-2
III	REPRESENTATIVE STAI SIMULATION DATA	III-1
IV	EVALUATION CRITERIA AND QUESTIONNAIRE FOR STOL TACTICAL AIRCRAFT INVESTIGATION (STAI)	IV-1
V	TEST AND EVALUATION PLAN FOR THE STAI (EBF) ON THE MOVING-BASE LARGE AMPLITUDE SIMULATOR	V-1

LIST OF ILLUSTRATIONS

Figure		Page
2-1	EBF General Arrangement	2-2
2-2	EBF Engine Nacelle/Wing Relationship	2-3
2-3	IBF-2 General Arrangement	2-4
2-4	MF/VT General Arrangement	2-9
2-5	MF/VT Engine Nacelle/Wing Relationship	2-12
2-6	EBF Horizontal Tail - cg Criteria	2-17
2-7	EBF n_z/α and $d\gamma/dV$ versus True Airspeed	2-18
2-8	IBF/VT n_z/α and $d\gamma/dV$ versus True Airspeed	2-19
2-9	MF/VT n_z/α and $d\gamma/dV$ versus True Airspeed	2-19
2-10	EBF Phugoid Damping	2-20
2-11	IBF/VT Phugoid Damping	2-21
2-12	MF/VT Phugoid Damping	2-21
2-13	EBF Short Period Frequency and Acceleration Sensitivity	2-22
2-14	IBF/VT Short Period Frequency and Acceleration Sensitivity	2-23
2-15	MF/VT Short Period Frequency and Acceleration Sensitivity	2-23
2-16	EBF Short Period	2-24
2-17	IBF/VT Short Period	2-24
2-18	MF/VT Short Period	2-25
2-19	EBF Longitudinal Static Stability	2-25
2-20	IBF/VT Longitudinal Static Stability	2-26
2-21	MF/VT Longitudinal Static Stability	2-26
2-22	EBF, IBF/VT, and MF/VT $\delta_{c/g}$ versus Airspeed	2-27
2-23	Preliminary Longitudinal Stability Augmentation System	2-32
2-24	Pitch Attitude Loop	2-32
2-25	EBF Pitch Root Locus at 80 Knots and 60 Degrees of Flaps	2-33
2-26	Step Thrust Command with Pitch Augmentation only	2-34
2-27	Step Flap Command with Pitch Augmentation only	2-34
2-28	Airspeed and Angle of Attack Control Loops	2-35
2-29	Step Thrust Command with no Interconnects	2-35
2-30	Step Flap Command with no Interconnects	2-35
2-31	Flap/Throttle Interconnection	2-37
2-32	Step Thrust Command with Complete Augmentation	2-40
2-33	Step Flap Command with Complete Augmentation	2-40
2-34	Frequency Response for Bare and Augmented Airframe	2-42
2-35	Baseline Lateral Directional Control System	2-43
2-36	Trim Data for EBF Right Outboard Engine Out (60 degrees of Flaps)	2-44
2-37	Trim Data for IBF Right Outboard Engine Out (60 degrees of Flaps)	2-45
2-38	Trim Data for VT Right Outboard Engine Out (60 degrees of Flaps, 60 degrees of Thrust Vector)	2-46

LIST OF ILLUSTRATIONS, Contd

Figure		Page
2-39	EBF Steady-State Sideslip Trim Data	2-48
2-40	IBF Steady-State Sideslip Trim Data	2-49
2-41	VT Steady-State Sideslip Trim Data	2-50
2-42	EBF Roll Mode Time Constant	2-51
2-43	EBF Spiral Mode Time to Double Amplitude	2-51
2-44	IBF Roll Mode Time Constant	2-52
2-45	IBF Spiral Mode Time to Double Amplitude	2-52
2-46	MF/VT Roll Mode Time Constant	2-53
2-47	MF/VT Spiral Mode Time to Double Amplitude	2-53
2-48	Response of Roll Rate to Step 1 Deg Aileron Input (Open Loop)	2-54
2-49	Response of Roll Rate to Step Full Scale Input (Closed Loop)	2-55
2-50	EBF Dutch Roll Characteristics	2-57
2-51	IBF Dutch Roll Characteristics	2-57
2-52	VT Dutch Roll Characteristics	2-58
2-53	EBF Roll Oscillations, Landing	2-59
2-54	EBF Sideslip Excursions, Landing	2-60
2-55	EBF Sideslip Excursions, Landing, STOL Parameters	2-61
2-56	EBF Roll Oscillations, Takeoff	2-62
2-57	EBF Sideslip Excursions, Takeoff	2-62
2-58	EBF Sideslip Excursions, Takeoff, STOL Parameters	2-63
2-59	EBF Roll-Rate Oscillations, Cruise	2-64
2-60	EBF Sideslip Excursions, Cruise	2-64
2-61	IBF Roll Oscillations, Landing	2-65
2-62	IBF Sideslip Excursions, Landing	2-66
2-63	IBF Sideslip Excursions, Landing, STOL Parameters	2-67
2-64	IBF Roll-Rate Oscillations, Takeoff	2-68
2-65	IBF Sideslip Excursions, Takeoff	2-68
2-66	IBF Sideslip Excursions, Takeoff, STOL Parameters	2-69
2-67	IBF Roll-Rate Oscillations, Cruise	2-70
2-68	IBF Sideslip Excursions, Cruise	2-70
2-69	VT Roll Oscillations, Landing	2-71
2-70	VT Sideslip Excursions, Landing	2-71
2-71	VT Sideslip Excursions, Landing, STOL Parameters	2-72
2-72	VT Roll Oscillations, Takeoff	2-73
2-73	VT Sideslip Excursions, Takeoff	2-73
2-74	VT Sideslip Excursions, Takeoff, STOL Parameters	2-74
2-75	VT Roll Oscillations, Cruise	2-75
2-76	VT Sideslip Excursions, Cruise	2-75
2-77	Modified Lateral Directional Control System	2-76
2-78	EBF Lateral Directional SAS, 80 Knots and Landing Flaps	2-77

LIST OF ILLUSTRATIONS, Contd

Figure		Page
2-79	EBF Roll Oscillations - Landing Effect of SAS Gains at 80 knots	2-78
2-80	EBF Sideslip Excursions - Landing Effect of SAS Gains at 80 knots	2-78
3-1	Flight Path Control Original Baseline	3-2
3-2	Revised Flight Path Baseline	3-2
3-3	Maximum Mechanical Flight Path System	3-3
3-4	Pitch Axis Control Original Baseline	3-4
3-5	Pitch Axis Revised Baseline	3-5
3-6	Pitch Axis Fly-by-Wire Mechanization	3-7
3-7	Lateral Directional Original Baseline	3-8
3-8	Lateral Directional Revised Baseline	3-9
3-9	Roll Axis Mechanical Mechanization	3-10
3-10	Lateral-Directional Fly-by-Wire Mechanization	3-11
4-1	STOL Simulator Cockpit	4-3
4-2	Close-up of Simulator Cockpit	4-3
4-3	Left-Hand Console Layout	4-4
4-4	Flight Instrument Panel Layout	4-5
4-5	Visual-Scene Vertical Geometry	4-6
4-6	Simulation Equipment	4-7
4-7	STOL MST Propulsion Dynamics	4-8
4-8	Thrust Response Schedules	4-9
4-9	Thrust Rate Limits	4-9
4-10	Power Response Time History	4-9
4-11	Control Stick Signal Shaping	4-12
4-12	QBAR Gain Schedule	4-13
4-13	Simulation Model of Wind Magnitude Versus Altitude	4-14
4-14	Large Amplitude Simulator	4-16
4-15	FBS Uncontrolled Pitch Response to a Pulse of δ_{stick} (3700-ft Altitude, $\gamma_{IC} = -7$ deg, Flaps = 60 deg, Gear Down)	4-18
4-16	MBS Uncontrolled Pitch Response to a Pulse of δ_{stick} (3700-ft Altitude, $\gamma_{IC} = -7$ deg, Flaps = 60 deg, Gear Down)	4-19
4-17	FBS Uncontrolled Pitch Response to a Pulse of δ_{stick} (12,500-ft Altitude, $\gamma_{IC} = 0$ deg, Flaps = 0 deg)	4-20
4-18	MBS Uncontrolled Pitch Response to a Pulse of δ_{stick} (12,500-ft Altitude, $\gamma_{IC} = 0$ deg, Flaps = 0 deg)	4-21
4-19	FBS Uncontrolled Roll Response to a Pulse of Lateral Stick (3700-ft Altitude, $\gamma_{IC} = -7$ deg, Flaps = 60 deg, Gear Down, Speed _{IC} = 80 knots)	4-22
4-20	MBS Uncontrolled Roll Response to a Pulse of Lateral Stick (3700-ft Altitude, $\gamma_{IC} = -7$ deg, Flaps = 60 deg, Gear Down, Speed _{IC} = 80 knots)	4-23

LIST OF ILLUSTRATIONS, Contd

Figure		Page
4-21	FBS Uncontrolled Roll Response to a Pulse of Lateral Stick (12,500-ft Altitude, $\gamma_{IC} = 0$ deg, Flaps = 0 deg, Gear Down, Speed = 200 knots)	4-24
4-22	MBS Uncontrolled Roll Response to a Pulse of Lateral Stick (12,500-ft Altitude, $\gamma_{IC} = 0$ deg, Flaps = 0 deg, Gear Down, Speed = 200 knots)	4-25
4-23	FBS Uncontrolled Yaw Response to a Pulse of Rudder Pedal (3700-ft Altitude, $\gamma_{IC} = -7$ deg, Flaps = 60 deg, Gear Down, Speed _{IC} = 80 knots)	4-26
4-24	MBS Uncontrolled Yaw Response to a Pulse of Rudder Pedal (3700-ft Altitude, $\gamma_{IC} = -7$ deg, Flaps = 60 deg, Gear Down, Speed _{IC} = 80 knots)	4-27
4-25	FBS Uncontrolled Yaw Response to a Pulse of Rudder Pedal (12,500-ft Altitude, $\gamma_{IC} = 0$ deg, Flaps = 0 deg, Gear Down, Speed = 200 knots)	4-28
4-26	MBS Uncontrolled Yaw Response to a Pulse of Rudder Pedal (12,500-ft Altitude, $\gamma_{IC} = 0$ deg, Flaps = 0 deg, Gear Down, Speed = 200 knots)	4-29
4-27	FBS Augmented Pitch Response to a Pulse of δ_{stick} (3700-ft Altitude, $\gamma_{IC} = -7$ deg, Flaps = 60 deg, Gear Down, Speed _{IC} = 80 knots)	4-30
4-28	MBS Augmented Pitch Response to a Pulse of δ_{stick} (3700-ft Altitude, $\gamma_{IC} = -7$ deg, Flaps = 60 deg, Gear Down, Speed _{IC} = 80 knots)	4-31
4-29	FBS Augmented Yaw Response to a Pulse of Rudder Pedal (3700-ft Altitude, $\gamma_{IC} = -7$ deg, Flaps = 60 deg, Gear Down, Speed _{IC} = 80 knots)	4-33
4-30	MBS Augmented Yaw Response to a Pulse of Rudder Pedal (3700-ft Altitude, $\gamma_{IC} = -7$ deg, Flaps = 60 deg, Gear Down, Speed _{IC} = 80 knots)	4-34

LIST OF TABLES

Table		Page
2-1	EBF Dimensional Data	2-5
2-2	EBF Group Weight Statement	2-6
2-3	IBF-2 Dimensional Data	2-7
2-4	IBF-2 Group Weight Statement	2-8
2-5	MF/VT Dimensional Data	2-10
2-6	MF/VT Group Weight Statement	2-11
2-7	Baseline Vehicle Mass Properties	2-15
4-1	Control Mode Switch Selections	4-10
4-2	Actuator Characteristics	4-11
4-3	Large Amplitude Flight Simulator System Summary	4-15
4-4	Cooper/Harper Handling Qualities Rating Scale	4-35

NOMENCLATURE

<u>Symbol</u>		<u>Units</u>
A_x	Total external force divided by weight along body axes, x	g's
A_y	Total external force divided by weight along body axes, y	g's
A_z	Total external force divided by weight along body axes, z	g's
b	Wing span	Ft
c, MAC	Mean Aerodynamic Chord	Ft
C_D	Drag Coefficient	
C_L	Lift Coefficient	
C_{ℓ}	Rolling Moment Coefficient	
$C_{L_{MAX}}$	Maximum Lift Coefficient	
C_m	Pitching Moment Coefficient	
C_n	Yawing Moment Coefficient	
C_{μ}	Thrust Coefficient	
G_1, G_2	Transfer functions of control system elements	
GT	Gross Thrust	Lb
h	Altitude	Ft
\dot{h}	Altitude	Ft/Sec
I_x	Moments of inertia about the c. g.	Slug/Sq Ft
I_y	Moments of inertia about the c. g.	Slug/Sq Ft
I_z	Moments of inertia about the c. g.	Slug/Sq Ft

NOMENCLATURE, Contd

<u>Symbol</u>		<u>Units</u>
I_{xz}	Product of inertia about the c. g.	Slug/Sq Ft
i_H	Stabilizer Incidence Angle	Deg
K	SAS Gain	Var
L_β	Dimensional rolling moment derivative with respect to β	$1/\text{Sec}^2$
L_p	Dimensional rolling moment derivative with respect to p	$1/\text{Sec}$
L_r	Dimensional rolling moment derivative with respect to r	$1/\text{Sec}$
L_{δ_r}	Dimensional rolling moment derivative with respect to δ_r	$1/\text{Sec}^2$
L_{δ_a}	Dimensional rolling moment derivative with respect to δ_a	$1/\text{Sec}^2$
$L_{\delta_{sp}}$	Dimensional rolling moment derivative with respect to δ_{sp}	$1/\text{Sec}^2$
L_{ENG}	Dimensional rolling moment derivative with respect to $\dot{\theta}_{ENG}$	Rad/Sec^2
l_T	Distance from MAC/4 to the 1/4 c of the horizontal tail	Ft
M_μ	Dimensional pitching moment derivative with respect to μ	$1/\text{Ft}\text{-Sec}$
M_w	Dimensional pitching moment derivative with respect to w	$1/\text{Ft}\text{-Sec}$
M_q	Dimensional pitching moment derivative with respect to q	$1/\text{Sec}$
$M_{\dot{w}}$	Dimensional pitching moment derivative with respect to \dot{w}	$1/\text{Sec}$

NOMENCLATURE. Contd

<u>Symbol</u>		<u>Units</u>
M_{δ_e}	Dimensional pitching moment derivative with respect to δ_e	1/Sec ²
M_{δ_F}	Dimensional pitching moment derivative with respect to δ_F	1/Sec ²
M_{THR}	Dimensional pitching moment derivative with respect to THR	1/Sec ² - %
M_x	Externally applied moments about the x axis	Ft-Lb
M_y	Externally applied moments about the y axis	Ft-Lb
M_z	Externally applied moments about the z axis	Ft-Lb
N_{β}	Dimensional yawing moment derivative with respect to β	1/Sec ²
N_p	Dimensional yawing moment derivative with respect to p	1/Sec
N_r	Dimensional yawing moment derivative with respect to r	1/Sec
N_{δ_r}	Dimensional yawing moment derivative with respect to δ_r	1/Sec ²
N_{δ_a}	Dimensional yawing moment derivative with respect to δ_a	1/Sec ²
$N_{\delta_{sp}}$	Dimensional yawing moment derivative with respect to δ_{sp}	1/Sec ²
N_{ENG}	Dimensional yawing moment derivative with respect to ENG	Rad/Sec ²
n_z	Normal acceleration	Ft/Sec ²
$n_{z/\alpha}$	Acceleration sensitivity parameter	Ft/Sec ²
p	Roll Rate	Deg/Sec or Rad/Sec
$P_{osc/p_{avg}}$	Roll oscillation parameter	

NOMENCLATURE, Contd

<u>Symbol</u>		<u>Units</u>
q	Pitch Rate	Deg/Sec
q	Dynamic Pressure	Lb/Sq Ft
q_t/q	Dynamic pressure ratio of horizontal tail to free stream	
r	Yaw rate	Deg/Sec or Rad/Sec
S	Wing area	Sq Ft
S, s	Laplace transform variable	1/Sec
T_z	Time to double amplitude of an experimental motion	Sec
T, TH, THR	Throttle position in percent of engine thrust	
u	Incremental forward body-axis velocity	Ft/Sec
V	True airspeed	Kts or Ft/Sec
w	Incremental downward body axis velocity	Ft/Sec
X_u	Dimensional X-axis force derivative with respect to u	1/Sec
X_w	Dimensional X-axis force derivative with respect to w	1/Sec
X_q	Dimensional X-axis force derivative with respect to q	Ft/Sec
$X_{\dot{w}}$	Dimensional X-axis force derivative with respect to \dot{w}	
X_{δ_e}	Dimensional X-axis force derivative with respect to δ_e	Ft/Sec ²
X_{δ_F}	Dimensional X-axis force derivative with respect to δ_F	Ft/Sec ²
X_{THR}	Dimensional X-axis force derivative with respect to THR	Ft/Sec ² - $\frac{q}{b}$

NOMENCLATURE, Contd

<u>Symbol</u>		<u>Units</u>
Y_{β}	Dimensional yawing moment derivative with respect to β	1/Sec
Y_p	Dimensional yawing moment derivative with respect to p	
Y_r	Dimensional yawing moment derivative with respect to r	
Y_{δ_r}	Dimensional yawing moment derivative with respect to δ_r	1/Sec
Y_{δ_a}	Dimensional yawing moment derivative with respect to δ_a	1/Sec
$Y_{\delta_{sp}}$	Dimensional yawing moment derivative with respect to δ_{sp}	1/Sec
Y_{ENG}	Dimensional yawing moment derivative with respect to ENG	1/Sec
Z_u	Dimensional Z-axis force derivative with respect to u	1/Sec
Z_q	Dimensional Z-axis force derivative with respect to q	Ft/Sec
Z_w	Dimensional Z-axis force derivative with respect to \dot{w}	
Z_{δ_e}	Dimensional Z-axis force derivative with respect to δ_e	Ft/Sec ²
Z_{δ_F}	Dimensional Z-axis force derivative with respect to δ_F	Ft/Sec ²
Z_{THR}	Dimensional Z-axis force derivative with respect to THR	Ft/Sec ² -%
<u>Greek</u>		<u>Units</u>
α	Angle of attack	Deg
$\dot{\alpha}$	$d\alpha / dt$	Deg/Sec
$\Delta\beta_{MAX/K}$	Sideslip excursion parameter	Deg
$\Delta\beta/C_1$	STOL sideslip excursion parameter	

NOMENCLATURE, Contd

<u>Greek</u>		<u>Units</u>
γ	Flight Path Angle	Deg
$d\gamma/\gamma V$	Flight Path Stability Parameter	Deg/Kt
δ_a	Aileron Deflection Angle	Deg, Rad
δ_e	Elevator Deflection Angle	Deg, Rad
$\delta_{e/g}$	Maneuver Stability Parameter	Deg/g
$d\delta_e/dV$	Static Stability Parameter	Deg/Kt
$d\delta_e/d\theta$	STOL Static Stability Parameter	
δ_F	Flap Deflection Angle	Deg
δ_H, δ_{STAB}	Stabilizer Incidence Angle	
δ_R	Rudder Deflection Angle	Deg, rad
δ_{sp}	Spoiler Deflection Angle	Deg, Rad
δ_{STICK}	Longitudinal Stick Deflection	Deg
ϵ	Downwash Angle	Deg
ζ	Damping Ratio of Complex Root	
η	Gross Thrust Vector Angle	Deg
θ	Pitch Angle	Deg, Rad
$\dot{\theta}, q$	Pitch Rate	Deg/Sec or Rad/Sec
τ	Control System Time Constants	Sec

NOMENCLATURE, Contd

<u>Greek</u>		<u>Units</u>
τ_R	Roll Mode Time Constant	Sec
ω	Natural Frequency of Complex Root	Rad/Sec
ϕ	Bank Angle	Deg
ϕ_{osc}/ϕ_{avg}	STOL Roll Oscillation Parameter	
$\phi/\beta \Big _d$	Ratio of ϕ to β in the Dutch Roll Mode	
ψ_β	Phase Angle of the Dutch Roll Sideslip Response	Deg
 <u>Subscripts</u>		
a	Aileron	
B	Body	
ENG	Engine Out	
e	Elevator	
f	Flap	
H	Horizontal Tail	
o	Trim Value	
ph	Phugoid	
SP	Short Period	
sp	Spoller	
THR	Throttle	
W	Wing	

SECTION 1

INTRODUCTION

This report presents the flight control technology aspects of the STOL Tactical Aircraft investigation conducted by the Convair Aerospace Division of General Dynamics. Baseline flight control systems were generated for each of three versions of the Medium STOL Transport. An externally blown flap (EBF), an internally blown flap with vectoring of non-diverted engine flow (IBF/VT), and a mechanical flap/vectored thrust (MF/VT) configuration were the three baseline vehicles used for the flight control studies.

The analyses used to generate the baseline control systems and the results thereof are presented in Section 2. Analytical models are defined and handling quality characteristics are plotted relative to applicable specifications. A preliminary stability augmentation system (SAS) is identified where required to satisfy handling quality specifications.

Section 3 presents the findings of the control system mechanization trade study. Baseline control systems were analyzed and revised to generate both a maximum-mechanical control implementation and a fly-by-wire implementation. Revised systems are diagrammed and a comparison of the mechanical versus a fly-by-wire version is discussed. A recommended system is described.

Validation of the baseline control systems was effected through extensive flight simulator evaluations using both fixed-base and moving-base simulators. Section 4 describes the flight simulators used and significant aspects of the simulation models. The larger part of this section deals with the pilot qualitative evaluations of the three STOL configurations. Evaluation criteria are described and pilot opinion data in the form of narrative description and Cooper/Harper ratings are presented. Evaluations on the moving-base simulator for the EBF version are compared to the fixed-base results for the same EBF configuration. Finally, there is pilot commentary regarding the relative merits of various levels of flight simulation for flight control studies, e.g., fixed base versus moving base.

The appendixes include descriptions of analytical programs, turbulence model adaptations, evaluation questionnaires, the evaluation test plan, and a collection of representative simulated flight run data.

SECTION 2

LOW SPEED CONTROL METHODS

This section covers the analyses performed to generate a baseline control system used in the control mechanization trades in Section 3 and the simulations of Section 4. The emphasis is on the generation of handling qualities, comparisons to the handling quality specifications, and in generating a stability augmentation system (SAS) to show compliance.

Included is a brief description of the three baseline vehicles and the analytical model used. The sources for the data base are referenced.

2.1 VEHICLE DESCRIPTION

The control analyses in this report concern three specific configurations. These are three of the six configurations described in detail in Reference 2-1, and are:

1. EBF. Externally blown jet flap with GE13/F2B cruise engines.
2. IBF-2. Internally blown jet flap with STF369 engines.
3. MF/VT. Mechanical flap plus vectored thrust with GE13/F2A cruise engines.

Reference 2-1 describes each of these vehicles, including general arrangement three-views, dimensions, weights, and mission performance. The criteria and analyses used for configuring and sizing the vehicles are also included, as well as the majority of the aerodynamic and propulsion data bases needed for control analyses. These configurations are presented briefly here to identify the data base and points of departure for the controls analyses. A significant modification was made to the IBF-2 vehicle described in Reference 2-1 due to controls analysis and simulation. The IBF-2 vehicle used in this report is assumed to have vectoring capability of the undiverted flow. This modification was needed to better match its propulsion capability to the landing configuration. Without vectoring, the low throttle setting to balance drag during the approach reduces the diverted flow and thus reduces the flow coefficient (C_{μ}) and maximum coefficient of lift ($C_{L_{max}}$).

2.1.1 EXTERNALLY BLOWN FLAP. The externally blown flap (EBF) configuration was sized using GE13/F2B engines scaled to a rated thrust of 18,600 pounds per engine for a takeoff gross weight of 148,200 pounds. General arrangement of the EBF configuration is shown in Figure 2-1. The engines are installed in single nacelles and use annular cascades to reverse thrust. Auxiliary engines are also

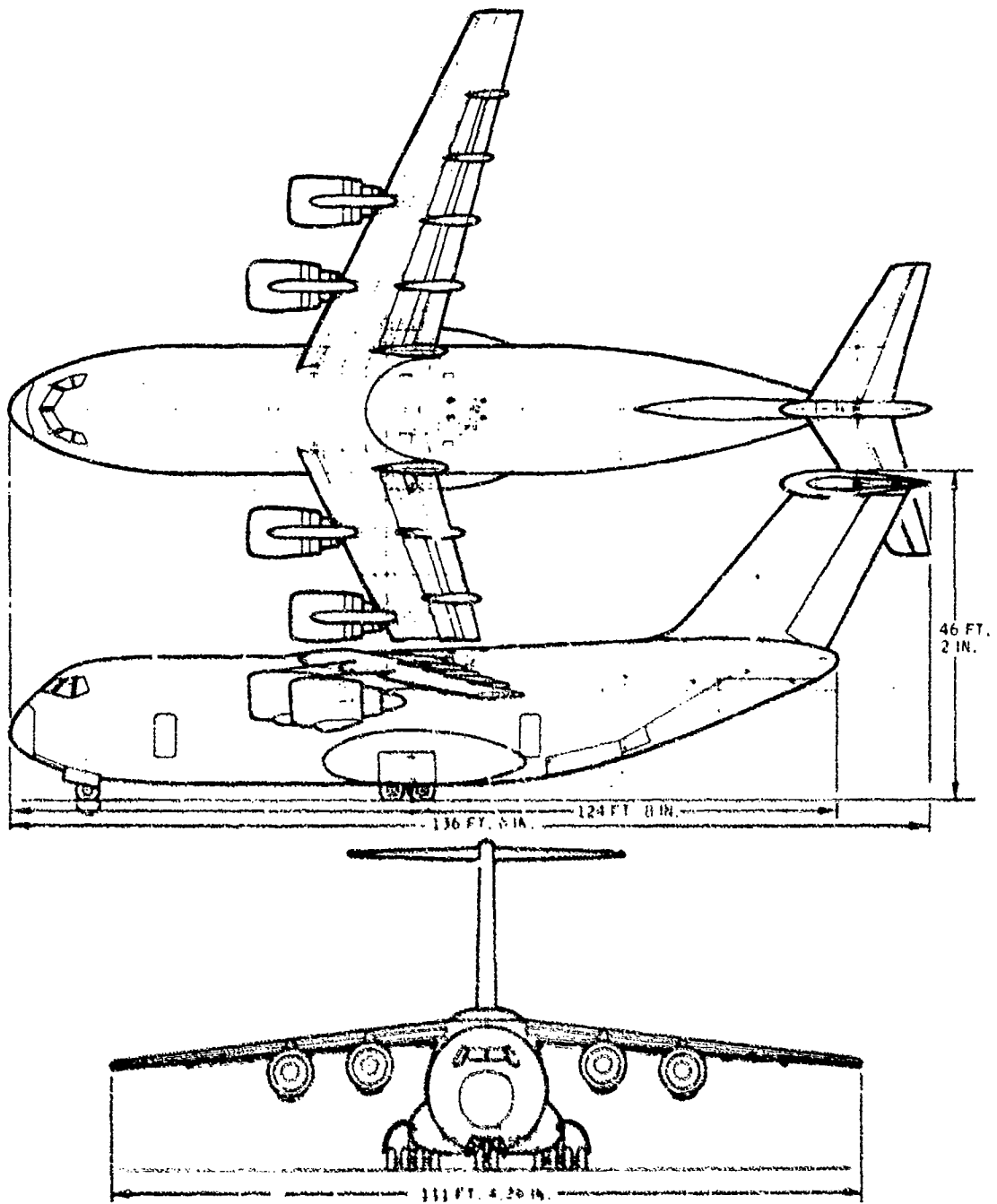


Figure 2-1. EBF General Arrangement

located in the fuselage to supply boundary layer control on the wing leading edge device for engine-out lateral control, on the elevator for longitudinal control, and on the rudder for engine-out directional control. Figure 2-2 shows a cross section of the engine nacelle/wing relationship to illustrate the features of the variable-geometry leading edge flap and the double-slotted trailing edge flap. Dimensional data and the weight statement are presented in Tables 2-1 and 2-2, respectively.

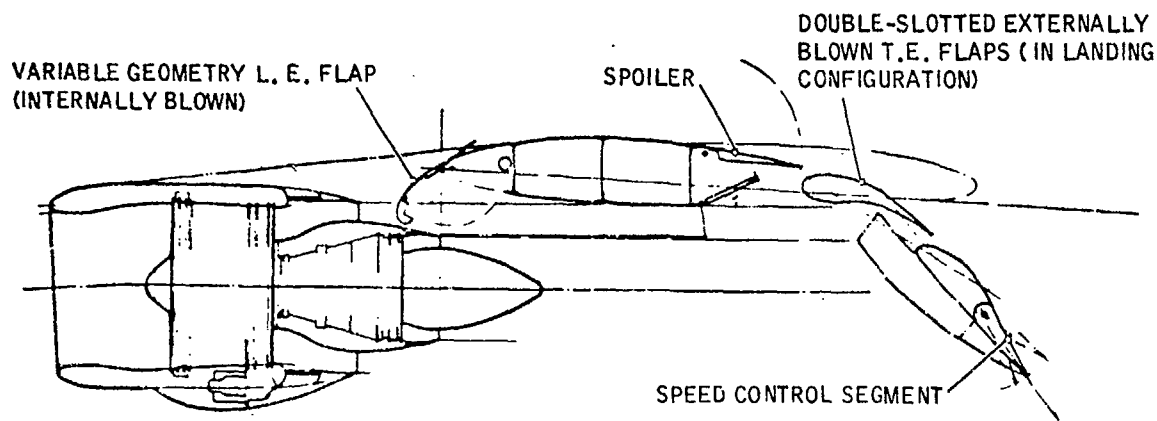


Figure 2-2. EBF Engine Nacelle/Wing Relationship

2.1.2 INTERNALLY BLOWN FLAP, IBF-2. The internally blown flap configuration (IBF-2) was sized using STF369 engines scaled to a rated thrust of 22,840 pounds per engine for a takeoff gross weight of 170,350 pounds. General arrangement is shown in Figure 2-3. The engines are installed in single nacelles and use annular cascades to reverse thrust. Dimensional data and the weight statement are presented in Tables 2-3 and 2-4, respectively.

2.1.3 MECHANICAL FLAP PLUS VECTORED THRUST. The mechanical flap plus vectored thrust configuration was sized using GE13/F2A cruise engines. A scaled engine thrust of 24,500 pounds was required for the selected takeoff gross weight of 168,750 pounds.

General arrangement of the MF/VT configuration is shown in Figure 2-4. The design used a twin-podded nacelle arrangement to accommodate the single-bearing thrust deflection devices. Auxiliary engines (two RB176-11s) were located in the fuselage to supply boundary layer control on the wing leading edge devices for high lift and on the elevator if required for additional longitudinal control. Figure 2-5 shows a cross section of the engine nacelle/wing relationship, illustrating the features of the variable-geometry leading edge flap and the triple-slotted trailing edge flap. Dimensional data and the weight statement are given in Tables 2-5 and 2-6, respectively.

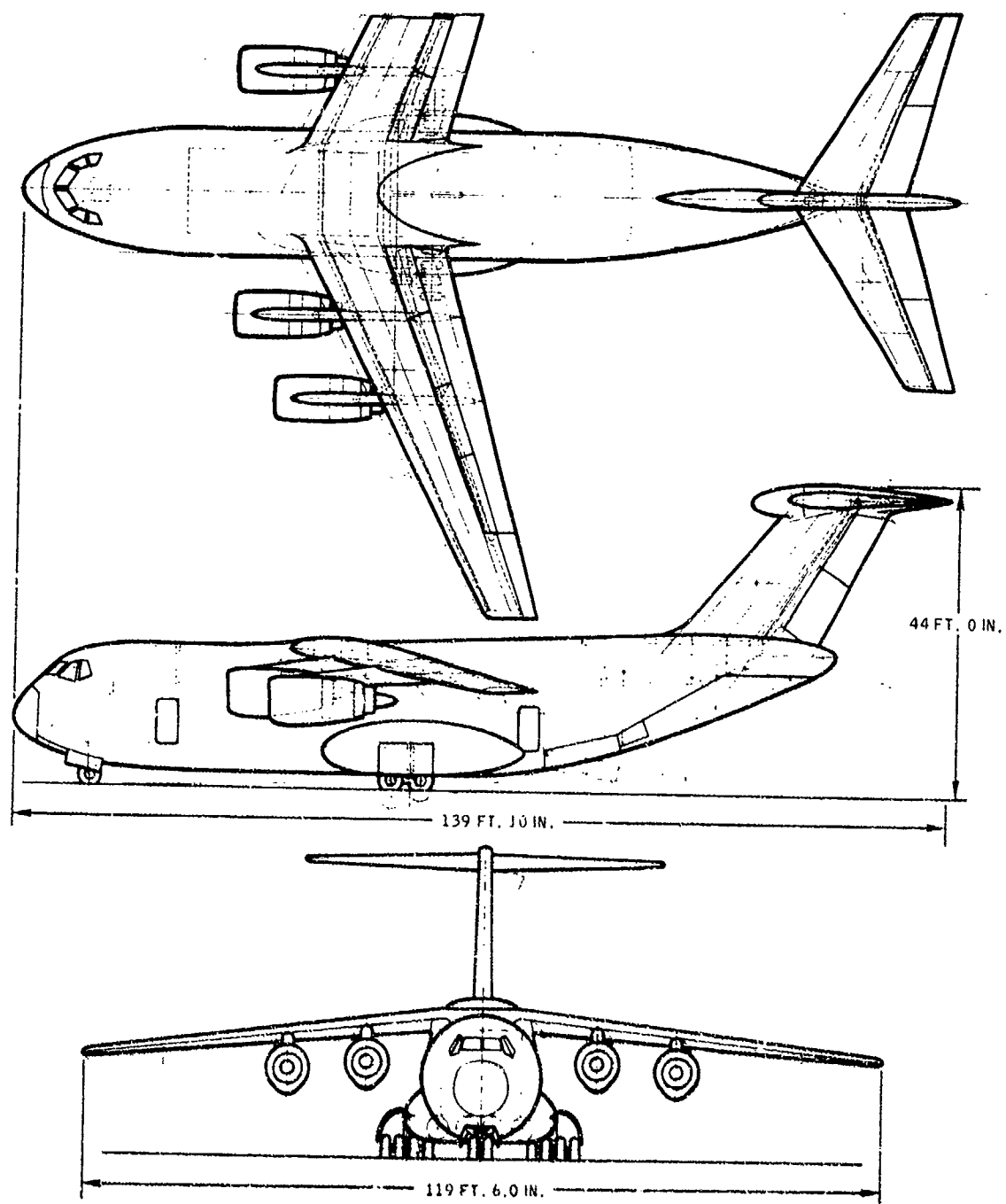


Figure 2-3. IBF-2 General Arrangement

Table 2-1. EBF Dimensional Data

Wing		Horizontal Tail	
Span	111.36 ft	Span	40.66 ft
Area	1550.00 ft ²	Area	367.33 ft ²
Aspect Ratio	8.00	Aspect Ratio	4.50
Taper Ratio	0.33	Taper Ratio	0.40
Incidence		Deflection	+5 to -10 deg
At Root	3.5 deg	Sweep at c/4	30 deg
At Tip	-1.0 deg	Chord	
Dihedral	-3.5 deg	Root	154.88 in.
Sweep at c/4	25.0 deg	Tip	61.95 in.
Chord		Mean Aerodynamic	115.06 in.
Root (at Aircraft Centerline)	250.60 in.	Airfoil Section	
Tip	83.45 in.	Root	64A012
Mean Aerodynamic	180.97 in.	Tip	64A008
Airfoil Section		Pivot Centerline	c/4 _{MAC}
Root (at W.S. 69.0)	64A3 (13.12)		
Tip	64A4 10	Elevator	
Leading Edge Device		Span	Full
(Variable Camber)		Chord	0.35
Span	Full	Deflection	+15 to -50 deg
Chord	0.155% c	Hinge Line	0.35c
Deflection	56 deg	Vertical Tail	
Trailing Edge Flap		Span	24.68 ft
Span	0.80 b/2	Area	510.0 ft ²
Chord	0.75c	Aspect Ratio	1.18
Deflection	60 deg	Taper Ratio	0.65
Spoilers		Sweep at c/4	39.0 deg
Span	0.80 b/2	Chord	
Chord	0.195c	Root	301.38 in.
Hinge	0.548c	Tip	195.00 in.
Deflection	60 deg	Mean Aerodynamic	252.37 in.
Alleron		Airfoil Section	64A012
Span	0.20 b/2	Rudder	
Chord	0.25c	Span	Full
Deflection	+50 deg	Chord	0.30c
Fuselage		Deflection	+50 deg
Length	136 ft, 4 in.		
Maximum Width	212 in.		
Cargo Envelope			
Length	55 ft		
Width	12 ft		
Height	12 ft		

Table 2-2. EBF Group Weight Statement

STRUCTURE	62704.6 lb	SYSTEMS AND EQUIPMENT	16386.4
Wing	20639.5		
Basic Structure	14758.0	Auxiliary Power Unit	525.2
Box Structure	10856.3	Instruments	602.5
Ribs + LE + TE	3056.1	Hydraulic and Pneumatic	725.2
Penalties	845.6	Electrical	2058.8
Secondary Structure	737.9	Avionics	2000.0
Flaps	3867.6	Armament	1200.0
Leading Edge Device	995.2	Furnishings	4504.0
Spoilers	280.8	Air Conditioning/Anti Ice	1741.4
Wing Fold	0.0	Auxiliary Gear	2959.2
Horizontal Tail	1411.2		
Vertical Tail	3488.7	WEIGHT EMPTY	93363.5
Body	25238.1		
Landing Gear	7107.6	Basic Operating Items	1829.0
Surface Controls	2012.3		
Nacelle	2807.0	BASIC OPERATING WEIGHT	95192.5
PROPULSION	14282.5		
Engines	9495.0	Payload	28000.0
Propulsion Systems	2943.2		
Thrust Reversers	2157.8	ZERO FUEL WEIGHT	123192.5
Inlets	163.2		
Exhaust	189.6	Fuel	25000.0
Cooling	83.2	Wing	25000.0
Lubrication	29.1	Fuselage	0.0
Starting	201.7		
Engine Controls	118.7	TAKEOFF GROSS WEIGHT	148192.5
Fuel System	1844.3		
Plumbing	872.6	DESIGN WEIGHT (lb)	148075.6
Pumps	212.8		
Distribution	230.0	MAXIMUM WEIGHT (lb)	148075.6
Vent	175.4		
Controls	23.1		
Refuel	101.3		
Dump	34.0		
Tankage	871.7		
Foam	480.0		
Sealing	124.2		
Cells	367.6		

Table 2-3. IBF-2 Dimensional Data

Wing		Horizontal Tail	
Span	119.50 ft	Span	25.20 ft
Area	17.85 ft ²	Area	453.94 ft ²
Aspect Ratio	8.00	Aspect Ratio	4.50
Taper Ratio	0.33	Taper Ratio	0.40
Incidence		Deflection	+5 to -10 deg
At Root	3.5 deg	Sweep at c/4	30 deg
At Tip	-1.0 deg	Chord	
Dihedral	-3.5 deg	Root	172.2 in.
Sweep at c/4	25.0 deg	Tip	68.9 in.
Chord		Mean Aerodynamic	128.0 in.
Root (at Aircraft Centerline)	279.0 in.	Airfoil Section	
Tip	89.5 in.	Root	64A012
Mean Aerodynamic	194.0 in.	Tip	64A008
Airfoil Section		Pivot Centerline	c/4 MAC
Root (at W.S. 69.0)	64A3 (13.12)		
Tip	64A4 10	Elevator	
Leading Edge Device		Span	Full
(Variable Camber)		Chord	0.35
Span	Full	Deflection	+15 to -50 deg
Chord	0.155% c	Hinge Line	0.35c
Deflection	56 deg		
Trailing Edge Flap		Vertical Tail	
Span	0.80 b/2	Span	27.81 ft
Chord	0.35c	Area	655.5 ft ²
Deflection	60 deg	Aspect Ratio	1.18
		Taper Ratio	0.65
		Sweep at c/4	39.0 deg
		Chord	
Spoilers		Root	342.5 in.
Span	0.80 b/2	Tip	223.0 in.
Chord	0.195c	Mean Aerodynamic	286.8 in.
Hinge	0.548c	Airfoil Section	64A012
Deflection	60 deg		
Aileron		Rudder	
Span	0.20 b/2	Span	Full
Chord	0.25c	Chord	0.30c
Deflection	±50 deg	Deflection	±50 deg
Fuselage			
Length	136 ft, 4 in.		
Maximum Width	212 in.		
Cargo Envelope			
Length	55 ft		
Width	12 ft		
Height	12 ft		

Table 2-4. IBF-2 Group Weight Statement

STRUCTURE		73186.6 lb	SYSTEMS AND EQUIPMENT		13864.6
Wing		24103.2	Auxiliary Power Unit		552.8
Basic Structure	18384.4	Instruments		737.2	
Box Structure	13141.3	Hydraulics and Pneumatic		859.4	
Ribs + LE + TE	3632.4	Electrical		2110.5	
Peralties	1610.7	Avionics		2000.0	
Secondary Structure	919.2	Armament		1200.0	
Flaps	3300.7	Furnishings		4504.0	
Leading Edge Device	1182.4	Air Conditioning/ Anti Ice		1842.6	
Spoilers	316.5	Auxiliary Gear		68.1	
Wing Fold	0.0	WEIGHT EMPTY		107086.1	
Horizontal Tail	1742.9	Basic Operating Items		1964.0	
Vertical Tail	4602.8	BASIC OPERATING WEIGHT		109050.1	
Body	26319.4	Payload		28000.0	
Landing Gear	8174.4	ZERO FUEL WEIGHT		137050.1	
Surface Controls	2334.0	Fuel		33300.0	
Nacelle	5910.0	Wing		33300.0	
		Fuselage		0.0	
PROPULSION	20014.9	TAKEOFF GROSS WEIGHT		170350.1	
Engines	14240.0	DESIGN WEIGHT (lb)		170300.0	
Propulsion Systems	3517.9	MAXIMUM WEIGHT (lb)		170300.0	
Thrust Reversers	2548.1	LANDING WEIGHT (lb)		153650.0	
Inlets	214.1				
Exhaust	234.1				
Cooling	100.5				
Lubrication	39.9				
Starting	262.5				
Engine Controls	118.7				
Fuel System	2257.0				
Plumbing	1027.1				
Pumps	257.1				
Distribution	280.3				
Vent	211.9				
Controls	26.6				
Refuel	210.3				
Dump	40.9				
Tankage	1239.9				
Foam	639.4				
Sealing	154.0				
Cells	436.6				

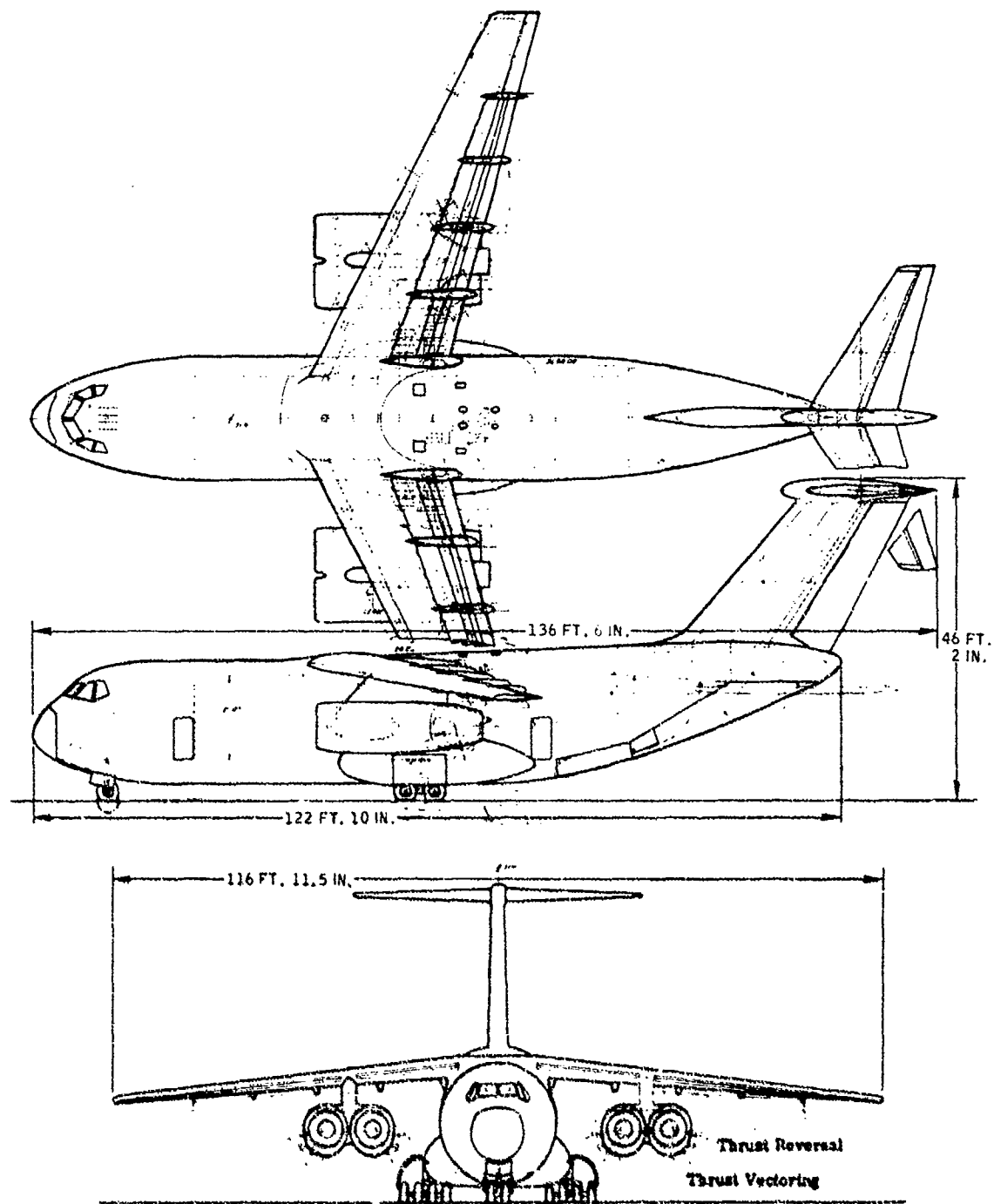


Figure 2-4. MF/VT General Arrangement

Table 2-5. MF/VT Dimensional Data

Wing		Horizontal Tail	
Span	116.96 ft	Span	43.76 ft
Area	1710.0 ft ²	Area	425.63 ft ²
Aspect Ratio	8.00	Aspect Ratio	4.50
Taper Ratio	0.33	Taper Ratio	0.40
Incidence		Deflection	+5 to -10 deg
At Root	3.5 deg	Sweep at c/4	30 deg
At Tip	-1.0 deg	Chord	
Dihedral	-3.5 deg	Root	166.5 in.
Sweep at c/4	25.0 deg	Tip	66.8 in.
Chord		Mean Aerodynamic	124.0 in.
Root (at Aircraft Centerline)	263.0 in.	Airfoil Section	
Tip	87.6 in.	Root	64A012
Mean Aerodynamic	190.0 in.	Tip	64A008
Airfoil Section		Pivot Centerline	c/4 MAC
Root (at W.S. 69.0)	64A3 (13,12)		
Tip	64A4 10	Elevator	
Leading Edge Device		Span	Full
(Variable Camber)		Chord	0.35
Span	Full	Deflection	+15 to -50 deg
Chord	0.155% c	Hinge Line	0.35c
Deflection	56 deg	Vertical Tail	
Trailing Edge Flap		Span	26.93 ft
Span	0.80 b/2	Area	614.59 ft
Chord	0.45c	Aspect Ratio	1.18
Deflection	60 deg	Taper Ratio	0.65
Spoilers		Sweep at c/4	39.0 deg
Span	0.80 b/2	Chord	
Chord	0.195c	Root	332.0 in.
Hinge	0.548c	Tip	216.0 in.
Deflection	60 deg	Mean Aerodynamic	278.0 in.
Aileron		Airfoil Section	64A012
Span	0.20 b/2	Rudder	
Chord	0.25c	Span	Full
Deflection	+50 deg	Chord	0.30c
Fuselage		Deflection	+50 deg
Length	136 ft. 4 in.		
Maximum Width	212 in.		
Cargo Envelope			
Length	55 ft		
Width	12 ft		
Height	12 ft		

Table 2-6. MF/VT Group Weight Statement

STRUCTURE		72096.0 lb	SYSTEMS AND EQUIPMENT		16716.6
Wing		23844.8	Auxiliary Power Unit		549.4
Basic Structure	17039.6	Instruments		732.2	
Box Structure	12750.2	Hydraulic and Pneumatic		822.5	
Ribs + LE + TE	3478.0	Electrical		2113.4	
Penalties	811.4	Avionics		2000.0	
Secondary Structure	852.0	Armament		1200.0	
Flaps	4537.6	Furnishings		4504.0	
Leading Edge Device	1224.6	Air Conditioning/Anti Ice		1827.4	
Spoilers	311.1	Auxiliary Gear		2967.5	
Wing Fold	0.0	WEIGHT EMPTY		110862.7	
Horizontal Tail	1662.4	Basic Operating Items		1887.5	
Vertical Tail	4345.0	BASIC OPERATING WEIGHT		112750.2	
Body	26250.5	Payload		28000.0	
Landing Gear	8103.2	ZERO FUEL WEIGHT		140750.2	
Surface Controls	2230.2	Fuel		28000.0	
Nacelle	5660.0	Wing		28000.0	
PROPULSION	22050.1	Fuselage		0.0	
Engines	13570.0	TAKEOFF GROSS WEIGHT		168750.2	
Propulsion Systems	6377.8	DESIGN WEIGHT (lb)		168817.4	
Thrust Reversers	5420.0	MAXIMUM WEIGHT (lb)		168817.4	
Inlets	207.3				
Exhaust	228.3				
Cooling	110.6				
Lubrication	38.5				
Starting	254.4				
Engine Controls	118.7				
Fuel System	2103.3				
Plumbing	1036.1				
Pumps	283.0				
Distribution	260.1				
Vent	233.4				
Controls	24.4				
Refuel	198.6				
Dump	36.6				
Tankage	1066.2				
Foam	537.6				
Sealing	135.2				
Cells	393.4				

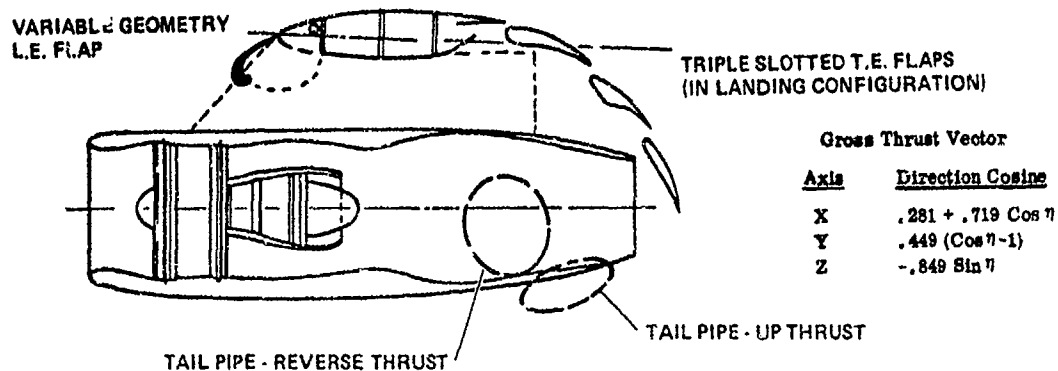


Figure 2-5. MF/VT Engine Nacelle/Wing Relationship

2.2 ANALYTICAL MODEL

Most of the analyses have been performed by digital computer, primarily using two existing programs:

1. TRIM-STAB, capable of performing six-degree-of-freedom (DOF) trim, separate longitudinal and lateral-directional linearized stability analyses about a trim point, and non-real-time, six DOF transients. This program is described in Appendix I.
2. Real-time piloted simulations, both fixed-base and moving-base, as described in Section 4.

This procedure requires an analytical model for each of the three vehicles. Subroutines were formulated to describe all forces and moments on the vehicles, based on these considerations:

1. Matching the data base as generated, primarily in Reference 2-1.
2. Maximum compatibility with existing programs.
3. Minimum reprogramming necessary to shift from one vehicle to another.
4. Minimum reprogramming necessary to shift from non-real-time programs to the real-time piloted simulations.

The following modules were generated as subroutines, separately, for each of the three vehicles where required. They contain all differences between the configurations.

2.2.1 WING/BODY LONGITUDINAL AERODYNAMICS. These subroutines include tabulated data that is interpolated to obtain the desired parameters. The outputs are C_L , C_D , C_m , q_t/q , ϵ , and $d\epsilon/d\alpha$. The inputs are angle of attack and flap angle. For the EBF vehicle, C_{μ} is also an input. For the IBF configuration, C_{μ} based on the diverted flow is an input. The data stored are points taken from the curves in Section 5 of Reference 2-1.

2.2.2 HORIZONTAL TAIL AERODYNAMICS. Contributions of the horizontal tail are included in a module that is common to all three vehicles. The principal data is tail lift coefficient as a function of tail angle of attack and elevator angle. The contribution of the elevator is given both with and without blowing, and is the data shown in Figure 96 of Reference 2-1.

Values of q ratio and downwash are determined in the wing/body module, and are different for each vehicle. Tail angle of attack is then computed by:

$$\alpha_H = \alpha_B - \epsilon + i_H + \frac{\dot{\theta} l_t}{V} + \frac{d\epsilon}{d\alpha} \dot{\alpha} \frac{l_t}{V}$$

Tail C_L and C_D are then evaluated. These are resolved to body axes and, based on the proper tail area and q ratio, converted to forces and moments about the aircraft cg.

2.2.3 LATERAL DIRECTIONAL AERODYNAMICS. This module includes the tabulated lateral directional data as it appears in Reference 2-1. Complete aircraft stability derivatives in stability axes are included. These are tabulated as functions of angle of attack and flap position. For the EBF vehicle, these are also functions of C_{μ} . For the IBF vehicle, these derivatives are functions of the C_{μ} computed from the diverted flow. The airframe derivatives are those due to sideslip, roll rate, and yaw rate. Control effectiveness is included (not as derivatives but as a control moment or force versus deflection) to accommodate nonlinearities. Aileron effectiveness is given two ways: with and without surface blowing. Spoiler effectiveness is particularly nonlinear and is stored as a four-dimensional function of angle of attack, flap angle, thrust coefficient, and spoiler deflection for both the EBF and IBF configurations. The runner effectiveness data base is the same for each vehicle, and is thus called as a separate subroutine.

This stability axis data about the quarter chord is then input to standard subroutines that convert them to body axes about the cg by translation and rotation for various time histories or linearized analyses.

2.2.4 PROPULSION. These subroutines are restricted to data for 2500 feet of altitude on a hot day (93°F). Data is generally stored as gross thrust and ram drag for full throttle as a function of velocity. It is stored as the unity scaled engine,

and the scale factors are stored separately. From Reference 2-1, the figure numbers for the hot-day data and the scale factors used are:

<u>Concept</u>	<u>Reference 2-1 Figure No. *</u>	<u>Scale</u>
EBF	49	0.815
IBF	67	1.015
MF/VT	65	1.1

The subroutines that describe each concept differ greatly in how the thrust-related forces are formulated. For the EBF, the outputs are:

1. Thrust coefficient based on gross thrust, $C_\mu = GT/qs$, which is used in the longitudinal wing body and the lateral directional subroutines.
2. Engine-out rolling moment, $\Delta C_\ell = f(\alpha, \delta_F, C_\mu)$
3. Engine-out yawing moment, $\Delta C_n = f(C_\mu)$

Ram drag effects for the EBF are all included in the data base as functions of C_μ , including drag, pitching moment, and sideslip derivatives.

The propulsion model for the MF/VT configuration is a self-contained momentum model. Gross thrust and ram drag magnitudes for full throttle are stored as functions of velocity. The centers of pressure for each component are estimated from the three-view and stored as constants. Gross thrust and ram drag are then resolved into three body-axis components, with gross thrust as a function of vector angle and ram drag as a function of angle of attack and sideslip angle. The vectoring assumed is the GE single-bearing thrust deflecting device, which results in significant side forces for each engine. These engines are installed side-by-side in paired pods as shown in Figures 2-4 and 2-5.

Moments about the cg are calculated in pitch, roll, and yaw from the force components and the stored centers of pressure. There is no asymmetry when all engines are operating equally except for sideslip ram drag effects. The model, however, accommodates an engine loss or differential throttle settings.

The propulsion model for the IBF vehicle is a split-flow type. Stored data consists of tabulated values of diverted gross thrust, undiverted gross thrust, and ram drag for full throttle as functions of velocity (Figure 67, Reference 2-1). The diverted gross thrust is used to compute a thrust coefficient, C_μ . This is used as a data

*The data in Figure 49 of Reference 2-1 as originally issued was in error. The correct 2500-foot hot day installed static thrust is 19,000 pounds for the unity scaled GE13/F2B engine.

argument in the other subroutines in the same manner as for the EBF vehicle except that a plenum and cross plumbing is assumed, and no engine-out rolling or yawing moments are evaluated due to the diverted flow.

The undiverted gross thrust and the ram drag are used in a momentum model. Component forces are calculated, centers of pressure determined, and moments calculated as for the MF/VT. The vectoring capability for this IBF vehicle (described in Paragraph 1.1) is included in the model as a pitch plane rotation of the gross thrust vector.

2.2.5 MASS PROPERTIES AND DIMENSIONS. This module includes the weights, cg, and moments and product of inertia for each vehicle using the mid-mission weights identified in Reference 2-1.

Some analysis was performed by arbitrary variation of one of these parameters; e.g., GW or cg, without altering the remainder of the baseline mass properties package. Also stored in this data package are the physical dimensions and areas required. Table 2-7 shows the baseline parameters used in the analyses and simulations.

Table 2-7. Baseline Vehicle Mass Properties

	EBF	IBF-2	VT/MF
Takeoff Weight (lb)	148,192	170,350	168,750
Mid-mission Weight (lb)	134,200	152,450	153,500
Fuselage station of cg (in.)	660.3	657.7	672.7
% MAC	20.1	19.0	26.8
Water Line (in.)	182.0	186.9	177.8
I_x (slug-ft ²)	1,144,000	1,468,000	1,574,000
I_y (slug-ft ²)	2,687,000	2,936,000	3,033,000
I_z (slug-ft ²)	3,459,000	3,966,000	4,141,000
I_{xz} (slug-ft ²)	322,500	276,700	293,500

2.2.6 LANDING GEAR. This module calculates the six-degree-of-freedom force and moment contributions of the main and nose landing gear. Since each of the three vehicles is designed around the same fuselage, and since the gear location is nominally the same for each, this module is common. Input data is included for each gear for: lumped spring constants, lumped damping constants, coefficients of friction, extended no-load coordinates for wheel center, and wheel radius.

This subroutine requires a set of direction cosines that relate aircraft position and attitude relative to the ground. It also includes aircraft linear and rotational velocities. The subroutine then calculates the deflection and rate of each gear from the no-load position and the gear load normal to the deflection. Finally, based on calculated skid angles, stored coefficients of friction, and input steering angles (if any), body axis forces and moments are calculated for each gear.

2.3 LONGITUDINAL HANDLING QUALITIES

In this section, the longitudinal handling qualities characteristics of the three vehicles are presented and compared to the handling quality specifications (MIL-F-8785B and MIL-F-83300). This data has been generated by the TRIM-STAB program described in Appendix I. The analytical model interpolates on tabulated non-linear aerodynamic data as discussed in Section 2.2. The trim-type data uses this continuous model. The linearized stability analyses are based on derivatives evaluated from the non-linear model at the trim point. Scatter vs. speed in any one of the plotted parameters in Sections 2.3 and 2.6 is not considered significant, but is primarily due to the process of evaluating local derivatives of the non-linear multi-dimensioned stored data. Most of the data presented is bare airframe data. A baseline longitudinal stability augmentation system (SAS) is developed in Paragraph 2.4; some of the curves in this discussion also include values with this nominal SAS.

Characteristics that had first-order effects on tail size were evaluated in establishing the baseline configurations in Reference 2-1. Decisions were made on tail size, including tail blowing. Figure 2-6 is repeated from Reference 2-1 as a starting point. The data base has been refined, but no attempt is made here to either update or completely review Reference 2-1. The most critical aft cg limit for the EBF is that marked Stability with Takeoff Flap-High α in Figure 2-6. This curve denotes the pitch-up characteristics (mostly a high $dc/d\alpha$ effect) that occur at high power settings, takeoff flaps, and high α and that reduce inherent stability. The steep slope of the curve shows that much additional tail area is needed to allow aft cg's and inherent stability at this flight condition. With the fairly elaborate SAS required for good flying qualities, this aft cg requirement is somewhat alleviated.

Two forward cg limits are shown: nose wheel liftoff and trimming high angles of attack with landing flap. These are both shown with and without elevator blowing, indicating that at least some of the tail blowing shown in the data base (Reference 2-1, Figure 96) will be required. The nominal cg is 20 percent for a tail area of 367 ft².

The data in this section is shown for each of the three vehicles. Since the handling quality characteristics for these vehicles are functions of power and high lift configuration, three specific flight configurations are also defined:

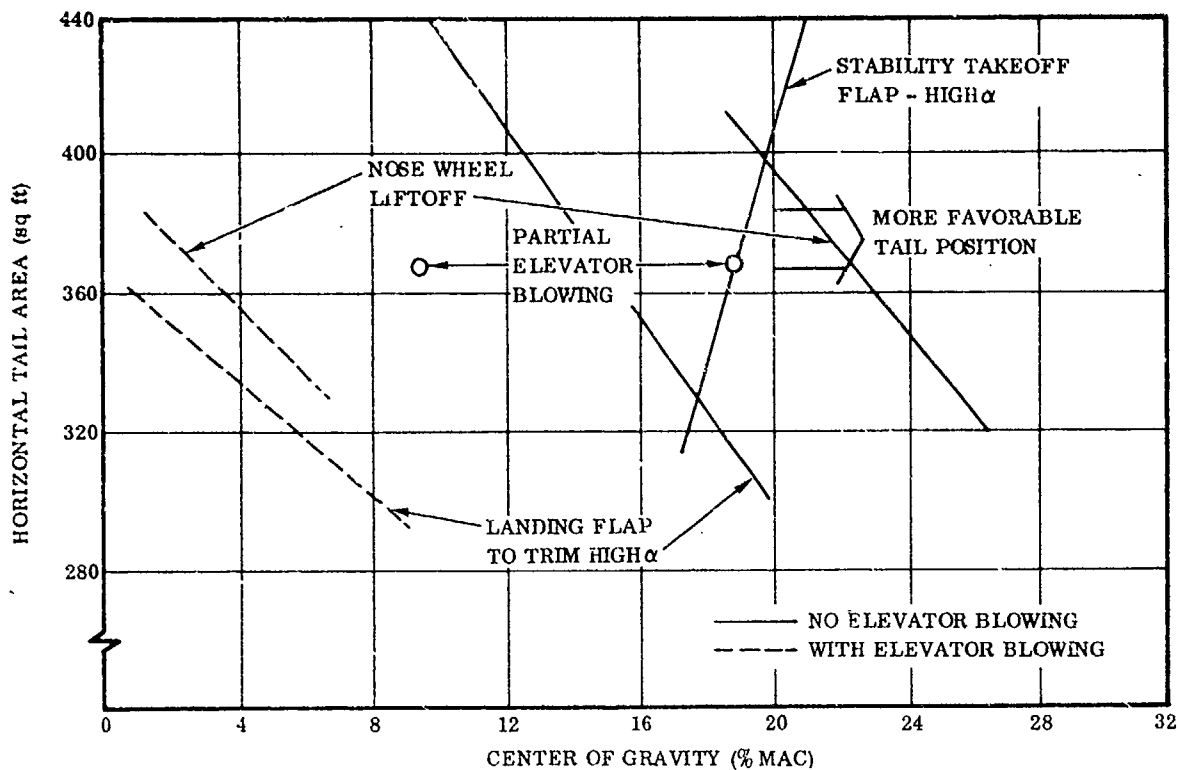


Figure 2-6. EBF Horizontal Tail - cg Criteria

1. Landing, Flaps at 60 degrees, Thrust Vector at 60 degrees for both the IBF/VT and MF/VT Vehicles. This is a Category C flight phase and corresponds to (L) of Reference 2-2 and (SL) of Reference 2-3. Trim conditions are a steady-state speed at a seven-degree descent and speeds from minimum to 100 knots.
2. Takeoff, Flaps at 30 degrees, Thrust Vector at 30 degrees for IBF/VT and MF/VT. This is also a Category C flight phase and corresponds to (TO) of Reference 2-2 and (ST) of Reference 2-3. Trim conditions are accelerating at full power ($\dot{V} > 0$) at $\gamma = 0$, and speeds from minimum to 160 knots.
3. Cruise, Flaps and Thrust Vector at 0 degrees, Power for Level Flight, Speeds from Minimum to 200 knots. This corresponds to (CR) Category B of Reference 2-2.

All cases use 2500 feet of altitude and a hot day (93° F). Where possible, longitudinal trim was by the stabilizer with the elevator at neutral. At speeds below 80 knots, the elevator was also used.

STOL vehicles such as MST must meet two handling quality specifications, References 2-2 and 2-3. In the cruise conditions, the aircraft specification applies; at minimum landing speeds, the V/STOL specification applies. Reference 2-2 refers to a discussion in Reference 2-4 on the establishment of V_{con} , the speed that establishes the demarcation. Three parameters are listed as potential measures of V_{con} : n_z/α , $d\gamma/dV$, and stall margin. Stall margin is difficult to establish with blown flaps, since $C_{L_{max}}$ is not sharply defined.

Figures 2-7 through 2-9 show plots of n_z/α and $d\gamma/dV$ for the three vehicles for cruise, takeoff, and landing configurations. As expected, the estimates of V_{con} vary, generally between 90 and 110 knots. Since the landing approach covers this speed regime, and since the landing approach has been emphasized in this contract work, responses are compared to specifications from both. It is generally assumed that below V_{con} the pilot will tend to use the STOL technique of controlling glide path with throttle, and above V_{con} he will use elevator. When SAS is used to give closed-loop characteristics that improve n_z/α and $d\gamma/dV$, V_{con} becomes especially confusing. The approach has been to use SAS so that both specifications are met, and to use piloted simulations to develop a preferred technique. The simulation program and results reported in Section 4 show the prevailing preference to be the STOL technique on landing approach.

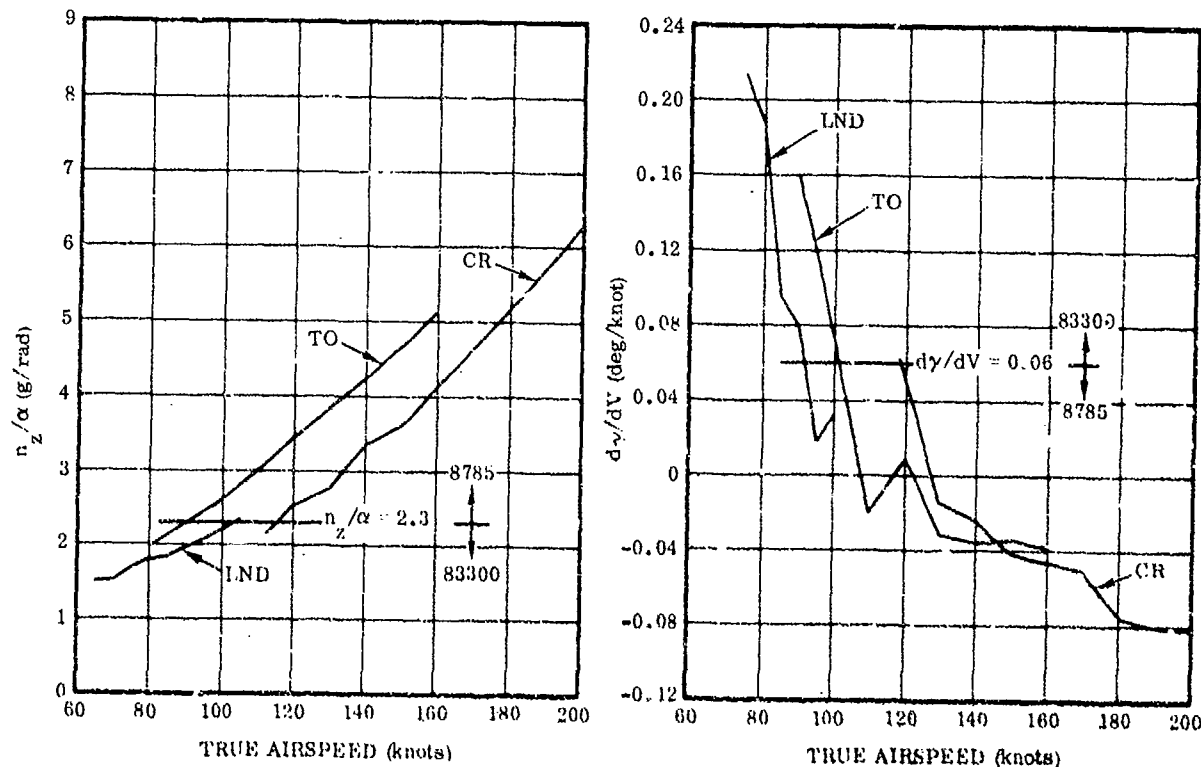


Figure 2-7. EBF n_z/α and $d\gamma/dV$ versus True Airspeed

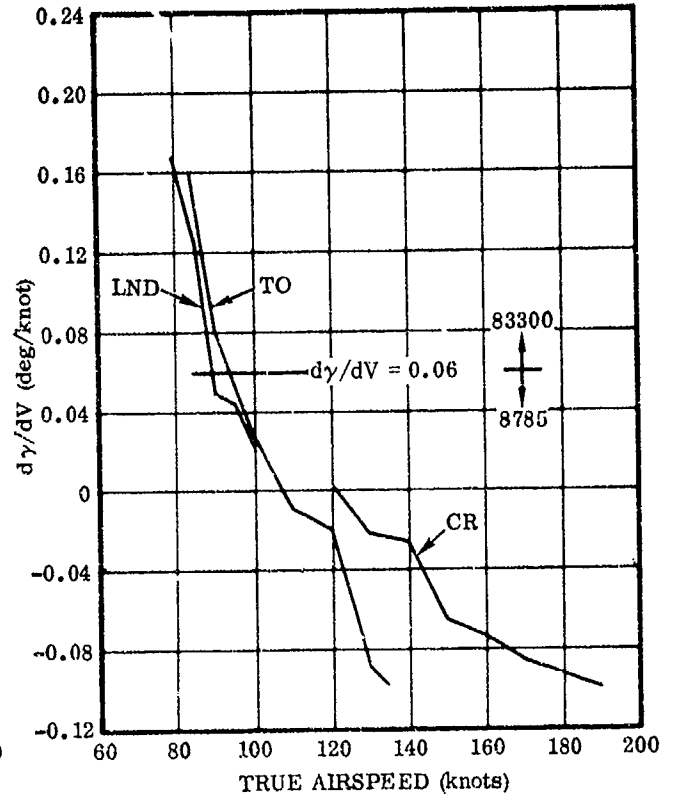
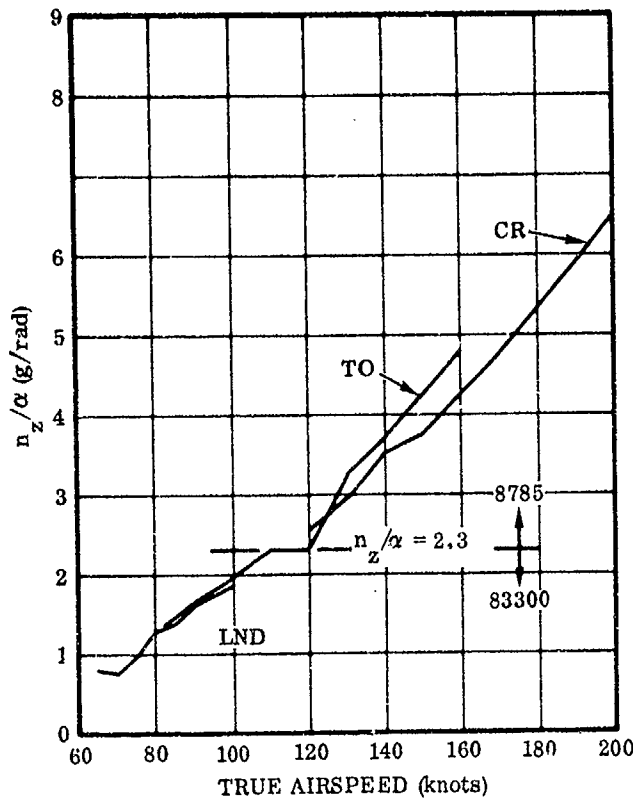


Figure 2-8. IBF/VT n_z/α and $d\gamma/dV$ versus True Airspeed

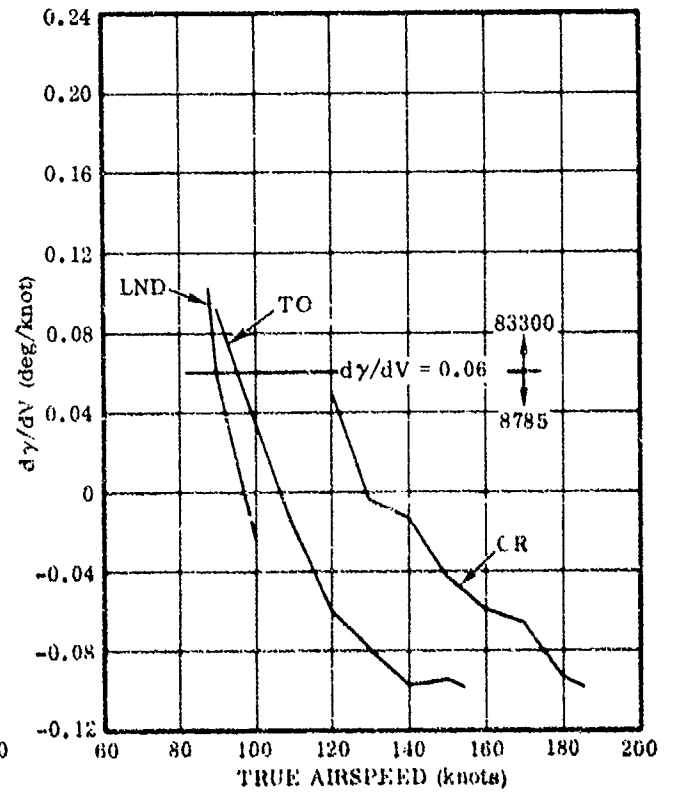
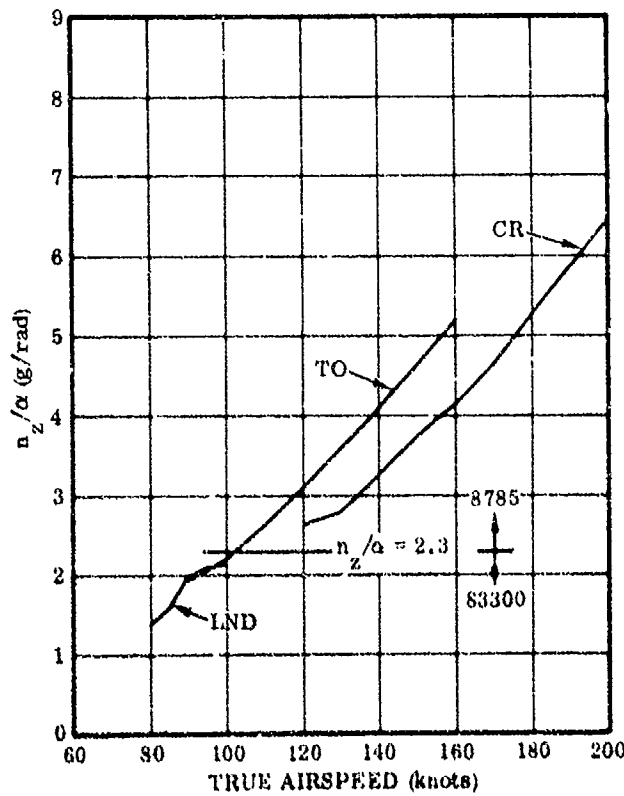


Figure 2-9. MF/VT n_z/α and $d\gamma/dV$ versus True Airspeed

Figures 2-10 through 2-12 show phugoid damping for all three vehicles. The boundaries from Reference 2-3, Paragraph 3.2.1.2 are shown. The requirement from Reference 2-2, Paragraph 3.3.2 is:

<u>Level</u>	<u>Requirement</u>
1	$\zeta > 0$
2	$T_2 < 12$
3	$T_2 < 5$

The EBF airframe is especially deficient. An artificial M_θ derivative due to pitch angle feedback to the elevator effectively damps the phugoid. The effect of the nominal gain schedule as determined in Paragraph 2.4 is also shown in these figures.

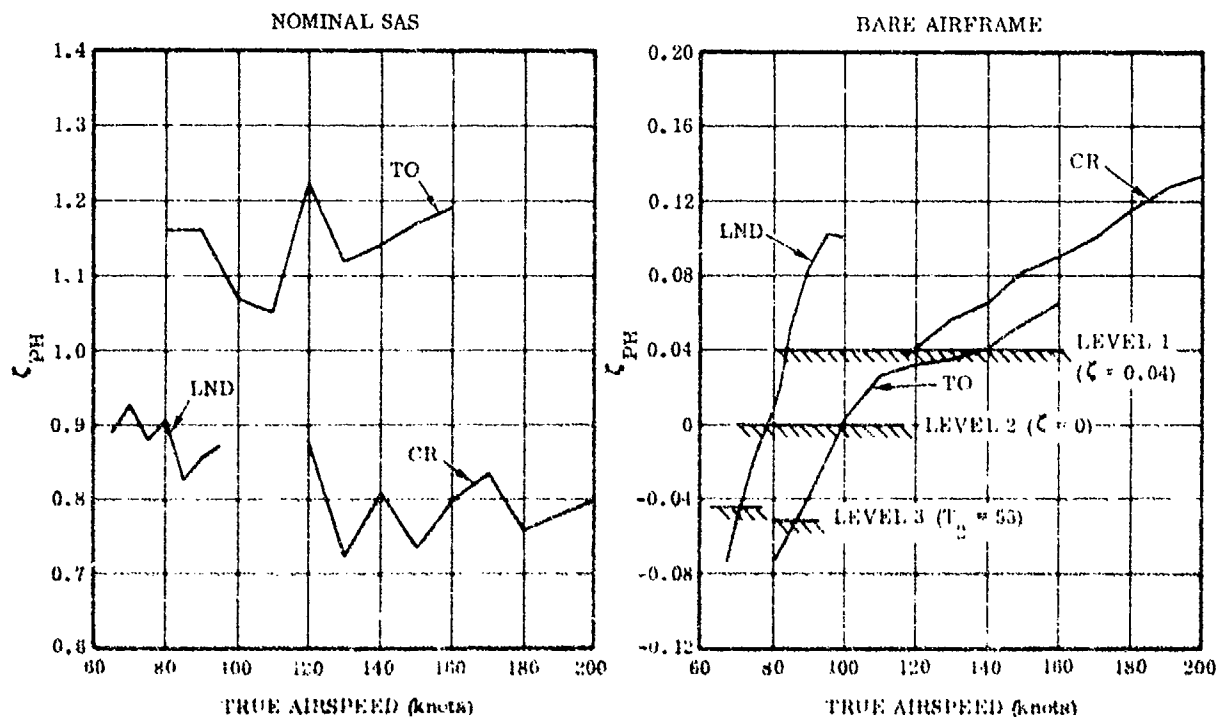


Figure 2-10. EBF Phugoid Damping

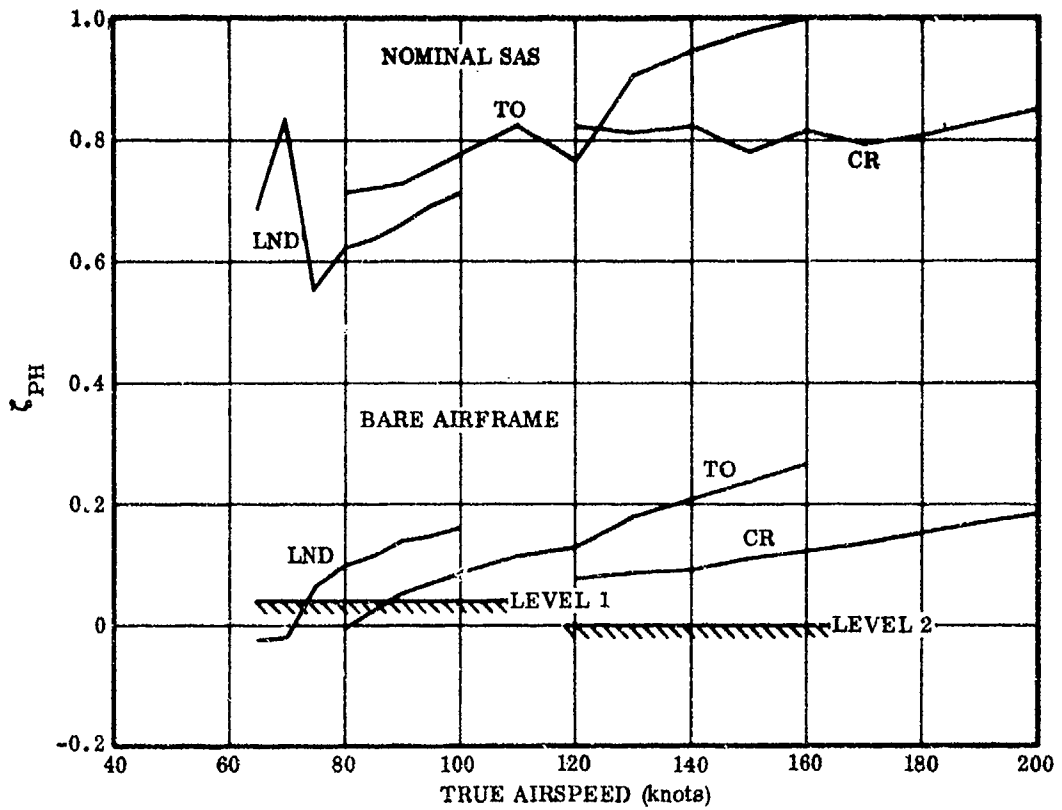


Figure 2-11. IBF/VT Phugoid Damping

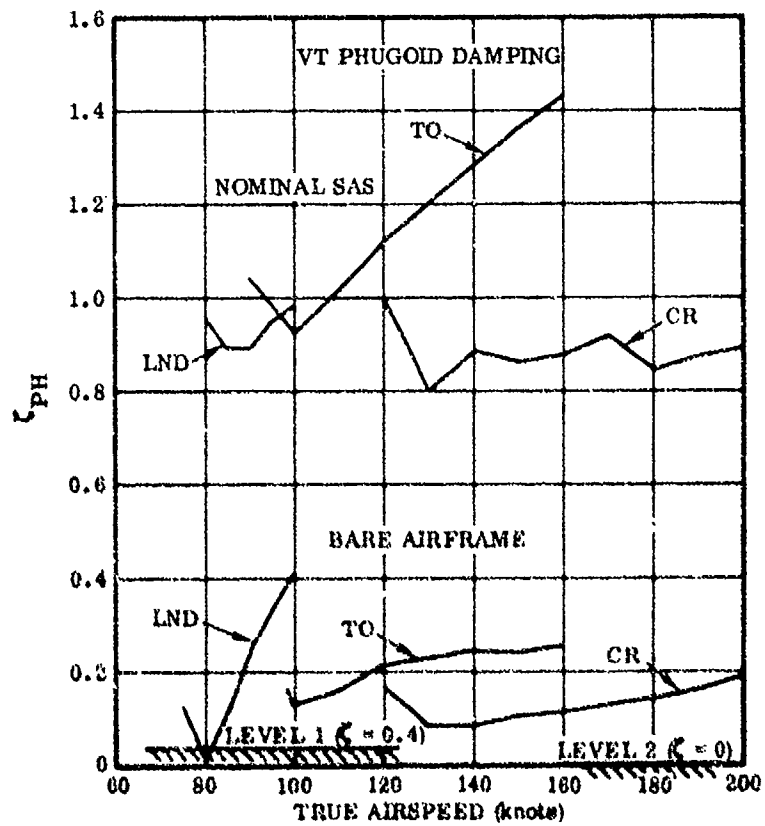


Figure 2-12. MF/VT Phugoid Damping

The short period responses are shown in Figures 2-13 through 2-18. The boundaries from Reference 2-2, Paragraph 3.2.2.1.1, are shown in Figures 2-13 through 2-15. As expected, the low speeds in both landing and takeoff fail to meet the Reference 2-3 specification. The responses do meet the Level 1 boundaries of Paragraph 3.3.2 of Reference 2-2, as shown in Figures 2-16 through 2-18. These are somewhat difficult to present, since the upper boundaries are functions of ω_n and ζ and the lower boundaries of n_z/α .

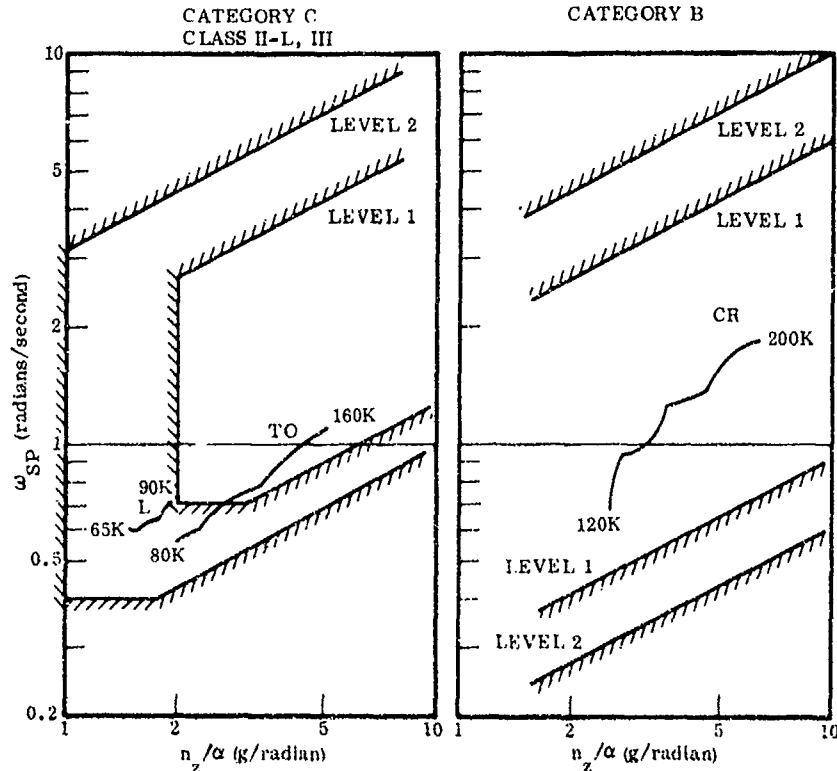


Figure 2-13. EBF Short Period Frequency and Acceleration Sensitivity

Longitudinal static trim data is shown in Figures 2-19 through 2-21. These are plots of the slopes calculated at each trim point, corresponding to changing trim speed with the elevator (without changing power). The term $d\delta_e/dV$ is specified to be stable in Paragraph 3.2.1.1 of Reference 2-3. Paragraph 3.3.1 of Reference 2-2 specifies both $d\delta_e/dV$ and $d\delta_e/d\theta$ for this maneuver.

Figure 2-22 shows δ_e/g for the three aircraft, as specified in Paragraph 3.2.2.2 of Reference 2-3. No detailed analysis of force gradients has been performed. A full power system is assumed, and no difficulty is anticipated in tailoring feel springs to meet the control force gradient specs, both in maneuvering flight (F_g/g) and speed trim (dF_g/dV and $dF_g/d\theta$). Since the position gradients look good, the combination of a q-spring and a fixed spring is almost certain to meet all of the specifications.

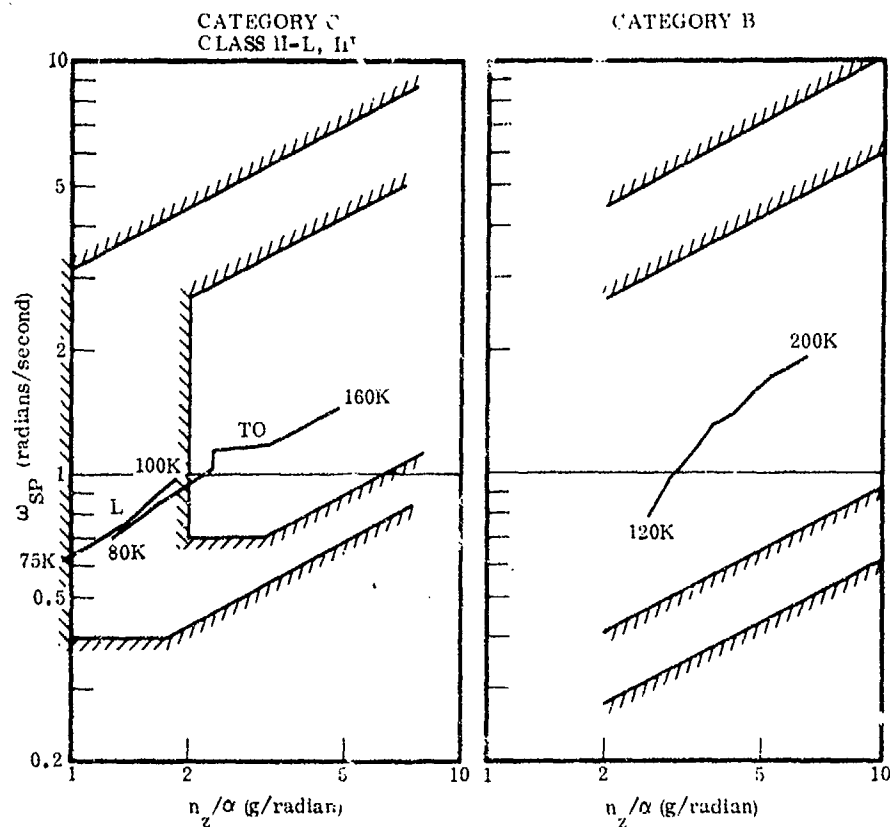


Figure 2-14. IBF/VT Short Period Frequency and Acceleration Sensitivity

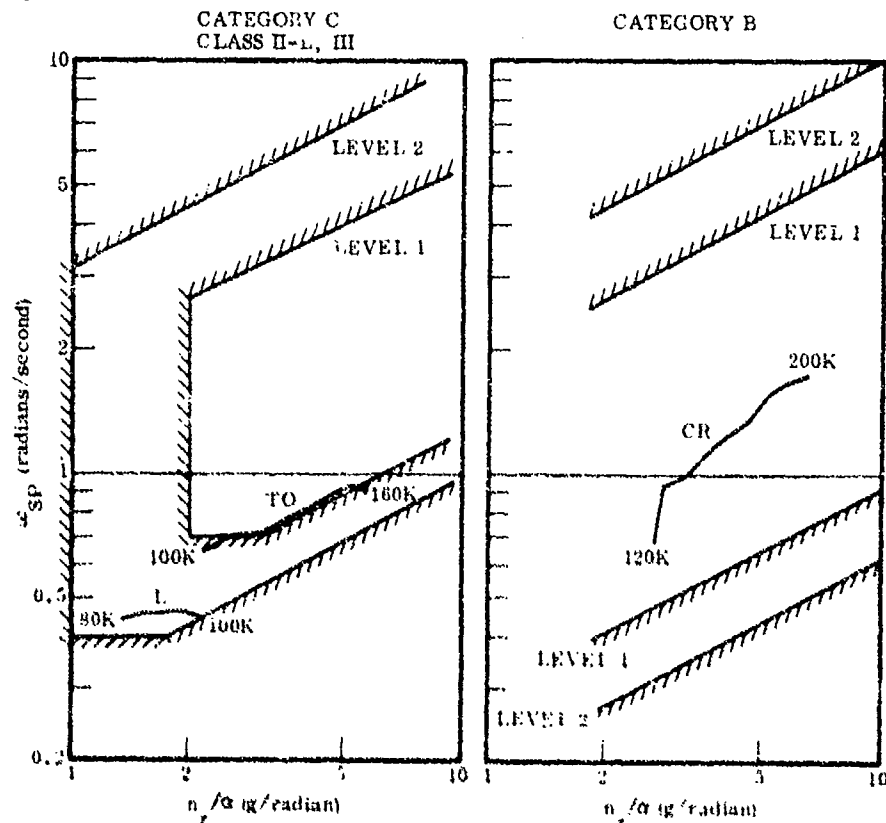


Figure 2-15. MF/VT Short Period Frequency and Acceleration Sensitivity

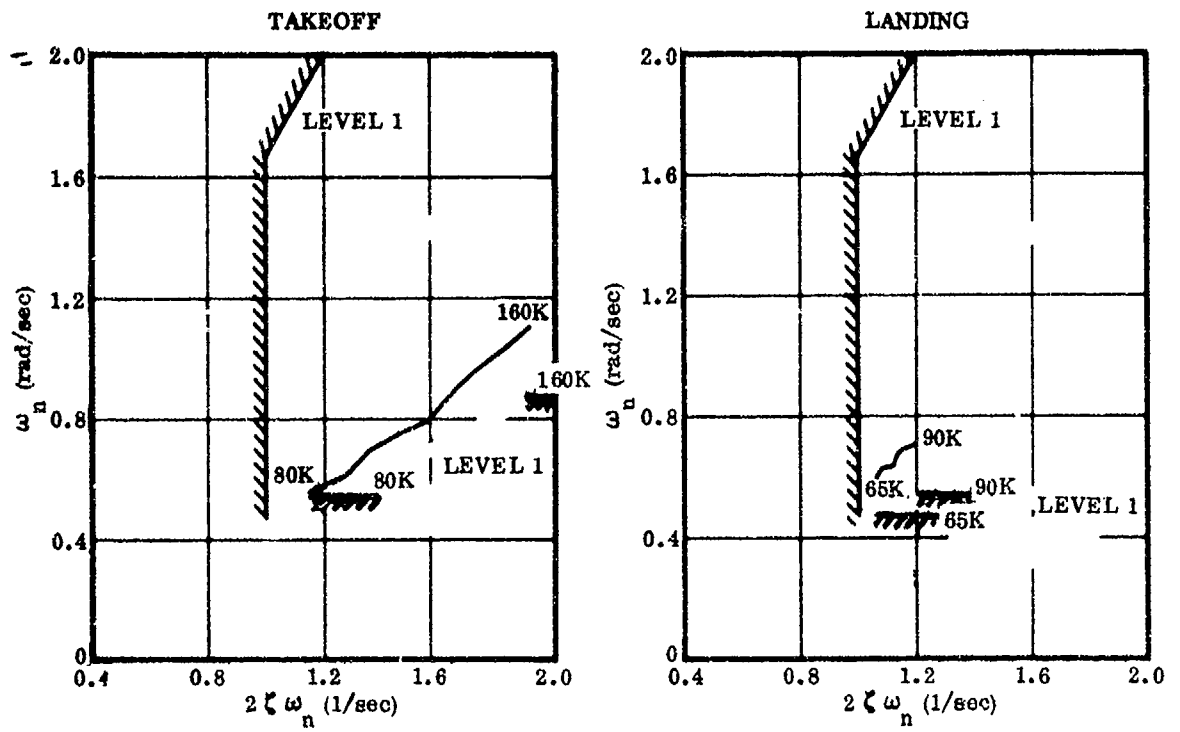


Figure 2-16. EBF Short Period

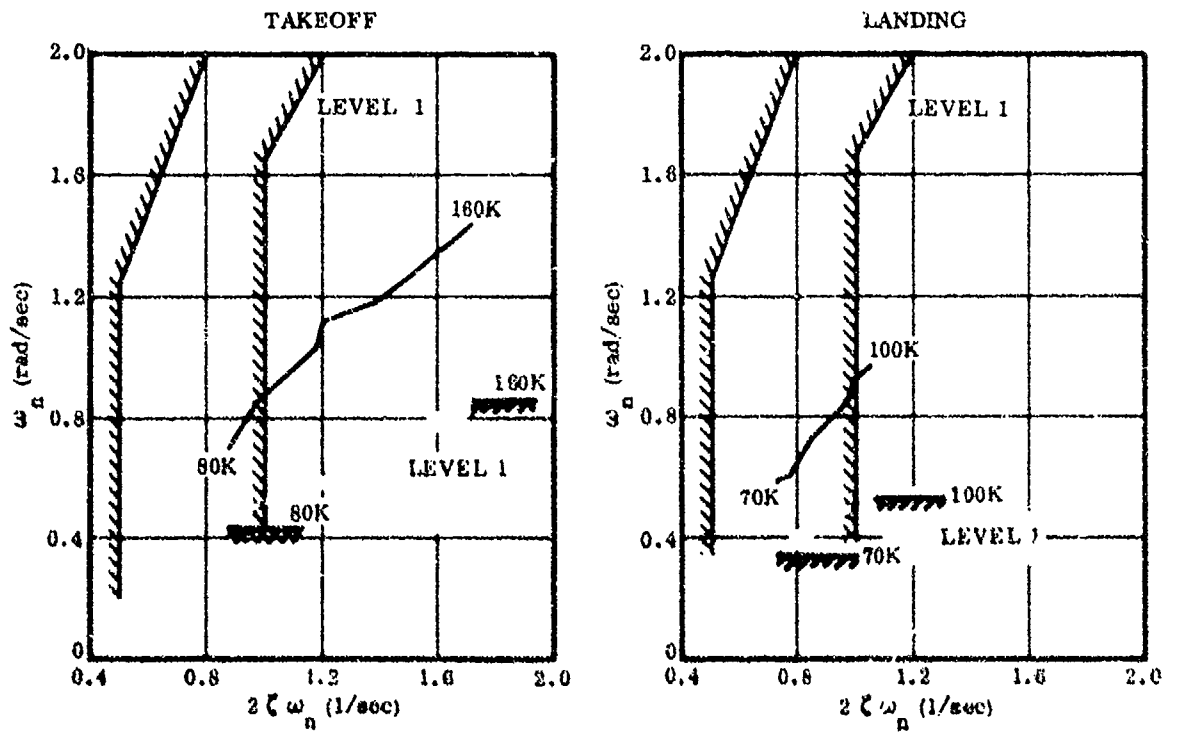


Figure 2-17. IBF/VT Short Period

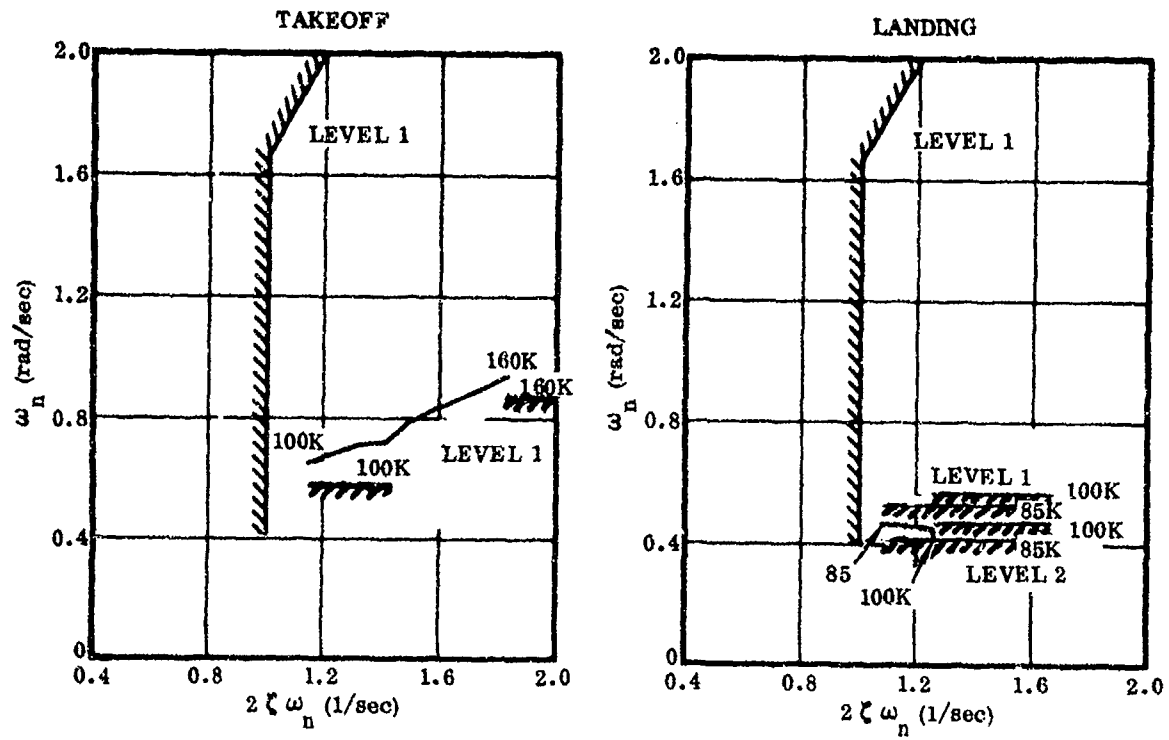


Figure 2-18. MF/VT Short Period

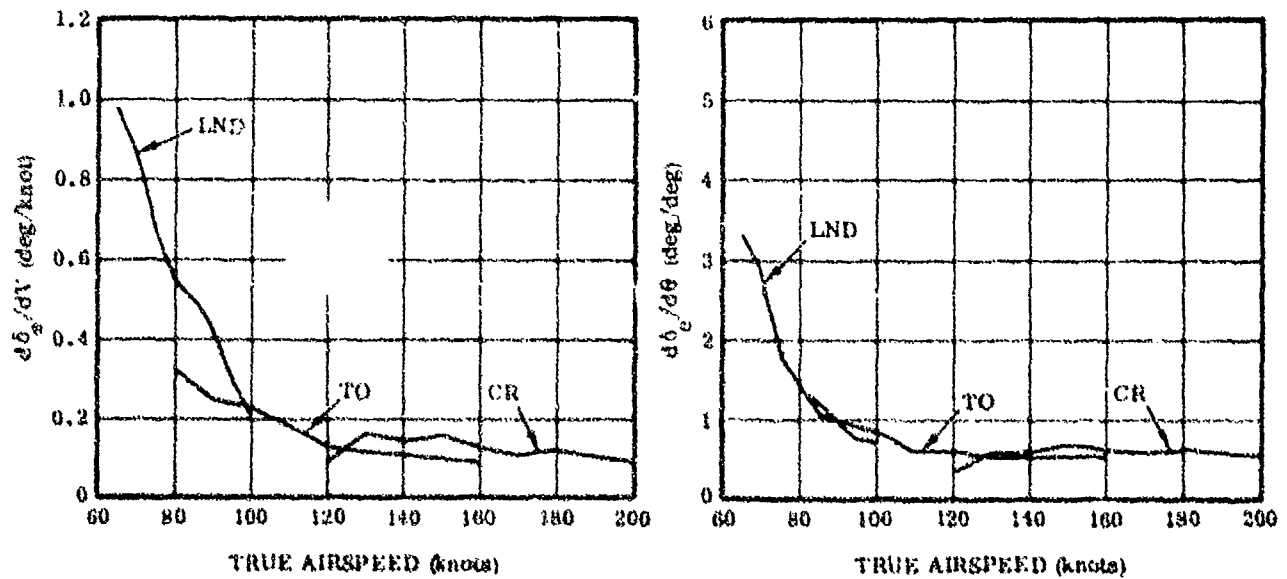


Figure 2-19. SBF Longitudinal Static Stability

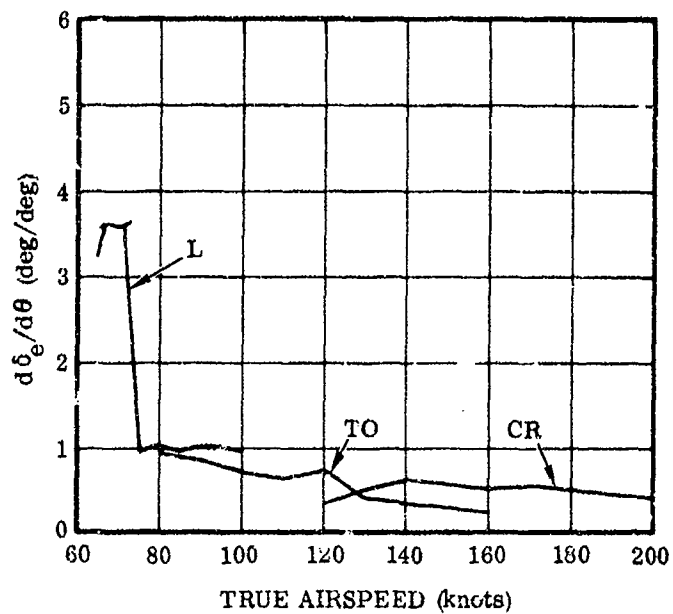
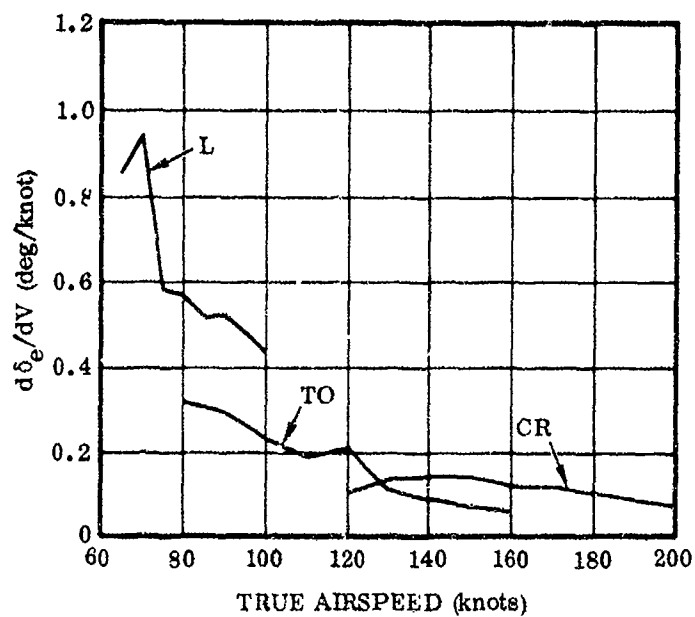


Figure 2-20. IBF/VT Longitudinal Static Stability

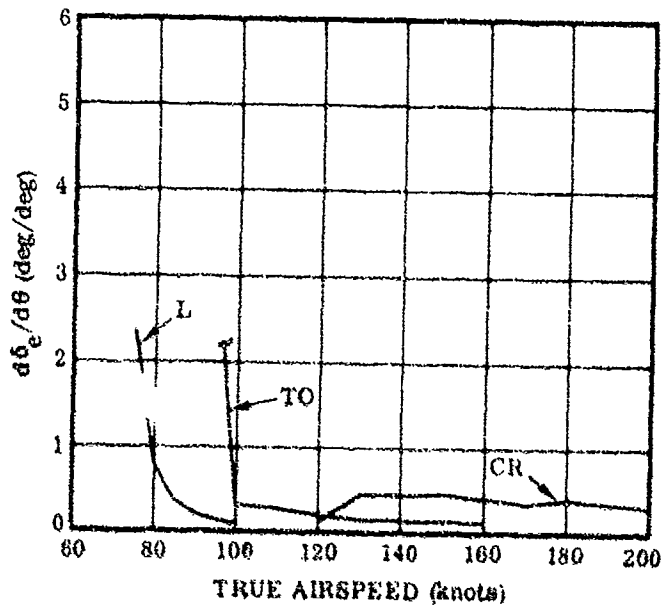
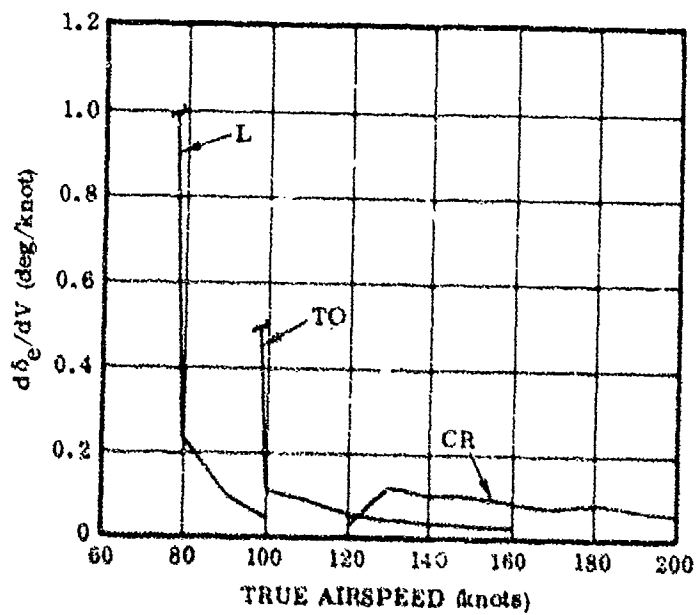


Figure 2-21. MF/VT Longitudinal Static Stability

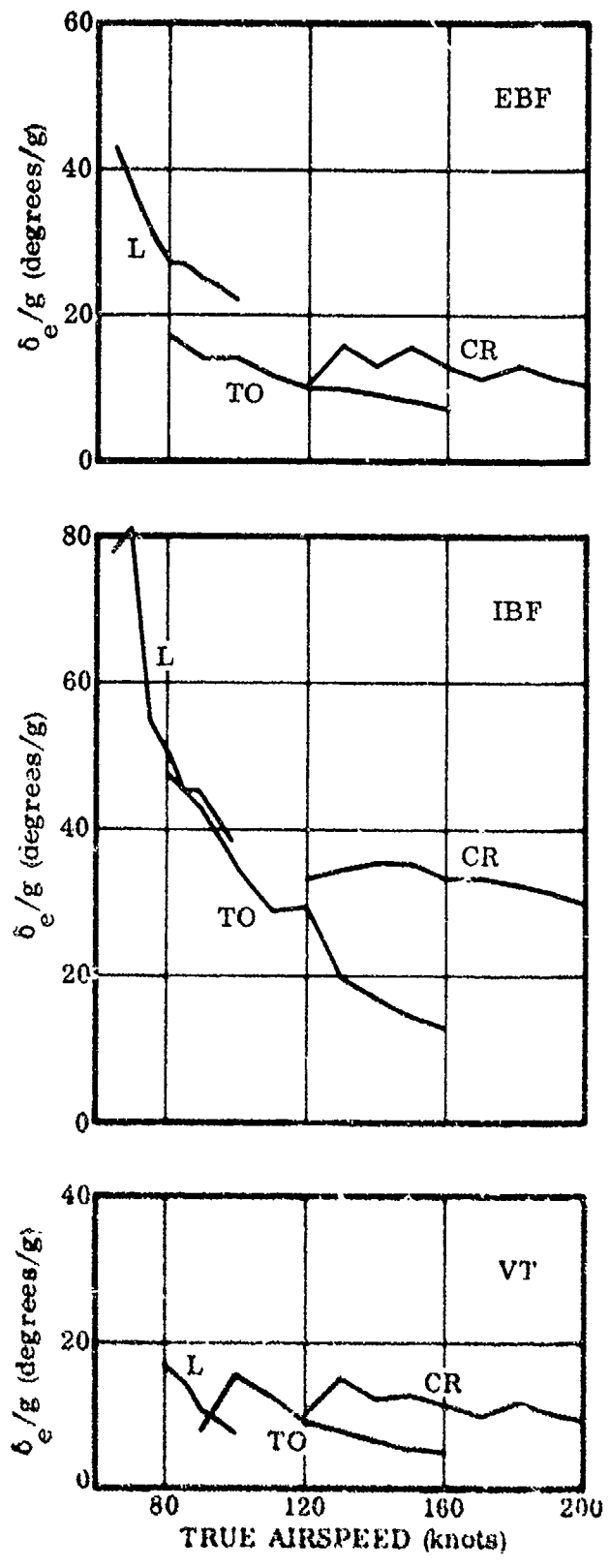


Figure 2-22. EBF, IBF/VT, and MF/VT δ_e/g versus Airspeed

2.4 LONGITUDINAL STABILITY AUGMENTATION

The longitudinal stability augmentation was performed in several stages over the period of the contract work. The major steps are to:

1. Select a critical flight condition, synthesize a complete system, and analytically determine all gains.
2. Verify and adjust gains in the manned simulation for the critical flight condition.
3. Synthesize nominal gain schedules for the attitude loop and calculate responses for all flight conditions and vehicles.
4. Examine flap and throttle feedback and cross-coupling gains using linearized analog unmanned simulations.
5. Verify all three vehicles in the approach condition using manned simulation.

This Paragraph (2.4) covers most of Steps 1, 2, and 3. The responses for Step 3 are in Paragraph 2.3. Step 4 is shown in Paragraph 2.5 and Step 5 in Section 4.

The flight condition emphasized for initial longitudinal stability augmentation of the EBF configuration was:

EBF Vehicle

Landing Flaps (60 deg)

Altitude = 2500 ft

Velocity = 80 knots

Gross Weight = 134,200 lb (mid-mission weight)

Glide Path = -7 deg

Trim values for this flight condition are:

$$\alpha_B = 6.10 \text{ deg}$$

$$\delta_{stab} = -0.89 \text{ deg}$$

Throttle = 75%

The analysis is based on numerical linear transfer functions determined about this trim point. The Convair Aerospace TRIM-STAB digital program is used for the majority of the analysis. A summary description of this program is given in Appendix I.

The stability derivatives for this condition are:

XU = -0.62834134816438E-01,
 ZU = -0.27709746480848E+00,
 MU = 0.14160557455776E-02,
 XW = 0.89235801142891E-01,
 ZW = -0.44509146964742E+00,
 MW = -0.15799230435313E-02,
 XQ = -0.54058586523037E+00,
 ZQ = -0.3718548677739E+01,
 MQ = -0.39321066770739E+00,
 XW00T = -0.2974462579E-02,
 ZW00T = -0.15157183868951E-01,
 MW00T = -0.17992459136563E-02,
 XCE = -0.48387979813798E-01,
 ZCE = -0.40102212567484E+01,
 MCE = -0.44260718259225E+00,
 XFL = -0.14898237952583E+02,
 ZFL = -0.23482176115694E+02,
 MFL = 0.30181251203754E-01,
 XTMR = 0.35152944314721E-01,
 ZTMR = -0.17161184827976E+00,
 MTMR = -0.959048846-1367E-03,

The matrix equations used are:

$$\begin{bmatrix} (s - X_u) & (q_o - X_w) & (w_o s + g \cos \theta_o) \\ -(q_o + Z_u) & [(1 - Z_w) s - Z_w] & [- (U_o + Z_q) s + g \sin \theta_o] \\ -M_u & (-M_w s - M_w) & (s^2 - M_q s) \end{bmatrix} \begin{bmatrix} u \\ w \\ \theta \end{bmatrix} = \begin{bmatrix} X_{\delta_o} & X_F & X_{TH} \\ Z_{\delta_o} & Z_F & Z_{TH} \\ M_{\delta_o} & M_F & M_{TH} \end{bmatrix} \begin{bmatrix} \delta_o \\ \delta_F \\ \delta_{TH} \end{bmatrix}$$

$$\begin{bmatrix} u \\ w \\ \theta \end{bmatrix} = \begin{bmatrix} u/\delta_o & u/\delta_F & u/\delta_{TH} \\ w/\delta_o & w/\delta_F & w/\delta_{TH} \\ \theta/\delta_o & \theta/\delta_F & \theta/\delta_{TH} \end{bmatrix} \begin{bmatrix} \delta_o \\ \delta_F \\ \delta_{TH} \end{bmatrix}$$

The numerical transfer functions are:

$$u/\delta_F(s) = N_{u_F} / D$$

$$D = 0.0343 \left[\left(\frac{s}{0.288} \right)^2 + \frac{2(0.008)s}{0.288} + 1 \right] \left[\left(\frac{s}{0.640} \right)^2 + \frac{2(0.879)s}{0.640} + 1 \right]$$

$$N_{u_E} = 6.1130 \left[\left(\frac{s}{1.007} \right)^2 + \frac{2(0.962)s}{1.007} + 1 \right] \left(\frac{s}{-123.0} + 1 \right)$$

$$N_{w_E} = -4.142 \left[\left(\frac{s}{0.260} \right)^2 + \frac{2(0.176)s}{0.260} + 1 \right] \left(\frac{s}{14.81} + 1 \right)$$

$$N_{\theta_E} = -0.0235 \left(\frac{s}{0.158} + 1 \right) \left(\frac{s}{0.336} + 1 \right)$$

$$N_{v_T} = 0.7027 \times 10^{-3} \left[\left(\frac{s}{0.586} \right)^2 + \frac{2(0.435)s}{0.536} + 1 \right] \left(\frac{s}{0.466} + 1 \right)$$

$$N_{w_T} = -0.0145 \left[\left(\frac{s}{0.276} \right)^2 + \frac{2(0.051)s}{0.276} + 1 \right] \left(\frac{s}{1.458} + 1 \right)$$

$$N_{\theta_T} = -0.1657 \times 10^{-4} \left[\left(\frac{s}{0.150} \right)^2 + \frac{2(0.892)s}{0.150} + 1 \right]$$

$$N_{u_T} = -1.636 \left[\left(\frac{s}{0.494} \right)^2 + \frac{2(0.838)s}{0.494} + 1 \right] \left(\frac{s}{0.443} + 1 \right)$$

$$N_{w_F} = -0.8102 \left[\left(\frac{s}{0.352} \right)^2 + \frac{2(-0.237)s}{0.352} + 1 \right] \left(\frac{s}{0.279} + 1 \right)$$

$$N_{\theta_F} = -0.01495 \left(\frac{s}{0.668} + 1 \right) \left(\frac{s}{-0.307} + 1 \right)$$

Paragraph 2.3 presents an evaluation of the bare airframe handling qualities, including this power approach condition. Items that are deficient are:

$$n_z / \alpha, d\gamma/dV, \omega_{SP}, \zeta_{PH}$$

In addition to the elevator, throttle and flaps are available for flight path and airspeed control. Reference 4, among others, indicates that pilots would like to control flight path with the throttle on a power approach, where significant lift is due to the throttle. However, the coupling of airspeed and flight path through each of these controls makes bare airframe control deficient.

A direct lift system via throttle control gives the pilot two distinct means of controlling flight path:

1. Heave control with the throttle, with minor pitch changes.
2. Pitch control with the elevator, which depends on an adequate n_z/α , to minimize α changes and make pitch changes result in flight path changes.

The equation $\gamma = \theta - \alpha$ expresses the two techniques, the heave control corresponding to changing γ with α and pitch control changing γ with θ .

The linear derivatives indicate the throttle to be a better direct lift control and the flaps as better speed control, as seen by:

$$\frac{Z_{THR}}{X_{THR}} = \frac{-0.1316}{+0.0351} = -3.75 \qquad \frac{Z_F}{X_F} = \frac{-23.48}{-14.89} = +1.575$$

Decoupling requirements between throttle and elevator along with transient responses are shown in 2.5.

Thus, the aims of the low speed longitudinal SAS development were defined as:

1. Improve phugoid damping, short period frequency, n_z/α , and $d\gamma/dV$ when controlling through the elevator.
2. Provide a throttle control that controls flight path with minimum disturbance to pitch angle and airspeed.
3. Provide an airspeed control through the flaps with minimum disturbances to pitch angle and angle of attack.

A primary man-in-the-loop simulator task has been identified to determine which of the two flight path control schemes results in better performance and pilot acceptance. Figure 2-23 is a block diagram of a preliminary longitudinal control system to meet these requirements. Considerable analysis was performed at the 80-knot EBF landing condition to set gains. These were then checked for other flight conditions of the EBF and for use in the other vehicles.

The first step in the analysis is to close a pitch attitude loop. Figure 2-24 is a block diagram of this loop, giving the numerical airframe transfer function for the selected flight condition and indicating K_θ and τ_θ to be the principal variables. Figure 2-25 shows a locus of the short period and phugoid roots for values of K_θ up to 6 and for τ_θ equal to 0, 1, and 2. On initial interpretation, values of $K_\theta = 0.64$ and $\tau_\theta = 0$ were selected as showing good damping of both phugoid and short period modes. However, early real-time simulation indicated this response to be extremely sluggish. Subsequently, values of $K_\theta = 4$ and $\tau_\theta = 1$ were selected as nominal values. Figure 2-25 indicates the response to be well damped in both modes and the short period to be significantly faster than for the original gain. Also, Figure 2-25 shows that $\pm 10\%$ changes in gain around the nominal also results in good responses, indicating sharp tuning is not required. For the nominal pitch loop, the K_θ gain of 4 at 80 knots is multiplied by an inverse-q schedule normalized to 1 at the 80-knot condition.

Along with a $\tau_\theta = 1$, these attitude loop gains are applied to other EBF flight conditions and to the IBF/VT and MF/VT vehicles. The SAS-on responses of Paragraph 2.3 include these gains.

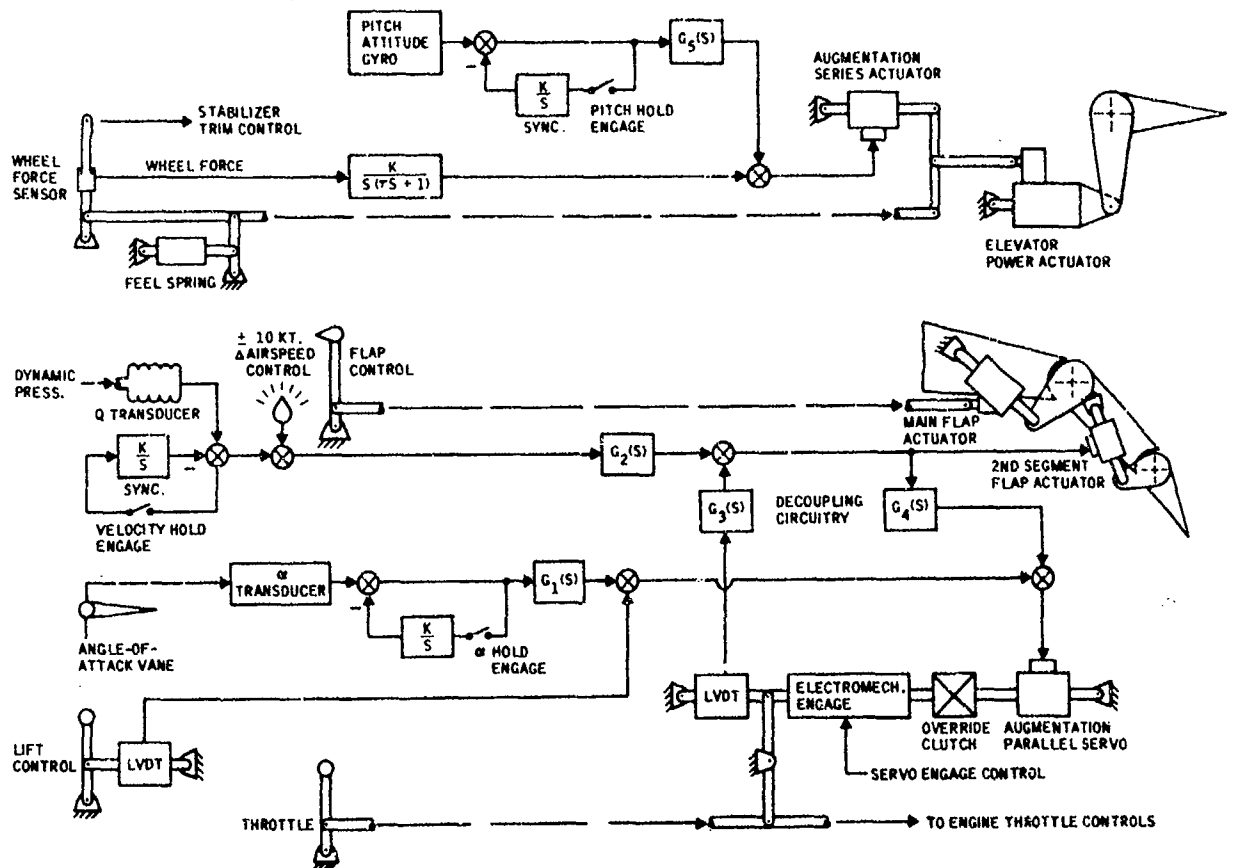


Figure 2-23. Preliminary Longitudinal Stability Augmentation System

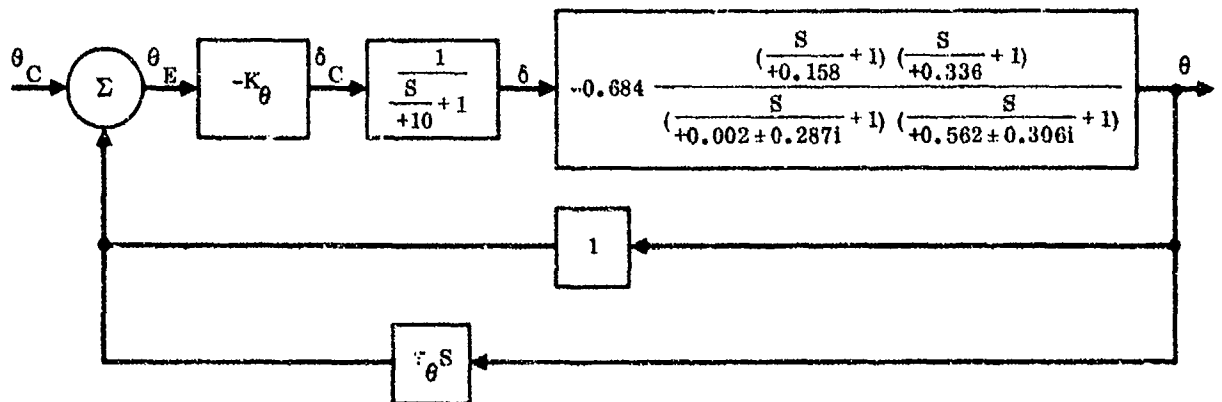


Figure 2-24. Pitch Attitude Loop

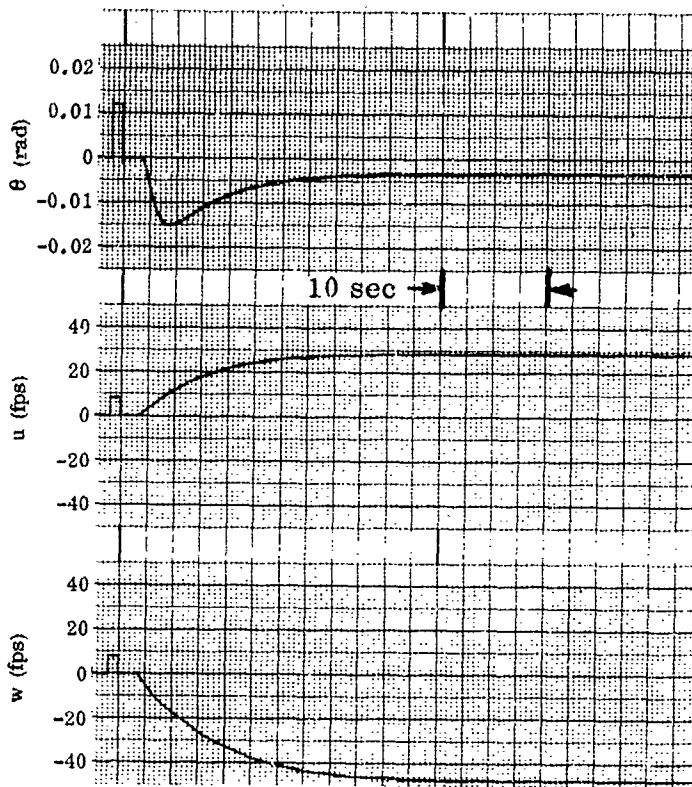


Figure 2-26. Step Thrust Command with Pitch Augmentation only

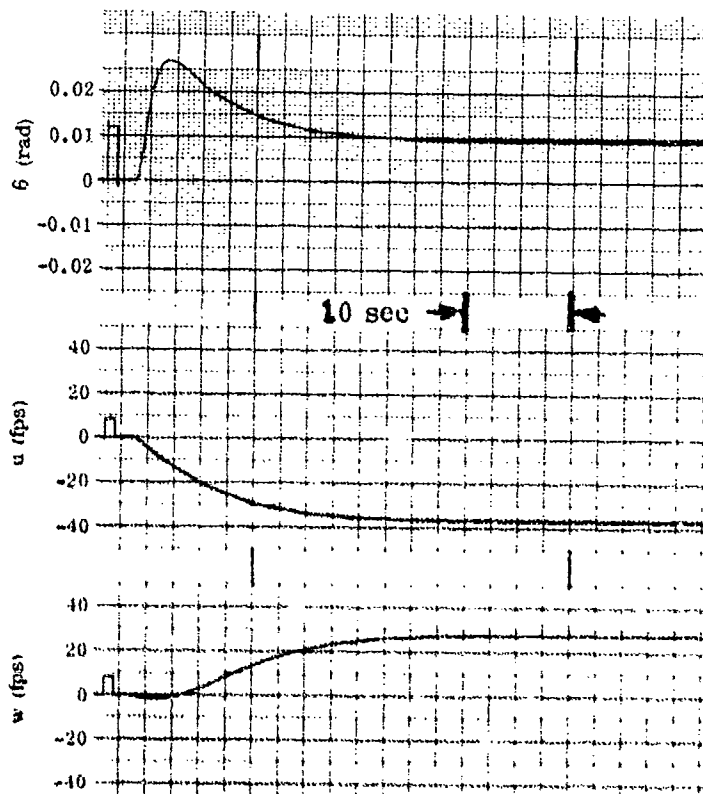


Figure 2-27. Step Flap Command with Pitch Augmentation only

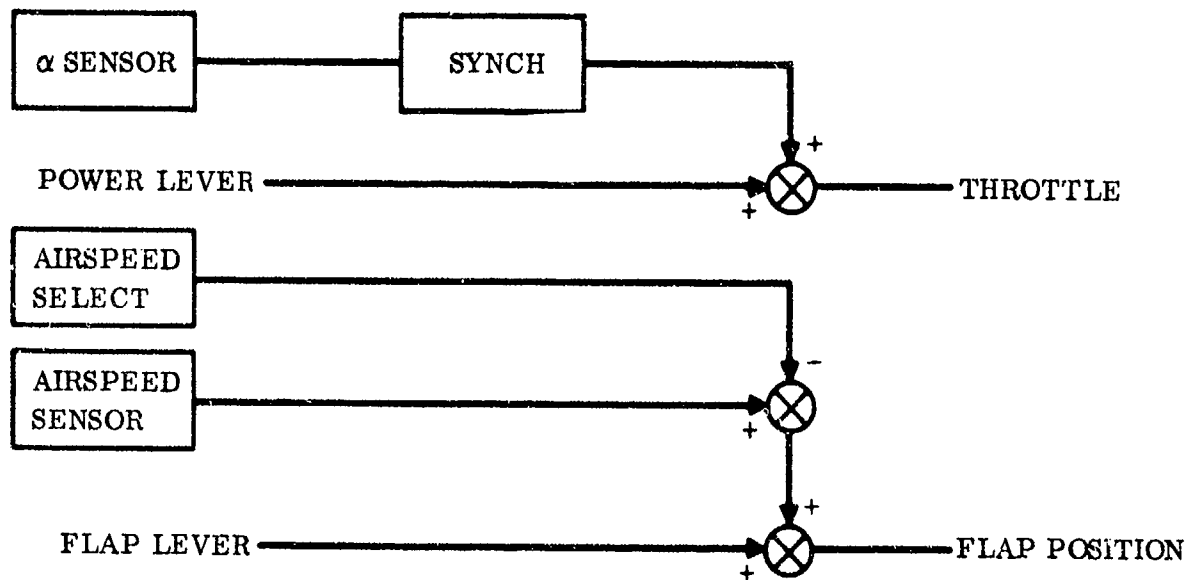


Figure 2-28. Airspeed and Angle of Attack Control Loops

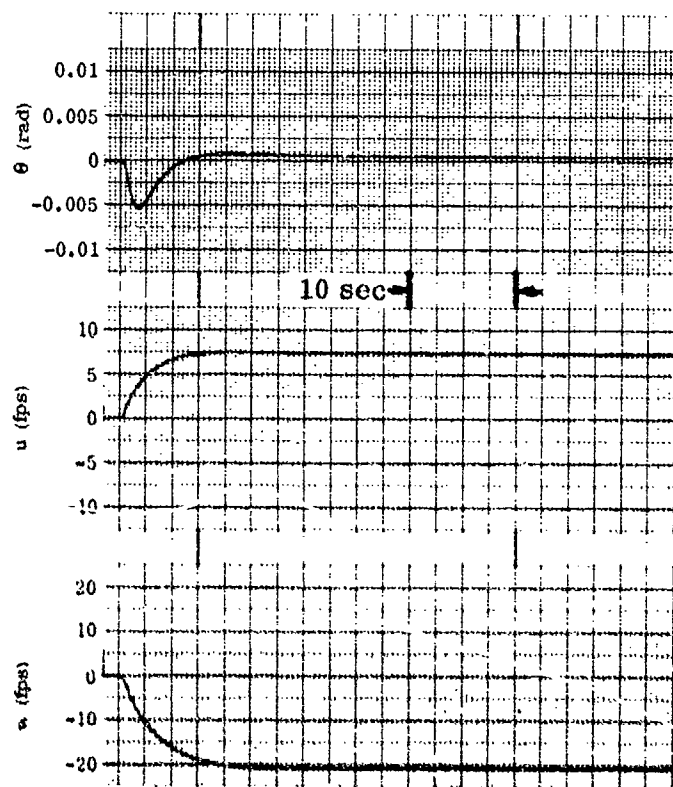


Figure 2-29. Step Thrust Command with no Interconnects

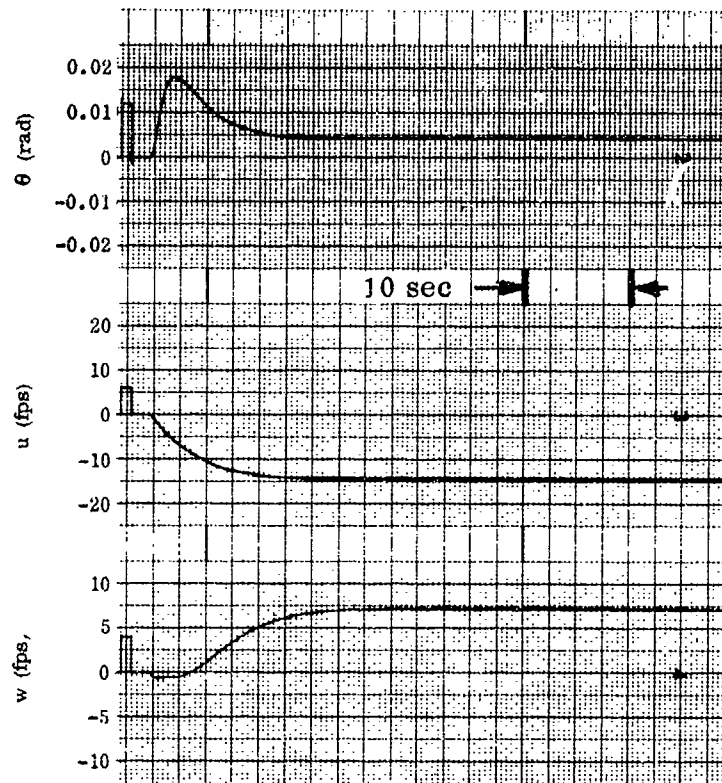


Figure 2-30. Step Flap Command with no Interconnects

such control loops, again for the MF/VT vehicle. Although somewhat less severe, the two-parameter response to a single control input is still significant. A side benefit of the loops is that the responses have been speeded up. It is therefore concluded that types of crosscoupling should be investigated to determine a combination of throttle and flap that can be commanded to essentially produce changes in w only, and a different combination that will give essentially forward speed changes only.

It would, of course, be ideal if a speed change command produced no change in w , either transient or steady-state, and if a w command produced no change in u . A brief investigation of the systems needed to attain these ideal decoupled responses indicated that extensive filtering would be needed to handle both the transient and the steady-state. Rather than go immediately to the most complex configuration, the conditions for setting the steady state at (or near) zero were investigated.

The block diagram for the steady-state interconnect approach is shown in Figure 2-31. Since none of the transfer functions of interest have free Laplace transform variable (s) in either numerator or denominator, the steady-state transfer function is simply the ratio of the zero-order terms of the numerator and denominator polynomials. Referring to Figure 2-31, the following relations can be written.

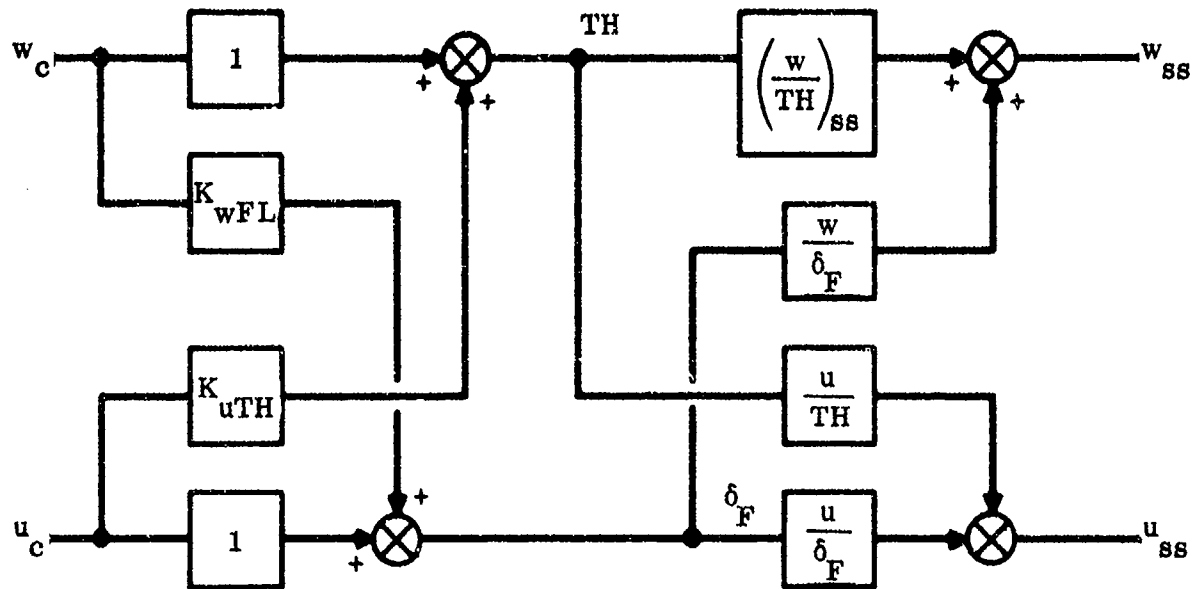


Figure 2-31. Flap/Throttle Interconnection

$$\begin{aligned}
 w_{ss} &= (w_c + K_{u_{TH}} u_c) \left(\frac{w}{TH} \right)_{ss} \\
 &\quad + (K_{w_{FL}} w_c + u_c) \left(\frac{w}{\delta_F} \right)_{ss}
 \end{aligned} \tag{2-1}$$

$$\begin{aligned}
 u_{ss} &= (u_c + K_{w_{FL}} w_c) \left(\frac{u}{\delta_F} \right)_{ss} \\
 &\quad + (K_{u_{TH}} u_c + w_c) \left(\frac{u}{TH} \right)_{ss}
 \end{aligned} \tag{2-2}$$

where:

w_{ss} and w_c are the steady-state and commanded incremental downward velocities.

u_{ss} and u_c are the steady-state and commanded incremental forward velocities.

$\left(\frac{w}{TH} \right)_{ss}$ and $\left(\frac{w}{\delta_F} \right)_{ss}$ are the steady-state transfer functions of w per throttle and w per flap.

$\left(\frac{u}{TH} \right)_{ss}$ and $\left(\frac{u}{\delta_F} \right)_{ss}$ are the steady-state transfer functions of u per throttle and u per flap.

$K_{w_{FL}}$ is the flap per w_c gain

$K_{u_{TH}}$ is the throttle per u_c gain

The desired contribution to w_{ss} from u_c in Equation 2-1 is zero, as:

$$K_{u_{TH}} u_c \left(\frac{w}{TH} \right)_{ss} + u_c \left(\frac{w}{\delta_F} \right)_{ss} = 0$$
$$K_{u_{TH}} = \frac{\frac{w}{-(\delta F)_{ss}}}{\left(\frac{w}{TH} \right)_{ss}}$$

Identical reasoning with u_{ss} and w_c in Equation 2-2 gives:

$$K_{w_{FL}} = \frac{-\left(\frac{u}{TH} \right)_{ss}}{\left(\frac{u}{\delta_F} \right)_{ss}}$$

To demonstrate the procedure, the following equations were obtained from MF/VT configuration digital computer runs with the pitch augmentation loop operative.

$$\left(\frac{w}{TH} \right)_{ss} = \frac{-1.197 \times 10^{-2}}{1.012 \times 10^{-1}} = -0.1183 \frac{\text{fps}}{\%}$$

$$\left(\frac{u}{TH} \right)_{ss} = \frac{7.63 \times 10^{-3}}{1.012 \times 10^{-1}} = 0.0753 \frac{\text{fps}}{\%}$$

$$\left(\frac{w}{\delta_F} \right)_{ss} = \frac{-6.28 \times 10^{-1}}{1.012 \times 10^{-1}} = -6.21 \frac{\text{fps}}{\text{rad}}$$

$$\left(\frac{u}{\delta_F} \right)_{ss} = \frac{-5.63 \times 10^{-1}}{1.012 \times 10^{-1}} = -5.56 \frac{\text{fps}}{\text{rad}}$$

$$K_{u_{TH}} = \frac{-(-6.21)}{-0.1183} = -52.5 \frac{\%}{\text{rad}}$$

$$K_{w_{FL}} = \frac{-(0.0753)}{-5.56} = 0.01354 \frac{\text{rad}}{\%}$$

Several things should be noted at this point, the first of which is the units of K. The diagram in Figure 2-31 was set up to express the w and u commands in terms of percent of power lever and radians of flap, respectively. The commands could have been expressed in fps, but since the pilot must make his inputs via percent power lever and angular displacement of flap, these latter input units were used. The second item of note is that the transfer functions used included closed-loop pitch augmentation. If pitch augmentation was not included, the problem would become one of determining six interconnects since throttle and flap influence attitude, which in turn influences forward and downward velocities. The third item is that the approach is not limited to decoupling u from power lever and w from flap; the same procedure can define interconnect gains such that the power lever controls speed and the flaps control w.

The dynamic responses using these gains are shown in Figure 2-32 for a power lever step and in Figure 2-33 for a step of flap input for the MF/VT vehicle. In both cases, the steady-state behavior is as desired. Figure 2-32 shows a very small u transient for a step of power lever. Since this transient would be even smaller for a more realistic pilot input, it appears that the steady-state approach without transient reducing filters is adequate to decouple u from the power lever. However, Figure 2-33 shows that the simple approach has given a comparatively large w transient in response to flap. Although this could be noticed in the presence of rapid speed corrections, the transient would not result in objectional control characteristics. The speed loop will generate most of the speed commands, and these can be expected to be smooth enough to excite only minimal transients. In any event, fair transient and good steady decoupling will prevent one variable from going into another variable and thereby undoing the original correction. In view of this, simple decoupling appears adequate.

The analysis was extended for the EBF vehicle to evaluate filtering. This analysis was performed using a combination of TRIM STAB and a graphics program with root locus and Bode plot options. TRIM-STAB was used to generate transfer functions of u and w to throttle commands and to flap commands, with the attitude loop closed. Then, using the graphics program, each of the pertinent transfer functions (G_1 , G_2 , G_3 , and G_4) in Figure 2-23 was represented by a gain and a first-order numerator over a first-order denominator. The frequency decade that included both the phugoid

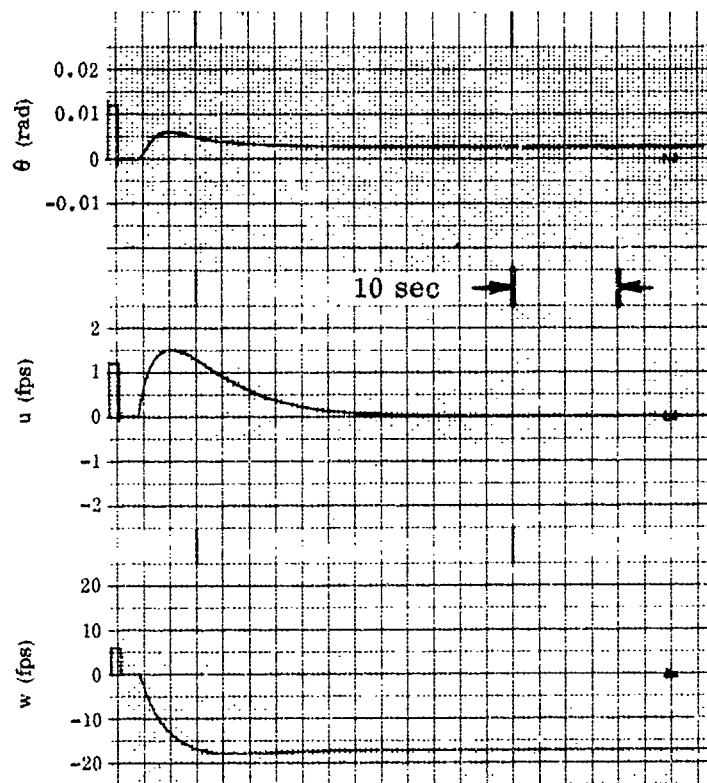


Figure 2-32. Step Thrust Command with Complete Augmentation

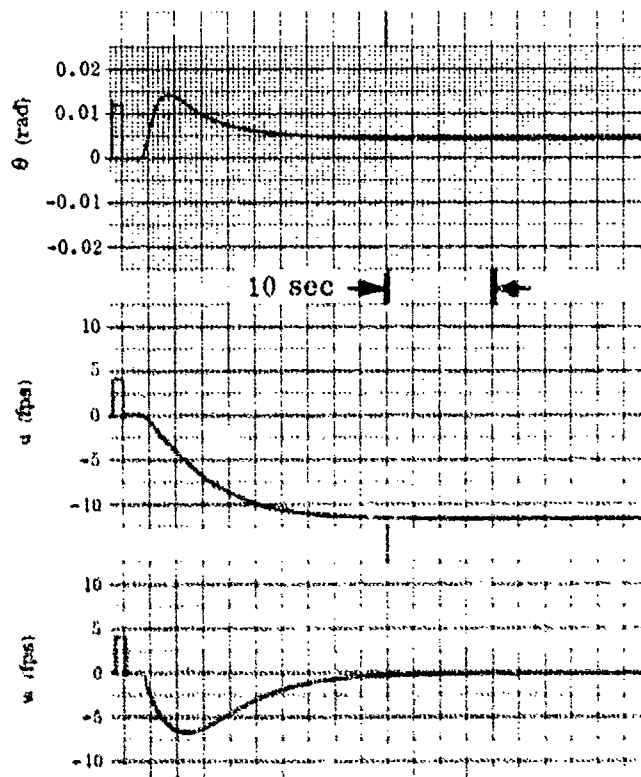


Figure 2-33. Step Flap Command with Complete Augmentation

and short period was then used for a graphics display and the analyst could vary each of these transfer functions while looking at a display such as Figure 2-34. The parameters plotted in Figure 2-34 are the amplitude in db for the variable w/u for a throttle input and for a flap input. This ratio should be large for a throttle input, corresponding to a large w change for a small velocity change. Similarly, a large negative db value corresponds to a large velocity change for a small flight path angle change. Figure 2-34 shows that the minimum closed-loop separation is about 40 db, from an open loop value of about 10 db. The phase plots are also available, and were used mostly to help approximate higher order "exact" decoupling with first order terms. The set of gains including second-order gust filters corresponding to Figures 2-34 and 2-23 are:

$$G_1(s) = \frac{2.36 \left(\frac{s}{0.75} + 1 \right)}{\left(\frac{s}{3} + 1 \right) \left(\frac{s}{6} + 1 \right)^2} \quad \%/deg$$

$$G_2(s) = \frac{4.84 \left(\frac{s}{0.3} + 1 \right)}{\left(\frac{s}{1.5} + 1 \right) \left(\frac{s}{7} + 1 \right)^2} \quad deg/knot$$

$$G_3(s) = \frac{-0.126}{\frac{s}{1.2} + 1} \quad deg/\%$$

$$G_4(s) = -1.22 \quad \%/deg$$

$$G_5(s) = 4(s + 1) \quad deg/deg$$

The transfer functions corresponding to these gains were mechanized on the manned simulator for the EBF vehicle as described in Section 4. The linearized analog results were used to update the crosscoupling from one vehicle to another, but the feedback gains were held constant.

2.6 LATERAL-DIRECTIONAL HANDLING QUALITIES

Lateral directional handling qualities have been calculated for all three vehicles for the speeds and flight conditions itemized in Paragraph 2.3. The nominal scheduled gains determined in Paragraph 2.7 were used to calculate SAS- α responses plotted in this discussion.

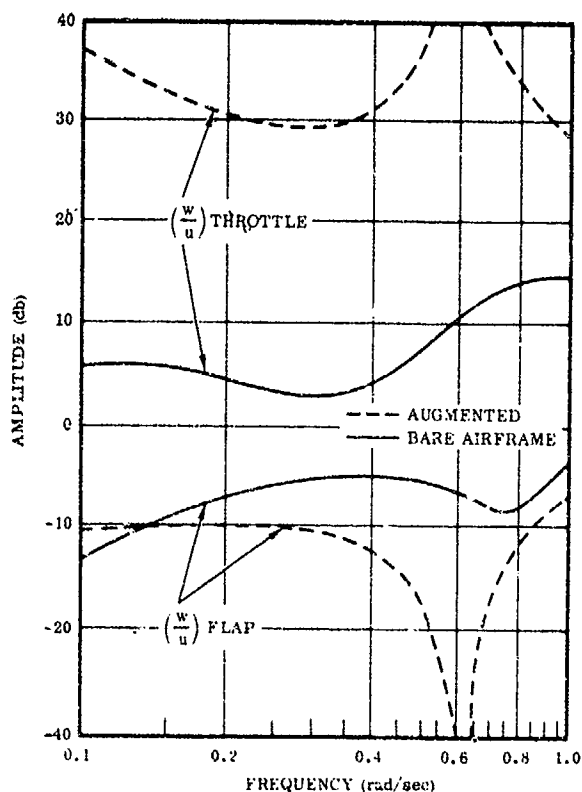


Figure 2-34. Frequency Response for Bare and Augmented Airframe

Figure 2-35 is a baseline lateral directional control system. The data in Figure 2-23 of Reference 2-1 shows that ailerons and spoilers are both required for EBF engine-out trim. The spoilers are mechanically driven and the ailerons are fly-by-wire, providing "aerodynamic mixing" as opposed to the mechanical series mixer required when mechanical inputs and fly-by-wire signals drive the same surface. Since there are problems in defining "bare airframe" handling qualities, the following ground rules have been chosen. For engine-out trim data, a fixed ratio of 60 degrees of spoiler to 100 degrees of aileron is used, although the control system would not always give this except at the point where lateral control runs out. The aerodynamic data base assumes 100 degrees (± 50 degrees) of aileron are available when surface blowing is actuated. For these engine-out calculations, the nonlinear spoiler data is used.

For the small-amplitude handling quality parameters, the aileron and spoiler effectiveness derivatives are based on small deflections. This is also true of the sideslip trim parameters. In those cases, responses are calculated separately for spoiler and aileron, giving a better basis for formulating a SAS.

2.6.1 ENGINE-OUT TRIM DATA. Figures 2-36 through 2-38 show engine-out characteristics for the three vehicles. These curves show that the EBF is the most

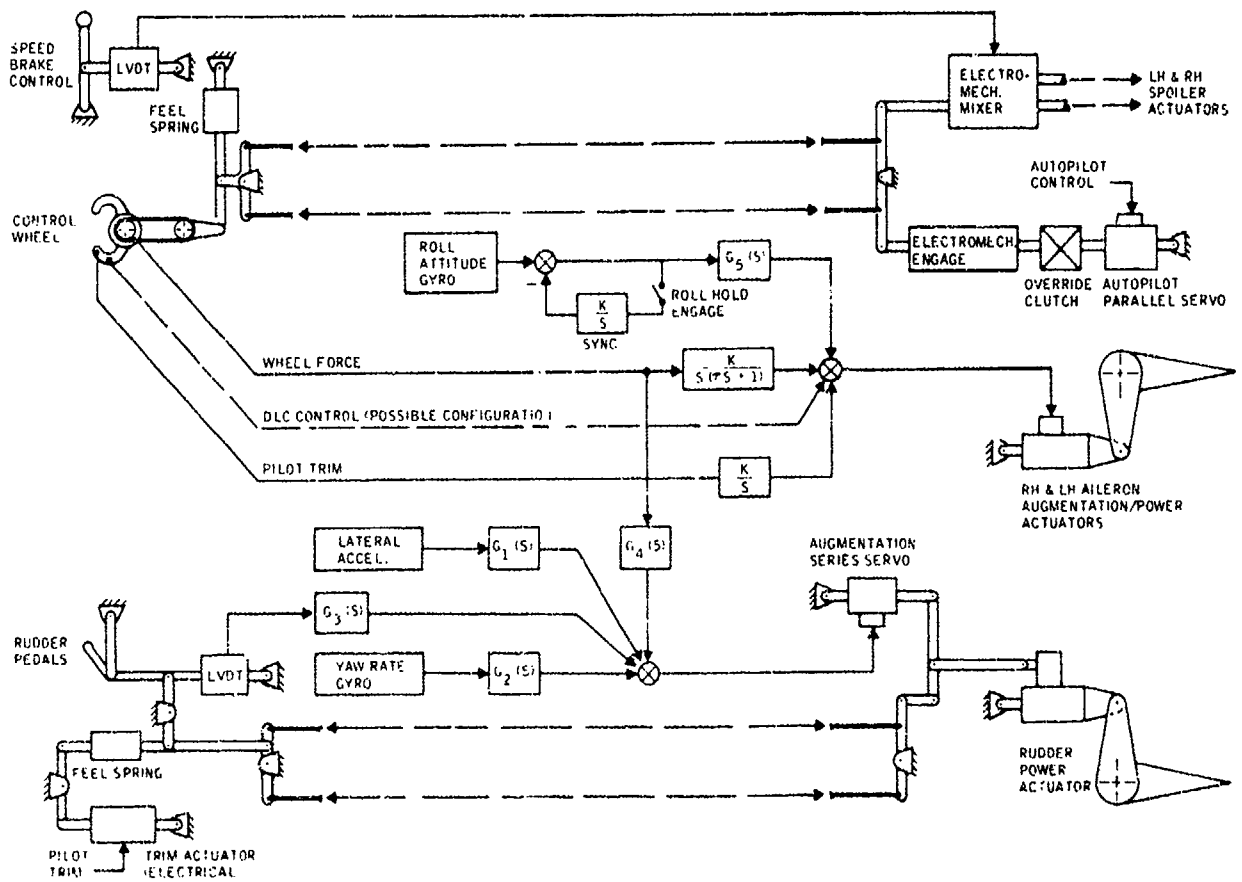


Figure 2-35. Baseline Lateral Directional Control System

critical of the three with neither IBF/VT nor MF/VT using all the available control. Flaps and thrust vector are adjusted for landing and power is 100 per cent. The data is shown for a range of speeds and sideslip angles. Takeoff calculations were not completed; these are less critical in roll but more so in yaw.

For the EBF, Figure 2-36 shows that at 66 knots and 5.5 degrees of sideslip, all yaw and roll control is used. The roll control becomes critical if less rudder or more β is used, due to dihedral effects. Likewise, yaw control becomes critical for less β . A sideslip of 5.5 degrees gives a balanced limit at 66 knots. These curves are based on using blowing, giving aileron effectiveness up to 100 degrees (± 50 degrees), together with 60 degrees of spoiler. No differential blowing of the leading edge or any maneuver margin above trim was assumed.

The IBF/VT data in Figure 2-37 reflects the plenum used and no asymmetric input due to the diverted flow. Only the undiverted tail pipe thrust excites the aircraft. The assumed IBF/VT vectoring reduces the yaw moment, and this data indicates that blowing is not needed for either aileron or rudder.

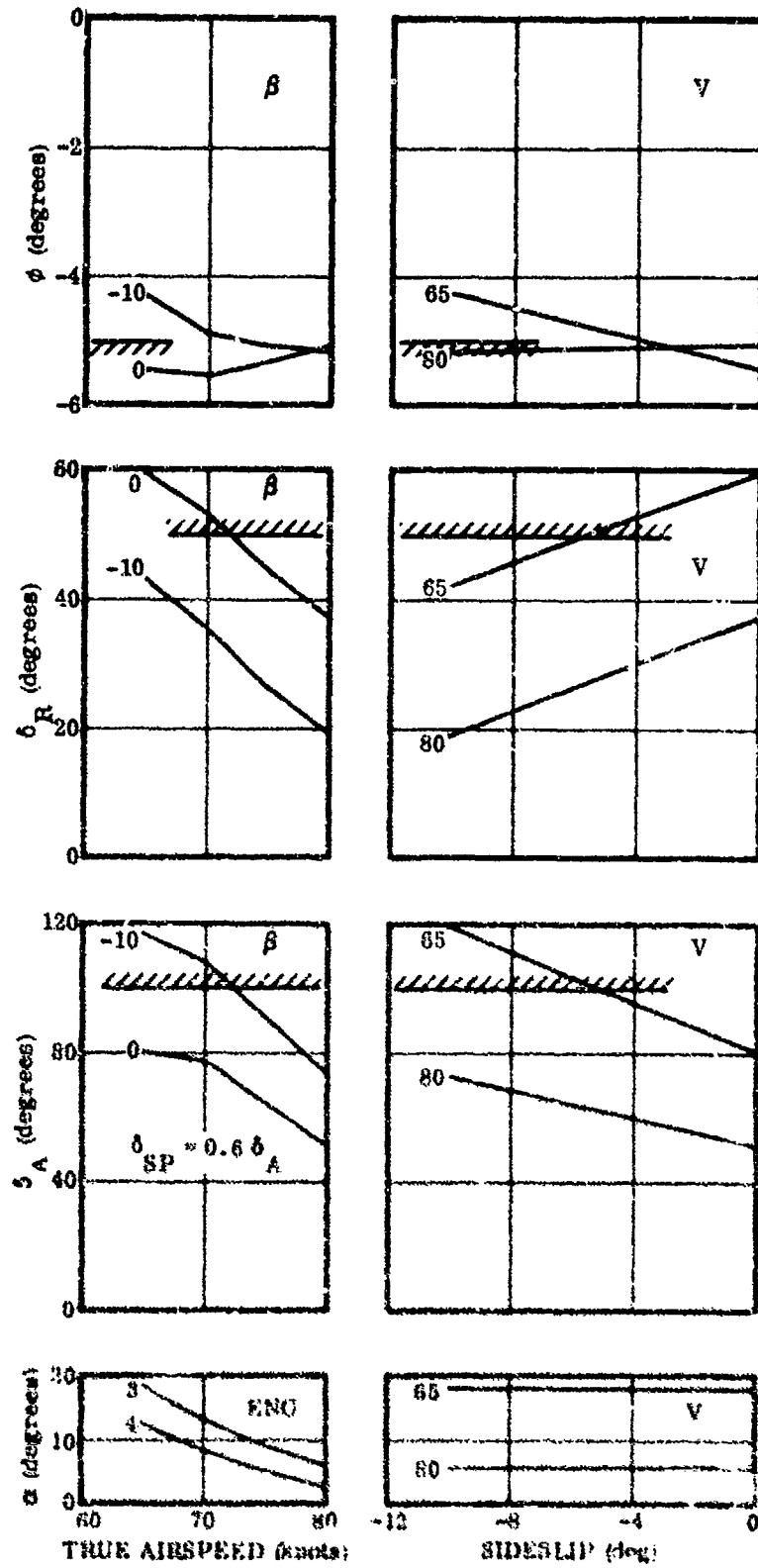


Figure 2-36. Trim Data for EBF Right Outboard Engine Out (60 degrees of Flaps)

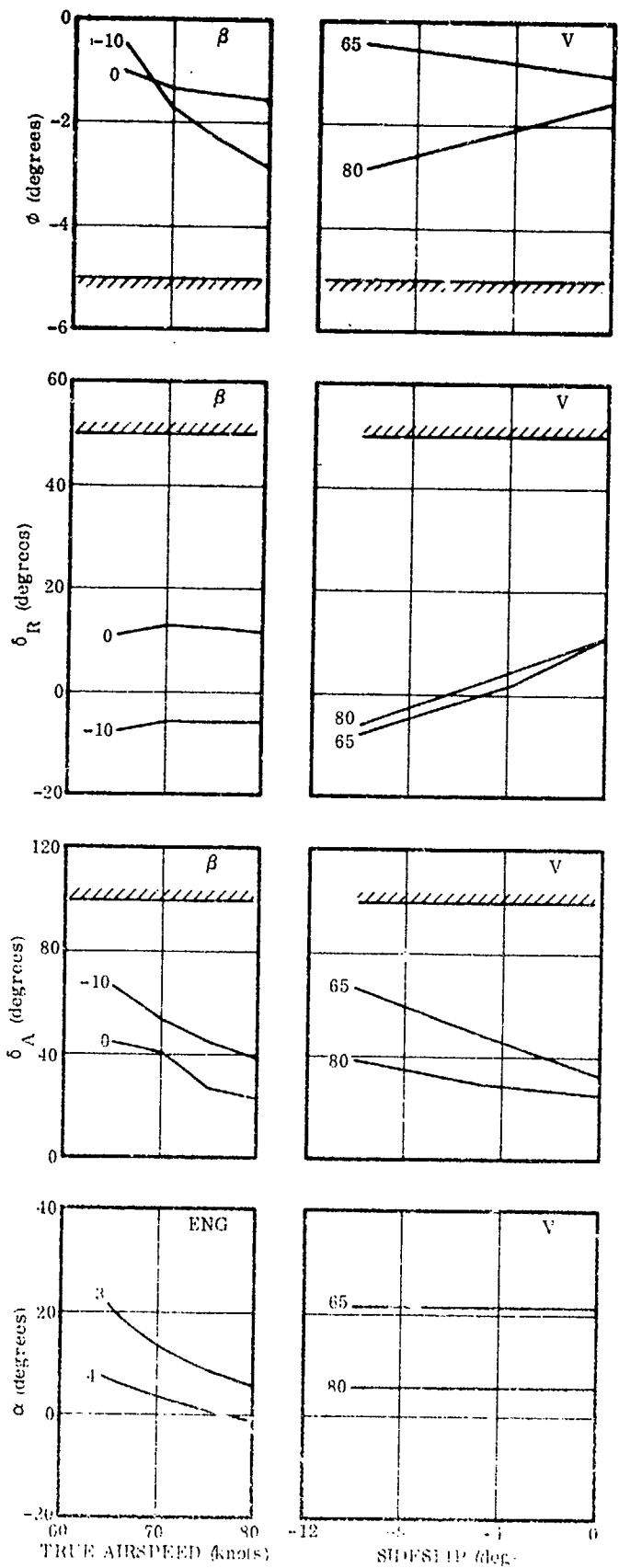


Figure 2-37. Trim Data for IBF Right Outboard Engine Out (60 degrees of Flaps)

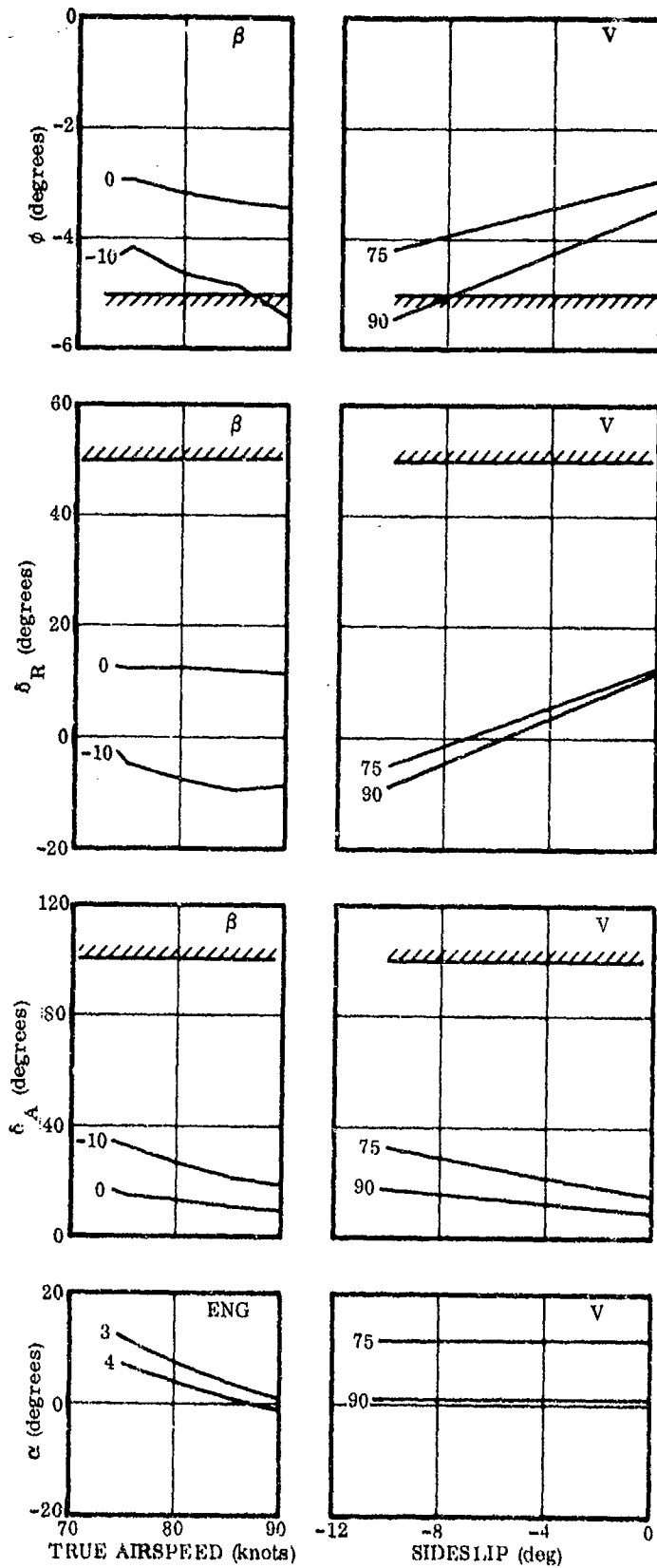


Figure 2-38. Trim Data for VT Right Outboard Engine Out (60 degrees of Flaps, 60 degrees of Thrust Vector)

The MF/VT data in Figure 2-38 reflects the unique single-bearing engine vectoring, which pivots outboard and down for the outboard engines as shown in Section 2.2.4. At 60 degrees, the thrust vector points near the cg to minimize engine-out rolling and yawing moments. A significant side force affects the trim bank angles, and may become critical on ground roll engine-out conditions. The data in Figure 2-38 shows that even with zero rudder, only 5 to 10 degrees of sideslip is needed and no excessive roll is required. If roll requirements tended to be excessive, then reducing β with δ_r would help.

Steady-state sideslip trim data for the three vehicles is shown in Figures 2-39 through 2-41. The figures indicate that all three vehicles are all stable in sideslip, requiring positive (left) rudder, negative (up right) roll control, and positive (right) bank angle to trim positive (right) sideslip, as prescribed in Paragraphs 3.3.11 and 3.3.6 of References 2-2 and 2-3, respectively.

Since the data in Figures 2-39 through 2-41 is based on linear derivatives for small deflections, it would not be appropriate to combine them for large-amplitude results (e.g., maximum crosswind capability). The spoiler data is the most nonlinear (Reference 2-1, Figure 152). The aileron and rudder data is more nearly linear, and the resultant δ_r/β for large values will lie between the aileron and spoiler data shown. With combined aileron and spoiler, the aileron will be somewhat less than that shown. Paragraphs 3.3.6 and 3.3.7 of MIL-F-8785B require at least 10 degrees sideslip. Thus, multiplying the largest δ_a/β or δ_r/β values shown by 10 would be a conservative estimate of control required for maximum sideslip. This is well within the limits of 100 degrees of δ_a and 50 degrees of δ_r .

2.6.2 ROLL MODE AND SPIRAL MODE. The roll mode and spiral mode bare airframe data for all three concepts is shown in Figures 2-42 through 4-47. The roll mode data shows that for the EBF and IBF vehicles, the time constants are better than Level 1 for all three flight configurations. For the MF/VT vehicle at lowest speeds in the landing mode, the time constant approaches the Level 1 value. This time constant is approximately equal to $1/L_p$, which is approximately inversely proportional to $C_{L\alpha}$. Thus, the one concept that does not increase $C_{L\alpha}$ by blowing shows up more nearly deficient.

The SAS assumed in Figure 2-36 and in Figure 2-77 Paragraph 2.7 has a large roll rate feedback, which greatly reduces this time constant. The closed-loop data is not shown in Figures 2-42, 2-44, and 2-46 because the high order of the closed loop (including spoiler and aileron actuator lags and yaw damper high-pass time constant) loses the one-to-one correspondence of any one real root to this time constant. Figures 2-48 and 2-49 shown typical open and closed loop response corresponding to the EBF 80-knot landing condition. Referring to Figure 2-77, Figure 48 represents an open-loop 1 degree δ_a input to the airframe. Figure 49 represents a unity ROLL C input, where ROLL C varies over the range ± 1 for full scale inputs. The output of these linearized responses in both cases is roll rate in deg/sec.

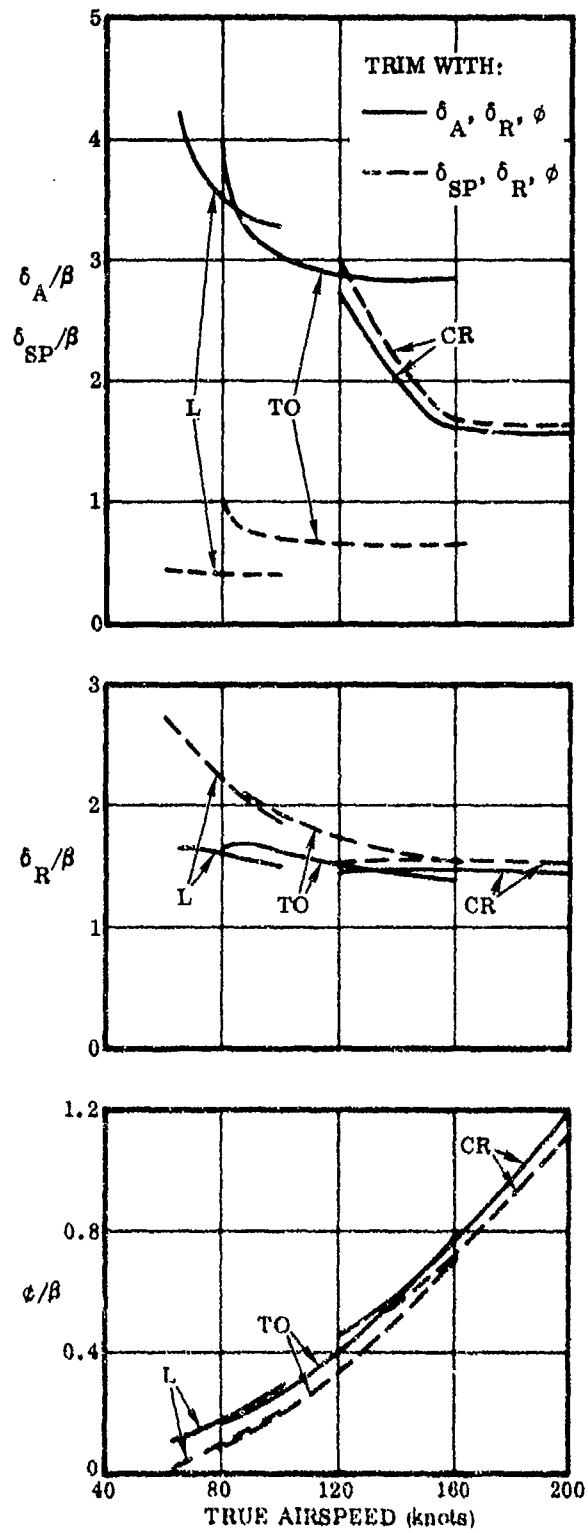


Figure 2-39. EBF Steady-State Sideslip Trim Data

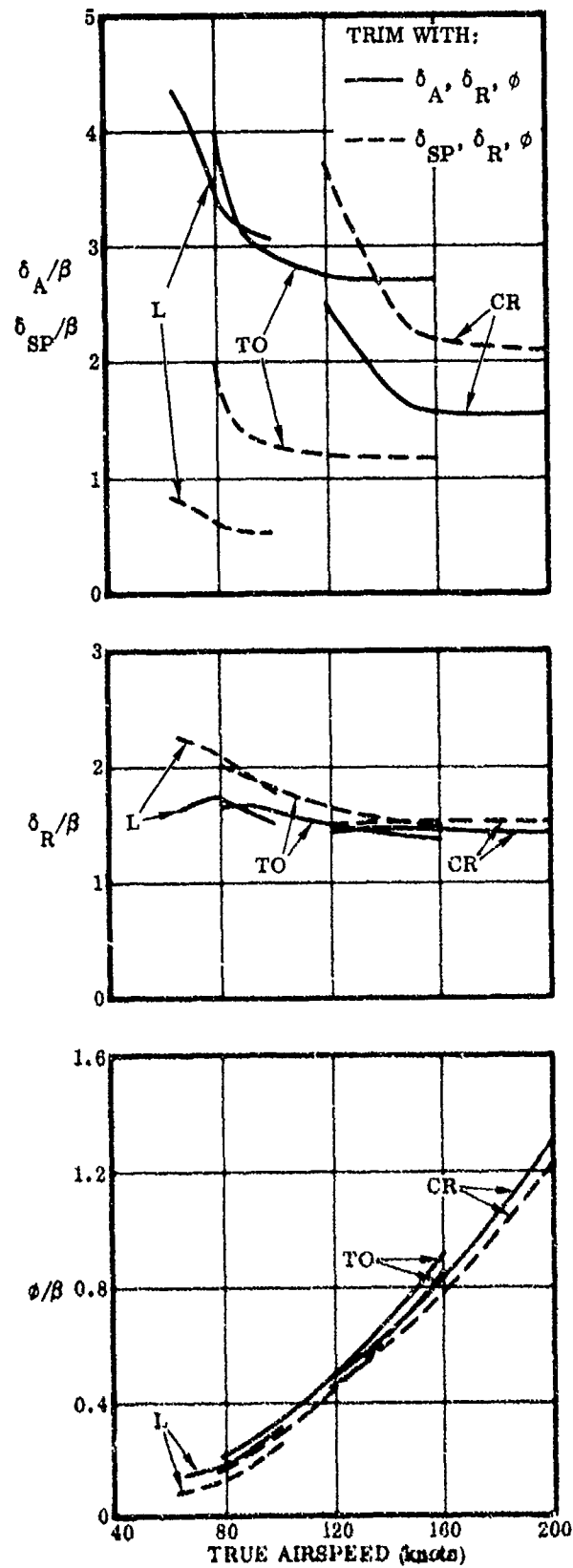
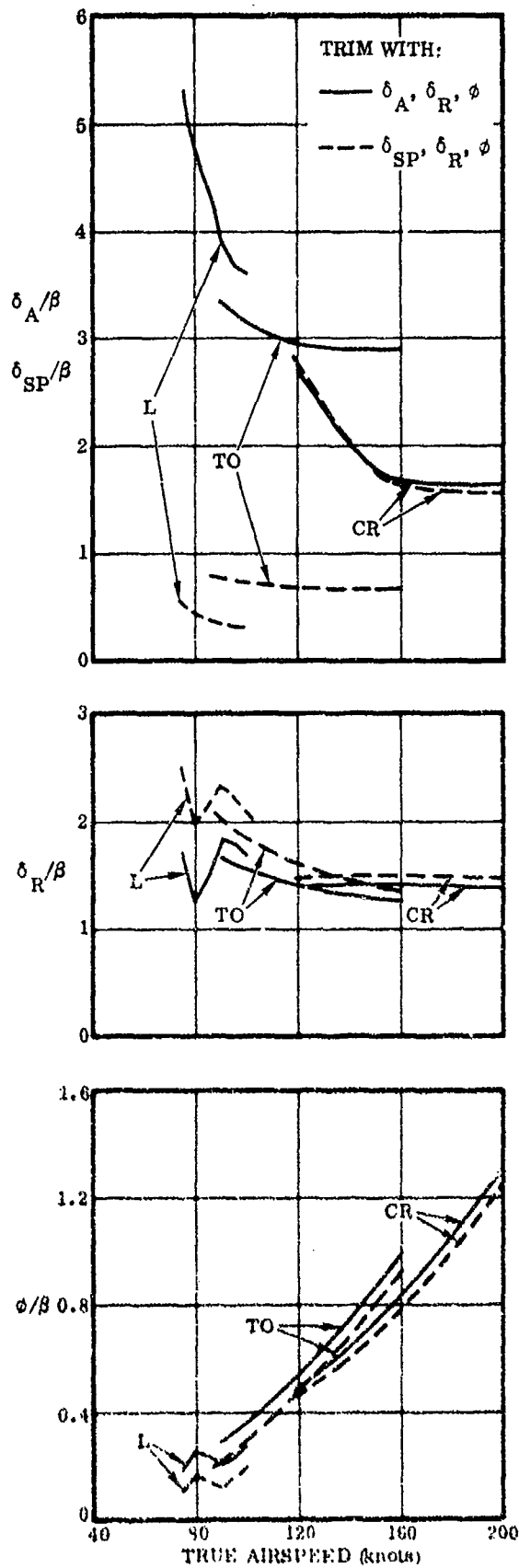


Figure 2-40. IBF Steady-State Sideslip Trim Data



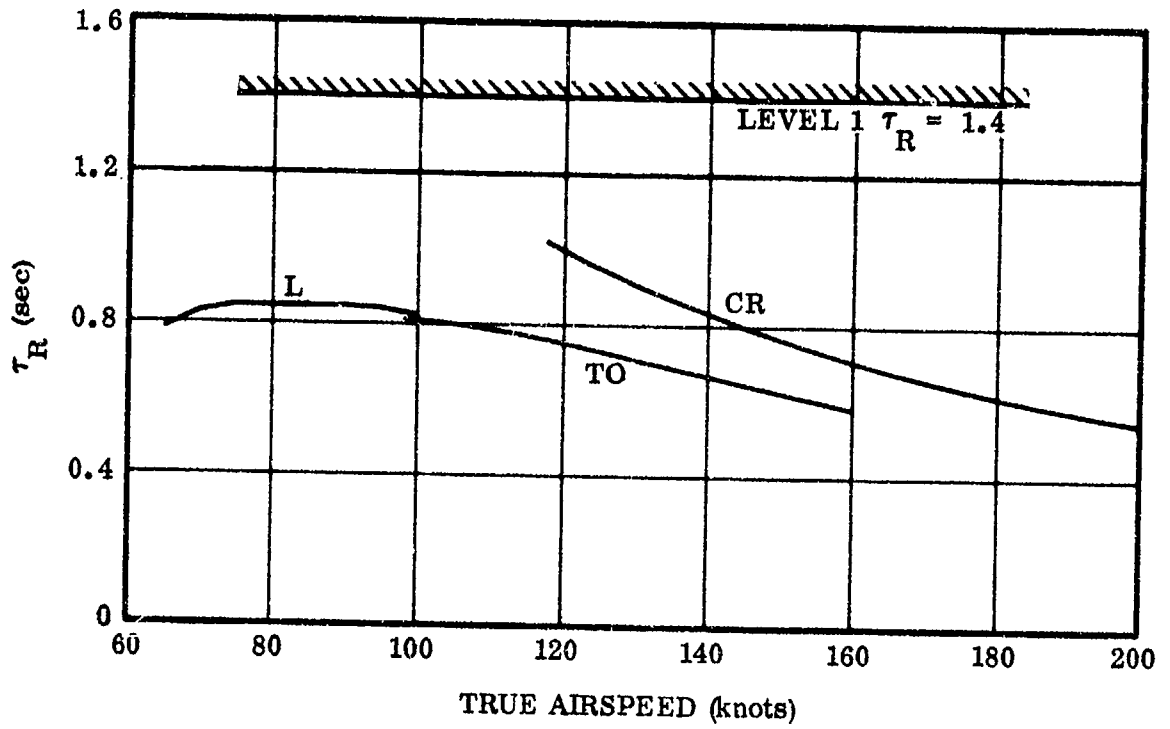


Figure 2-42. EBF Roll Mode Time Constant

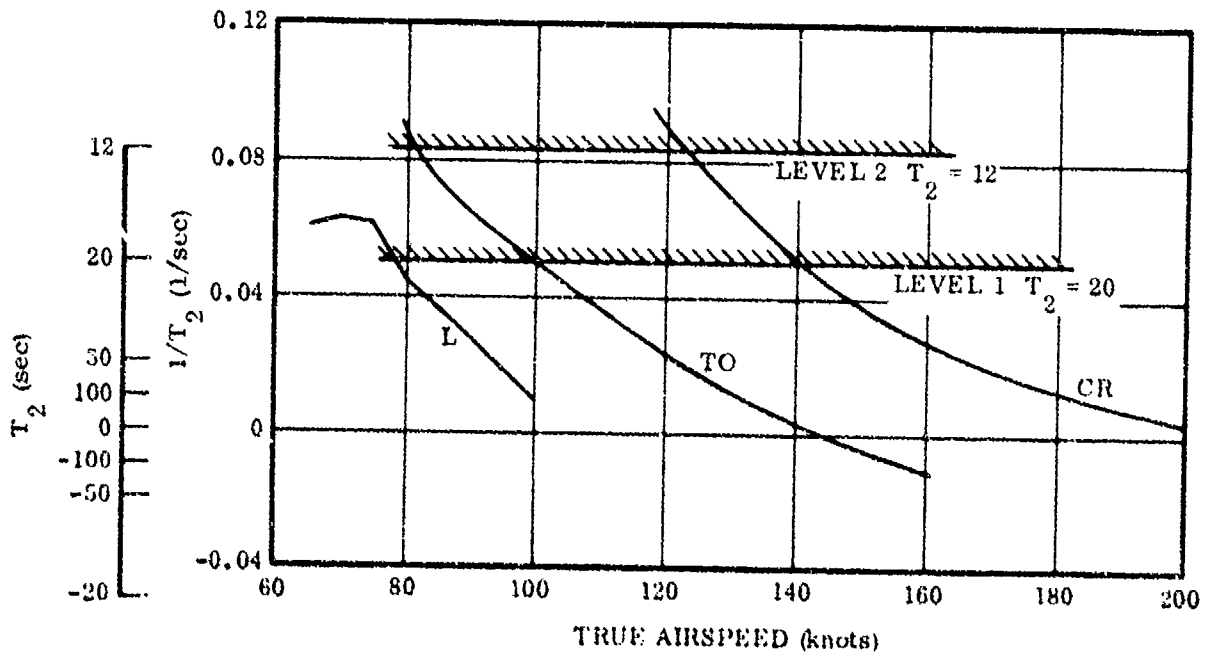


Figure 2-43. EBF Spiral Mode Time to Double Amplitude

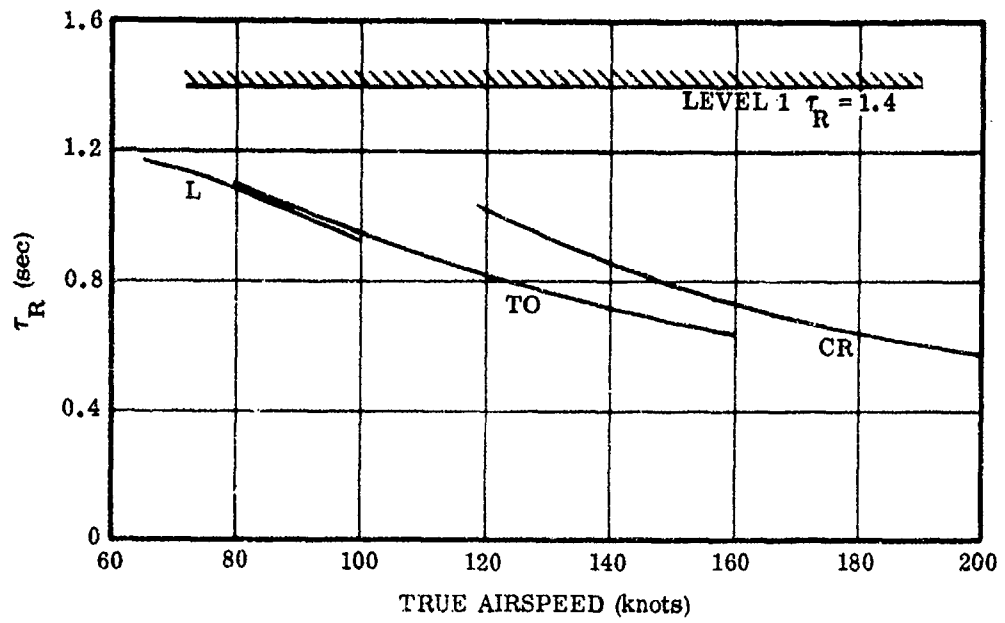


Figure 2-44. IBF Roll Mode Time Constant

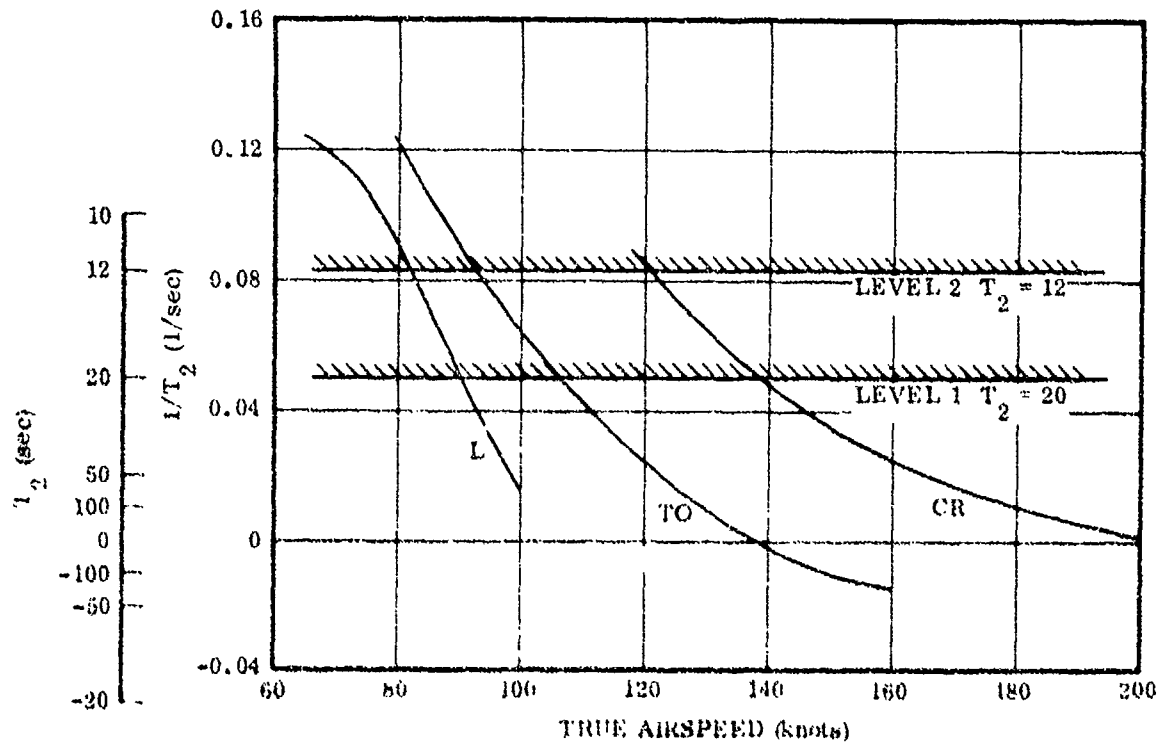


Figure 2-45. IBF Spiral Mode Time to Double Amplitude

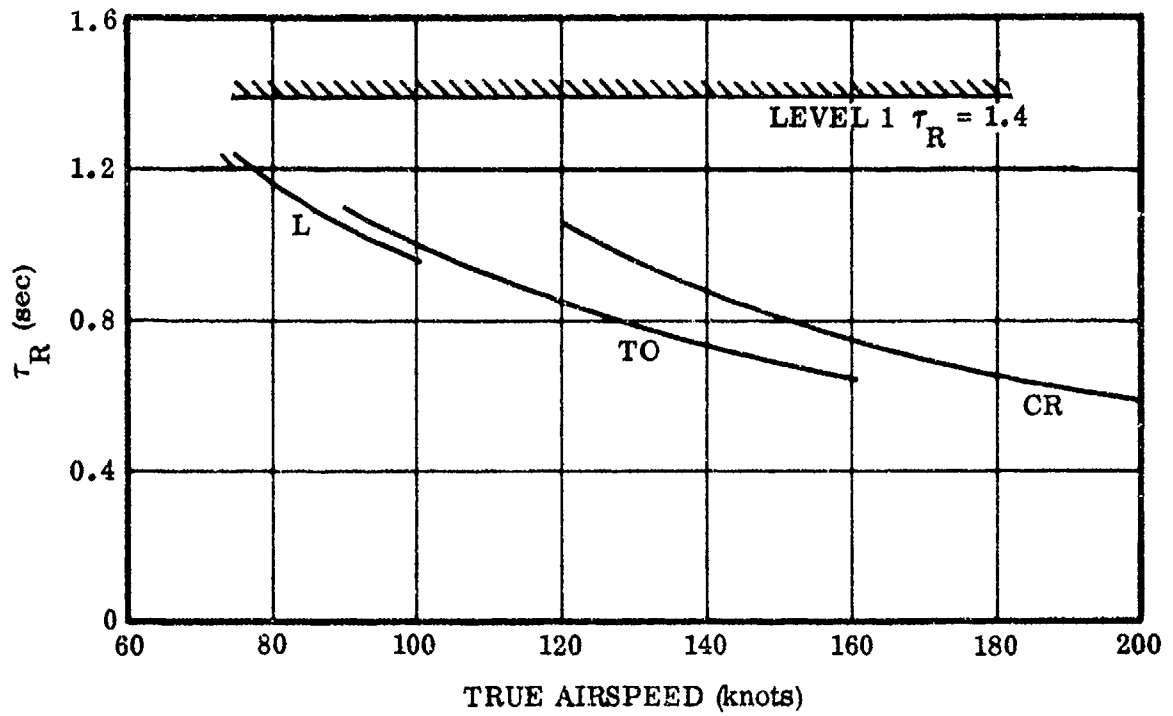


Figure 2-46. MF/VT Roll Mode Time Constant

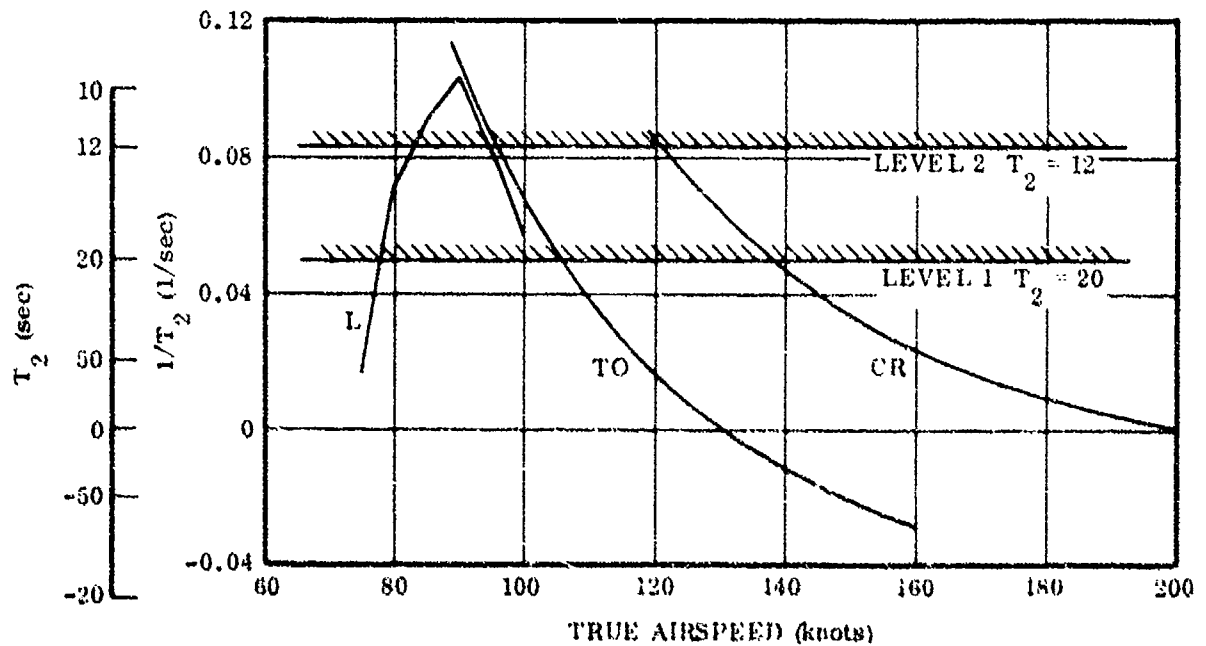


Figure 2-47. MF/VT Spiral Mode Time to Double Amplitude

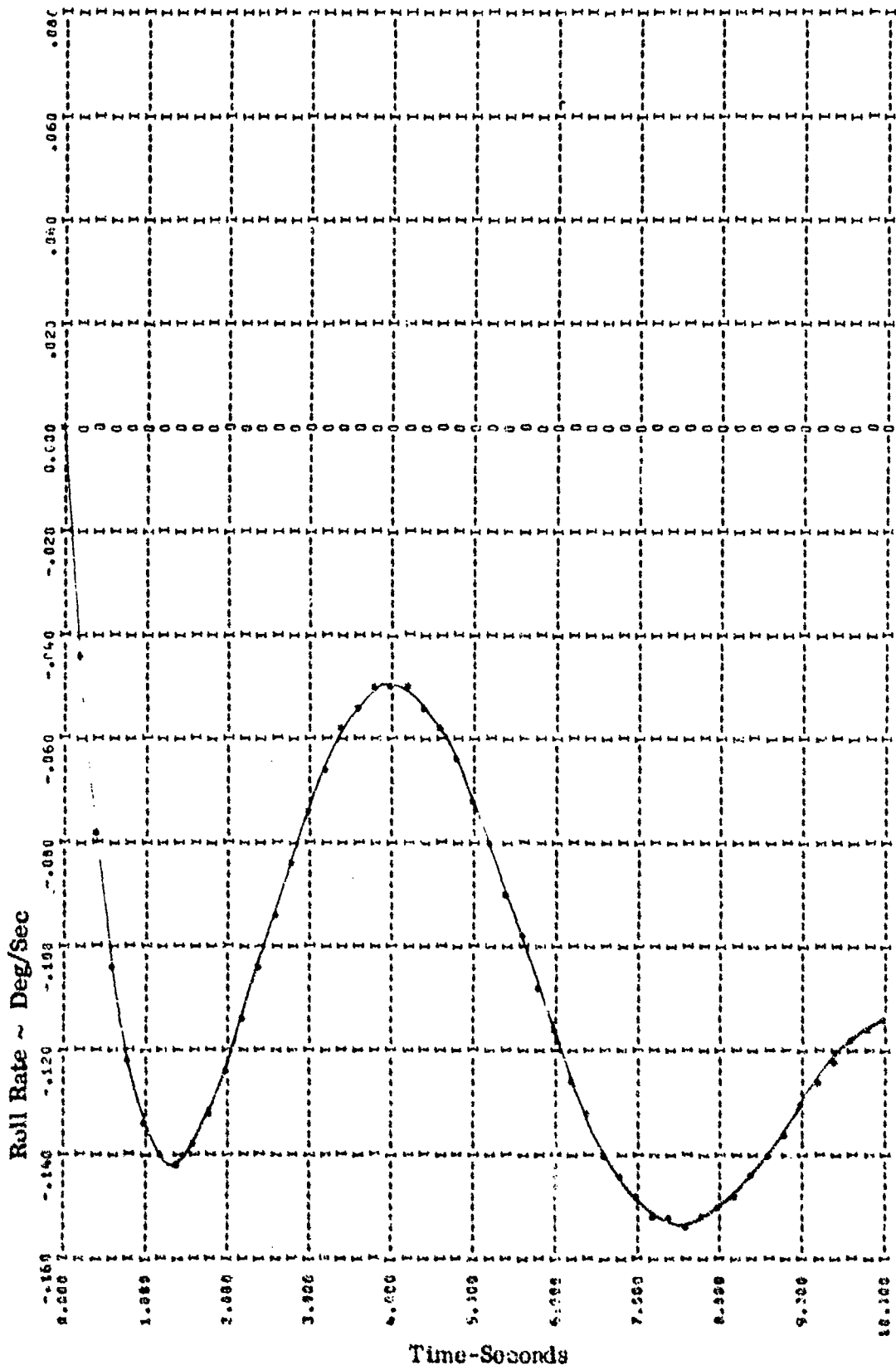


Figure 2-48. Response of Roll Rate to Step 1 Deg Aileron Input (Open Loop)

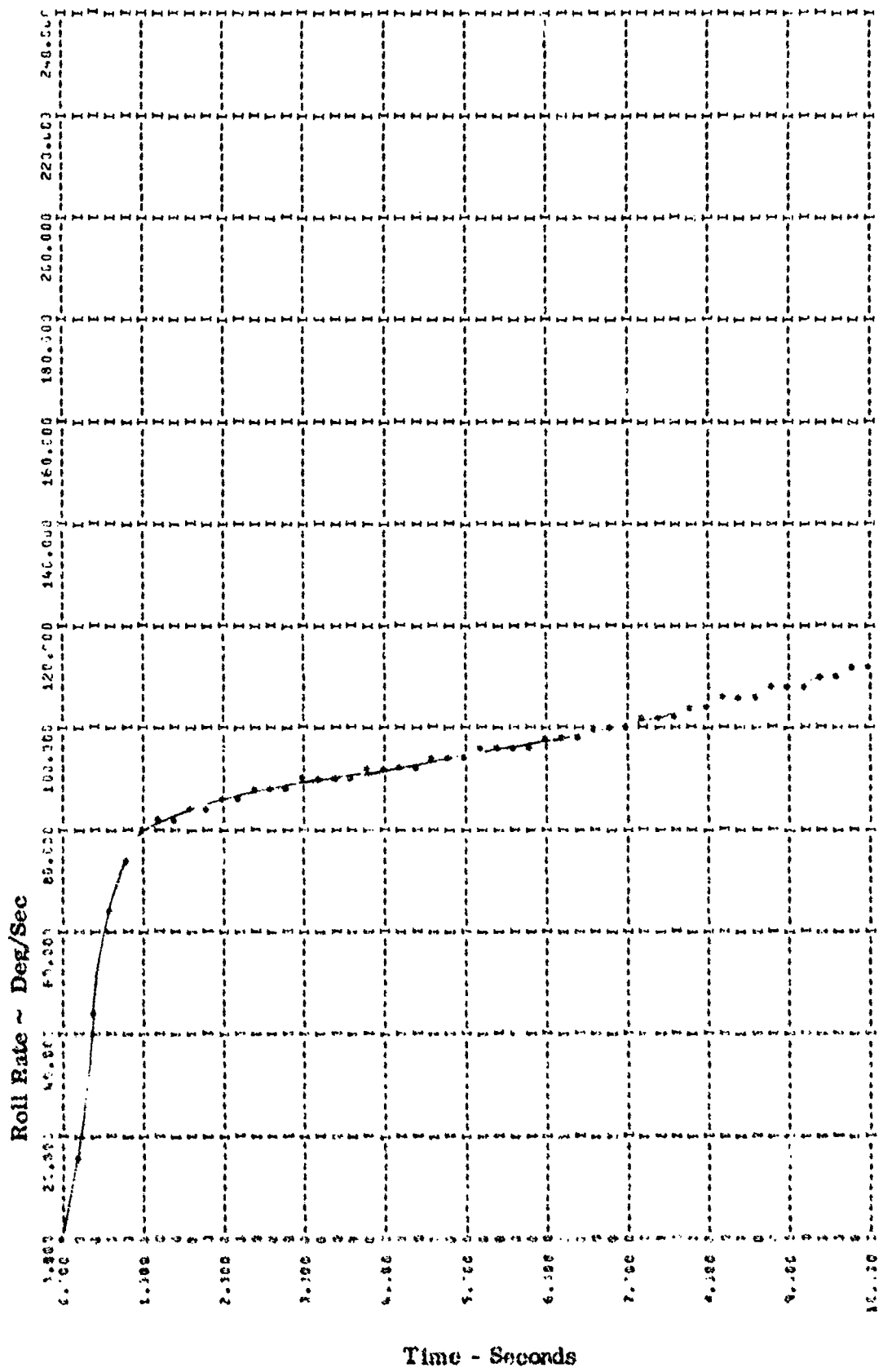


Figure 2-49. Response of Roll Rate to Step Full Scale Input (Closed Loop)

Dutch roll characteristics are shown in Figures 2-50 through 2-52 for the three vehicles. The specification values from References 2-2 and 2-3 are shown. The bare airframe responses in EBF landing and takeoff configurations meet the specifications in Reference 2-2, but not those in Reference 2-3. The other two vehicles meet both specifications in landing, takeoff, and cruise. Values for the nominal SAS are also shown in Figures 2-50 through 2-52 for each vehicle. This SAS corresponds to the gain schedules identified as nominal in Paragraph 2.7. The SAS-on responses far exceed the Level 1 specifications. Simulations indicate that the SAS-off responses are worse than these comparisons show, as discussed in Section 4.

Roll-rate oscillation, bank-angle oscillation, and sideslip excursion data is shown in Figures 2-53 through 2-76. Data is shown for the landing and takeoff configurations for the parameters from References 2-2 and 2-3. Bare airframe data is shown for both aileron and spoiler inputs. The results for the normal SAS from Paragraph 2.7 are also shown.

Roll-rate oscillation data is in the form of p_{osc}/P_{avg} versus $\psi\beta$. P_{osc} and P_{avg} are calculated from the transient response of roll rate to a roll control step. These step responses are calculated from the linearized matrix from which the dutch roll, roll mode, and spiral mode roots are determined. Although the specifications define P_{osc} as measured by the absolute peaks of the total response, close approximations are obtained from the residues of the dutch roll component only. An alternative form of the aircraft specification and the form of the V/STOL spec is ϕ_{osc}/ϕ_{avg} , measured from a bank angle response to a roll control pulse input. Using the linearized response, these two forms are mathematically identical, and are interchangeable with the $\psi\beta$ value shifted by the angle $(90 \text{ deg} + \sin^{-1} \zeta)$.

The sideslip excursion parameter $\frac{\Delta\beta_{max}}{K}$ is calculated from the sideslip responses to a step and the bank angle response to a step. It is shown for landing, takeoff, and cruise, for aileron and spoiler inputs, and for a roll input with nominal SAS. The sideslip excursion parameters from Reference 2-2 are also shown for landing and takeoff. These are $\frac{\Delta\beta}{\phi_1}$ and $\left| \frac{\Delta\beta}{\phi_1} \right| \times \left| \frac{\phi}{\beta} \right|_d$, calculated from sideslip and bank angle responses to pulse roll inputs.

2.7 LATERAL DIRECTIONAL SAS

The lateral directional SAS, like the longitudinal, was developed for the EBF vehicle at 80 knots in a landing approach configuration. The trim conditions delineated

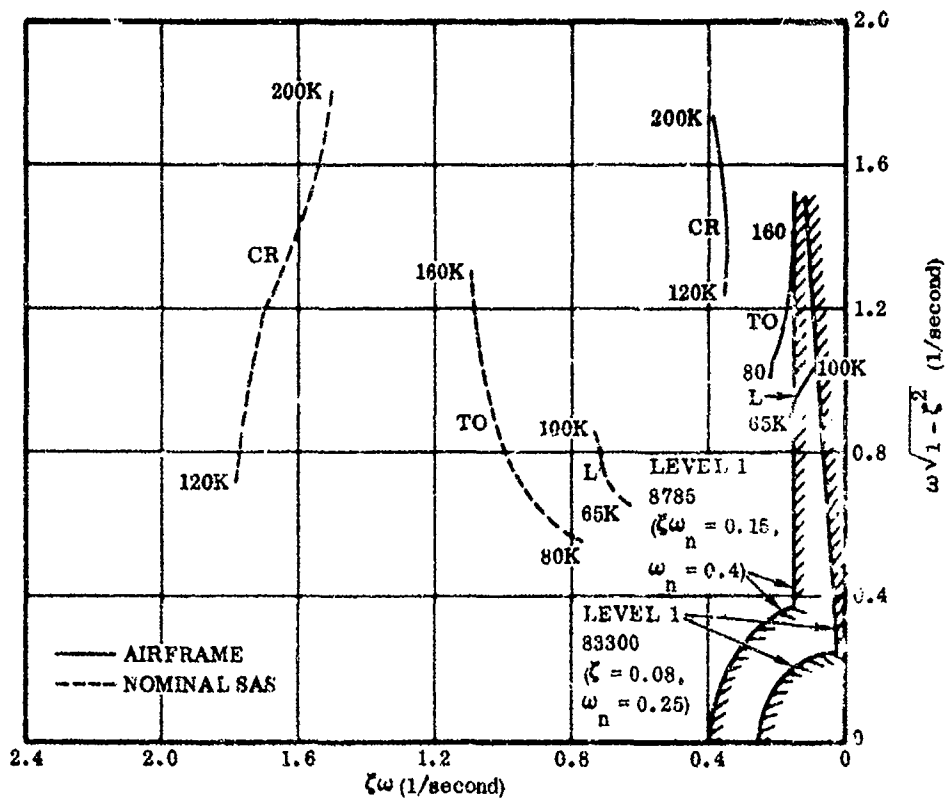


Figure 2-50. EBF Dutch Roll Characteristics

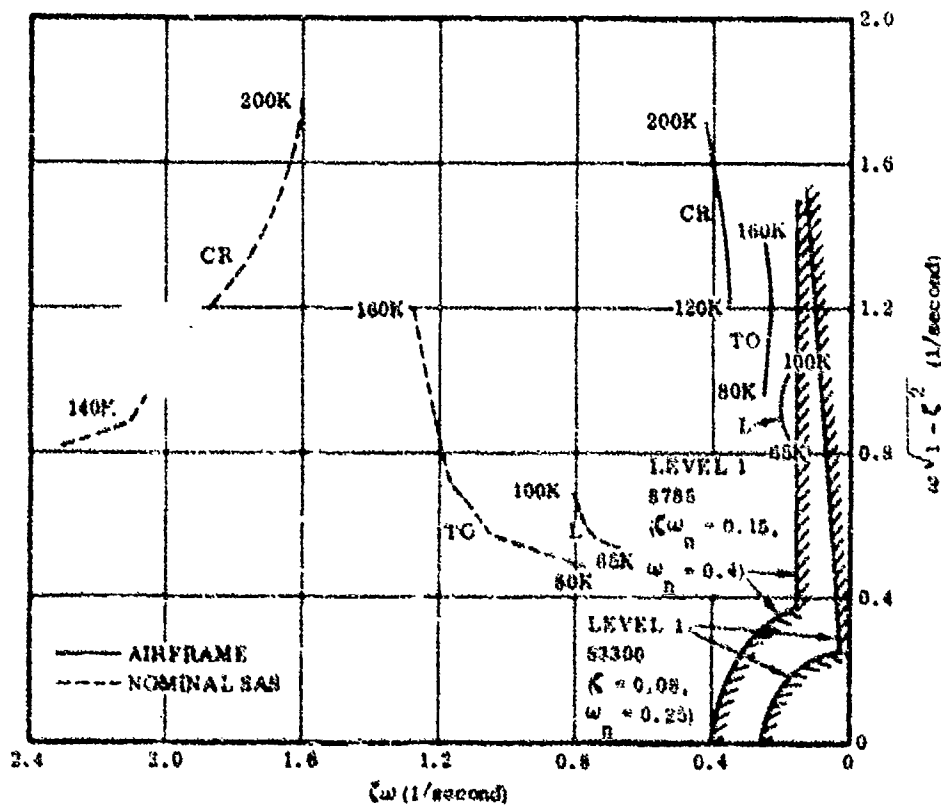


Figure 2-51. IBF Dutch Roll Characteristics

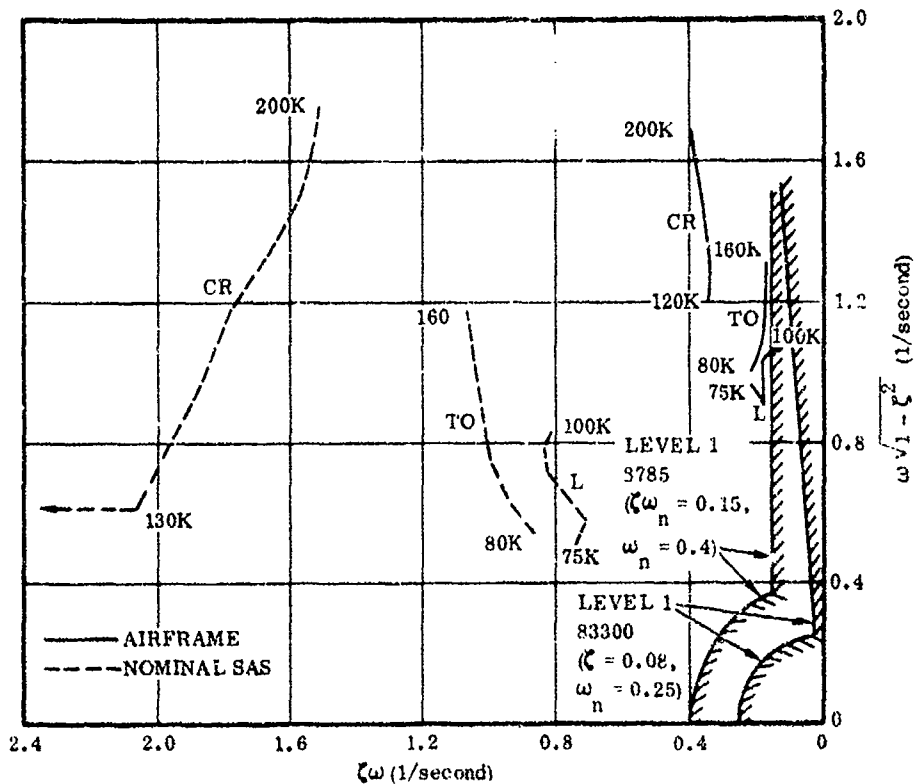


Figure 2-52. VT Dutch Roll Characteristics

in Paragraph 2.4 are used. The block diagram of Figure 2-36 was the starting point for this analysis, and was modified to Figure 2-77. The numerical dimensional derivatives for this flight condition are:

YR	+ -0.913123173007281-C1.	NDR	+ -1.748217395776956+11.
LR	+ -0.176471706731967+C1.	YDR	+ 0.11.
NR	+ 0.416195649491796+C1.	LDR	+ -0.25545419161797+10.
YR	+ 0.675177467-1.207-C1.	NDR	+ 0.424766176405718-C1.
LR	+ -0.11338677418197+C1.	YNSP	+ 0.4.
LW	+ -0.74299797370-1.11-C1.	LNSP	+ -0.1794016754117+C1.
YR	+ 0.37956277711057-C1.	NNSP	+ -1.4-318464711627-C1.
LW	+ 0.349702842430779+C1.	YENG	+ 0.11.
NR	+ -0.26171784711979+C1.	LENG	+ 0.749714549713768+C1.
YDR	+ 0.719797740364037-C1.	NEUC	+ 0.110761119437647+11.
LDR	+ 0.246796446421947+C1.		

Sideslip feedback was considered better over the speed range than lateral acceleration, especially at approach speeds. A roll attitude hold and a roll rate loop had both been mechanized, but the rate loop was preferred by the pilot and the SAS was analyzed on this basis.

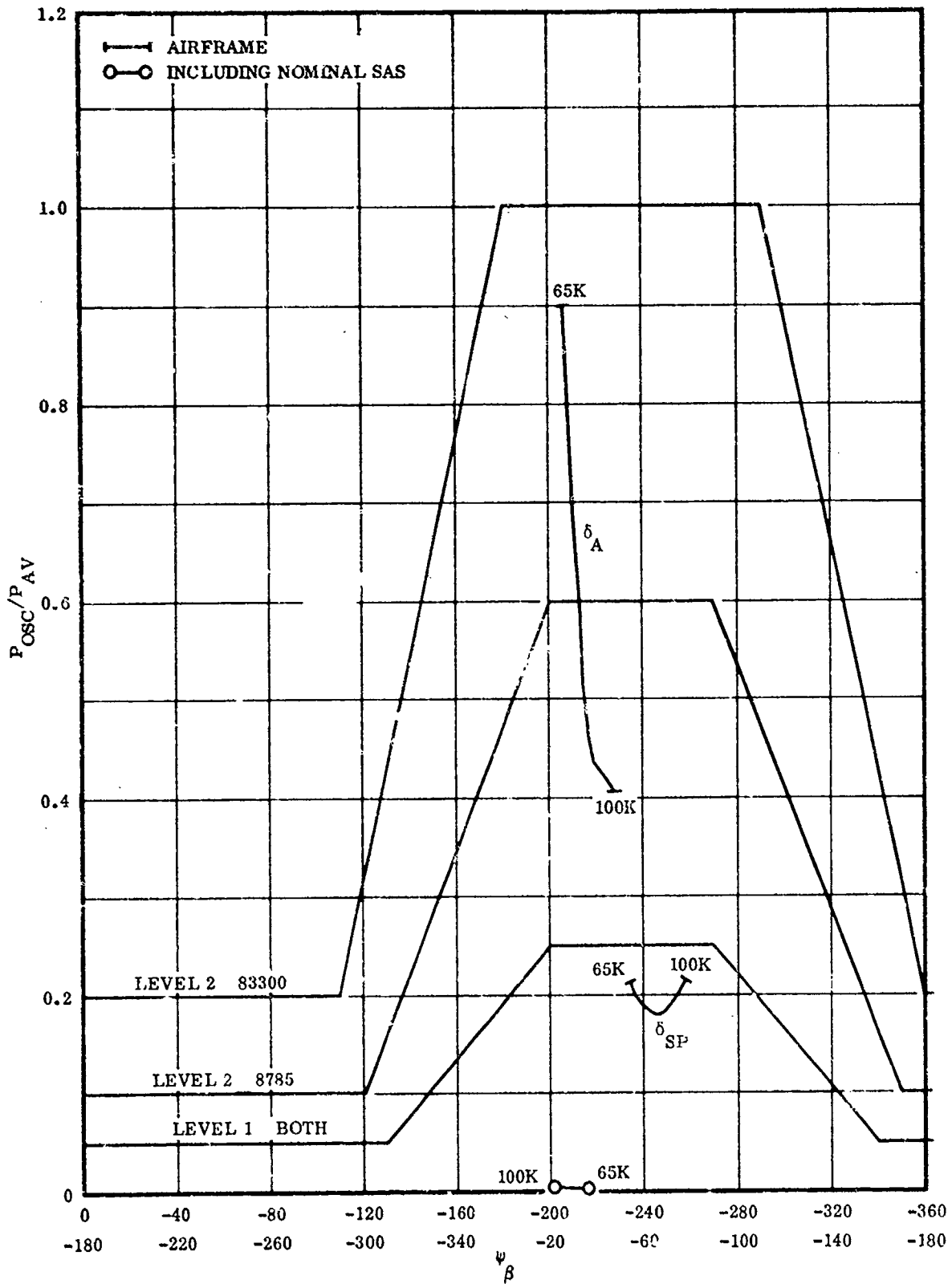


Figure 2-53. EBF Roll Oscillations, Landing

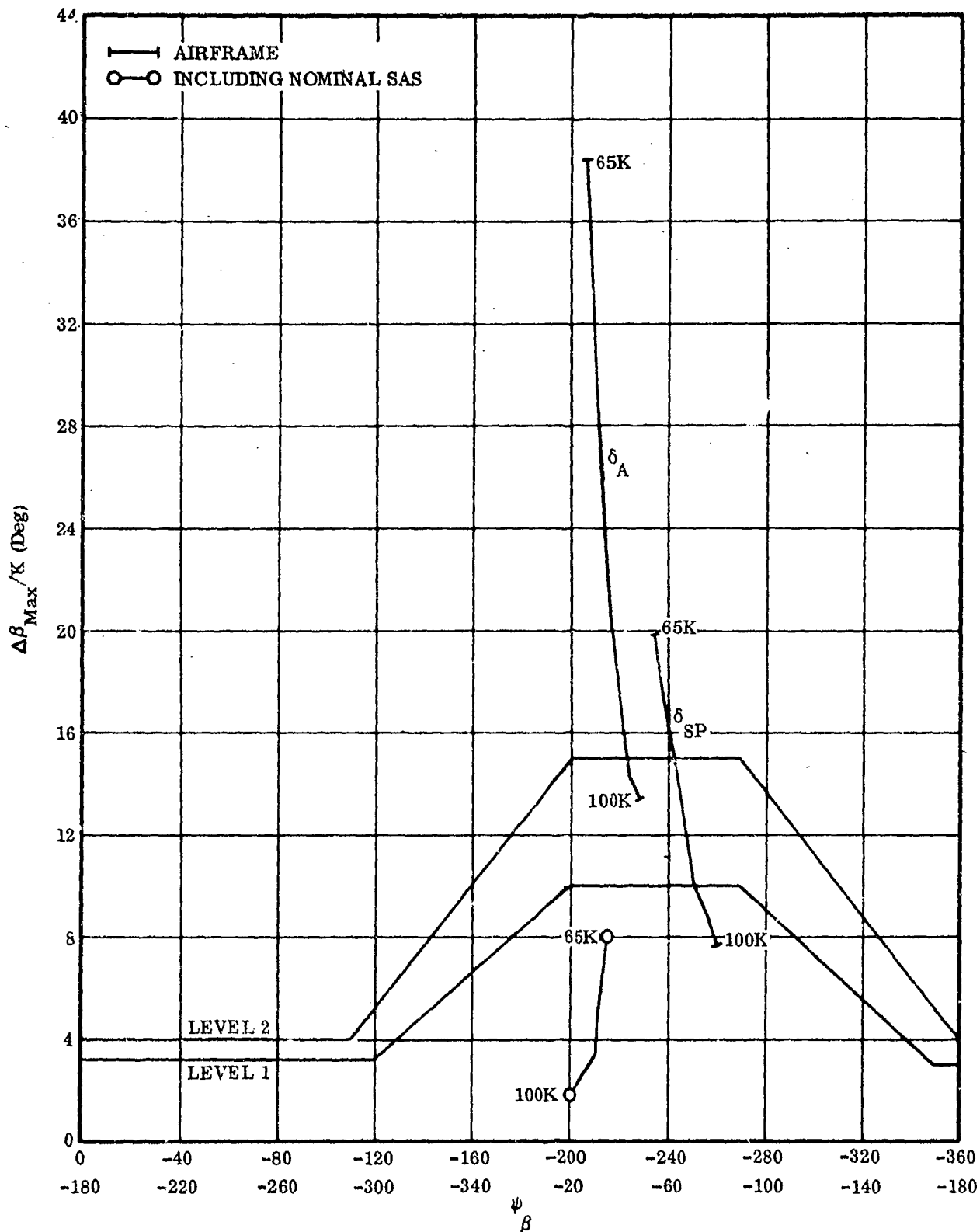


Figure 2-54. EBF Sideslip Excursions, Landing

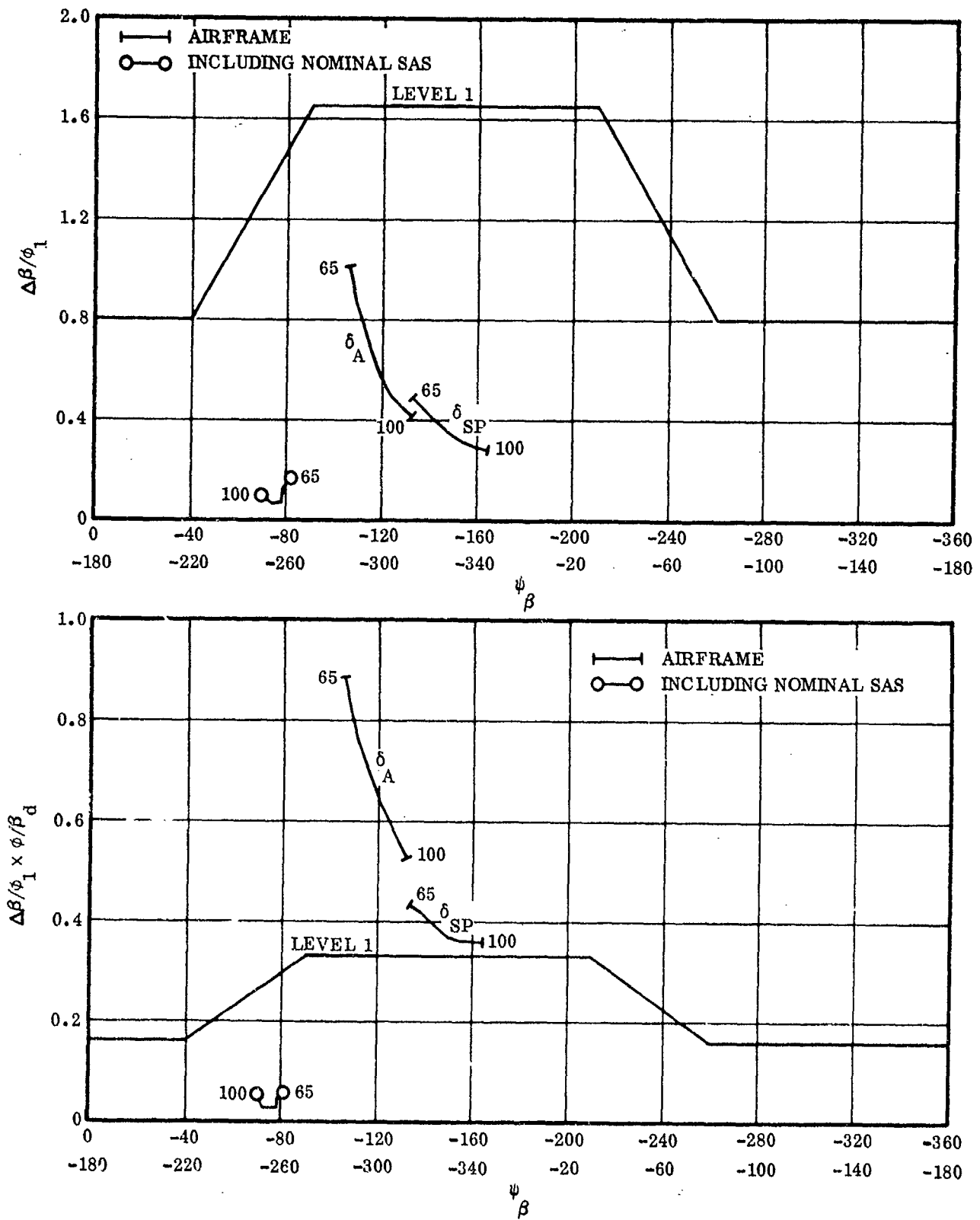


Figure 2-55. EBF Sideslip Excursions, Landing, STOL Parameters

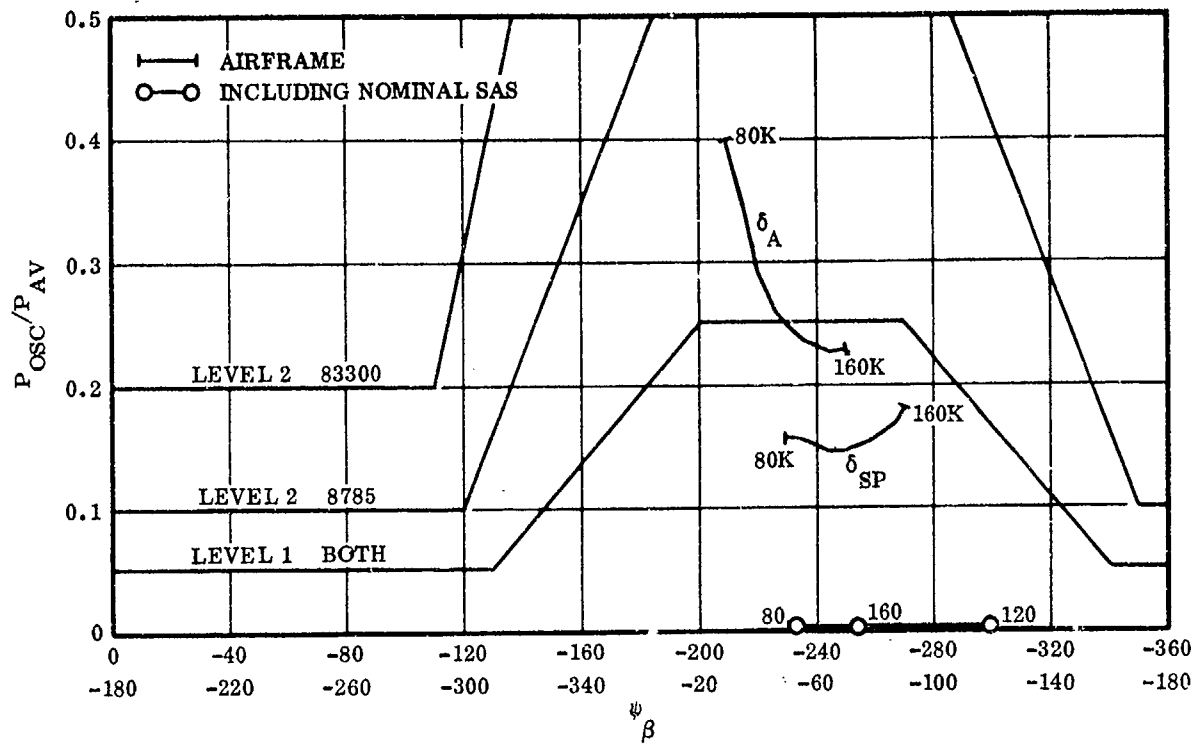


Figure 2-56. EBF Roll Oscillations, Takeoff

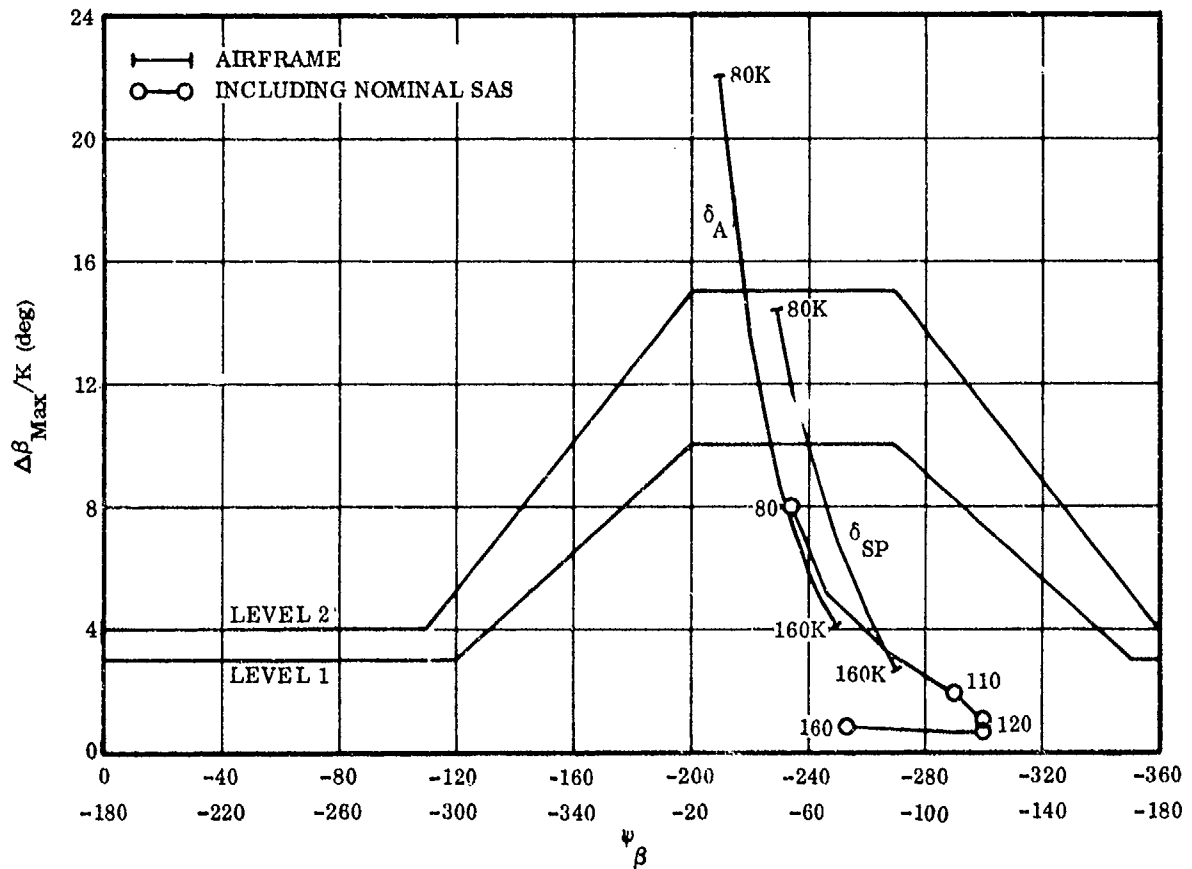


Figure 2-57. EBF Sideslip Excursions, Takeoff

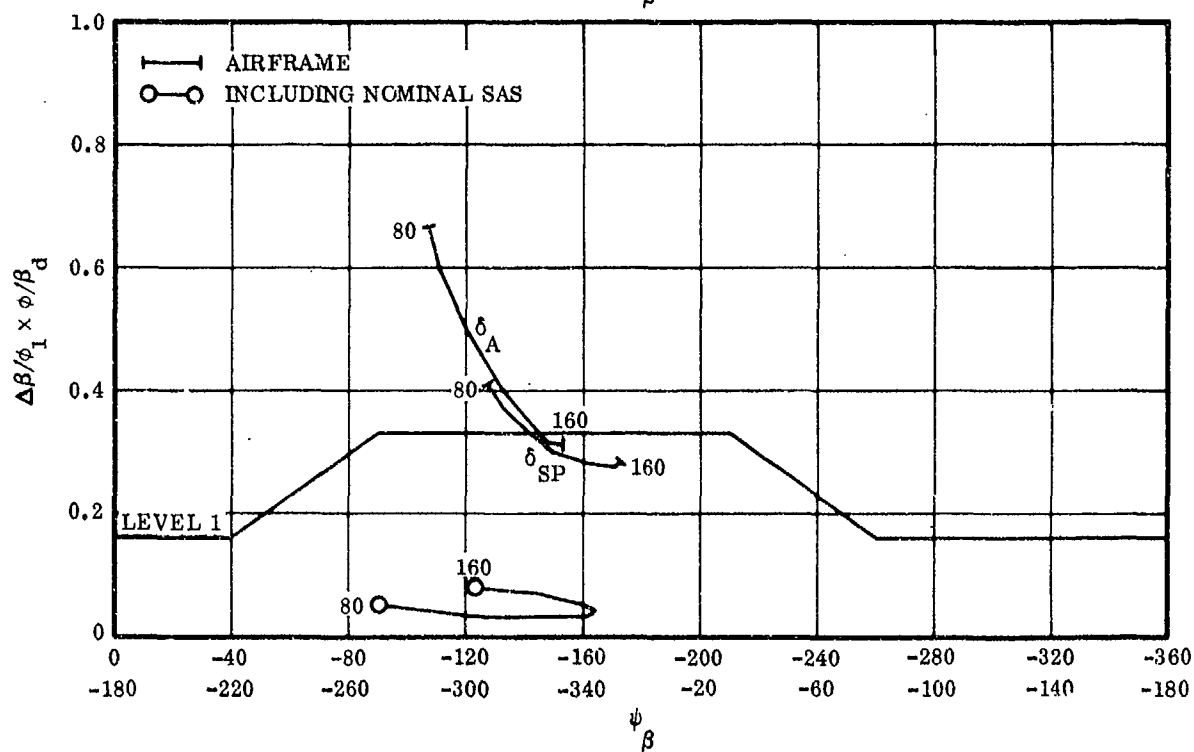
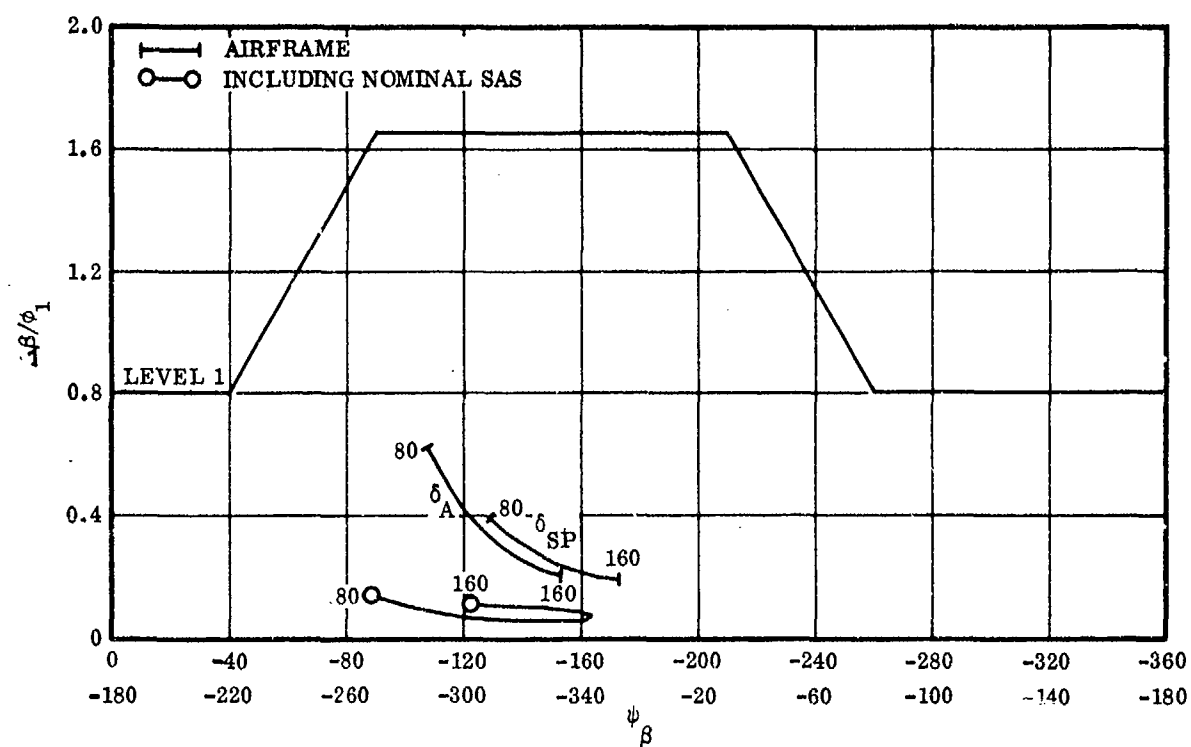


Figure 2-58. EBF Sideslip Excursions, Takeoff, STOL Parameters

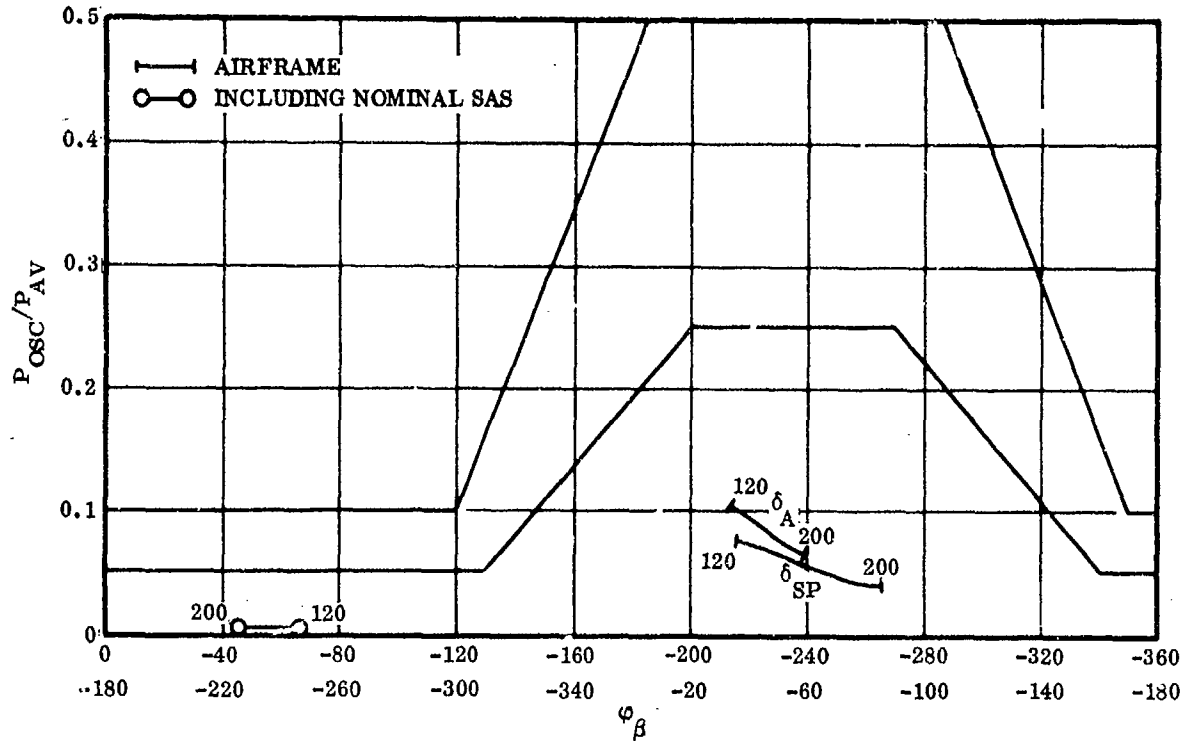


Figure 2-59. EBF Roll-Rate Oscillations, Cruise

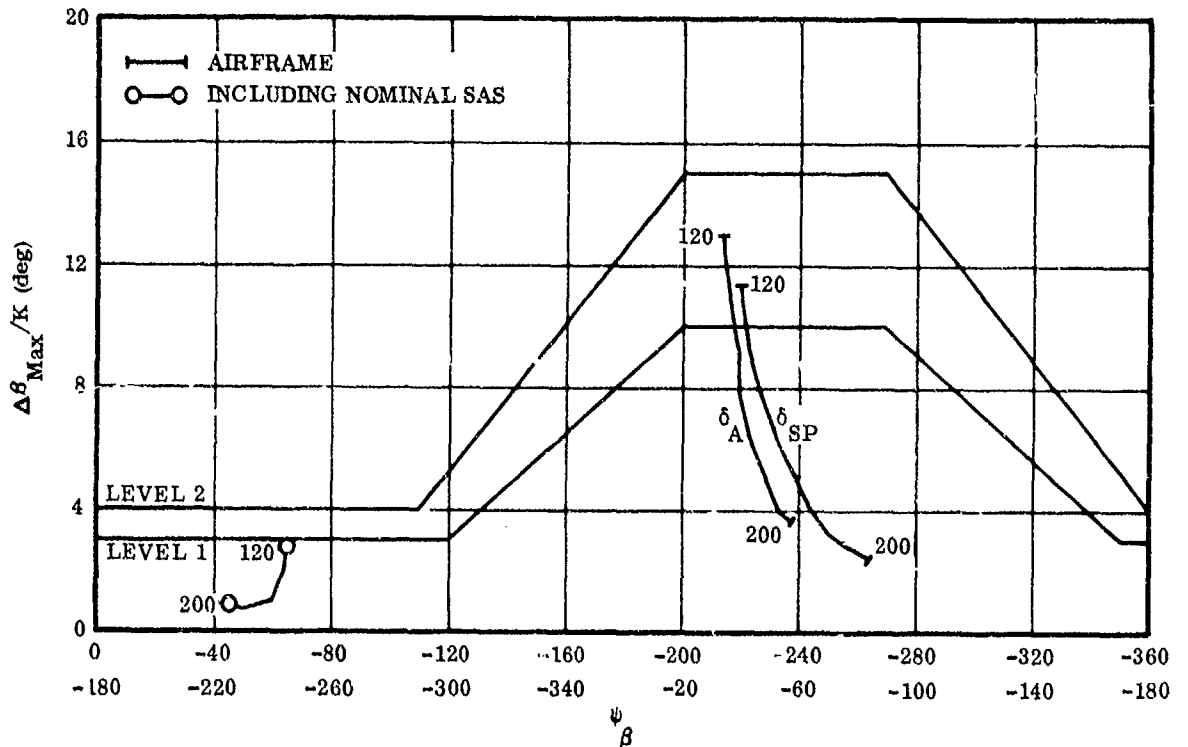


Figure 2-60. EBF Sideslip Excursions, Cruise

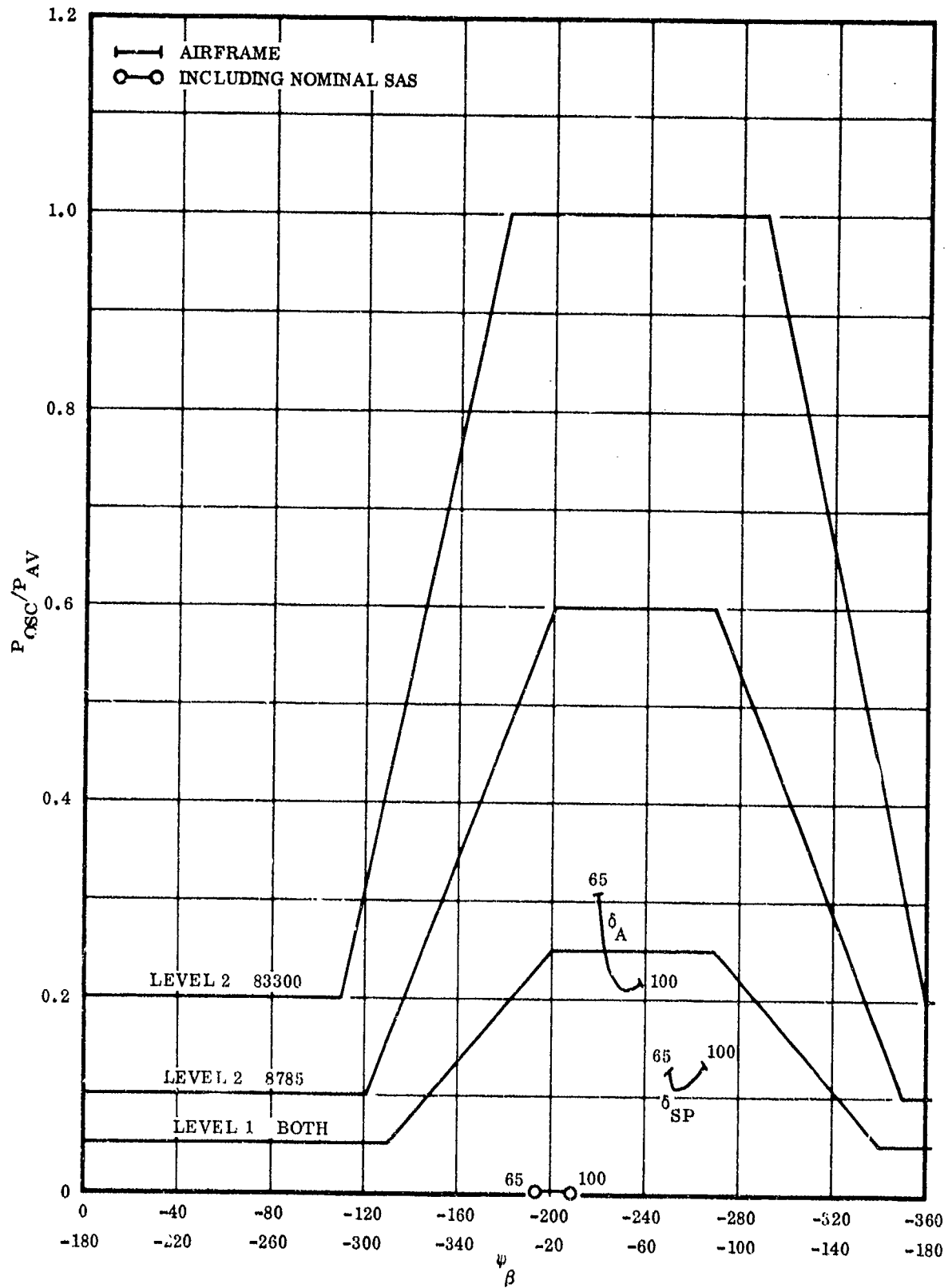


Figure 2-61. IBF Roll Oscillations, Landing

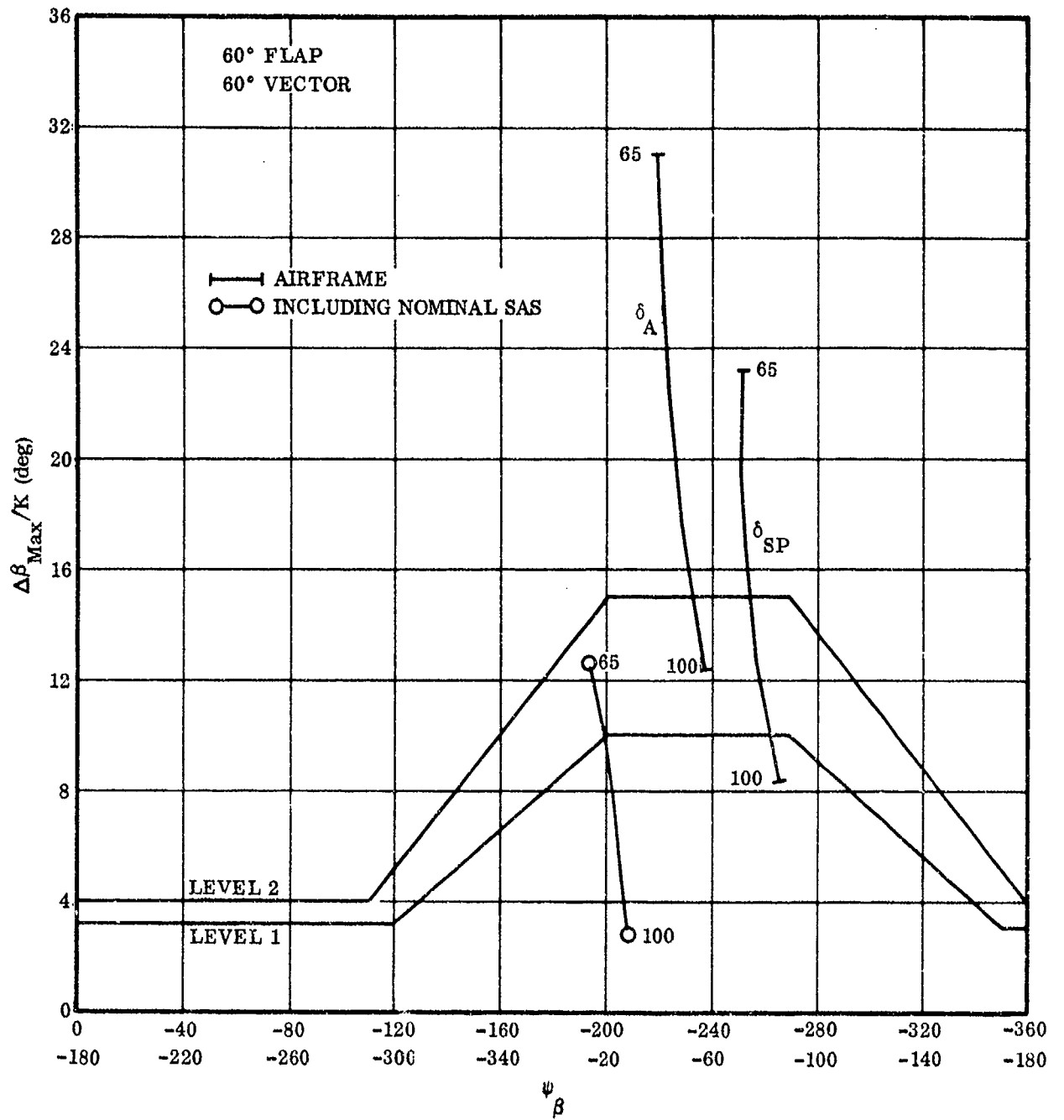


Figure 2-62. IBF Sideslip Excursions, Landing

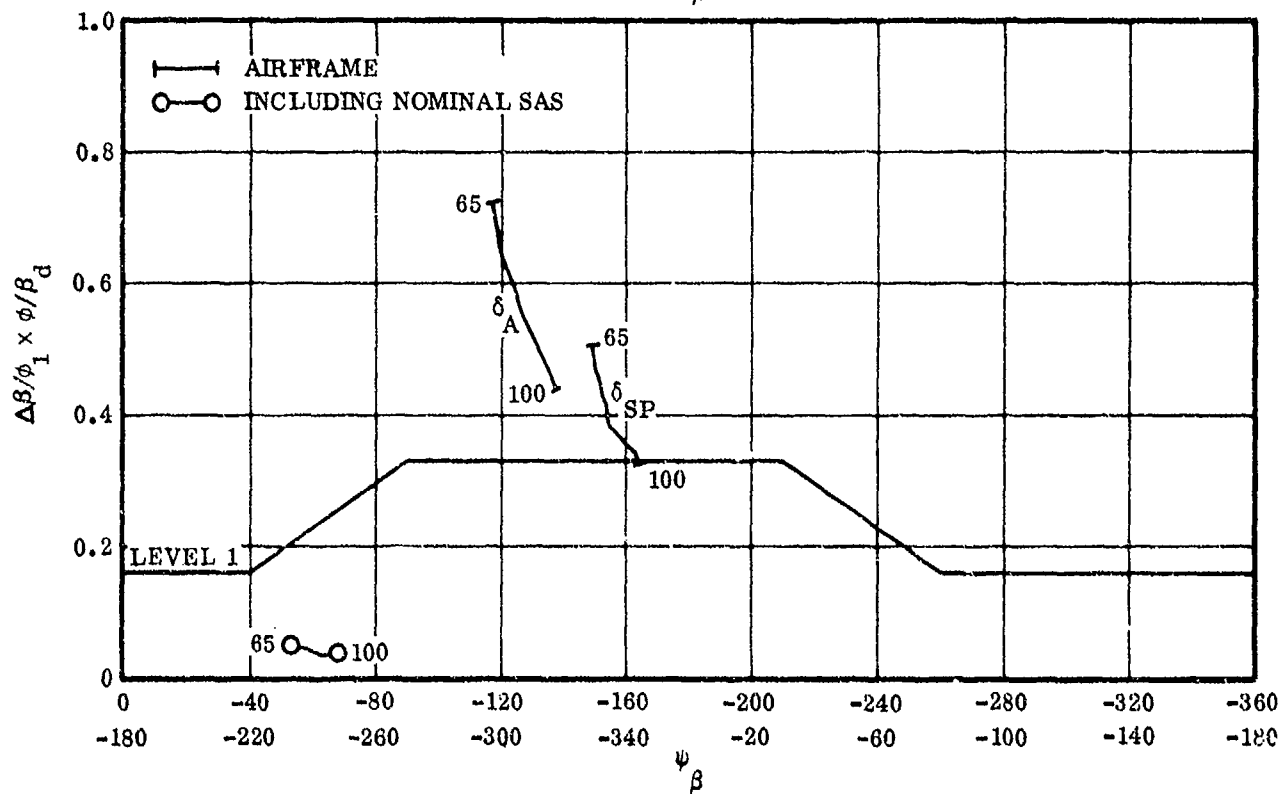
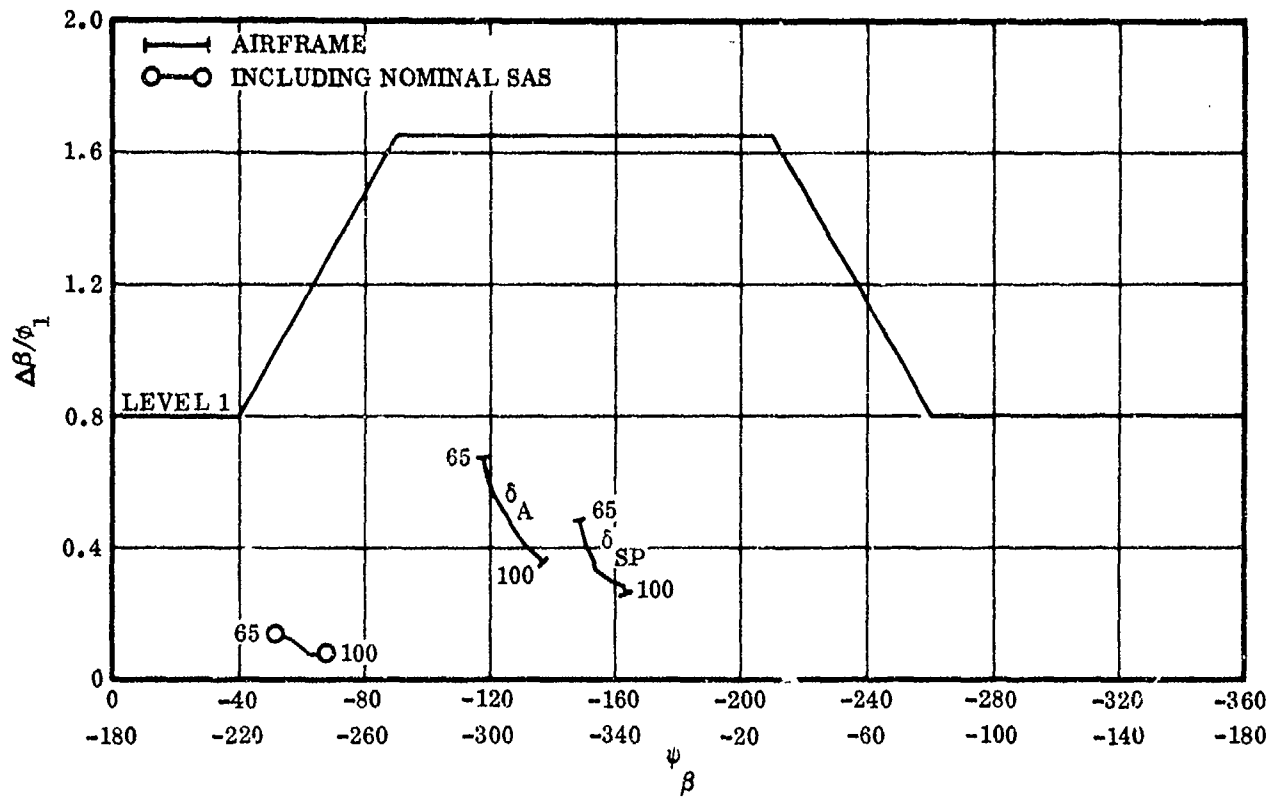


Figure 2-63. IBF Sideslip Excursions, Landing, STOL Parameters

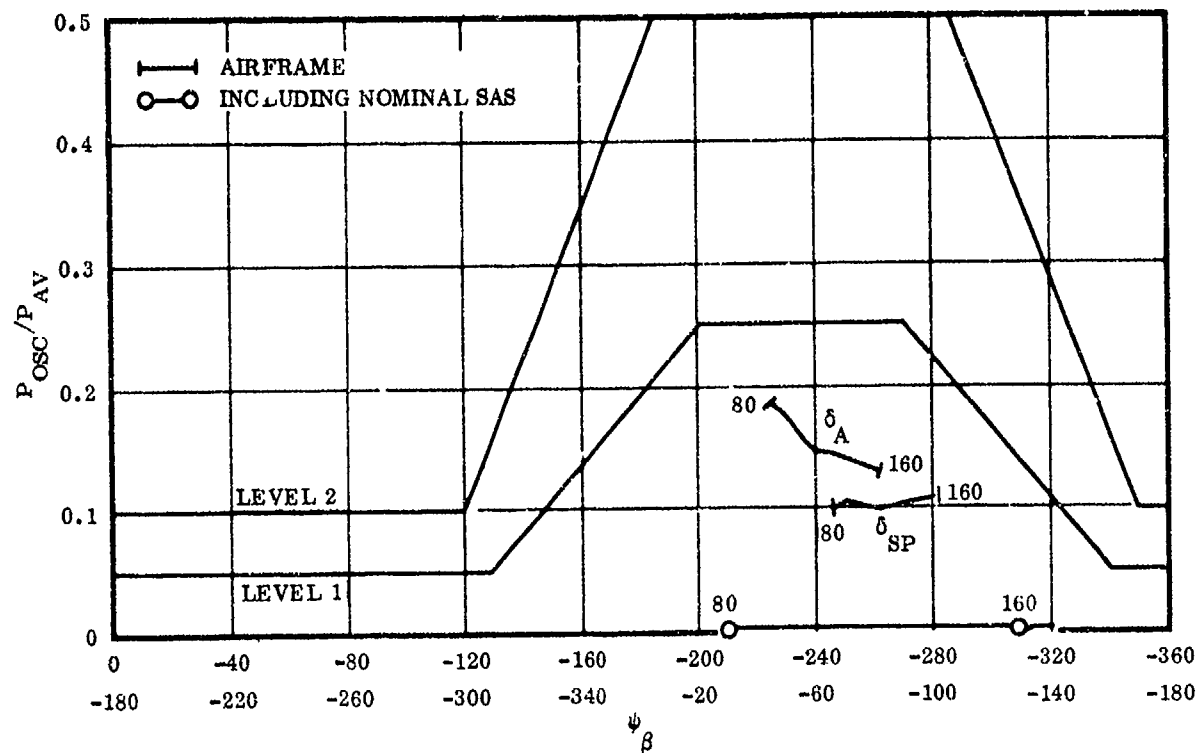


Figure 2-64. IBF Roll-Rate Oscillations, Takeoff

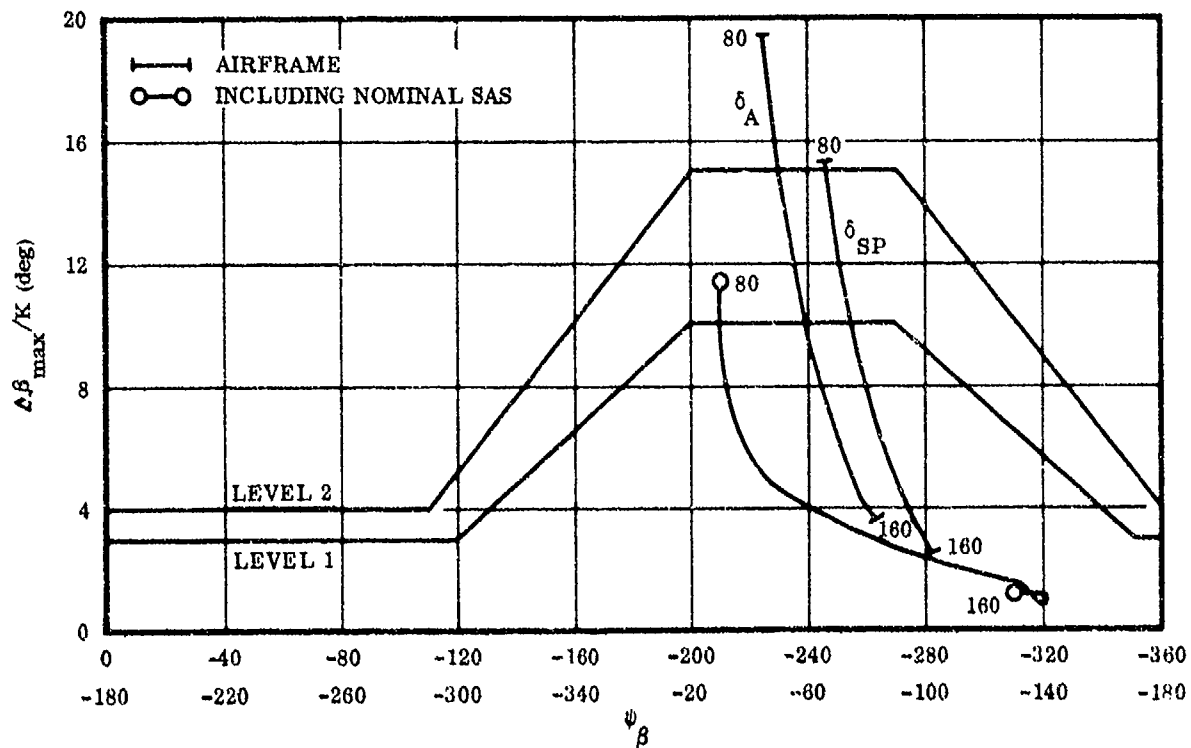


Figure 2-65. IBF Sideslip Excursions, Takeoff

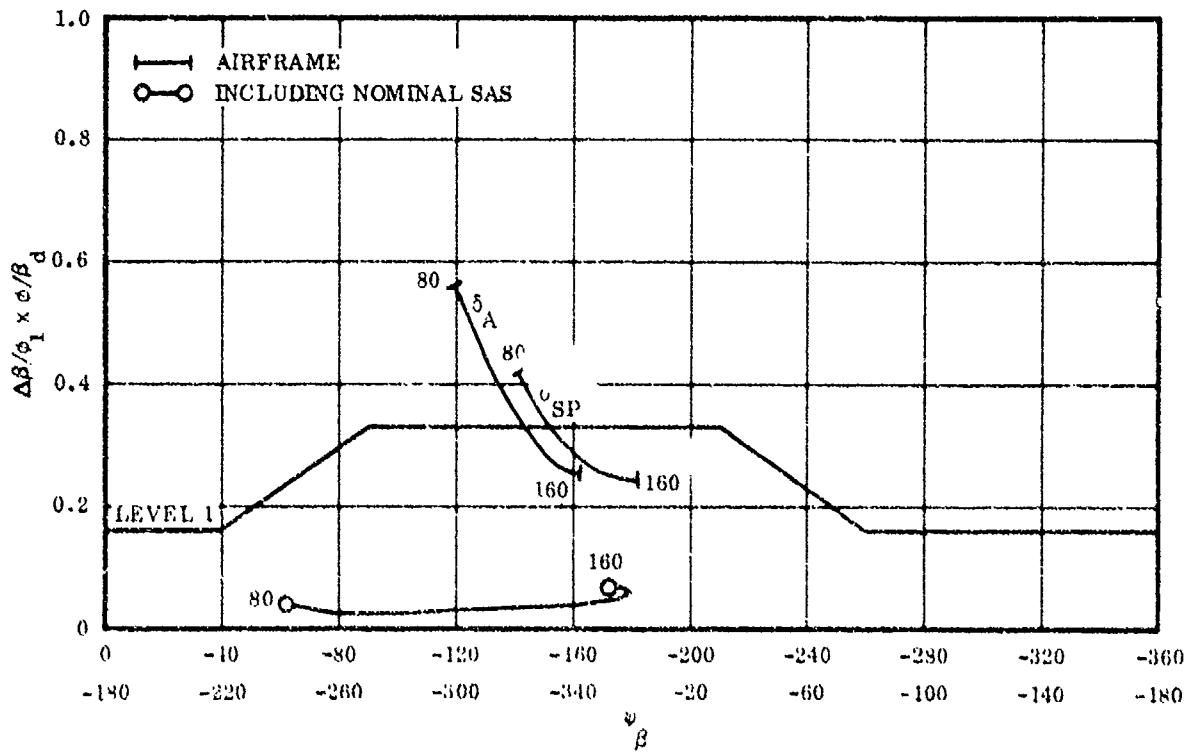
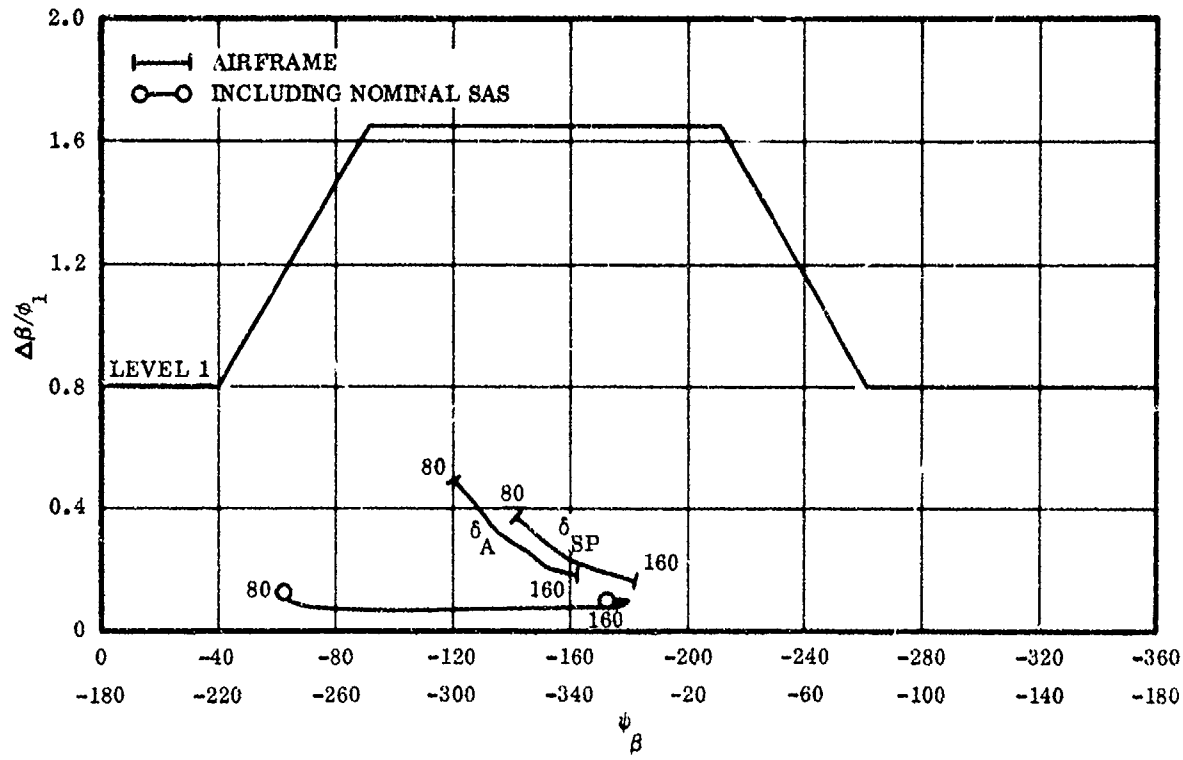


Figure 2-66. IBF Sideslip Excursions, Takeoff, STO Parameters

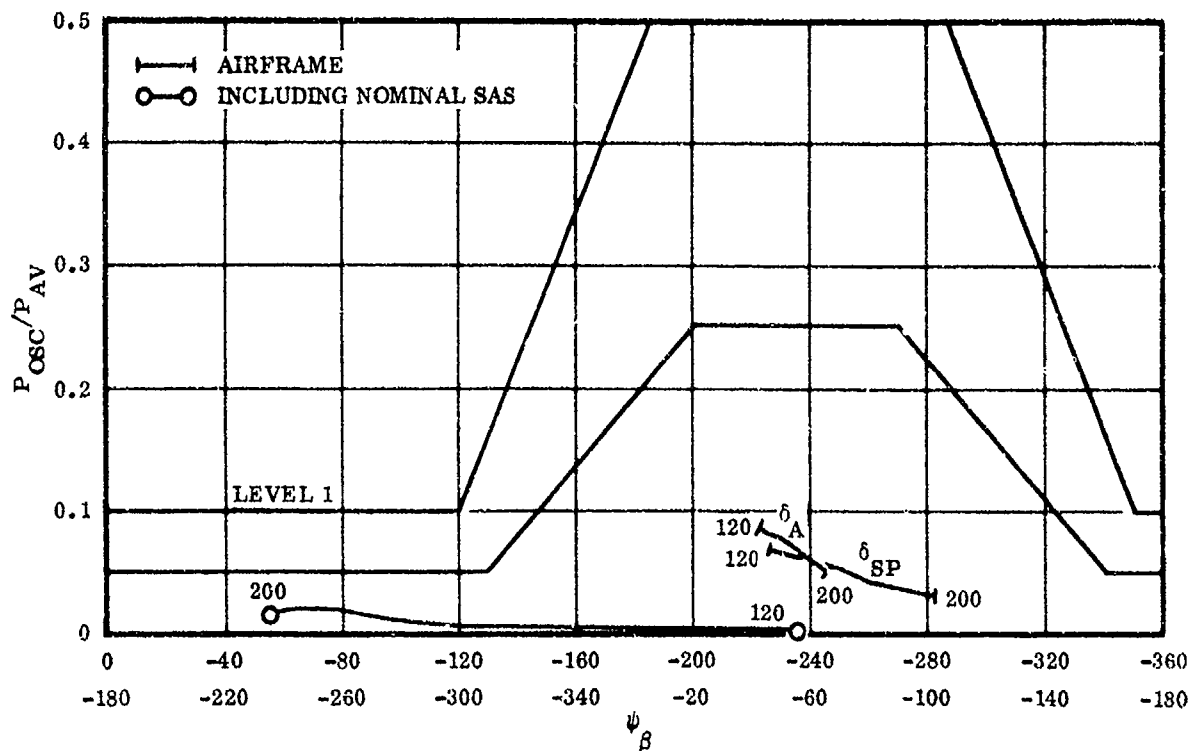


Figure 2-67. IBF Roll-Rate Oscillations, Cruise

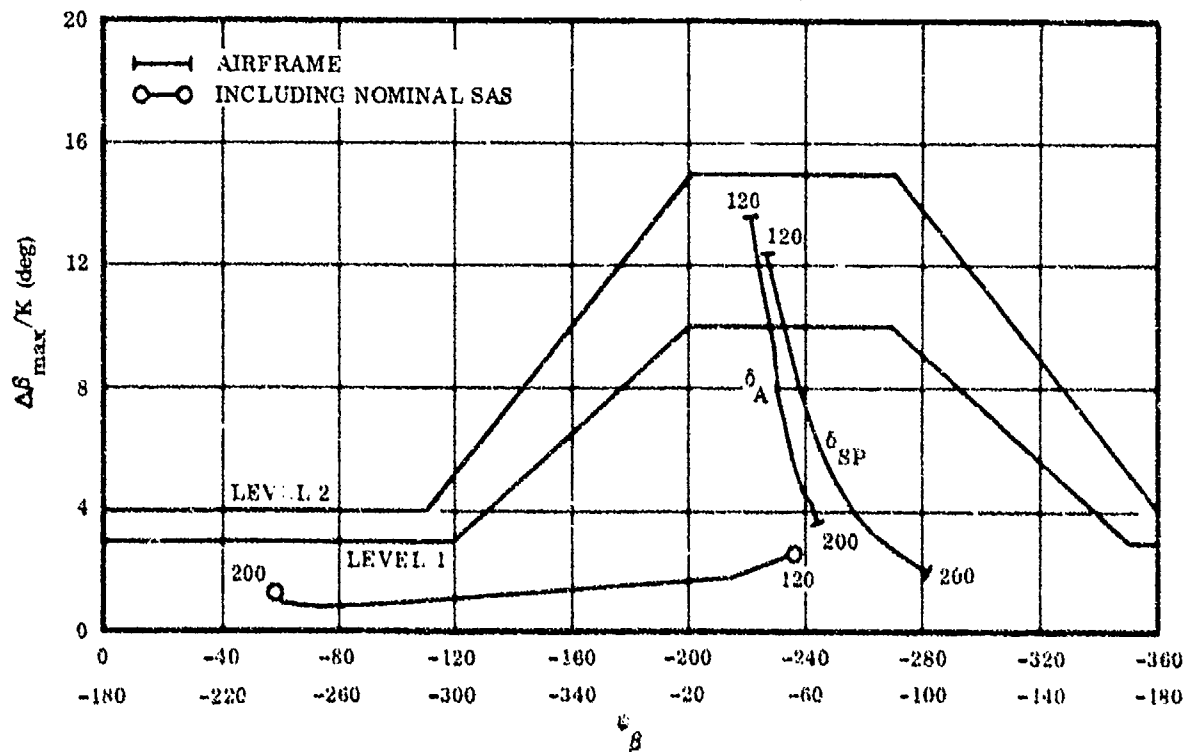


Figure 2-68. IBF Sideslip Excursions, Cruise

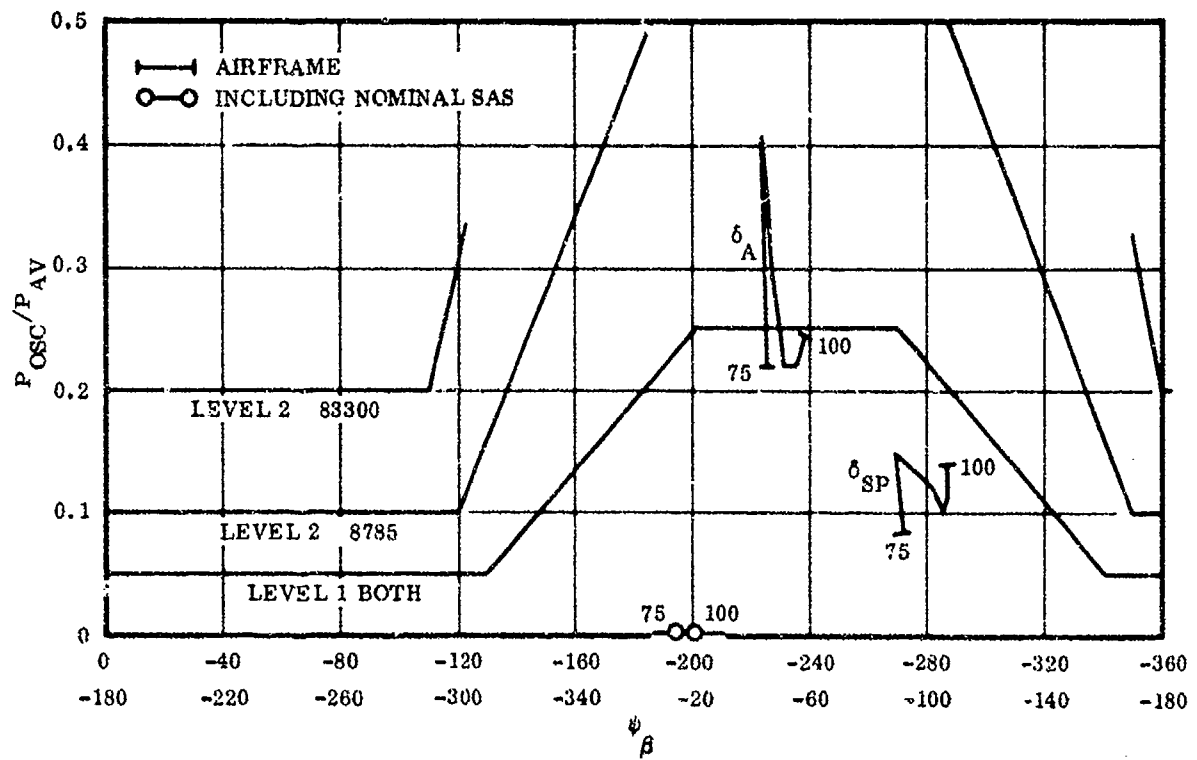


Figure 2-69. VT Roll Oscillations, Landing

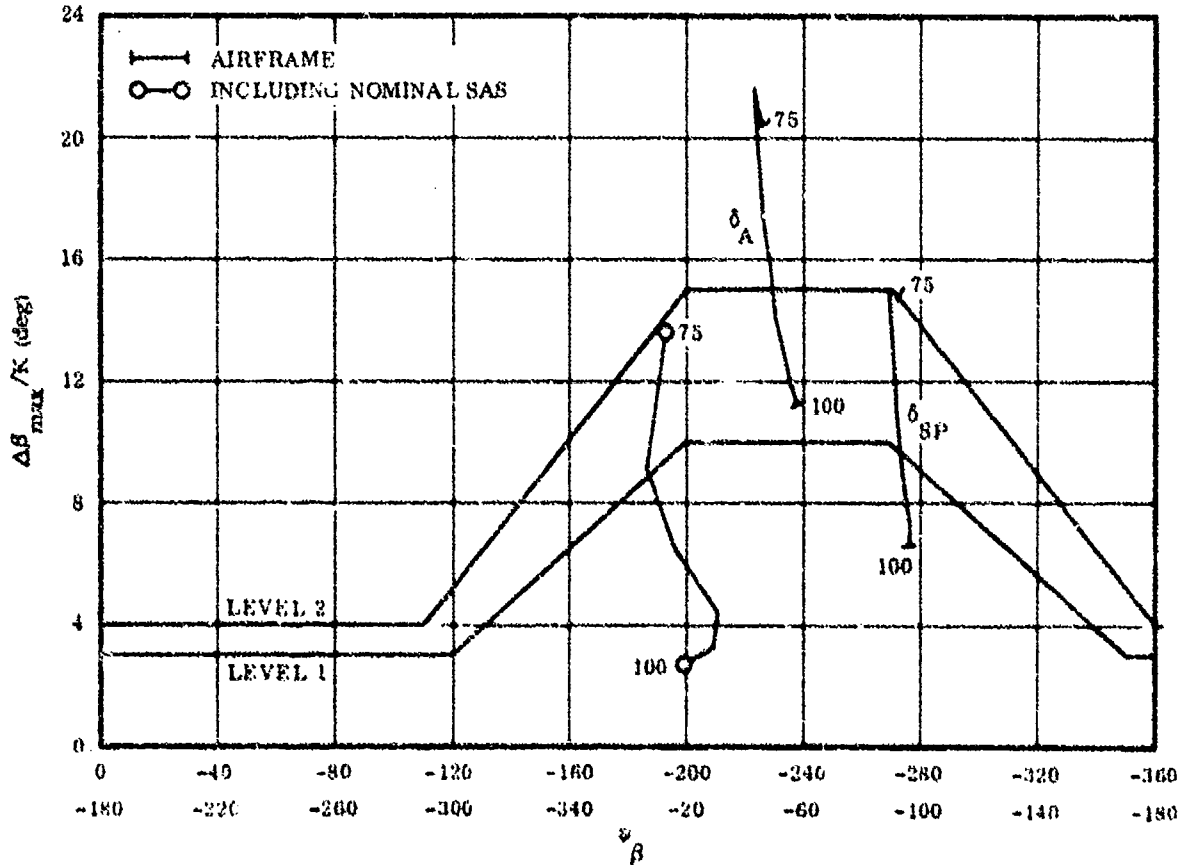


Figure 2-70. VT Sideslip Excursions, Landing

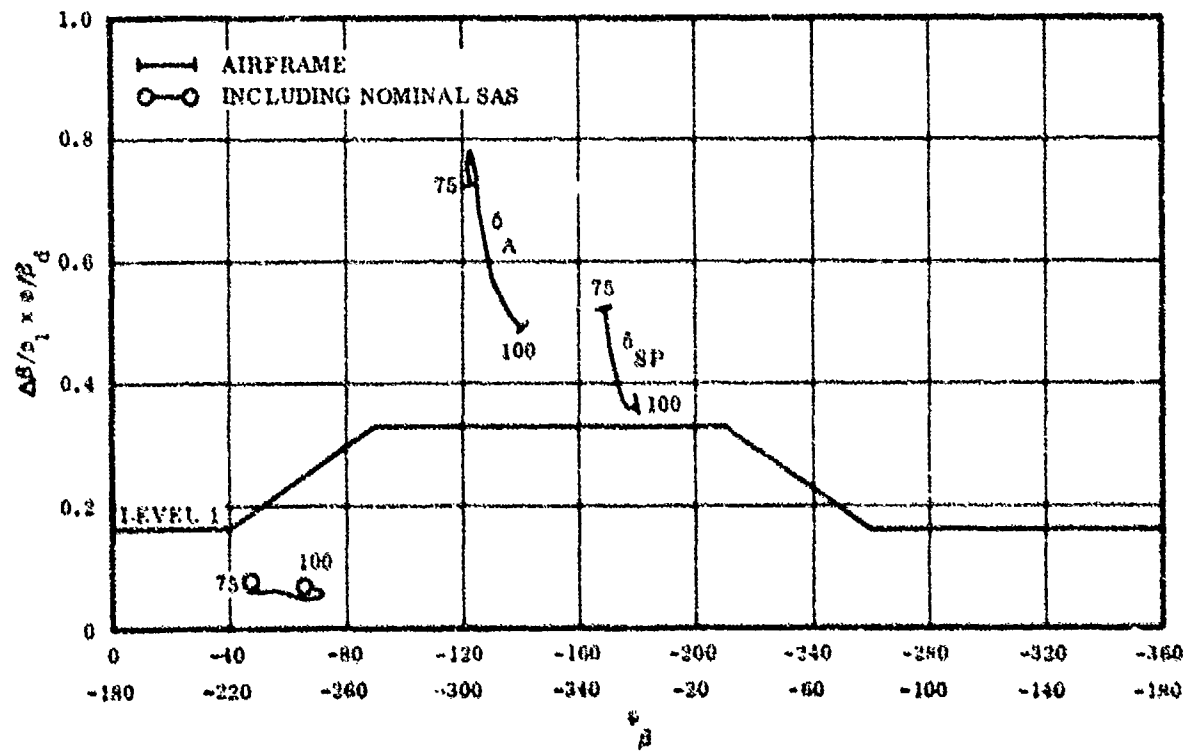
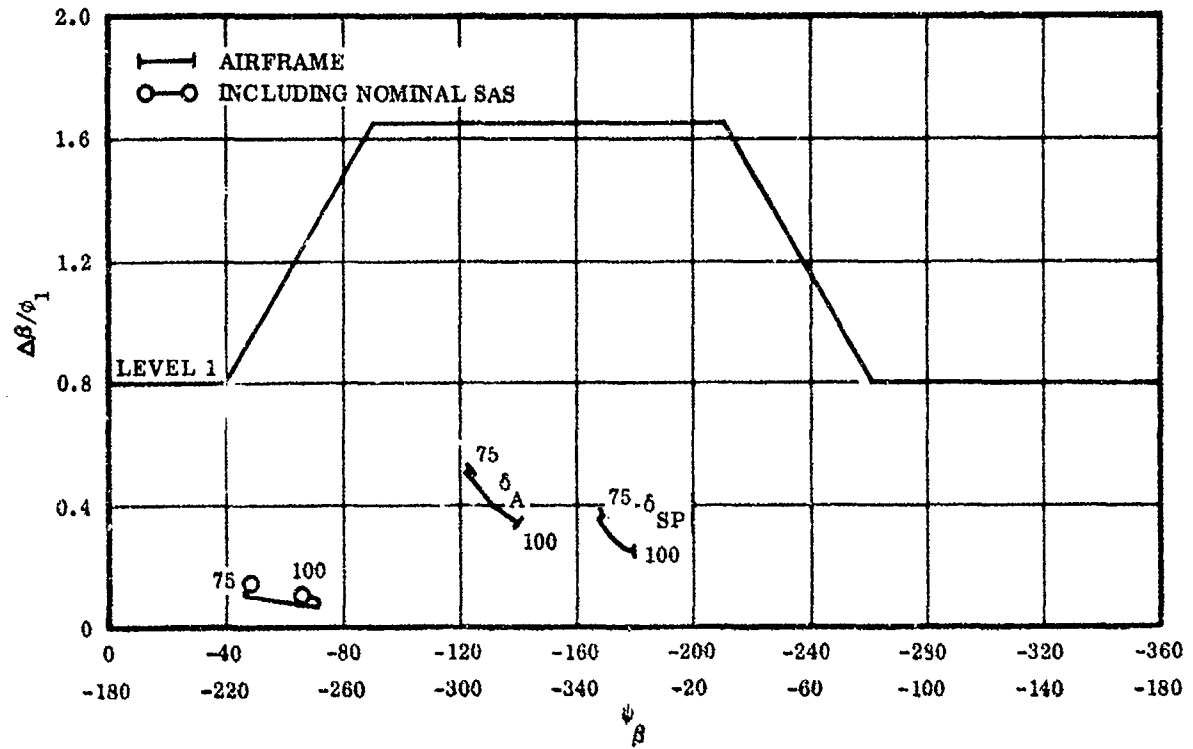


Figure 2-71. VT Sideslip Excursions, Landing, STOL Parameters

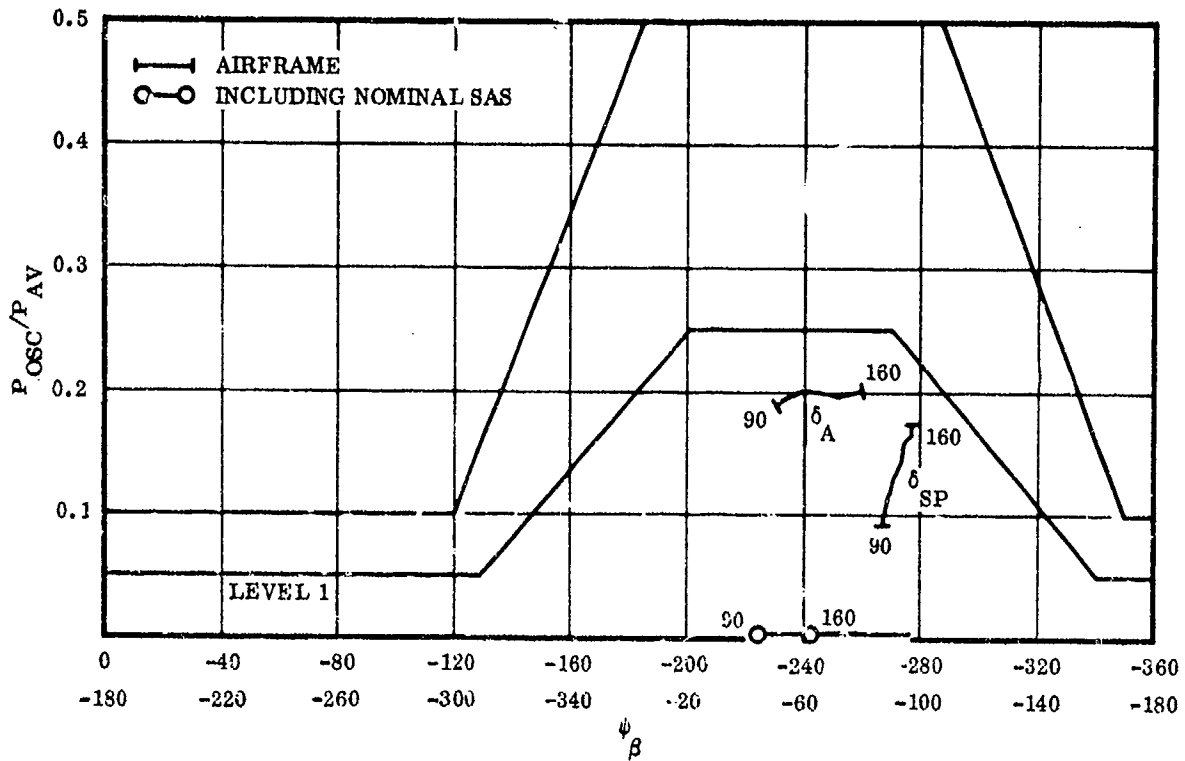


Figure 2-72. VT Roll Oscillations, Takeoff

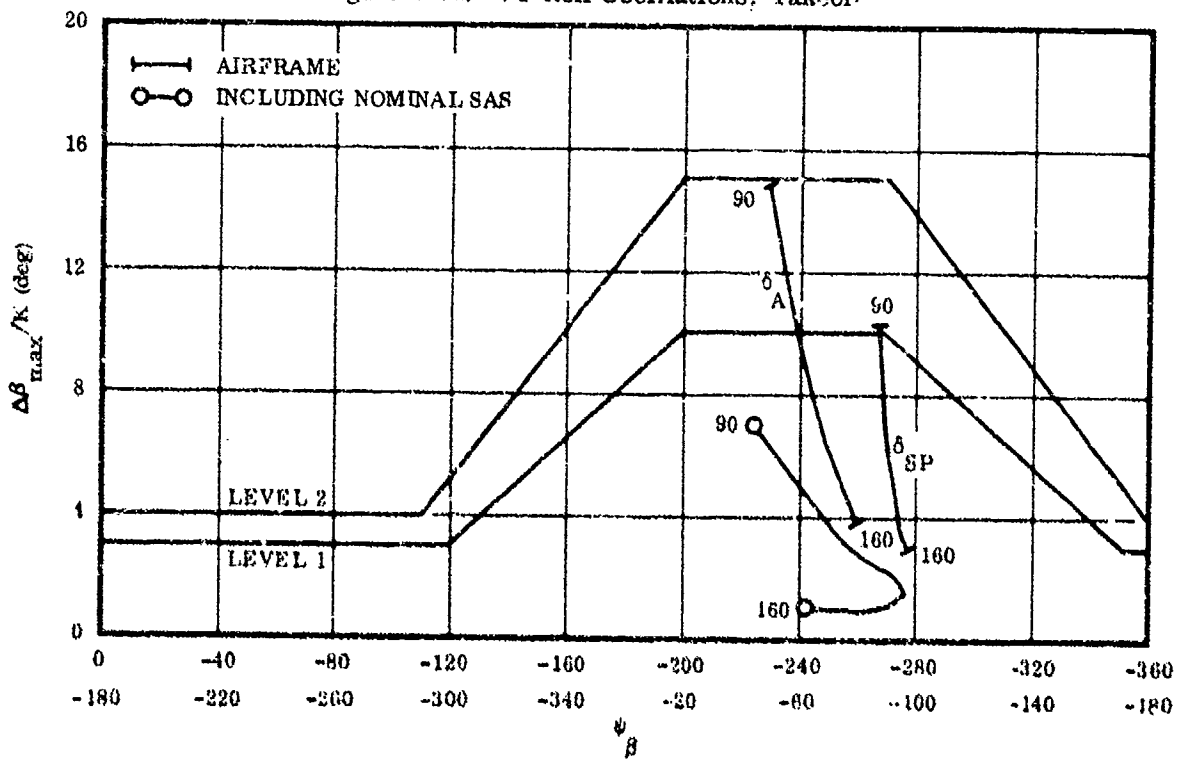


Figure 2-73. VT Sideslip Excursions, Takeoff

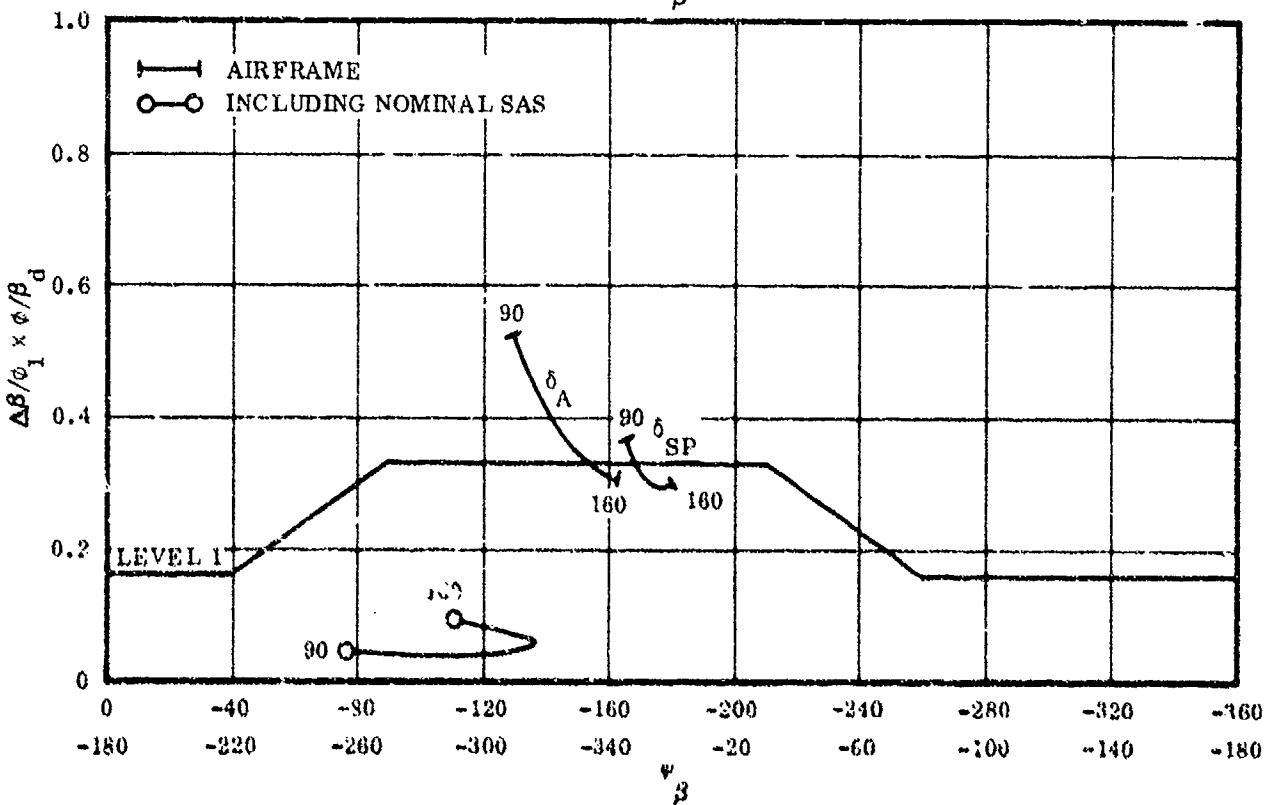
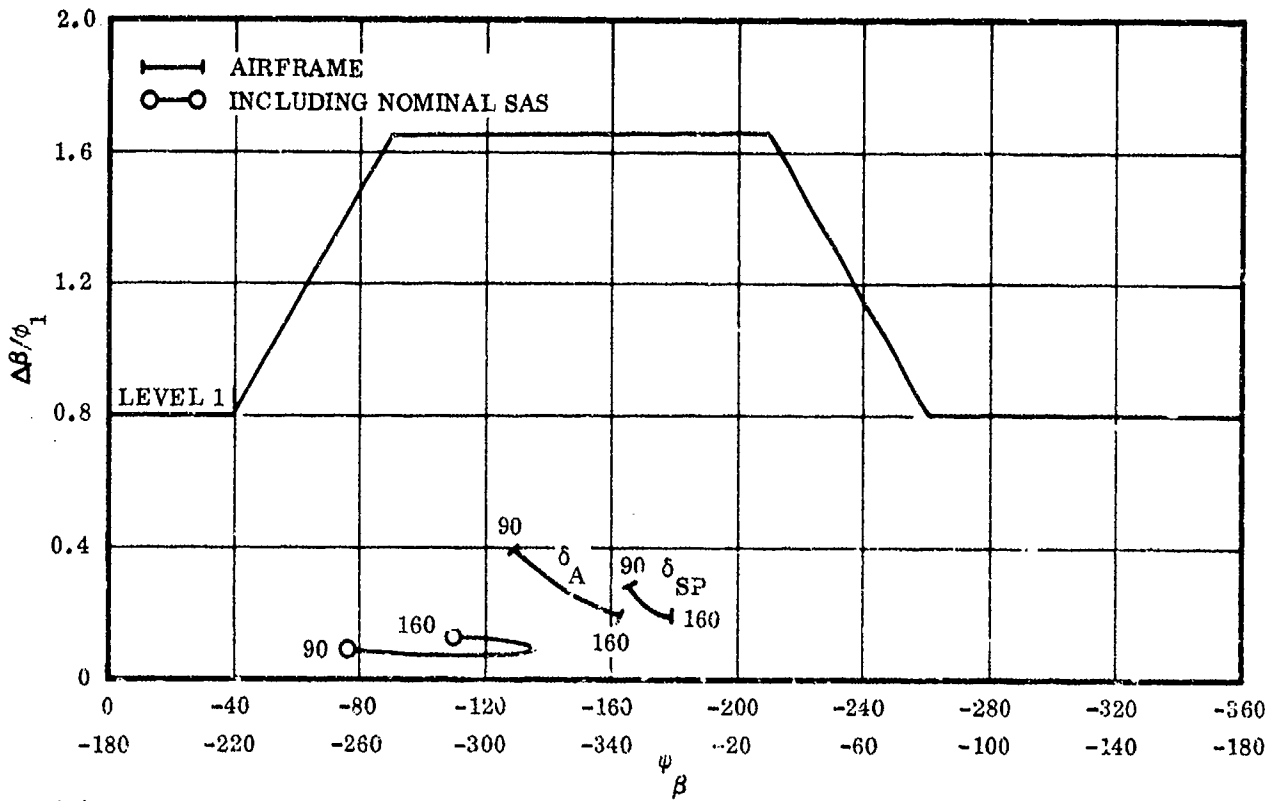


Figure 2-74. VT Sideslip Excursions, Takeoff, STOL Parameters

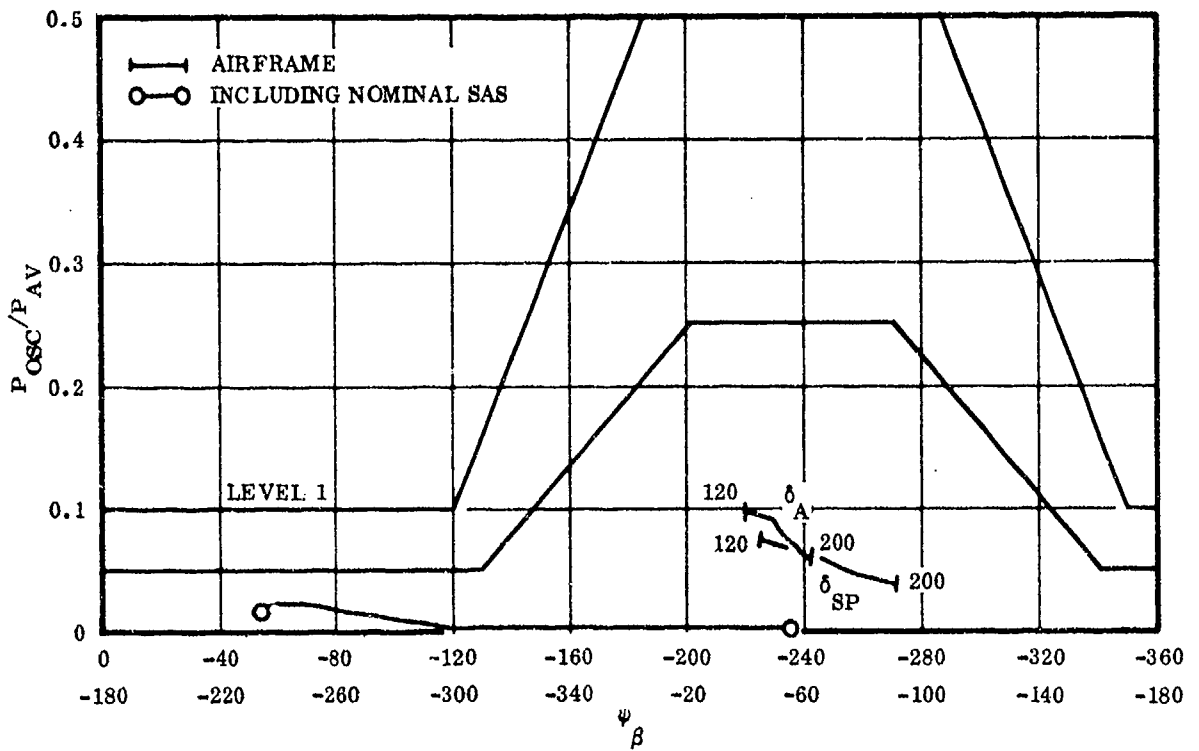


Figure 2-75. VT Roll Oscillations, Cruise

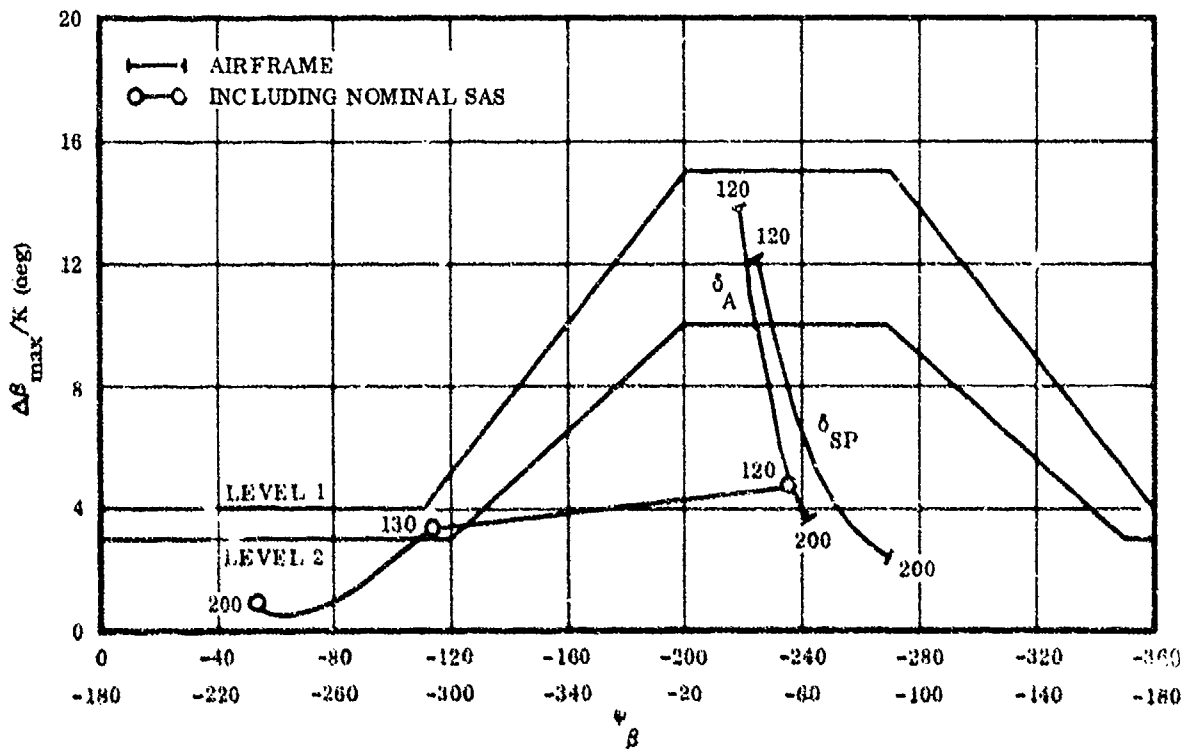


Figure 2-76. VT Sideslip Excursions, Cruise

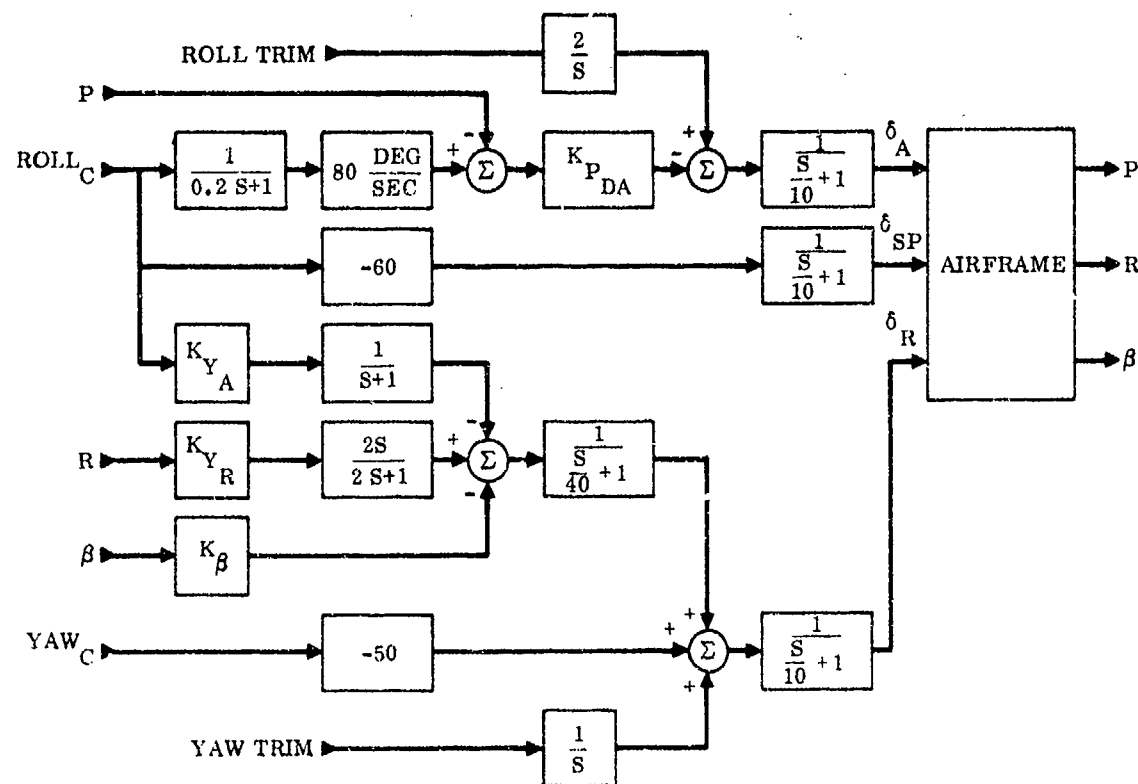


Figure 2-77. Modified Lateral Directional Control System

Deficiencies in the bare airframe responses are primarily in dutch roll, in roll oscillations, and in sideslip excursions. The spiral mode is near neutral stability. Gains and time constants were established by digital analysis, a combination of linearized root locus, and real-time responses. Figure 2-78 shows a locus of the roots of the dutch roll as the set of gains is varied jointly from zero to two times nominal. The nominal gains for this plot are:

$K_{P_{DA}}$	= 10	deg/(deg/sec)	Aileron Input
K_{β}	= 5	deg/deg	} Rudder Inputs
K_R	= 5	deg/(deg/sec)	
K_{YA}	= 200	deg/full lateral stick	

Since K_{YA} is a numerator term, its value does not affect the roots. The data shows the nominal gain to give a well damped, reasonably high frequency response. The spiral mode is hardly changed. The roll mode root ($S = \frac{1}{T}$) is seen to rapidly increase.

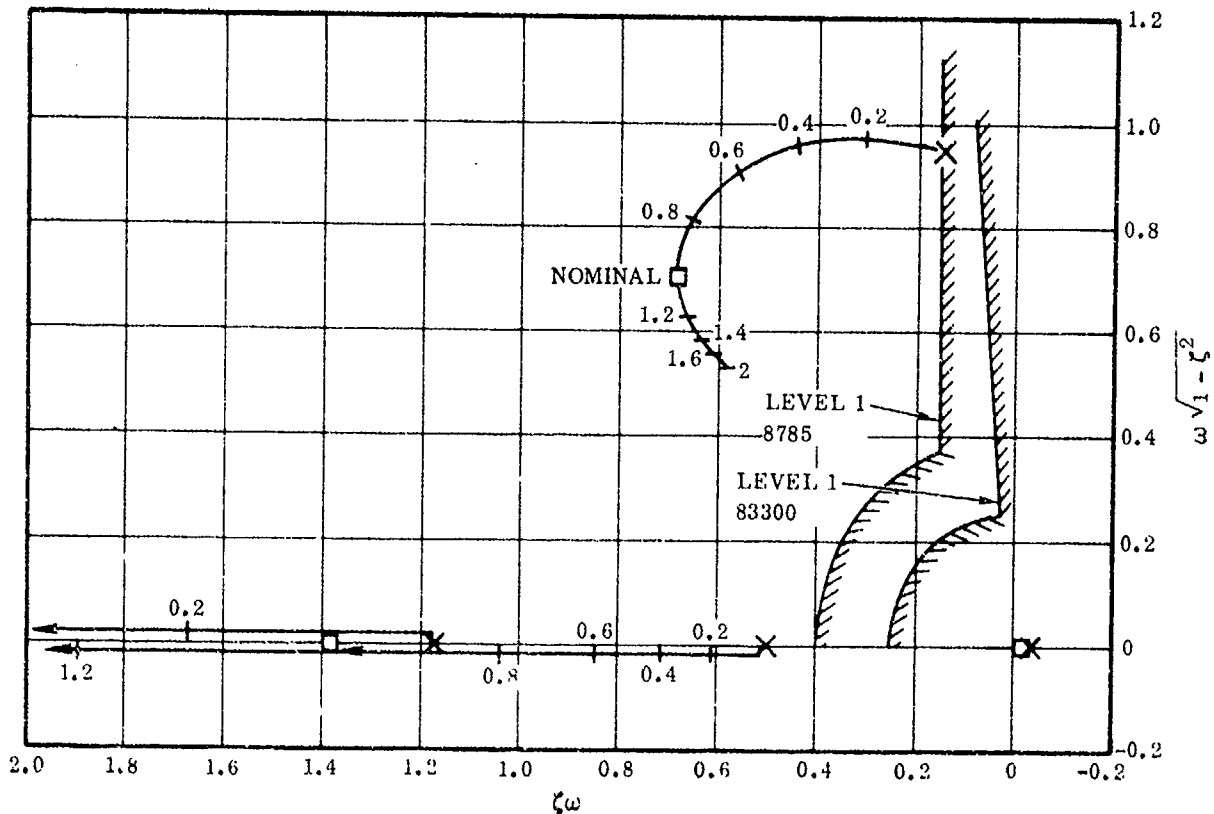


Figure 2-78. EBF Lateral Directional SAS, 80 knots and Landing Flaps

Figures 2-79 and 2-80 show the closed-loop sideslip excursions and roll oscillations. The zero-gain point should coincide with the spoiler bare airframe response, since the spoiler is mechanical and the aileron is all fly-by-wire (aerodynamic summing). The shift is the additional actuator lags accounted for in the closed-loop analysis. Curve A is the simultaneous increase of all four gains, K_R , $K_{P_{DA}}$, K_β , and K_{Y_A} . Curve B is obtained by varying only K_{Y_A} , the roll-to-rudder cross-coupling gain, while keeping the others at nominal. This curve shows that the sideslip excursion parameter is very sensitive to this gain. However, the roll oscillation parameter is so well damped that the variations are all well within the Level 1 boundary.

These nominal gains are assumed to have inverse-q schedules with invariant time constants. These are the conditions for the lateral directional responses labelled SAS in Paragraph 2.6.

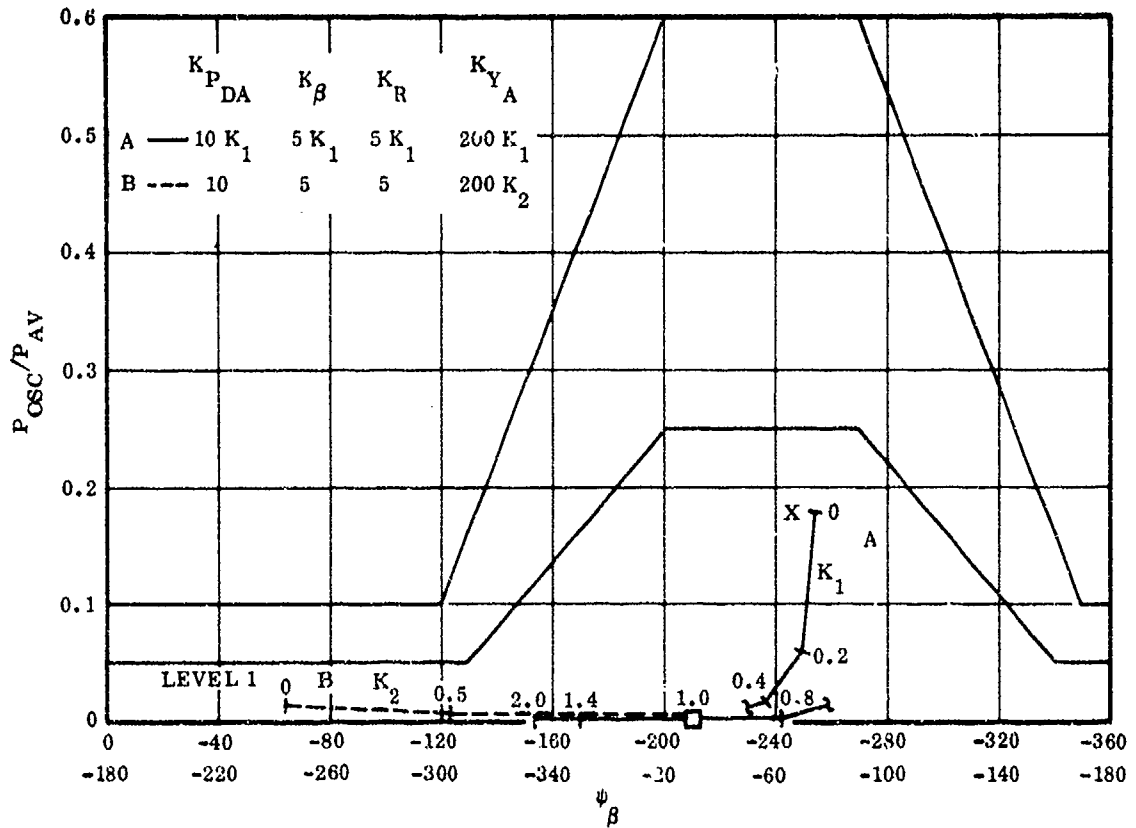


Figure 2-79. EBF Roll Oscillations - Landing Effect of SAS Gains at 80 knots

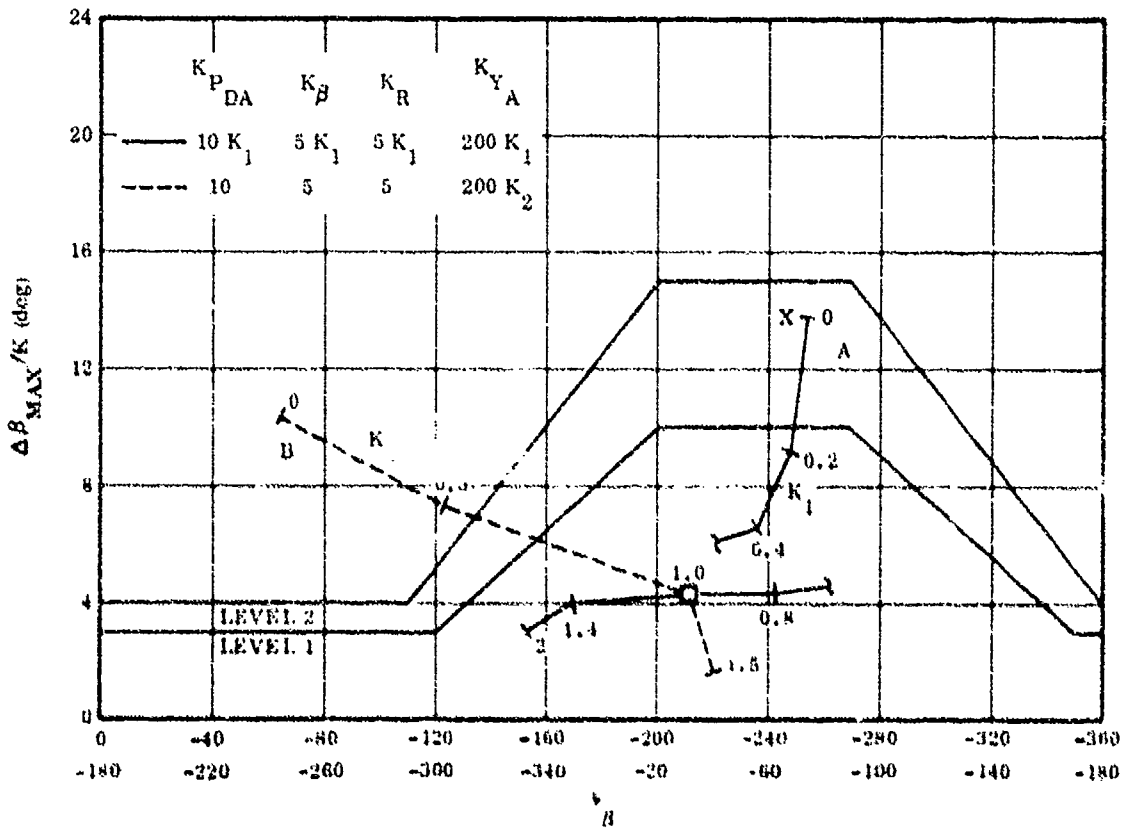


Figure 2-80. EBF Sideslip Excursions - Landing Effect of SAS Gains at 80 knots

SECTION 3

CONTROL SYSTEM MECHANIZATION TRADE STUDIES

The procedure used in the control system mechanization trade studies was to:

1. Examine the baseline system to establish requirements.
2. Modify the baseline mechanization to reflect the benefits of later knowledge.
3. Prepare mechanizations for both a maximum mechanical and a fly-by-wire approach.
4. Review the various mechanizations to establish the selected system.

3.1 FLIGHT PATH CONTROL SYSTEM

The basic features of the flight path control portion of the longitudinal system are an angle-of-attack hold loop, an airspeed hold loop, and flap-to-throttle and throttle-to-flap interconnects.

The original baseline flight path control system as used in the simulation is shown in Figure 3-1. As utilized in this study, there is appreciable dependence on electronic techniques: the angle-of-attack and speed loops both require synchronization, the flap-to-throttle and throttle to-flap interconnects must be disconnected for conventional flight, and there is a variable limiter on the automatic inputs to the throttle. Further, the lead filters on angle of attack and airspeed would almost certainly be electronic. In view of this, the original baseline has been shown as fly-by-wire. The purpose of the variable limiter is to ensure that the pilot can command full throttle even if the automatic systems are trying to reduce power. Its desirability was not specifically investigated on the simulator, although the pilots made no adverse comments. Thus, it has not been firmly established that this device is a requirement for the class of aircraft under investigation. Features such as this which were used on the simulation are taken as requirements for this study.

The first modification to the baseline simulation was to eliminate one of the two servoactuators driving into the flap power actuators. Although either actuator will provide adequate backup for the other in the mechanical summation, the second actuator for trim inputs only and the accompanying mechanical summer are unnecessary.

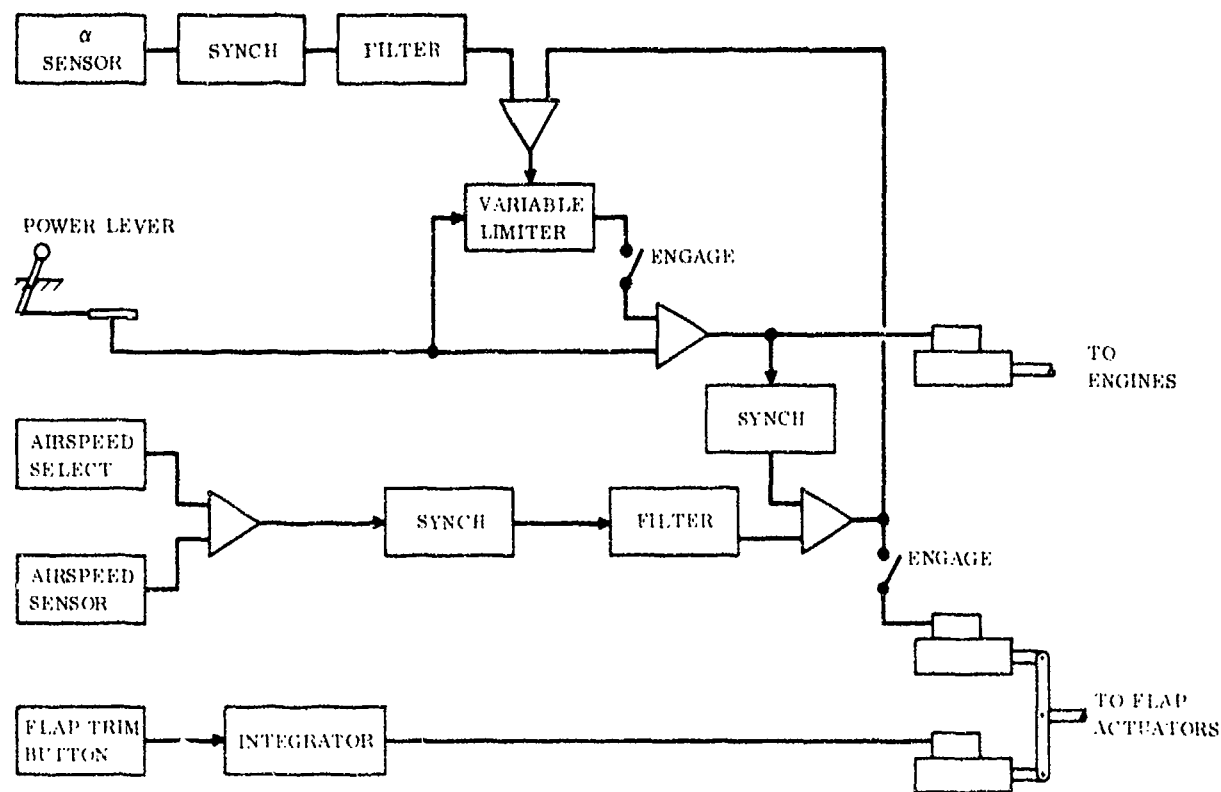


Figure 3-1. Flight Path Control Original Baseline

The second change is a rearrangement of the crossfeeds to eliminate feeding the signal to one flap servoactuator around into the throttle and then back into the same flap servoactuator. The rearrangement shown in Figure 3-2 gives the same transfer function as the baseline configuration, although internal gains will be somewhat different to achieve the same end-to-end gains. An added benefit of the rearrangement is the elimination of one synchronizer.

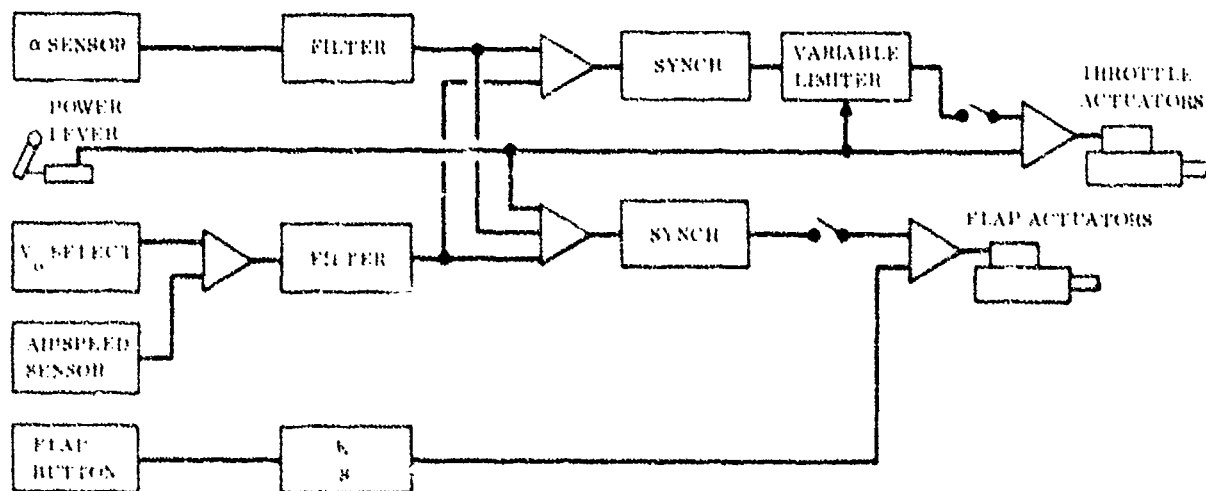


Figure 3-2. Revised Flight Path Baseline

The maximum mechanical version of the flight path control system is shown in Figure 3-3. Mechanical linkage is used from the throttle to the engines and from the

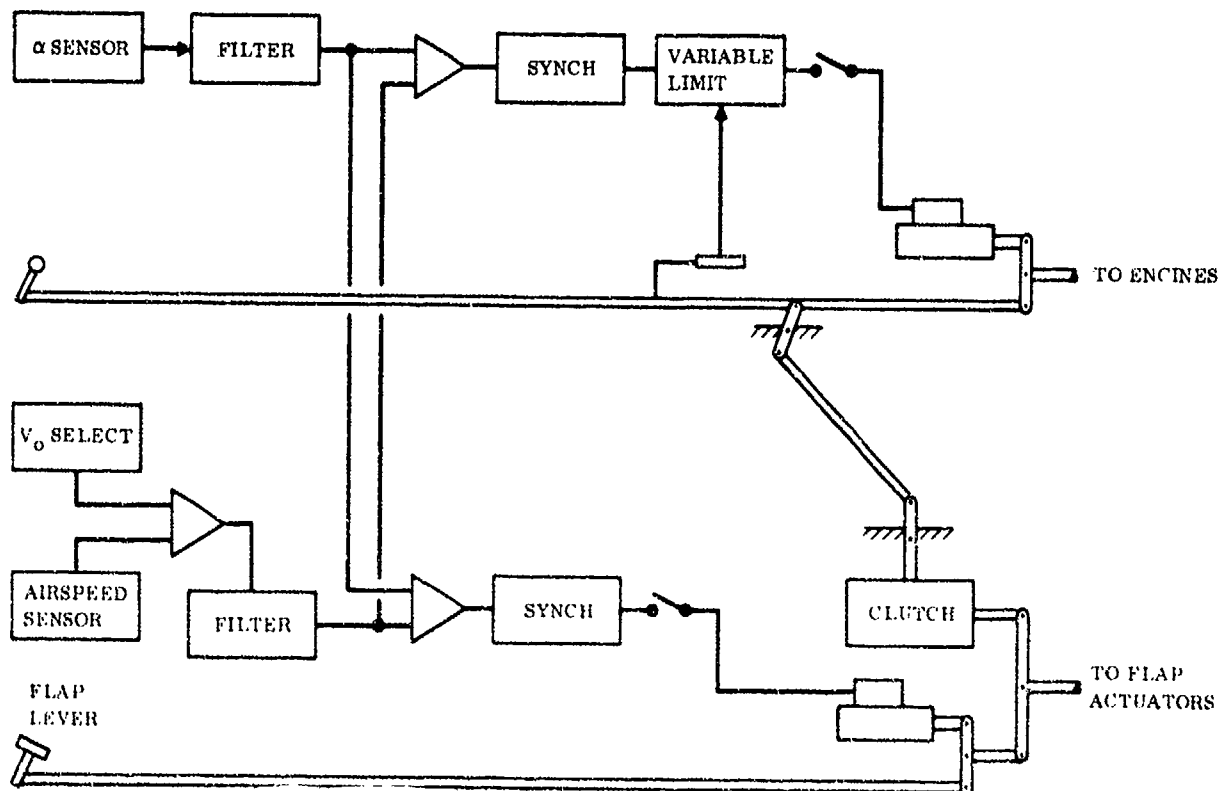


Figure 3-3. Maximum Mechanical Flight Path System

flap lever to the flap actuators. Series-type servoactuators are used to add the automatic inputs to the respective paths. The angle-of-attack and speed loops both use transducers with electrical outputs that must be converted to mechanical motion by the servoactuators. Therefore, electrical crosscoupling is used for the automatic loops since there would be no advantage in having these crosscouplings operative if the rest of the automatic system is inoperative. On the other hand, the interconnect from the power lever to the flaps is useful during STOL approach without the automatic system; use of flaps to adjust longitudinal velocity (u) will produce a disturbance in vertical velocity (w), but this can be controlled by the throttle without appreciable coupling back into u if the throttle-to-flap interconnect is operative. Provision is included to declutch the mechanical interconnect for conventional flight.

3.2 PITCH ATTITUDE SYSTEMS

In addition to the usual requirement for improving short-period damping, the pitch system for the three configurations under consideration must separate, in a frequency sense, the short period and the phugoid behavior. The pitch system, of course, must also provide pitch moment trim capability.

There is still another choice to be made for the maximum mechanical stabilizer mechanization: should the stabilizer actuator be a linear piston and cylinder or a hydraulic motor and screw jack? The appeal of the screw jack is that it can be made irreversible such that there is no drastic trim change in the event of hydraulic failure. However, this feature of irreversibility and the corresponding inefficiency causes objections to screw jacks in that many small motions, such as would result from augmentation system inputs, cause excessive wear. Since the aircraft under consideration is dependent on hydraulics anyway, screw jack irreversibility offers essentially no failure protection but does give increased actuator loads. Everything considered, the piston and cylinder configuration is better for horizontal stabilizer actuation.

Trim inputs could be mechanical, with cables from a wheel at the pilot's station providing a position to one end of a summing beam and a servoactuator from the augmentation system driving the other. This arrangement is not given serious consideration because if the problem of backup for the servoactuator could be solved, both the servoactuator and the input linkage would need excessive authority so they could subtract from each other to provide the required position. In summary, the maximum mechanical stabilizer mechanization consists of a linear power actuator with mechanical feedback, a servoactuator for providing mechanical inputs to the power servo, and an electronic integrator that receives signals from a trim button and the augmentation and provides the electrical input to the servoactuator.

3.2.4 FLY-BY-WIRE. Fly-by-wire mechanization of the pitch control system is shown in Figure 3-6. Because of the existing elements of the augmentation system, the change to the elevator channel block diagram consists only of removing the stick-to-elevator mechanical linkage and the mechanical summer. A change would be required in the dynamic pressure (q) schedule, but this does not change the diagram. Since elevator channel summing is performed electronically, there is no backup problem and the feel and centering elements can be placed near the control column where breakout and friction can be best controlled.

The horizontal stabilizer mechanization of the revised baseline is controlled by electronics and could be classed as fly-by-wire. However, it appears that a more desirable system can be obtained with very little change. As previously stated, a position power servo is preferred because of integration quality considerations. If the stick position signal were added into the stabilizer position command, an independent backup to the elevator would result. Providing full equivalent elevator capability in terms of time constant and surface rate would place excessive requirements on the hydraulic system, but matching time constants and rates would not be required. In the more mechanical diagrams, the automatic elevator channel puts in the desired elevator position and in so doing effectively removes any unwanted mechanically generated pilot inputs. Similarly, in the system of Figure 3-6, if

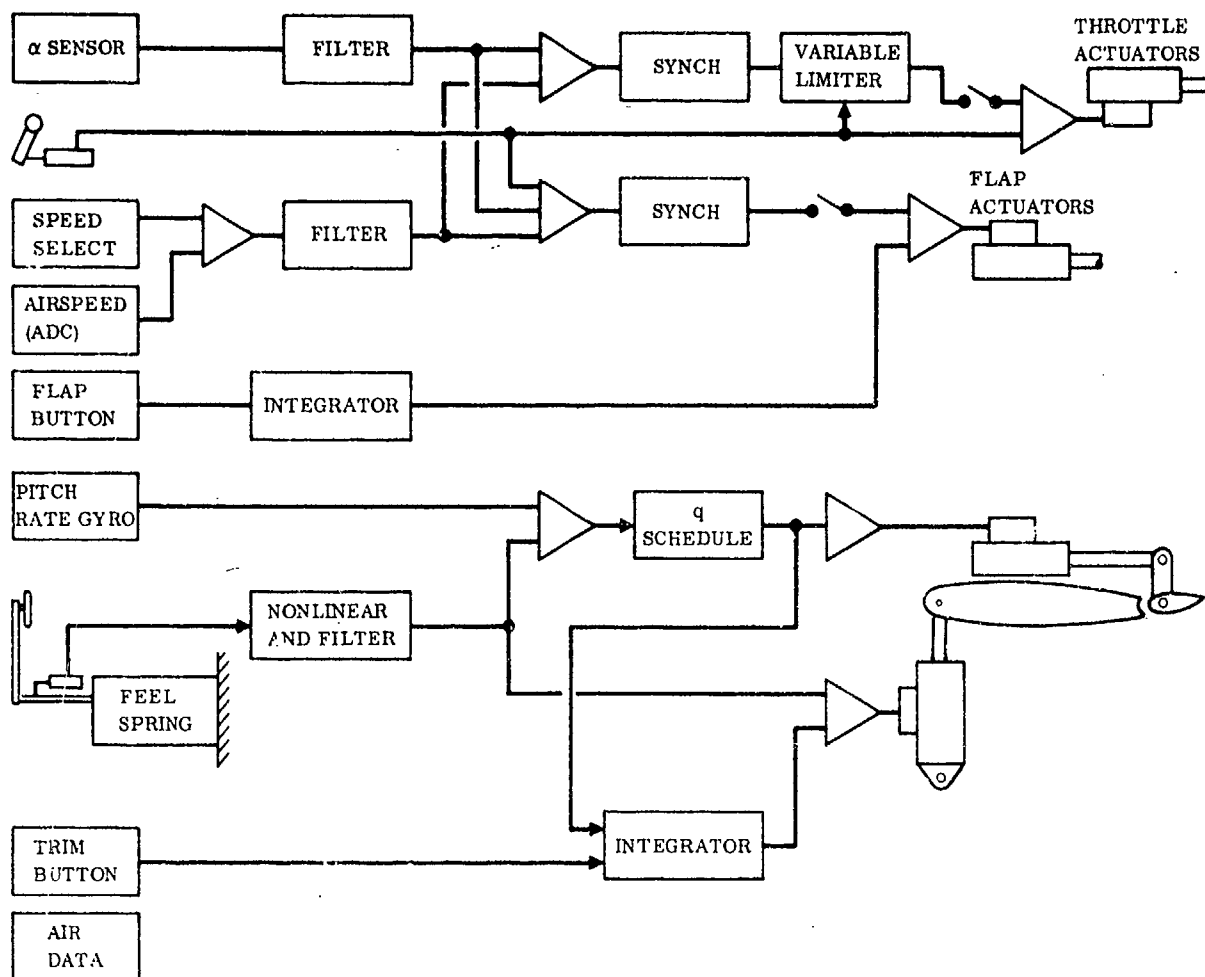


Figure 3-6. Pitch Axis Fly-by-Wire Mechanization

the horizontal stabilizer is at the "wrong" position because of a slow time constant or a rate limit, the automatic elevator channel will make adjustments so that the aircraft pitch response is as commanded by stick position. If the elevator has been disabled by battle damage or other causes, the limited stabilizer rate may limit the short landing capability of the aircraft, but the alternative is an undesirable increase in hydraulic system power during normal operations.

3.3 LATERAL DIRECTIONAL SYSTEM

The lateral system is relatively straightforward, as the basic augmentation requirements are met by the use of either roll attitude or roll rate. As usual, the directional system is more complex and requires a yaw rate gyro, a sideslip sensor, and an aileron/rudder interconnect.

3.3.1 ORIGINAL BASELINE. Figure 3-7 shows the original baseline lateral directional control system. Lateral trim and all lateral automatic functions are carried on the ailerons, with the spoilers an unscheduled function of pilot input.

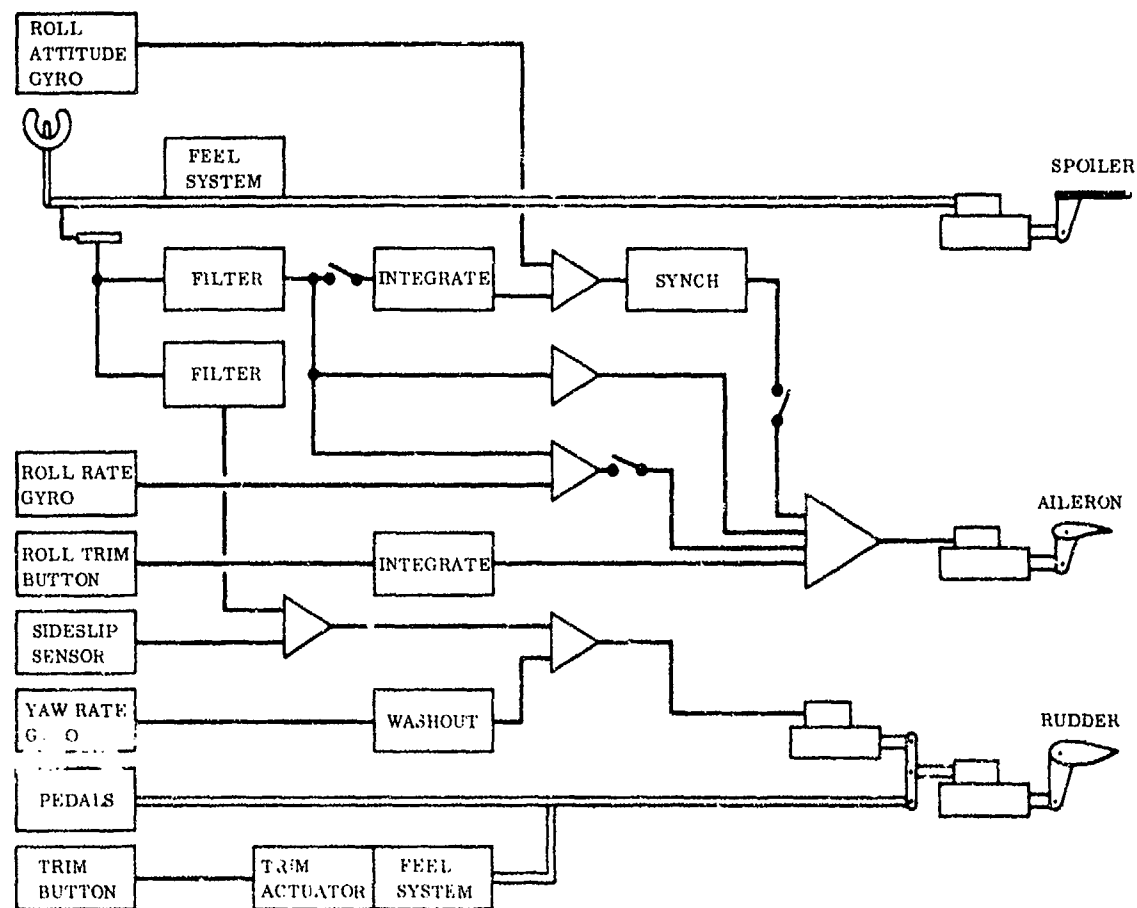


Figure 3-7. Lateral-Directional Original Baseline

Two basic lateral control modes are provided: an attitude-hold mode where roll attitude is summed with integrated wheel position and a simple proportional loop where wheel position is summed with roll rate to provide an aileron command. Aileron trim is carried on an electronic integrator, the ailerons are fly-by-wire, and the spoilers are all mechanical input.

The directional system has the rudder pedals mechanically summed with the output of a servoactuator to provide the input to the rudder power servo. Inputs to the servoactuator are control wheel position and sideslip for turn coordination and washed-out yaw rate for damping. To avoid a second mechanical summation, rudder trim is provided by driving the pedal feel and centering mechanism with a trim actuator.

3.3.2 REVISED LATERAL-DIRECTIONAL BASELINE. The integrator arrangement used in the simulation worked well on the digital computer used for the simulation, but a diagram change is required to obtain a mechanizable system. The problem is that in the "attitude" mode, the wheel integrator and the trim integrator are independent and a situation could arise where both were carrying very large signals

that subtract to give the desired aileron command. However, one would eventually saturate and a loss of aileron control could result. This problem is eliminated during the general rearrangement as discussed in the following paragraphs.

The revised lateral directional baseline is shown in Figure 3-8. As for the pitch axis, the attitude gyro is replaced with a rate gyro and the pilot input integrator that provided the rate command is incorporated into the trim integrator. There is a rate gyro available for the roll control system, however, so an instrument is eliminated rather than replaced. The revised system provides the same steady-state transfer function as the original, but the roll-attitude-to-aileron transfer function has more transient lead. If this additional lead proves undesirable, it can be readily compensated by a lag filter after the roll-rate gyro. Once again, although the diagram of Figure 3-3 contains fewer elements and interconnections than Figure 3-7, the dynamics and steady-state performance can be made identical.

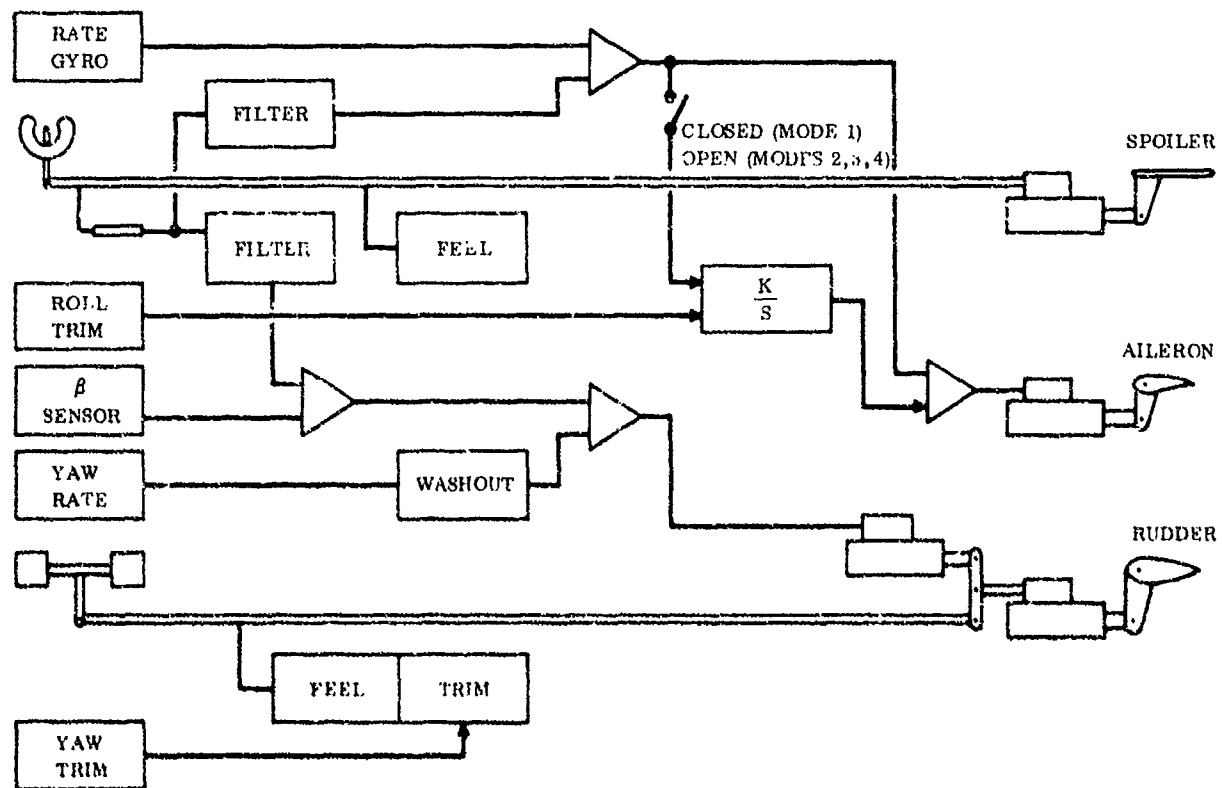


Figure 3-8. Lateral Directional Revised Baseline

3.3.3 MAXIMUM MECHANICAL. The maximum mechanical mechanization of the roll control system is shown in Figure 3-9. With the possible exception of a mechanical aileron rudder interconnect, the revised baseline directional system is already maximum mechanical and the yaw portion of the diagram has not been repeated. The mechanical connection from wheel to aileron will require at least one mechanical summing mechanism so that automatic signals can be combined with

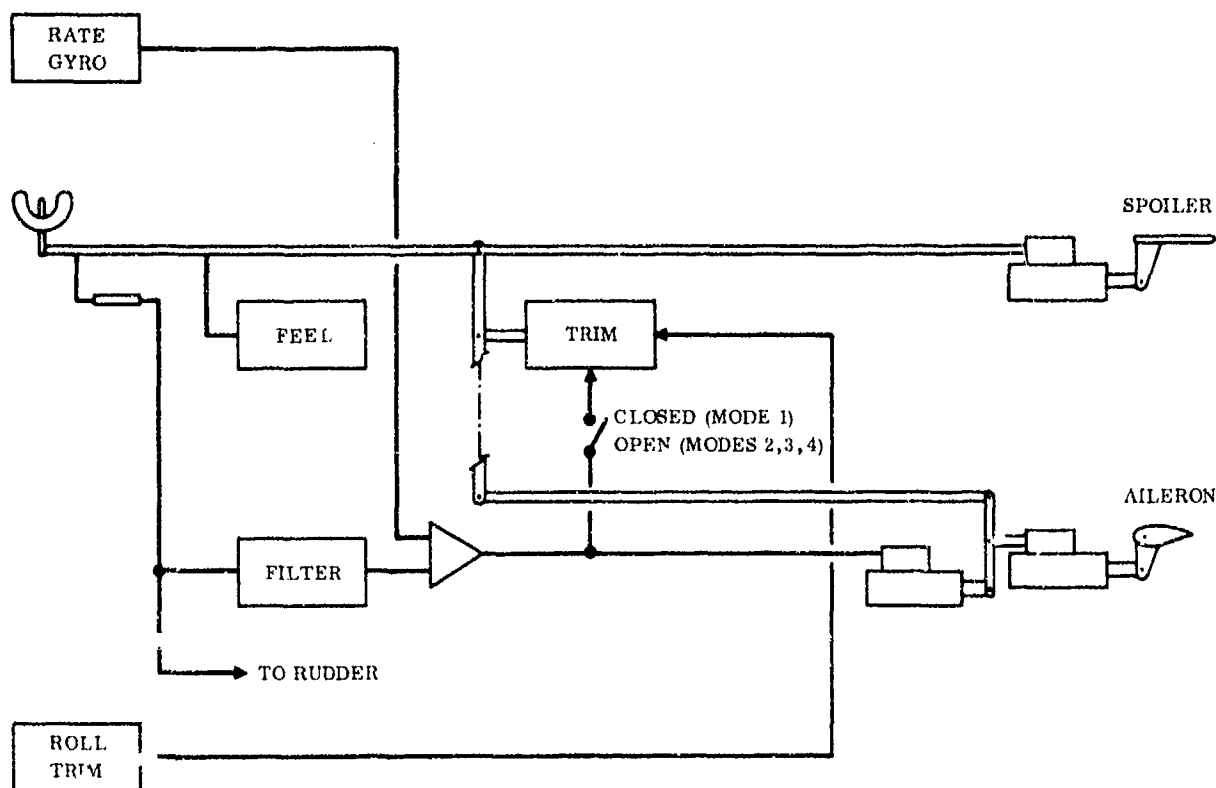


Figure 3-9. Roll Axis Mechanical Mechanization

the pilot's input. There are actually two options available for the trim input: a separate trim actuator could be used (which would require another summing mechanism) or the trim signal could be put into the system via the servoactuator. Using the servoactuator would give a "cleaner" system with only one summation, but the actuator must have relatively large authority so as to carry both trim and automatic inputs. The separate trim actuator and the second summing point have been shown, since this approach is generally more compatible with the mechanical philosophy of using a limited-authority, high-response actuator for the damper signals and a limited-rate, high-authority actuator for trim. The aileron/rudder interconnect is electrical, since all required elements would be present even if the mechanical interconnect was used. Further, the interconnect rudder authority requirements are such that the rudder servoactuator authority is not changed appreciably.

3.3.4 FLY-BY-WIRE. The fly-by-wire mechanization of the lateral directional system is shown in Figure 3-10. There is an option as to just how the spoilers are used. In the baseline systems, the spoilers received pilot inputs only and all automatic signals went to the ailerons. If the spoilers are to be controlled electronically, however, there is little or no additional complication in also using them for the non-trim portion of the automatic signals. Roll trim is not carried on the spoilers because of drag considerations. By choosing to use the spoilers as part of the automatic system, enhanced roll control can be maintained even if the ailerons are

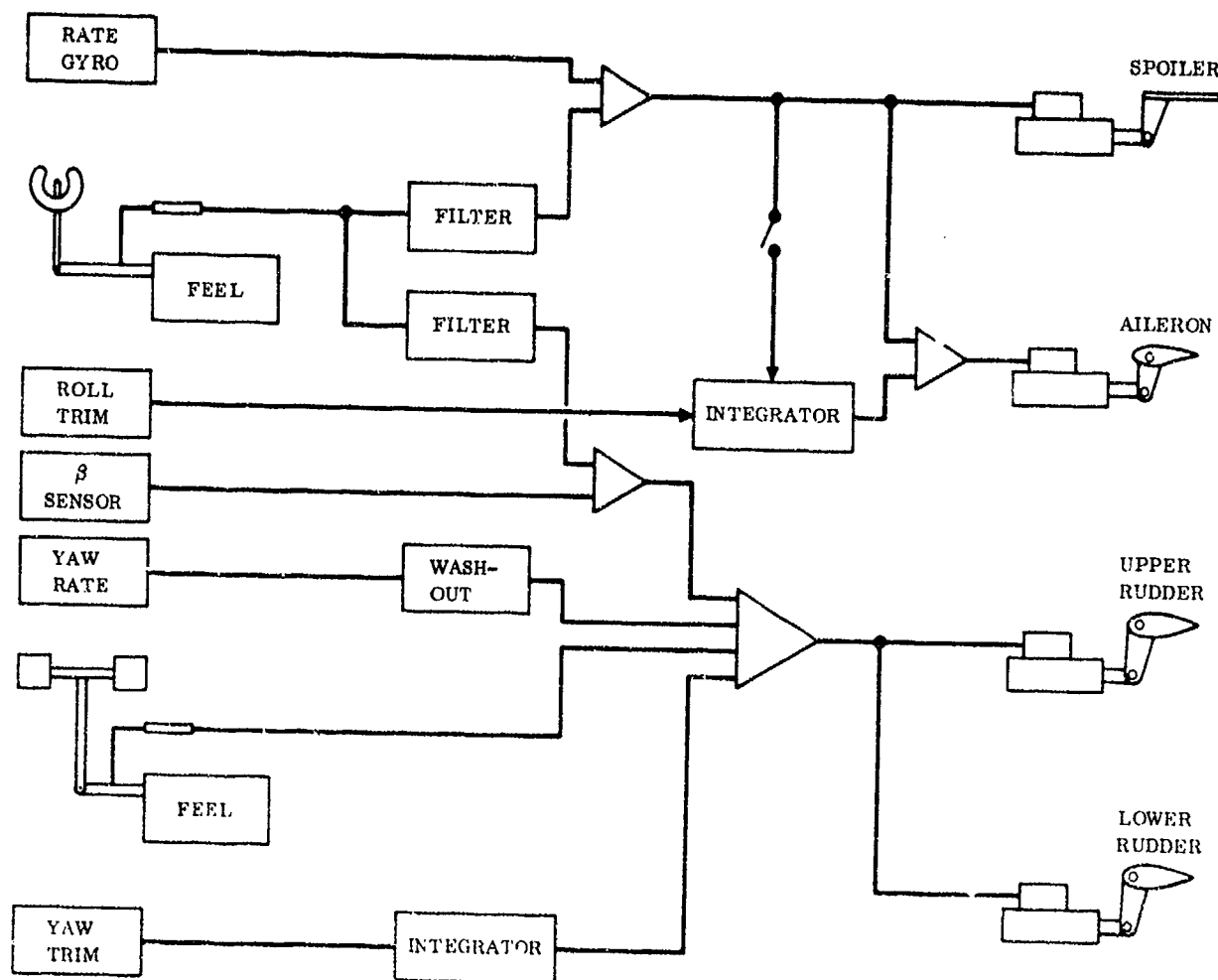


Figure 3-10. Lateral-Directional Fly-by-Wire Mechanization

disabled by battle damage. Of course, the pilot would have to exert a constant force on the wheel to hold trim, but this would be a relatively minor increased pilot workload following a failure.

In reviewing the control surface backup capabilities of the fly-by-wire mechanizations, the rudder is the only surface that does not have an alternative to provide control in the event of battle damage. (Either the elevator or the horizontal stabilizer can be used for pitch control and either spoiler or aileron can provide roll control.) To eliminate this shortcoming in the directional axis, a split rudder with separate power servos for each section was chosen. Severe damage to one of the rudder sections could, of course, limit short or high-crosswind landings but the aircraft could still be flown to a larger field and landed safely.

3.4 SYSTEM SELECTION

Selecting a specific system frequently involves at least a moderate amount of emotion and prejudice. However, an attempt at a rational appraisal of the relative merits of the more mechanical versus fly-by-wire mechanizations is presented in the following paragraphs.

3.4.1 MECHANICAL VERSUS FLY-BY-WIRE COMPARISON. The first point considered is in favor of the mechanical approach: the aircraft can be controlled without electronic augmentation. A statically unstable aircraft as found in some control configured vehicle (CCV) designs has not been used here and the few undesirable aircraft characteristics are slow enough to be controlled by the pilot. As compared to the conventional aircraft control system, however, more extensive modification of bare airframe handling qualities is required.

Reviewing the mechanizations indicates that either approach will work reasonably well with proper design. Accepting the fact that augmentation and the interconnects are required, the only basic problem appears to be that of providing adequate force reaction for the servoactuators in the summing mechanisms of the mechanical implementation. Although not previously discussed, using the horizontal stabilizer as a position control to provide backup for elevator damage can be incorporated mechanically, but not quite so cleanly as in the fly-by-wire approach. This, coupled with a split rudder, can give a mechanical system with backup for all maneuvering control surfaces. If having the automatic signals on the spoilers in the event of aileron damage is desired, the mechanical approach could provide this capability by adding a summing linkage and a servoactuator to the spoiler linkage. In view of these considerations, it is concluded that there are no overriding considerations to dictate that the control system must be either fly-by-wire or mechanical with fairly extensive augmentation.

3.4.2 RECOMMENDED SYSTEM. Since extensive augmentation is necessary to achieve the required handling qualities, much of a fly-by-wire system is correspondingly required. Further, the basic short field mission of the aircraft would be compromised by failure of all or part of the augmentation system, so it is reasonable to assume that the augmentation system will have enough redundancy to approach a fly-by-wire system in reliability. The more mechanical version would already contain appreciable fly-by-wire features to achieve the required augmentation and decoupling. The full fly-by-wire system is chosen as the recommended system primarily on this consideration. There are many side benefits, such as eliminating the mechanical summing mechanisms and placing the feel system close to the pilot's control without attaching appreciable linkage to compromise desirable centering and friction characteristics.

Mechanization using the mechanical linkages should not be discounted entirely. Direct mechanical connections between the pilot's controls and the power serves, coupled with limited-authority servoactuators, places the pilot in maximum command of emergency situations and the adaptable human operator has often demonstrated a unique ability to cope with these situations. Thus, fly-by-wire is recommended, but the more mechanical approach is a close second and should be given full consideration in future configurations.

SECTION 4

FLIGHT SIMULATION

Flight simulations were conducted using both fixed-base and moving-base simulation facilities to permit pilot evaluation of flight control performance and general handling qualities of the three STOL transport configurations; i. e., externally blown flap (EBF), internally blown flap (IBF), and vectored thrust (VT). Approximately 120 simulated flight hours were accumulated at the fixed-base facility with the following distribution among the three configurations:

EBF	80 hours	(These are not simulator facility occupancy
IBF	20 hours	hours but are the cumulative simulated flight
VT	20 hours	times for productive evaluation runs.)

Moving-base simulation studies, which followed the fixed-base studies, were confined to the EBF configuration. Approximately 30 hours of productive moving-base evaluation were accomplished. In all, well over 3000 data runs were flown.

The results of simulated flight evaluations and conclusions derived therefrom are presented in this report. Also included are detailed descriptions of the flight simulation implementation, hardware, evaluation tasks and procedures, and pertinent data samples. General objectives of the flight simulation tasks were to:

1. Evaluate flight control performance and general handling qualities of the alternative STOL configurations for terminal flight phase operations.
2. Modify the design and/or control scheme as required to provide a level of STOL flight control performance and handling qualities for which pilot evaluations can be made using Cooper/Harper rating techniques.
3. Evaluate alternative flight control techniques for accomplishing flight path control during the applicable subcategories of STOL flight associated with the terminal flight phase. Determine the most effective techniques.
4. Evaluate overall control design and assess the suitability of the flight control scheme to provide acceptable handling quality ratings for STOL flight under operational conditions. This is to include adverse environmental conditions, critical system failures (e. g., engine out), and evaluation of off-nominal flight maneuvers.

5. Conduct flight simulations using both fixed-base and moving-base simulator cockpits to determine the significance of moving-base flight simulation on pilot evaluations obtained in a fixed-base simulator.

4.1 FLIGHT SIMULATORS

The two simulator facilities are described in this section. General implementation of the STOL transport flight simulator at both the fixed-base simulator (FBS) and the moving-base simulator (MBS) consisted of a hybrid (digital plus analog computers) representation of the aircraft, its subsystems, flight geometry, visual scene, atmospheric effect, etc. Program software differences necessitated by computer equipment limitations at the MBS facility are discussed in a later section.

4.1.1 FIXED-BASE SIMULATOR. The fixed-base simulator was developed using equipment available at the Convair Aerospace Hybrid Simulation Laboratory in San Diego. Characteristics of this simulator are described in the following sections.

4.1.1.1 Physical Characteristics. An existing cockpit was modified extensively to provide a baseline STOL cockpit configuration. A single pilot station was devised representing one-half of a STOL transport cockpit. The control arrangement provided a center-stick for pitch and roll inputs (with conventional trim button), standard rudder pedals with rudder trim, and a single throttle at the left console for propulsion control. The force-deflection characteristics of the center-stick and pedals were provided by simple spring assemblies. Nominal linear gradients established were:

Stick Gradient (Pitch)	4.3 lbf/in.
Stick Gradient (Roll)	3.7 lbf/in.
Pedal Gradient (Yaw)	40.0 lbf/in.

The pilot's seat and flight controls were arranged in general accordance with Military Standard MS33574, Dimensions, Basic, Cockpit, Stick Controlled, Fixed Wing Aircraft. The seat/instrument panel relation was designed to provide the pilot with a nominal look-down angle of 25 degrees (as in a helicopter) to accommodate the steeper descent angles expected for STOL approaches. At the left console, switches were provided for selection of control augmentation modes, computer control, data control options, and engine failure initiation. General cockpit arrangement is shown in Figures 4-1 through 4-3.

A half-cockpit instrument panel was constructed using state-of-the-art flight instruments in a rather conventional T-pattern. An attitude deviation indicator (ADI) and compass were centered in line with the pilot's seat, flanked by an airspeed indicator and an altimeter. The airspeed indicator used was an older version because it provided better airspeed resolution (3.6 degrees of dial angle per knot). A rate-of-climb indicator was rescaled to provide vertical velocity information. It and an



Figure 4-1. STOL Simulator Cockpit

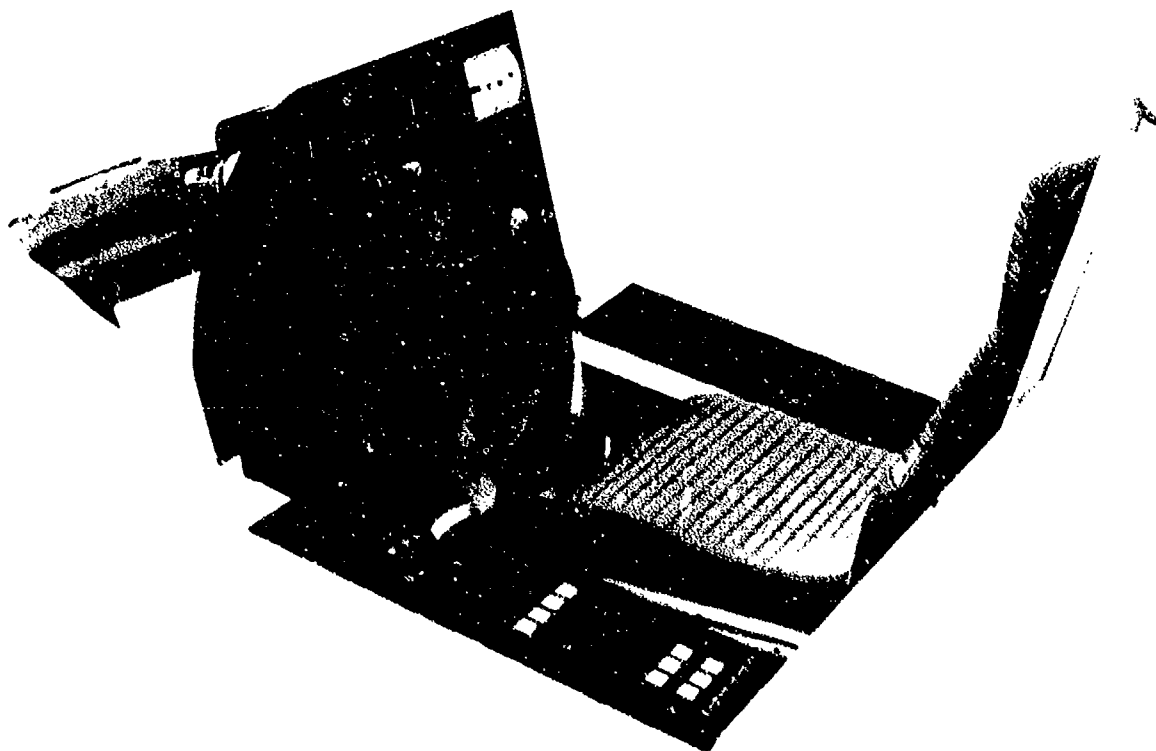


Figure 4-2. Close-up of Simulator Cockpit

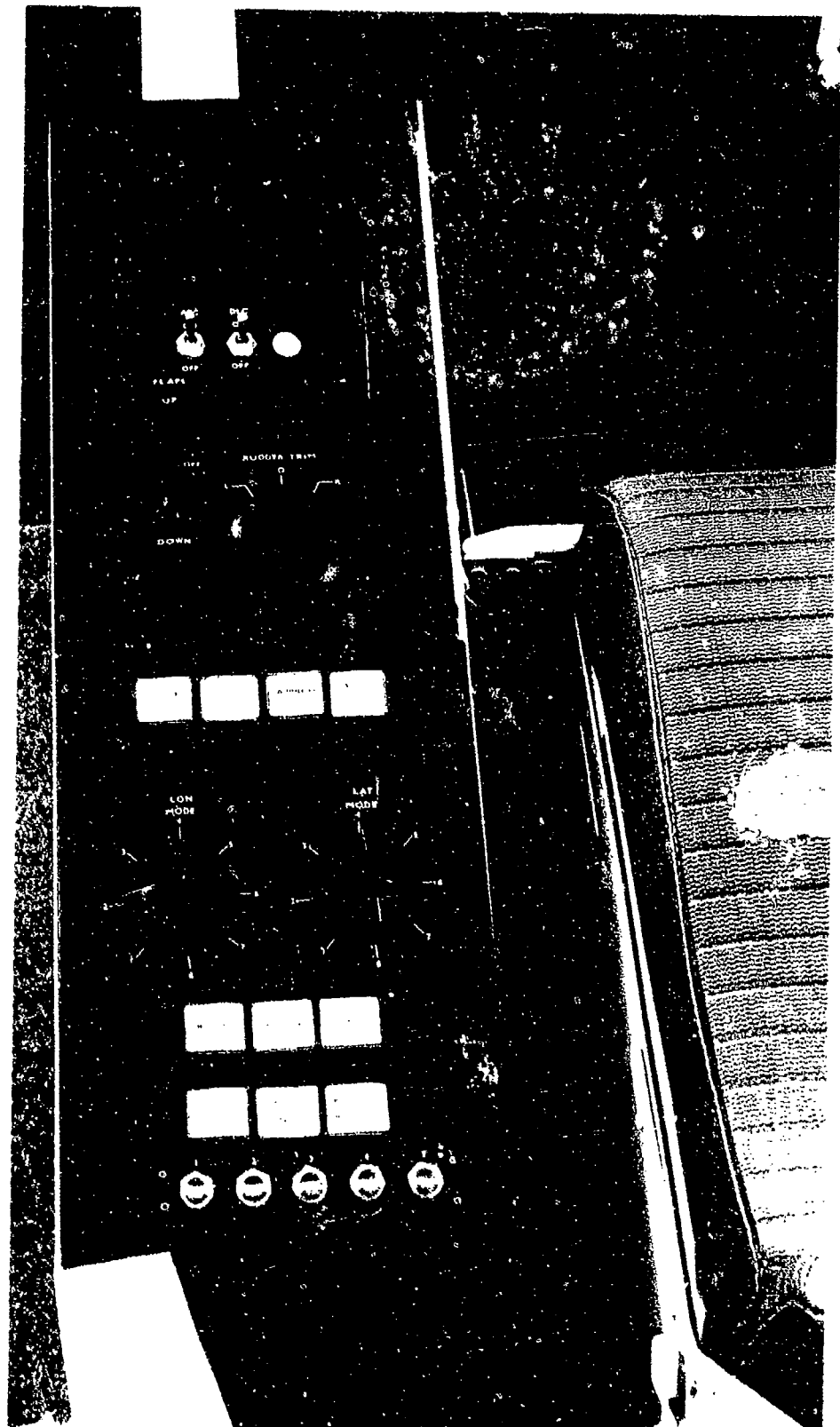


Figure 4-3. Left Hand Console Layout

angle-of-attack indicator were placed to the sides of the compass location. Figure 4-4 shows the flight instrument panel layout before the ADI was replaced by a more modern

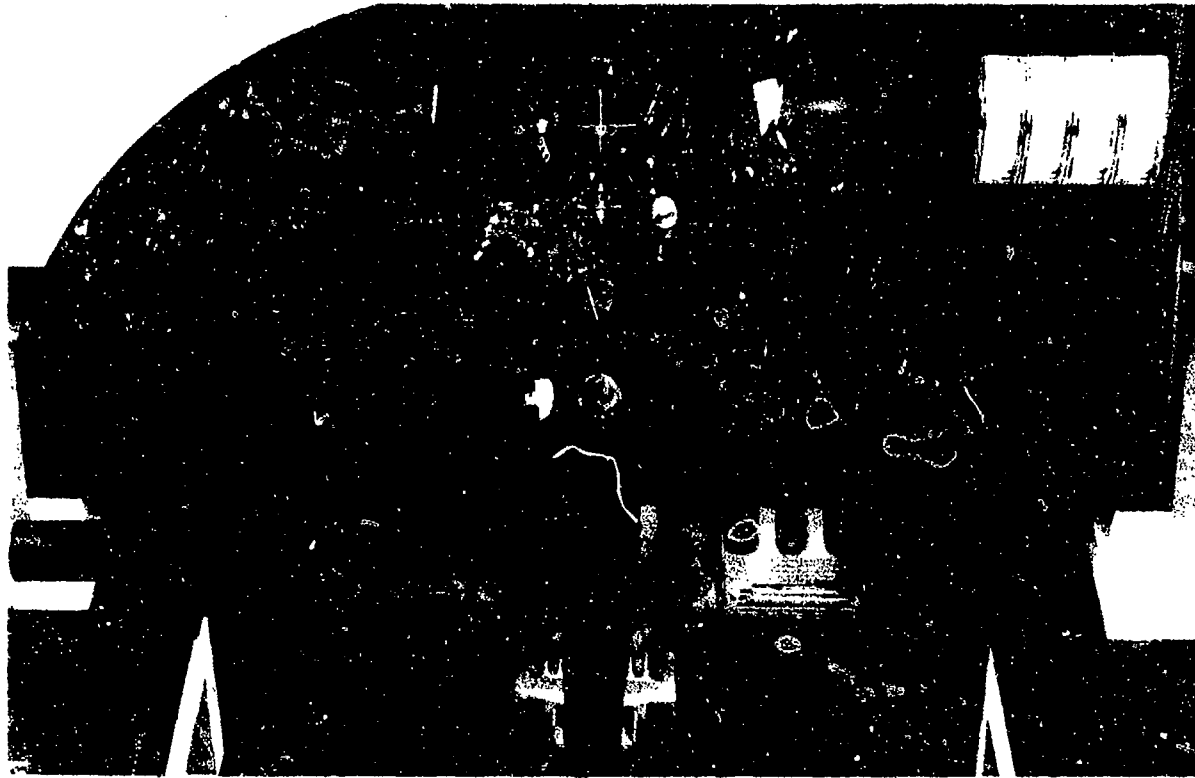


Figure 4-4. Flight Instrument Panel Layout

unit and before the compass was replaced by an horizontal situation indicator (HSI). The radar altimeter was later relocated to the right of the barometric-type altimeter. The digital indicating instrument just below the airspeed indicator showed the commanded airspeed when in the Autospeed mode. Changes to this commanded airspeed were effected through a slewing switch on the throttle handle, which can be seen in Figure 4-3.

A visual scene display was added to the fixed-base simulator by mounting a closed-circuit television monitor ahead of the pilot station. An airport terrain model (scaled to 1 inch = 64 feet) was televised to provide the visual scene for simulated flight operations. An optics system and television camera was controlled by the computer to represent the aircraft motions in the terrain model scale. The airport model included a 1500-foot-long by 60-foot-wide STOL runway (superimposed on a larger existing runway). Other terrain features included taxiways, airport buildings, and low-lying cloud formations near the horizon beyond the airport. The monitor-to-eye distance of the installation was designed to reproduce the correct viewing angles on the visual display. Limitations of the monitor area restricted viewing angles to 15 degrees either side of the aircraft nose and to a maximum vertical angle of 24 degrees. The center of the vertical look angle was depressed approximately 8 degrees, such

that the vertical field of view was 4 degrees above and 20 degrees below the aircraft X-axis (or nose position). Motion limitations of the terrain model and related equipment restricted simulated flight (using the visual scene for reference) to a wedge-shaped airspace extending forward of the runway. This airspace is defined as shown below; Figure 4-5 shows the vertical aspects of these limitations.

Maximum Range = 30,000 feet
 Maximum Bearing = ± 10 degrees
 Altitude Limits = (Range - 1500) (tan 5 deg) \pm 650 feet
 (Must be > 0)

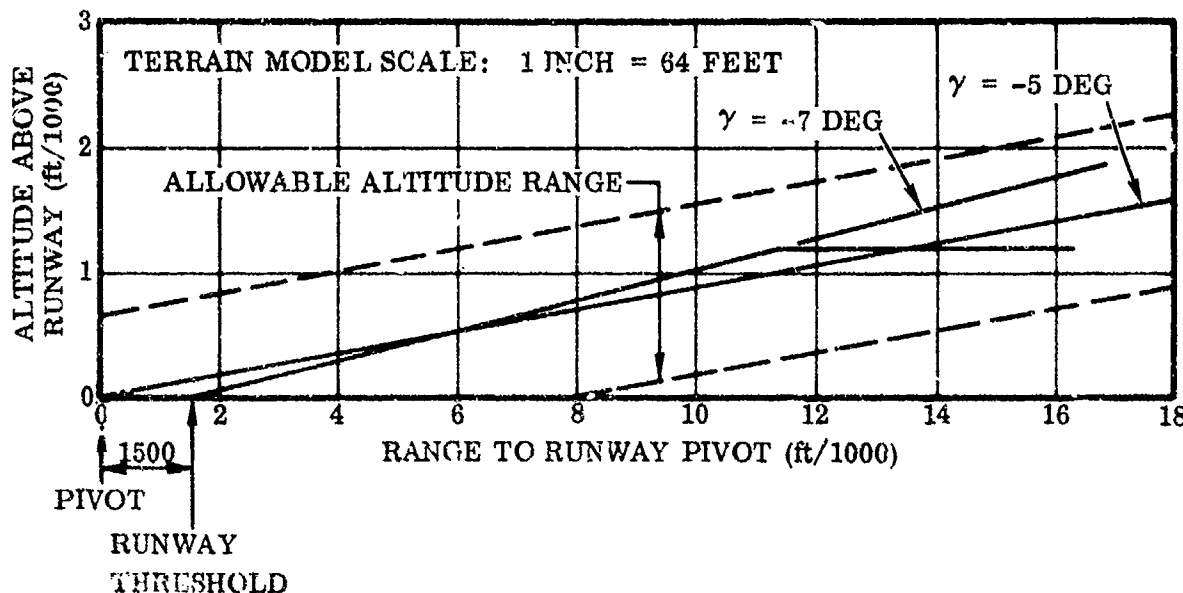


Figure 4-5. Visual-Scene Vertical Geometry

4.1.1.2 Computing Equipment. This simulation uses a CDC 6400 digital computer which, for real-time operation, interfaces with an SDS 930/COMCOR 5000 hybrid computer to provide communication with the simulator cockpit and display subsystem. Figure 4-6 shows the interconnection of various simulation hardware components.

The teletype identified in Figure 4-6 serves as a monitor of hybrid operations. It signals computer seconds remaining, sequence and run number, roll-in and roll-out messages, and abort and hybrid-ready messages. The teletype can also be used to modify any significant program parameters that must be changed during a simulation session. Output data is stored during the run and provided in tabulated form by a line printer after the run. Print intervals can be specified through the teletype. Continuous 8-channel strip chart recordings are available from analog recorders.

4.1.1.3 Simulation Implementation and Validation. The STOL simulations developed for this study were substantially digital. Analog equipment was used to process cockpit control signals and to condition flight instrumentation signals, thus making the

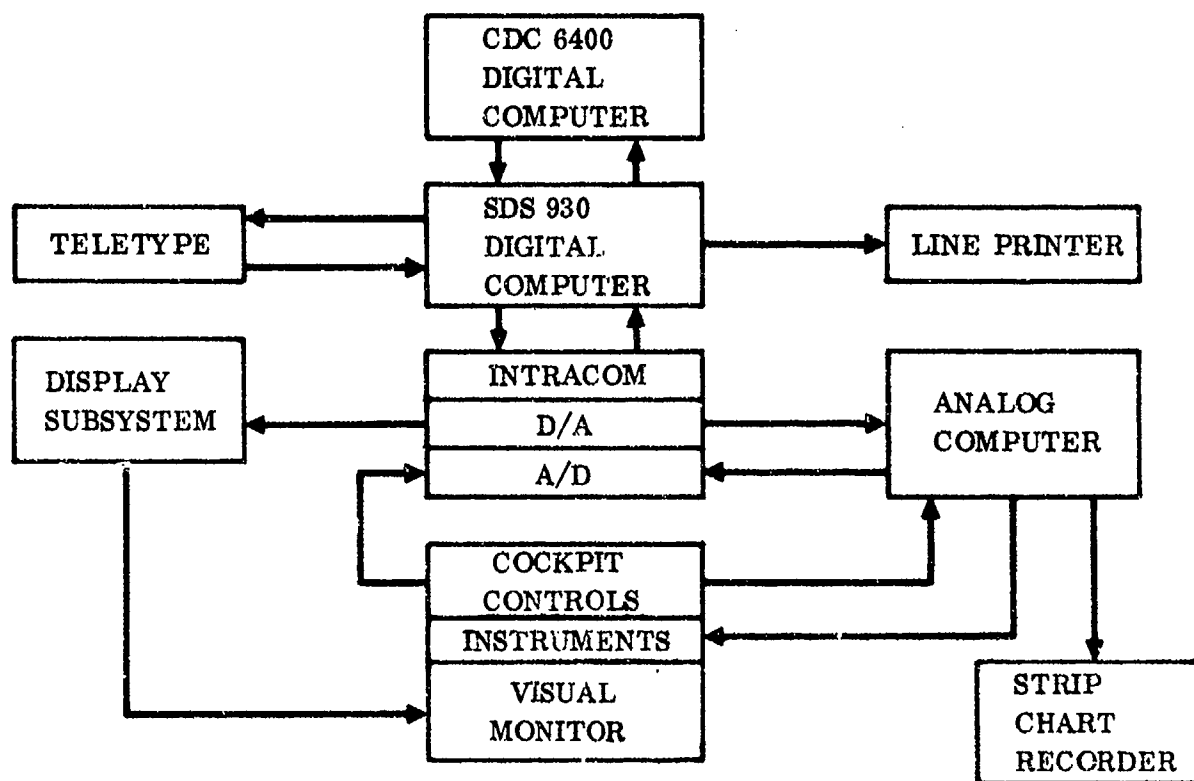


Figure 4-6. Simulation Equipment

overall implementation hybrid. The majority of computations were performed in the CDC 6400, which has a frame time (one complete cycle of all computations) between 15 and 20 milliseconds exclusive of data storage time for line printer output. When data storage (for later printout) was required, frame time increased to 65 to 70 milliseconds. By "padding" the shorter cycles of computation, an average frame time of 50 milliseconds was provided. Updating the solution 20 times per second was found suitable for the dynamic characteristics of the represented vehicle and its subsystems.

Software programming for this STOL simulation was developed from an existing six-degree-of-freedom real-time simulation. Software was organized to facilitate the changing of STOL configurations. Only 4 out of over 50 subroutines had to be changed to produce an alternative STOL configuration once the EBF version had been implemented and validated. Simulation programming was validated by obtaining non-real-time responses to specific control inputs in both unaugmented and augmented control modes. These were checked against responses to identical inputs from an established six-degree-of-freedom, non-real time digital program used earlier for analytical studies of that particular STOL configuration. Validation was performed for each STOL configuration simulated.

Non-linear aerodynamic data was stored in multi-dimensioned tables. Table look-up techniques were used to give the represented vehicle large-amplitude motion capabilities. Aerodynamic forces and moments were based on the atmospheric properties

of the 1962 Air Force-Navy Standard Hot Atmosphere. (Data from ANA Bulletin 421.) Landing operations were assumed to be on a field 2500 feet above mean sea level. Total body-axis moments and forces included inputs from the control elements, the propulsion system, and the landing gear. Modelling of these subsystems is discussed in later sections.

Vehicle motion and position data was provided through integration of the equations of motion. Resolution of parameters between body and earth coordinate systems was achieved using direction cosine matrices. Quaternion rates were generated and integrated to provide continuous computation of the direction cosines and Euler angles. This technique avoids the gimbal-lock problem of integrating Euler angles directly and reduces the number of integrations required when generating direction cosines directly. The aircraft was automatically trimmed longitudinally prior to each run by deflection of the horizontal stabilizer. Because the pilot's power lever was not servo-driven, it was necessary to set the power lever to the trim power setting at the start of a run. This was facilitated by simple instrumentation at the cockpit.

Engine power dynamics were modelled to an existing dynamic engine model with generally applicable characteristics, as shown in Figure 4-7. The propulsion system

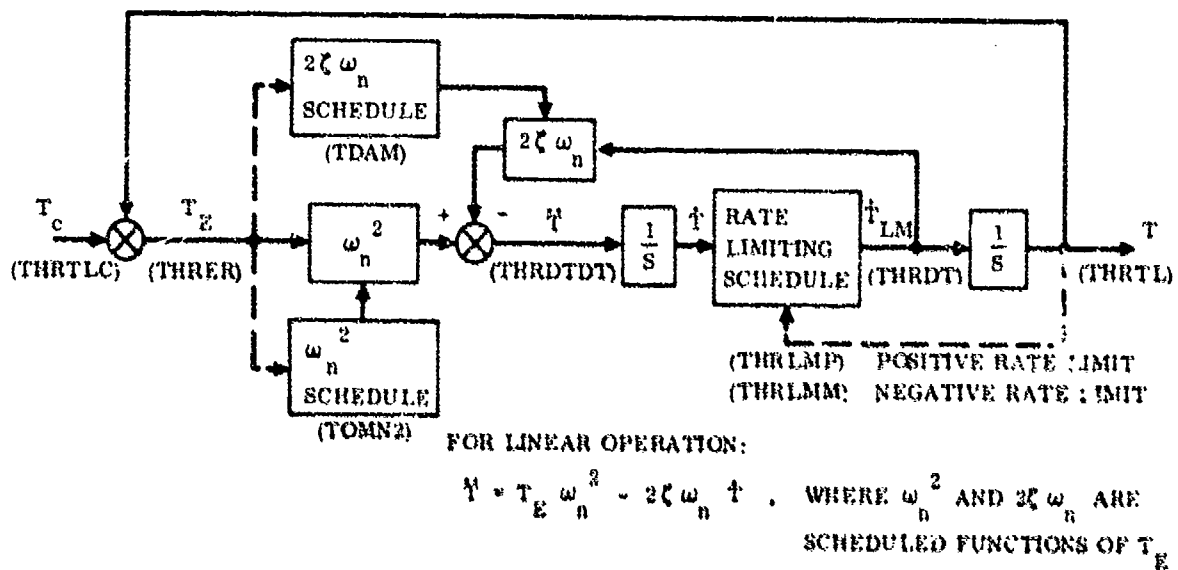


Figure 4-7. STOL MST Propulsion Dynamics

is represented as a second order, non-linear system whose response is a function of power level, power increment, and direction of power change. The schedules of natural frequency, damping, and rate limits are shown in Figures 4-8 and 4-9. Figure 4-10 is a time history of the modelled power response to a sequence of power command changes.

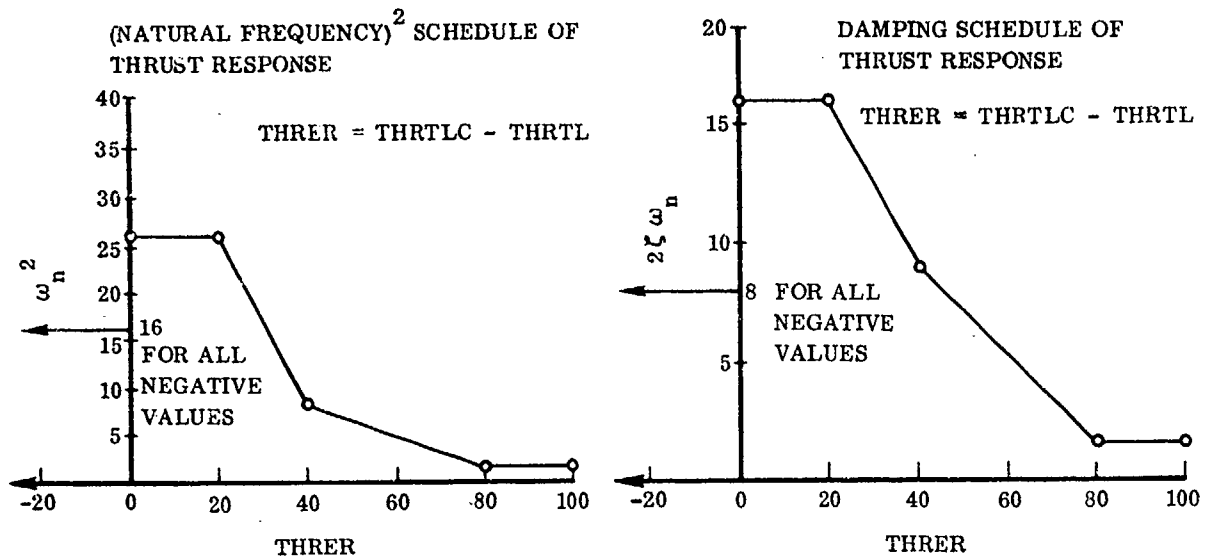


Figure 4-8. Thrust Response Schedules

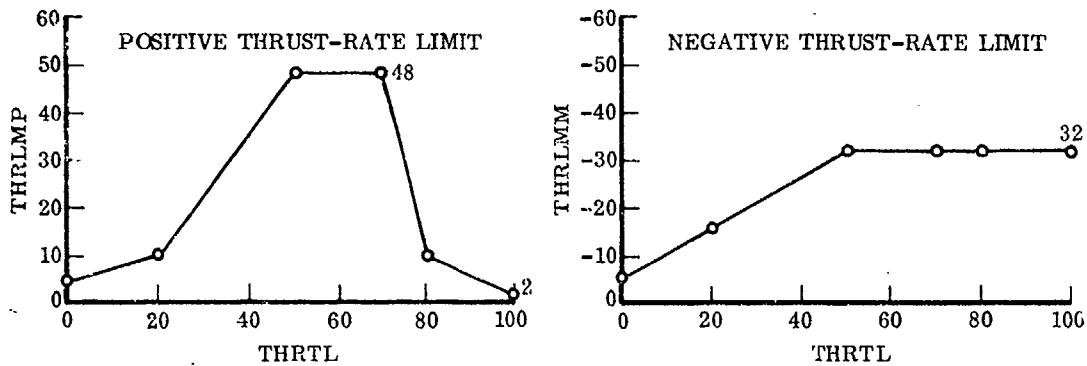


Figure 4-9. Thrust Rate Limits

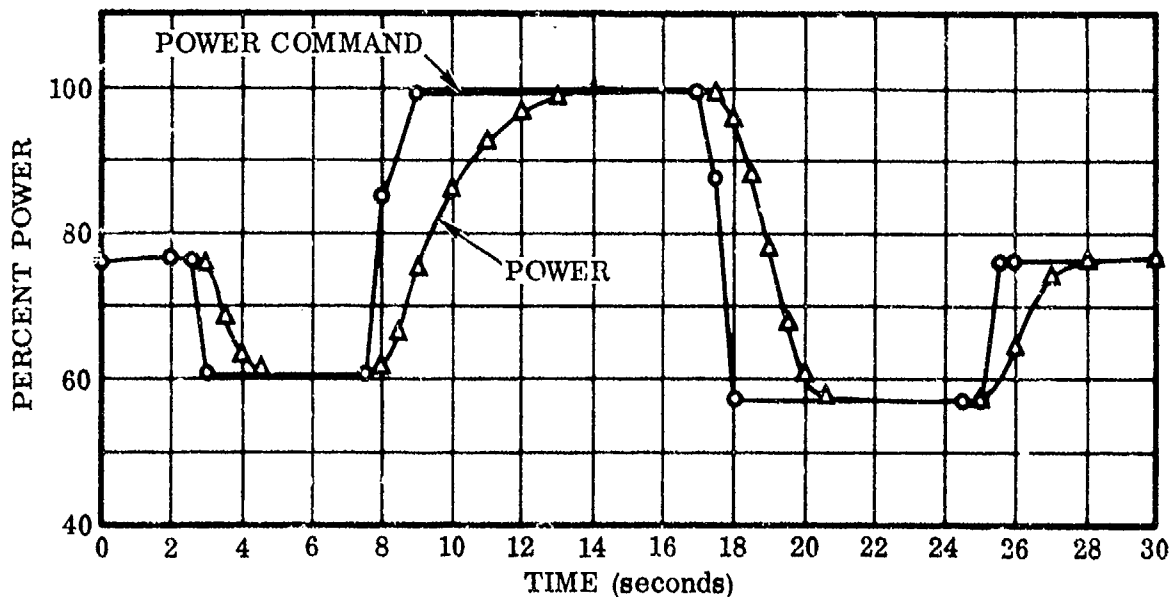


Figure 4-10. Power Response Time History

The landing gear was modelled to generate forces and moments in body-axis coordinates based on inputs from each of two main and one nose gear assemblies. Static gear deflection was assumed to be proportional to applied force, and a linear damping force proportional to gear deflection rate was assumed. A damping constant was assigned to produce a damping ratio of about 0.7. Nose wheel steering was implemented to be controlled through the rudder pedals. The software can provide for braking inputs, but the capability was not used for this simulation.

In implementing the simulation baseline control system, the lateral modes were selectable at one multiposition switch (MODELAT) in the cockpit and the longitudinal modes were selectable at another (MODELON). Five positions at each switch were activated. Position 5 provided only basic airframe controls (i.e., no augmentation). Decreasing numbers generally added augmentation features, with Position 1 including provision for automatic flight. The full-augmentation mode evaluated in this work was Position 2 in both lateral and longitudinal axes. Table 4-1 shows the augmentation

Table 4-1. Control Mode Switch Selections

MODELON		(Longitudinal Control)			
Switch Position					
5	BA				(Basic Airframe - Elevator Control)
4	BA	+	CA		(Control Augmentation)
3	BA	+	CA	+	X (Throttle-to-Flap Crossfeed)
* 2	BA	+	CA	+	X + Y (Flap plus Alpha Error-to-Throttle Crossfeed)
1	BA	+	CA	+	X + Y + PGUID (Auto)
MODELAT		(Lateral Control)			
Switch Position					
5	BA				(Basic Airframe - Spoiler Control)
4	BA				
3	BA				
2	BA	+	$\dot{\phi}_C$		(Aileron Control)
1	BA	+	ϕ_C	+	RGUID (Auto) (Aileron Control)
		(Directional Control)			
5	BA				(Basic Airframe - Rudder Control)
4	BA	+	YD		(Yaw Damper)
3	BA	+	YD	+	TC (Turn Coordinator)
* 2	BA	+	YD	+	TC
1	BA	+	YD	+	TC

* Full-Augmentation Mode

features provided in the various switch positions. Two push-to-select switches were made available to the pilot to select the AUTOSPEED and the APPROACH functions. These were assumed to be operationally selectable functions chosen by the pilot in relation to the flight situation. AUTOSPEED provided automatic control of airspeed through modulation of flap deflection. The commanded airspeed was the airspeed at engagement or, as later modified, at the pilot's discretion through the throttle slewing switch. Flaps had to be extended at least 40 degrees for this function to be operable. If flaps were retracted, this function was faded out at 40 degrees. The APPROACH function provided the crossfeeds for decoupling heave and pitch effects of control inputs. This mode was available only if the MODELON switch was at Position 2 or 1. When MODELON switch was at 2 (or 1) and APPROACH was deactivated, the MODELON switch function became equivalent to Position 4; i.e., pitch augmentation only. To simplify the go-around procedures, an automatic flap reduction circuit was implemented using the trigger switch for initiation of the action. When the power lever was at 98 percent or higher and the trigger switch was depressed, the flaps would retract to the flap switch (FLPSW) setting, a value chosen to minimize altitude loss after go-around initiation (nominally 40 degrees).

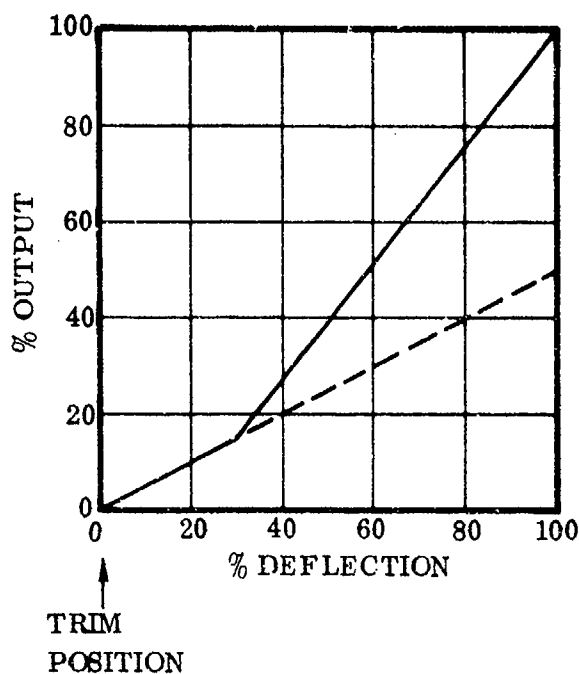
All control surfaces were assumed to be fully powered by hydraulics. Surface-positioning dynamics and all other control actuator dynamics were assumed to exhibit first-order characteristics. Representation of these included actuator rate and position limits. Characteristics of the various actuators are shown in Table 4-2.

Table 4-2. Actuator Characteristics

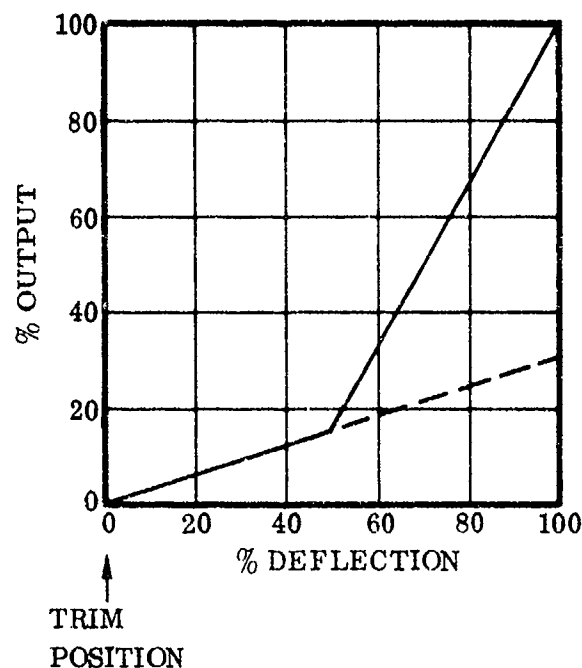
Surface	Max Rate (deg/sec)	Loop Gain (1/sec)	Deflection Limits (degrees)	
Aileron	120.0	10.0	100.0	-100.0
Rudder	75.0	10.0	50.0	- 50.0
Elevator	50.0	10.0	50.0	- 50.0
Stabilizer	2.0	5.0	10.0	- 15.0
Flap	5.0	4.0	70.0	0.0
Spoiler	180.0	10.0	60.0	- 60.0
Rudder Servo	75.0	40.0	25.0	- 25.0
Elevator Servo	50.0	40.0	20.0	- 20.0
Thrust Servo	20.0	5.0	100.0	- 0.0
Flap Servo	10.0	4.0	10.0	- 10.0

The loop gain shown is the reciprocal of the first-order time constant assigned. Pitch and roll signals from the stick were fed into a nonlinearization subroutine with variable characteristics. Pitch and roll signals were both nonlinearized to desensitize control stick motions around the neutral or trimmed position. This was found to be very desirable during the earliest evaluations. Figure 4-11 shows the nonlinear schedules used for the control stick; the rudder signal did not require

shaping. A small electrical dead zone was employed to mask the effects of friction when no force was applied to the pilot's controls, ensuring zero output for zero input.



PITCH SIGNAL SHAPING
(SYMMETRICAL ABOUT TRIM POSITION)



ROLL SIGNAL SHAPING
(SYMMETRICAL ABOUT TRIM POSITION)

Figure 4-11. Control Stick Signal Shaping

Augmentation gains were established for the STOL approach configuration (at 80 knots). At the higher dynamic pressures prior to transition, instability occurred until a gain schedule was incorporated. Gains of the augmentation subsystems were modified by a function of dynamic pressure to accommodate the higher speed conditions. Figure 4-12 shows the gain schedule and the table of gains used to approximate the schedule for this simulation. Gain variation with flap deflection may serve equally well to solve the problem, but this was not evaluated.

A turbulence model was implemented using an existing digital turbulence subroutine. This subroutine modelled turbulence in accordance with MIL-F-8785B and also provided for both Gaussian and non-Gaussian noise. Reference 4-1 describes the characteristics of the digital subroutine on which the turbulence model of this simulation was based. The MIL-F-8785B turbulence model was found to be too severe for realistic simulation work, and was even worse when the simulation task required low altitude flight as in approach and landing. Consequently, the turbulence model was modified to avoid the extreme effects of approaching the ground, and the general scaling of the gust components was reduced based on conversations with personnel at Cornell Aeronautical Laboratory and on qualitative pilot evaluations regarding

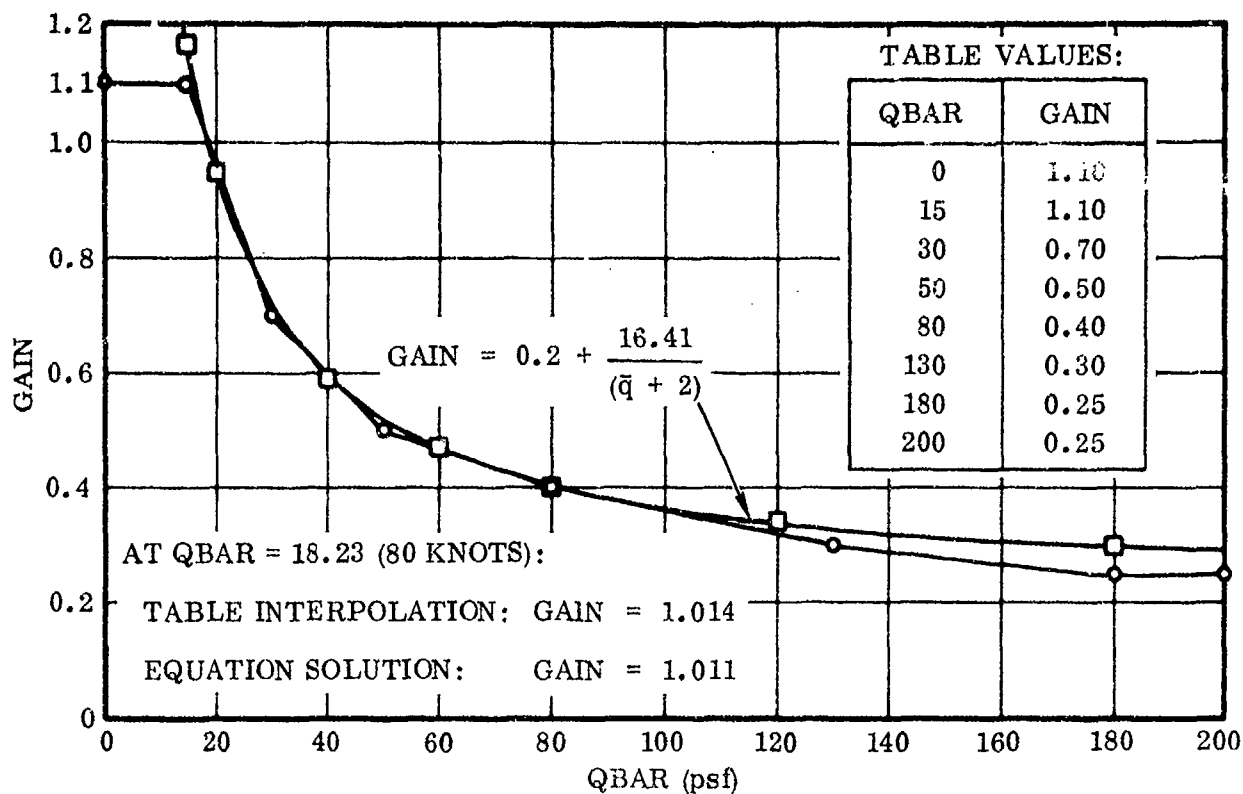


Figure 4-12. QBAR Gain Schedule

reasonable amounts of turbulence for the simulation tasks scheduled. A detailed account of the modifications adopted for this work is presented in Appendix II.

A wind model, independent of the turbulence representation, was generated for cross-wind approaches. Wind direction could be assigned any compass heading, and magnitudes were stored in a table whose entering argument was altitude. The values used were taken from a table of mean wind values in Reference 4-2. Figure 4-13 shows the tabulated values of wind velocity versus altitude used for this work. Where records of evaluation runs in Appendix III indicate wind to be at "30 KTS," it was actually this variable wind model which was used. At the minimum altitude (aircraft on the ground), the mean wind was about 12 knots. At 1200 feet above ground level, the mean wind value was about 43 knots.

Experience with the fixed-base simulation visual display demonstrated that it was difficult to judge lateral displacement from the runway centerline at the initial approach distance. Also, the visual display limitations made it very difficult to interpret the simulation flight path angle versus the desired flight path angle. To compensate for these difficulties, flight director signals were generated and displayed on the ADI.

4.1.2 MOVING-BASE SIMULATOR. The moving-base simulator facility used for this work was the Large-Amplitude Flight Simulator located at the Aircraft Division of the Northrop Corporation, Hawthorne, California. This facility includes a flight simulation computing laboratory and other supporting laboratories and workshops.

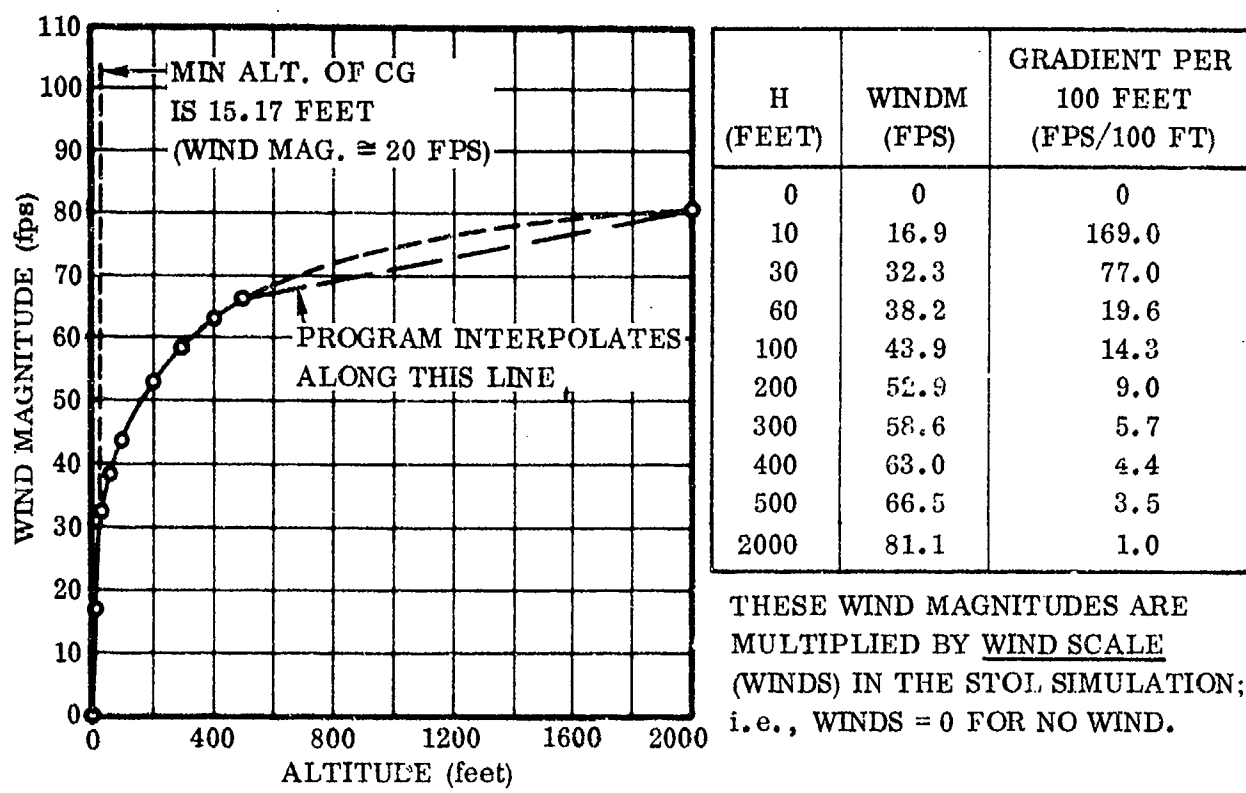


Figure 4-13. Simulation Model of Wind Magnitude Versus Altitude

4.1.2.1 Physical Characteristics. The large-amplitude simulator (LAS) shown in Figure 4-14 uses a cockpit gimbal system mounted on a 30-foot-long beam that, in turn, is supported by a single two-axis base gimbal on a fixed support pedestal. The LAS and its wide-angle viewing system consist of a five-degree-of-freedom beam-type motion subsystem that carries a single-place cockpit, the projectors (for sky/earth/horizon and runway or target image), and the display screen of the visual display subsystem as a unit on the end of the beam. Other elements of the simulator system, not mounted on the beam, include the hydraulic supply system, the runway (or target) image generation subsystem, and the monitor and control console. The remaining elements of the moving-base simulator facility are contained in the hybrid computer system (EAI-8900) located in an adjacent building and in the related software programs. Northrop developed these programs to drive the motion subsystem and the runway (or target) image subsystem and to perform daily dynamic and diagnostic checks of the various subsystems. Table 4-3 lists the general capabilities of the motion, visual, and control subsystems.

The cockpit used for this simulation work was an existing fighter type, single-place cockpit equipped with a center-stick, rudder pedals, and a conventional throttle lever. Stick and rudder pedal forces were provided hydraulically under computer control. The force-deflection characteristics were programmed to the same

Table 4-3. Large Amplitude Flight Simulator System Summary

	Cockpit Translation		Cockpit Rotation		
	Vertical	Horizontal	Pitch	Roll	Yaw
MOTION SYSTEM					
Displacement (Full Mechanical Travel)	± 13 ft	± 13 ft	± 32 deg	± 30 deg	± 28 deg
No Load Velocity	13 ft/sec	9 ft/sec	0.95 rad/sec	1.1 rad/sec	1.3 rad/sec
Stall Acceleration (Other Servos Stationary)	2.5 g	1.35 g	15.7 rad/sec ² Up 21.5 rad/sec ² Down	4.6 rad/sec ²	8.6 rad/sec ²
Looks Like a 4 Hz, 0.7 Damped Second-Order System					
VISUAL SYSTEM					
Field of View of Screen	210 deg Lateral		-60 deg To +77 deg Vertical (Nominal)		
Earth/Sky Projection	3 degrees of Freedom, Continuous Rotation				
Target Projection	15-deg Field of View Anywhere Within Screen Field of View				
Target Image Generation	Aircraft: 3 Dimensional Model Viewed by TV Camera				
	Other: Line Drawings on CRT Viewed by TV Camera Runway and Terrain View				
CONTROL SYSTEM					
Stick and Rudder Pedal Forces Provided Hydraulically Under Computer Control					

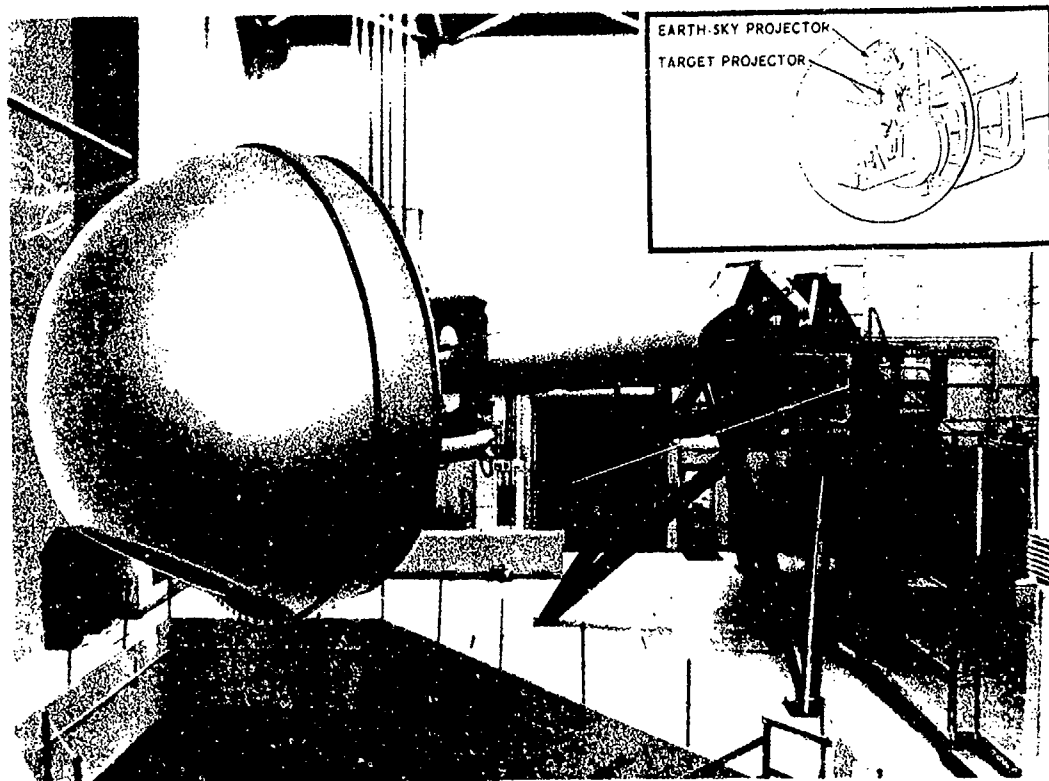


Figure 4-14. Large Amplitude Simulator

characteristics as for the fixed-base simulator (FBS) tasks. Provision for pilot selection of the AUTOSPEED and APPROACH modes was made in a manner similar to that for the FBS cockpit. Other controls were operated at the computer station. The variation in cockpit features from the FBS cockpit were not significant enough to warrant the cost and time delays of developing an exact duplicate.

Flight instrumentation was somewhat different from that of the FBS cockpit. An existing instrument panel (in daily use on alternate work shifts) was modified slightly to provide the same flight information as the FBS instrumentation. Resolution of airspeed was slightly more coarse and the placement of certain instruments was different, but the ADI and HSI were identically located. The minor influence of these variations far offset the considerable expense and lost time that would have been incurred in exactly duplicating the FBS cockpit instrumentation. Pilot opinion was that the differences in flight instrumentation at the MBS required a little more familiarization time, but after that the differences did not significantly influence the evaluations.

The MBS facility includes a wide-angle visual system (WAVS). In addition to the large hemispherical viewing screen and the beam-mounted projectors, visual equipment includes a target image generator subsystem that provides the video information supplied to the target projector. For this work, a simple runway model was televised in lieu of a target model and superimposed onto the earth-sky image. The runway

model had motion capabilities to simulate various horizontal and vertical approach angles. The mechanization was limited, however, and the minimum altitude simulated was about 30 feet above ground level (AGL). Terrain features surrounding the runway were minimal and the target projector was limited to projection of a rather narrow image (i.e., a 15-degree cone of view centered about the runway model).

4.1.2.2 Computing Equipment. The flight simulation computing laboratory that supports the MBS facility includes extensive electronic, solid-state equipment able to accommodate a broad variety of detailed engineering and scientific problem investigations. One EAI 8900 Integrated Hybrid System was used in implementing the MBS for this program. This system consisted of:

- 8800 Analog Computer & Control Console
- 8400 Digital Computer (32K core)
- 64 Analog-to-Digital (A/D) Interface Channels
- 96 Digital-to-Analog (D/A) Interface Channels

Simulator motions were monitored using a COMCOR 175 and two rectilinear 8-channel strip chart recorders. Problem input parameters were tabulated on a high-speed line printer, and output parameters were recorded using the strip chart recorders.

4.1.2.3 Simulation Implementation and Validation. Simulation of the STOL (EBF version) transport at the MBS facility was implemented in the same way as for the fixed-base simulator (FBS), except for minor differences dictated by computing equipment differences and/or limitations. The more significant of these are discussed later. The MBS implementation was validated by submitting that simulation to the same series of control pulses as used at the FBS and comparing the aircraft responses. The 12 test responses taken included uncontrolled (no augmentation) and augmented control modes in pitch, roll, and yaw axes for two flight conditions: STOL approach conditions and 10,000-foot cruise conditions. Figures 4-15 through 4-26 show un-augmented responses to control pulses for pitch, roll, and yaw inputs for both FBS and MBS. The FBS pitch response of Figure 4-15 was made early in the fixed-base work and is slightly less damped than the MBS response. The software was corrected when it was found that the $\dot{\alpha}$ computation was overlooked in setting up the real-time software. Addition of that computation produced the same response as for the MBS; this was later verified. Instrumentation of stick deflection (δ_{stick}) was recorded with different scale factors and the apparent magnitude difference should be discounted. As shown in Figures 4-15 and 4-16, elevator pulses are the same. The same is true regarding the rudder pedal deflection scale factors - the rudder deflections are alike.

Figures 4-27 and 4-28 show FBS and MBS pitch responses of the augmented aircraft. These illustrate the effect of some limitations of the MBS computer system. The

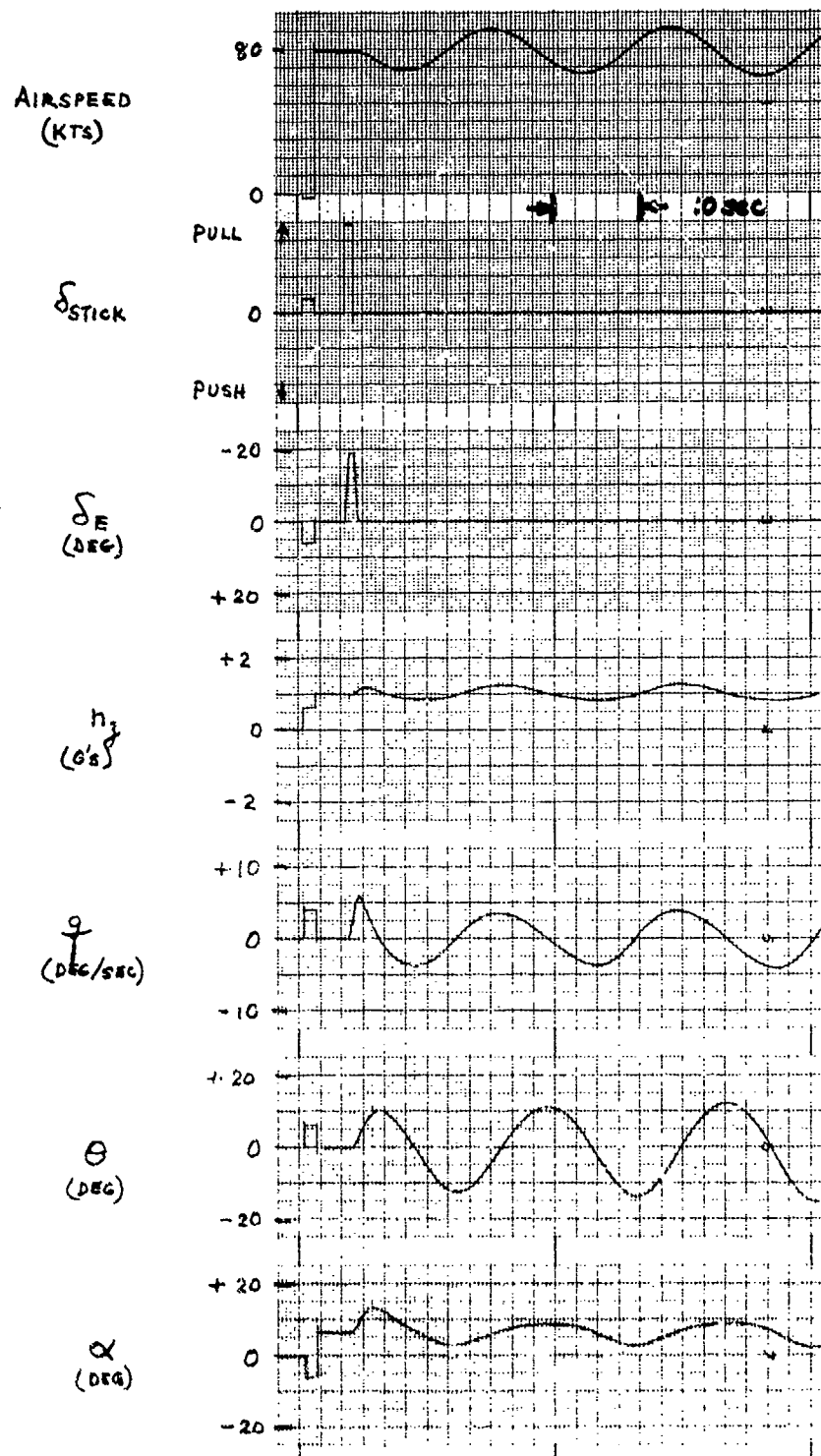


Figure 4-15. FRS Uncontrolled Pitch Response to a Pulse of δ_{stick}
 (3700-ft Altitude, $\gamma_{IC} = -7$ deg, Flaps = 60 deg, Gear Down)

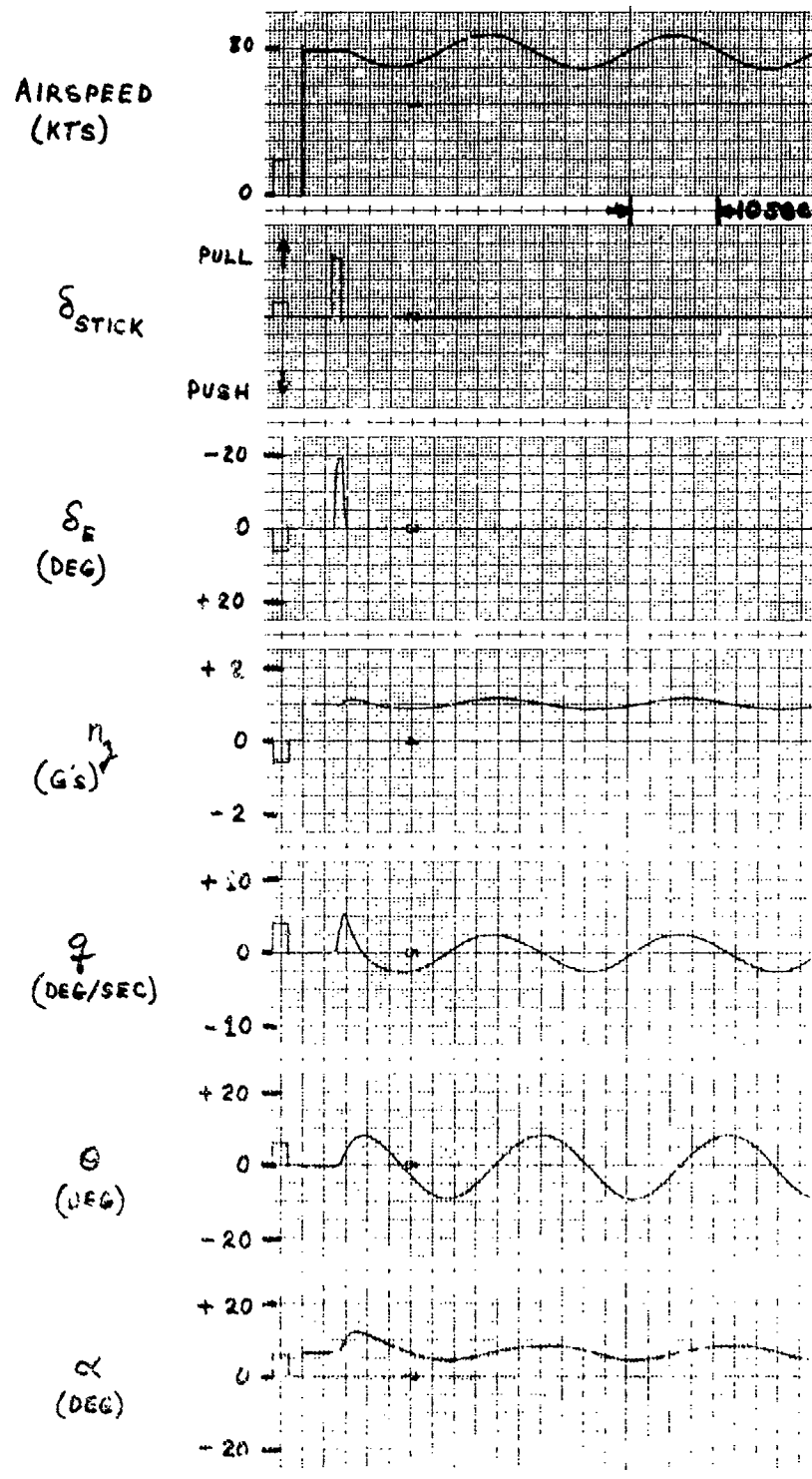


Figure 4-16. MBS Uncontrolled Pitch Response to a Pulse of δ_{stick} ; (3700-ft Altitude, $\gamma_{IC} = 7$ deg, Plane = 0 deg, Gear Down)

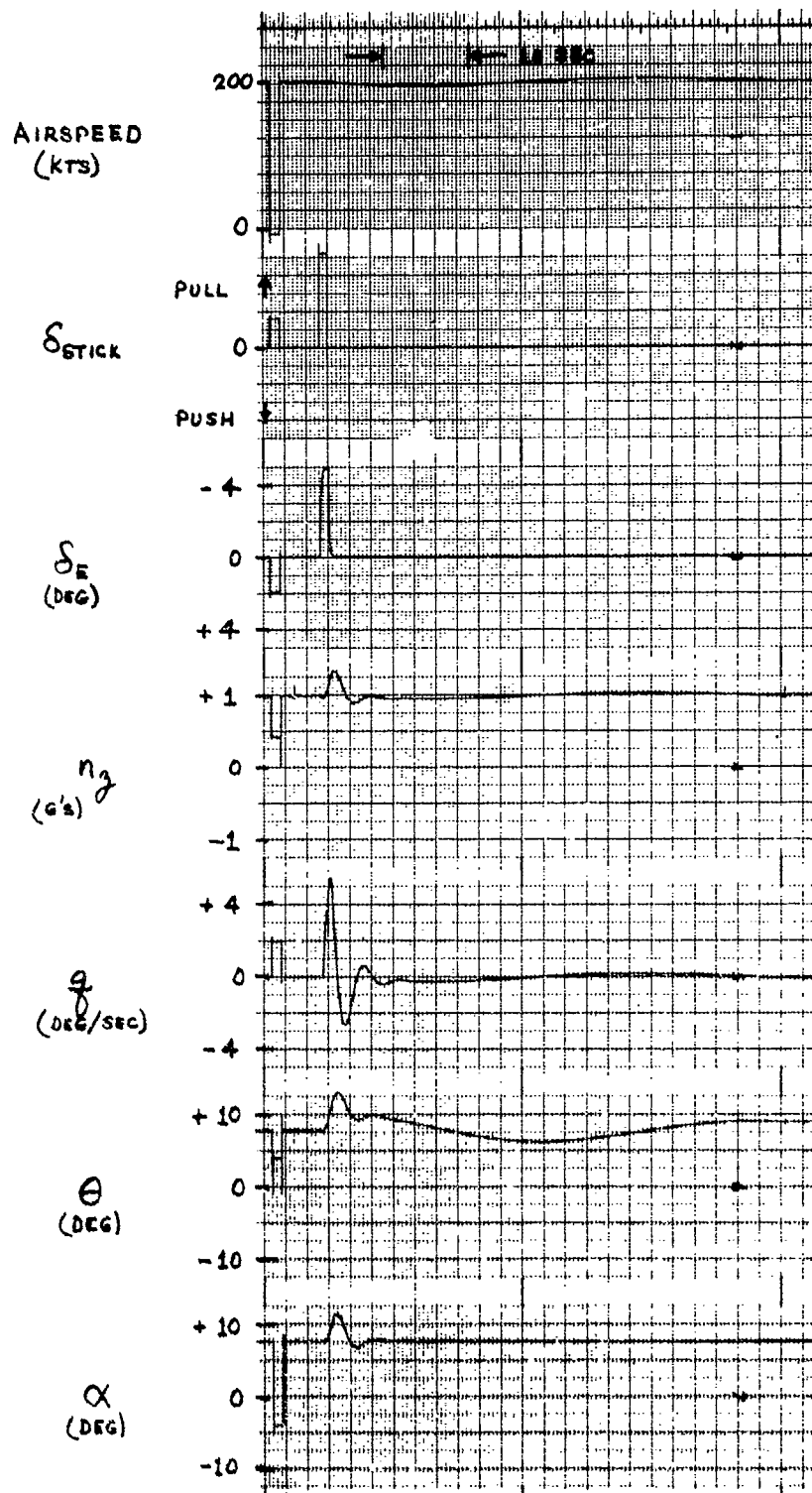


Figure 4-17. FBS Uncontrolled Pitch Response to a Pulse of δ_{stick} (12,500-ft Altitude, $\gamma_{IC} = 0$ deg, Flaps = 0 deg)

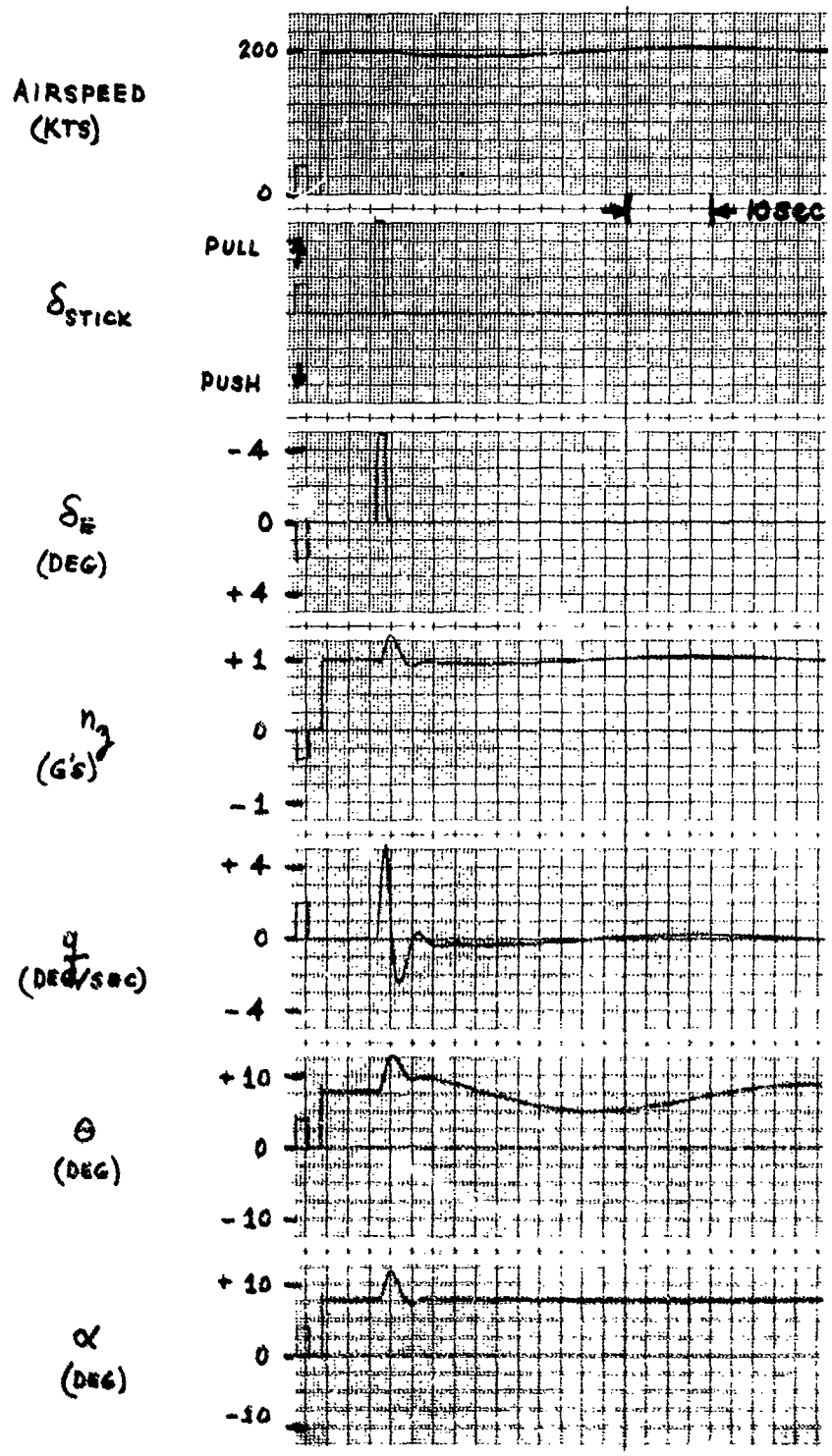


Figure 4-18. MBS Uncontrolled Pitch Response to a Pulse of δ_{stick}
 (12,500-ft Altitude, $\gamma_{IC} = 0$ deg, Flaps = 0 deg)

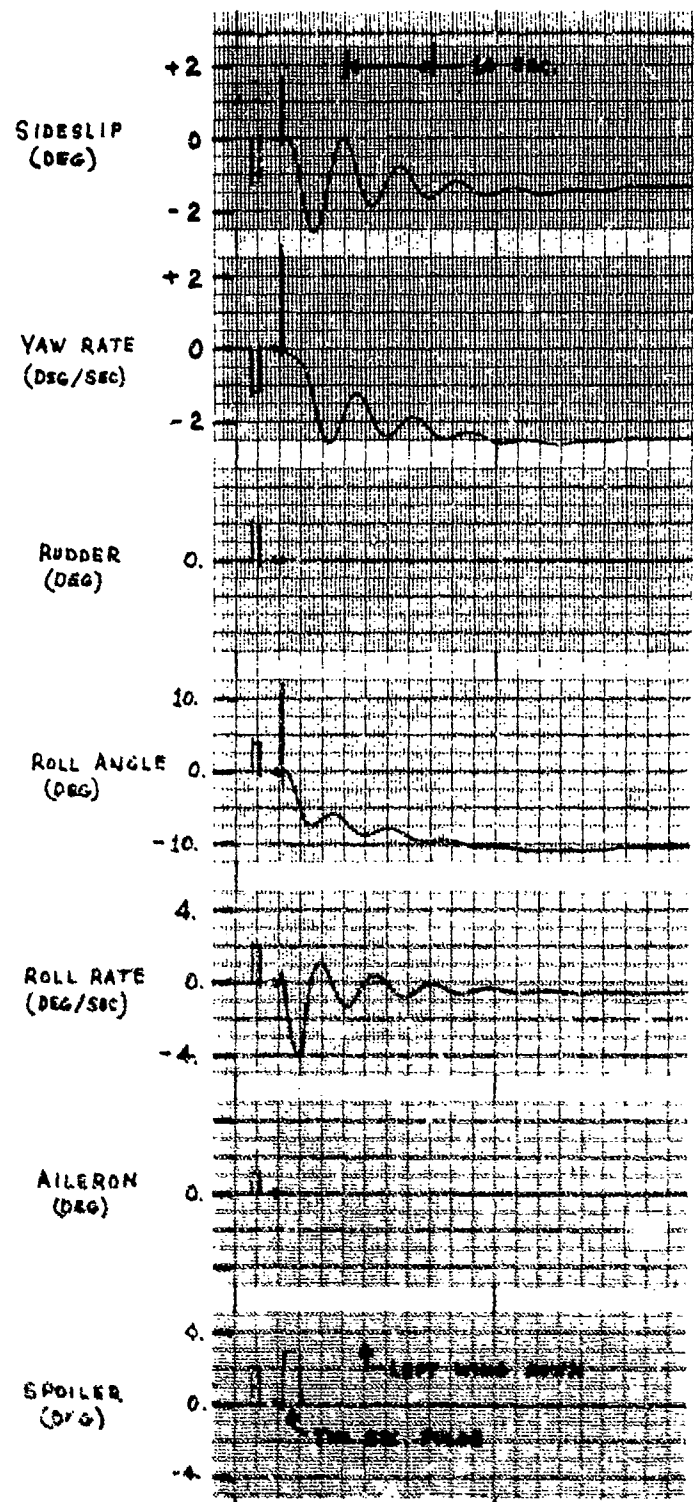


Figure 4-19. FBS Uncontrolled Roll Response to a Pulse of Lateral Stick
 (3000-ft Altitude, $\gamma_{IC} = -7$ deg, Flaps = 60 deg, Gear Down,
 Speed_{IC} = 80 knots;

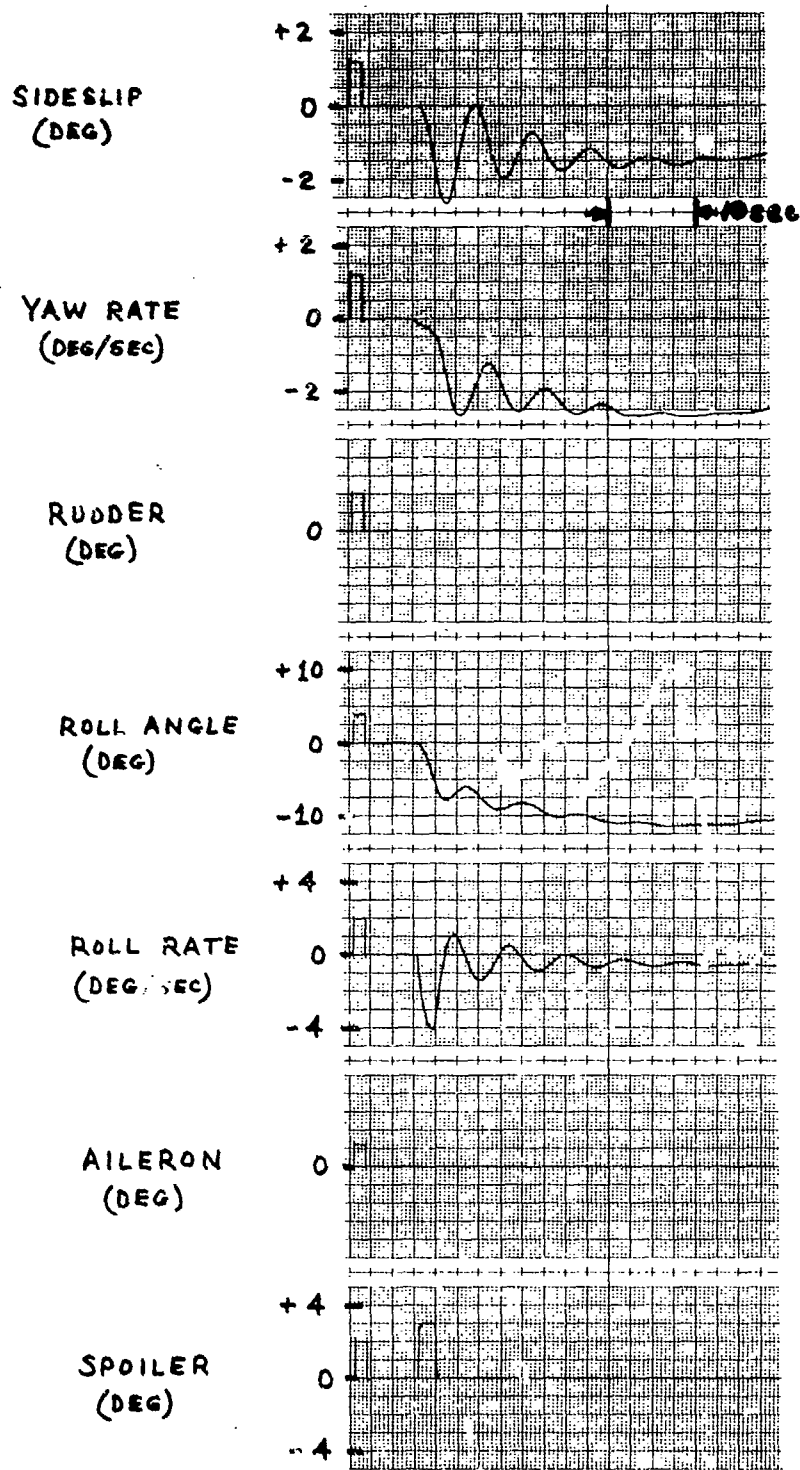


Figure 4-20. MBS Uncontrolled Roll Response to a Pulse of Lateral Stick (3700-ft Altitude, $\gamma_{IC} = -7$ deg, Flaps = 60 deg, Gear Down, Speed_{IC} = 80 knots)

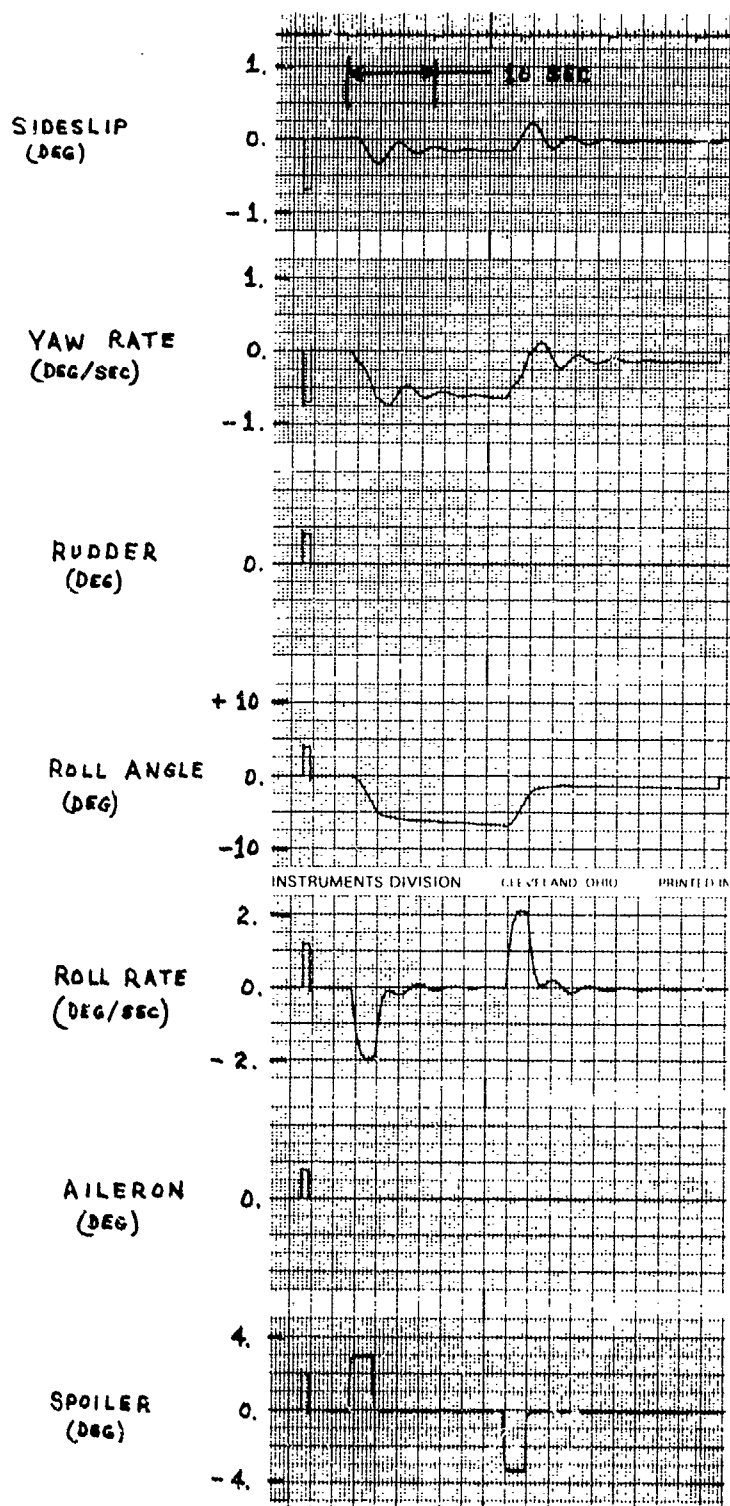


Figure 4-21. FBS Uncontrolled Roll Response to a Pulse of Lateral Stick (12,500-ft Altitude, $\gamma_{IC} = 0$ deg, Flaps = 0 deg, Gear Down, Speed = 200 knots)

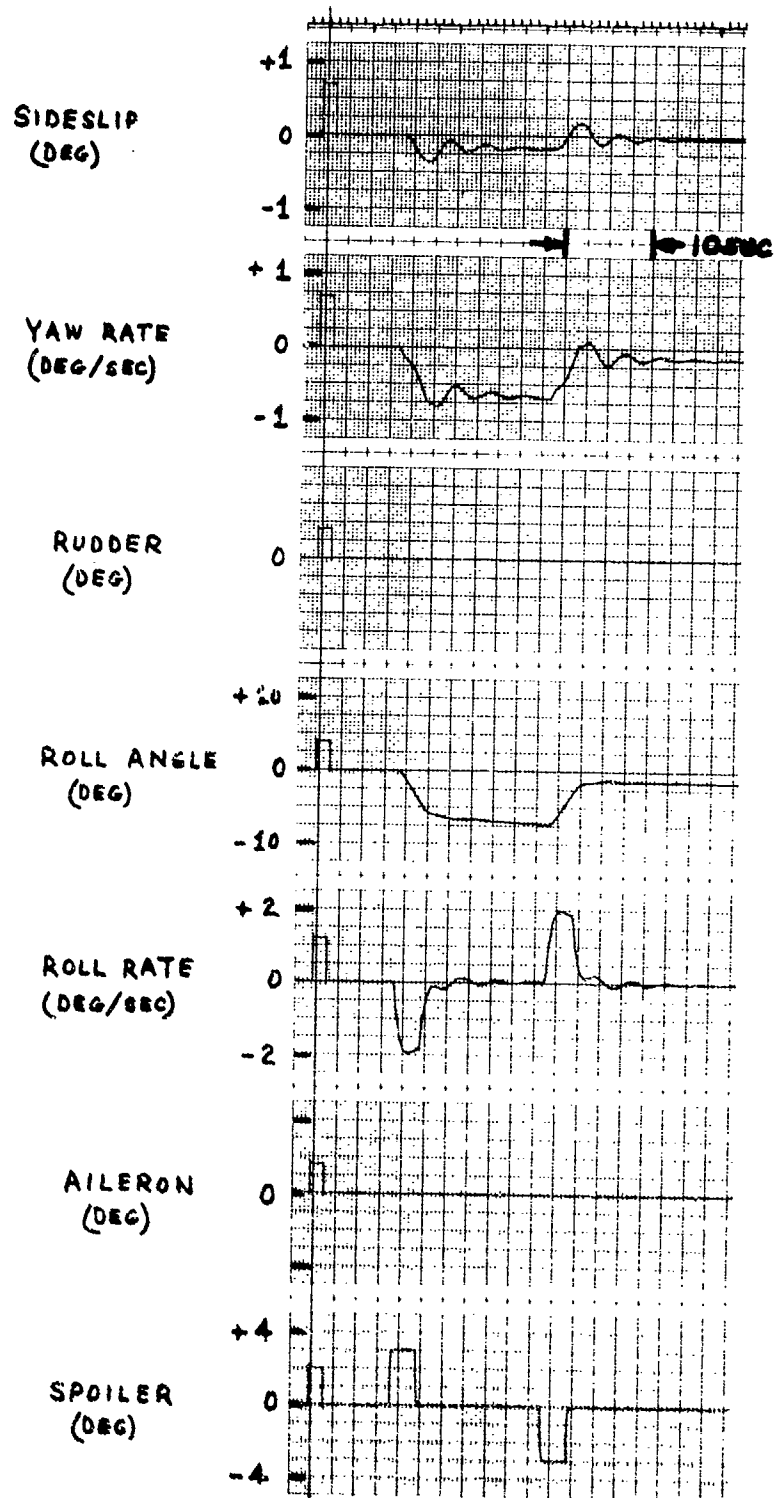


Figure 4-22. MBS Uncontrolled Roll Response to a Pulse of Lateral Stick (12,500-ft Altitude, $\gamma_{IC} = 0$ deg, Flaps = 0 deg, Gear Down, Speed = 200 knots)

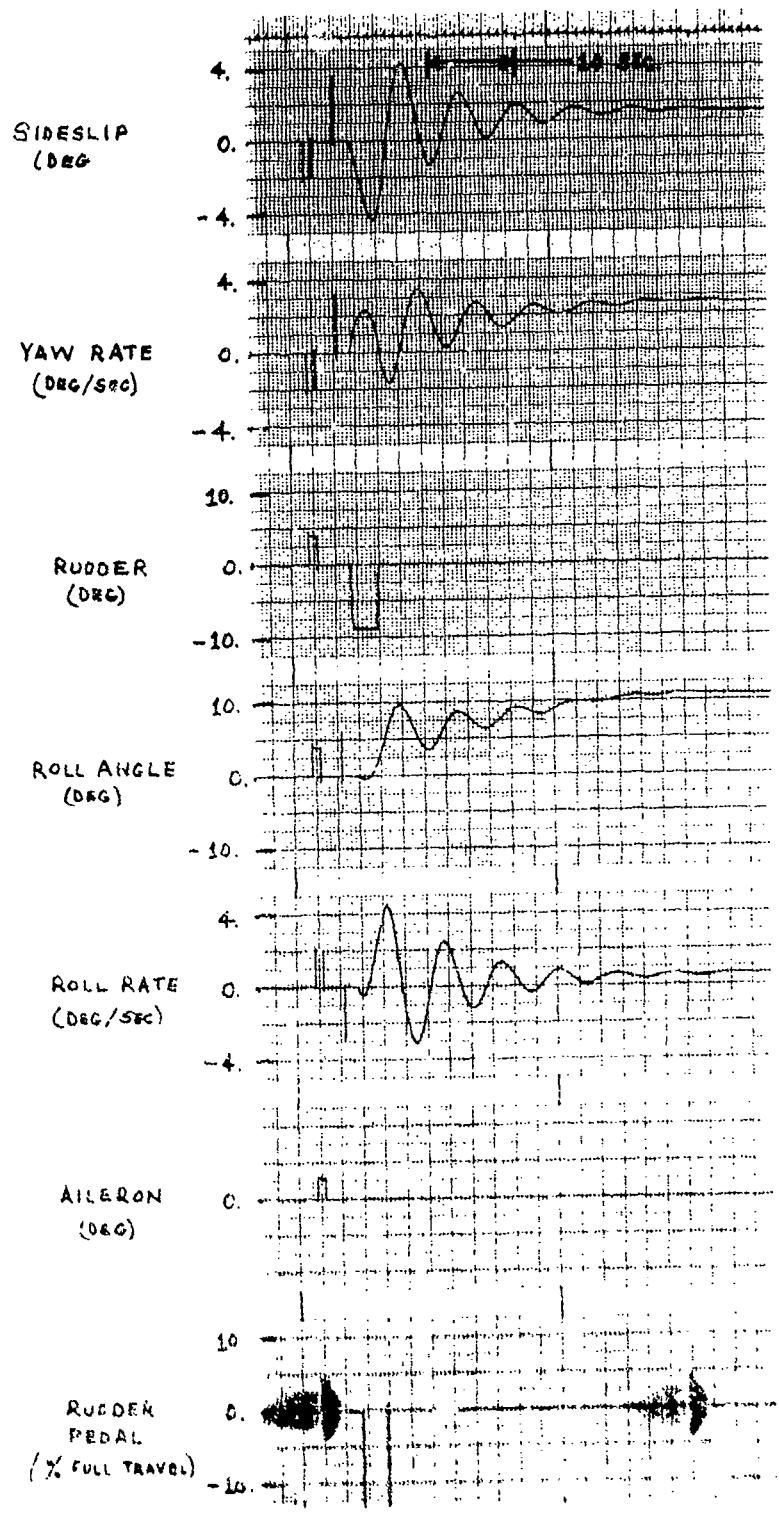


Figure 4-23. PRS Uncontrolled Yaw Response to a Pulse of Rudder Pedal
 (3700-ft Altitude, $\gamma_{IC} = -7$ deg, Flaps = 60 deg, Gear Down,
 Speed_{IC} = 40 knots)

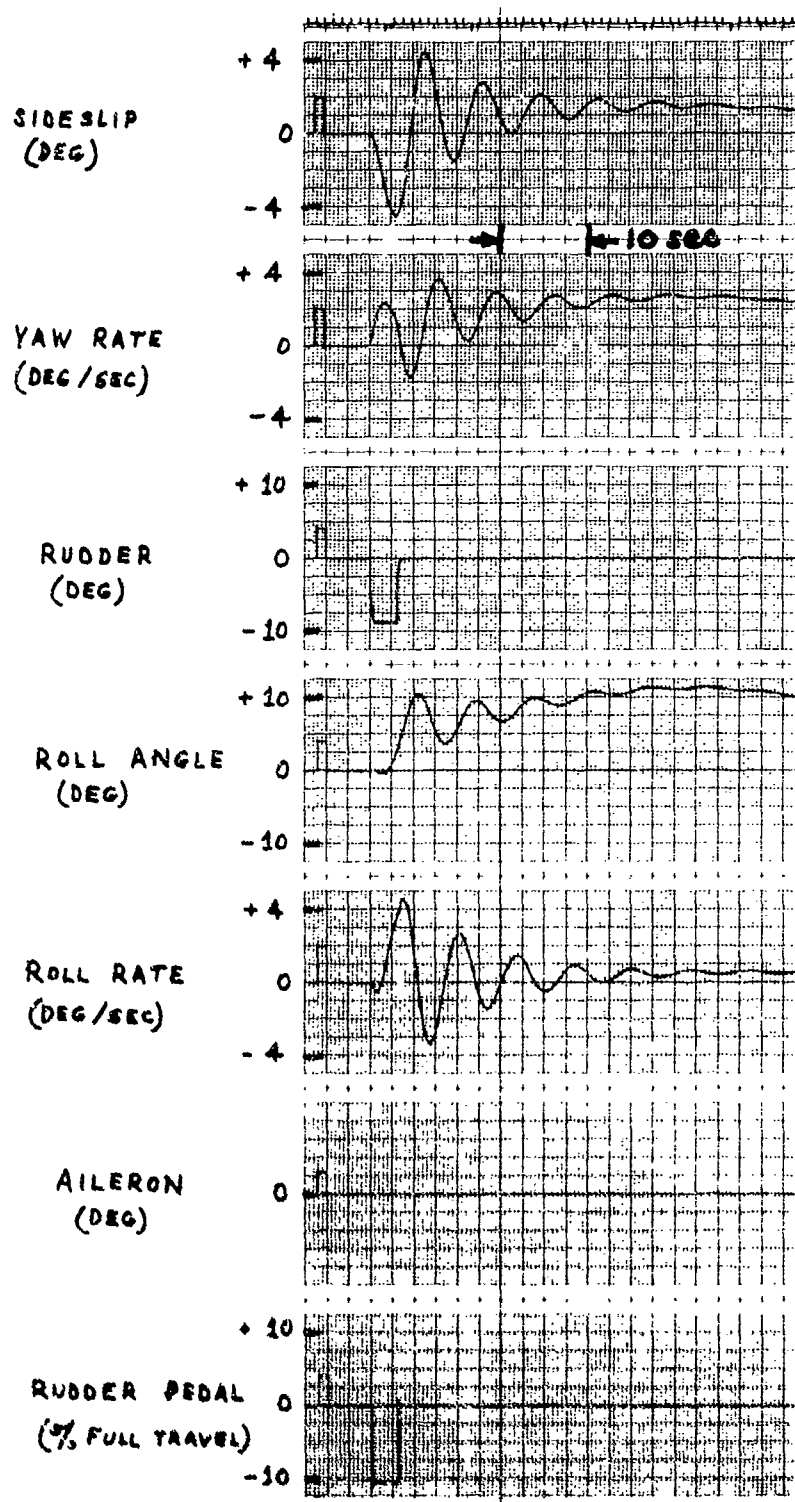


Figure 4-24. MBS Uncontrolled Yaw Response to a Pulse of Rudder Pedal (8700-ft Altitude, $\gamma_{IC} = -7$ deg, Flaps = 60 deg, Gear Down, Speed_{IC} = 80 knots)

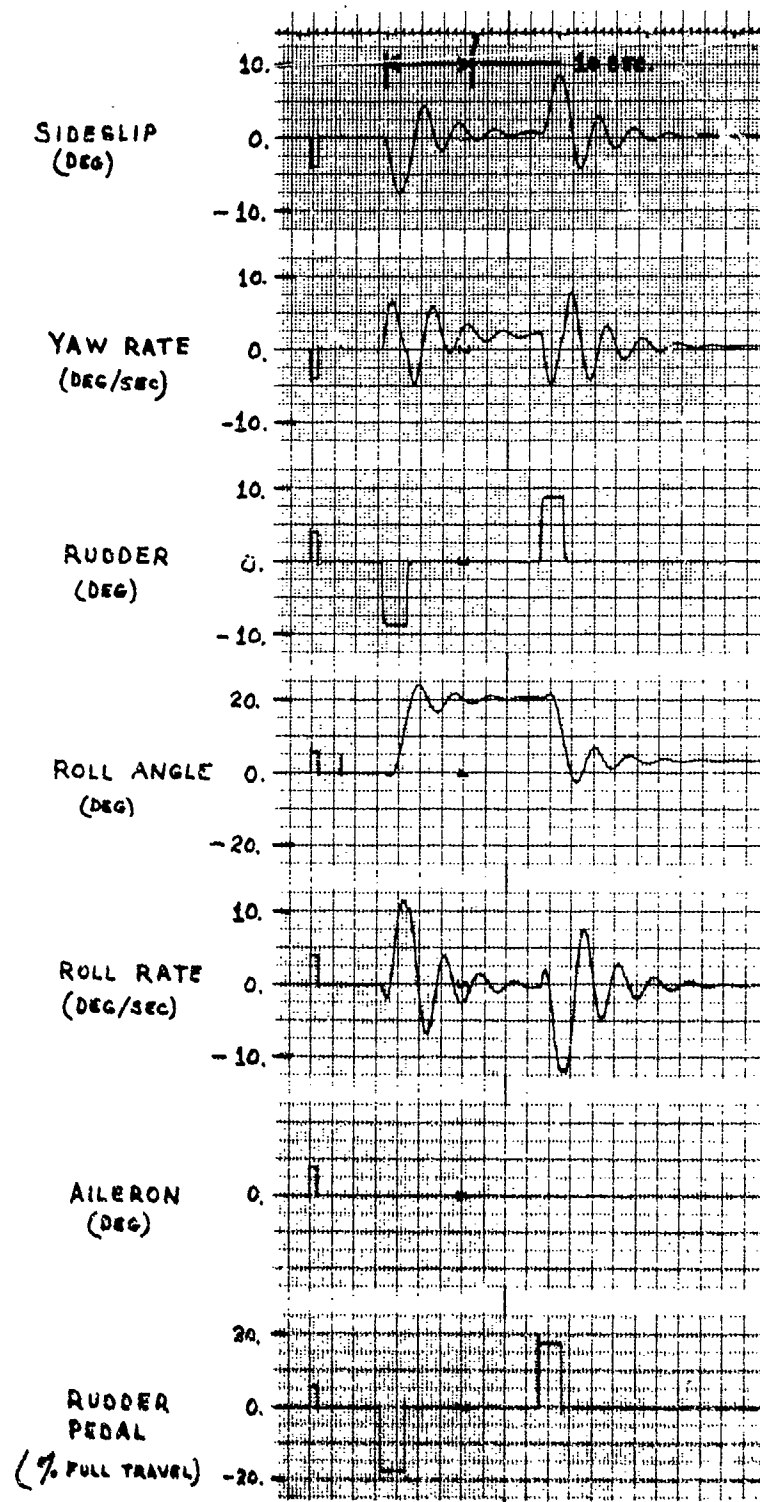


Figure 4-25. FBS Uncontrolled Yaw Response to a Pulse of Rudder Pedal
 (12,500-ft Altitude, $\gamma_{IC} = 0$ deg, Flaps = 0 deg, Gear Down,
 Speed = 200 knots)

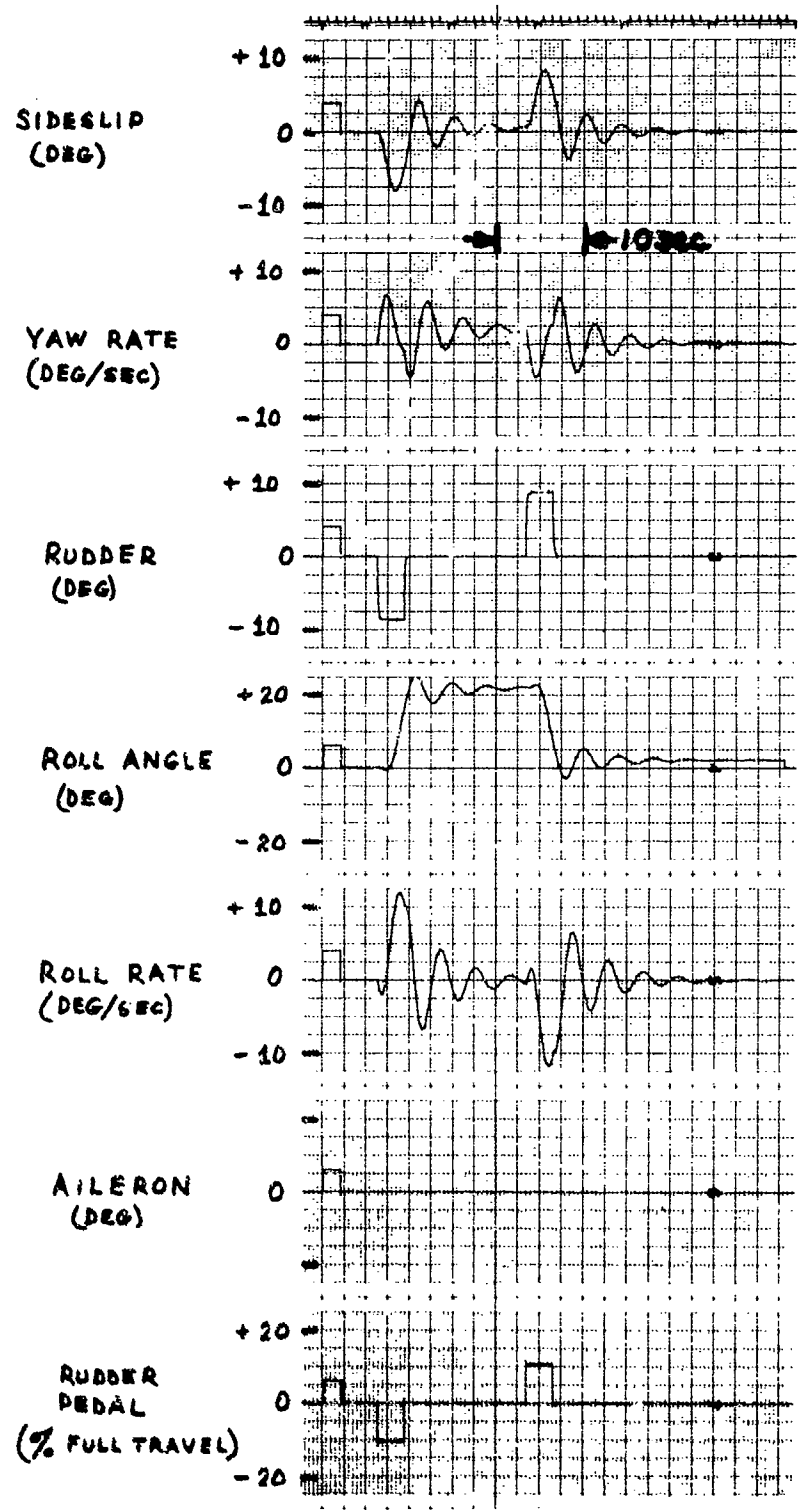


Figure 4-26. MBS Uncontrolled Yaw Response to a Pulse of Rudder Pedal (12,500-ft Altitude, $\gamma_{IC} = 0$ deg, Flaps = 0 deg, Gear Down, Speed = 200 knots)

AIRSPPEED
(KTS)

δ_{STICK}
(% FULL TRAVEL)

δ_E
(DEG)

$\dot{\alpha}$
(G's)

$\dot{\theta}$
(DEG/SEC)

θ
(DEG)

α
(DEG)

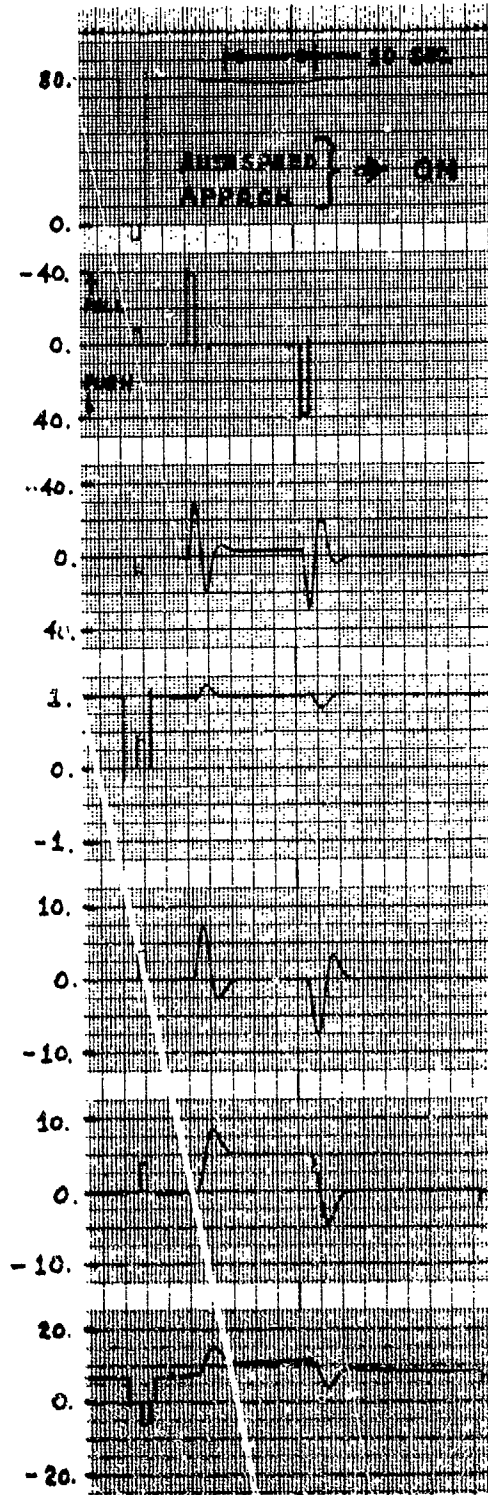


Figure 4-27. FBS Augmented Pitch Response to a Pulse of δ_{stick}
(3700-ft Altitude, $\gamma_{IC} = -7$ deg, Flaps = 60 deg, Gear
Down, Speed_{IC} = 80 knots)

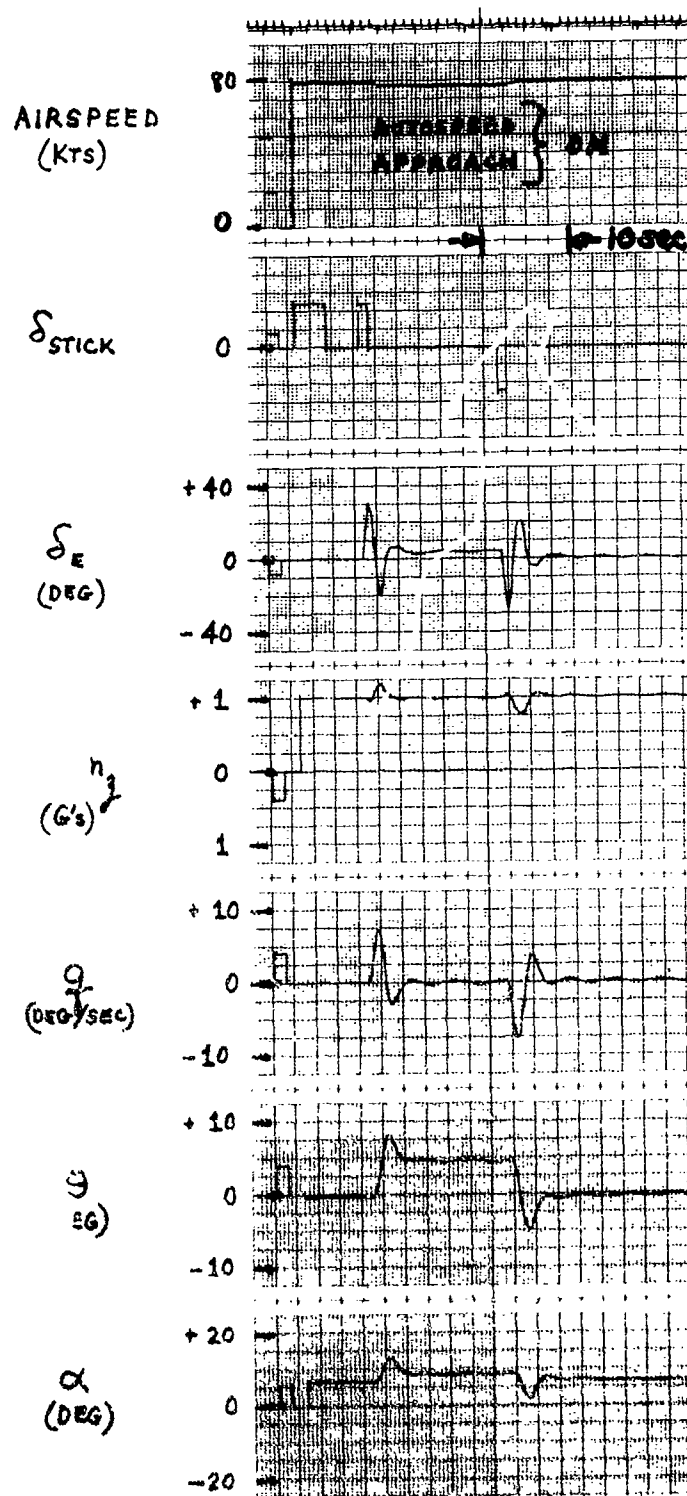


Figure 4-28. MBS Augmented Pitch Response to a Pulse of δ_{stick}
 (3700-ft Altitude, $\gamma_{IC} = -7$ deg, Flaps = 60 deg, Gear
 Down, Speed_{IC} = 80 knots)

small oscillations that follow the transient responses for the MBS are the result of a dynamic reaction between elevator servo dynamics and the computer frame time for this problem. Because of the slower computer speed at the MBS, the frame time required to execute all computations once was about five times longer than for the FBS with identical software. The software program was reduced in length by careful elimination of certain computations not essential to the moving-base evaluation work. The responses of Figure 4-28 were obtained using the reduced software program with the noted results. Frame time had been reduced to 69 milliseconds, the minimum that would accommodate turbulence and engine failure simulation in conjunction with basic flight operations. This updating of the problem parameters approximately 16 times per second was too infrequent to accommodate the assumed elevator servoactuator response bandwidth of nearly 6.4 Hertz. The rudder servoactuator had been assigned the same response bandwidth, and oscillations were also observed in the rudder responses. With the turbulence model off and normal engine operation, it was possible to reduce the frame time of the MBS program to 58 milliseconds and the oscillations did not appear. The expedient adopted to solve the problem was to alter the servoactuator implementation to produce instantaneous response to input signals. This permitted full simulation capability at the MBS within the 69 millisecond frame time. Figures 4-29 and 4-30 show the FBS and MBS aircraft responses to a rudder pedal pulse. The MBS response was taken after the removal of rudder servo dynamics, and there are no post-transient oscillations as were seen in Figure 4-28. The augmented responses of Figures 4-29 and 4-30 are essentially identical, as were the roll and pitch responses after the high-performance servoactuator dynamics were removed.

The changes to software made to reduce frame time at the MBS were generally to eliminate logic and unnecessary computations. Line printer data storage, for instance, was not required. In the control subroutines, alternative system gains and network parameters and the associated logic were removed. Also, control modes not to be evaluated were removed. The Gaussian form of turbulence was chosen, since the non-Gaussian form required more frame time to generate. This choice was partly based on the pilot opinion that the difference between the two seemed negligible.

4.2 STAI PILOT QUALITATIVE EVALUATION

The simulated flight evaluations of the three STOL aircraft configurations, which included externally blown flap (EBF), internally blown flap (IBF), and vectored thrust (VT) versions, were generally based on an Experiment Design plan prepared in the early stages of this work. This section includes a summary of the pilot's qualitative comments collected over the evaluation period. Additional data includes test plans, evaluation criteria, and a representative sample of the data runs, which appear in the appendixes.

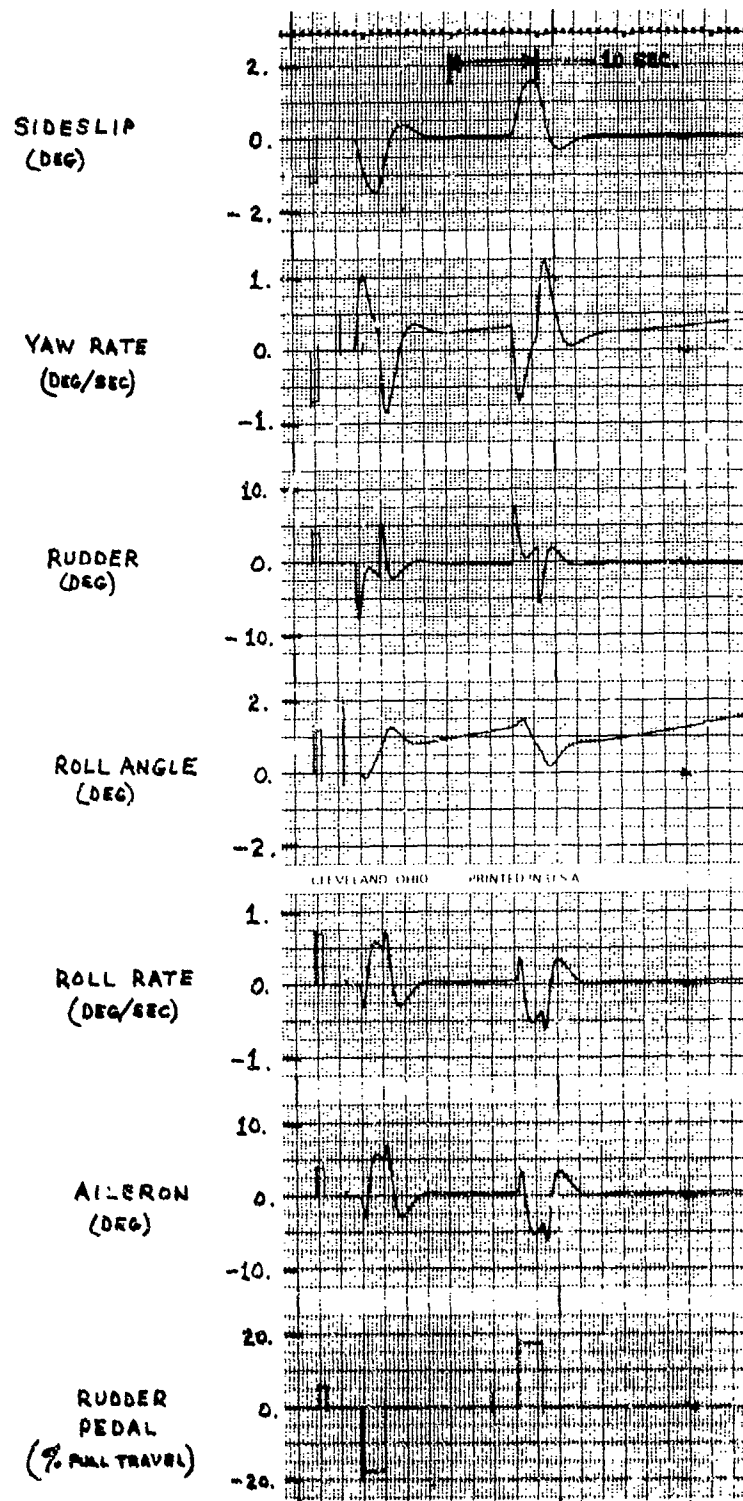


Figure 4-29. FBS Augmented Yaw Response to a Pulse of Rudder Pedal
 (3700-ft Altitude, $\gamma_{IC} = -7$ deg, Flaps = 60 deg, Gear Down,
 Speed_{IC} = 80 knots)

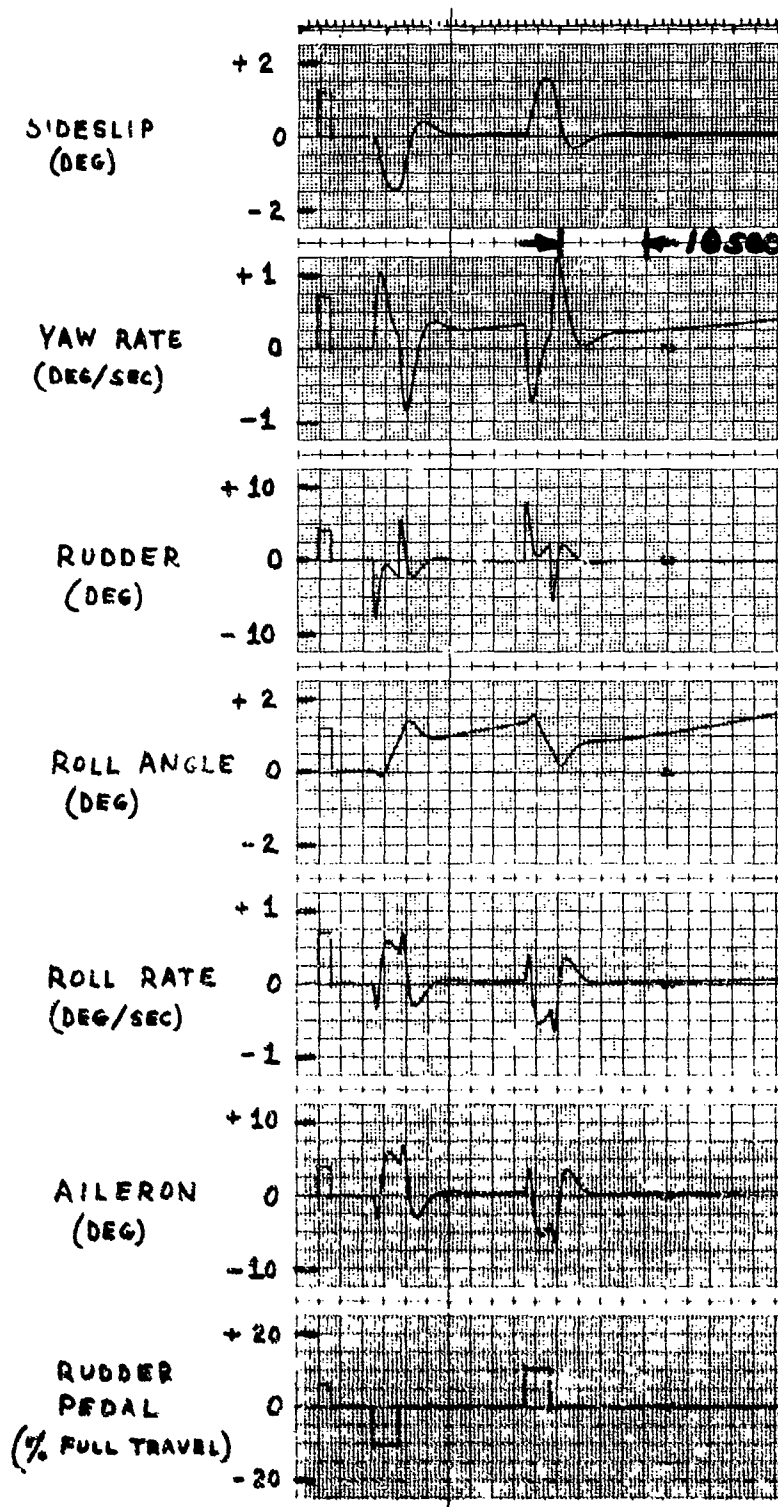
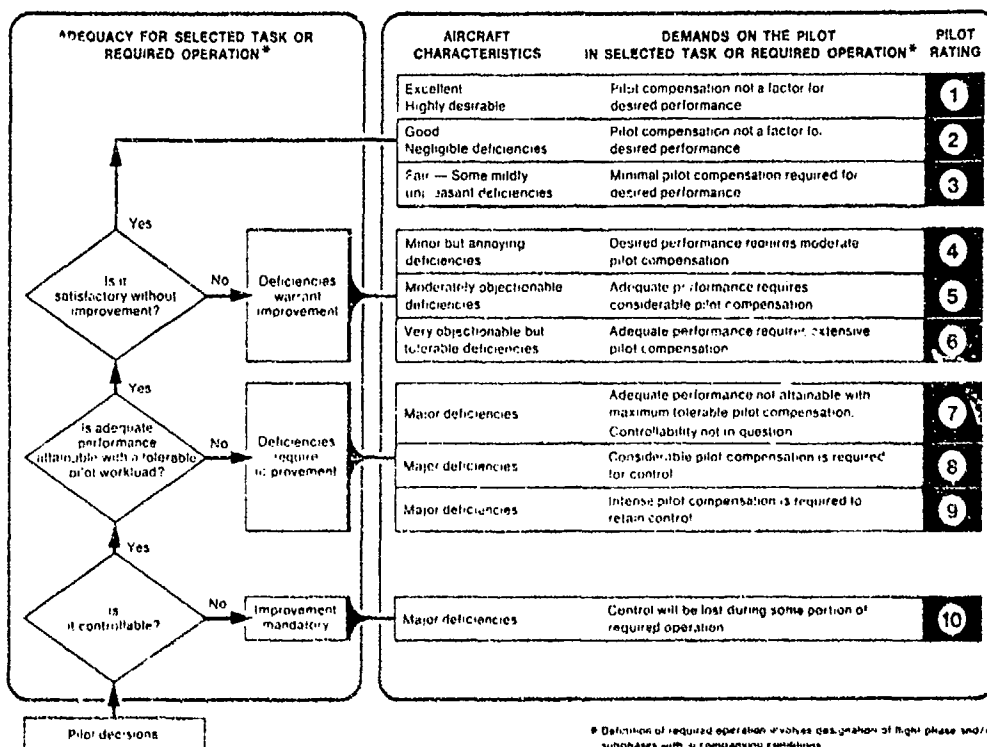


Figure 4-30. MBS Augmented Yaw Response to a Pulse of Rudder Pedal
 (3700-ft Altitude, $\gamma_{IC} = -7$ deg, Flaps = 60 deg, Gear Down,
 Speed_{IC} = 80 knots)

The evaluations recorded throughout this program were those of a highly qualified engineering test pilot assigned especially for this work. A graduate of the USAF test pilot school, the evaluation pilot was experienced in use of the Cooper/Harper (C/H) rating scale, Table 4-4, which was used extensively in this work. His primary flight experience background includes USAF and USN fighter aircraft, with secondary experience in utility, transport, bomber, and helicopter aircraft. In each STOL

Table 4-4. Cooper/Harper Handling Qualities Rating Scale



version evaluated, a large number of simulated flight runs were flown for orientation to minimize the effects of a learning curve on pilot ratings. Evaluations were recorded after these orientation sessions. The original intent was to have two pilots perform the simulation tasks but, because of the very large number of tests, it was decided to limit the evaluations to one engineering test pilot. It was also concluded that a single pilot's evaluations would provide better continuity to the comments, better comparative evaluations of the alternative STOL configurations, and better comparative observations as to fixed-base versus moving-base simulator effectiveness.

The Terminal Flight Phase as defined in MIL-F-8785-ASG and MIL-F-83300 provided the scope of the evaluation. This flight phase was further divided into subcategories of approach, flare/touchdown, go-around, and transition. Except for the flare/touchdown subcategory, each of the three general aircraft configurations were evaluated over each of these subcategories. The flare/touchdown subcategory was evaluated only for the externally blown flap configuration because there was no ground

effect data for any of the configurations during the evaluation period. Over 150 hours of piloted simulation and 3000 data runs were accomplished during the total evaluation program.

Simulation facilities, cockpit instrumentation, data facilities, and control systems (including definitions of APPROACH and AUTOSPEED modes) are described in other sections of this volume.

Evaluation of the approach subcategory of the terminal flight phase began with the STOL final approach configuration established and the aircraft trimmed on a -7 degree flight path angle. The aircraft was located two miles from touchdown about 50 feet below the -7 degree desired glide path and 200 feet to the right of the localizer centerline parallel to the runway. The evaluation was performed until a 100-foot decision height was reached. Qualitative evaluation included the ability to control flight path angle on the glide slope precisely, control airspeed precisely, maintain alignment with the runway, and maintain visibility over the aircraft nose. Adequacy of the information displayed and the control techniques required in performing the maneuvers were also part of the evaluation. The techniques used included:

1. STOL. Control airspeed with pitch, control flight path angle with power.
2. Conventional. Control airspeed with power, control flight path angle with pitch.
3. Flapping. Control airspeed with power and pitch, control flight path angle with incremental flap adjustment.

Cooper/Harper (C/H) ratings were used extensively during this phase of qualitative evaluation to register pilot opinions as to controllability and desirability. The task was evaluated for VFR conditions, where desired glide path information was displayed by the horizontal needle on the ADI flight director and runway alignment was performed visually on the 60- by 1500-foot target runway. Steering information was available through the vertical needle on the ADI flight director.

Evaluation of the go-around subcategory of the terminal flight phase examined techniques and configurations carried from the approach subcategory evaluation. The evaluation began at a simulated 100-foot decision height (DH) on the -7 degree glide path and centerline and covered the flight until the aircraft was climbing back through the simulated DH. The aircraft was initially trimmed in the STOL approach configuration. The techniques used included:

1. Power addition only.
2. Power addition and pitch rotation simultaneously, followed by flap retraction upon reaching target pitch attitude.

3. Simultaneous power addition, pitch rotation, and flap retraction.

Depending on the technique used, the aircraft was reconfigured to a lesser flap angle during the go-around procedure. This configuration was assumed to be maintained throughout a subsequent GCA pattern until arriving at the position to begin re-configuration for another approach. Many of the tested reconfiguration combinations were eliminated early in the investigation, as they failed to effect a recovery in less than 100 feet. The remaining combinations were evaluated on the following criteria.

1. Airspeed

No large or rapid airspeed losses.
No airspeed loss preferable.
Airspeed increase and acceleration preferable.

2. Altitude

Minimum altitude loss preferable.
Time below 100 feet at a minimum.

3. Attitude

A positive attitude increase was felt to be psychologically preferred.
A nominal 3 deg/sec attitude increase appears very comfortable.
Ability to track a new attitude.
Attitude increase over 15 degrees not felt desirable from a visibility-over-the-aircraft-nose standpoint nor from an IFR-flying viewpoint.

4. Flight Path Angle

Positive and immediate increase in flight path angle.
Smooth and constant increase in flight path angle to a maximum value of at least 2 degrees positive.
No tendency to sag or reverse direction during flight path angle increase.

Although quantitative data was produced, it was generally handled in a qualitative fashion after meeting minimum values due to the many tradeoffs that had to be made to determine recommended procedures and control parameter values.

Evaluation of the flare/touchdown subcategory of the terminal flight phase for the externally blown flap examined techniques and configurations carried from the approach and go-around subcategory evaluation. Although ground effect data was not available for the evaluation, the effects of pitching moments and negative ground effect that must be overcome by control techniques and procedures were considered. The

evaluation began at various flare heights using radar altimetry from a trimmed -7 degree glide slope STOL configuration. The evaluation continued to landing gear touchdown. The techniques used were:

1. Flare to final pitch attitude by pitching only.
2. Flare with power addition only.
3. Flare to final pitch attitude by pitching and power addition to overcome probable negative ground effect (≈ 10 percent power addition).

Flare height evaluation above 100 feet was discontinued early in the study. These altitudes not only increased air distances significantly but caused large dispersions in sink rate at touchdown, as there was a marked tendency to balloon the aircraft. In addition, having a flare height above a 100-foot decision height did not appear to be operationally desirable. Flaring for touchdown could be accomplished without a pitch change by full power addition (Technique 2), which produced acceptable touchdown sink rates but left no margin for any negative ground effects. It also produced increased air distances as compared to other techniques. A pitch change technique was required if acceptable air distances (distance from a 50-foot height to touchdown) and touchdown sink rates were to be obtained for other than nominal laboratory test conditions. The following evaluation criteria were used to evaluate landing performance for the techniques and configurations of this subcategory.

1. Airspeed. Airspeed decrease at touchdown desired but of minor importance compared to minimizing air distances.
2. Flare Height. As wide a band of flare heights as possible to achieve acceptable performance and allow for varying terrain conditions.
3. Attitude. A nominal 3 deg/sec attitude change rate appeared desirable. Attitude increase over 15 degrees not desirable from a visibility-over-the-nose standpoint or from a probable geometry-limited touchdown attitude for structural clearance.
4. Air Distance. Most important parameter to minimize total stopping distance.
5. Touchdown Sink Rate. A mean value of less than 10 feet/sec was desirable from a design standpoint.

Evaluation of the transition subcategory of the terminal flight phase covered the transition to a STOL approach configuration in order to conduct a STOL approach to landing. This subcategory was divided into two phases. Phase I included transition from a cruise flight condition to an intermediate configuration and flight condition where final transition to the approach glide path could begin. Phase II included the transition

to a STOL final approach configuration and establishment of the aircraft on the approach glide path. The intermediate configuration and flight condition achieved in the Phase I transition was reverted to in executing a missed approach or go-around maneuver or for flying a typical GCA box pattern. A total transition from cruise configuration to an established approach glide path in one step was also evaluated. The following techniques were used.

1. Initial Transition. Cruise configuration through initial transition configuration change.
2. Final Transition. Initial transition configuration through final transition configuration change on the approach glide path.
3. Total Transition. Total transition from cruise configuration through final transition configuration change on the approach glide path.

The final flap setting for the approach configuration was carried from the previous subcategory evaluations as the final flap position that produced the best overall performance and response. The intermediate flap position to begin the final transition was carried from the go-around subcategory evaluation recommendation. Operationally, this flap position was suitable for flying typical GCA patterns and provided satisfactory handling qualities at reasonable power levels. It also minimized the large pitch changes that occurred during flap changes between 0 degree and the intermediate position. If desired, the aircraft could be configured to the 0-degree flap position for flying GCA patterns, but this is probably undesirable operationally unless tactical conditions warrant higher speeds associated with the 0-degree flap setting.

Although this subcategory evaluation used some quantitative data for purposes of analysis, it was largely handled by qualitative judgement using C/H ratings. Criteria used in the evaluation included:

1. Minimum power changes with no tendency to reverse power changes.
2. Minimum stick action with gradual change characteristics and minimal stick reverses.
3. Positive but no immediate large pitch change requirement with no tendency to reverse pitch action.
4. Ability to capture glide slope smoothly and quickly.
5. Minimal tendency to climb during configuration changes and ability to hold altitude with minimal stick and power adjustments.

4.2.1 EXTERNALLY BLOWN FLAP (EBF) EVALUATION. The EBF configuration was evaluated using the Convair Aerospace fixed-base simulator for the four sub-categories discussed in the preceding paragraphs: approach, go-around, flare/touchdown, and transition.

4.2.1.1 EBF Approach. The STOL technique using 60 degrees of flaps at 80 knots without the APPROACH and AUTOSPEED modes allowed accurate and precise control with satisfactory response characteristics to pitch needle deviation (± 15 degrees) by power changes alone. The tendency to overshoot the desired flight path when making large corrections by power alone was very slight, although evident in attempting to find the trim power setting required. This was only a minor annoyance, as the tendency to overshoot damped quickly as the flight path errors were reduced. The pitch-attitude-hold mode of the control stick allowed precise pitch attitude control even with large power changes. It also appeared to allow good control of airspeed during large power changes, although a large reduction in power to correct flight path errors tended to allow airspeed to decrease 2 to 3 knots off the 80-knot trim airspeed. Power additions, once the airspeed had been lost, had very little effect in correcting the airspeed although it gave a large corresponding decrease in flight path angle. Use of pitch to correct for the 2- to 3- knot loss was effective, although a relatively long time was involved in making the airspeed correction. This decrease in pitch attitude also appeared more effective in changing flight path angle which, together with power, would correct the airspeed error. This resulted in an increase in pilot workload to the extent that usually there was no feeling or desire to make a rapid correction to the airspeed error but rather to set a trend condition of pitch and power that would eventually resolve the error. The use of a large power correction alone to effect a change in flight path angle had very little effect on airspeed, with a typical increase of about 1 knot. This condition was rated at 3.

The STOL technique using 60 degrees of flaps at 80 knots with APPROACH and AUTOSPEED modes proved to be among the most accurate of all methods examined. Pilot task loading was minimal and natural enough to allow an excellent feeling of control and response. The APPROACH and AUTOSPEED modes, although probably not required for these flight conditions, are desirable features in reducing pilot concentration and task loading as compared to the same tasks without these modes. The same minor annoyance of finding a trim power setting also existed. This condition was rated at 2-1/2. The conventional technique using 60 degrees of flaps at 80 knots without the APPROACH and AUTOSPEED modes was acceptable, but increased the pilot workload and concentration greatly. This did not appear to be a natural method of control. Deviations and control inputs were large, with only a slight tendency to reduce the deviations as the flight progressed. The control inputs appeared to be chasing the deviations, giving the feeling that flying this method was like flying an actual aircraft in moderately turbulent conditions. It appeared desirable to attempt to trim the longitudinal axis due to the low frequency of these deviations. Constant reference to the thrust indicator was required to attempt to fly closely around the known trim conditions. This condition was rated at 6.

The conventional technique using 60 degrees of flaps at 80 knots with the APPROACH and AUTOSPEED modes was better than without the modes, but did not reach the level of the STOL technique without these modes. Although airspeed deviations were less than 2 knots, pitch variations were only slightly less than without the APPROACH and AUTOSPEED modes. This reduced the pilot tasks slightly, but still required considerable effort in pitch control. The glidepath deviations were less, but a constant requirement to decrease the pitch attitude (-4 degrees) of the aircraft was apparent as the aircraft approached the flare point. This was slightly uncomfortable, although the situation was certainly acceptable. This condition was rated at 5.

The flapping technique using 60 degrees of flaps at 80 knots proved to be uncontrollable for conditions both with and without the APPROACH and AUTOSPEED modes. For very small deviations below the glide path, there is no flap adjustment possible as the flaps are already at the maximum lift condition of 60 degrees. For very small deviations above the glide path, a flap angle decrease will increase the glide path angle to correct the error. If this correction is not large enough initially, the error appears to diverge further. This requires another decrease in flap position which, although initially effective in reducing error, allows the airspeed to increase substantially (10 to 15 knots), which again makes the flight path shallow. As power is reduced to correct the airspeed error, control input oscillations begin, making control of the aircraft impossible. This condition was rated at 10.

The STOL technique using 45 degrees of flaps at 80 knots without the APPROACH and AUTOSPEED modes required a trim power setting of 61 percent as compared to 76 percent with 60 degrees of flaps. This allowed a more rapid correction of large glidepath deviations. Attendant small errors were as closely controlled as when 60 degrees of flaps were used, but with a subtle feeling of better control of flight path angle. Power changes created a slightly increased rate of airspeed change, but the magnitudes did not appear to be noticeably larger than with the 60 degrees of flaps. This caused some initial concern with thoughts of overcontrol, but no problems occurred. The chief effect of 45 degrees of flaps was to cause a deterioration in the lateral-directional-handling qualities. This deterioration appeared to be in the form of problems in turn coordination by large β excursions with limited damping and a roll oscillation problem. As a result, there was an increased requirement on pilot concentration to maintain runway alignment. This condition was rated at 4.

The STOL technique using 45 degrees of flaps at 80 knots with the APPROACH and AUTOSPEED modes again allowed decreased pilot attention to airspeed control, although the requirement for close control of airspeed without these modes has not been apparent for the conditions examined thus far. The problems of turn coordination and roll oscillation were again obvious, which tended to overshadow the desirable rapid response of glide path angle to changes of power. This condition was rated at 3-1/2.

The conventional technique using 45 degrees of flaps at 80 knots without the APPROACH and AUTOSPEED modes presented the same general problem as when 60 degrees of flaps were used, although it caused wider pitch oscillations to control flight path angle. The same annoyance of a loosening of the lateral-directional characteristics caused a still further increase in pilot workload and concentration, all of which caused this configuration to be termed unacceptable. This condition was rated at 7.

The conventional technique using 45 degrees of flaps at 80 knots with the APPROACH and AUTOSPEED modes appeared acceptable, although considerable pilot attention was required to achieve this acceptability. The comments concerning the 60-degree flap condition are generally applicable for the 45-degree flap, with the addition of the decreased desirability of the lateral-directional handling qualities and the requirement for larger pitch changes for glide path angle corrections. This condition was rated at 6.

The flapping techniques using flaps nominally at 45 degrees at 80 knots with and without the APPROACH and AUTOSPEED modes was initially somewhat improved over the 60 degrees of flaps condition, although the flight deteriorated to the extent that controllability was obviously lacking. For small errors, positive corrections could be made by raising and lowering the flaps incrementally about a set value, but interaction of the lift/drag relationship of the flaps and the throttle required maximum skill for control. If pitch needle deviations became large (> 3 to 5 degrees), the interactions were much too degrading to allow positive control. This condition was rated at 10.

Since the STOL technique was the obvious choice, further work used only this method. Also, because of excellent airspeed and glidepath control without the APPROACH and AUTOSPEED modes, it was decided to continue the investigation in the approach subcategory without these modes. Although this was consistently thought to offer a C/H rating of 1/2 less than when these modes were used, it offered a more identifiable pattern of responses for evaluation.

The 50 degrees of flaps at 80 knots condition constituted an improvement in the lateral-directional-handling qualities as compared to the 45-degree setting. The rapid response to throttle coupled with precision control of both large and small errors made the 50-degree setting slightly more desirable than the 60-degree configuration. This condition was rated at 2-1/2.

Using 55 degrees of flaps at 80 knots also improved the lateral directional-handling qualities over the 50-degree setting, although only slightly. An improvement in overall rating was offset by the slight tendency toward a more sluggish response of power to flight path angle control. This condition was rated at 2-1/2.

The use of 45 and 60 degrees of flaps at 85 knots showed good controllability aspects but there was an annoying tendency to show too rapid an increase in airspeed due to power changes for flight path angle corrections. This again appeared to be bound by a ± 3 -knot margin, but the general feeling was one of discomfort because things appeared to be moving too fast both in flight path angle corrections as well as in speed responses. This did not appear to warrant further evaluation. These conditions were rated at 3-1/2.

Using 45 and 60 degrees of flaps at 75 knots showed the same deterioration of lateral-directional-handling qualities as in the 80 knot/45 degrees of flap setting, probably due to the higher angle of attack. Trim power for 45 degrees of flaps was 77 percent as compared with 82 percent for 60 degrees of flaps. The deterioration in glide path angle response to power at 60 degrees of flaps for large glide path deviations was obvious in moving to the higher trim power setting, giving less than well behaved characteristics. These did not appear to be desirable conditions for further evaluation, and were rated at 4.

The lack of enthusiasm about the APPROACH and AUTOSPEED modes was due to three characteristics. The first was an appearance of insensitivity of airspeed to small (± 2 to 3 degrees) pitch changes, although it was easier to lose 2 to 3 knots than to gain airspeed. Once the airspeed was lost, an uncomfortable pitch change (> 4 degrees) was required for precise flight-path following. When the airspeed had degraded 2 to 3 knots, however, the trim setting appeared to settle down and no more airspeed was lost. The second characteristic was the addition of a pitch-attitude-hold capability in the longitudinal axis. This tended to minimize any longitudinal oscillations and thus minimized further loss of airspeed due to those oscillations. It also appeared to subdue the effects of the short-period frequency and the phugoid being so close together. The third characteristic was the lack of a turbulence model at the time of the EBF evaluation. The addition of turbulence could necessitate the need for these modes.

The effectiveness of pitch attitude control of airspeed was demonstrated by reverting to the bare airframe and flying without the attitude-hold feature. This also demonstrated the importance of knowing the trim attitude for a particular configuration, airspeed, and aircraft weight. Approaches were made with 50 degrees of flaps at 80 knots with the ADI attitude indicator offset about +9 degrees from the zero reference. Difficulty was encountered, and increased pilot concentration was required to hold airspeed within 5 knots and the flight director indicator (FDI) glide path needle deflections within 5 degrees. A C/H rating of 7 was assigned to this condition because of the pilot's tendency to oscillate without finding a trim point, even though it was known that +9 degrees would result in a fairly stable airspeed of 80 knots. In addition, to the reduced pitch damping of the unaugmented control mode, the lack of an attitude reference mark at the +9 degree attitude contributed to the tendency to oscillate. The next run was accomplished under the same conditions except that the 0-degree reference point on the ADI was used as the 80-knot trim attitude. This showed a marked decrease in pilot workload with considerable improvement in accuracy.

allowing a C/H rating of 5. Knowing that the trim airspeed attitude was at the 0-degree ADI position rather than at + 9 degrees demonstrated the large benefit that could be achieved by knowing and being able to set the trim attitude reference to 0 degrees for the variable parameters of the aircraft. This allowed reasonable control and capture of airspeed, with resultant reasonable control of flight path angle by virtue of power control.

4.2.1.2 EBF Go-Around. The test data indicated that 60 to 70 feet of altitude loss was as good as could be obtained. A pitch rate increase to 6 deg/sec from a nominal comfortable 3 deg/sec produced no noticeable decrease in altitude loss although it tended to produce considerable oscillation in trying to stabilize on the target pitch attitude. The power-addition-only technique was not investigated in depth because the power addition introduced a transient pitchdown rate sufficient to excite a longitudinal dynamic mode with a period of about 15 seconds. Techniques 2 and 3 were evaluated fully, with 3 becoming the desired technique. Technique 2 was continued, however, as it produced data of a safety nature describing the flight results if the flaps were delayed upon initiating a go-around condition. For Technique 3, the flap rates investigated did not appear to be a factor in achieving recommended procedures and parameters. If Technique 2 was used, however, the flap rate value of 5 deg/sec produced the best characteristics, largely by minimizing airspeed losses. For Technique 3, performance appeared insensitive to combinations of APPROACH and AUTOSPEED modes. For Technique 2, it was desirable to keep the airspeed-hold feature in operation until reaching the final flap position to prevent excessive airspeed loss. Airspeed losses were greater at the 60-degree initial flap setting than at the 50-degree initial setting when the APPROACH and AUTOSPEED modes were not used.

Remaining comments in this paragraph apply to Technique 3, since it became the baseline technique. Flight path angle response was very sensitive to final flap position; a 40-degree final flap setting was found to be the desired value. This sensitivity increased and performance deteriorated beginning with a 60-degree initial flap position and going to a 50-degree initial flap setting. Although lower final flap settings (< 40 degrees) allowed a very rapid and desirous airspeed increase, it did so by allowing the flight path angle to sag and to have dangerous reversal characteristics. Airspeed increase with the 40-degree final flap setting was better at a 55-degree initial flap setting. There was thus a compromise between a desirable airspeed increase characteristic and an undesirable altitude loss. At the 50-degree initial flap setting, airspeed increase was negligible with no noticeable increase in flight path angle or decrease in altitude loss as compared to other flap settings, although the time below the 100-foot decision height was slightly less (14 seconds) than for the 55- and 60 degree initial flap settings (17 and 18 seconds, respectively). The 55-degree initial flap setting with the 40-degree final flap setting appeared to offer the best overall characteristics. The 40-degree final flap setting was a satisfactory configuration for continuing a GCA pattern for another approach. The aircraft could

accelerate safely to climb or cruise speed by manually raising the flaps from 40 degrees to 0 degrees at an average rate of 1.5 deg/sec to continue the climb while accelerating in airspeed. An automatic function for retracting flaps beyond the 40 degree stop, which was judged satisfactory, was also investigated. This scheme would allow the flaps to retract all the way based on maintaining a designated minimum positive flight path angle during retraction. Relief of pilot work load was the primary advantage offered by this feature.

The go-around target attitude was investigated to examine the sensitivity to undershooting and overshooting the target attitude. The undershoot investigation of the target attitude of 10 degrees by 5 degrees for the 60- and 55-degree initial flap settings showed that about 100 feet of altitude would be lost. However, the aircraft could accelerate approximately 20 knots by the time the aircraft had climbed backed through its decision height of 100 feet (about 22 seconds). The general operational tendency, however, would probably be an error in overshoot of target attitude. Again, the 60- and 55-degree initial flap settings gave similar results for pitch overshoots, which showed this to be a safe error. There was a desirable tendency for the airspeed increase to be greater for the 55-degree initial flap setting.

Technique 2 simulated the effects of a delay in flap retraction upon initiating a go-around. As found in Technique 3; this technique showed a nominal altitude loss of 60 to 70 feet. Using the 55-degree initial flap setting with Technique 2, the APPROACH and AUTOSPEED modes proved valuable by minimizing airspeed losses and time spent below the 100-foot decision height (3 knots loss and 24 seconds below 100 feet as compared to 9 knots loss and 32 seconds below 100 foot without these modes). For the 60-degree initial flap setting using the APPROACH and AUTOSPEED modes, the values were similar to the 55-degree initial flap setting without the APPROACH and AUTOSPEED modes. Again, the 55-degree initial flap setting appeared to offer safety for this type of potential pilot error.

The recommendation is to use Technique 3 with an initial flap setting of 55 degrees, going to 40 degrees at a flap rate of 5 deg/sec during the go-around procedure. A pitch attitude change of 10 degrees should be accomplished. The C/H rating for the go-around was a satisfactory 3.

4.2.1.3 EBF Flare/Touchdown. Data generally indicated that the minimum air distance obtainable within the desired touchdown sink rate was 350 to 375 feet. Analytic calculations showed that a total stopping distance of 1800 feet is required for worst-case weight and cg locations. This distance includes 400 feet of air distance, leaving 1400 feet as the total ground distance. If total runway plus overrun distance is 2000 feet, air distances up to 600 could theoretically be used but air distance should be minimized for any recommended technique or configuration.

Pitch rate variations were evaluated from 2 to 7 deg/sec. The slower pitch rates had very little effect on air distance covered or touchdown sink rate as long as the pitch attitude change was at least 5 degrees immediately before touchdown. The faster pitch rates could be used at the lower flare heights (60 feet), although this was considered a maximum-effort technique for which timing was critical. For as little as ± 10 feet about a 60-foot flare height, the aircraft would suffer a hard landing or balloon at these initial altitudes. With the higher pitch rates, there was also a marked tendency to overshoot the target attitude and to begin pitch oscillations.

There were only slight differences in landing performance when APPROACH and AUTOSPEED modes were active. This was because the interconnections compensate each other when pitching to flare; i. e., the flaps are raised 10 degrees automatically to minimize speed loss but the power is increased about 10 percent to compensate for lift reduction due to the flap action. Although these modes are primarily for the approach subcategory, they have little effect on landing performance. Results indicate there is no requirement to turn them off for the flare and touchdown subcategory if they are being used in the approach phase. This differs from the conclusion drawn in the go-around phase where it is recommended to turn these modes off for optimum go-around results. Runs with flap settings of 55 and 60 degrees showed no discernible difference in landing performance. The effect on touchdown sink rate by having the APPROACH and AUTOSPEED modes active depended on pitch attitude change and flare initiation height. For a small attitude change starting at the lower flare-initiation height, rate of sink at touchdown was slightly greater with the modes active than without. However, when a higher pitch attitude change was employed, the rate of sink at touchdown was somewhat less (by about 2 ft/sec) with the modes active. There was no appreciable difference in air distance with the modes active or inactive for runs employing similar techniques.

An increase in either pitch attitude change greater than 5 degrees or in flare height above 70 feet tended to increase air distance with a decrease in touchdown sink rate. This ranged from an air distance of 375 feet at an 11 ft/sec touchdown sink rate at 5 degrees of pitch attitude change and a 70-foot flare height to a severe ballooning effect at 20 degrees of pitch attitude change and a 100-foot flare height. The minimum sink rate of 4.5 ft/sec occurred at 15 degrees pitch attitude change and an 80-foot flare height. Increasing either the pitch attitude change to 20 degrees or the flare height to 90 feet caused the aircraft to balloon, which increased air distances about 125 feet and sink rate to a nominal value of 8 ft/sec. Using 10 degrees as a reference pitch attitude change for flare heights between 70 feet and 90 feet showed air distances increasing from 350 to 525 feet, with respective touchdown sink rates of 10 and 6.5 ft/sec. This appeared to be the best pitch attitude change for variations in flare height due to operational considerations to provide the best overall landing performance. Operational tolerances such as pitch attitude change variations between 5 and 15 degrees still gave the desired landing performance.

The optimum and recommended conditions are thus a 10-degree pitch attitude change occurring at a flare height of 80 feet to give a nominal value of 400 feet air distance and 6 ft/sec touchdown sink rate. This technique carries with it the recommendation from the go-around and approach subcategory evaluations of an initial flap setting of 55 degrees. Also, this technique and configuration can be flown equally well with or without the APPROACH and AUTOSPEED modes.

A slight power addition of 10 percent was used with this recommended technique and configuration to reflect the ability of a power increase to overcome the probable negative ground effects. This power addition reduced the touchdown sink rate to 3 ft/sec, demonstrating the adequacy of power to overcome these effects. The control system was considered adequate to handle probable aircraft pitching moments resulting from ground effects.

The recommended techniques and configurations with operational variations considered will safely warrant a C/H rating of 3, with pitch attitude changes greater than 15 degrees dropping the C/H rating to 4.

4.2.1.4 ERF Transition. This discussion covers three types of transition: final, initial, and total.

4.2.1.4.1 Final Transition. This evaluation included initiation at airspeeds from 125 to 80 knots. The faster flap rate of 5 deg/sec was regarded as inferior to the lower flap rates because the pitch change required to maintain altitude is too rapid. The 5 deg/sec flap rate also created annoying and sometimes objectionable pitch reversals, causing an added pilot workload. The slower flap rates gave the pilot the impression of being in better control during the transition. The flap rate of 1.5 deg/sec was listed as unsatisfactory because it extended the transition time, although it was an easy transition to control. The 3 deg/sec flap rate produced the best overall C/H ratings. C/H ratings of 4, 4, and 3 accompanied the respective flap rates of 5, 1.5, and 3 deg/sec at 115 knots. The remaining discussions of final transition pertain to the 3 deg/sec flap rate.

Although final transition to the approach glide slope could be performed acceptably from initial airspeeds of 80 to 125 knots, the final transition for this study was initiated only between 90 and 115 knots. In evaluating the final transition at an initial airspeed of 80 knots, there was a large and immediate pitchdown requirement of about 12 degrees, with a power reduction requirement of nearly 17 percent from the 86 percent level required for trimmed level flight. These actions required critical coordination and timing by the pilot and were considered objectionable, resulting in a C/H rating of 5. The associated angle of attack at 80 knots was also fairly high (14 degrees). At an initiation speed of 125 knots, which also rated a C/H value of 5, the aircraft gave an uncomfortable feeling of flying nose low with an angle of attack of -1 degree. In addition, the transition caused both pitch and stick reversals (to prevent initially climbing) and a subsequent excessively steep glide slope angle. The total pitch change reversal was 10 degrees.

At initial airspeeds of 90 and 115 knots, the C/H rating was 3, indicating that this range of initial airspeeds produced satisfactory results. The 90-knot initial airspeed was satisfactory in that it produced positive and smooth results within about 12 seconds. A power reduction requirement of 7 percent and a pitch change requirement of 8 degrees with no reversals appeared comfortable and were easily controlled. At 115 knots, the pitch change requirements were even smoother and more easily followed. The pitch attitude required from the beginning of final transition to the pitch attitude required at the end of the transition was only 1 degree, although a non-objectionable intervening pitch reversal of 4 degrees was required. There was no power change requirement throughout the transition with this condition, as the trim power setting was the same from the beginning of the transition to that required on the glide slope. This was felt to be a very desirable characteristic. The 115 knot initial airspeed transition, however, required nearly 33 seconds to complete. This would require about 400 feet of vertical glide slope information to be displayed by the glide slope bar to key the start of final transition. At 125 knots initial airspeed, this would require about 1200 feet of the same information due to both the increased speed and the increased time to complete the final transition.

The recommended technique, therefore, is to initiate final transition at airspeeds between 90 and 115 knots, with a flap rate of 3 deg/sec. Flight director computations should include the additional vertical glide slope information required to allow the transition to be initiated in a timely fashion.

4.2.1.4.2 Initial Transition. This evaluation included the range of initial airspeeds from 170 to 140 knots. Initial transition proved to be a more troublesome task than final transition. None of the flap rates investigated were given a satisfactory C/H rating. A flap rate of 5 deg/sec at 155 knots was unacceptable with a C/H rating of 7. With the higher flap rates, large and rapid pitch changes with large pitch reversals were required. Although this condition was controllable, pilot compensation was very high; even with the high compensation, altitude control was very poor. The 1.5 deg/sec flap rate at 155 knots was not satisfactory, but was awarded an acceptable C/H rating of 4. The nearly 50 seconds needed at this condition was not detrimental for initial transition, but pilot workload was greater than required for an initial transition at 145 knots and 3 deg/sec. At the 155 knot, 1.5 deg/sec flap rate condition, pitch reversals were slight and easily compensated by the pilot. Using a 3 deg/sec flap rate at 155 knots created a peak pilot demand that tended to be slightly higher than the 1.5 deg/sec flap rate. This condition rated a C/H value of 5. At 145 knots and 3 deg/sec flap rate, pitch reversals were not evident although the total attitude change of 15 degrees was an annoying characteristic, as it was at 155 knots. The 145 knot, 3 deg/sec flap rate condition was rated 4. At 170 knots, the 3 deg/sec flap rate was rated acceptable (C/H = 6) due to objectionable pitch reversal characteristics.

The recommendation for initial transition is to initiate the transition between 145 (over-the-nose visibility restriction) and 155 knots at flap rates between 1.5 and 3 deg/sec. The airspeed envelope could probably be extended safely beyond 155 knots by using a flap rate value of 1.5 deg/sec, although this was not investigated. Even at flap rate values up to 3 deg/sec, it was felt that the airspeed envelope could be extended safely up to 170 knots if a deterioration of precision flying and increased pilot workload proved acceptable to the operational agency. Starting initial transition below 140 knots was not desirable even assuming that visibility would be adequate, because the 15-degree angle of attack cut into the gust margin of safety for stability and control.

4.2.1.4.3 Total Transition. This transition, using an initial airspeed of 155 knots and a 3 deg/sec flap rate, was acceptable but at a rating of 6. It presented an unsatisfactory demand on pilot concentration and workload even though there was no doubt about safety, and was not considered a precise method of intercepting the glide path for the approach. Transition to a STOL configuration should therefore be effected in two separate steps. The intermediate flap position for the two-step transition technique should be 40 degrees for the EBF configuration.

4.2.2 INTERNALLY BLOWN FLAP (IBF) EVALUATION. Flight simulator evaluations of the IBF configuration were conducted for two versions. Preliminary evaluations using a simple IBF version were unacceptable and gave way to a modified version in which the non-diverted engine flow was vectored downward at the same angle as the nominal flap setting.

4.2.2.1 IBF Approach. Evaluation of the simple IBF configuration produced some unacceptable characteristics. In general, at speeds of 70 to 100 knots for flap angles of 60, 70, and 80 degrees, the aircraft flew much the same as did the externally blown flap configuration. Engine response, however, was unacceptable due to the large time constant effective at the lower trim thrust levels. Initial attempts at acquiring and following a -7 degree flight path angle received a C/H rating of 9. The engine response lagged sufficiently to cause a great deal of power lever overcontrol, which at times nearly diverged into an out-of-control condition. Practice and discipline at setting the power at the required power setting between 30 and 40 percent and using small incremental changes interspersed by time delays produced C/H ratings of 6 in this mechanical and controlled situation. Adding a drag device to bring the required power setting up to a nominal 60-percent setting could conceivably produce satisfactory ratings for these configurations. (The control difficulties discussed here resulted from the low trim power settings required for this configuration. At these lower power settings, the engine response to power change commands is quite sluggish. The addition of drag brakes, which would increase trim power requirements, was evaluated in a non-real-time simulation of this configuration. It was found that, for the slow approach speeds desired, speed brakes of the largest reasonable size did not generate sufficient drag to increase the trim power settings to a range where engine response was significantly better.)

In addition, the flight path angle versus airspeed characteristics at the desired STOL approach speeds produced a sharply deteriorated control condition upon loss of airspeed at constant power settings. The aircraft handled and responded well for airspeeds of 85, 90, and 95 knots at respective flap angles of 80, 70, and 60 degrees, all of which produced angle-of-attack values of about 14 degrees. However, any decrease in airspeed with constant power settings of as little as 2 knots led to stall conditions with angle of attack exceeding 25 degrees. It appeared that as the airspeed decreased, causing the angle of attack to exceed a nominal 16 degrees, a subsequent increase in airspeed by as much as 5 knots did not halt the increasing angle of attack before exceeding a 20-degree angle of attack. This was unacceptable from an operational consideration of turbulence and workload at these STOL airspeeds. Higher airspeeds must, therefore, be used with the IBF configuration to avoid this adverse control situation. An AUTOSPEED mode should also be used. This mode could be initiated automatically when configuring to a STOL approach. The higher airspeeds, however, appear to defeat the primary advantage of the STOL concept. This IBF configuration would have to be improved before suitable C/H ratings of handling qualities could be generated.

4.2.2.2 IBF/VT Approach. The simulated IBF aircraft using vectored thrust (VT) handled and performed much like the EBF configuration, with great improvement over the IBF not incorporating partial vectoring of thrust. (For the IBF/VT configuration, the undiverted engine flow was vectored downward at an angle proportional to the nominal flap deflection; i. e., AUTOSPEED flap motions were not a factor in the angle of vectoring.) One major difference was noted, however: there was a positive pitching moment with an increase in power that proved annoying during precise flying. This pitch-up motion was a nominal 3 to 4 degrees with a power increase of about 10 percent. A power reduction of the same amount, however, produced only a 1- to 2-degree pitch-down attitude, tending to cause slight power overcontrolling. As the aircraft pitched due to a power addition to correct to the glide slope, the horizontal needle on the ADI seemed to move indicating that a further increase in power was required. This problem appeared to diminish slightly through experience, but it was still noticeable throughout the evaluation at all flap positions. The problem tended to become more aggravated at the lower flap settings, which required lower power settings to maintain a -7 degree flight path angle. Operating at these lower power settings involved longer time constants for power response, further contributing to the apparent power oscillations in correcting glide slope errors. The APPROACH and AUTOSPEED modes contributed to more precise flying and a reduction of pilot workload throughout the evaluation, especially at the lower flap angles (as compared to the EBF configuration).

The higher flap angles (up to 70 degrees) allowed flying at slower airspeeds (down to 70 knots) at an acceptable rating. However, these lower airspeeds without the

APPROACH and AUTOSPEED modes caused airspeed dispersions up to 4 knots in some cases, which were annoying and caused an increased pilot workload in providing more precise control of airspeed. At 70 degrees of flaps and 80 knots, the aircraft was acceptably controllable although the pitch attitude gave an uncomfortable impression of flying nose-down throughout the approach. Angle of attack for this condition was 3 degrees, as compared to 7 degrees at 70 knots and 70 degrees of flaps. At 60 degrees of flaps and 80 knots, the aircraft appeared more lightly damped in the dutch roll mode at a +12-degree angle of attack than in the 70-degree flap conditions. The 50 degrees of flap at 90 knots condition with a 15-degree angle of attack appeared about the same as at 60 degrees of flaps. A compromise of 65 degrees of flaps at 80 knots produced the best overall C/H rating of 3.

Representative C/H ratings (with and without APPROACH and AUTOSPEED modes) are shown below.

Flaps (deg)	Airspeed (knots)	With Modes	Without Modes
50	80	4	5
50	90	4	4 1/2
60	80	3 1/2	4
70	70	4	5
70	75	4	4 1/2
70	80	4	4 1/2
65	80	3	3 1/2

The aircraft was also evaluated using conventional aircraft techniques, whereby airspeed was controlled by power and glide path by pitch attitude. This technique was unsatisfactory, resulting in a decrease in the C/H to 6 for 65 degrees of flaps and 80 knots.

Engine-out conditions using 65 degrees of flaps and 80 knots during the approach were considerably improved over the EBF configuration. Although sudden loss of an engine produced very noticeable roll and yaw, it was controllable to the extent that a failure at 800 feet AGL could be controlled and the approach could be continued to touchdown. A bank angle of 8 degrees would balance the aircraft into steady straight flight with no rudder force required. The APPROACH and AUTOSPEED modes proved very beneficial in controlling airspeed to negligible errors during and after the failure. This condition warranted a C/H rating of 6.

Turbulence evaluation using the Convair Aerospace modified MIL SPEC turbulence model indicated that controllability was not in question at 65 degrees of flaps and 80 knots. Extensive pilot compensation, however, was required for adequate performance. The longitudinal gusts, although very noticeable on the airspeed indicator,

seemed to null around 80 knots of airspeed. The vertical gusts caused the most challenging problem in tracking the glide slope. The lateral gusts continually excited the dutch roll mode, but was controllable throughout. A C/H value of 6 was assigned with the APPROACH and AUTOSPEED modes connected, and a C/H value of 7 was assigned when the modes were not used. With the APPROACH mode on, angle-of-attack changes would tend to automatically make the proper power correction to stay on the glide path. Coupled with manual attempts at correcting power for deviations in glide path, there was a tendency to overcontrol with manual participation. By setting a throttle lever angle that corresponded to the required normal trim power, manual power adjustments could for the most part be neglected. Using this technique tended to cause a reversion back to conventional aircraft techniques whereby glide path corrections could be better controlled by small pitch changes and airspeed was controlled by the AUTOSPEED function. This was not observed on flights without turbulence.

Further work in this area is recommended, as the observations suggest one technique of control when turbulence is encountered and another when turbulence is not encountered, leading to possible confusion in operational situations. The overall condition recommended is 65 degrees of flaps and 80 knots for the approach subcategory using the AUTOSPEED mode as desired.

4.2.2.3 IBF/VT Go-Around. The IBF/VT configuration during the go-around subcategory evaluation performed almost identically to the EBF configuration. Some differences were noted, however. The chief problem lay in finding a flap angle to be used as a final flap angle after retraction from 65 degrees such that airspeed would increase during go-around reconfiguration, the flight path angle would not droop and change directions, and a minimum of altitude would be lost.

A 45-degree final flap configuration proved the best compromise. Using the recommended procedure of retracting flaps to 45 degrees at the same time a positive pitch attitude and throttle increase were initiated, the aircraft could readily climb back to nearly +7 degrees flight path angle. Airspeed would increase nearly 8 knots and a maximum of 60 feet of altitude would be lost. This occurred regardless of whether the APPROACH and AUTOSPEED modes were used. Flap rates were investigated from 8 deg/sec to 1 deg/sec. The slower flap rates detracted both from the desired airspeed increase and the smooth and steady increase of flight path angle up to its maximum value. The higher flap rates appeared to offer the more desirable performance. Pitch attitude changes from 0 to 15 degrees offered a tradeoff between time spent below 50 feet (which was longer at the lower pitch attitude changes) and a desired increase in airspeed (which was higher at the lower pitch attitude changes). A pitch attitude change of 10 degrees was recommended.

The operational problem of delaying flap retraction until pitch attitude is obtained was evaluated. This condition was not as flexible as that in the EBF evaluation.

The IBF/VT aircraft was very sensitive, in that all flap rates produced a significant loss in airspeed before airspeed began to increase as well as a reversal tendency of the flight path angle. A 7 deg/sec flap rate minimized these conditions when the APPROACH and AUTOSPEED modes were connected. The same evaluation without these modes produced unacceptable results of a 10-knot loss in airspeed and a reversal of flight path angle back to nearly level flight before the aircraft began accelerating again. Since the 7 deg/sec flap rate again proved best, it is recommended for all operations.

For the go-around, a reconfiguration to 45 degrees of flaps from the initial flap setting of 65 degrees is recommended. A pitch attitude change of +10 degrees using a flap rate of 7 deg/sec with APPROACH and AUTOSPEED modes connected is also recommended. This was felt sufficient to warrant a C/H rating of 3 except for the condition where APPROACH and AUTOSPEED modes are not available and the possibility of a late flap retraction could occur. This latter set of conditions rated a C/H value of 7, indicating that system design should ensure against these occurrences.

4.2.2.4 IBF/VT Transition. Performing transition in the IBF/VT configuration proved to be more difficult than in the EBF configuration. In general, the IBF/VT configuration was more difficult to control precisely, reversals appeared more abrupt, and the change in technique from conventional aircraft control of attitude, airspeed, and flight path angle to the recommended STOL techniques was more apparent and required greater mental concentration to effect the change of techniques.

4.2.2.4.1 Total Transition. Complete transition from conventional flight to the STOL configuration in a continuous manner was judged unacceptable, primarily because of stick reversals (especially at 170 knots) and the difficulty in capturing the -7 degree flight path angle at 80 knots. Flap rates greater than 1.5 deg/sec greatly complicated control during the transition. Transition to the final STOL configuration should definitely be conducted in two phases. Phase I includes the transition to a 45-degree flap position, which is also the flap angle recommended for go-around. The final configuration includes the flap change from 45 to 65 degrees. Representative C/H ratings for total transition are shown in the following list. In general, higher flap rates resulted in poorer C/H ratings for the total transition maneuver.

Initial Airspeed (knots)	Final Airspeed (knots)	Flap Rate (deg/sec)	C/H Rating
140	80	1.5	6
170	80	1.5	8

4.2.2.4.2 Final Transition. In the second phase of a two-phase transition, airspeeds from 90 to 110 knots were considered the most acceptable initial speeds for configuring to a STOL mode at 80 knots on a -7 degree flight path angle. Although the 80-knot

initial speed point was considered acceptable, considerable pilot attention and technique were involved to prevent loss of airspeed. The airspeed range from 90 to 110 knots was not judged satisfactory because of the timing and precision of technique involved between when to make power reductions and when to start pitch-down action to intercept the glide slope and stabilize at 80 knots. At an initial airspeed of 110 knots, flight data appeared to be approaching a limit at which the interactions and reversals would become slightly confusing and for which control would resort more to a mechanical flying task rather than a precise control task. Although this was not readily apparent from the data, it was felt that at 120 knots the reversals in pitch, although slight, plus the power and pitch reversals required, detracted from performance and required extensive pilot compensation for acceptability. An evaluation of flap rates higher than 5 deg/sec also gave generally unsatisfactory results. The main objection was that trim change requirements occurred too fast for safe operational control as compared to the flap rate of 1.5 deg/sec at the same airspeeds. Representative C/H ratings for the final transition are:

Initial Airspeed (knots)	Final Airspeed (knots)	Flap Rate (deg/sec)	C/H Rating
80	80	1.5	5
90	80	1.5	4
100	80	1.5	4
110	80	1.5	4-1/2
120	80	1.5	6
90	80	3	5
110	80	3	6

4.2.2.4.3 Initial Transition. This area proved the most troublesome and resulted in low C/H ratings. The most noticeable problem occurred during the final few degrees of flap deflection. As mentioned in the introductory comment, the change from conventional aircraft control techniques to STOL techniques was very apparent, with highly objectionable pilot compensation required. This condition was about the same for all airspeeds evaluated at the 1.5 deg/sec flap rate, and increasing the flap rates caused unacceptable C/H ratings. With all the pitch and stick reversals, it was extremely difficult to maintain altitude during the early part of the maneuver. This portion of the transition was rated marginally acceptable to unacceptable for use in precise control during IFR conditions. Therefore, initial transition should be conducted well before intercepting the final course to landing, such as on a downwind leg of a GCA or perhaps at an intermediate altitude on a TACAN approach. Representative C/H ratings are:

Initial Airspeed (knots)	Final Airspeed (knots)	Flap Rate (deg/sec)	C/H Rating
140	100	1.5	6
155	100	1.5	6
170	100	1.5	6
140	100	5	7
170	100	3	7

The recommended procedure for transitioning to the STOL configuration is to conduct it in two phases. Initial transition should begin between 140 and 170 knots, stabilizing between 90 and 110 knots. Flaps should be lowered from 0 to 45 degrees at a flap rate of 1.5 deg/sec. Final transition should include the final flap lowering from 45 to 65 degrees, also at 1.5 deg/sec, and should be initiated between 90 and 110 knots, stabilizing at 80 knots on the -7-degree glide slope. Guidance information on the flight director needles should be available to give the proper lead for initiating the final STOL configuration change so as to intercept and hold the glide slope.

4.2.3 VECTORED THRUST (VT) EVALUATION. This discussion covers approach, transition, and go-around evaluations of the pure vectored-thrust configuration (no internally blown flaps).

4.2.3.1 VT Approach. In general, the simulated aircraft handled and performed as well as the EBF configuration. Flying the approach at 85 knots proved to be easier than at 80 knots, primarily in stability in tracking the glide path using STOL techniques. Although the VT configuration generally handled better at 85 knots, stability on the glide path deteriorated as the flap angle was decreased below 70 degrees. The configuration at 70 degrees of flaps at 85 knots was highly satisfactory and earned a C/H rating of 2-1/2; the configuration at 70 degrees of flaps at 80 knots was also judged satisfactory with a C/H rating of 3. The slightly poorer C/H rating for 80 knot operation was the result of the lower trim power setting for that airspeed. Engine response characteristics were more sluggish and an annoying increase in pilot power lever activity was required at the lower airspeed.

Airspeed control was good throughout, with only slight sensitivity to power changes. The response of airspeed to pitch attitude changes was also acceptable. Typical power changes produced slight airspeed changes, usually less than 2 knots, and small pitch changes. With the APPROACH and AUTOSPEED modes engaged, this was not a problem and the C/H ratings with these modes improved to a satisfactory 3 for these same configurations. During evaluation of this subcategory, tests were conducted using the pitch augmentation system to determine the margins for pitch maneuvers. At the 80-knot trim airspeed for the range of flap settings tested, a positive pitch change of more than 2.5 to 3 degrees would result in an increasing angle-of-attack situation leading to loss of control. Starting with an 85-knot trim airspeed, a 5-degree positive pitch change could be made and it was possible to

restabilize the aircraft on its original -7 degree flight path angle. The ability to achieve this restabilized flight deteriorated with decreasing flap angle. (These pilot observations clearly relate to the non-linear gamma/velocity characteristics of this configuration. The positive pitch attitude change, maintained by the pitch augmentation system, reduces airspeed and the negative $d\gamma/dV$ parameter increases sharply at the "knee" of the gamma/velocity curve. The region of this knee in terms of airspeed is a function of flap deflection and power setting. Increased flap angle and power setting drive the knee region toward lower airspeeds.) Although the pitch maneuver criterion may be considered similar to specifying an approach speed in percent of stall speed, an important difference was observed. The rate-command/attitude-hold pitch system has proved to be highly desirable for the terminal flight phase. Using this system, the pilot tends to use the pitch attitude for both command and performance information. The airspeed indicator becomes more of an instrument to cross-check for trend and precision airspeed changes. Thus, it is probably more important to establish an attitude change margin than to establish an airspeed margin.

The approach evaluation using the modified gust model without the APPROACH and AUTOSPEED modes dropped the C/H rating to an unsatisfactory level. The primary problem was in achieving and holding proper runway alignment. The aircraft was in a continuous roll oscillation. Although the dutch roll was well damped, it was easily excited. Once excited, the control inputs that were applied seemed to be out of phase and extensive concentration was required, with periodic cross-controlling to achieve runway alignment. It was difficult to determine whether this was the result of a long time constant or the fact that the gusts continually excited the dutch roll. With the APPROACH and AUTOSPEED modes, the C/H ratings dropped to an unacceptable value. There appeared to be little control of flight path available to the pilot, who seemed to be out of phase and fighting the automatic power changes resulting primarily from alpha changes using the APPROACH mode system. Because the pilot appeared to be fighting the power loop, an attempt was made to let the automatic feature work for itself. To do this, the pilot set a medium power level and flew pitch corrections when needed to adjust to the flight path. This was also considered unacceptable.

The bare airframe with no augmentation was also evaluated, resulting in occasional out-of-control conditions. This was evaluated without the gust model. The pilot could only make very slight and cautious corrections, which almost always resulted in a divergent condition. Large corrections nearly always resulted in rapid loss of control.

Investigation of the engine-out condition with the augmented airframe indicated that the vectored thrust configuration was well behaved. Although both were acceptable, the 85-knot conditions were considered slightly better than the 80-knot conditions. Only a slight roll and yaw occurred when the engine was lost. These could quickly be controlled, although there was some difficulty in achieving and holding balanced

flight conditions. Balancing of side forces seemed to be very sensitive to bank angle, causing difficulty in maintaining precise control. With normal pilot training, the operational aircraft suffering an engine loss above 800 feet could be safely controlled on the approach to arrive in a position for a safe landing.

Representative C/H ratings for VT approach evaluations are:

Flap Setting (deg)	Airspeed (knots)	Technique	Approach/Autospeed Mode On	C/H Rating
70	85	STOL	No	2-1/2
60	85	STOL	No	3-1/2
50	85	STOL	No	3-1/2
70	80	STOL	No	3
60	80	STOL	No	3-1/2
70	85	STOL/Gusts	No	6
70	80	STOL/Gusts	No	6
70	85	STOL/Gusts	Both	8
70	85	Conv/Gusts	Both	9
70	85	B. A/F*	No	9-1/2
70	85	STOL/EO**	No	5
70	80	STOL/EO	No	6

* Bare airframe

** Engine out

The configuration recommended for further evaluation is 70 degrees of flaps at 85 knots.

4.2.3.2 VT-Go-around. This subcategory compared very favorably to the EBF and IBF/VT configurations. The go-around procedure was the same as for the other configurations, and was considered straightforward, easily controlled, and repeatable. This overall subcategory was judged a C/H rating of 3, the same as the other configurations.

Unlike the IBF/VT configuration, however, go-around performance did not appear sensitive to variations in the flap rates evaluated as long as a 10 degree or greater pitch attitude change occurred. At less than this pitch attitude change, performance deteriorated as the flap rate increased over 1.5 degrees/second. A pitch attitude change of 15 degrees was considered uncomfortable and undesirable since it did not improve performance. When the flaps were raised to 40 degrees at the same time go-around was initiated, there appeared to be little difference between the 70 degrees of flaps/80-knot condition and the 70 degrees of flap/85-knot condition.

If raising the flaps was delayed until pitch attitude had changed 10 degrees, the 70 degrees of flaps/85-knot condition provided the better performance margins.

Go-arounds initiated upon sudden loss of a critical engine could be easily and safely handled. The 70 degrees of flaps/85-knot condition was far superior to the 70 degrees of flaps/80-knot condition, primarily in the amount of altitude lost in the recovery. The 85-knot condition suffered only a 90-foot altitude loss as compared to a normal 60-foot loss for all engines operating. Airspeed loss was very slight, with a subsequent airspeed increase trend observed.

For the VT go-around, a reconfiguration to 40 degrees of flaps from 70 degrees at a flap rate of 5 deg/sec is recommended. At an initial airspeed of 85 knots, a positive 10-degree pitch attitude change should be accomplished using a nominal 3 deg/sec pitch rate. Flaps-up should be initiated upon go-around initiation.

4.2.3.3 VT Transition. The VT configuration was better balanced than the EBF or IBF/VT configurations. Control was better throughout, over a wider range of flap rates. As with the IBF/VT configuration, there was a point in the transition that required some concentration to shift from conventional to STOL techniques.

4.2.3.3.1 Total Transition. Continuous transition from conventional flight to the STOL configuration on the -7 degree flight path could be accomplished acceptably. This was the only configuration examined that was rated acceptable for this type of transition. This acceptability rapidly decreased, however, as flap rates increased above 1.5 deg/sec or initial airspeed increased above 155 knots. It took nearly a full minute to complete the total transition at 155 knots using 1.5 deg/sec. While this was not considered unacceptable from an operational viewpoint, it does require longer-lead glide path information for good intercept results. Having this long time requirement minimizes the flexibility of the pilot to counter changing environment conditions by simply requiring a long period of concentration upon this task. It is therefore recommended that transition be performed in more than one step. Representative C/H ratings for the total transitions evaluated are:

<u>Initial Airspeed</u> (knots)	<u>Final Airspeed</u> (knots)	<u>Flap Rate</u> (deg/sec)	<u>C/H</u> <u>Rating</u>
155	85	1.5	4-1/2
155	85	3	6

4.2.3.3.2 Final Transition. This was a very easy and likeable transition task. There were practically no control reversals, and confusing control requirements were nonexistent. The acceptable airspeed range for initiation of final transition at a flap rate of 5 deg/sec was small as compared to lower flap rates. At 3 deg/sec, the desirable initial airspeed range was from 90 to 120 knots, although it was almost

satisfactory from 85 to 125 knots. Further decreasing the flap rate to 1.5 deg/sec showed no beneficial effect. In fact, the slower flap rate tended to make the required airspeed bleed rate almost too slow, especially at the higher initiation airspeeds. At the 3 deg/sec flap rate, the overall transition was nearly optimum at the 105- to 115-knot initiation airspeed range. There was only a slight pitch attitude change required throughout the final transition, with power serving as an excellent control for flight path angle change from 0 degrees to the -7 degree glide path. Representative C/H ratings for final transition are:

Initial Airspeed (knots)	Final Airspeed (knots)	Flap Rate (deg/sec)	C/H Rating
85	85	5	5
95	85	5	3
125	85	5	4-1/2
85	85	3	3-1/2
105	85	3	2-1/2
125	85	3	4
95	85	1.5	3
115	85	1.5	3-1/2

4.2.3.3.3 Initial Transition. Like the IBF/VT configuration, this was more troublesome than the final transition task and was also very sensitive to flap rate. Acceptable ratings over the airspeed test range from 140 to 170 knots could only be achieved at 1.5 deg/sec flap rate. A power reduction to combat the tendency of the aircraft to balloon while the flaps were being lowered was effective, although it tended to be objectionable. It was uncomfortable to have to manipulate the throttle in the approximately 20 percent thrust range. The power response at these values was very sluggish and added to the difficulty of the task. Pitch changes were adequately controlled by considerable pilot concentration, with only a slight tendency to exhibit reversals. At the 3 deg/sec flap rate, it took nearly idle power plus an unacceptable amount of pilot compensation for pitch changes at the higher airspeeds. Representative C/H ratings for initial transitions are:

Initial Airspeed (knots)	Final Airspeed (knots)	Flap Rate (deg/sec)	C/H Rating
140	105	1.5	4-1/2
155	105	1.5	4-1/2
170	105	1.5	6
155	105	3	6

The recommended procedure for transitioning to the STOL configuration is to conduct it in two phases. The initial transition should be initiated between 140 and 170 knots,

stabilizing between 90 and 120 knots. During this phase, the flaps should be lowered from 0 to 40 degrees at 1.5 deg/sec. The second phase or final transition should include the final flap lowering from 40 to 70 degrees at 3 deg/sec. This phase should be initiated between 90 and 120 knots, stabilizing at 85 knots on the -7 degree glide-slope. Proper lead guidance should be available on the flight director needles to direct timely initiation of the final transition to intercept the glideslope.

4.2.4 EBF EVALUATION ON THE LARGE AMPLITUDE SIMULATOR (LAS). The evaluation on the LAS consisted largely of moving-base evaluations, with some fixed-base evaluations for comparison to the Convair Aerospace fixed-base results and to examine differences between the LAS moving-base and fixed-base results. In general, the results of the moving-base simulations verified earlier Convair Aerospace fixed-base results.

4.2.4.1 EBF Approach on the LAS. There was very little difference between the LAS moving-base and Convair Aerospace fixed-base results. Variations in pitch attitude as a result of flap angle and airspeed combinations were better represented in the LAS fixed-base and moving-base evaluations. This was manifested by a feeling of an extreme and uncomfortable nose-high condition using 45 degrees of flaps to a slight feeling of diving at the ground with 60 degrees of flaps. Pitch variations using conventional approach techniques were occasionally large, requiring a moderate to intense degree of compensation by the pilot using the moving-base. The C/H ratings were not significantly different from fixed-base work, although the reasons were more readily identified using the moving base.

Applying the gust model made the STOL technique of flying the approach stand out very clearly as the desirable technique as compared to conventional technique. The C/H ratings varied as much as 2, going from 6 for STOL techniques to 8 (unacceptable) for conventional techniques using the same mode combinations. The APPROACH mode by itself on runs without gusts appeared to make the task more difficult. When used with the gust model, however, it appeared to be trying to damp out some of the the glide slope variations. Without the gust model, the APPROACH mode seemed to fight the pilot inputs. When the pilot applied power to climb to the glide slope, for example, the system would apparently also look at the angle of attack (which would be decreasing) and try to retard the power. The reason it appeared to help with the gust model applied was because the system looked at the perturbations and applied corrections that tend to limit the amplitude of the error. The system could normally perform these maneuvers better than the pilot. In any case, undue criticism of the APPROACH mode and its function is unjustified at this time. Additional work should be accomplished to refine this mode to determine its full capability. The primary reason for the low C/H ratings with the gust model applied was the relatively poor glide path control. Runway alignment did not appear to cause more than a moderate (acceptable) degree of pilot compensation.

Because of the dramatic effects when a critical outboard engine was lost during an approach, considerable attention was given this area. In general, the engine-out evaluation concluded that an engine loss at 800 feet AGL using a 2-second delay for recovery initiation and attempting to continue the approach to arrive at a repeatable and controllable flare point produced overall unacceptable results. The C/H ratings varied from 7 at a 45-degree flap setting to 10 using 60 degrees of flaps, regardless of the modes used. These evaluations were conducted by leaving the flaps in their existing position.

By raising the flaps to 45 degrees or less and increasing the approach speed, the C/H ratings perhaps could have increased to an acceptable value, although this was not attempted. Beginning at 55 degrees of flaps, the power margin seemed to be slight and was felt to be insufficient for safe repeatable performance. After aircraft control was established following an engine loss, it was difficult to get back to the runway in the altitude remaining. Holding runway alignment proved extremely difficult, as bank angle variations of as little as 2 or 3 degrees produced large side forces.

Evaluations were also performed to determine when corrective controls should be initiated. In addition to the two-second delay, a one-second delay and a minimum time delay condition were evaluated to examine the potential for an automatic system that could be armed on the approach. If an engine loss occurred, this system would put inputs into control surfaces to enhance recovery and minimize aircraft motion excursions. A delay in corrective action of one second or less was found to produce acceptable C/H ratings for recovery of attitude control. The difference between the minimum time delay and a one-second delay was slight. Although motion excursions were obviously less for the minimum time delay, the pilot tended to overcontrol on the initial correction control inputs as compared to a delay of one second. This was felt to be as a result of seeing and feeling the motion for at least one second, during which good approximations of the amount of control and coordination needed could be better judged. When delaying over one second, the C/H ratings suffered greatly. Sufficient advantage for using some automatic system with arming capability to enhance engine-out recovery is felt to warrant further design work in this area.

Engine-out investigations with a bare airframe using both a one-second delay and a two-second delay received C/H ratings of 10, regardless of flap position. There was simply not enough control authority available to continue the approach while correcting back to the runway centerline for the lower flap positions. At the higher flap position, there was insufficient control authority to regain control of the aircraft.

The bare airframe investigation for normal approaches without the gust model or engine-out conditions indicated that the basic airframe was well behaved, with a C/H rating of 4. The chief annoyance was that positive power applications produced negative pitching moments, which tended to cause oscillations that continually excited the longitudinal dynamic modes (although they were satisfactorily controlled).

Bare airframe evaluations of off-nominal cg and weight conditions (± 10 percent) using STOL techniques were considered acceptable. Considerable pilot compensation was required, however, as a result of the negative pitching moments due to power increases for the forward cg, heavier weight condition. The apparent stability decrease at this condition was what might be expected in the aft cg, lighter weight condition. The aft cg, lighter weight condition required less pilot compensation and was more desirable. Evaluating the augmented aircraft with the same STOL techniques produced the same ratings as normal cg and weight conditions to slightly less desirable for the forward cg, heavier weight condition. Power available was considered marginal using 60 degrees of flaps. Again, the negative pitching moment due to power increases caused considerable difficulty in achieving adequate performance. The net effect was to produce one continuous glidepath oscillation fed by power changes and pitch changes. (The increased pilot work load for the unaugmented aircraft with the forward cg, heavier weight condition was due to a decrease in longitudinal dynamic stability. Later analysis determined this to be the result of a simulation trim discrepancy. The software logic that adjusts the horizontal stabilizer to trim the aircraft prior to a run did not ensure against trimming on the back side of the stabilizer's lift curve. For the forward cg, heavier weight condition, this did occur and contributed a destabilizing influence.)

Evaluation of the approach using 90-degree crosswinds up to 30 knots mean value combined with the gust model produced some question as to whether the pilot could consistently arrive at the flare point for touchdown. Glidepath control was normal for the conditions evaluated, but the principal difficulty was in achieving runway alignment and timing the decrab maneuver for landing. It was difficult to determine when runway lineup had been achieved and to hold this alignment against varying wind conditions as altitude was lost. More critical, however, was the timing of the decrab maneuver for landing. Although generally satisfactory, timing was considered too sensitive for daily operational use. With the wind and gust model applied, an automatic decrab system or a system that does not require a decrab maneuver would be required for operational use. Flying these environmental models using conventional techniques highlighted the undesirableness of these techniques. The pilot was at the limit of concentration, such that any problem occurring during the approach with these environmental models would require a go-around to maintain aircraft control. (The wind profile used for this work was relatively severe. It was the mean wind profile that would be exceeded less than 5 percent of the time at Cape Kennedy and was extrapolated for altitudes greater than 500 feet AGL. For the 90-degree crosswind used, the approximate crab angle for an approach at 80 knots would be 28 degrees at 1200 feet AGL, reducing to 18 degrees at a nominal flare altitude of 100 feet and to 10 degrees immediately prior to touchdown.)

BEST AVAILABLE COPY

4.2.4.2 EBF Go-Around on the LAS. The evaluation of go-around performance on the LAS produced results nearly identical to the Convair Aerospace fixed-base results. The motions of the moving-base simulator added little if anything to pilot assessment of the difficulty of performing the maneuver or of the merits of various procedures. One exception to this general opinion was that when pitch attitude changes reached or exceeded 15 degrees, the motion cues stimulated a feeling of undesirably large nose-up attitudes for the situation under evaluation.

The evaluations examined go-around performance and handling qualities with a critical engine out. Although the go-around procedure called for an initial flap retraction to 40 degrees, this did not provide adequate performance in terms of ability to gain altitude or to prevent loss of airspeed. By using the stick trigger switch to command further flap retraction (i. e., by "milking" the flaps up gradually in small increments from 40 to about 25 degrees), a significant increase in performance could be achieved. The automatic system evaluated on the Convair Aerospace fixed-base simulator, which commanded further flap retraction when flight path angle exceeded a designated minimum positive value, would have greatly benefitted the evaluation. In any case, there would be an altitude loss of about 300 feet before a positive climb could be effected. In other words, the aircraft is committed to land when it descends to 300 feet AGL. This is not desirable, because it is almost certain that the aircraft would not touch down on the runway because of the side forces developed during engine failure (two-second delay) and while corrective control is being applied. Adequate control of the aircraft could be achieved (largely because of flap retraction), but the aircraft would no longer be lined up with the runway.

The other go-around evaluations showed an insignificant difference from the norm achieved in the Convair Aerospace fixed-base simulation work. The only significant area was with the forward cg, heavier weight condition. This condition exhibited a very objectionable tendency to oscillate in pitch if the pitch rate exceeded the normal 3 to 4 deg/sec by 2 or 3 deg/sec.

4.2.4.3 EBF Transition on the LAS. Results of the LAS transition evaluation were also similar to the Convair Aerospace fixed-base results. The techniques did not vary significantly between the two simulators, although the LAS moving-base produced certain subtle effects that were not observed on the fixed-base simulator. These effects were primarily in the pilot reaction to aircraft attitude changes during transition maneuvers, and were caused by motion and peripheral vision cues. The coordination required to prevent climbing during the transition at the higher flap rates was perhaps better defined on the moving base, although the task still presented the same degree of difficulty. Introduction of the gust model produced only minor changes. With turbulence, it seems to take slightly longer to get established on the proper glide slope. In addition, the rate of climb indicator, while providing a good sensitivity ratio for approaches, was deemed too sensitive for transitions with the gust model. The standard sensitivity ratio on present indicators would be

preferred for operational transition. The transition maneuver was evaluated under assumed operational conditions using a 90-degree heading offset and different initial altitudes. The technique for transitioning to an intermediate flap position and airspeed was found to vary somewhat over the range of initial airspeeds examined. This variation in technique with different initial airspeeds is undesirable. The situation was improved somewhat by using flap rates of 3 deg/sec or less.

4.3 MOVING BASE VERSUS FIXED BASE EVALUATION

Evaluation of the STOL transport EBF configuration between fixed-base simulation and moving-base simulation produced many effects and subtleties that are difficult to describe and nearly impossible to quantify. The oft-stated opinion that "moving base simulation produces better engineering results the more the flight task changes from steady straight flight to maneuvering flight" should be reemphasized as important. The better the simulation, whether fixed base or moving base, the better will be the qualitative results, and quantification of results will be enhanced as well. If not well modelled and executed, the moving-base simulation could cause evaluations to be less accurate than those obtained on a good fixed-base simulation. For example, while evaluating the EBF configuration on the moving-base simulator, a confusing effect was observed during steady level flight before beginning the transition to STOL approach conditions. After several runs, it was discovered that the simulator cockpit was experiencing a slight pitch-up rate with no associated indication on the cockpit instruments or data recording facility. This was confusing because it imparted to the pilot that a pitch rate, a power increase, or a longitudinal acceleration was occurring. This was not observed in the fixed-base simulation. Once the problem was recognized, the effects were ignored and were not considered further in the evaluation. This was apparently an example of an inaccurate drive equation and was relatively simple to identify. If this type of drive equation error were buried in some coupled mode of flight, it could conceivably influence qualitative as well as quantitative results. It may be difficult to ferret out these non-realistic movements in an engineering development program, and engineering judgement and perhaps design solutions could be adversely affected. Motion drive equations are not required for fixed-base simulation, and small inaccuracies in visually represented motion are less likely to influence pilot evaluations because they are somewhat difficult to resolve. This is not to say that engineering simulation should be fixed-base because mechanization errors are better hidden. It does point out, however, that moving-base simulation requires great care in the development and execution of the constrained-motion drive equations because of the pilot's sensitivity to motion cues. In any case, sufficient software engineering should be conducted to minimize these degrading potentials to within the bandwidth of errors expected in any simulation program.

In general, Cooper/Harper ratings on the same equipment in the same time period were the same to one point better for the LAS than for the fixed-base simulation. For the conditions evaluated, however, the rating differences were never sufficient

to cause a jump across major decision points (such as 3 to 4 or 6 to 7). When comparing the LAS fixed-base results with the Convair Aerospace fixed-base simulation results, the ratings at Convair Aerospace were scattered around the LAS results. This scatter ran from one point better to two points worse on the Convair Aerospace fixed-base facility. Part of this difference can be attributed to additional training provided by the additional evaluation work and part by the difference of the time period in which the evaluations were conducted.

One major factor, however, was felt to contribute significantly to the differences. During an evaluation on the LAS with fixed-base operation, the earth/sky contrast part of the video projection system failed leaving only the target runway and surrounding terrain features. Fortunately the run being evaluated was a reasonably difficult task for which explicit memories remained from the evaluation on the Convair Aerospace fixed-base simulator. Quite dramatically, the situation seemed to focus back on these memories and the critique conducted during the prior evaluation. From this and other experience, there seem to be three definite levels of simulation for pilot-in-the-loop evaluations where visual presentations are available.

The first of these is a fixed-base simulator that incorporates video projection of a fixed target but is limited by an included viewing angle of only a few degrees. This is only slightly better than a video presentation and is probably the least expensive of the three simulation levels. This first level is quite useful for gross design studies that require maneuvers primarily associated with closing on the fixed target or performing longitudinal maneuvers with perturbation studies of lateral or directional motion. Even this usage is limited, because the visual effects are stimulating only a portion of the visual sense of perception. The difficulty is that the pilot must wait until the movement has built to a sufficient value that position effects can be detected visually and a correction can be made, if needed. The limitation noted here is particularly bad for lateral motion. For non-maneuvering flight, the lateral information delay created by the pilot's dependence on limited visual information led to a small-amplitude lateral-directional limit cycle, which ceased when the pilot released the control stick. For some time, the pilot believed the problem to be caused by a poor turn coordinator; however, when IFR approaches were simulated, the lateral-directional oscillations were not present. A chief criticism of this level of simulation for approach or landing is that the visual system creates an effect of almost accelerating forward to the runway as the runway or decision point is approached. The missing critical items are the rate cues provided by lateral peripheral vision from the cockpit. It becomes difficult to judge runway alignment or the amount of control correction required to correct to the runway and to provide for accurate timing of turn rollout initiation to bracket the runway centerline.

The second level of simulation is achieved by providing wrap-around or wide-angle horizon cues to a first-level simulation. Qualitatively, this provides nearly a 70 percent improvement over the first level of simulation. If cloud features move

relative to the aircraft motion and horizon and if scattered terrain features with vertical development are provided, meaningful improvement can again be realized (to perhaps an 80 percent improvement over level one). Because of the many features seen with various perspectives, this level of simulation achieves nearly optimum advantage of the visual sense. The ability of sight to grasp a spectrum of events or relative motion in reference to a wide-angle horizon and to interpret it without pause provides such realism to the pilot that he relies very little on his other senses. This is especially true for the lower frequency events occurring during roll maneuvers, slightly less for pitch and yaw, and essentially not applicable for translation in any direction. Interpretation capability during the EBF evaluation in the LAS moving-base simulator (but without motion drives activated) was sufficient to allow thorough understanding of the control system and to provide engineering judgement with a significant improvement in accuracy over the first level of simulation. Although the rating differences between this level and the first level were inconsequential (perhaps for the reasons mentioned earlier), the chief gain was that the evaluation pilot could make more incisive judgements and comments. In other words, he may react to a particular aircraft response nearly the same regardless of the simulation level, but with the second level he can understand and communicate more thoroughly just why he likes or dislikes the aircraft response. The peripheral cues along with the additional visual features is felt to be the reason for this.

The third level of simulation provides for level two visual presentations with the addition of a moving-base capability. The larger the amplitude of movement capability, of course, the closer the actual aircraft movement can be simulated. The amount of movement that should be included is difficult to assess, but it must stimulate the senses sufficiently to allow accurate representation of the initial movement effects. Since a moving-base simulation must be constrained, the lack of motion after reaching the limits may actually confuse the evaluation pilot. This occurred during engine-out evaluations of the EBF configuration, causing the evaluation pilot to revert entirely to the visual sense of perception and to consciously ignore the movement sensation until back into steady straight flight. The initial effects of movement probably allowed an additional 20 to 30 percent improvement over the second level of simulation, and raised the evaluation pilot's confidence in providing qualitative ratings. Perhaps the most important aspect of motion is that the pilot feels the initial aircraft response to control inputs and is less likely to overcontrol during simulated flight. This overcontrol did exist to a noticeable degree during the second level of simulation.

The importance of this realistic feel is borne out in an observation by the Chief Pilot of American Airlines while the test pilot on this study was evaluating the Boeing 747 moving-base simulator. He observed that typically, as in an actual aircraft, the pilot can be seen to make control movements without seeing any visual movement. In other words, simulator movement allows the senses to react before the need is seen in the visual presentation. Although the observation was made in reference to

moving-base simulators used in pilot training, it is equally valid for engineering simulators. Evaluations conducted on the moving-base simulator demonstrated this phenomenon clearly; the effect of pilot sensitivity to physical motion was that the lateral-directional limit cycle was eliminated and lateral control was easier. This raises a question as to accuracy of pilot work-load evaluations in fixed-base versus moving-base simulators. Fine resolution of work-load effects is not usually essential for development work normally performed on fixed-base simulators. For a careful assessment of pilot work-load, however, the motion cues of the moving-base simulator may prove significant.

Probably the most important characteristic of the moving-base simulator is its ability to impart short-term translational motion cues to the pilot. Interpreting these motions from visual presentations is very difficult and evidently includes an effective time lag while visual interpretation is being performed. By stimulating the pilot's sense of feel, the moving-base simulator permits a better evaluation of control devices that produce linear accelerations in the aircraft; e.g., drag-increase devices, power effects, side-force-generating devices, and direct lift devices. These must be considered meaningful areas for evaluation — as important as any of the attitude control devices. If these or similar devices are present on the aircraft to be simulated, an increase in capability of nearly 100 percent over the second level of simulation is provided by moving-base simulation due to the difficulty in visual perception of the effects of these devices. Additional benefit was achieved with the moving-base simulation during evaluation of the EBF configuration. Better aircraft control was achieved with positive damping of external disturbances during runs with the turbulence model and where relatively large amplitude aircraft excursions (10 degrees or greater) were needed. With the motion being fed back to the pilot, the tendency to overcontrol was minimized with a subsequent improvement in the C/H ratings.

As stated earlier, the EBF configuration was evaluated better with the third level of simulation than with the second level, although the difference was not sufficient to change the conclusion design. Other evaluation programs or different aircraft could, of course, justify the need for the third level of simulation for the reasons mentioned earlier. For example, an evaluation of a helicopter conducted with an exceptionally good visual simulation coupled with a very limited moving-base capability proved the need for even a very limited amount of motion. While flying a specific task on this simulator with the moving base active, the C/H rating was at 5. When the moving-base portion was deactivated while retaining the full visual presentation, the flight quickly went out of control and was rated at 10. While the reason for the drastic change was not fully evaluated, there are evidently situations in which at least a limited amount of moving base capability is required.

SECTION 5

CONCLUSIONS AND RECOMMENDATIONS

The following conclusions and recommendations resulted from the flight control technology studies.

1. Simulated flight operations for the internally blown flap (IBF) version were totally unacceptable in the presence of even mild disturbances at low approach speeds desired for STOL operations. A modification was incorporated that vectored the non-diverted engine flow at the angle of the nominal flap deflection. This proved quite acceptable and was the basis for all subsequent IBF/VT simulation activities.
2. Longitudinal low speed control analysis showed all three (EBF, IBF/VT, and MF/VT) configurations to have adequate control power but deficient handling qualities, specifically in flight path stability, acceleration sensitivity, phugoid damping, and short period frequency. A stability augmentation system (SAS) was synthesized so that the closed-loop handling qualities meet the specifications of both MIL-F-8785 (conventional aircraft) and MIL-F-83300 (V/STOL aircraft). The longitudinal SAS consists of a pitch loop to the elevator, a throttle flight path loop (APPROACH), an airspeed loop to the flaps (AUTO-SPEED), and appropriate cross coupling.

Lateral-directional low speed control analysis showed all three configurations to have adequate roll and yaw control power. Engine-out control characteristics for the EBF configuration are marginal. Handling quality analysis shows deficiencies for all three vehicles in dutch roll stability, spiral stability, and roll-induced sideslip excursions. A lateral-directional SAS was synthesized to meet both specifications.

Flight simulator results showed that all three configurations could be flown without augmentation under nominal flight conditions with moderate to large increase in pilot workload. The addition of the augmentation features improved pilot ratings to acceptable or satisfactory levels for all three configurations.

3. The AUTOSPEED function, provided by modulation of flap position in the STOL-approach configuration, proved an efficient speed control. Its use was not considered important under ideal environmental conditions, but it was very helpful and was rated essential in the presence of turbulence and/or wind shear.

4. The APPROACH function, designed to decouple aircraft responses to stick and throttle inputs, was considered helpful under turbulent conditions and of questionable value for smooth conditions. Optimization of the decoupling effects will make this feature an asset for STOL operations under all environmental conditions.
5. In regard to piloting techniques for STOL terminal area flight operations, there is clearly a preference for the STOL mode of flight path control (i. e., power lever adjustments for flight path error corrections with relatively constant pitch attitude maintained by a pitch-attitude-hold mode and airspeed regulated by the AUTOSPEED function). Pilot workload is significantly reduced with this concept. Mechanization of this control scheme requires simpler decoupling provisions because the power level is inherently a better control of vertical velocity than forward velocity when the aircraft is in the low-speed, STOL configuration.
6. For voluntary (four-engine) go-around, all three configurations required some flap reduction from the full STOL-approach configuration to minimize altitude loss after go-around initiation. For the baseline data used, the minimum altitude loss was between 60 and 70 feet. This required a high level of pilot activity. Conversely, an automatic feature that reduced the flaps to the correct intermediate setting reduced the pilot activity requirement significantly.
7. Failure of the critical engine in a STOL-approach produced significant variation among the three STOL configurations. For the EBF, it was considerably more difficult to regain control of attitude. During recovery, departure from the desired approach path was so great that a go-around on three engines was often required. Altitude loss was greatest for the EBF version and least for the MF/VT version. Cooper/Harper ratings assigned to evaluations were poor when a two-second delay preceded recovery attempts. An automatic system with an arming capability for STOL approach is highly desirable to enhance engine-out recovery.
8. Transition from cruise to STOL-approach using constant flap deflection rates proved to be a challenging pilot task. Considerable control activity by the pilot was required during transition flight since no constant flap rate would result in trimmed lift, drag, and pitching moment throughout the maneuver. It is recommended that the transition be performed in two steps, with an intermediate configuration and speed used to maneuver the glide path engage point to alleviate these control difficulties. Again, this is a piloting task problem that can be simplified by the use of automatic features to perform or assist in the transition maneuver.

9. The mechanization trade study concluded that fly-by-wire mechanization is preferred over the more mechanical version, primarily because the more mechanical version would require significant fly-by-wire features to achieve the required augmentation and decoupling. The maximum mechanical implementation is rated a close second choice.
10. The Cooper/Harper ratings assigned during flight simulator evaluations did not show any one of the STOL configurations to be significantly superior to the others. For the subcategories of flight simulation, the ratings given were quite comparable (except for the loss of a critical engine during STOL approach). Because the IBF/VT and MF/VT configurations showed superior engine-out characteristics over the EBF version, the aggregate of pilot ratings for these configurations was probably somewhat better.
11. Pilot evaluations using the rate-command/attitude-hold pitch system showed a tendency to use the pitch attitude indicator for both command and performance information. It was suggested that for STOL flight operations it may be more important to establish an attitude change margin for maneuvering limits than to rely on the traditional speed margins.

SECTION 6

REFERENCES

- 2-1 STOL Tactical Aircraft Investigation Configuration Definition Report, Convair Aerospace Division of General Dynamics, Contract F33615-71-C-1754 CDRL item 0002, 15 December 1971.
- 2-2 Flying Qualities of Piloted V/STOL Aircraft, MIL-F-83300, 31 December 1970.
- 2-3 Flying Qualities of Piloted Airplanes, MIL-F-8785B (ASG), 7 August 1969.
- 2-4 Background Information and User Guide for MIL-F-83300-Military Specification-Flying Qualities of Piloted V/STOL Aircraft, AFFDL-TR-70-88, March 1971.
- 4-1 Turbulence Generator for Flying Quality Investigation, G. R. Friedman, Convair Aerospace memo, 1971.
- 4-2 Terrestrial Environment (Climatic) Criteria Guidelines for Use in Space Vehicle Development, NASA Technical Memo, TM-X-64589, 1971 Revision.

APPENDIX I

CONVAIR AEROSPACE TRIM-STAB DIGITAL COMPUTER PROGRAM

APPENDIX I

CONVAIR AEROSPACE TRIM-STAB DIGITAL COMPUTER PROGRAM

TRIM-STAB is a Fortran IV program that has evolved at Convair over many years. The program interfaces with an AERO subroutine, which is generated for the specific class of vehicles being analyzed. Data is stored in the AERO subroutine so that for specified inputs, total force and moment coefficients are computed. The TRIM-STAB program (Figure I-1) can be used in a symmetrical three-degree-of-freedom mode or with six degrees of freedom. A thrust subroutine gives gross thrust and C_{μ} for specified throttle, speed, and altitude. Linear interpolations between stored data points are used. Data is stored as functions of one, two, or three variables. For the EBF vehicle the nonlinear data of Reference 2-1 is stored as:

$$\begin{array}{l}
 C_L = f(\alpha, C_{\mu}, \delta_F) \\
 C_D = f(\alpha, C_{\mu}, \delta_F) \\
 C_m = f(\alpha, C_{\mu}, \delta_F) \\
 \epsilon = f(\alpha, C_{\mu}, \delta_F) \\
 C_{L_H} = f(\alpha_H, \delta_H)
 \end{array}
 \left. \begin{array}{l} \\ \\ \\ \\ \end{array} \right\} \begin{array}{l} \text{TAIL-OFF PARAMETERS} \\ \\ \\ \text{TAIL CONTRIBUTIONS} \end{array}$$

In general, it is preferred to determine moments from stored force and CP data, but stored moment data is used when more convenient or more available. Tail angle of attack is computed from

$$\alpha_H = \alpha - \epsilon + \delta_H + (\dot{\theta} + d\epsilon/d\alpha \dot{\alpha}) l_t/V$$

thus accounting for $\dot{\theta}$ and $\dot{\alpha}$ effects.

The trimming procedure is based on an iterative linear simultaneous closure of three or six degrees of freedom. A square matrix of accelerations due to increments from an assumed first guess in each of the trim variables is generated. Four passes through AERO are required to generate the matrix equation:

$$\begin{bmatrix} \dot{u}/TH & \dot{u}/\alpha & \dot{u}/\delta_H \\ \dot{w}/TH & \dot{w}/\alpha & \dot{w}/\delta_H \\ \dot{q}/TH & \dot{q}/\alpha & \dot{q}/\delta_H \end{bmatrix} \begin{bmatrix} \Delta TH \\ \Delta \alpha \\ \Delta \delta_H \end{bmatrix} = - \begin{bmatrix} \dot{u}_{SS} \\ \dot{w}_{SS} \\ \dot{q}_{SS} \end{bmatrix}$$

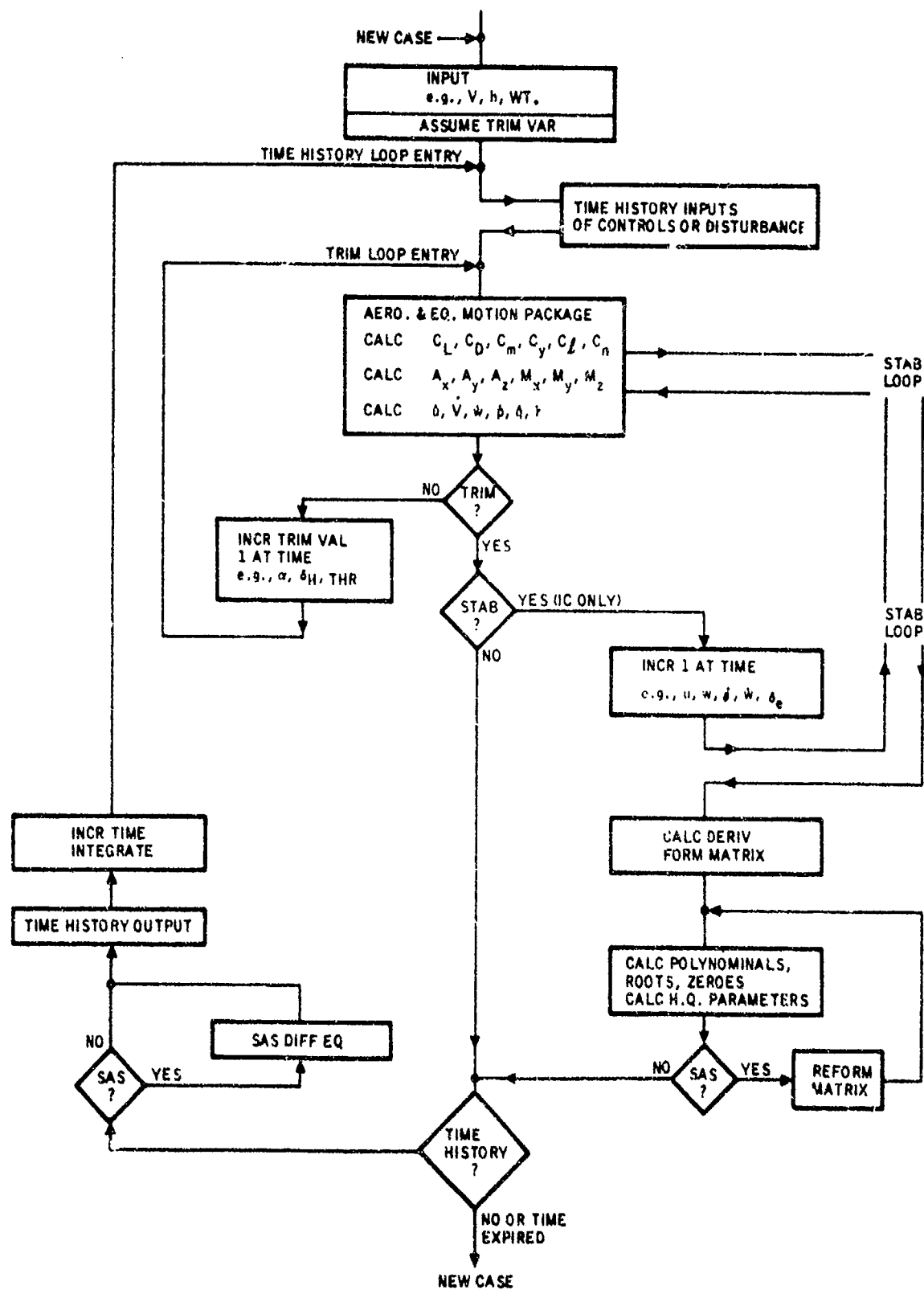


Figure I-1. TRIM-STAB Program Flow.

This equation is inverted to solve for the three increments to form a second iteration. Few problems have been encountered in trimming a variety of vehicles. A combination of trimming very near the stall, extremely nonlinear data, and bad initial guesses can force runs to be repeated.

The STAB portion of the program is used after a trim is established. The body axis variables, including u , w , \dot{w} , $\dot{\theta}$, δe , δ_H , δ_{FL} , and throttle, are perturbed one at a time. Dimensional derivatives are computed and printed out.

Matrices are formed and characteristic roots, as well as zeros, for any selected numerators are calculated. For the longitudinal data both a 3 x 3 fourth-order matrix and a 2 x 2 second-order short-period matrix are formed. The polynomial constants are used to calculate such parameters as $d\delta e/dV$ and $d\gamma/dV$ in the former case and n_Z/α and $\delta e/g$ in the latter.

Transients to steps can be calculated from residues. The residues can be used to calculate such handling quality parameters as $POSC/PAVG$.

The program can also use the stored nonlinear data and by numerical integrations generate time histories for any specified initial condition or time history input, such as engine failures.

APPENDIX II

MODIFICATIONS TO MIL-F-8785B TURBULENCE MODEL FOR
STAI SIMULATION TASKS

APPENDIX II
MODIFICATIONS TO MIL-F-8785B TURBULENCE MODEL FOR
STAI SIMULATION TASKS

I. INTRODUCTION

The STOL Tactical Aircraft Investigation (STAI) studies require, as a part of the flight simulation tasks, the use of a low-altitude, non-gaussian turbulence model for pilot evaluation of the candidate STOL configurations. Digital implementation of a Dryden spectral form turbulence model using MIL-F-8785B rms values and scale lengths produced unreasonably severe turbulence simulation at and near ground levels. Modifications were made to the MIL-F-8785B rms and scale length parameters to provide an acceptable turbulence model for use in the STAI Simulation tasks. Details of the problem and the modifications made to improve the model are presented in this report.

II. DESCRIPTION OF THE PROBLEM

A number of problems arose in the course of digitally implementing a non-gaussian turbulence model for use in the simulation tasks of this program. Early attempts to activate turbulence were completely unsuccessful. Mean values of gust components departed dramatically from zero and rms values did not match expected values. These early problems were traced to the irregular integration intervals used in the real-time simulation program and modification to the software corrected these deficiencies. In seeking out the cause of these discrepancies, the digitally-generated noise (both Gaussian and non-Gaussian noise generators were developed) was analyzed and verified repeatedly. Yet when the Dryden form filtering specified in MIL-F-8785B was used the turbulence simulation became so severe at near-ground altitudes as to make landing on the runway nearly impossible. With the correctness of the noise generation already well confirmed, attention centered on the filter form. Plots of the specified scale lengths for the three gust components were made. These plots for L_u , L_v and L_w are shown in figures 1, 2 and 3, respectively. They are identified by the notated reference to MIL-F-8785B. Clearly each of these scale lengths goes to zero at ground level. Also plotted were the rms values (σ_u , σ_v and σ_w) of the gust components. These are shown in figures 4 and 5. The dramatic upsweep of σ_u and σ_v results from the way that the gust component scale lengths of the MIL-spec approach zero as the aircraft approaches the ground.

III. SOLUTION DESCRIPTION

One alternative, allowed by the MIL-spec, to avoid this problem is to fix the scale lengths and rms values to their 500 feet-above-ground values thus providing a simulation of relatively constant turbulence conditions. This seems to be a rather significant compromise of the near-ground turbulence situation. Recent crosswind landing studies conducted at Convair used a turbulence model developed from extensive low-altitude wind data compiled by NASA. The turbulence effects of this study were considered to be quite typical and it was therefore determined to adapt the MIL-F-8785B turbulence model to incorporate the near-ground turbulence characteristics defined in NASA document TM X-64589. Linear approximations of the low-altitude gust component scale lengths derived by Fichtl, et al in TM X-64589 were designed to coincide with the MIL-F-8785B values for a 1750 foot altitude above ground level. These "Modified Schedules" can be seen in figures 1, 2 and 3 along with the NASA specified schedules. Note that the NASA schedules of scale length are held constant at the 60 foot altitude values when at or below 60 feet above ground level. Rms values of the gust components are defined the same as in the MIL-spec. For this simulation the value of σ specified in MIL-F-8785B was used, with the zero altitude value extrapolated to be 6.8 fps. The modified values of σ_u and σ_v are plotted on Figure 4. It can be noted that these values are significantly higher than the NASA values of Figure 4. This is due to the desire of having the low-altitude values coincide with the MIL-F-8785B spec. at 1750 feet above ground. Figure 6 is a plot of σ^2/L for all three schedules. Note that all three turbulence models use the relationship that -

$$\frac{\sigma_u^2}{L_u} = \frac{\sigma_v^2}{L_v} = \frac{\sigma_w^2}{L_w}$$

For an assumed typical approach speed of 80 knots (135 ft/sec) the corner frequencies of the gust component filters change with altitude and are plotted in figures 7, 8 and 9.

IV. VALIDATION AND APPLICATION

Non-Gaussian and Gaussian noise sources were passed through the shaping filters whose parameters were varied as already described to produce the gust components for the simulation task. Generated noise distributions were plotted against calculated values and found to match quite well. Turbulence spectra and output distributions to Gaussian noise were plotted and verified to be close to exact solutions. Results of this validation work are reported in GD/Convair Internal Memo AD-71-62, "Turbulence Generator for Flying Quality Investigation", G. R. Friedman. The selection of scale factors to be

applied to the magnitude of the gust components was established through qualitative evaluation using the fixed-base simulator. The significant parameters for judgement were visual observations of the visual scene and flight instruments. It was found that, when the turbulence components were introduced at unity scale factor, turbulence responses of the aircraft were unreasonably severe relative to actual flight experience. All gust component scale factors were reduced to 0.5 and the w and v gust responses were still considered too large. Scale factors which were eventually settled upon as acceptable were 0.5, 0.3 and 0.3 for the u, v, and w gust components, respectively.

FIGURE 1
L_U VERSUS ALTITUDE

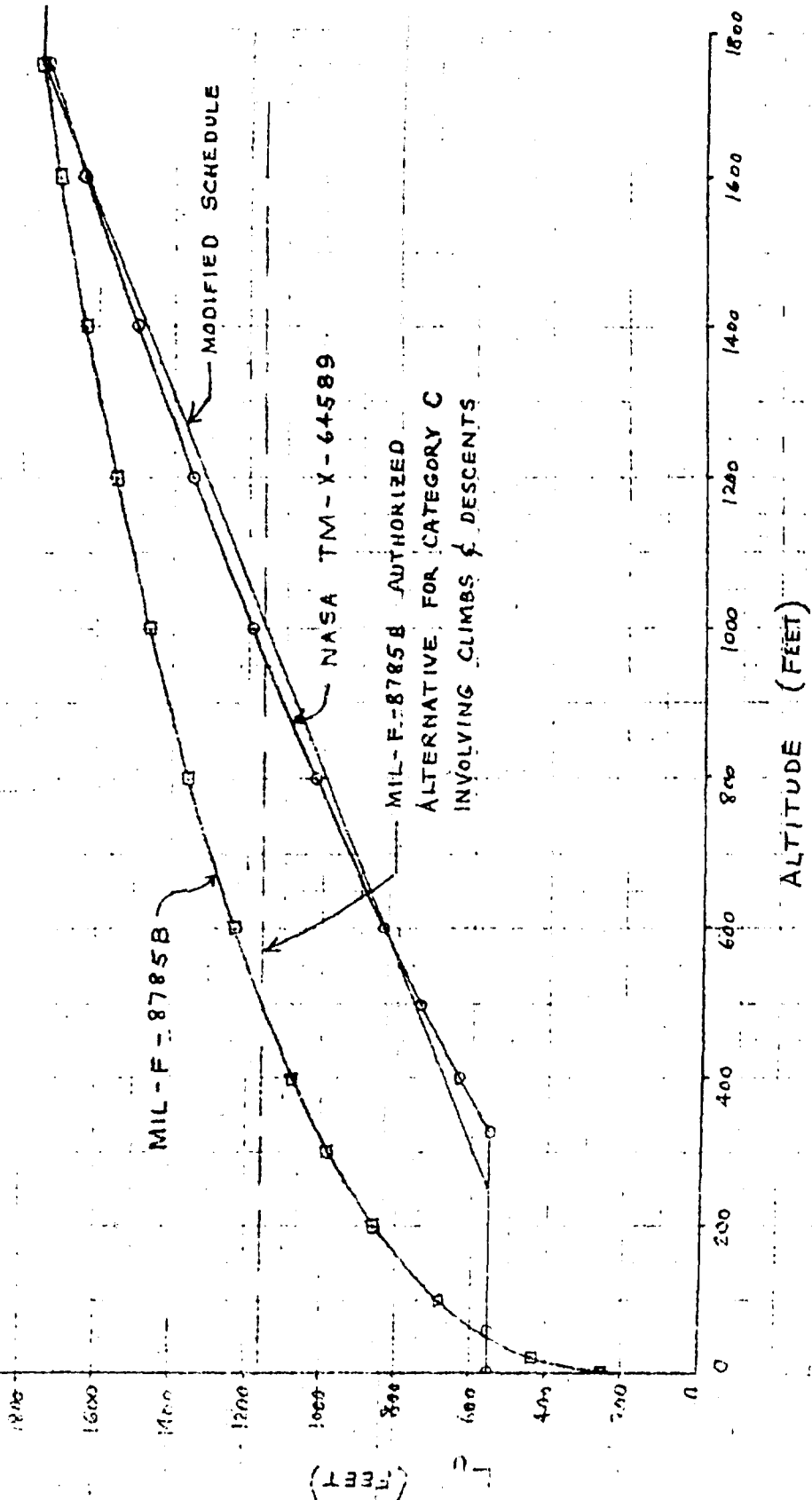


FIGURE 2
L_v VERSUS ALTITUDE

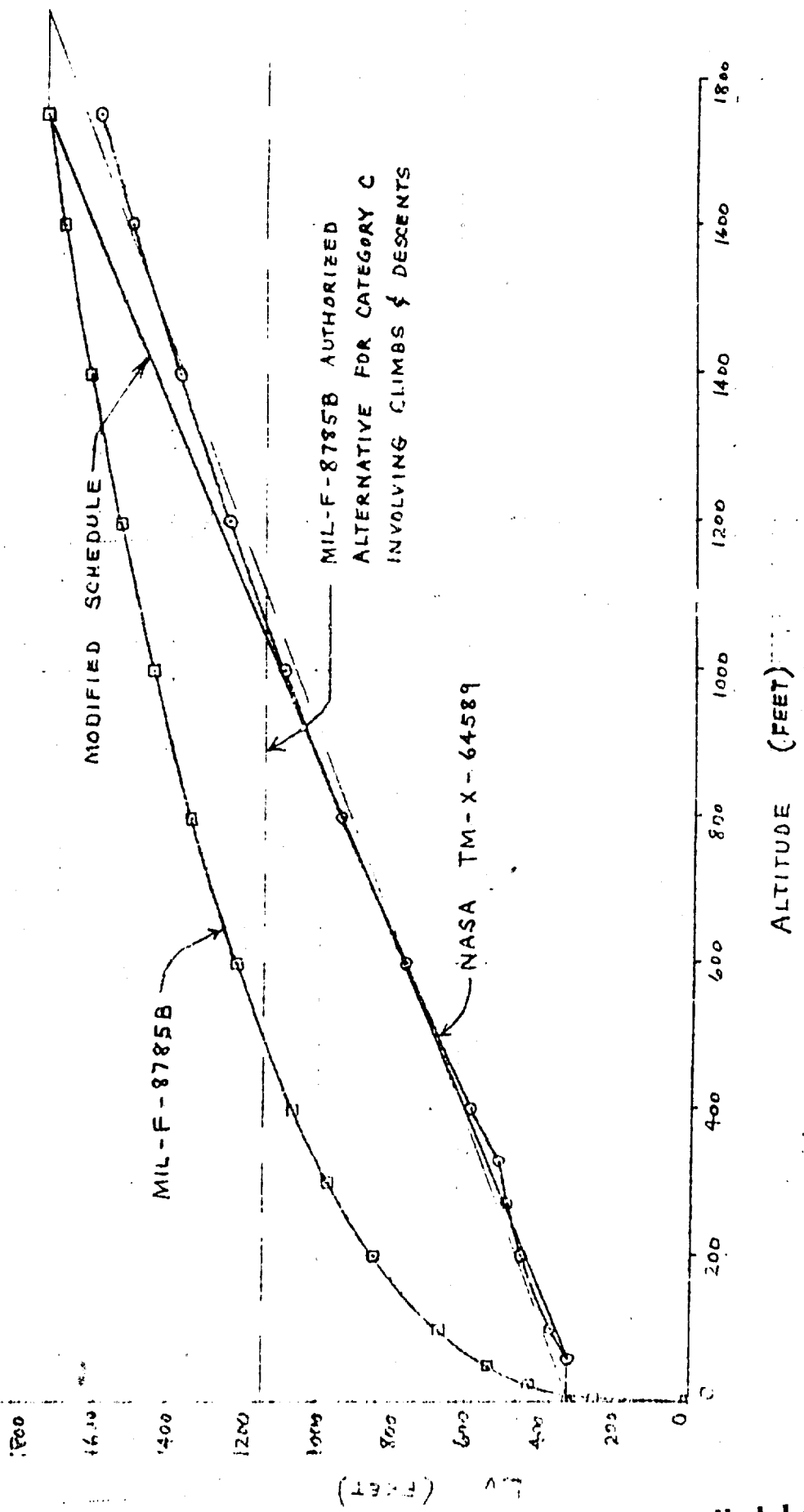


FIGURE 3
L_w VERSUS ALTITUDE

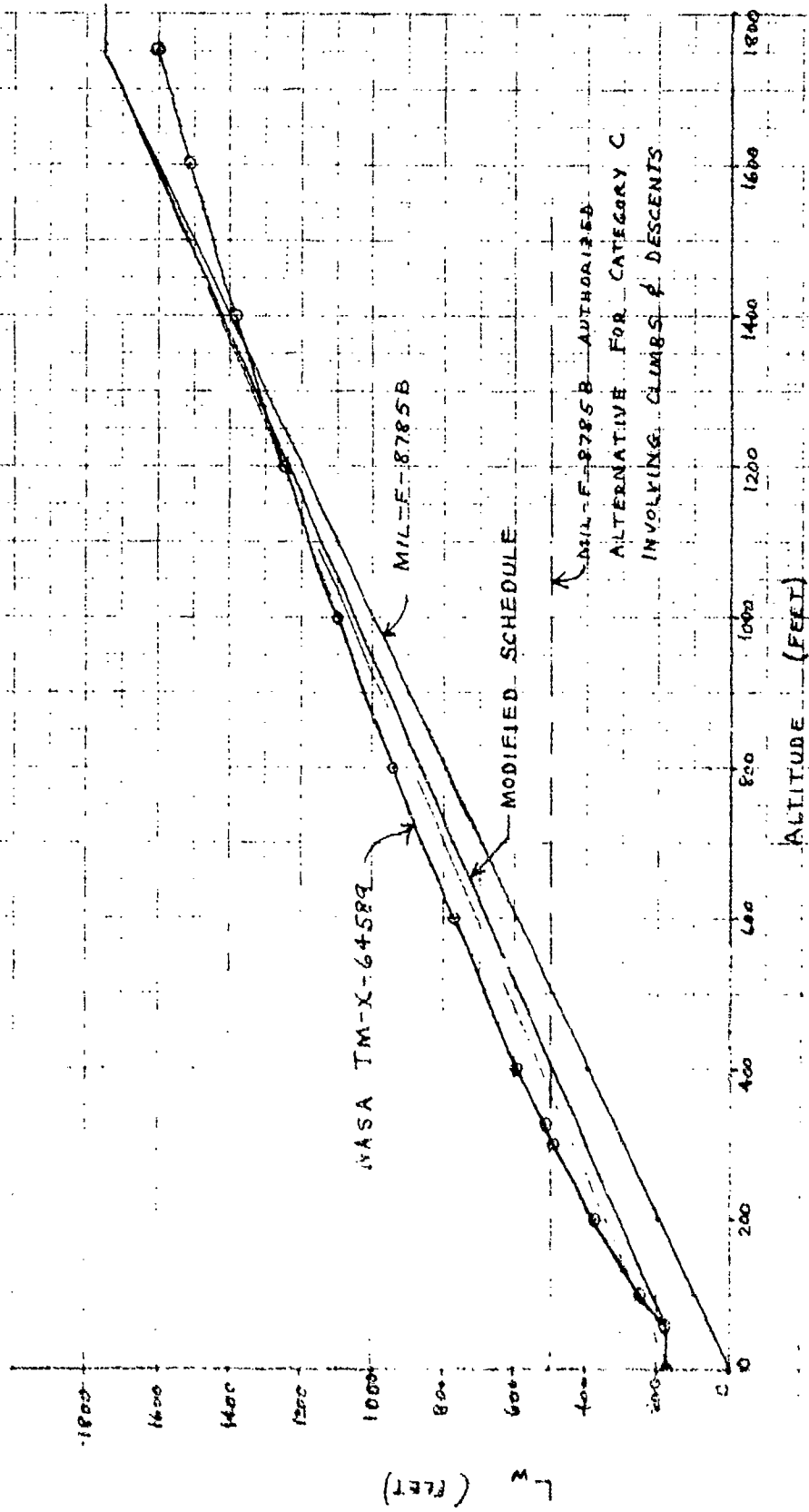


FIGURE 4
 σ_u & σ_v VERSUS ALTITUDE

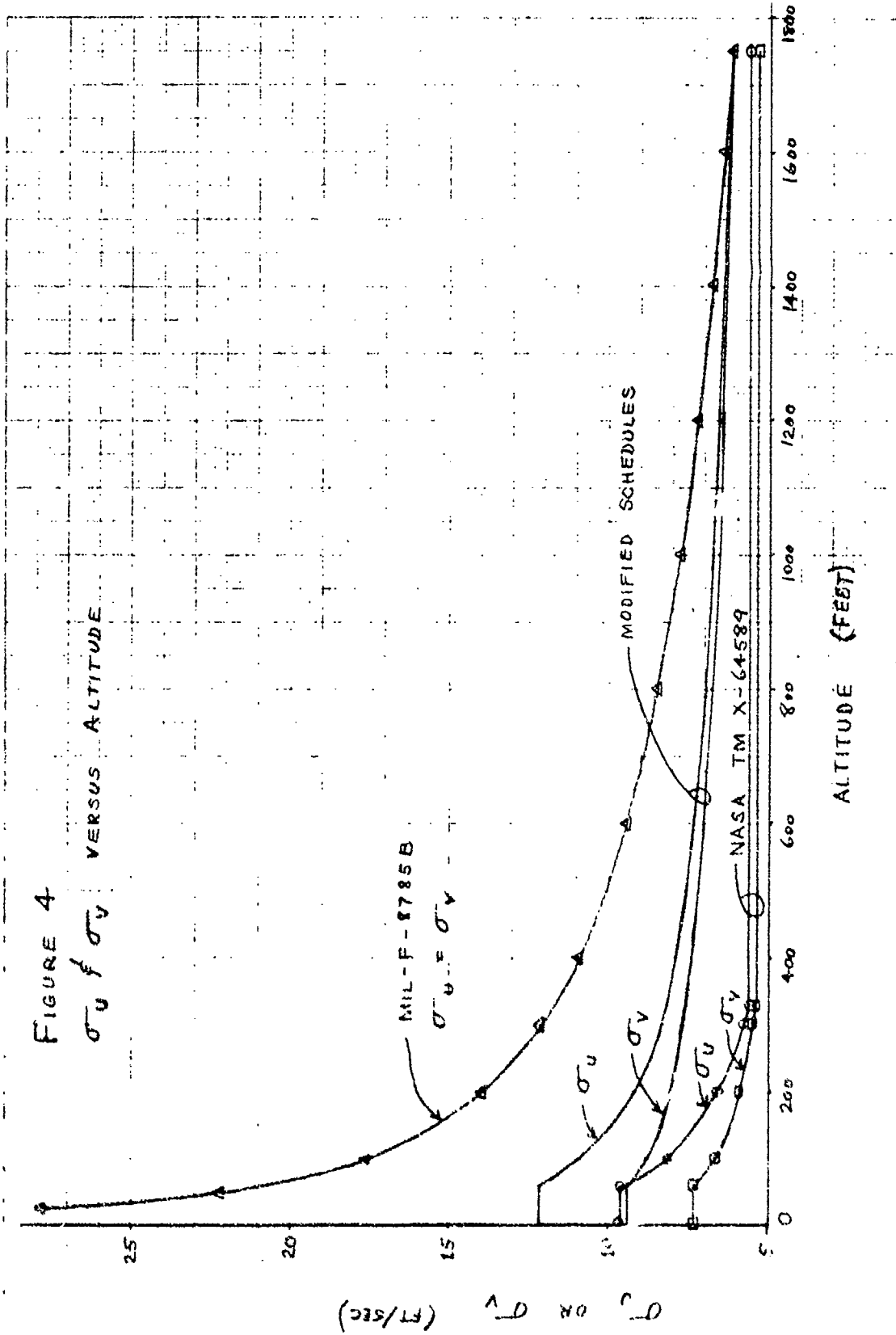


FIGURE 5
 σ_w VERSUS ALTITUDE

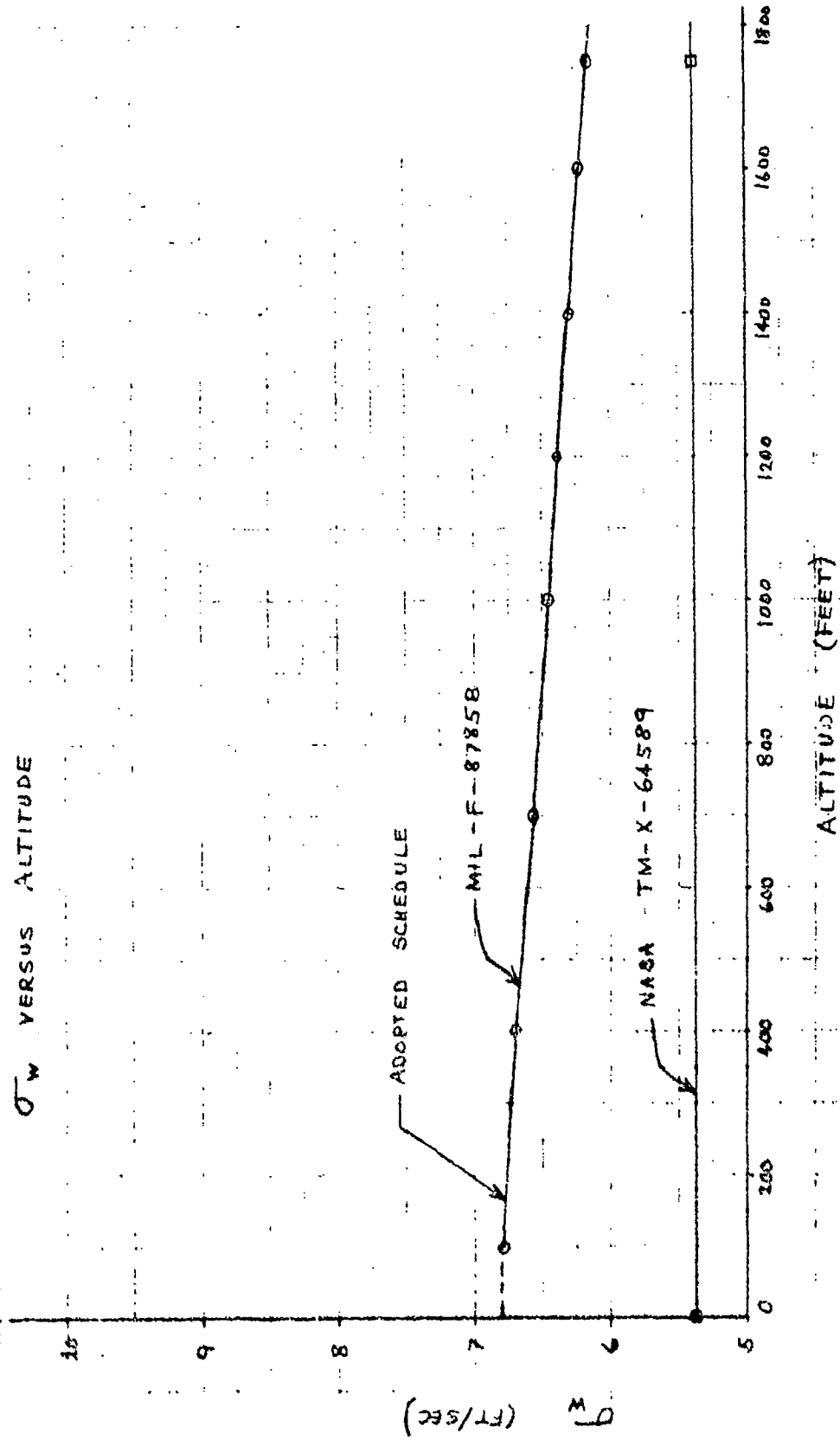


FIGURE 6
 σ^2/L VERSUS ALTITUDE

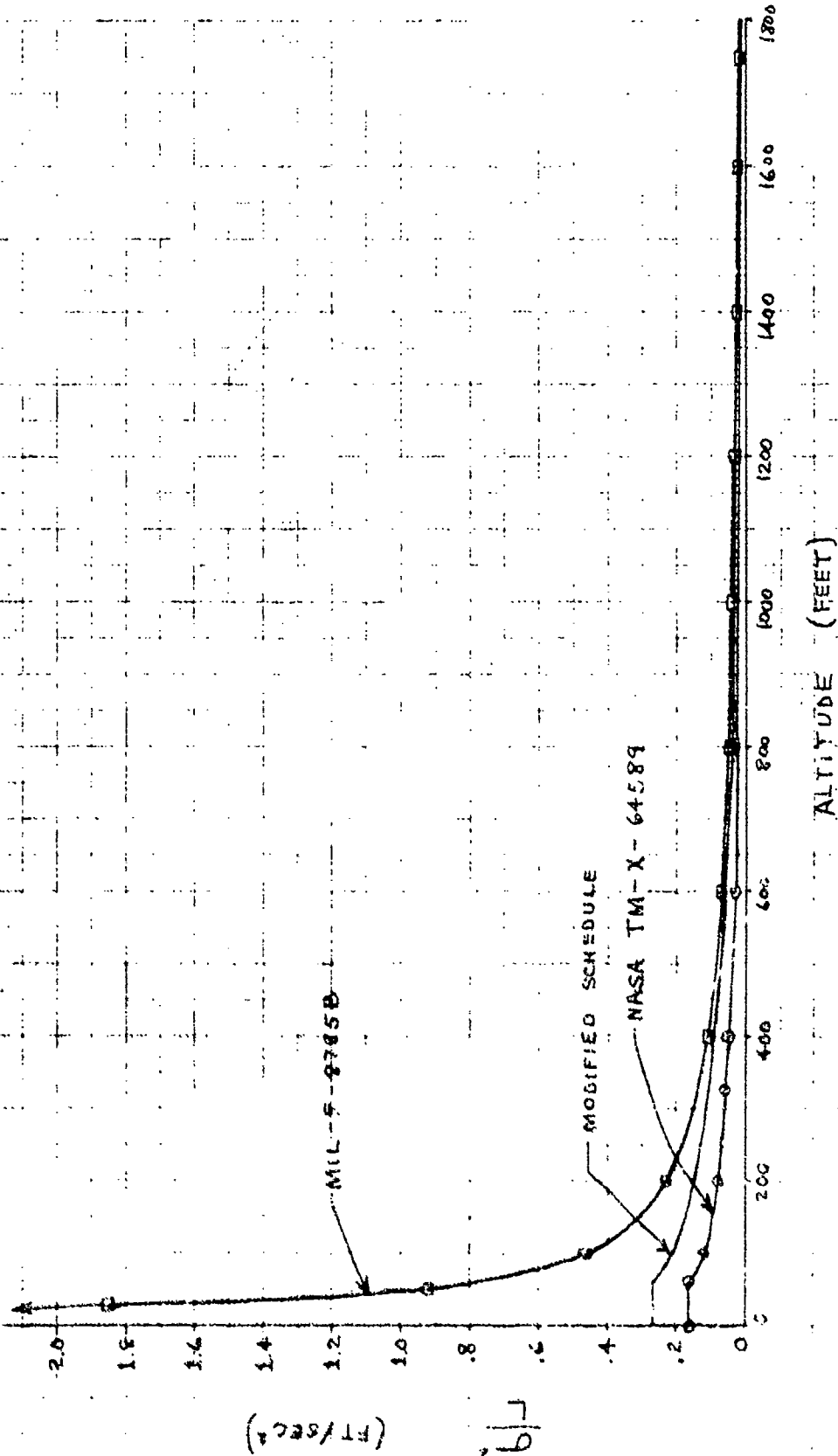


FIGURE 7 LONGITUDINAL GUST CORNER FREQUENCY
 (ω_u) VERSUS ALTITUDE FOR VEL. = 135 FPS (80 KTS)

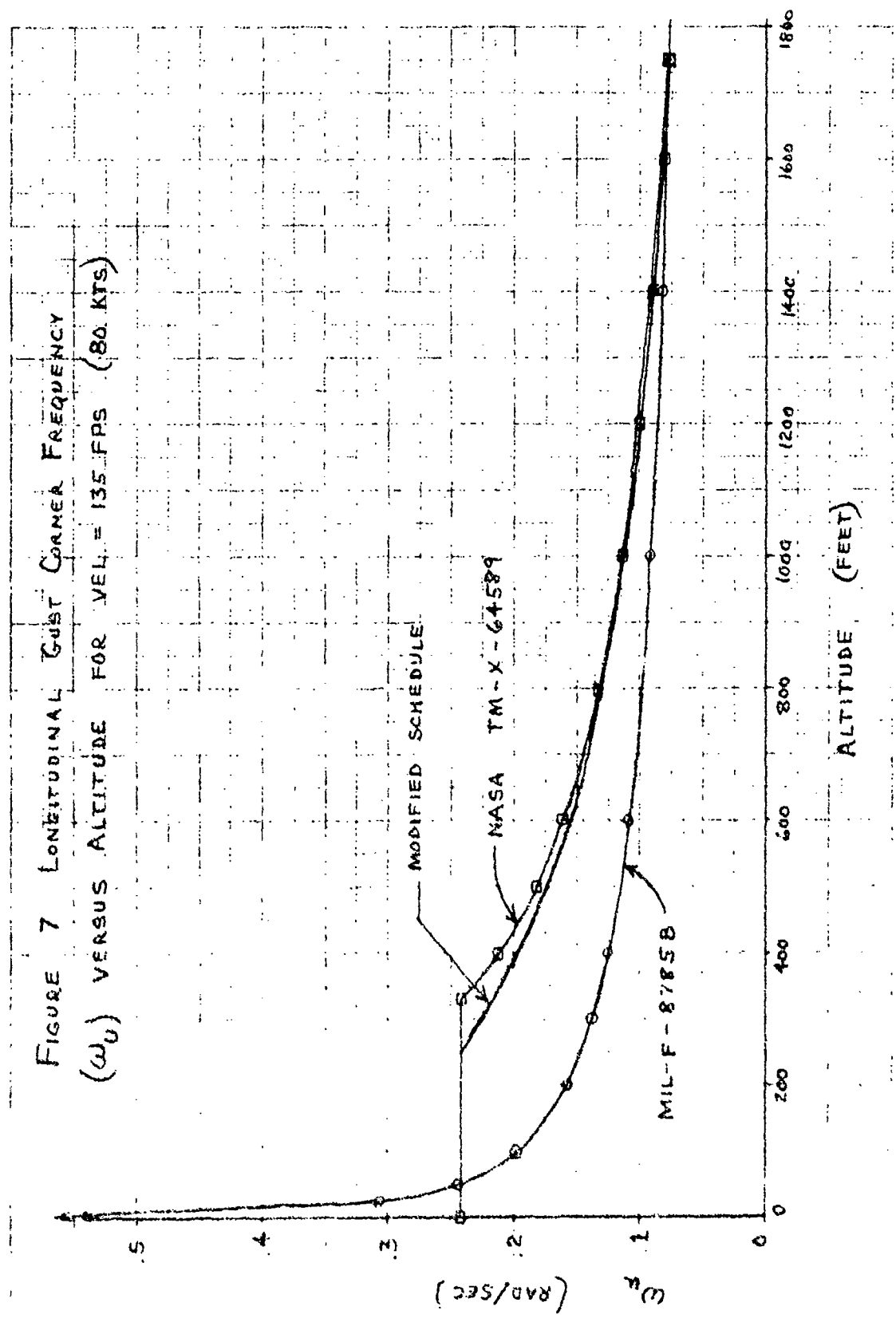


FIGURE 8 SIDE GUST CORNER FREQUENCY
 (ω_{Tr}) VERSUS ALTITUDE FOR VEL. = 135 FPS (80 KTS).

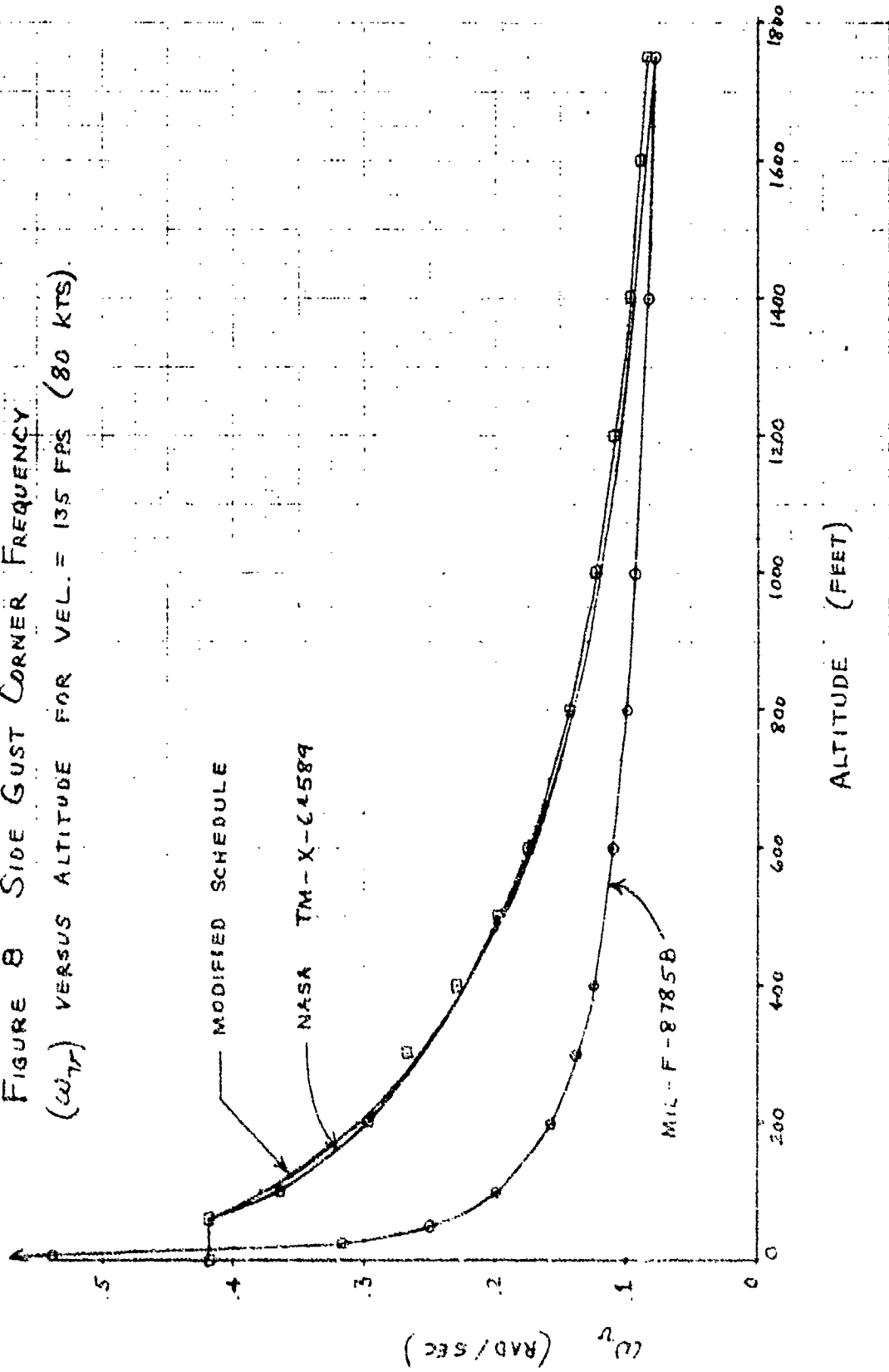
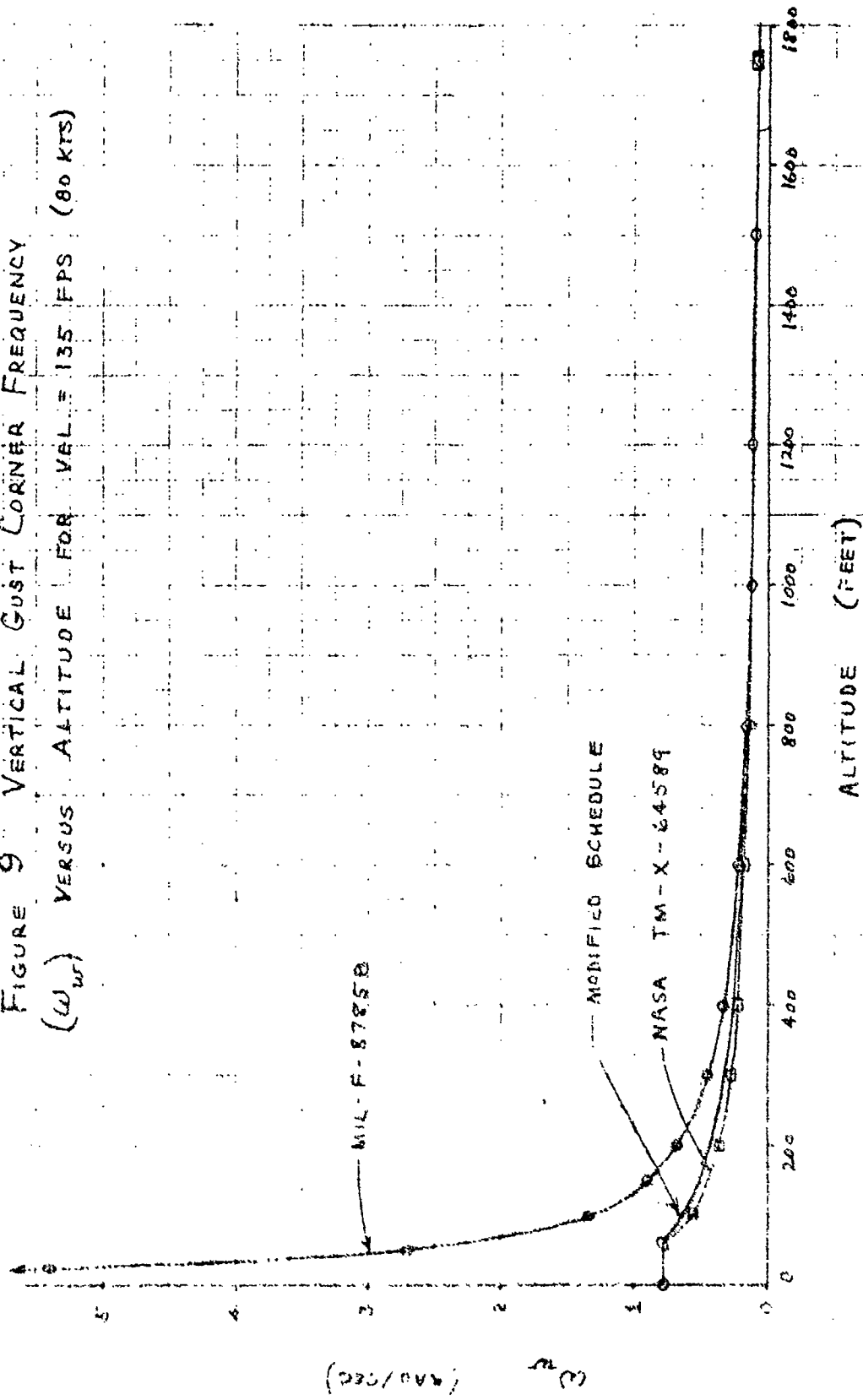


FIGURE 9 VERTICAL GUST CORNER FREQUENCY
 (ω_{WF}) VERSUS ALTITUDE FOR $V_{REF} = 135$ FPS (80 KTS)



APPENDIX III

REPRESENTATIVE STAI SIMULATION DATA

APPENDIX III

REPRESENTATIVE STAI SIMULATION DATA

The data runs in this appendix (which constitute about five percent of the total data) reflect material that is representative of the significant findings used for pilot recommendations. They show the effects of technique, environment, configuration parameters, and the use of varying levels of simulation hardware. The data does not show many of the combinations and considerations eliminated early in the evaluations.

The evaluations progressed from simulations of the externally blown flap, internally blown flap (with and without partial vectoring of thrust), and vectored thrust configurations on the Convair Aerospace fixed-base simulator to fixed-base and moving-base evaluations of the externally blown flap configuration on the large amplitude simulator (LAS). The LAS fixed-base evaluation of the externally blown flap (EBF) configuration was used to establish a data base for identical data runs accomplished on the Convair Aerospace fixed-base simulator. These fixed-base runs were then evaluated for those identical data runs to determine the significance of using a moving-base simulator for future evaluations. The data was generally the same regardless of the type of simulation used, although the accompanying qualitative comments were usually more incisive for the LAS moving base where a significant amount of motion was being simulated. The similarity of LAS fixed-base data runs and the moving-base runs was shown only for a small representative sample. Data runs that were primarily performance orientated (such as in the go-around subcategory) were not shown for the LAS, as they were not sensitive to that type of simulation.

Four subcategories of the terminal flight phase were investigated: approach, flare/touchdown, go-around, and transition. The approach subcategory included glide path following from the first correction to the proper glide path and centerline from an initial flight path angle and heading parallel to the desired paths. This continued to approximately 100 feet above ground level (AGL) to arrive at a point from which a subsequent maneuver to flare and touchdown could be accomplished. The flare/touchdown subcategory began with the aircraft stabilized on the glideslope and centerline in a position to initiate the flare. It continued through the flare until touchdown had been achieved. This subcategory was evaluated only on the Convair Aerospace fixed-base simulator and is of questionable value because of the lack of ground-effect data at the time of the evaluations. The go-around subcategory began with the aircraft stabilized on the glideslope and centerline. Go-around was initiated at a sufficient height to preclude inadvertent ground contact and continued through to the point at which the aircraft was climbing back through the go-around initiation height or it was evident that a successful go-around could not be accomplished.

The transition subcategory began with the aircraft in conventional cruise flight with the gear down and included all airspeed and flap changes necessary to arrive on the glidepath in the landing approach configuration. The transition subcategory was evaluated in three separate ways: total transition, initial transition, and final transition. Total transition included one continuous configuration and airspeed change from cruise to approach flight. Because of the difficulty in precise flying through this transition, it was decided to break the transition into two phases. Initial transition included the transition from cruise flight to an intermediate flap angle and airspeed that was identical to those used in the go-around subcategory. An aircraft so configured could conceivably be used for flying a GCA pattern or it could be configured to these intermediate conditions on a base leg. Final transition included the final airspeed and flap changes to the STOL configuration for intercepting and arriving on the proper glideslope for the landing approach.

Where applicable, the Convair Aerospace fixed-base simulation data runs are referenced to the LAS data runs. These are cross-correlated in Table III-1 to show which runs are identical by listing the run numbers for the two simulators on the same line, with the page number directly following the applicable simulator type and run number.

The following abbreviations and definitions are used in this appendix.

δ_F	Flap position (degrees)
$\dot{\delta}_F$	Flap movement rate (deg/sec)
$i \delta_F$	Initial flap position (degrees)
$f \delta_F$	Final flap position (degrees)
A/S	Airspeed (knots)
$i A/S$	Initial airspeed (knots)
$f A/S$	Final airspeed (knots)
$\Delta\theta$	Plus pitch attitude change (degrees)
$\dot{\theta}$	Pitch Rate
	NOM \approx 4 deg/sec
	SLOW \approx 2 deg/sec
	FAST \approx 7 deg/sec

MODES	Control System Configuration
	NO Normal: pitch attitude hold, turn coordination plus pitch, lateral and directional damping
	A/S Autospeed button plus NO
	APP Approach button plus NO
	BOTH Autospeed and approach button plus NO
	B. A/F Bare airframe, with no augmentation or damping
TECH	Control Technique
	CONV Conventional aircraft control of airspeed and flight path angle (γ by pitch, airspeed by power)
	STOL STOL aircraft control of airspeed and flight angle (γ by power, airspeed by pitch)
COND	Conditions of Aircraft or External Source
	30 KT Variable 90-degree crosswind with mean value of 30 knots
	G With gust model
	EO-2 SEC With critical engine out - 2-second delay
	UP 40 Flaps raised to 40 degrees simultaneous with go-around pitch maneuver
	PITCH 40 Flaps raised to 40 degrees after pitch maneuver ($\Delta\theta$) complete
	FWD Most forward cg location
	AFT Most aft cg location
	Lightest aircraft weight
	HVY Heaviest aircraft weight
CFB	Convair Aerospace Fixed-Base Simulation
LAS	Large Amplitude Simulation
	M. B. Moving base
	F. B. Fixed base
EBF	Externally blown flap aircraft configuration
IBF/VT	Internally blown flap with partial thrust vectoring configuration
VT	Vectored thrust configuration

LONG	Longitudinal parameters
LAT	Lateral directional parameters
FLARE HT	Flare initiation altitude (feet above touchdown)
C/H	Cooper/Harper pilot rating
γ	Flight path angle (degrees)
γ CONTROL BY POWER	STOL technique
γ CONTROL BY PITCH	Conventional technique
FULL AUG CONTROL	Using AIRSPEED and APPROACH modes
PITCH AUG ONLY	No AIRSPEED and APPROACH modes
DECISION HEIGHT	Altitude at which go-around is initiated
δ STICK	Pilot's control stick displacement
δ ELEV	Elevator position
q	Pitch rate
θ	Pitch attitude
β	Sideslip angle
r	Yaw rate
δ RUDDER	Rudder position
ϕ	Bank angle
p	Roll rate
δ AILERON	Aileron position
δ SPOILER	Spoiler position
δ FLAP	Flap position
AGL	Above ground level (feet)

Table III-1. Run Cross-Correlation and Location

EXTERNALLY BLOWN FLAP (EBF)

Approach Subcategory

Convair Fixed Base (CFB)

<u>δF</u>	<u>Airspeed</u>	<u>Technique</u>	<u>Modes</u>	<u>CFB Runs</u>	<u>Page No.</u>	<u>LAS Runs</u>	<u>Page No.</u>
60	80	STOL	Both	A	III-12	-	
60	80	Conv	Both	B	III-13	A36 M.B.	III-18
60	80	Conv	No	C	III-14	A24 M.B.	III-19
45	80	STOL	No	D	III-15	A2 M.B.	III-20
55	80	STOL	No	F	III-16	A8 M.B.	III-21
60	80	STOL	No	G	III-17	A6 M.B.	III-23

Large Amplitude Simulator (LAS)

<u>δF</u>	<u>Air. speed</u>	<u>Technique</u>	<u>Modes</u>	<u>CFB Runs</u>	<u>Page No.</u>	<u>LAS Runs</u>	
60	80	Conv	Both	B	III-13	A36 M.B.	III-18
50	80	Conv	No	C	III-14	A24 M.B.	III-19
45	80	STOL	No	D	III-15	A2 M.B.	III-20
55	80	STOL	No	F	III-16	A8 M.B.	III-21
60	80	STOL	No	G	III-17	A6 F.B.	III-22
60	80	STOL	No	G	III-17	A6 M.B.	III-23
55	80	STOL/G	No	None	-	A53 M.B.	III-24
55	80	Conv/G	No	None	-	A54 M.B.	III-25
45	80	STOL/EO-2 sec	No	None	-	A69 (Long.) M.B.	III-26
45	80	STOL/EO-2 sec	No	None	-	A69 (Lat.) M.B.	III-27
55	80	STOL/EO-2 sec	No	None	-	A77 (Long.) M.B.	III-28
55	80	STOL/EO-2 sec	No	None	-	A77 (Lat.) M.B.	III-29
60	80	STOL/EO-2 sec	No	None	-	A81 (Long.) M.B.	III-30
60	80	STOL/EO-2 sec	No	None	-	A81 (Lat.) M.B.	III-31
55	90	STOL	B. A/F	None	-	A77 M.B.	III-32
55	90	STOL/G	B. A/F	None	-	A91 (Long.) M.B.	III-33
55	80	STOL/G	B. A/F	None	-	A91 (Lat.) M.B.	III-34
55	80	STOL/EO-2 sec	B. A/F	None	-	A95 (Long.) M.B.	III-35
55	80	STOL/EO-2 sec	B. A/F	None	-	A95 (Lat.) M.B.	III-36
55	80	STOL/30 kt	No	None	-	CW 1 M.B.	III-37
55	80	STOL/30 kt/G	No	None	-	CW 3 M.B.	III-38
55	80	STOL/30 kt/G	B. A/F	None	-	CW 6 M.B.	III-39

Table III-1. Run Cross-Correlation and Location, Cont

Flare/Touchdown Subcategory

Convair Fixed Base (CFB)

δF	Technique	Flare Height	$\Delta\theta$	CFB Runs	Page No.	LAS Runs
55	Normal $\dot{\theta}$	80	5	A	III-40	None
55	Normal $\dot{\theta}$	80	15	C	III-40	None
55	Normal $\dot{\theta}$	80	10	F	III-40	None
55	Normal $\dot{\theta}$	70	10	D	III-41	None
55	Normal $\dot{\theta}$	80	10	B	III-41	None
55	Normal $\dot{\theta}$	90	10	E	III-41	None
55	Fast $\dot{\theta}$	80	10	I	III-42	None
55	Slow $\dot{\theta}$	80	10	J	III-42	None
60	Normal $\dot{\theta}$	80	10	L	III-42	None
55	+10% Power, Normal $\dot{\theta}$	80	10	G	III-43	None
55	+10% Power, Normal $\dot{\theta}$	80	10	H	III-43	None
55	Full Power	80	0	K	III-43	None

Go-Around Subcategory

Convair Fixed Base (CFB)

δF	Airspeed	$\dot{\delta F}$	Technique	$\Delta\theta$	$\dot{\theta}$	Modes	CFB Runs	Page No.	LAS Runs
55	80	5	Up 40	10	Nom	Both	F	III-44	None
55	80	5	Up 40	10	Fast	Both	M	III-44	None
55	80	5	Up 40	5	Nom	Both	L	III-45	None
55	80	5	Up 40	15	Nom	Both	B	III-45	None
50	80	5	Up 40	10	Nom	Both	D	III-46	None
60	80	5	Up 40	10	Nom	Both	G	III-46	None
55	80	5	Pitch 40	10	Nom	Both	H	III-47	None
55	80	5	Pitch 40	10	Nom	No	J	III-47	None

Large Amplitude Simulator (LAS)

δF	Airspeed	$\dot{\delta F}$	Technique/ Condition	$\Delta\theta$	$\dot{\theta}$	Modes	CFB Runs	Page No.	LAS Runs	Page No.
55	80	5	Up 40/EO- 2 sec	10	Nom	No	None	-	G35 M.B.	III-48

Table III-1. Run Cross-Correlation and Location, Cont

Transition Subcategory

Convair Fixed Base (CFB)

<u>i Airspeed</u>	<u>f Airspeed</u>	<u>δF</u>	<u>$i \delta F$</u>	<u>$f \delta F$</u>	<u>CFB Runs</u>	<u>Page No.</u>	<u>LAS Runs</u>	<u>Page No.</u>
140	115	3	0	40	A	III-49	IT2 M. B.	III-58
135	115	3	0	40	B	III-49	IT6 M. B.	III-59
170	115	3	0	40	C	III-50	IT10 M. B.	III-60
155	115	5	0	40	D	III-50	IT7 M. B.	III-61
155	115	1.5	0	40	E	III-51	IT5 M. B.	III-62
80	80	3	40	55	F	III-52	FT2 M. B.	III-63
90	80	3	40	55	G	III-52	FT6 M. B.	III-64
115	80	3	40	55	H	III-53	FT10 M. B.	III-65
125	80	3	40	55	I	III-53	FT14 M. B.	III-66
90	80	5	40	55	J	III-54	FT7 M. B.	III-67
115	80	5	40	55	K	III-54	FT11 M. B.	III-68
115	80	1.5	40	55	L	III-55	FT9 M. B.	III-69
115	80	3	0	55	M	III-56	TT5 M. B.	III-70

Large Amplitude Simulator (LAS)

<u>i Airspeed</u>	<u>f Airspeed</u>	<u>δF</u>	<u>$i \delta F$</u>	<u>$f \delta F$</u>	<u>CFB Runs</u>	<u>Page No.</u>	<u>LAS Runs</u>	
140	115	3	0	40	A	III-49	IT2 F. B.	III-57
140	115	3	0	40	A	III-49	IT2 M. B.	III-58
155	115	3	0	40	B	III-49	IT6 M. B.	III-59
170	115	3	0	40	C	III-50	IT10 M. B.	III-60
155	115	5	0	40	D	III-50	IT7 M. B.	III-61
155	115	1.5	0	40	E	III-51	IT5 M. B.	III-62
80	80	3	40	55	F	III-52	FT2 M. B.	III-63
90	80	3	40	55	G	III-52	FT6 M. B.	III-64
115	80	3	40	55	H	III-53	FT10 M. B.	III-65
125	80	3	40	55	I	III-53	FT14 M. B.	III-66
90	80	5	40	55	J	III-54	FT7 M. B.	III-67
115	80	5	40	55	K	III-54	FT11 M. B.	III-68
115	80	1.5	40	55	L	III-55	FT9 M. B.	III-69
155	80	3	0	55	M	III-56	TT5 M. B.	III-70

Table III-1. Run Cross-Correlation and Location, Cont

INTERNALLY BLOWN FLAPS WITH PARTIAL VECTORING (IBF/VT)

Approach Subcategory

Convair Fixed Base (CFB)

<u>δF</u>	<u>Airspeed</u>	<u>Technique</u>	<u>Modes</u>	<u>CFB Runs</u>	<u>Page No.</u>	<u>LAS Runs</u>
60	80	STOL	No	B	III-72	None
65	80	STOL	No	C	III-73	None
70	75	STOL	No	D	III-74	None
65	80	STOL	Both	F	III-75	None
65	80	Conv	Both	H	III-76	None
65	80	STOL/EO-2 sec	Both	I	III-77	None
60	80	STOL/G	No	J	III-78	None
60	80	STOL/G	Both	K	III-79	None

Go-Around Subcategory

Convair Fixed Base (CFB)

<u>i δF</u>	<u>Airspeed</u>	<u>δF</u>	<u>Technique</u>	<u>Δθ</u>	<u>θ</u>	<u>Modes</u>	<u>CFB Runs</u>	<u>Page No.</u>	<u>LAS Runs</u>
65	80	5	Up 45	5	Nom	No	K	III-80	None
65	80	5	Up 45	15	Nom	No	L	III-80	None
65	80	5	Up 45	10	Nom.	No	D	III-81	None
65	80	7	Up 45	10	Nom	No	H	III-81	None
65	80	5	Up 45	10	Fast	No	F	III-82	None
65	80	3	Pitch 45	10	Nom	Both	M	III-82	None
65	80	5	Pitch 45	10	Nom	Both	N	III-83	None
65	80	7	Pitch 45	10	Nom	Both	C	III-83	None
65	80	5	Pitch 45	10	Nom	No	P	III-84	None
65	80	5	Up 45/EO- 2 sec	10	Nom	Both	Q	III-84	None

Table III-1. Run Cross-Correlation and Location, Cont

VECTORED THRUST (VT)

Transition Subcategory

Convair Fixed Base (CFB)

<u>i Airspeed</u>	<u>f Airspeed</u>	<u>δF</u>	<u>$i \delta F$</u>	<u>$f \delta F$</u>	<u>CFB Runs</u>	<u>Page No.</u>	<u>LAS Runs</u>
155	100	1.5	0	45	B	III-85	None
170	100	1.5	0	45	C	III-87	None
170	100	3	0	45	E	III-87	None
80	80	1.5	45	65	A	III-88	None
100	80	1.5	45	65	C	III-89	None
120	80	1.5	45	65	E	III-90	None
110	80	3	45	65	G	III-91	None
170	80	1.5	0	65	B	III-92	None

Approach Subcategory

Convair Fixed Base (CFB)

<u>δF</u>	<u>Airspeed</u>	<u>Technique</u>	<u>Modes</u>	<u>CFB Runs</u>	<u>Page No.</u>	<u>LAS Runs</u>
70	85	STOL	No	A	III-94	None
70	80	STOL	No	D	III-95	None
70	85	STOL/G	No	F	III-96	None
70	85	Conv/G	Both	H	III-97	None
70	85	STOL/G	Both	I	III-98	None
70	95	B. A/F	No	J	III-99	None
70	85	STOL/EO-2 sec	No	K	III-100	None

Go-Around Subcategory

Convair Fixed Base (CFB)

<u>$i \delta F$</u>	<u>Airspeed</u>	<u>δF</u>	<u>Technique</u>	<u>$\Delta \theta$</u>	<u>$\dot{\theta}$</u>	<u>Modes</u>	<u>CFB Runs</u>	<u>Page No.</u>	<u>LAS Runs</u>
70	85	5	Up 40	5	Nom	No	D	III-101	None
70	85	5	Up 40	15	Nom	No	E	III-101	None
70	85	5	Up 40	10	Nom	No	F	III-102	None
70	85	7	Up 40	10	Nom	No	H	III-102	None
70	85	5	Pitch 40	10	Nom	Both	K	III-103	None
70	85	7	Pitch 40	10	Nom	Both	L	III-103	None
70	85	5	Up 40/EO-2 sec	10	Nom	Both	M	III-104	None
70	80	5	Up 40/EO-2 sec	10	Nom	Both	N	III-104	None

Table III-1. Run Cross-Correlation and Location, Cont

Transition Subcategory

Convair Fixed Base (CFB)

<u>i Airspeed</u>	<u>f Airspeed</u>	<u>δF</u>	<u>$i \delta F$</u>	<u>$f \delta F$</u>	<u>CFB Runs</u>	<u>Page No.</u>	<u>LAS Runs</u>
155	105	1.5	0	40	B	III-105	None
155	105	3	0	40	D	III-106	None
115	85	1.5	40	70	H	III-107	None
85	85	5	40	70	A	III-108	None
85	85	3	40	70	D	III-109	None
105	85	3	40	70	E	III-110	None
95	85	1.5	40	70	G	III-111	None
155	85	1.5	0	70	A	III-112	None

EXTERNALLY BLOWN FLAPS

(EBF)

AIRSPED
(KTS)

δ_{STICK}
(% FULL TRAVEL)

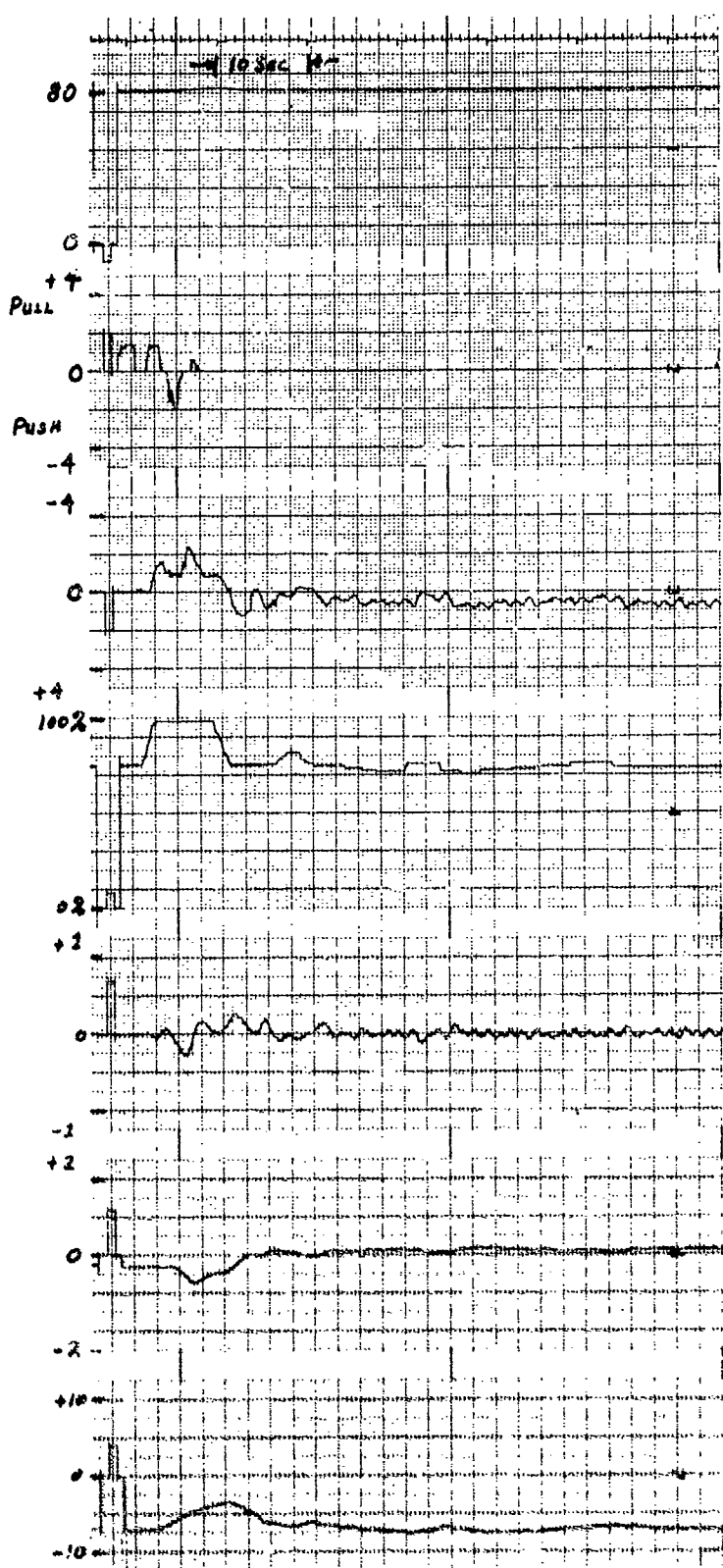
δ_{ELEV}
(DEG)

THROTTLE
(% THRUST)

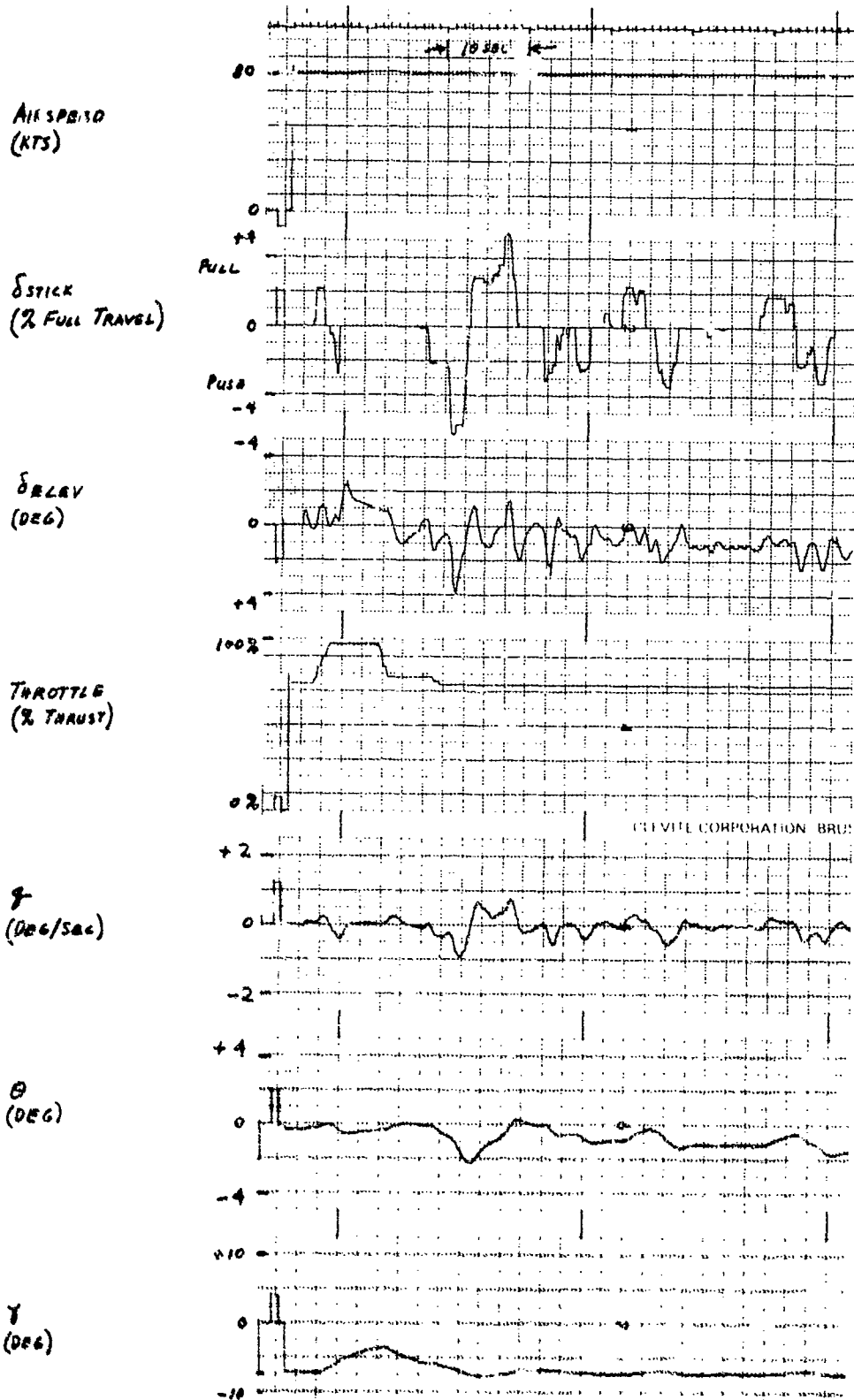
$\dot{\gamma}$
(DEG/SEC)

θ
(DEG)

γ
(DEG)



EBF APPROACH. RUN A. C/H = 2 1/2. $\gamma = -7^\circ$. Flaps = 60°.
 γ CONTROL BY POWER. FULL AUG CONTROL.



EBF APPROACH. RUN B. $C/N = 5$. $\gamma = -7^\circ$. FLAPS = 60° .
 δ CONTROL BY PITCH. FULL AUG. CONTROL.

AIRSPPEED
(KTS)

$\delta_{\text{SIC}}^{\text{C}}$
(% FULL TRAVEL)

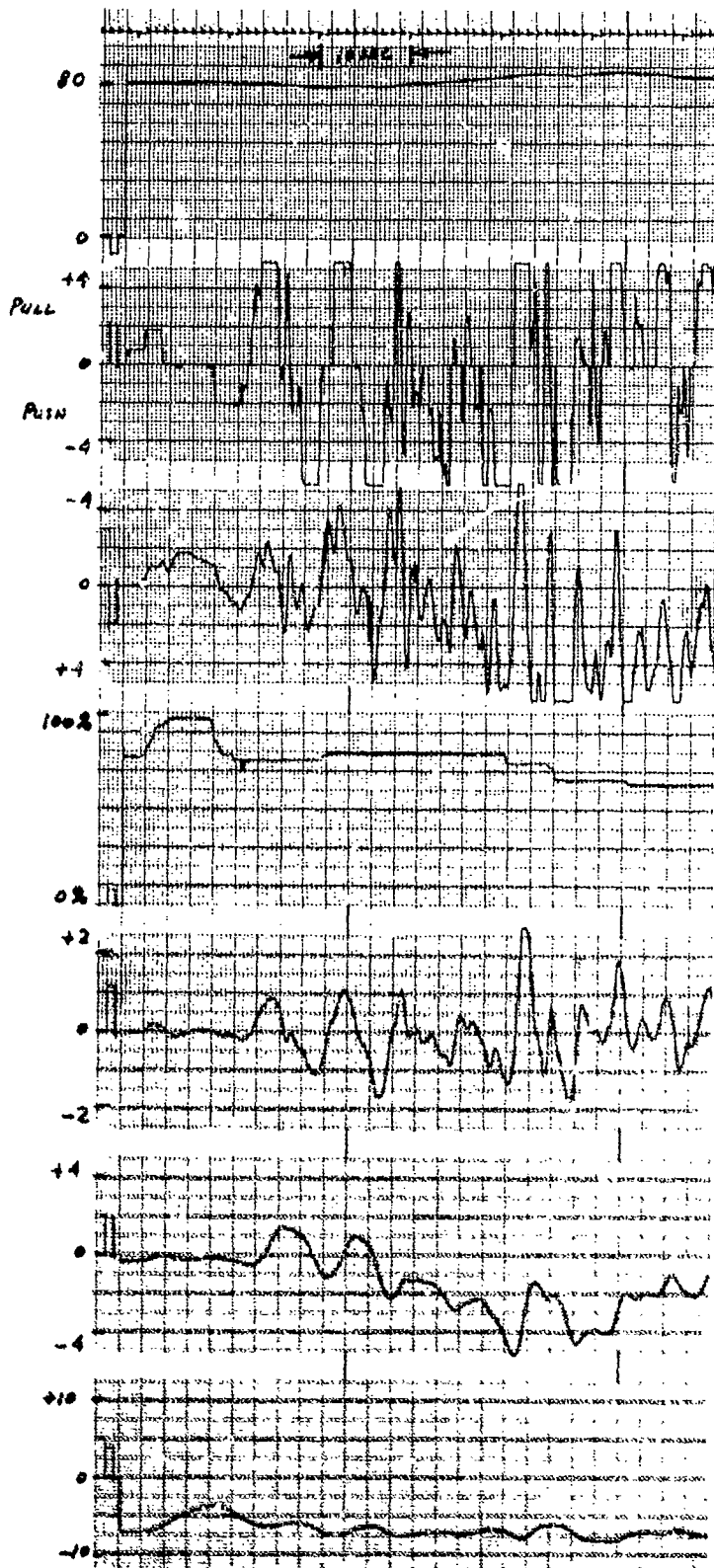
$\delta_{\text{SELY}}^{\text{C}}$
(DEG)

THROTTLE
(% THRUST)

$\dot{\gamma}$
(DEG/SEC)

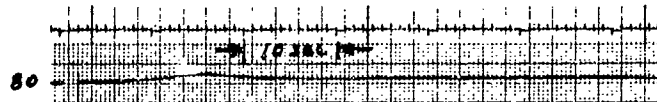
$\dot{\theta}$
(DEG)

$\dot{\phi}$
(DEG)



EBF APPROACH. RUNC. C/H = 6. $\gamma = -7^\circ$. FLAPS = 60°
 γ CONTROL BY PITCH. PITCH AUG CONTROL ONLY

AIRSPED
(KTS)



δ STICK
(% FULL TRAVEL)

PULL

0

PUSH

-4

-4

δ LEV
(DEG)

0

+4

THROTTLE
(% THRUST)

100%

0%

+1

$\dot{\gamma}$
(DEG/SEC)

0

-1

+10

θ
(DEG)

0

-10

+10

γ
(DEG)

0

-10

EXT APPROACH. RUN D. W/C 4. FLAPS = 45° $\gamma = -7^\circ$
 γ CONTROL BY POWER PITCH AUG ONLY.

AIRSPEED
(KTS)

δ STICK
(% FULL TRAVEL)

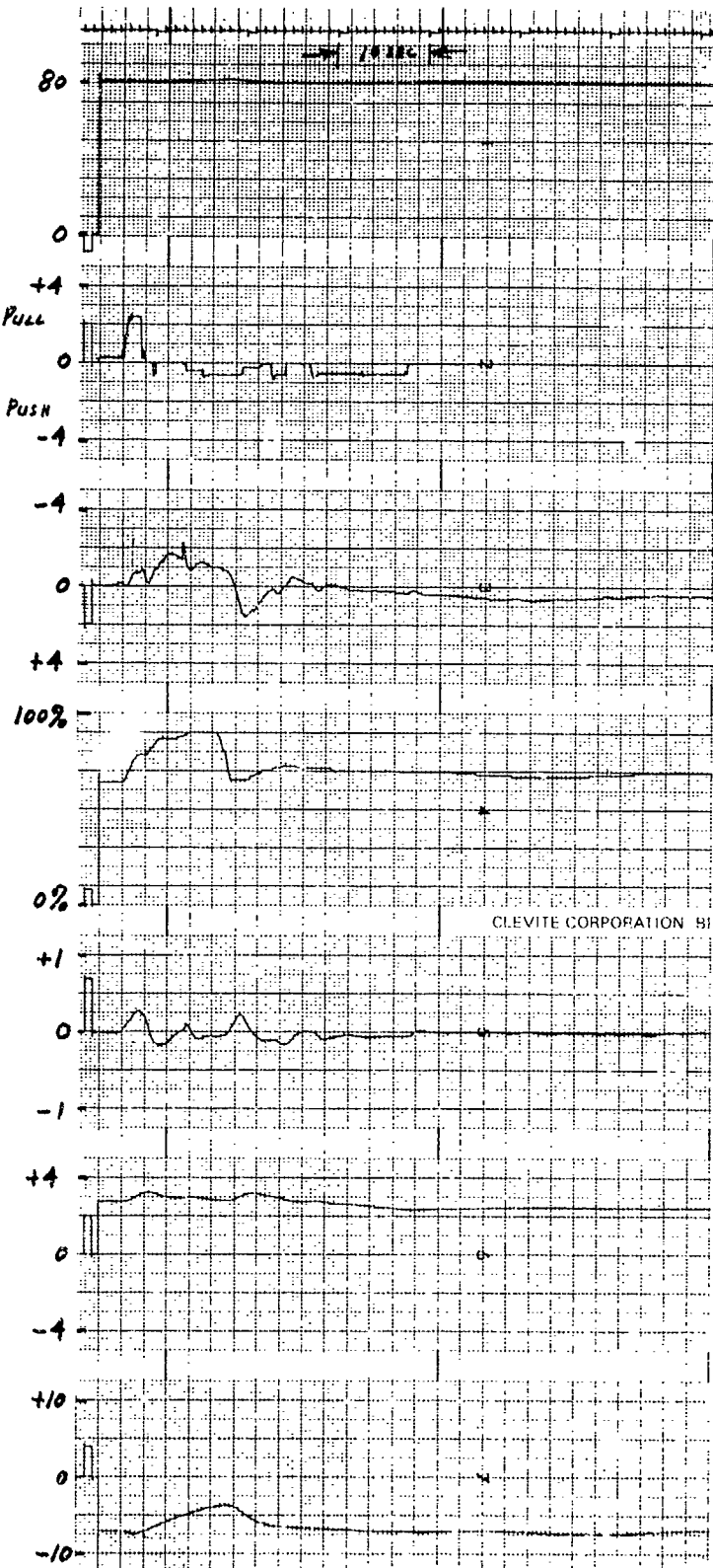
δ ELEV
(DEG)

THROTTLE
(% THRUST)

$\dot{\theta}$
(DEG/SEC)

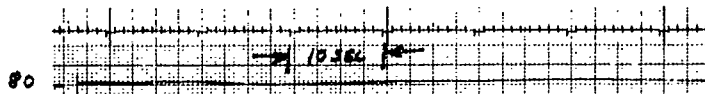
θ
(DEG)

γ
(DEG)

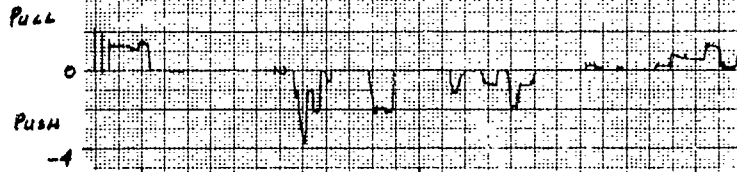


EBF APPROACH. RUN F. C/H = 2 1/2. $\delta = -7^\circ$. FLAPS = 55°.
 γ CONTROL BY POWER. PITCH AUG. ONLY.

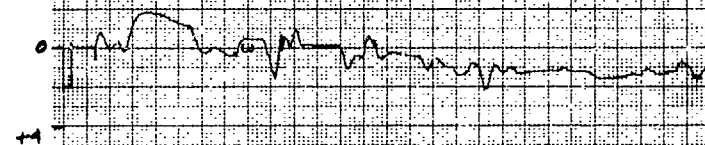
AIRSPEED
(KTS)



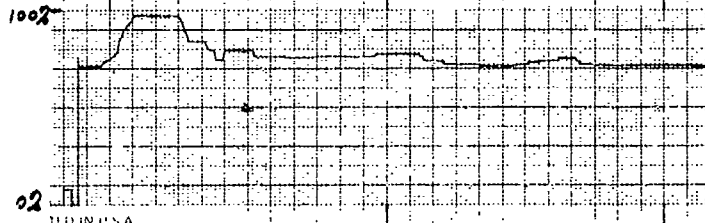
δ STICK
(% FULL TRAVEL)



δ ELEV
(DEG)



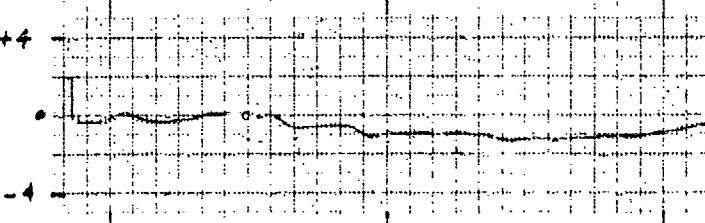
THROTTLE
(% THRUST)



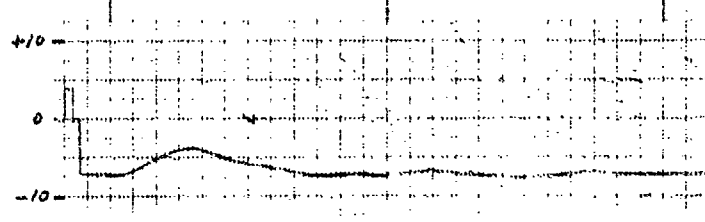
$\dot{\delta}$
(DEG/SEC)



θ
(DEG)



γ
(DEG)



EBF APPROACH. RUNG. C/N = 3. $\gamma = -7^\circ$. FLAPS = 60°.
 γ CONTROL BY POWER. PITCH. AUG. ONLY.

AIRSPEED
(KTS)

δ STICK
(% FULL TRAVEL)

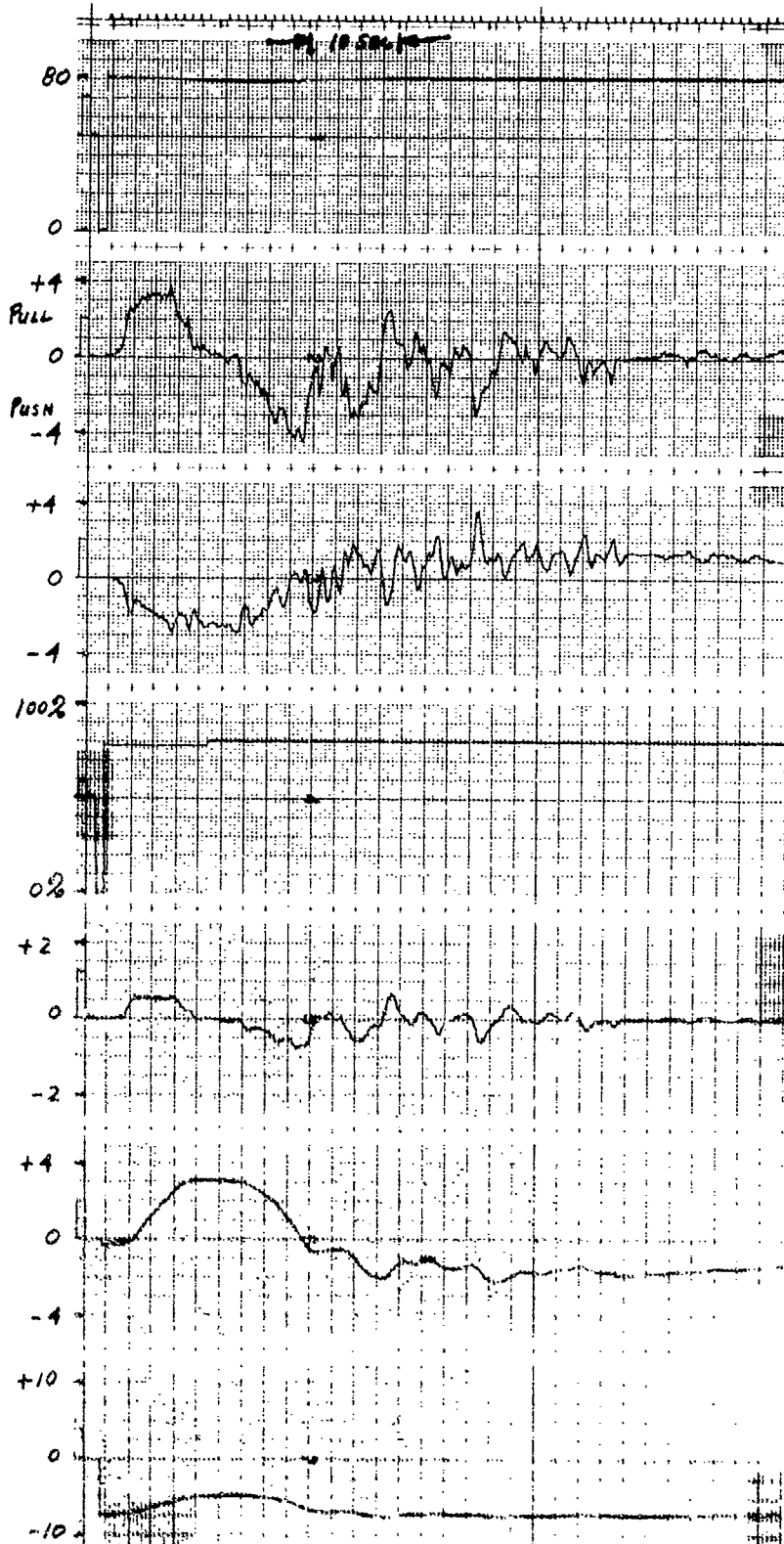
δ ELEV
(DEG)

THROTTLE
(% THRUST)

$\dot{\theta}$
(DEG/SEC)

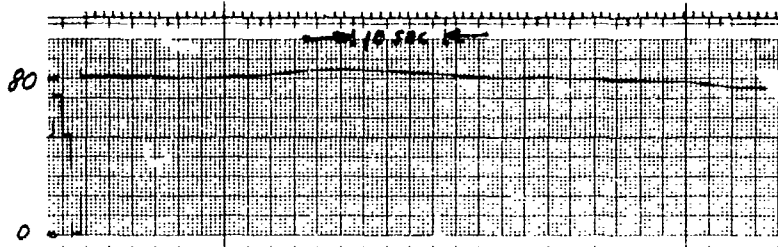
θ
(DEG)

γ
(DEG)

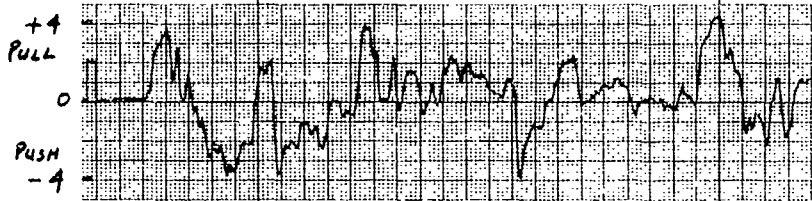


EBF APPROACH. RUN A36. C/H = 4. $\gamma = -7^\circ$. FLAPS = 60°.
Y CONTROL BY PITCH. FULL AUG. CONTROL.
L.A.S. — M.B.

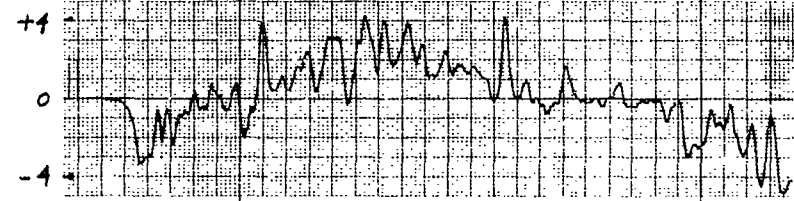
AIRSPPEED
(KTS)



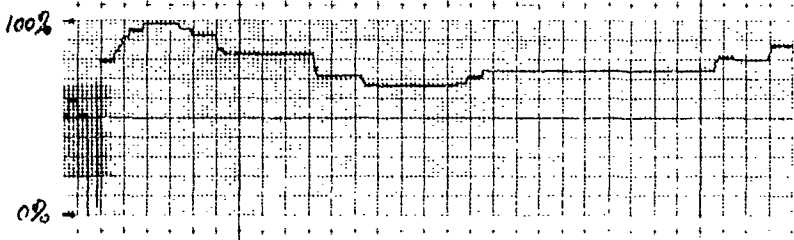
δ STICK
(% FULL TRAVEL)



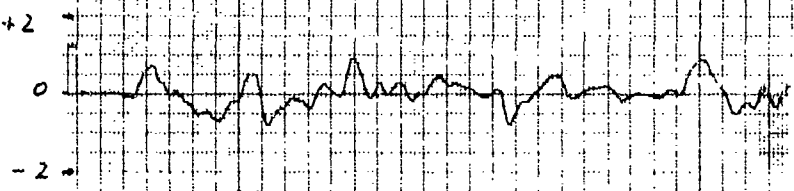
δ ELEV
(DEG)



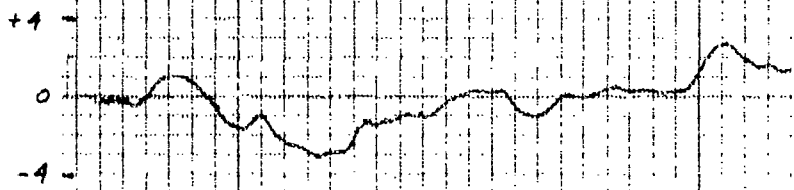
THROTTLE
(% THRUST)



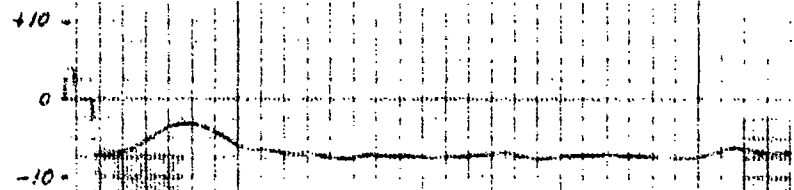
$\dot{\gamma}$
(DEG/SEC)



θ
(DEG)

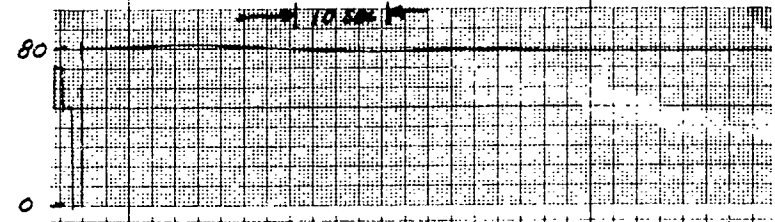


γ
(DEG)



EBF APPROACH. RUN A24. $CH=5$. $\gamma = -7^\circ$. FLAPS = 60°.
 γ CONTROL BY PITCH PITCH AUG. ONLY.
L.A.S. - M. B.

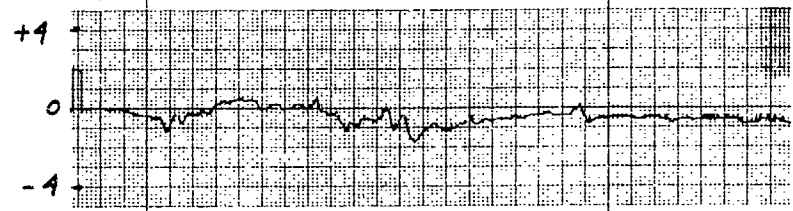
AIRSPEED
(KTS)



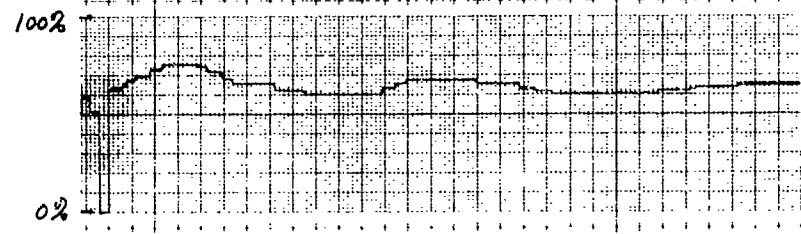
δ_{STICK}
(% FULL TRAVEL)



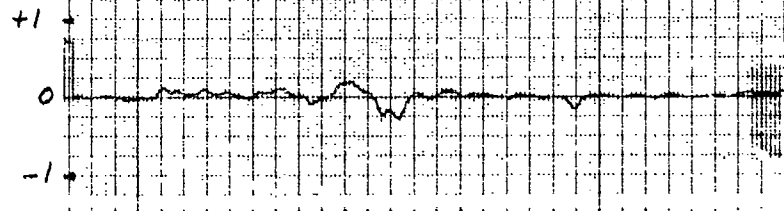
δ_{ELEV}
(DEG)



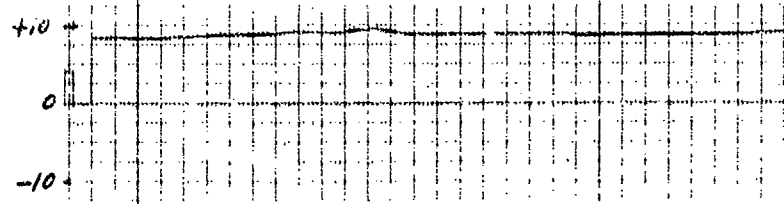
THROTTLE
(% THRUST)



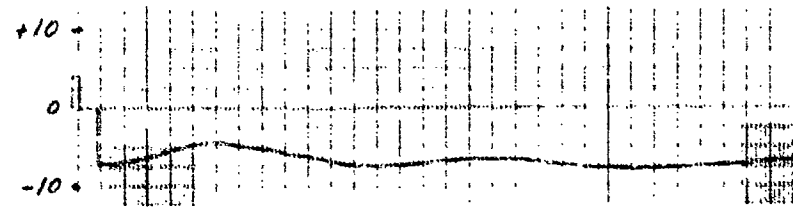
$\dot{\gamma}$
(DEG/SEC)



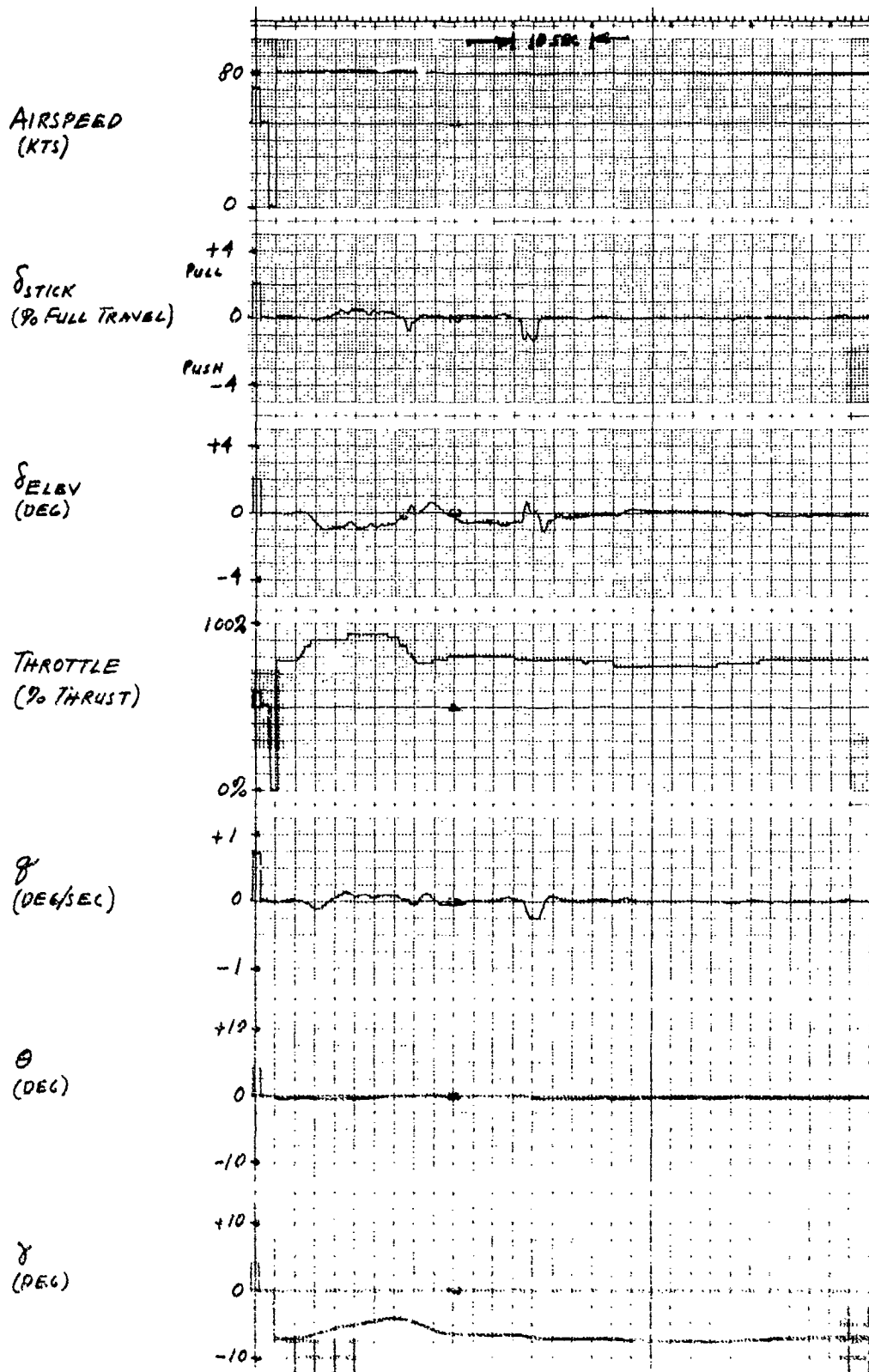
θ
(DEG)



γ
(DEG)

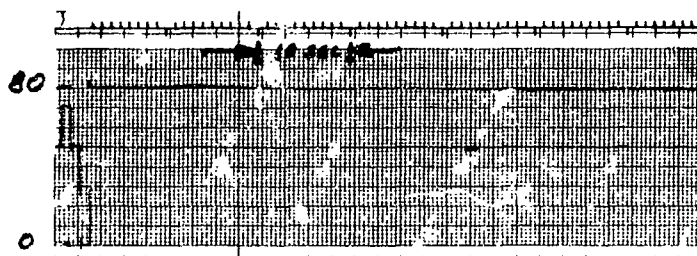


EBF APPROACH. RUN A2. $U/H = 3\frac{1}{2}$. $\gamma = -7^\circ$. FLAPS = 45° .
 γ CONTROL BY POWER. PITCH AUG. ONLY.
 L.A.S. - M.B.



EBF APPROACH. RUN AB. C/H = 2 1/2. $\gamma = -7^\circ$. FLAPS = 60°.
 γ CONTROL BY POWER. PITCH AUG. ONLY.
 L.A.S. - M.B.

AIRSPED
(KTS)



δ_{STICK}
(% FULL TRAVEL)

+4
PULL
0
PUSH
-4



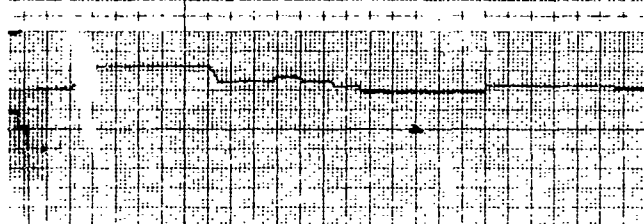
δ_{ELEV}
(DEG)

+4
0
-4



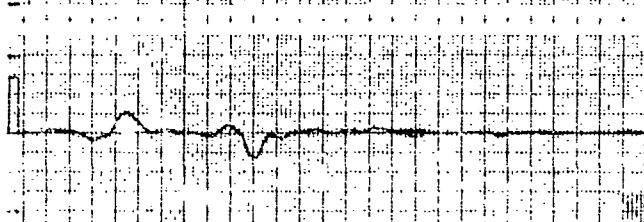
THROTTLE
(% THRUST)

100%



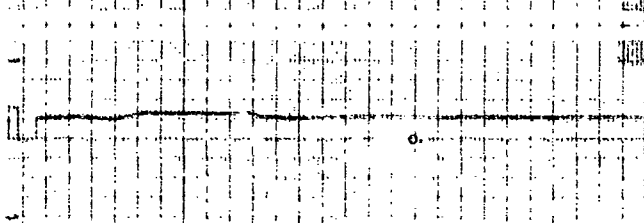
$\dot{\theta}$
(DEG/SEC)

+1
0
-1



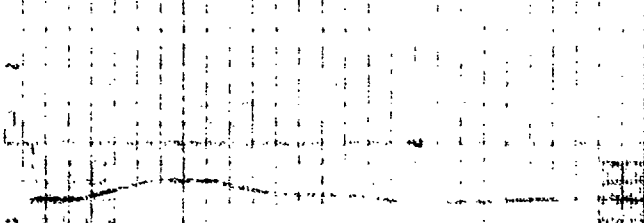
θ
(DEG)

+10
0
-10



γ
(DEG)

+10
0
-10



EBF APPROACH RUN 46. $L/H = 2\frac{1}{2}$ $\alpha = -7^\circ$; FLAPS = 55%
 δ CONTROL BY POWER. PITCH AND ONLY
L.A.S. - F B

BRUSH INSTRUM

AIRSPEED
(KTS)

80

0

δ_{STICK}
(% FULL TRAVEL)

+1
Pull

0
Push
-1

δ_{ELEV}
(DEG)

+1

0

-1

THROTTLE
(% THRUST)

100%

0%

γ
(DEG/SEC)

+1

0

-1

θ
(DEG)

+10

0

-10

ψ
(DEG)

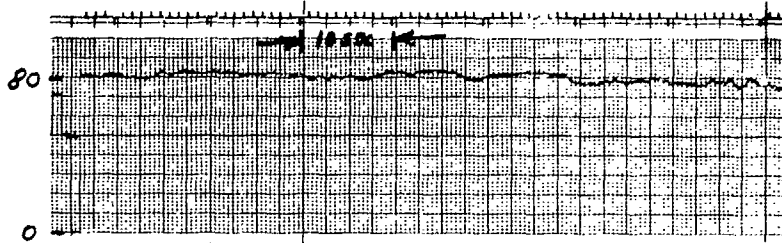
+10

0

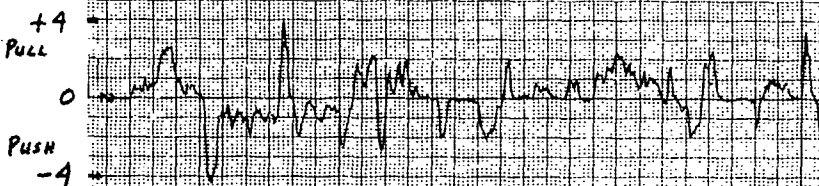
-10

EMP APPROACH RUN AT CR=2 X-75 FEARS. 50"
L CONTROL R1 POWER PITCH AXIS ONLY
L/A 3 - 14.3.

AIR SPEED
(KTS)



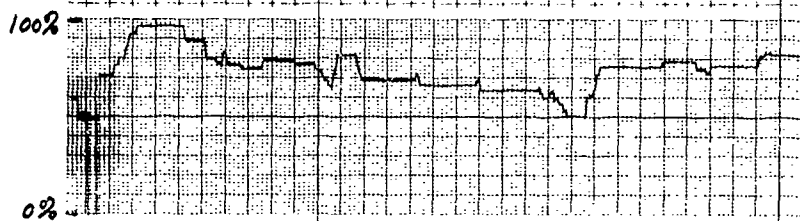
δ STICK
(% FULL TRAVEL)



δ ELEV
(DEG)



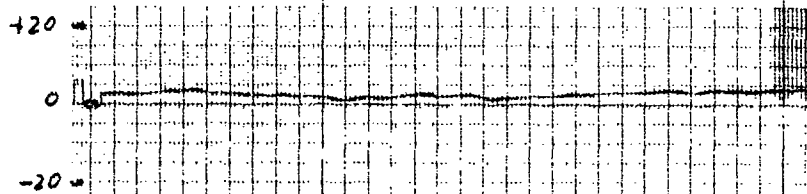
THRUSTLE
(% THRUST)



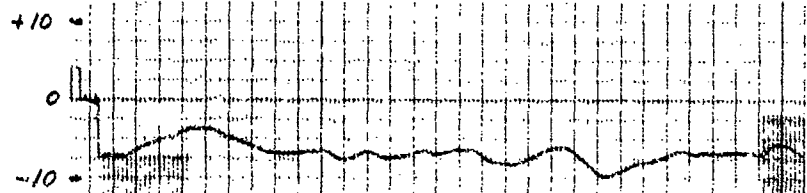
$\dot{\theta}$
(DEG/SEC)



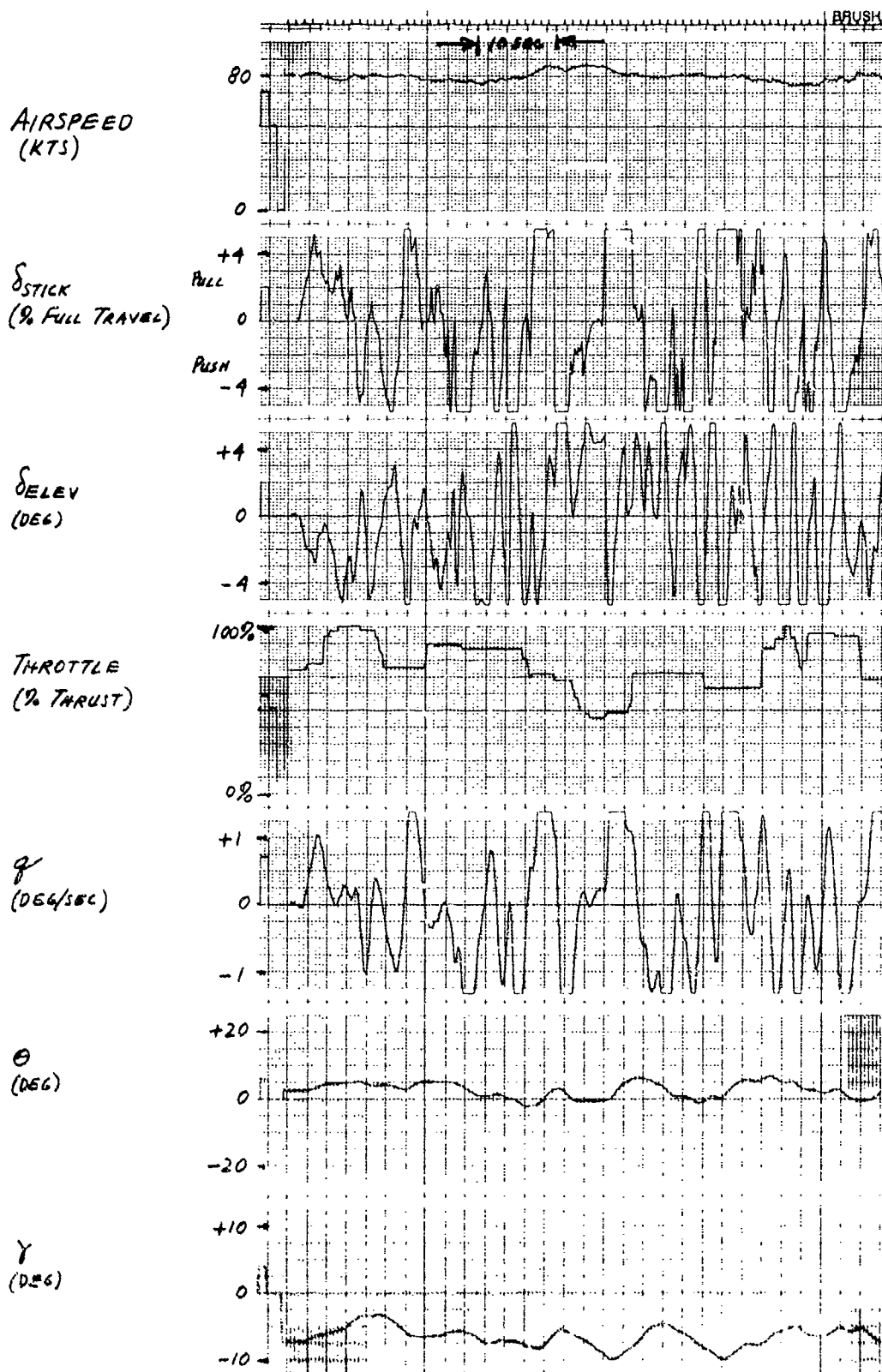
θ
(DEG)



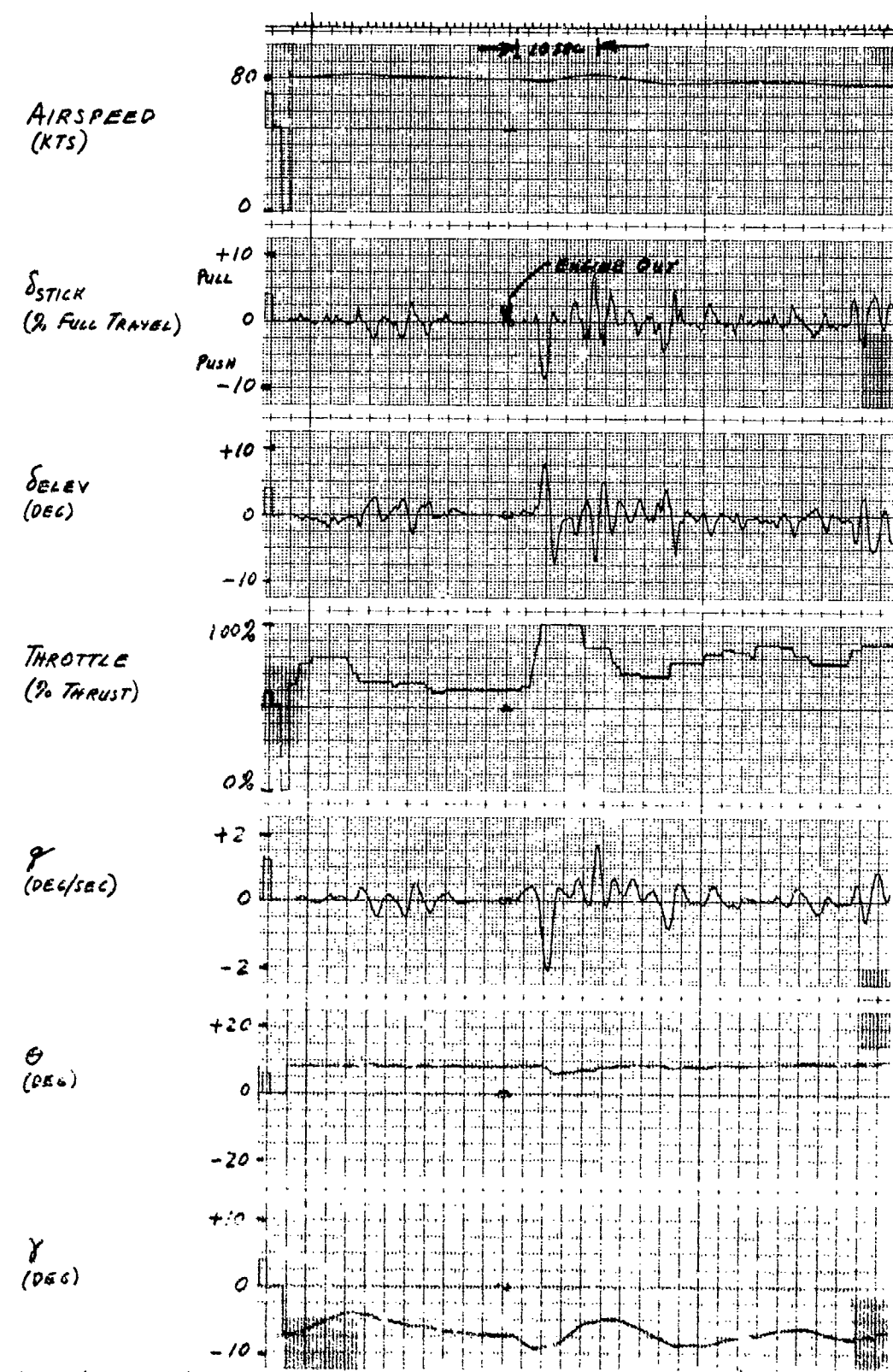
γ
(DEG)



EBF APPROACH. RUN A53. C/H = 6 1/2. $\gamma = -7^\circ$. FLAPS = 55°.
 γ CONTROL BY POWER. PITCH AUG. ONLY.
L.A.S. - M.B. GUST MODEL.

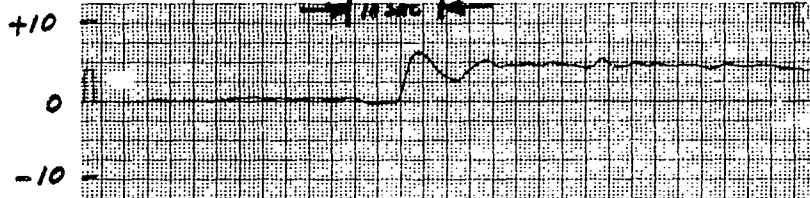


EBF APPROACH. RUN A54. C/H = 8. $\delta = -7^\circ$. FLAPS = 55°.
 δ CONTROL BY PITCH. PITCH AUG 2.17.
 L.A.S. - M.B. GUST MODEL.



EBF APPROACH. RUN A 69. C/M = B. $\gamma = -7^\circ$. FLAPS = 45°.
 γ CONTROL BY POWER. PITCH AUG. ONLY.
 L.A.S. - M.B. ENGINE OUT.

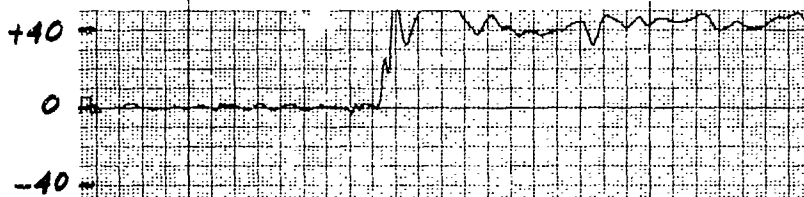
β
(DEG)



γ
(DEG/SEC)



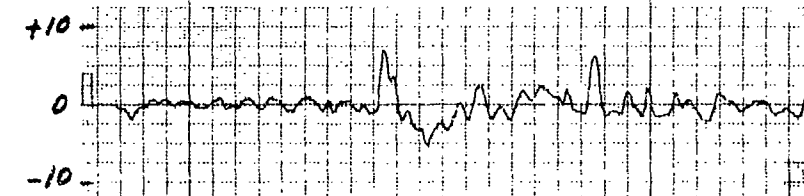
δ_{RUDDER}
(DEG)



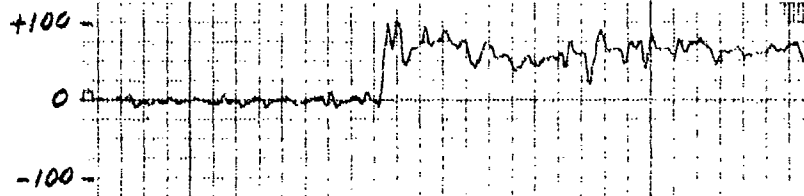
ϕ
(DEG)



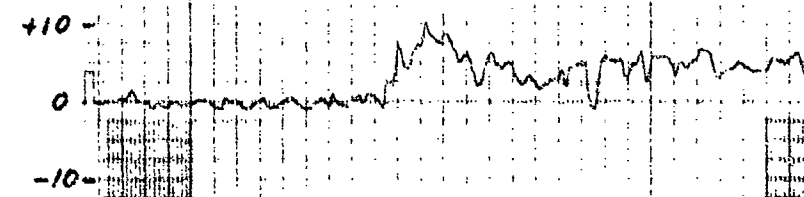
p
(DEG/SEC)



$\delta_{AILDRON}$
(DEG)

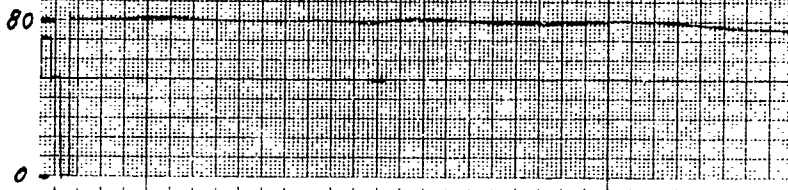


δ_{SPNLND}
(DEG)

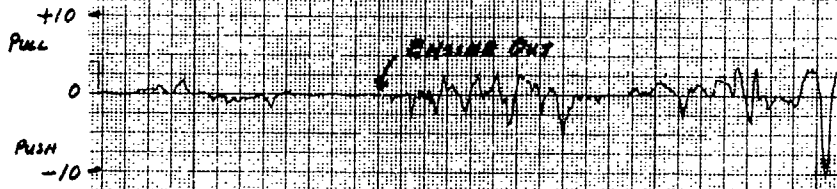


EBF APPROACH. RUN A 69. $C/H = B$. $\gamma = -7^\circ$. FLAPS = 45° .
 γ CONTROL BY POWER. PITCH AUG. ONLY.
 L.A.S. - M.B. ENGINE OUT.

AIRSPEED
(KTS)



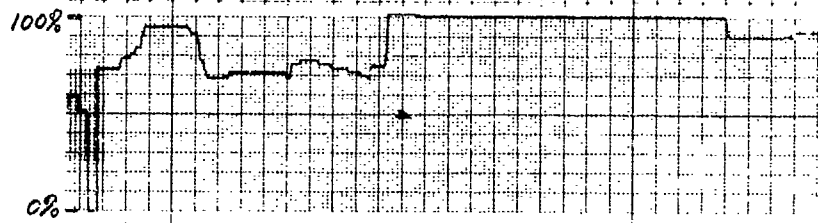
δ_{STICK}
(% FULL TRAVEL)



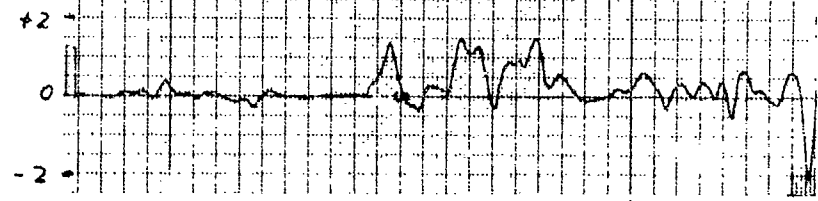
δ_{ELEV}
(DEG)



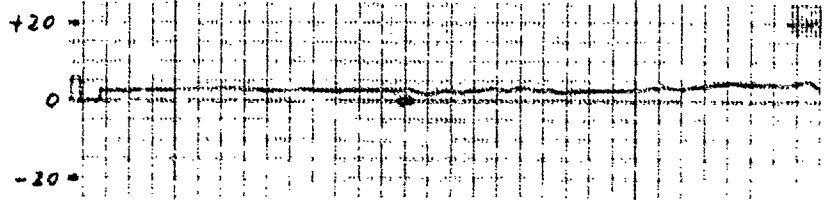
THROTTLE
(% THRUST)



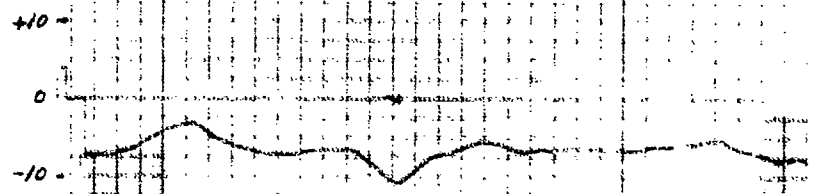
$\dot{\gamma}$
(DEG/SEC)



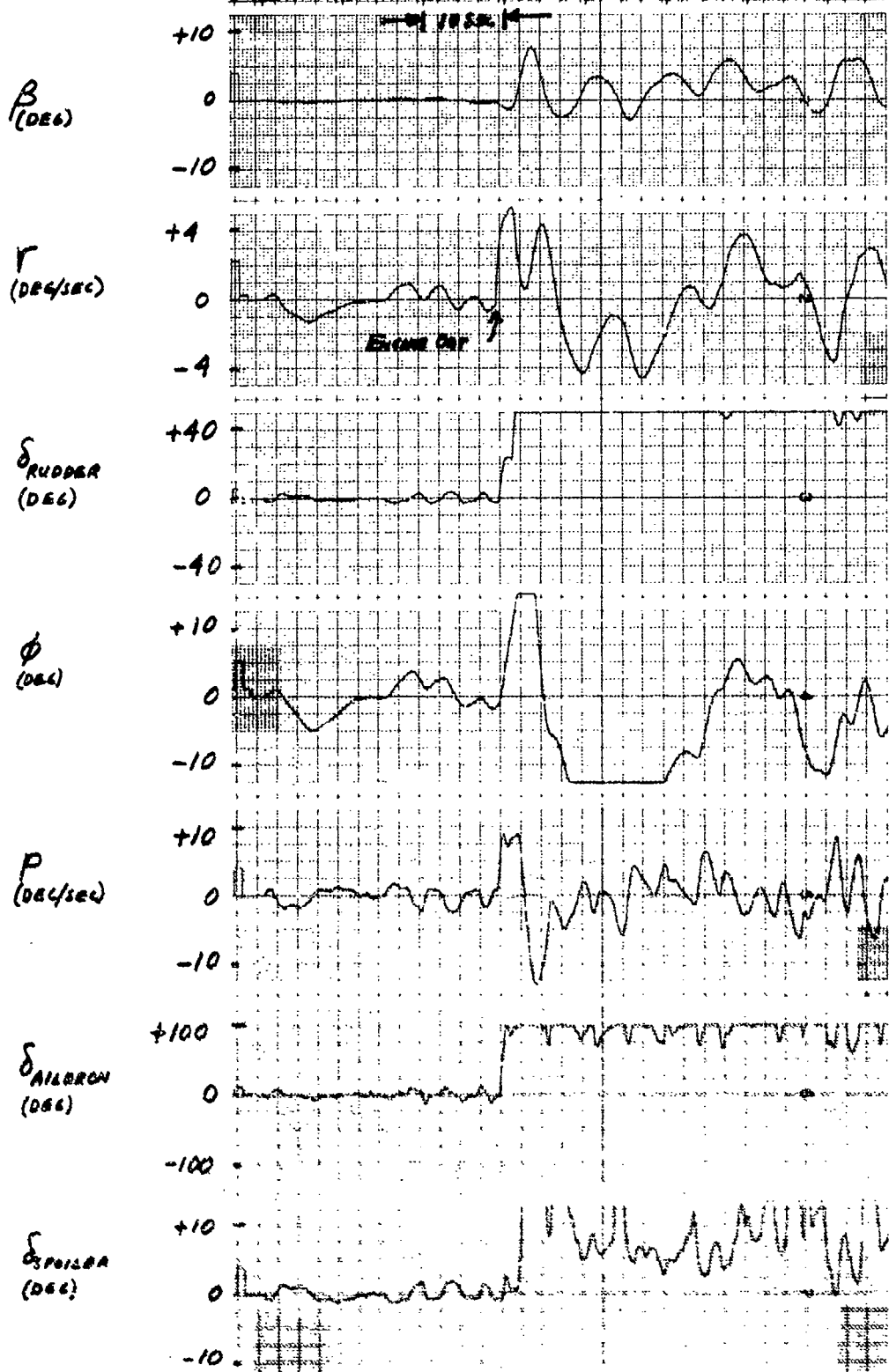
θ
(DEG)



γ
(DEG)

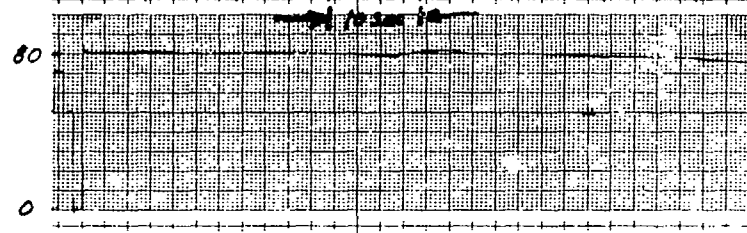


EBF APPROACH. RUN A 77. $\gamma/H = 9$. $\gamma = -7^\circ$ FLAPS = 55"
 γ CONTROL BY POWER. PITCH AUG. ONLY.
 L.A.S. - M.B. ENGINE OUT.

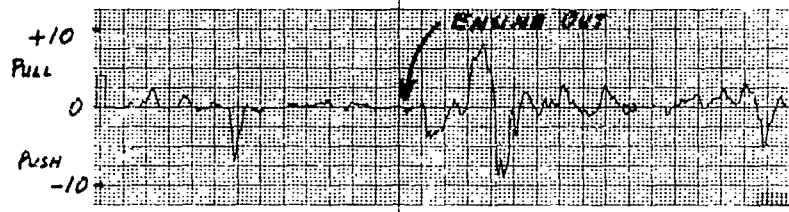


ESF APPROACH. RUN 77. $\gamma_H = 7$. $\gamma = -7^\circ$. FLAPS = 55°.
 γ CONTROL BY POWER. PITCH AUG. ONLY.
 L.A.S. - M.B. ENGINE OUT.

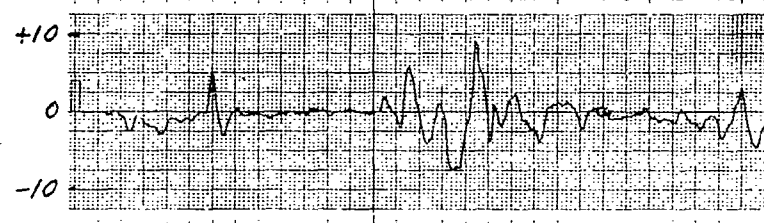
AIR SPEED
(KTS)



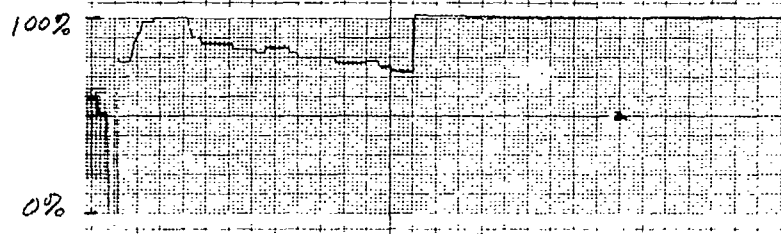
δ STICK
(% FULL TRAVEL)



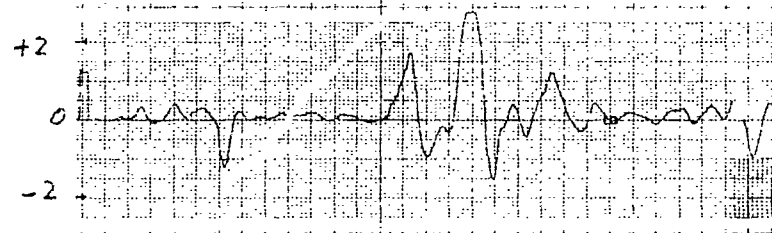
δ ELEV
(DEG)



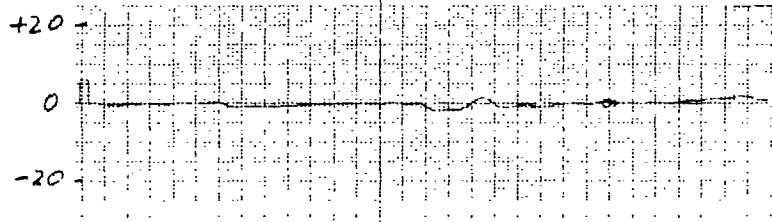
THROTTLE
(% THRUST)



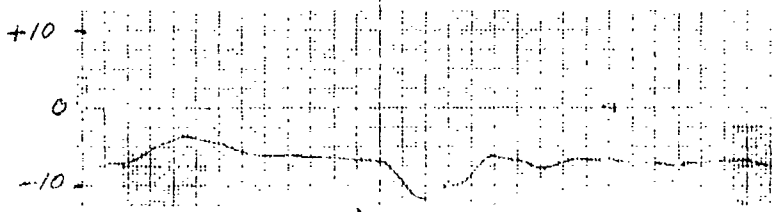
$\dot{\gamma}$
(DEG/SEC)



θ
(DEG)



γ
(DEG)



EBF APPROACH RUN A 91 C/H=10. $\delta = -7^\circ$ FLAPS = 30"
 γ CONTROL BY POWER. PITCH AUC ONLY
 L.A. - M.S. ENGINE OUT

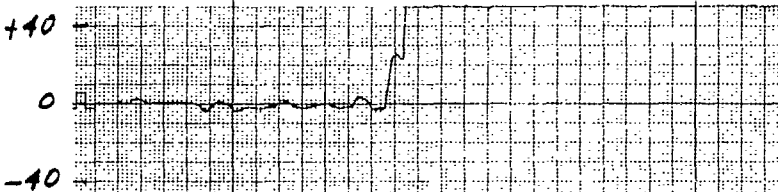
β
(DEG)



γ
(DEG/SEC)



δ_{RUDDER}
(DEG)



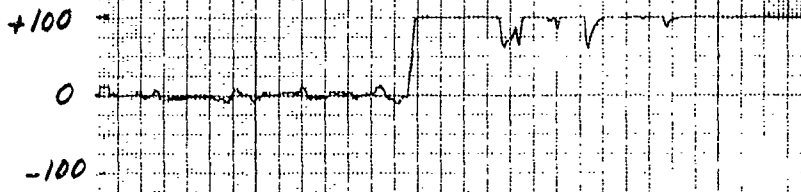
ϕ
(DEG)



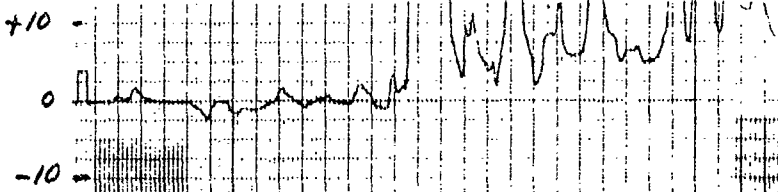
ρ
(DEG/SEC)



δ_{AILERON}
(DEG)

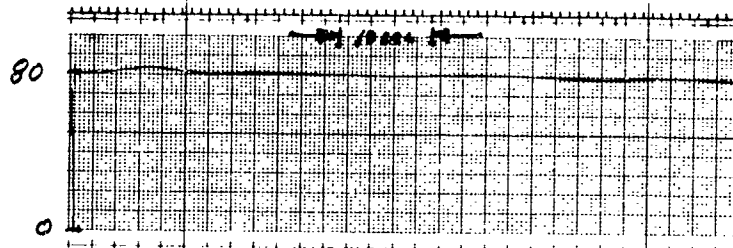


δ_{SPOILER}
(DEG)

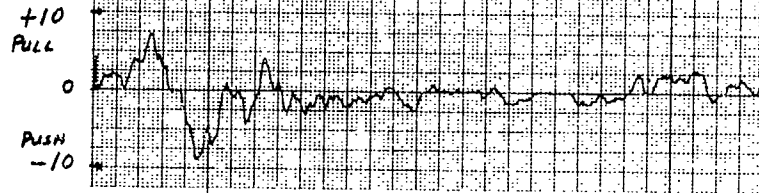


EBF APPROACH. RUN AB1. $q_H = 10$. $\delta = -7^\circ$. FLAPS = 60° .
 γ CONTROL BY POWER. PITCH AUG. ONLY.
 L.A.S. - M.B. ENGINE OUT.

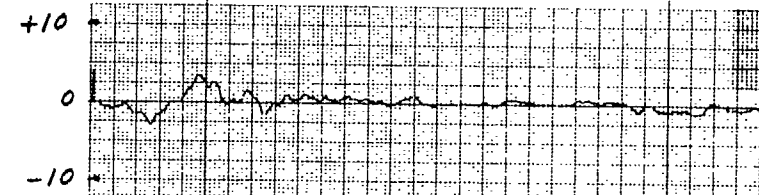
AIR SPEED
(KTS)



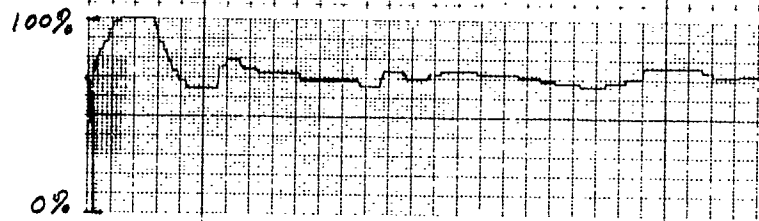
δ_{STICK}
(% FULL TRAVEL)



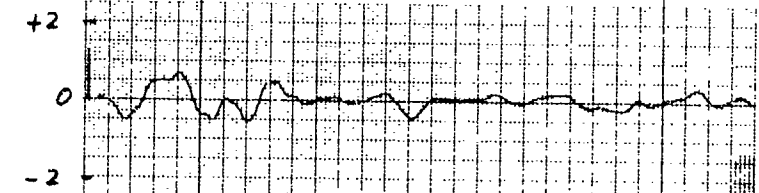
δ_{ELEV}
(DEG)



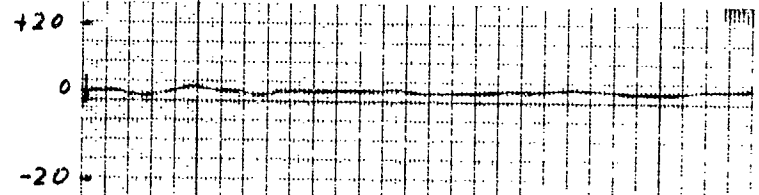
THROTTLE
(% THRUST)



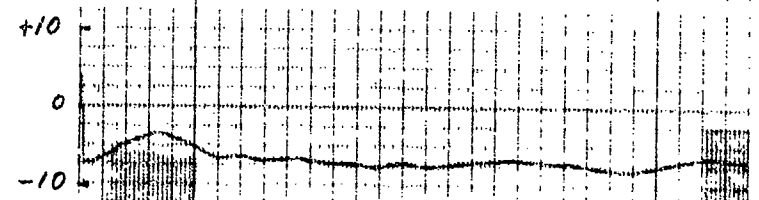
$\dot{\gamma}$
(DEG/SEC)



θ
(DEG)



γ
(DEG)

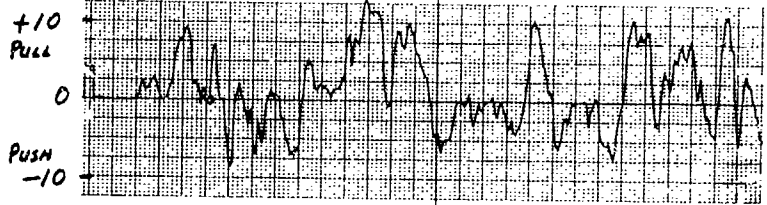


EBF APPROACH. RUN A B7. C/H = 4. $\gamma = -7^\circ$. FLAPS = 55°.
Y CONTROL BY POWER. BARE AIRFRAME.
L.A.S. - M. B.

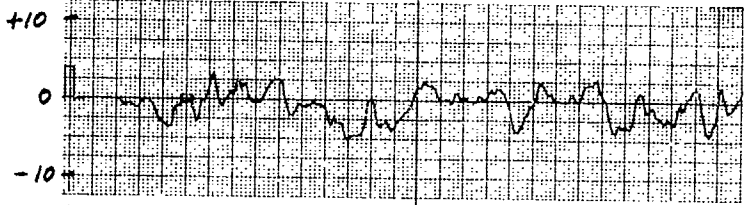
AIR SPEED
(KTS)



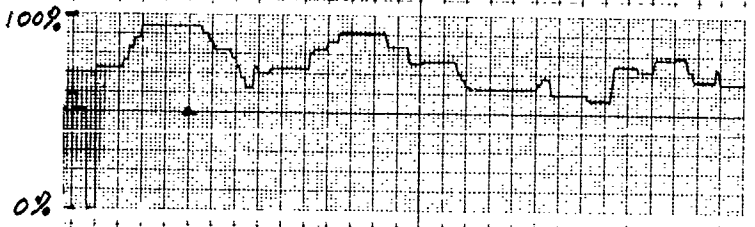
δ_{STICK}
(% FULL TRAVEL)



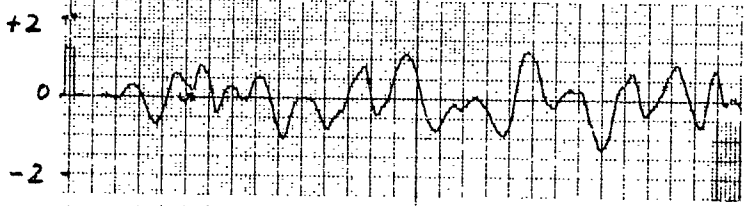
δ_{ELEV}
(DEG)



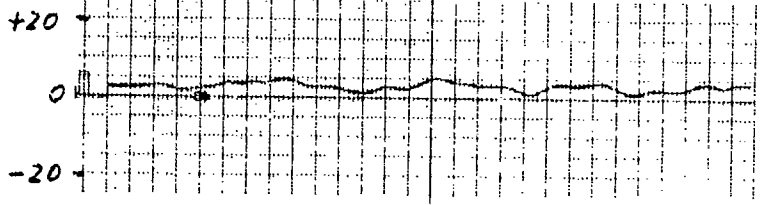
THROTTLE
(% THRUST)



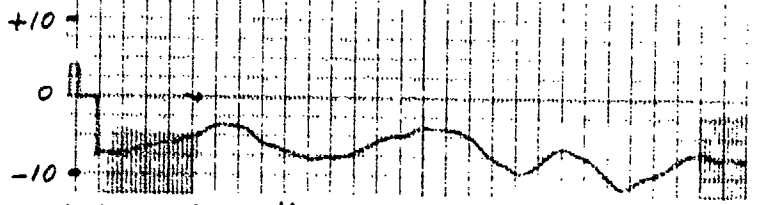
$\dot{\gamma}$
(DEG/SEC)



θ
(DEG)



γ
(DEG)

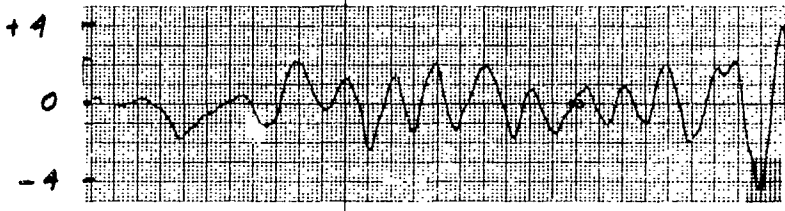


EBF APPROACH. RUN A 91. C/H = 7 1/2. $\gamma = -7^\circ$. FLAPS = 55°.
 γ CONTROL BY POWER. BARE AIRFRAME.
 L.A.S. - M.B. GUST MODEL.

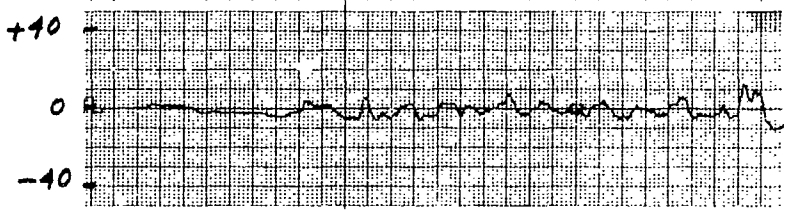
β
(DEG)



γ
(DEG/SEC)



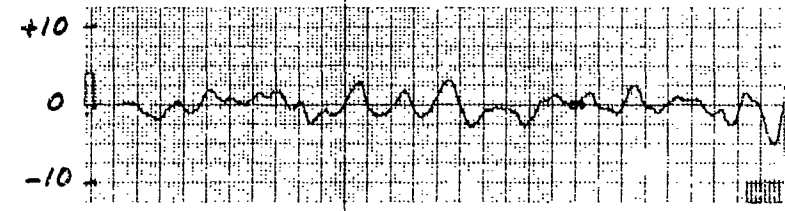
δ_{RUDDER}
(DEG)



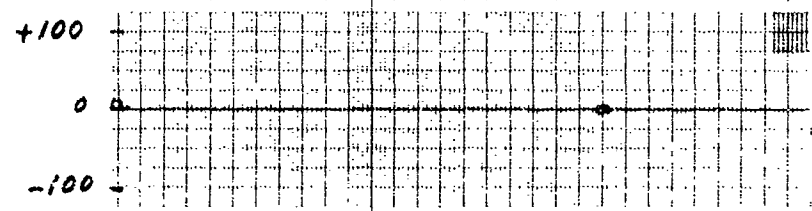
ϕ
(DEG)



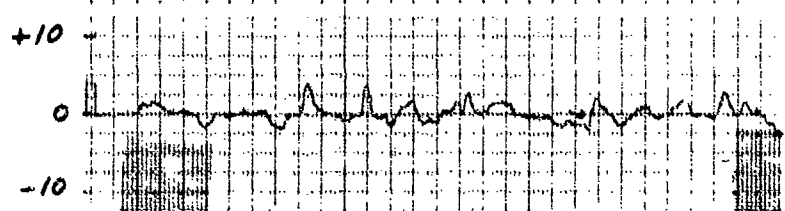
p
(DEG/SEC)



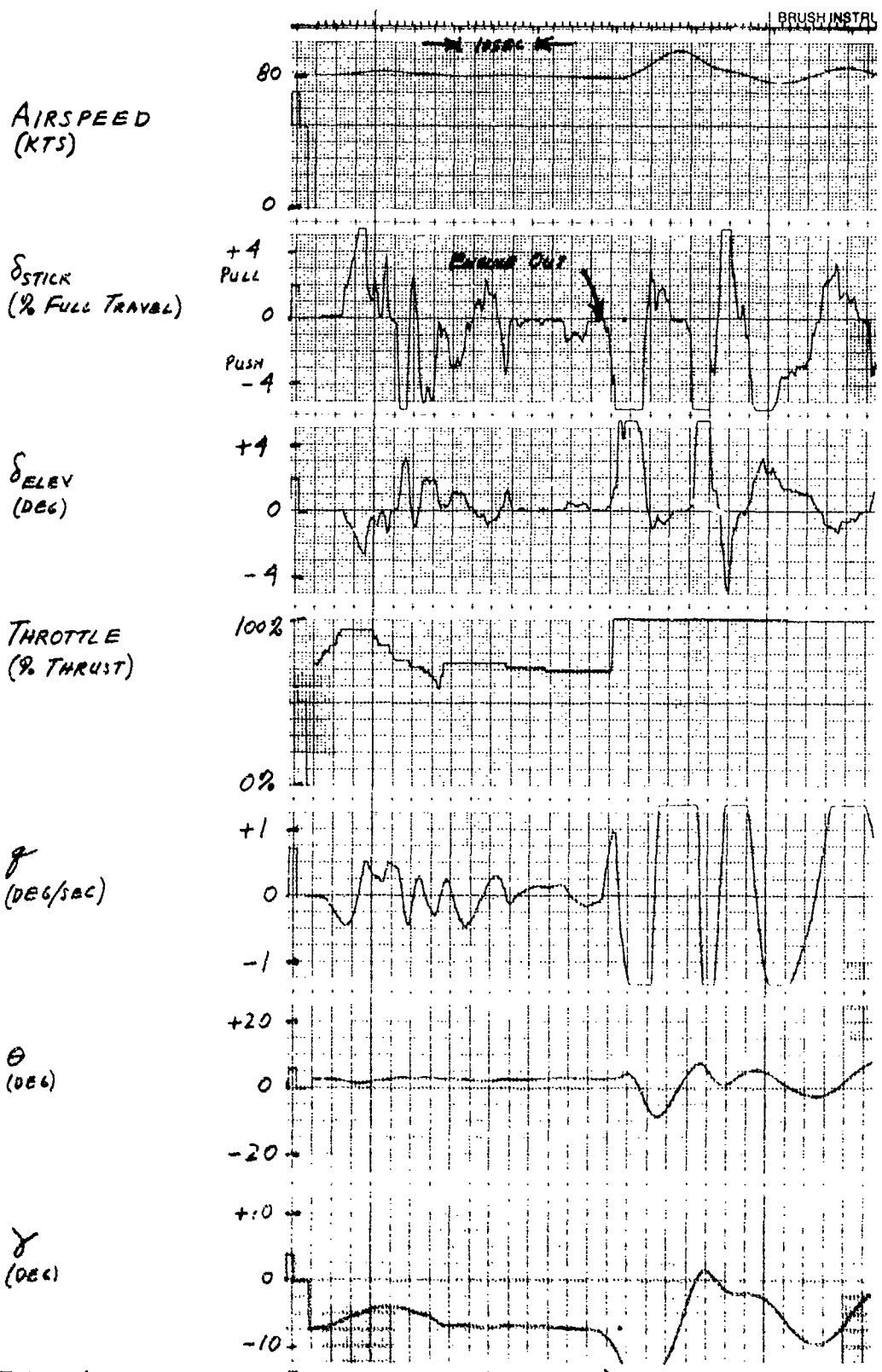
$\delta_{AILERON}$
(DEG)



$\delta_{SPOILER}$
(DEG)

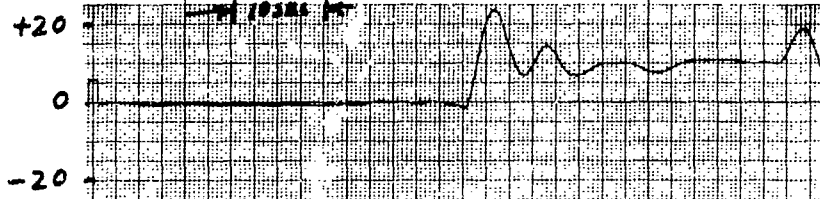


EBF APPROACH. RUN A 91. C/H = 7 1/2. $\gamma = .7^\circ$. FLAPS = 55°.
 γ CONTROL BY POWER. BARE AIRFRAME.
L.A.S. - M. B. GUST MODEL.

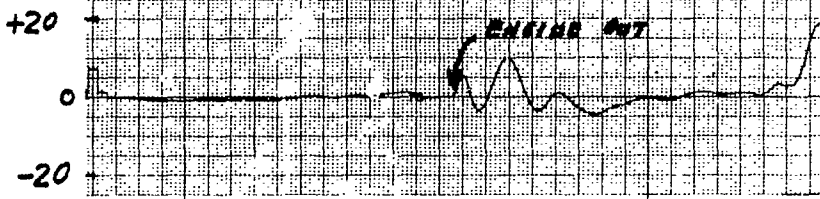


EBF APPROACH. RUN A95. $C/M = 10$. $\gamma = -7^\circ$. FLAPS = 55° .
 γ CONTROL BY POWER. BARE AIRFRAME.
 L.A.S. - M.B. ENGINE OUT

β
(DEG)



γ
(DEG/SEC)



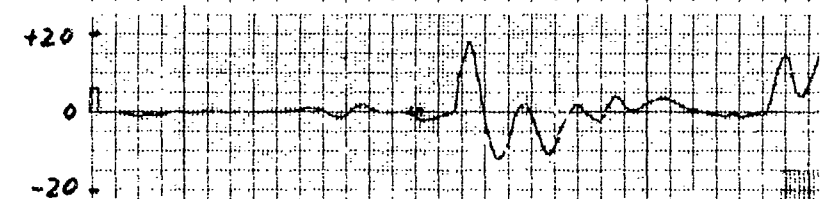
δ_{RUDDER}
(DEG)



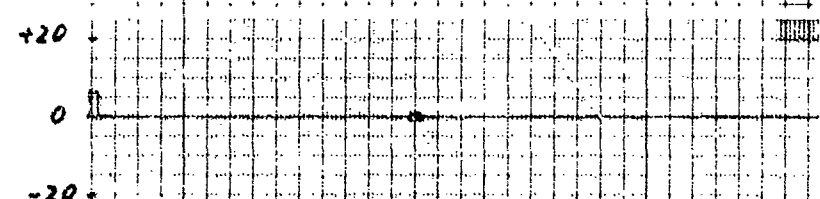
ϕ
(DEG)



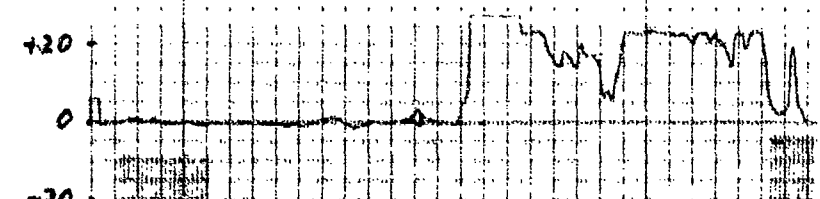
p
(DEG/SEC)



$\delta_{AILERON}$
(DEG)



$\delta_{SPOILER}$
(DEG)



EBF APPROACH. RUN A95. $C/N = 10$. $\gamma = -7^\circ$. FLAPS = 55° .
 γ CONTROL BY POWER. BARE AIRFRAME.
 L.A.S. - M. B. ENGINE OUT.

AIRSPEED
(KTS)

80
70

δ STICK
(% FULL TRAVEL)

+20
PULL

PUSH
-20

ALTITUDE
(FT. ALL)

1200

700

THROTTLE
(% THRUST)

100%

0%

δ FLAPS
(DEG)

55

0

θ
(DEG)

+20

0

-20

γ
(DEG)

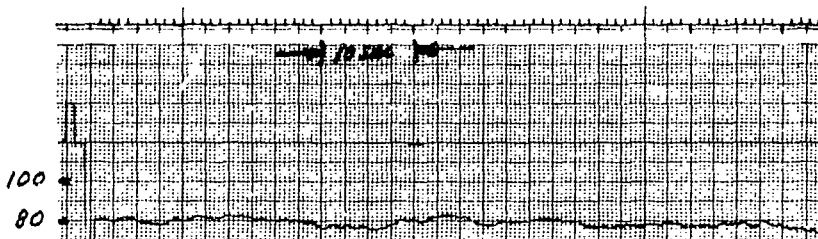
+40

0

-10

EBF APPROACH. RUN CW 1. C/H = 5 1/2. $\gamma = -7^\circ$. FLAPS = 55.
 γ CONTROL BY POWER. PITCH AUG. ONLY. L.A.S. - M.B.
WIND FROM 90° RIGHT AT 30 KTS.

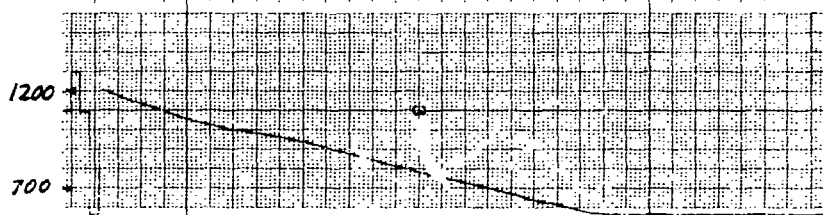
AIRSPEED
(KTS)



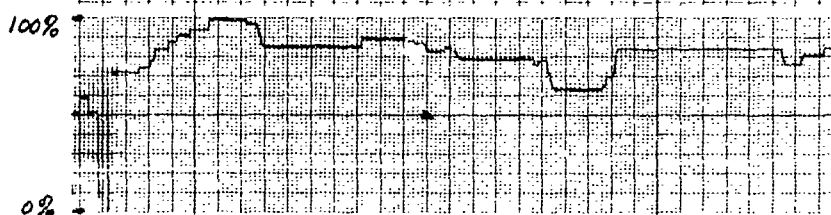
δ_{STICK}
(% FULL TRAVEL)



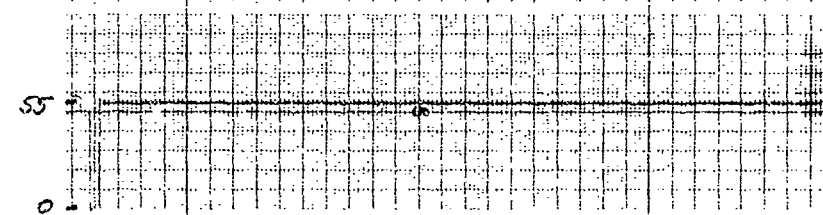
ALTITUDE
(FT. AGL)



THROTTLE
(% THRUST)



δ_{FLAPS}
(DEG)



θ
(DEG)



γ
(DEG)



EBF APPROACH. RUN CW 3. C/H = 6. $\gamma = -7^\circ$. FLAPS = 55° .
 γ CONTROL BY POWER PITCH AUG. ONLY. LAS. - M.B.
WIND FROM 90° RIGHT AT 25 KTS WITH GUST MODEL.

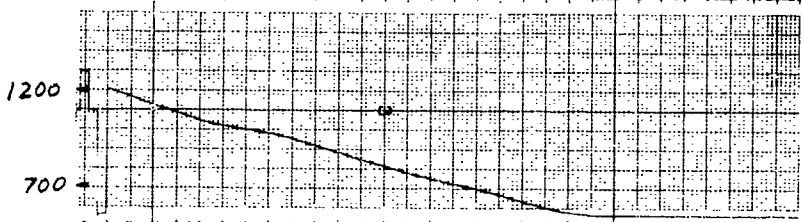
AIR SPEED
(KTS)



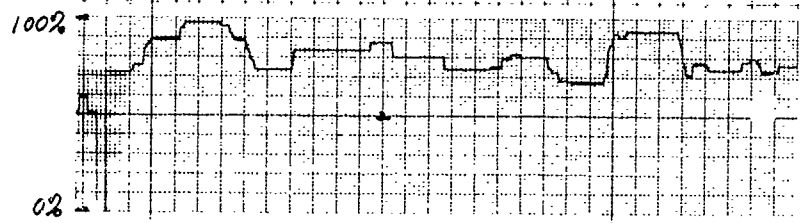
δ STICK
(% FULL TRAVEL)



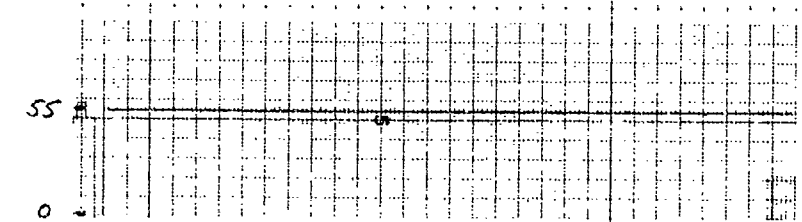
ALTITUDE
(FT. AGL)



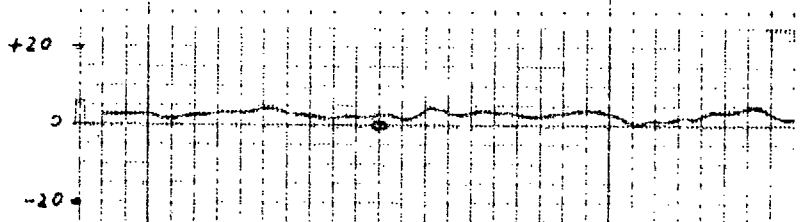
THROTTLE
(% THRUST)



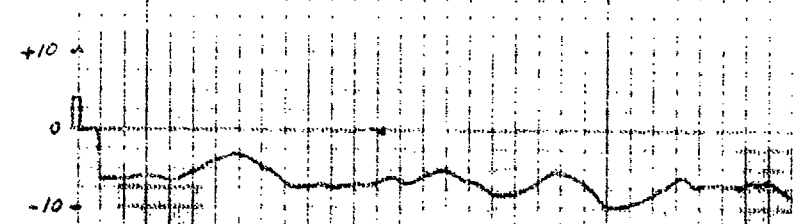
δ FLAPS
(DEG)



θ
(DEG)



γ
(DEG)



EBF APPROACH. RUN C/W G. L/H = B. $\gamma = -7^\circ$. FLAPS = 55° .
 γ CONTROL BY POWER. BARE AIRFRAME. L.I.S. - M.B.
WIND FROM 90° RIGHT AT 25 KTS WITH GUST MODEL.

AIRSPEED
(KTS)

STICK
(% FULL TRAVEL)

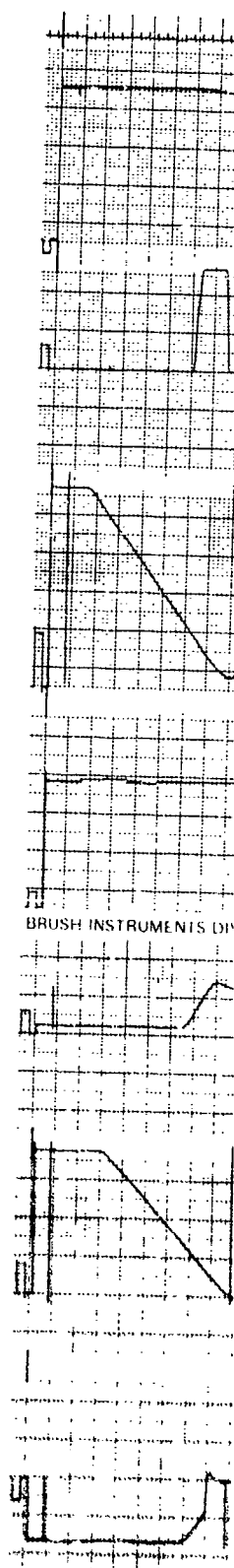
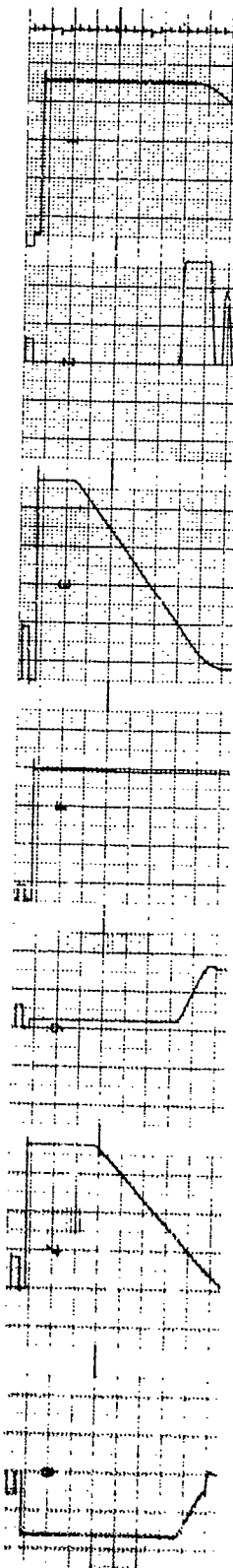
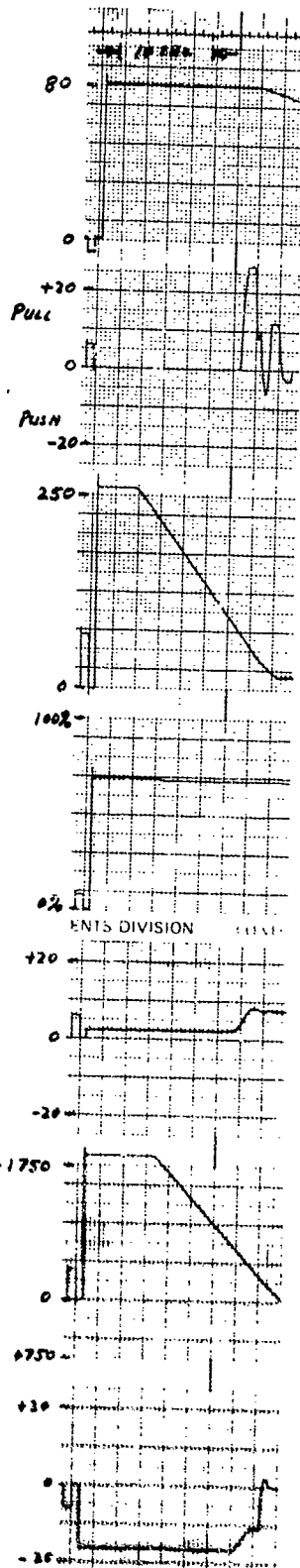
ALTITUDE
(FT. AGL)

THROTTLE
(% THRUST)

θ
(DEG)

RANGE TO
THRESHOLD
(FT.)

\dot{h}
(FT/SEC)



EBF FLARE/TOUENDOWN.
C/H = 3.
FLAPS = 55°
FLARE ALTITUDE =

PITCH AUG ONLY.
RUN A.
= 80 FT.

PITCH AUG ONLY.
RUN C.
= 80 FT.

FULL AUG. CONTROL.
RUN F.
= 80 FT.

AIRSPPEED
(KTS)

δ STICK
(% FULL TRAVEL)

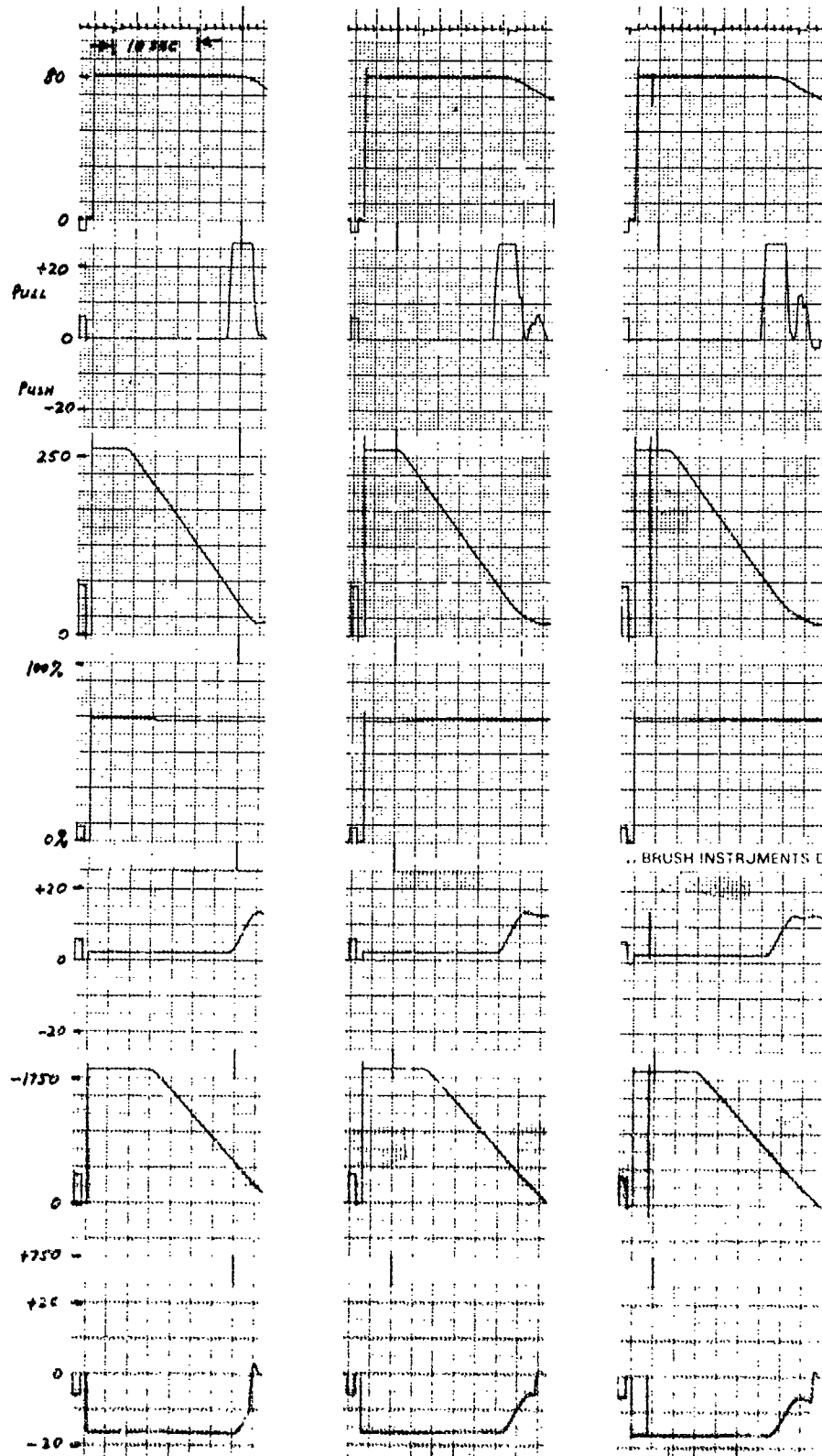
ALTITUDE
(FT. AGL)

THROTTLE
(% THRUST)

θ
(DEG)

RANGE TO
THRESHOLD
(FT.)

\dot{h}
(FT/SEC)



EBF FLARE/TOULNDOWN. PITCH ANG. ONLY.
C/H = 3.
FLAPS = 55°
FLARE ALTITUDE = 70 FT.

PITCH ANG ONLY.
RUN B.
= 80 FT.

PITCH ANG ONLY.
RUN E.
= 90 FT.

AIRSPED
(KTS)

δ STICK
(% FULL TRAVEL)

ALTITUDE
(FT. AGL)

THROTTLE
(% THRUST)

θ
(DEG)

RANGE TO
THRESHOLD
(FT.)

h
(FT/SEC)

EBF FLARE/TWINDOWN. PITCH AUG. ONLY.
C/H = 3. FAST PITCH RATE.
FLAPS = 55°. RUN I.
FLARE ALTITUDE = 80 FT.

PITCH AUG. ONLY.
SLOW PITCH RATE.
RUN J.
= 80 FT.

PITCH AUG ONLY.
FLAPS = 60°. RUN L.
= 80 FT.

AIR SPEED
(KTS)

δ STICK
(% FULL TRAVEL)

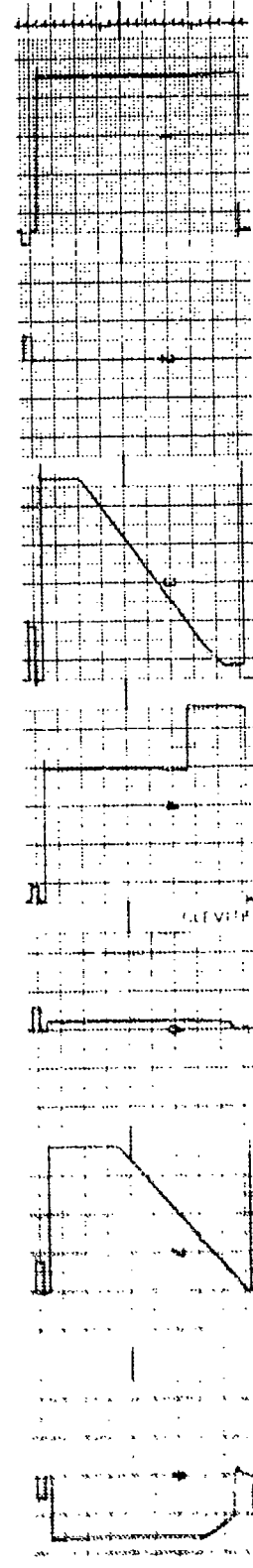
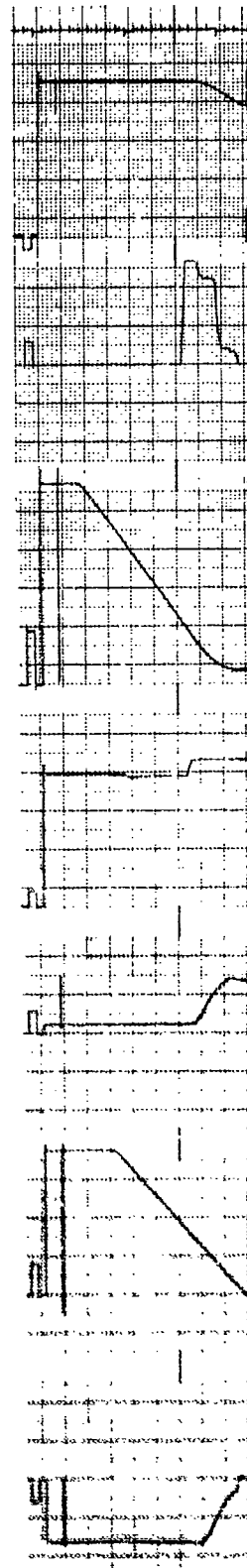
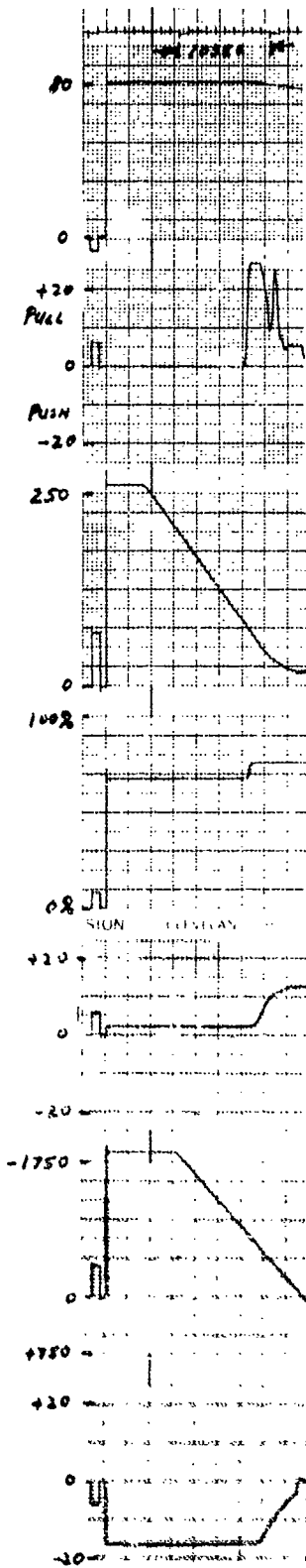
ALTITUDE
(FT. AGL)

THROTTLE
(% THRUST)

θ
(DEG)

RANGE TO
THRESHOLD
(FT.)

h
(FT/SEC)

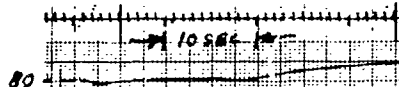


EBF FLARE/TOUCHDOWN. FULL AUG. CONTROL.
 $C_{L4} = 3$. 10% THRUST INCREASED.
 FLAPS = 55°. RUN G.
 FLARE ALTITUDE = 80 FT.

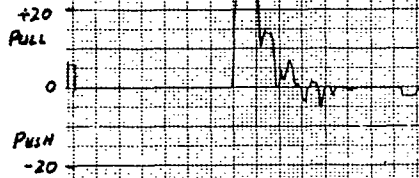
PITCH AUG. ONLY. 10% THRUST INCREASED.
 RUN H.
 = 80 FT.

PITCH AUG. ONLY. FULL THRUST.
 RUN K.
 = 80 FT.

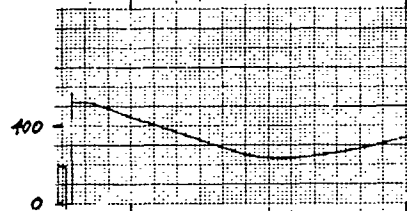
AIR SPEED
(KTS)



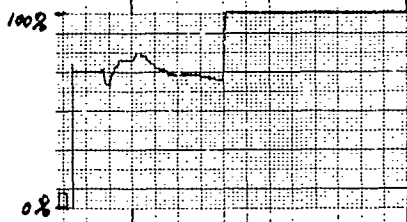
δ STICK
(% FULL TRAVEL)



ALTITUDE
(FT. AGL)



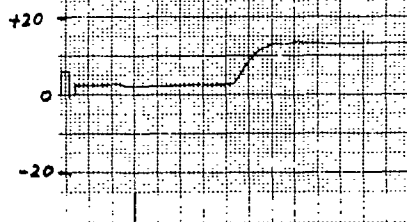
THROTTLE
(% THRUST)



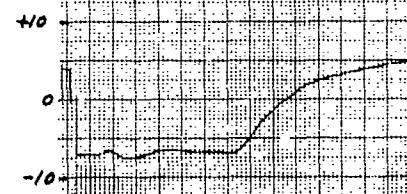
FLAPS
(DEG)



θ
(DEG)

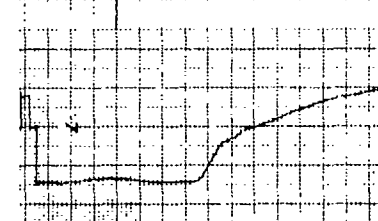
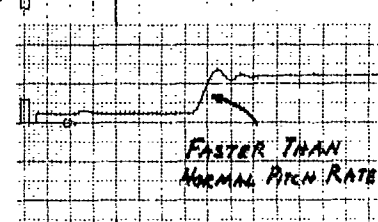
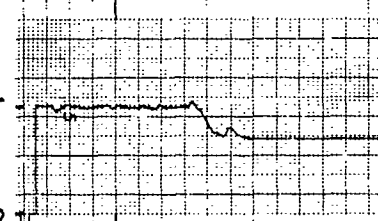
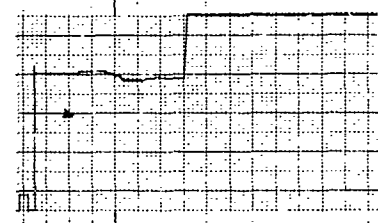
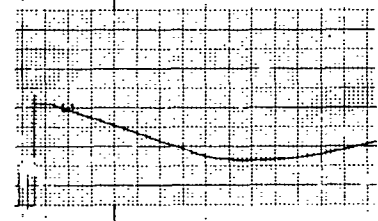
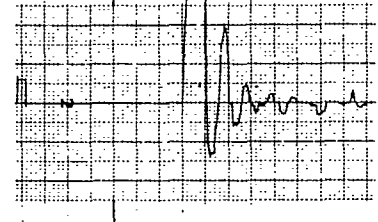
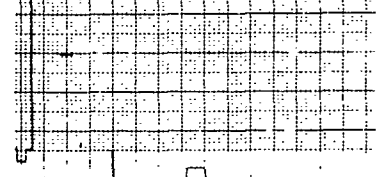
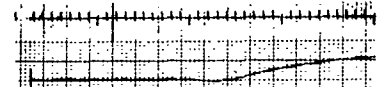


γ
(DEG)

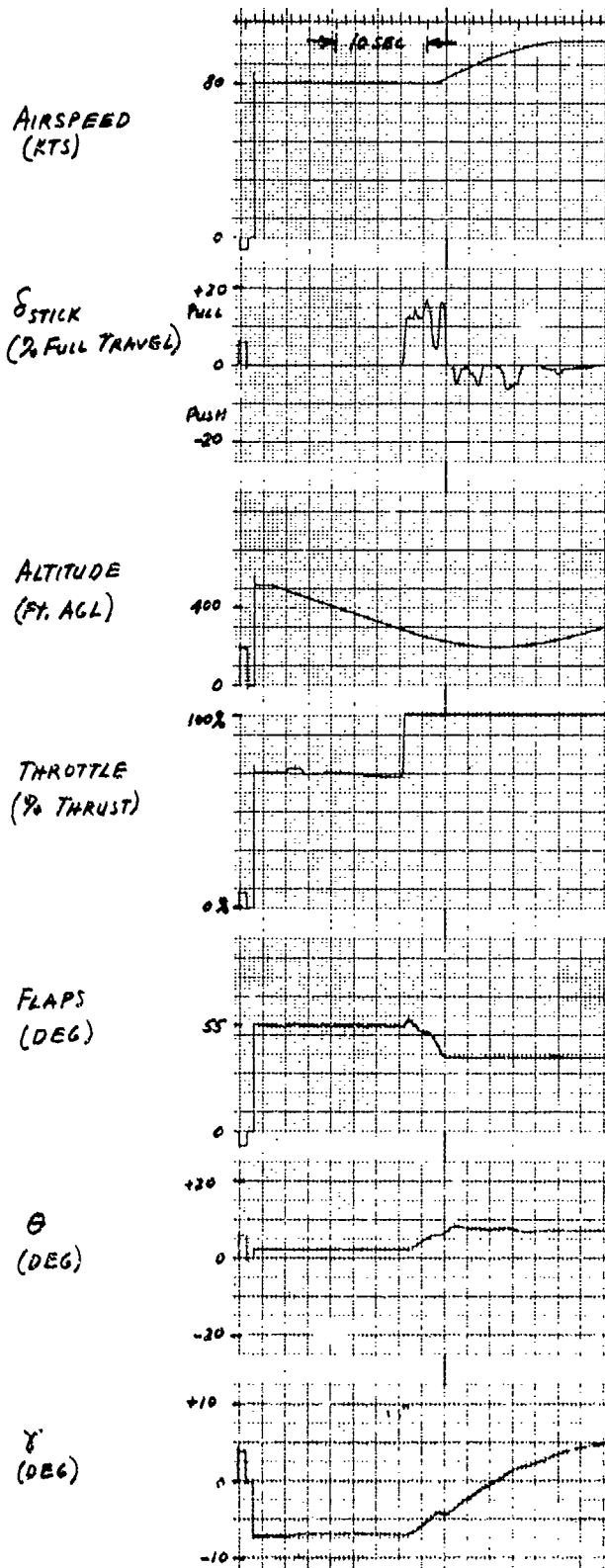


EBF GO-AROUND.
C/H = 3.
DECISION HEIGHT
= 300' AGL.

PITCH AND FLAPS UP.
FULL AUG. CONTROL.
FLAP RATE = 5 DEG/SEC.
RUN F.

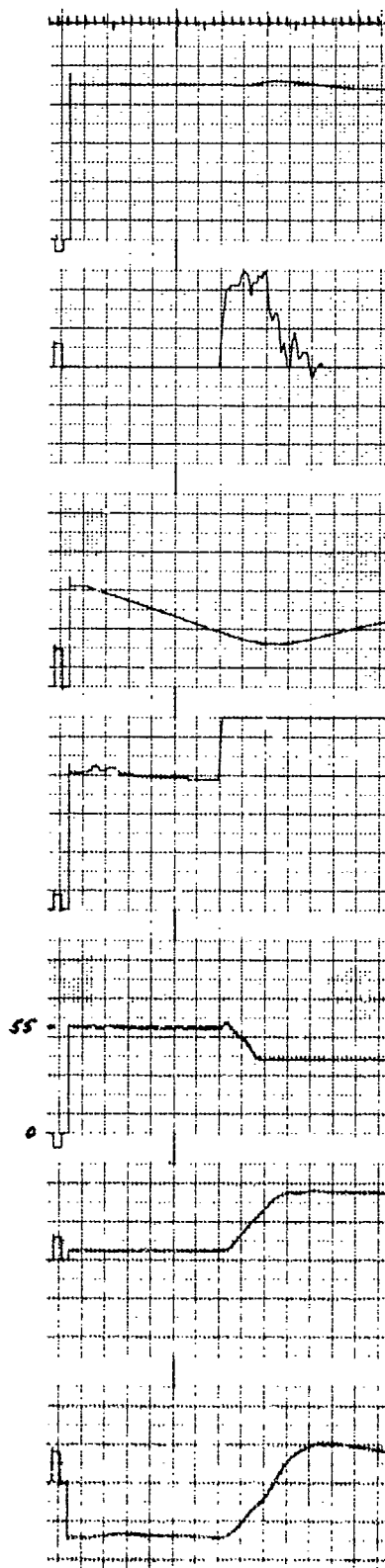


PITCH AND FLAPS UP.
FULL AUG. CONTROL.
FLAP RATE = 5 DEG/SEC.
RUN M.



EBF GO-AROUND.
 $\gamma/H = 3$.
 DECISION HEIGHT
 = 300' AGL.

PITCH AND FLAPS UP.
 FULL AUG. CONTROL.
 FLAP RATE = 50 DEG/SEC.
 RUN A.



PITCH AND FLAPS UP.
 FULL AUG. CONTROL.
 FLAP RATE = 50 DEG/SEC.
 RUN B.

AIRSPEED
(KTS)

δ_{STIC}
(% FULL TRAVEL)

ALTITUDE
(FT. AGL)

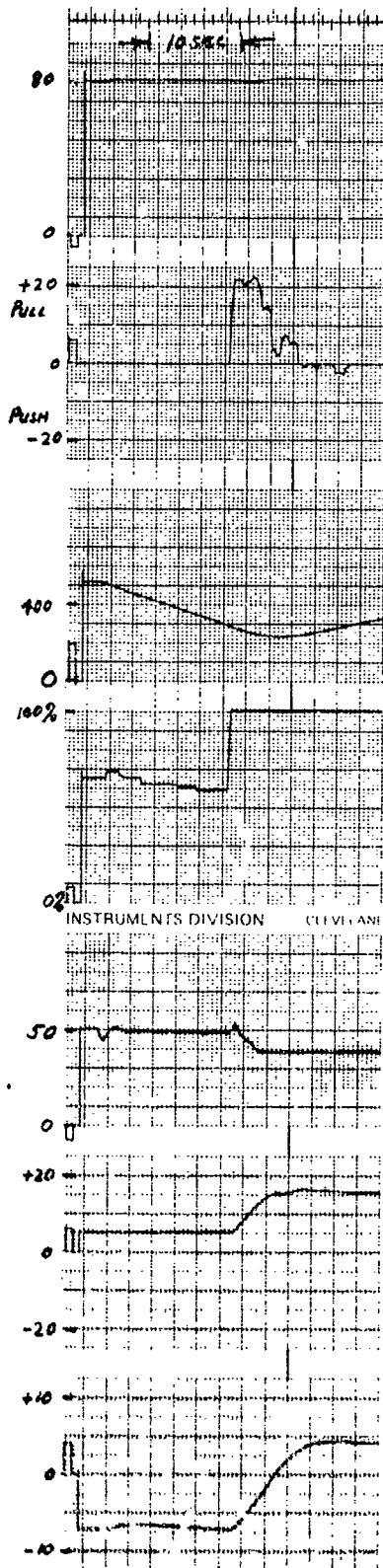
THROTTLE
(% THRUST)

FLAPS
(DEG)

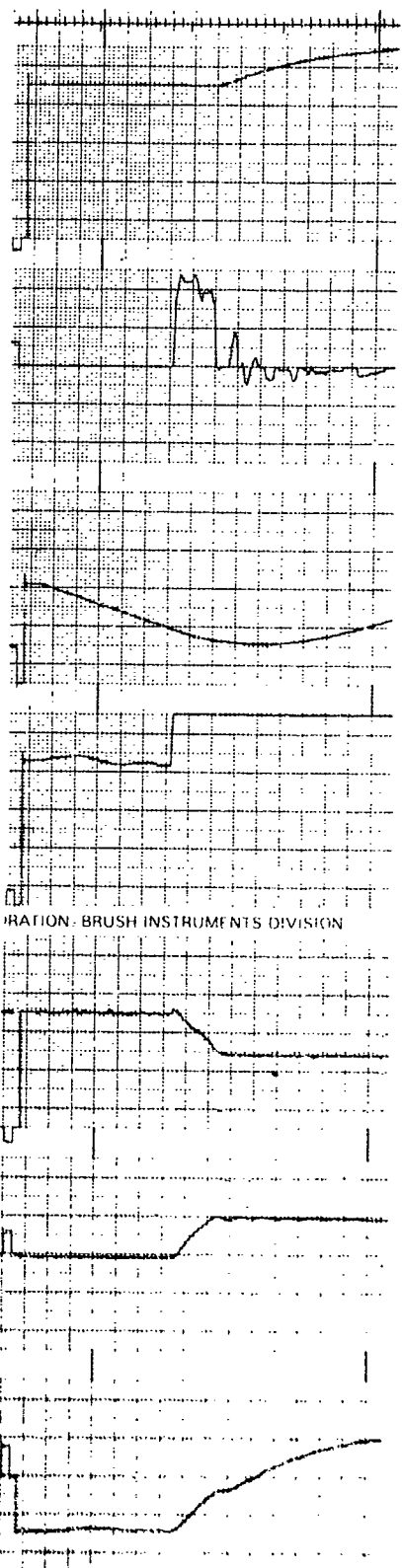
θ
(DEG)

γ
(DEG)

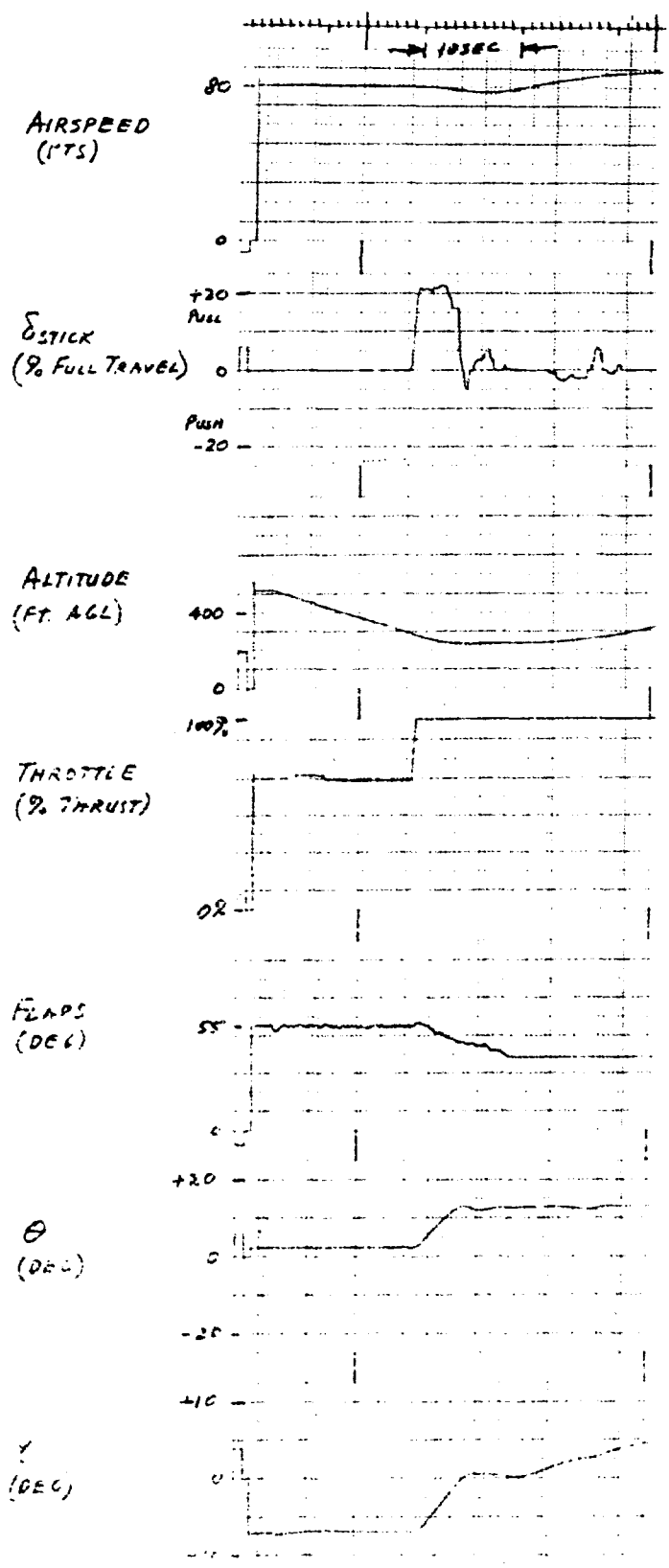
EBF GO-AROUND.
C/H = 3.
DECISION HEIGHT
= 300' AGL.



PITCH AND FLAPS UP.
FULL AUG CONTROL.
FLAP RATE = 5 DEG/SEC.
RUN D.

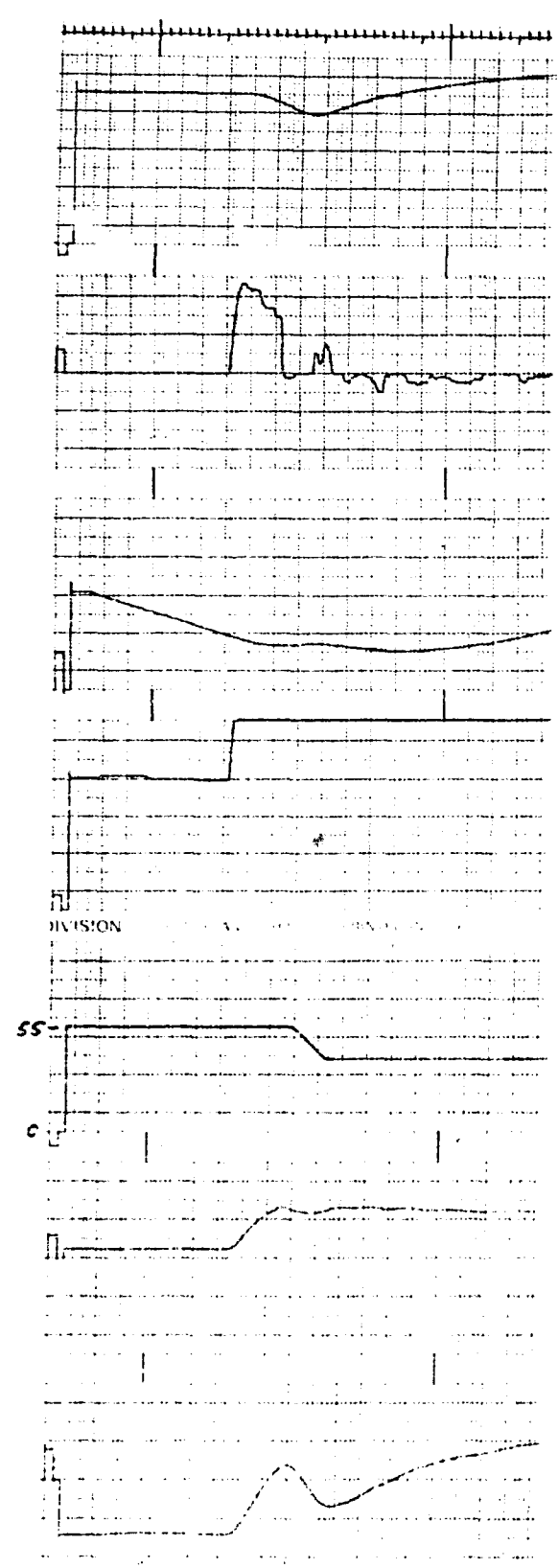


PITCH AND FLAPS UP.
FULL AUG CONTROL.
FLAP RATE = 5 DEG/SEC.
RUN G.



SEE COMMENTS
 20-100
 20-100
 20-100

PITCH THEN FLAPS UP
 FULL ROD CONTROL
 FLAP RATE = 5 DEG/SEC
 RUN II



PITCH THEN FLAPS UP.
 PITCH AUG. ONLY.
 FLAP RATE = 5 DEG/SEC
 RUN I.

AIRSPPEED
(KTS)

δ STICK
(% FULL TRAVEL)

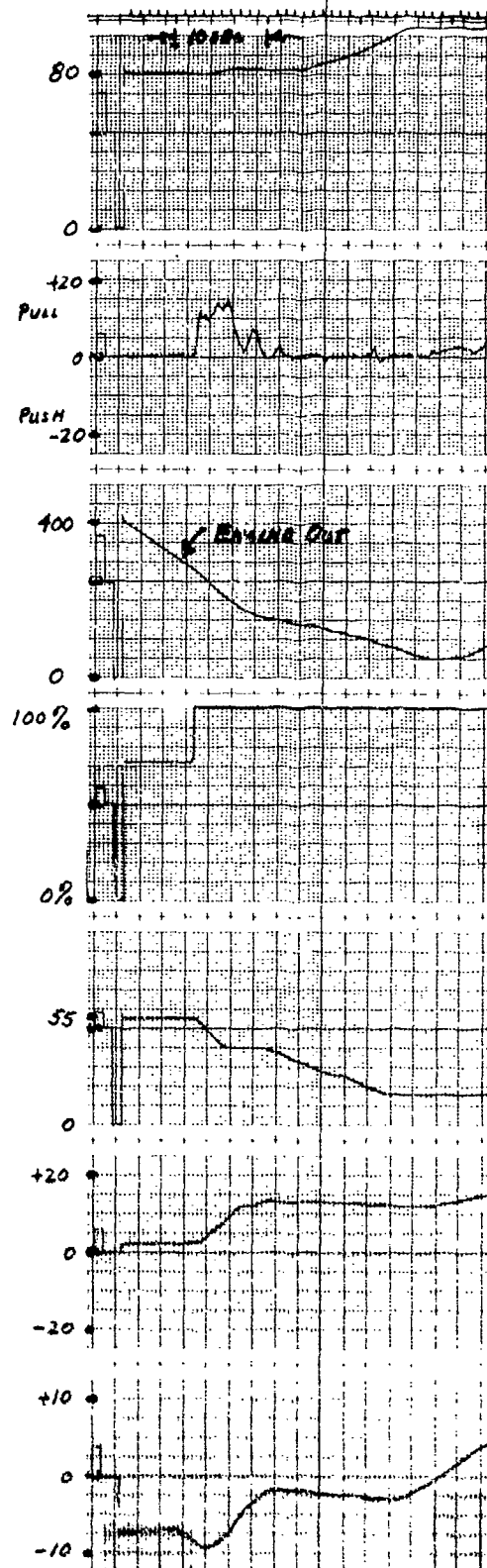
ALTITUDE
(FT. AGL)

THROTTLE
(% THRUST)

FLAPS
(DEG)

θ
(DEG)

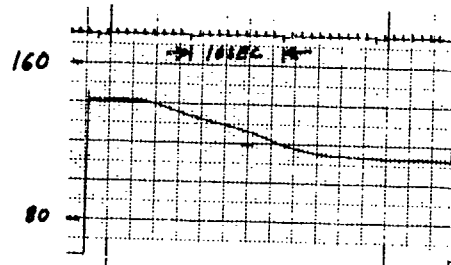
γ
(DEG)



EBF GO-AROUND. C/H = 7.
L.A.S. - M.B.
ENGINE OUT HEIGHT = 300' AGL.
DECISION HEIGHT = 300' AGL.

PITCH AND FLAPS UP.
PITCH AUG. ONLY.
FLAP RATE = 5 DEG/SEC.
RUN 635.

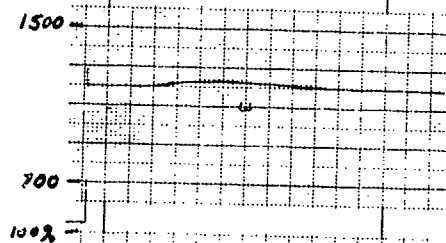
AIRSPPEED
(KTS)



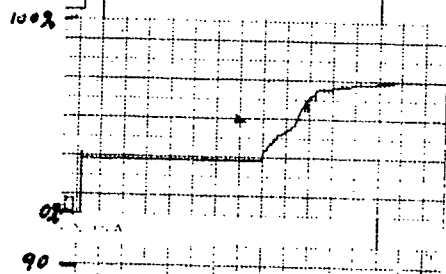
δ_{STICK}
(% FULL TRAVEL)



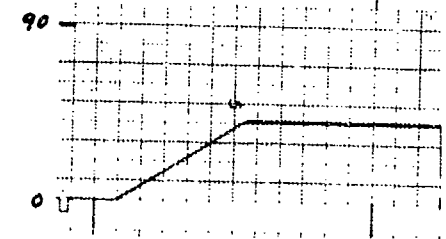
ALTITUDE
(FT AGL)



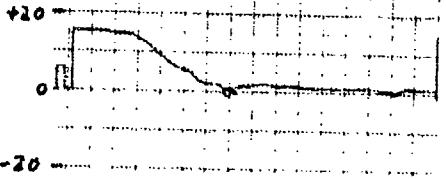
THROTTLE
(% THRUST)



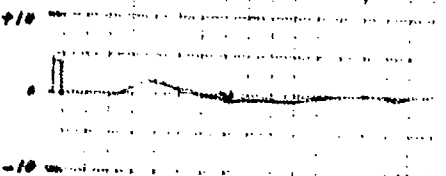
δ_{FLAP}
(DEG)



θ
(DEG)

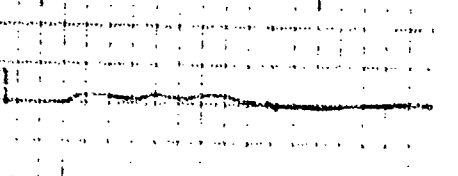
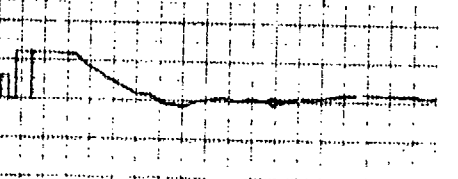
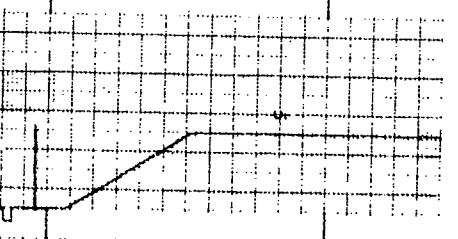
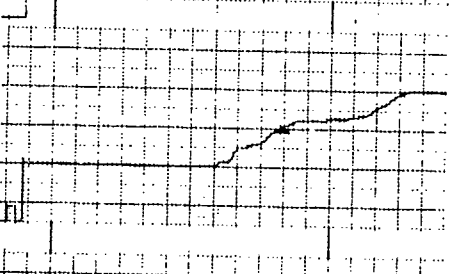
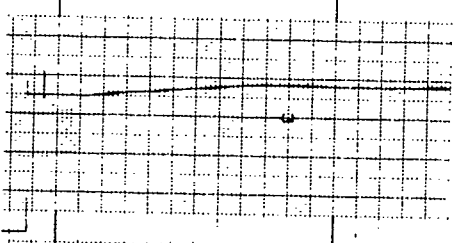
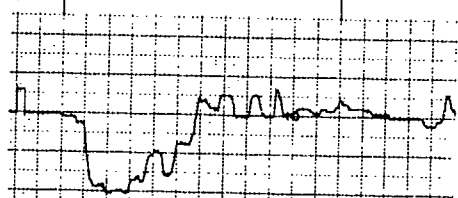
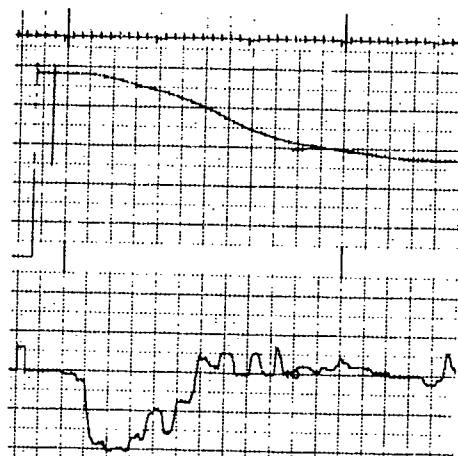


γ
(DEG)



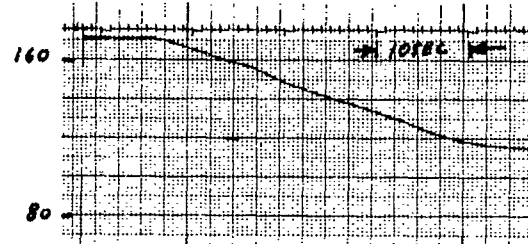
EBF INITIAL TRANSITION.
FLAPS 0 TO 40 DEGREES.
FINAL AIRSPEED = 115 KTS.

FLAP RATE = 3 DEG/SEC.
C/H = 7 (LIMITED VISIBILITY).
RUN A.



FLAP RATE = 3 DEG/SEC.
C/H = 5.
RUN B.

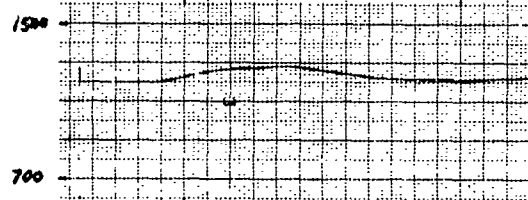
AIRSPPEED
(KTS)



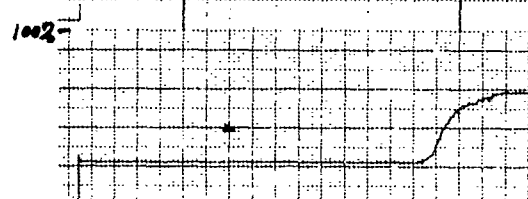
δ STICK
(% FULL TRAVEL)



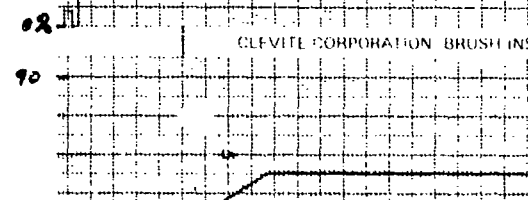
ALTITUDE
(FT. AGL)



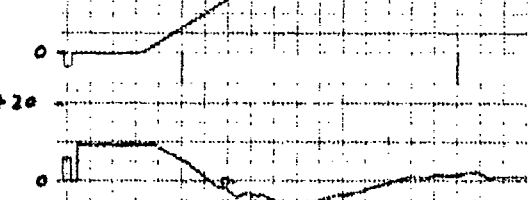
THROTTLE
(% THRUST)



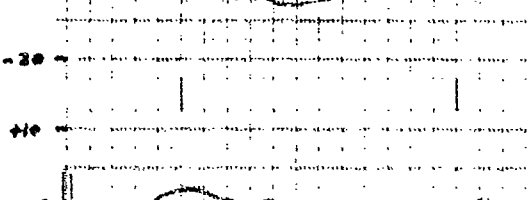
δ FLAP
(DEG)



θ
(DEG)

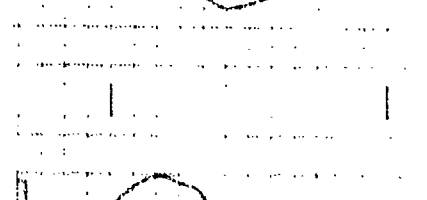
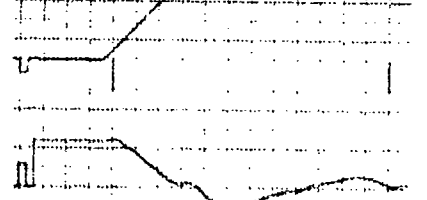
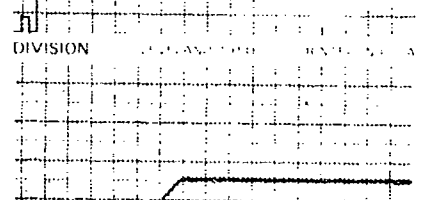
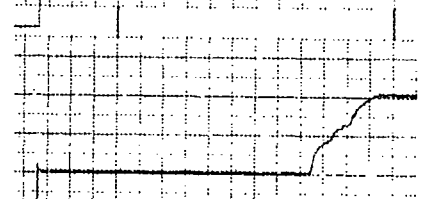
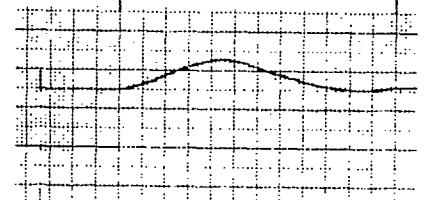
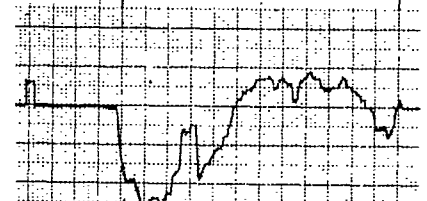
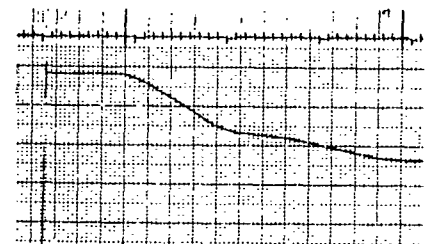


γ
(DEG)



EBF INITIAL TRANSITION.
FLAPS 0% TO 45 DEGREES.
FINAL AIRSPEED 115 KTS.

FLAP RATE = 3 DEG/SEC.
C/N = 6.
RUN C.



FLAP RATE = 5 DEG/SEC.
C/N = 7.
RUN D.

AIRSPPEED
(KTS)

160

80

+20

PULL

δ STICK
(% FULL TRAVEL)

0

PUSH

1500

ALTITUDE
(FT. AGL)

700

100%

THROTTLE
(% THRUST)

0%

90

δ FLAP
(DEG)

0

+20

θ
(DEG)

-20

γ
(DEG)

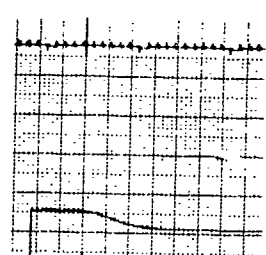
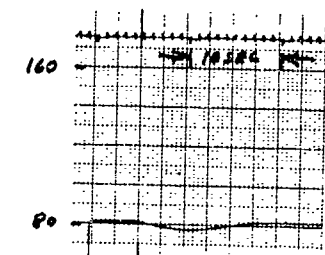
+20

-20

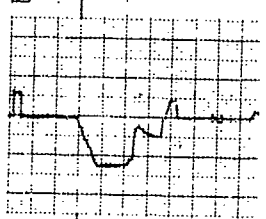
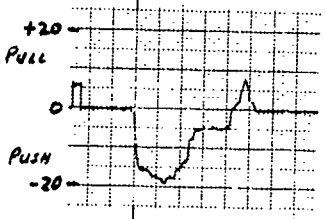
EBF INITIAL TRANSITION.
FLAPS 0 TO 40 DEGREES.
FINAL AIRSPEED = 115 KTS.

FLAP RATE = 1.5 DEG/SEC.
CH = 4.
RUN E.

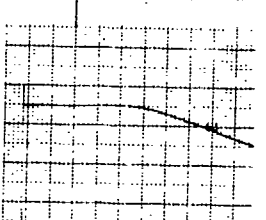
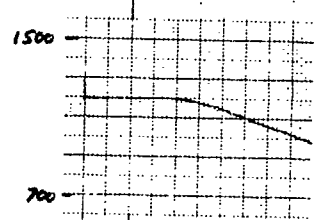
AIRSPPEED
(KTS)



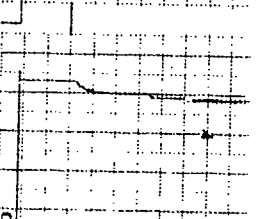
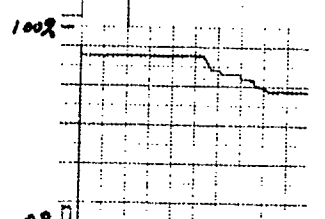
δ STICK
(% FULL TRAVEL)



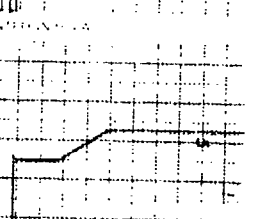
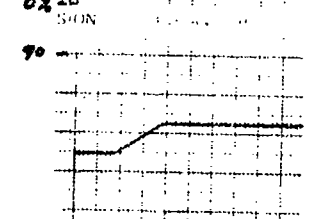
ALTITUDE
(FT. AGL)



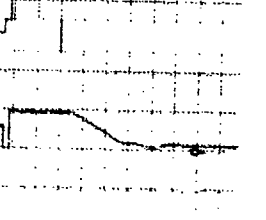
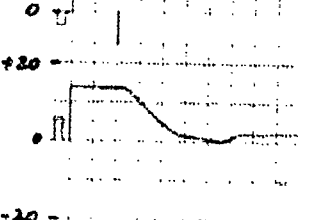
THROTTLE
(% THRUST)



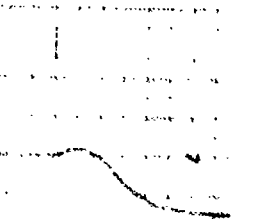
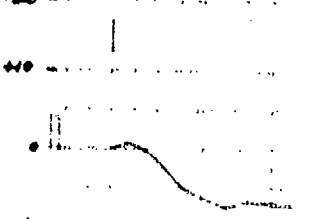
δ FLAP
(DEG)



θ
(DEG)



γ
(DEG)

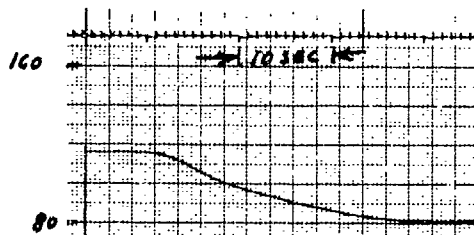


EBF FINAL TRANSITION
FLAPS 40 to 55 DEGREES.
FINAL AIRSPEED = 80 KTS. RUN F

FLAP RATE = 3 DEG/SEC.
C/N = 5

FLAP RATE = 3 DEG/SEC.
C/N = 3
RUN G

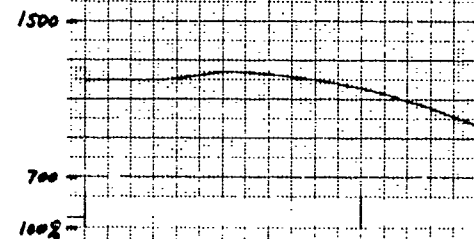
AIRSPEED
(KTS)



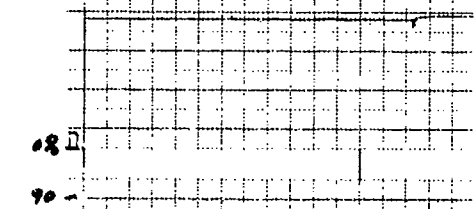
δ STICK
(% FULL TRAVEL)



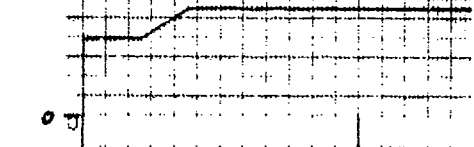
ALTITUDE
(FT. AGL)



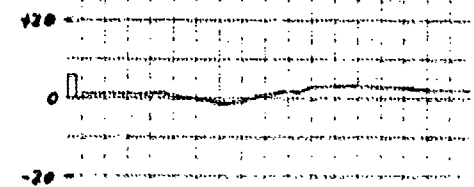
THROTTLE
(% THRUST)



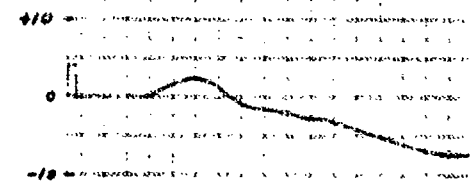
δ FLAP
(DEG)



θ
(DEG)

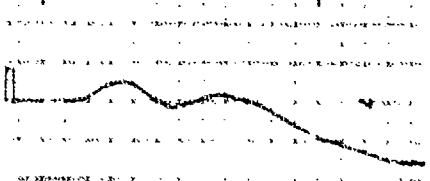
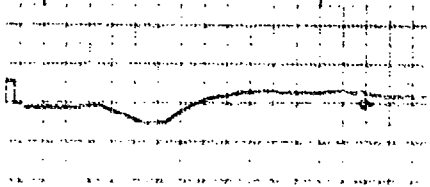
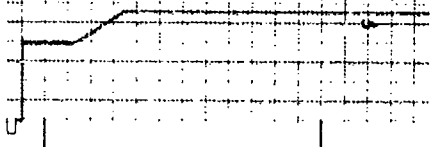
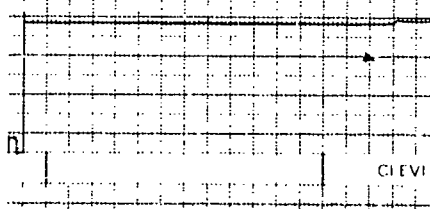
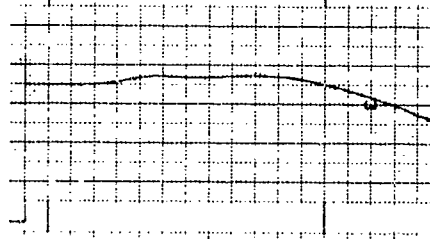
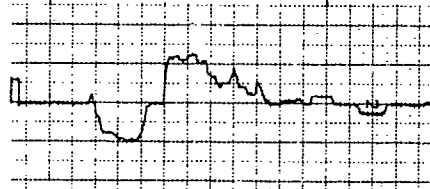
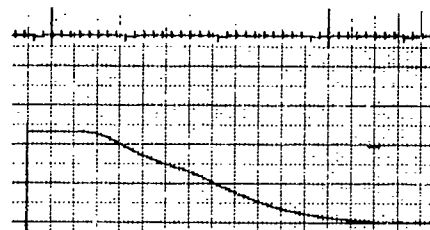


γ
(DEG)



EBF FINAL TRANSITION.
FLAPS 40 TO 55 DEGREES.
FINAL AIRSPEED = 80 KTS.

FLAP RATE = 3 DEG/SEC.
C/N = 3.
RUN H.



FLAP RATE = 3 DEG/SEC.
C/N = 5.
RUN I.

AIRSPED
(KTS)

160

80

δ STICK
(% FULL TRAVEL)

+20
PULL

0
PUSH

1500

ALTITUDE
(FT. ALL)

700

1000

THRUSTLE
(% THRUST)

0%

90

δ FLAP
(DEG)

0

θ
(DEG)

+30

-30

+10

γ
(DEG)

-10

CBF FINAL TRANSITION
FLAPS 40 TO 55 DEGREES
FINAL AIRSPEED 70 KTS

FLAP RATE 15 DEGREE/SEC
CIN 15
RUN 7

FINAL AIRSPEED 70 KTS
CIN 15
RUN 7

AIRSPED
(KTS)

δ STICK
(% FULL TRAVEL)

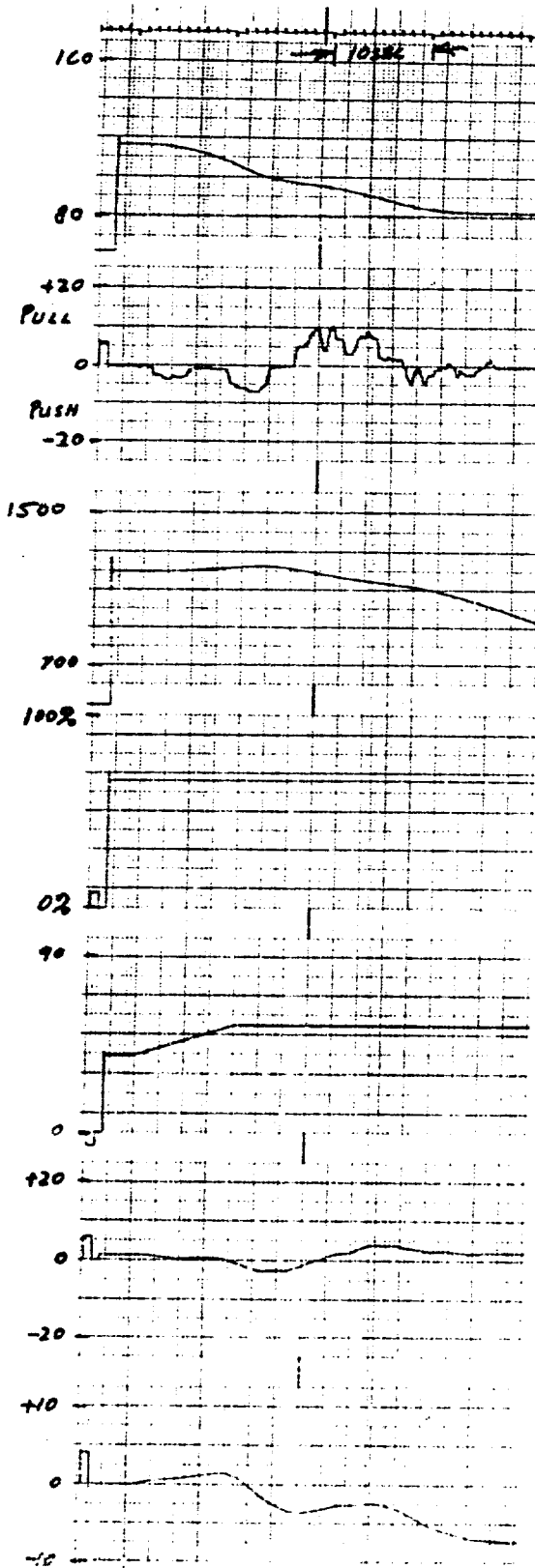
ALTITUDE
(FT. ALL)

THROTTLE
(% THRUST)

δ FLAP
(DEG)

θ
(DEG)

γ
(DEG)



END FINAL TRANSITION.
FLAPS 40% TO 0 DEGREES
FINAL AIRSPEED = 80 KTS

FLAP RATE = 1.5 DEG/SEC
C_Y = 0
RUM L

AIRSPED
(KTS)

δ STICK
(% FULL TRAVEL)

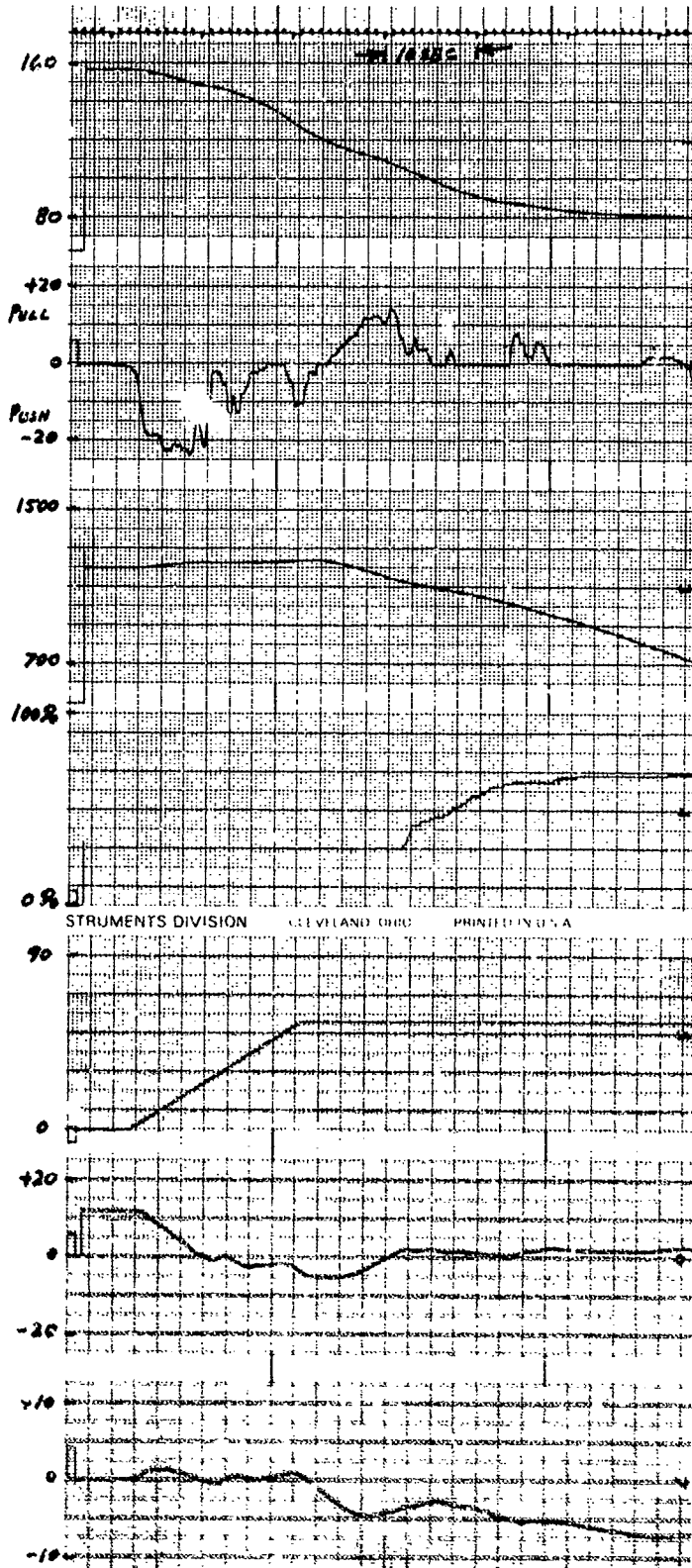
ALTITUDE
(FT. AGL)

THRITTLE
(% THRUST)

δ FLAP
(DEG)

θ
(DEG)

γ
(DEG)



EBF TOTAL TRANSITION.
FLAPS 0 TO 55 DEGREES.
FINAL AIRSPEED = 80 KTS.

FLAP RATE = 3 DEG/SEC.
C/N = 6.
RUN M.

AIRSPPEED
(KTS)

160

80

δ STICK
(% FULL TRAVEL)

+20

PULL

0

PUSH

-20

ALTITUDE
(FT. AGL)

1500

700

THROTTLE
(% THRUST)

100%

0%

δ FLAP
(DEG)

90

0

θ
(DEG)

+20

0

-20

γ
(DEG)

+10

0

-10

EBF INITIAL TRANSITION.
FLAPS 0 TO 40 DEGREES.
FINAL AIRSPEED = 115 KTS.
L.A.S. - F.B.

FLAP RATE = 3 DEG/SEC.

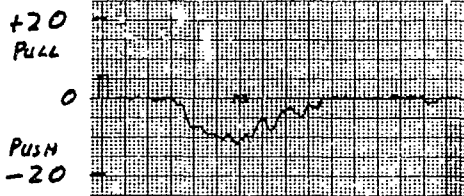
G/H = 6.

RUN IT-2.

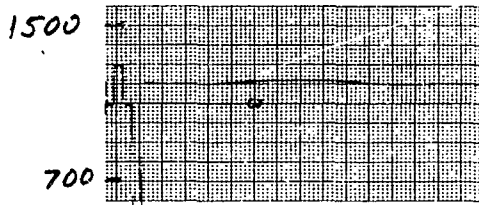
AIRSPEED
(KTS)



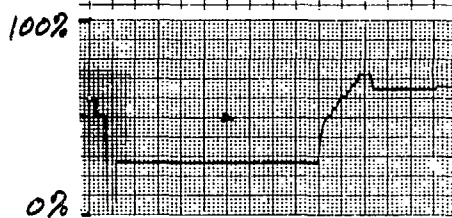
δ_{STICK}
(% FULL TRAVEL)



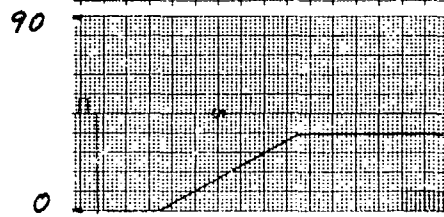
ALTITUDE
(FT. AGL)



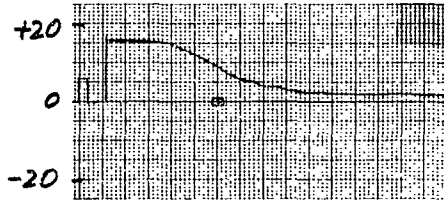
THROTTLE
(% THRUST)



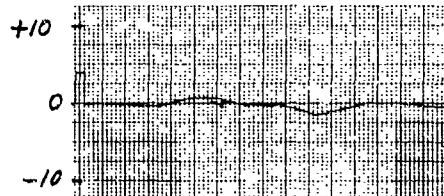
δ_{FLAP}
(DEG)



θ
(DEG)



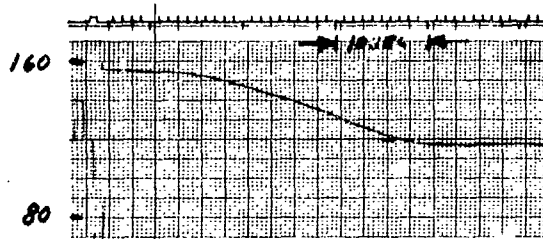
γ
(DEG)



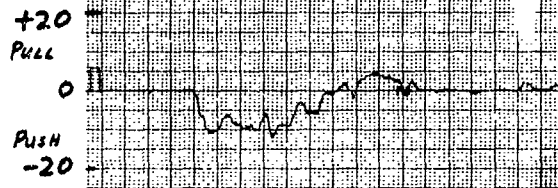
EBF INITIAL TRANSITION.
FLAPS 0 TO 40 DEGREES.
FINAL AIRSPEED = 115 KTS.
L.I.S - M. B.

FLAP RATE = 3 DEG/SEC.
CH = 5.
RUN IT 2.

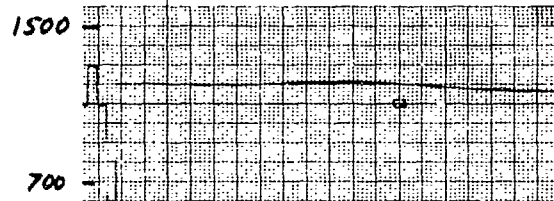
AIR SPEED
(KTS)



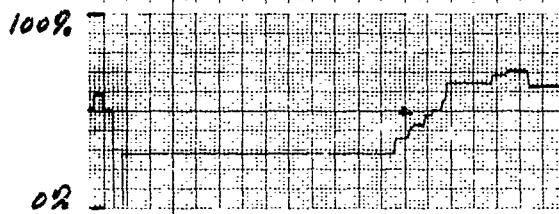
δ_{STICK}
(% FULL TRAVEL)



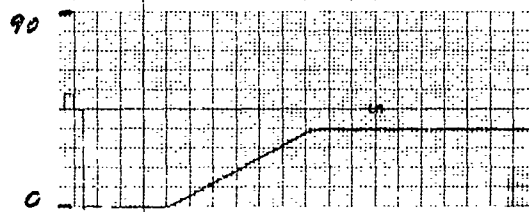
ALTITUDE
(FT. AGL)



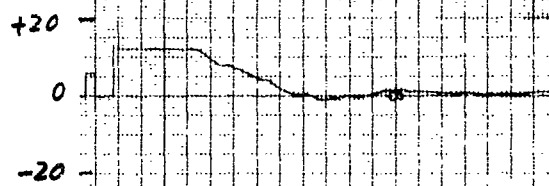
THROTTLE
(% THRUST)



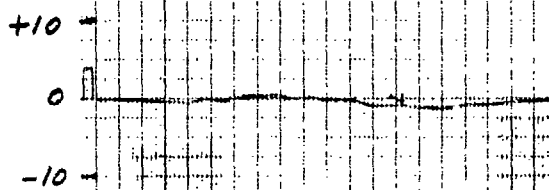
δ_{FLAP}
(DEG)



θ
(DEG)



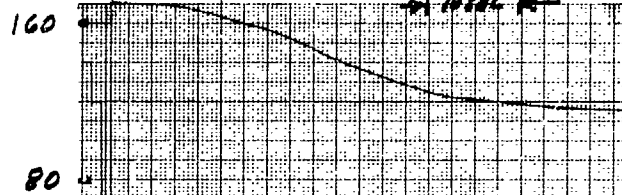
γ
(DEG)



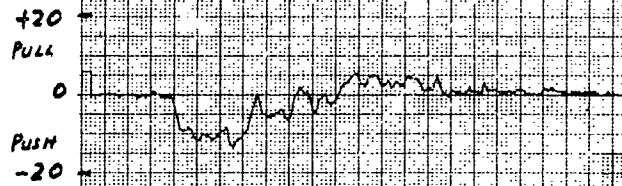
EBF INITIAL TRANSITION.
FLAPS 0 TO 40 DEGREES.
FINAL AIRSPEED = 115 KTS.
L.A.S. - M.B.

FLAP RATE = 3 DEG/SEC.
C/H = 6.
RUN IT-6.

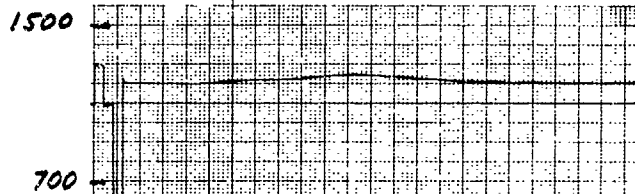
AIRSPPEED
(KTS)



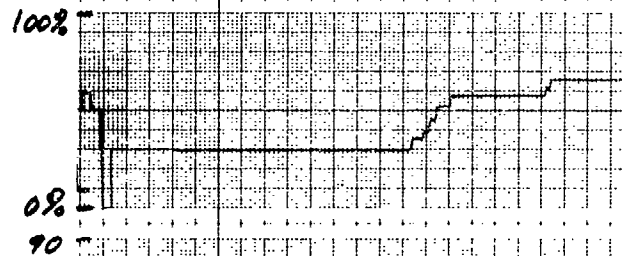
δ_{STICK}
(% FULL TRAVEL)



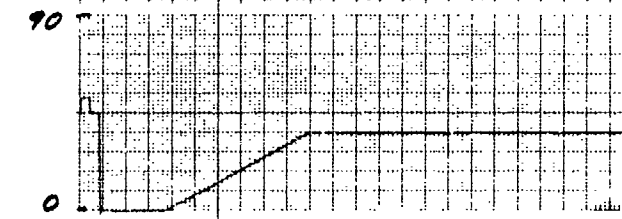
ALTITUDE
(FT. AGL)



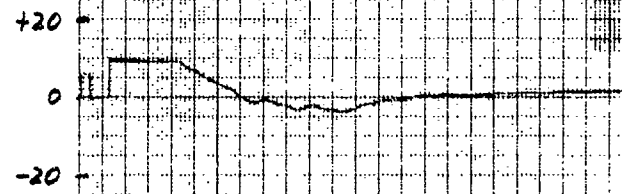
THROTTLE
(% THRUST)



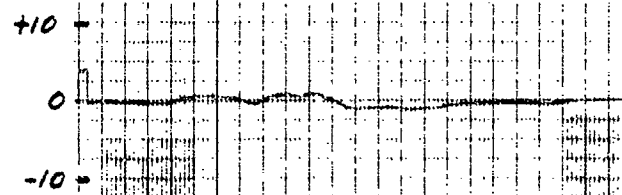
δ_{FLAP}
(DEG)



θ
(DEG)



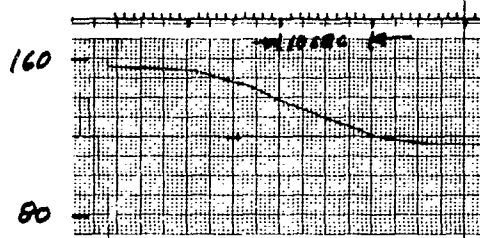
γ
(DEG)



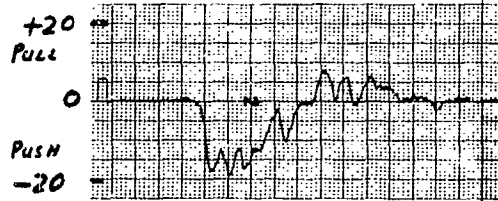
EBF INITIAL TRANSITION.
FLAPS 0 TO 40 DEGREES.
FINAL AIRSPEED = 115 KTS.
L.A.S. - M.B.

FLAP RATE = 3 DEG/SEC.
C/H = 5.
RUN IT 10.

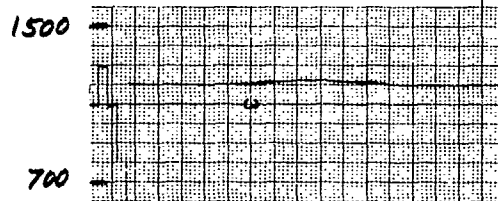
AIRSPPEED
(KTS)



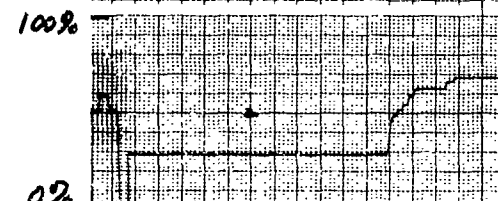
δ STICK
(% FULL TRAVEL)



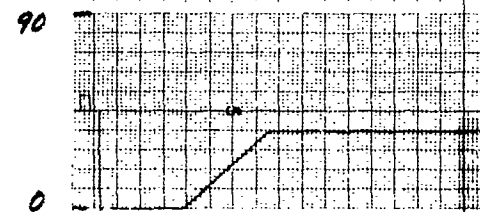
ALTITUDE
(FT. AGL)



THROTTLE
(% THRUST)



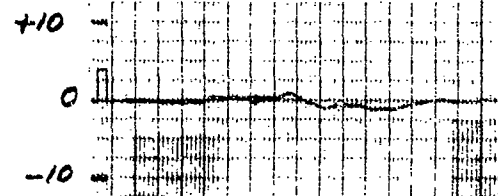
δ FLAP
(DEG)



θ
(DEG)



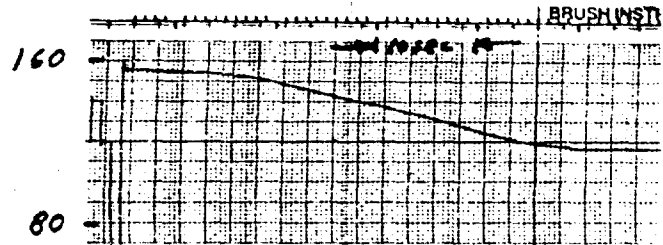
γ
(DEG)



EBF INITIAL TRANSITION.
FLAPS 0 TO 40 DEGREES.
FINAL AIRSPEED = 115 KTS.
L.A.S. - M. 8.

FLAP RATE = 5 DEG/SEC.
C/H = 7.
RUN IT 7.

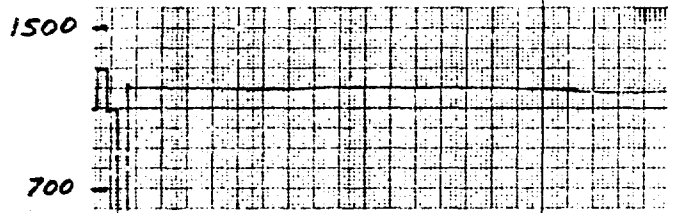
AIR SPEED
(KTS)



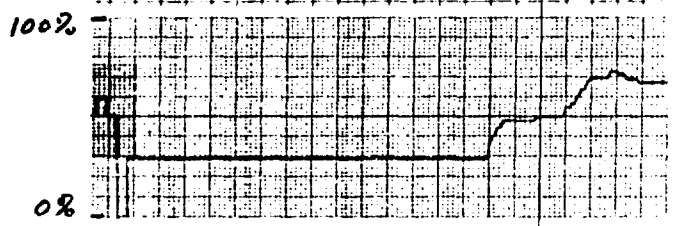
δ_{STICK}
(% FULL TRAVEL)



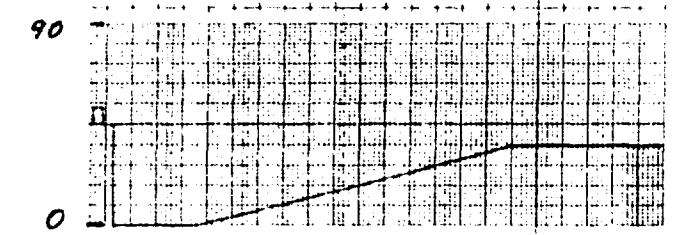
ALTITUDE
(FT. AGL)



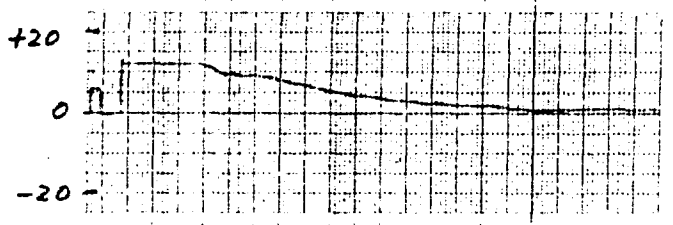
THROTTLE
(% THRUST)



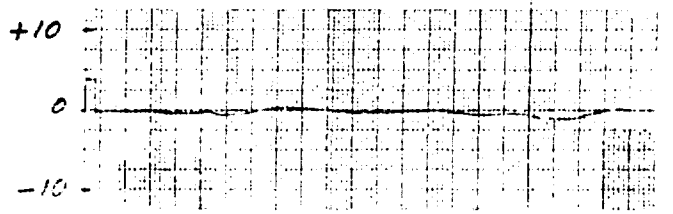
δ_{FLAP}
(DEG)



θ
(DEG)



γ
(DEG)



EBF INITIAL TRANSITION.
FLAP 0 TO 40 DEGREES
FINAL AIRSPEED = 115 KTS.
L.A. - M.B.

FLAP RATE = 1.5 DEG/SEC
S/R = 4 1/2
KUN I.T.S.

AIRSPPEED
(KTS)

160

80

δ STICK
(% FULL TRAVEL)

+20

PULL

0

PUSH

-20

ALTITUDE
(FT. AGL)

1500

700

THROTTLE
(% THRUST)

100%

0%

δ FLAP
(DEG)

90

0

θ
(DEG)

+20

0

-20

γ
(DEG)

+10

0

-10

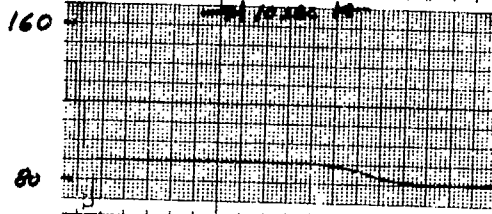
EBF FINAL TRANSITION.
FLAPS 40 TO 55 DEGREES
FINAL AIRSPEED = 80KTS.
L.A.S. - M.B.

FLAP RATE = 3 DEG/SEC.

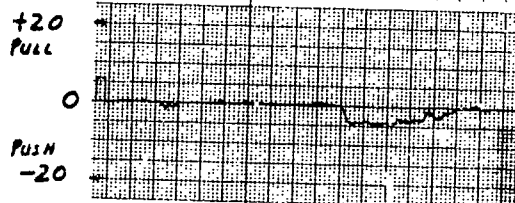
C/H = 5.

RUN FT 2.

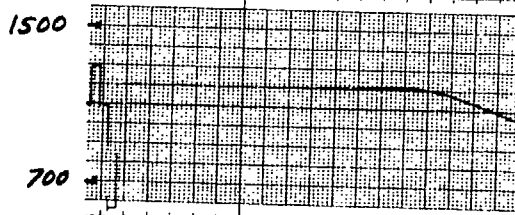
AIRSPEED
(KTS)



δ STICK
(% FULL TRAVEL)



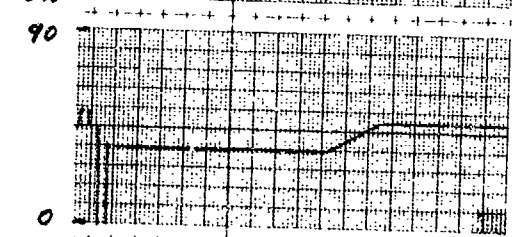
ALTITUDE
(FT. AGL)



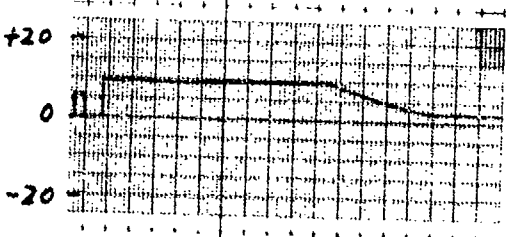
THROTTLE
(% THRUST)



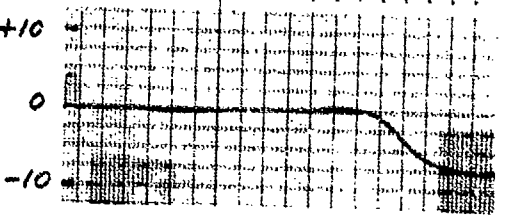
δ FLAP
(DEG)



θ
(DEG)



γ
(DEG)



EBF FINAL TRANSITION.
FLAPS 40 TO 55 DEGREES.
FINAL AIRSPEED = 80KTS.
L.A.S. - M.B.

FLAP RATE = 3 DEG/SEC.
L/H = 2 1/2.
RUN FTG.

AIRSPPEED
(KTS)

160

80

δ_{STICK}
(% FULL TRAVEL)

+20
PULL

0

PUSH
-20

ALTITUDE
(FT. ALL)

1500

700

THROTTLE
(% THRUST)

100%

0%

δ_{FLAP}
(DEG)

90

0

θ
(DEG)

+20

0

-20

γ
(DEG)

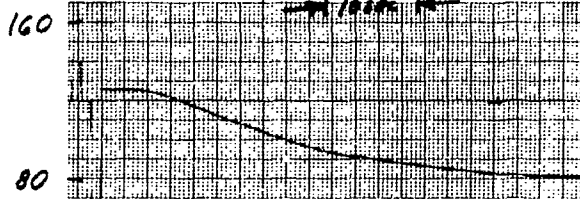
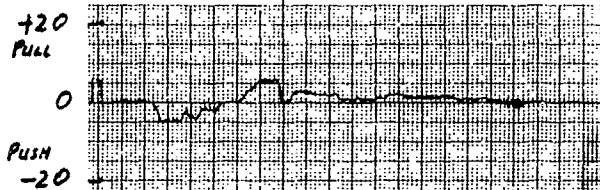
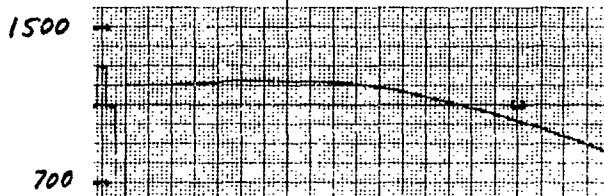
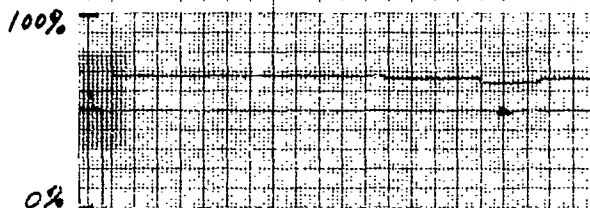
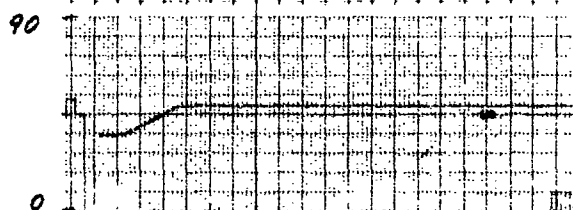
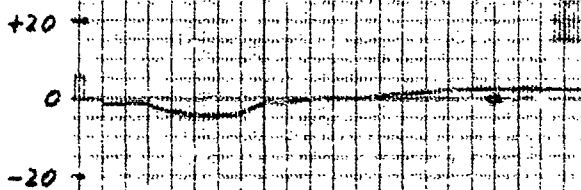
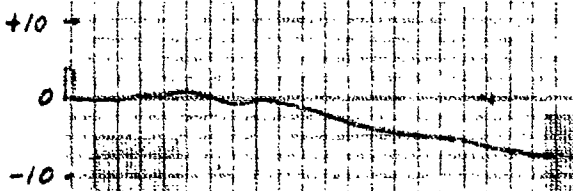
+10

0

-10

EBF FINAL TRANSITION.
FLAPS 40 TO 55 DEGREES.
FINAL AIRSPEED = 80 KTS.
L.A.S - M. B.

FLAP RATE = 3 DEG/SEC
L/H = 3.
RUN FT 10.

AIRSPEED
(KTS) δ STICK
(% FULL TRAVEL)ALTITUDE
(FT. AGL)THROTTLE
(% THRUST) δ FLAP
(DEG) θ
(DEG) γ
(DEG)

EBF FINAL TRANSITION.
 FLAPS 40 TO 55 DEGREES.
 FINAL AIRSPEED = 80 KTS.
 L.A.S. - M.B.

FLAP RATE = 3 DEG/SEC.
 C/H = A.
 RUN FT 1A.

AIRSPEED
(KTS)

δ_{STICK}
(% FULL TRAVEL)

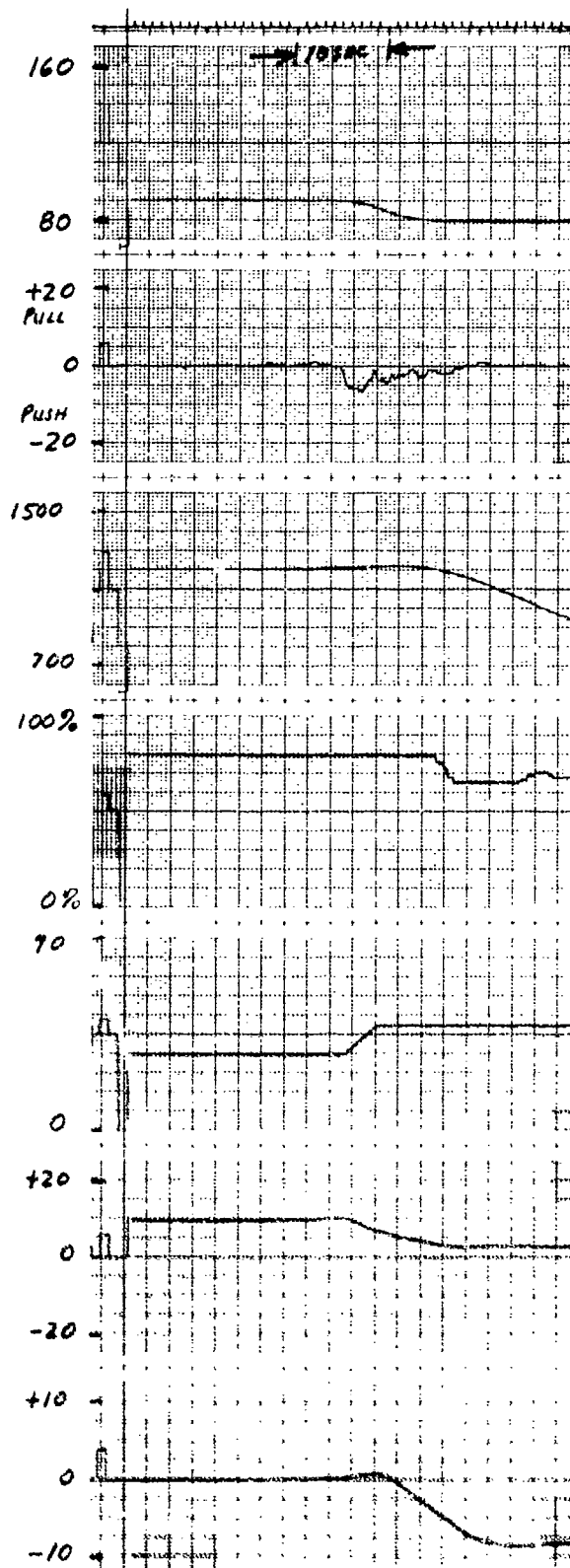
ALTITUDE
(FT. AGL)

THROTTLE
(% THRUST)

δ_{FLAP}
(DEG)

θ
(DEG)

γ
(DEG)



EBF FINAL TRANSITION.
FLAPS 40 TO 55 DEGREES.
FINAL AIRSPEED = 80 KTS.
L.A.S - M.B.

FLAP RATE = 5 DEG/SEC.
C/N = 3 1/2.
RUN FT 7.

AIRSPEED
(KTS)

160

80

δ STICK
(% FULL TRAVEL)

+20

PULL

0

PUSH

-20

ALTITUDE
(FT. AGL)

1500

700

THROTTLE
(% THRUST)

100%

0%

90

δ FLAP
(DEG)

0

θ
(DEG)

+20

0

-20

γ
(DEG)

+10

0

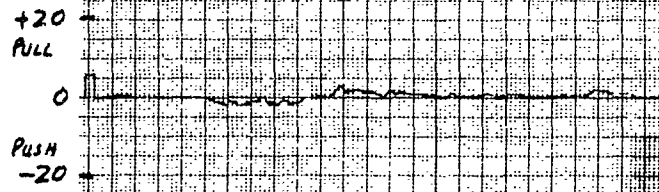
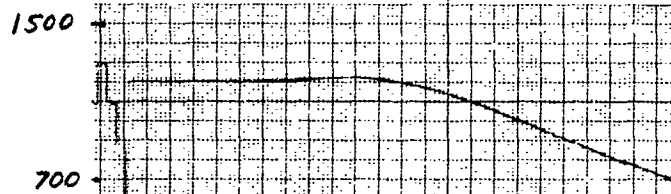
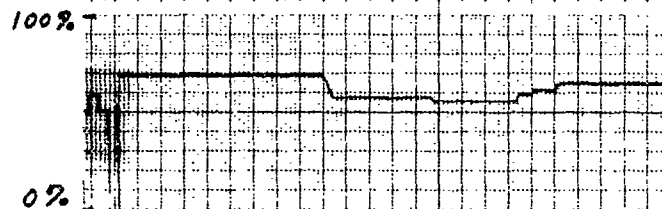
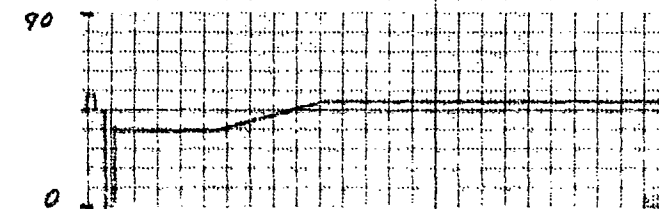
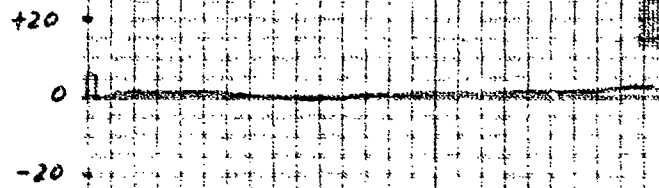
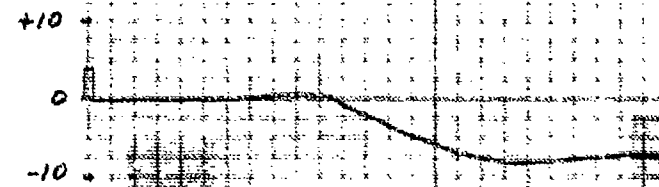
-10

EBF FINAL TRANSITION.
FLAPS 40 TO 55 DEGREES.
FINAL AIRSPEED = 80 KTS.
L.A.S. - M.B.

FLAP RATE = 5 DEG/SEC.

C/N = A.

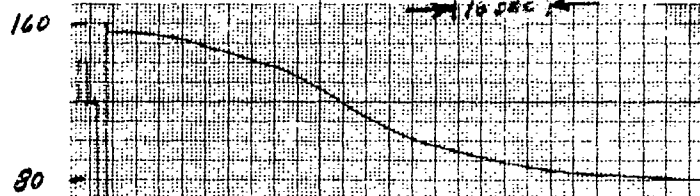
RUN FT 11.

AIRSPEED
(KTS) δ STICK
(% FULL TRAVEL)ALTITUDE
(FT. ALL)THROTTLE
(% THRUST) δ FLAP
(DEG) θ
(DEG) γ
(DEG)

EBF FINAL TRANSITION.
 FLAPS 40 TO 55 DEGREES.
 FINAL AIRSPEED = 80 KTS.
 L.A.S. - M. B.

FLAP RATE = 1.5 DEG/SEC.
 $\gamma/H = 3$
 RUN FT 9.

AIR SPEED
(KTS)



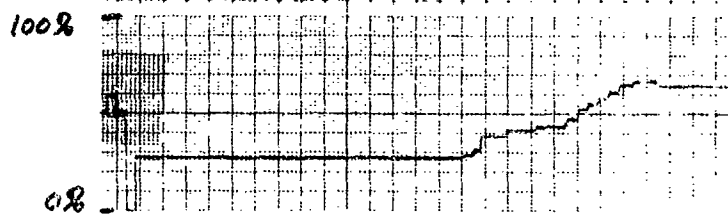
δ_{STICK}
(% FULL TRAVEL)



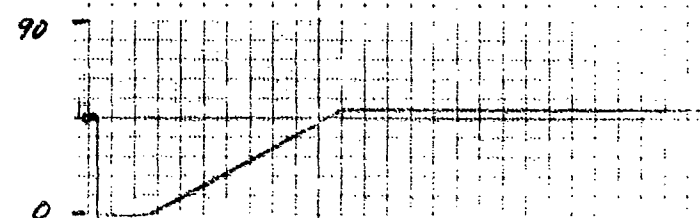
ALTITUDE
(FT. AGL)



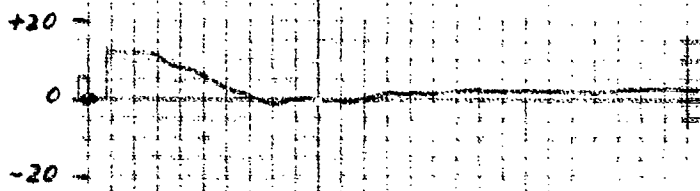
THROTTLE
(% THRUST)



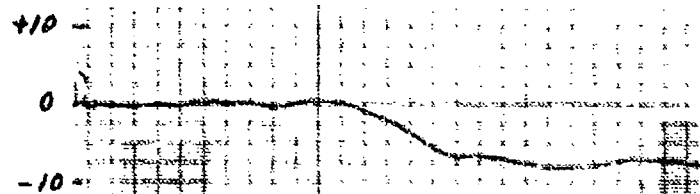
δ_{FLAP}
(DEG)



θ
(DEG)



γ
(DEG)

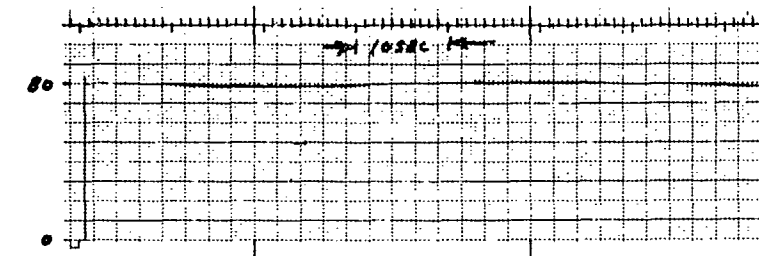


EBF TOTAL TRANSITION.
FLAPS 0 TO 55 DEGREES.
FINAL AIRSPEED = 80 KTS.
L.A.S. - M.B.

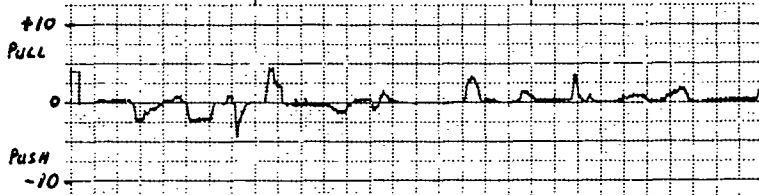
FLAP RATE = 3 DEG/SEC.
 $C/M = 5$.
RUN TTS.

INTERNALLY BLOWN FLAP
WITH PARTIAL
THRUST VECTORING
(IBF/VT)

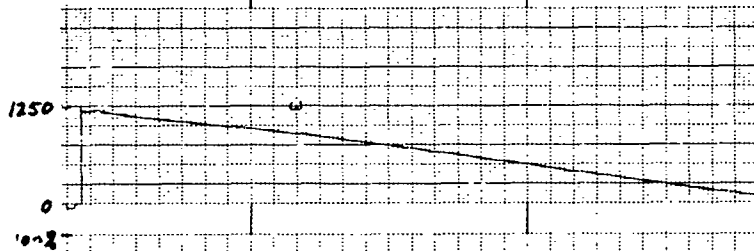
AIRSPPEED
(KTS)



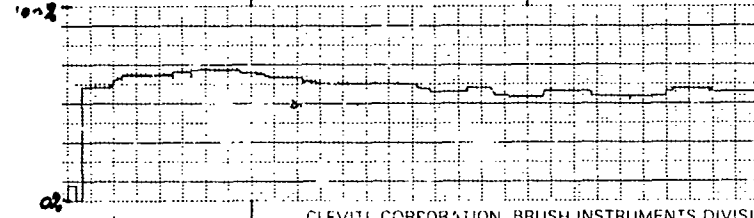
δ_{STICK}
(% FULL TRAVEL)



ALTITUDE
(FT. AGL)

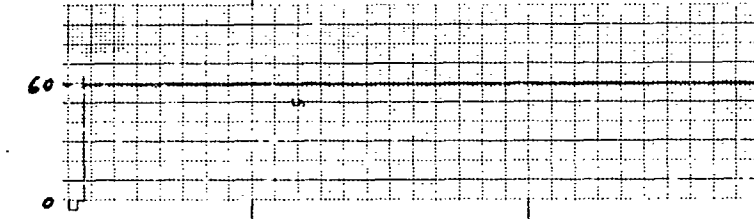


THROTTLE
(% THRUST)

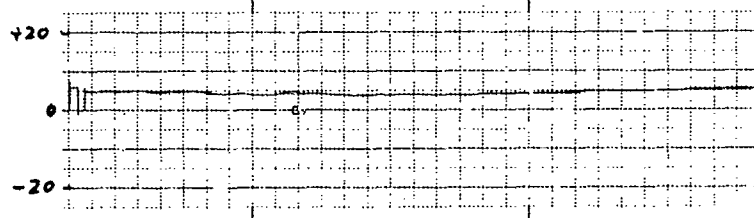


CLEVELAND CORPORATION BRUSH INSTRUMENTS DIVISION

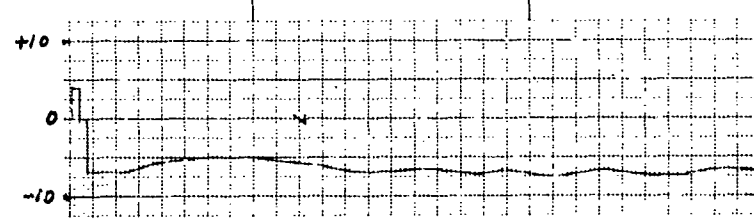
δ_{FLAP}
(DEG)



θ
(DEG)



γ
(DEG)



IBF/VT APPROACH. C/H = 4. $\gamma = -7^\circ$. γ CONTROL BY POWER.
RUN B. PITCH AUG ONLY.

AIRSPPEED
(KTS)

δ STICK
(% FULL TRAVEL)

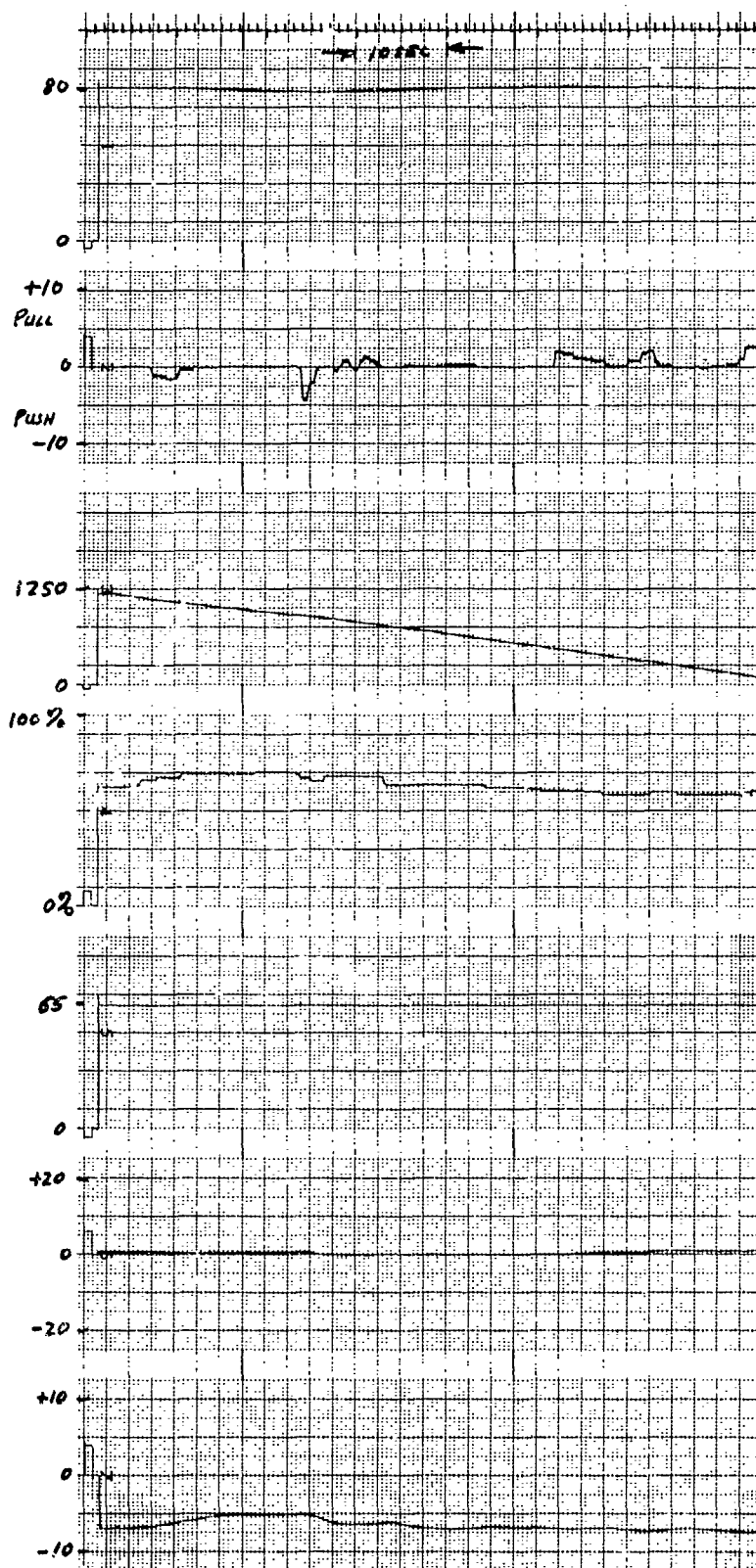
ALTITUDE
(FT. AGL)

THROTTLE
(% THRUST)

δ FLAP
(DEG)

θ
(DEG)

γ
(DEG)



IBF/NT APPROACH. C/H = 3 1/2. $\gamma = -7^\circ$. γ CONTROL BY POWER.
RUNC. PITCH AUG. ONLY.

AIRSPED
(KTS)

δ STICK
(% FULL TRAVEL)

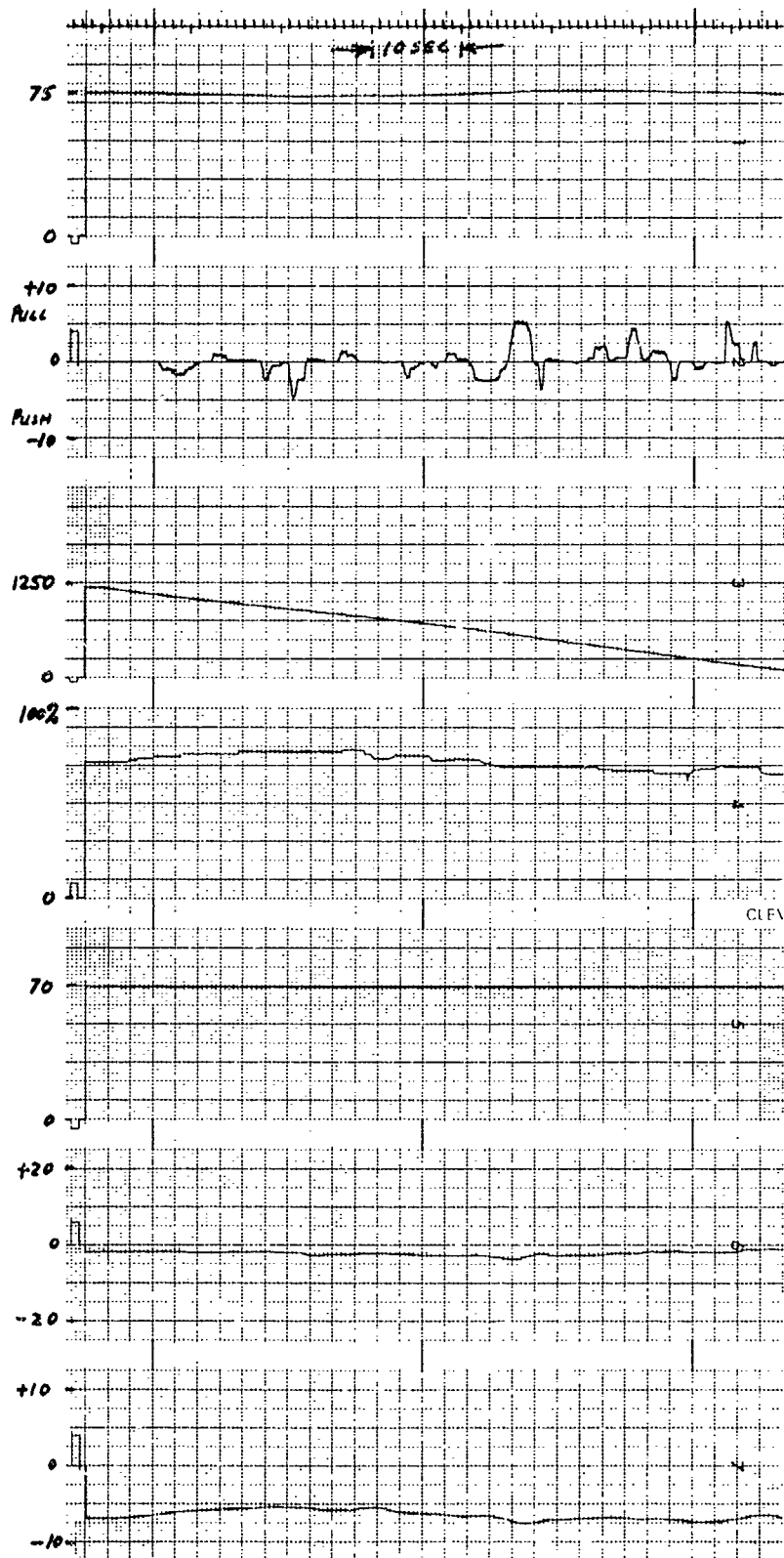
ALTITUDE
(FT. AGL)

THROTTLE
(% THRUST)

δ FLAP
(DEG)

θ
(DEG)

γ
(DEG)



IBF/NT APPROACH. C/H = 4 1/2. $\gamma = -7^\circ$. γ Control BY POWER
RUN D. PITCH AUG. ONLY.

AIRSPED
(KTS)

δ STICK
(% FULL TRAVEL)

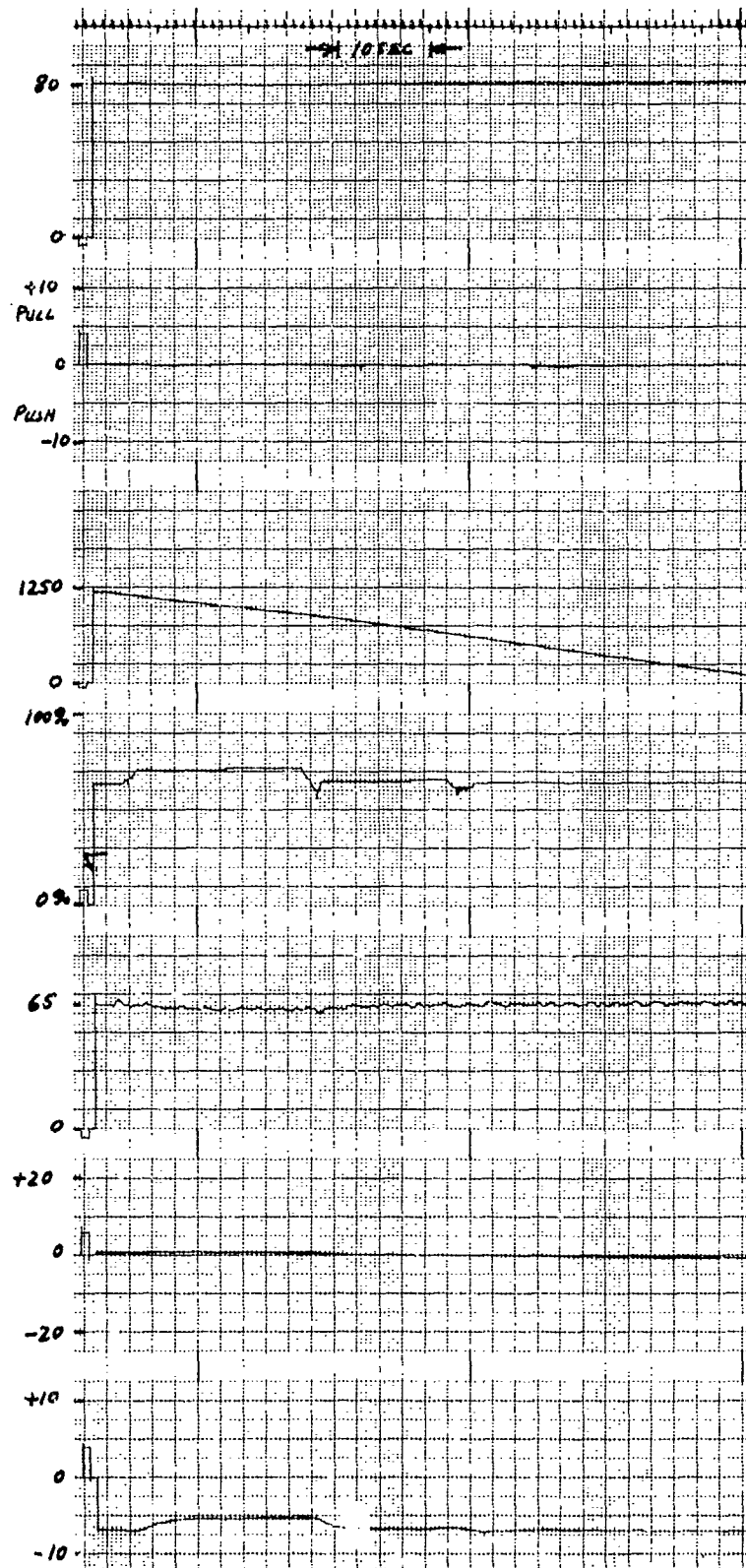
ALTITUDE
(FT. AGL)

THROTTLE
(% THRUST)

δ FLAP
(DEG)

θ
(DEG)

γ
(DEG)



IBF/VT APPROACH. C/H = 3. $\gamma = -7^\circ$. γ CONTROL BY POWER.
RUN F. FULL AUG. CONTROL.

AIRSPPEED
(KTS)

δ_{STICK}
(% FULL TRAVEL)

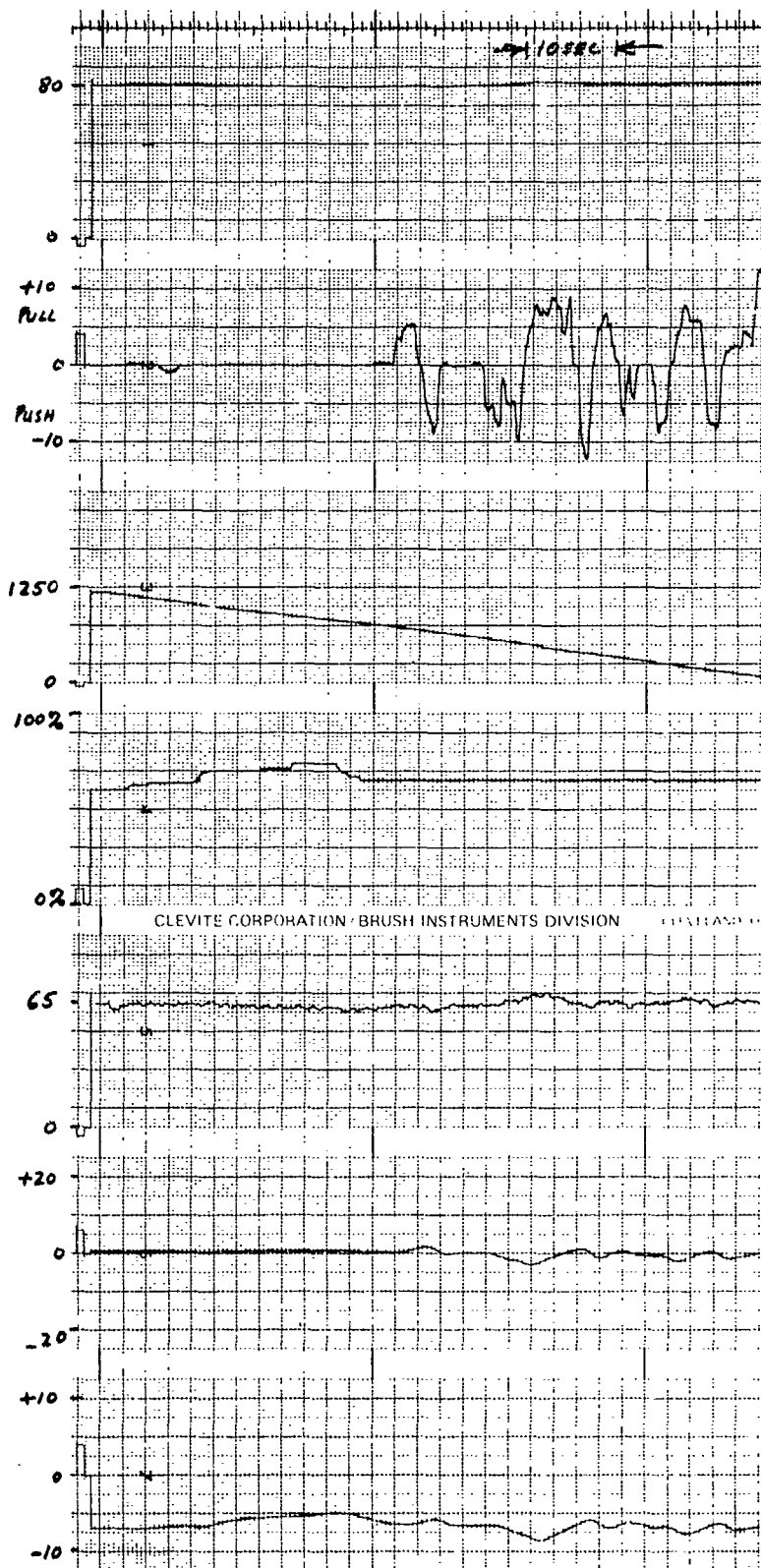
ALTITUDE
(FT. AGL)

THROTTLE
(% THRUST)

δ_{FLAP}
(DEG)

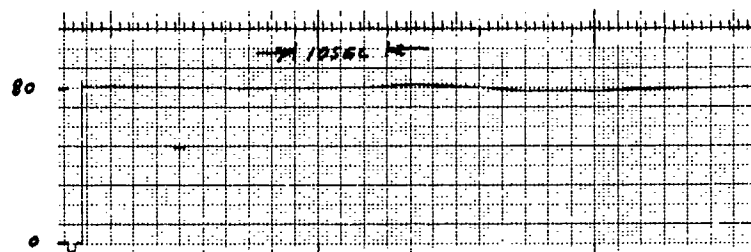
θ
(DEG)

γ
(DEG)



IBFVT APPROACH. C/H = 6. $\gamma = -7$. γ CONTROL BY PITCH.
RUN H. FULL AUG. CONTROL.

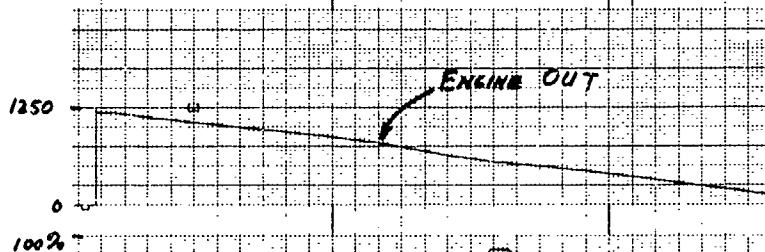
AIRSPEED
(KTS)



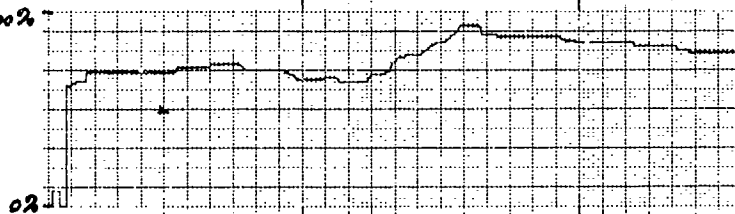
δ STICK
(% FULL TRAVEL)



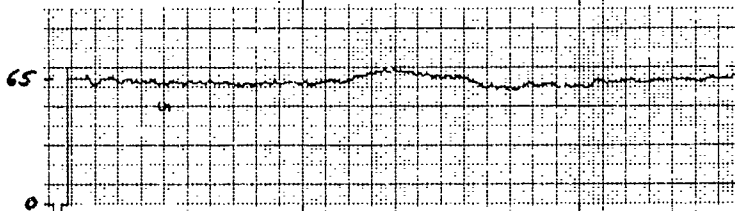
ALTITUDE
(FT. AGL)



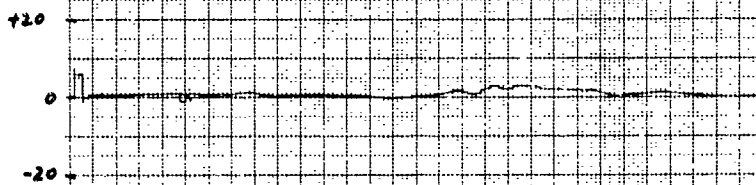
THROTTLE
(% THRUST)



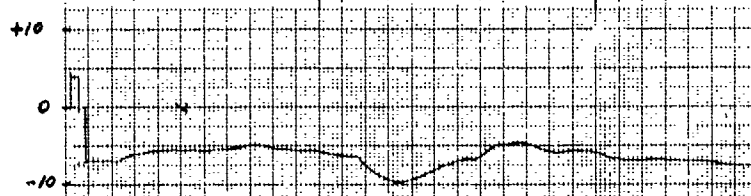
δ FLAP
(DEG)



θ
(DEG)

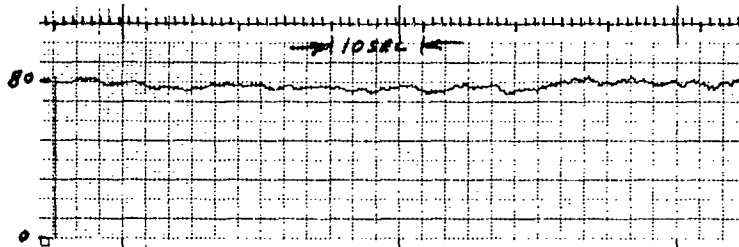


γ
(DEG)

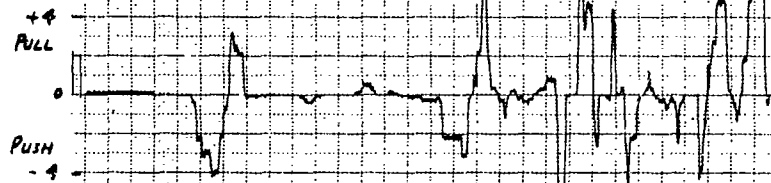


IBFNT APPROACH. C/H = 6. $\gamma = -7^\circ$. γ CONTROL BY POWER.
RUN I. ENGINE OUT APPROACH. FULL AUG. CONTROL.

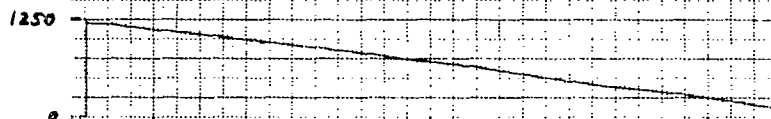
AIRSPEED
(KTS)



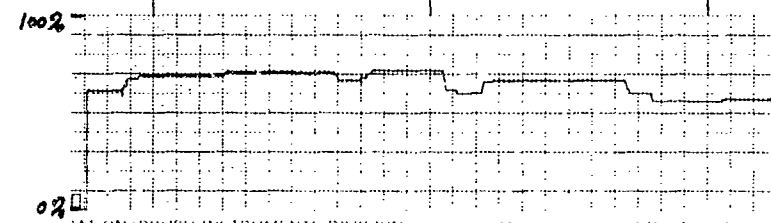
δ STICK
(% FULL TRAVEL)



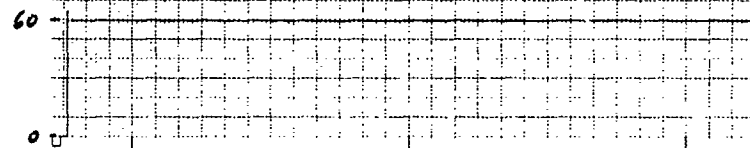
ALTITUDE
(FT. AGL)



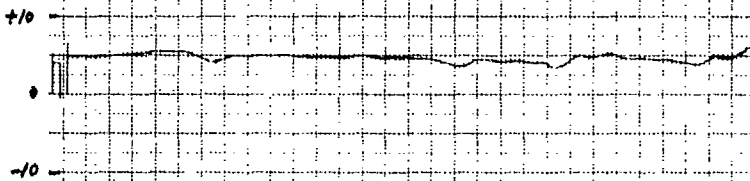
THROTTLE
(% THRUST)



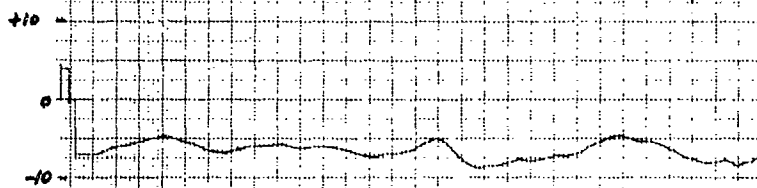
δ FLAP
(DEG)



δ
(DEG)



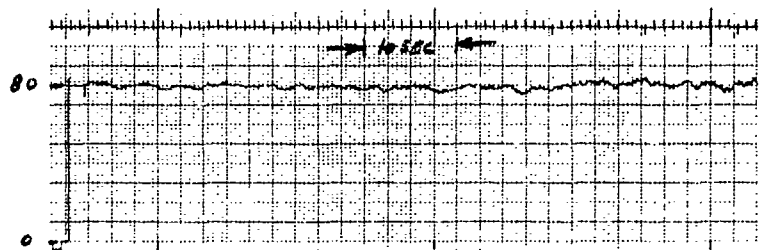
γ
(DEG)



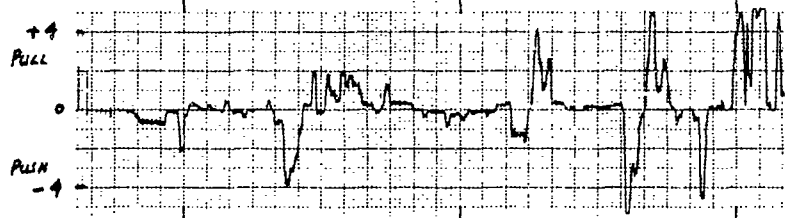
IBF/VT APPROACH. C/H 7. $\gamma = -7^\circ$ γ CONTROL BY POWER.

RUN J. TURBULENCE. PITCH AUG. ONLY.

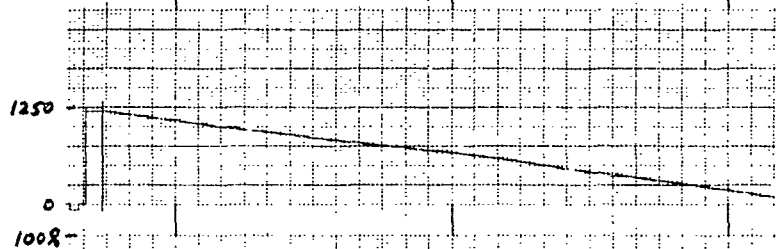
AIRSPPEED
(KTS)



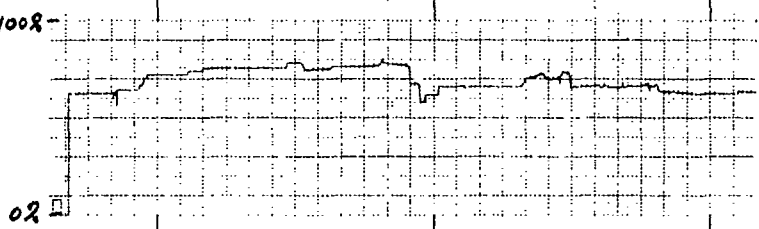
δ_{STICK}
(% FULL TRAVEL)



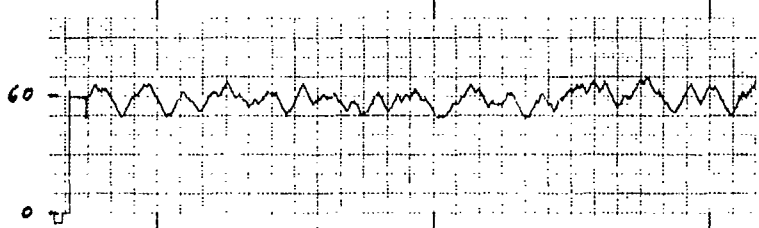
ALTITUDE
(FT. AGL)



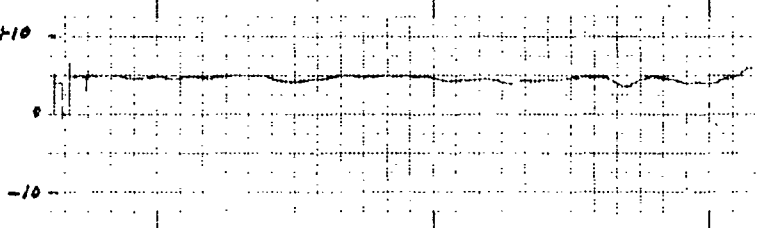
THROTTLE
(% THRUST)



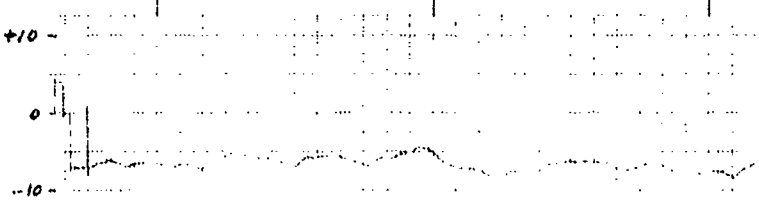
δ_{FLAP}
(DEG)



θ
(DEG)



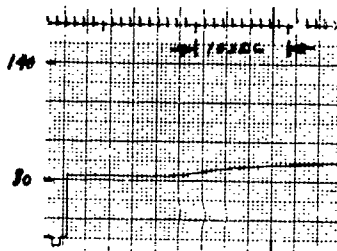
γ
(DEG)



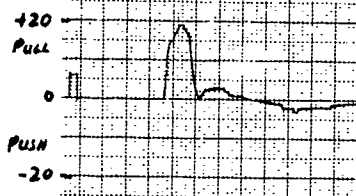
5.95 FT APPROACH $C/H = 6$ $\gamma = -7^\circ$ γ CONTROL BY POWER.

PUN K. FULL AUG. CONTROL

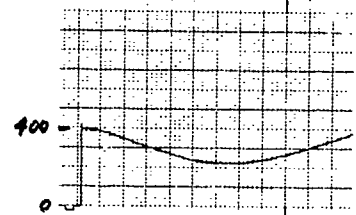
AIRSPED
(KTS)



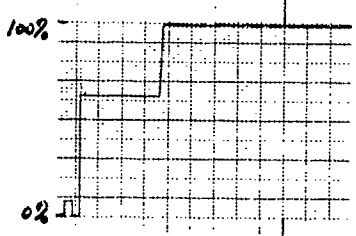
δ STICK
(% FULL TRAVEL)



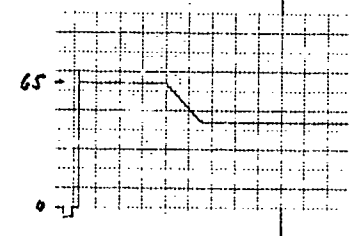
ALTITUDE
(FT. AGL)



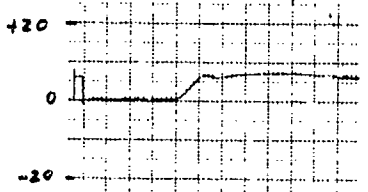
THROTTLE
(% THRUST)



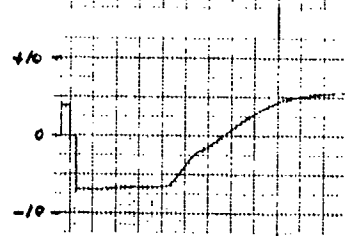
FLAPS
(DEG)



θ
(DEG)

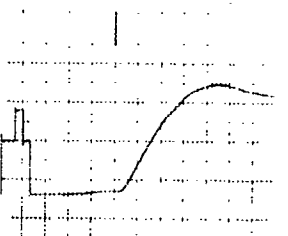
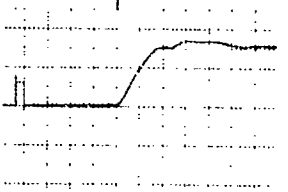
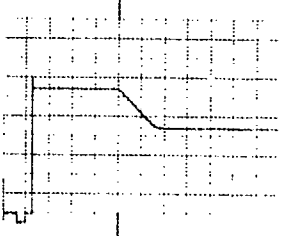
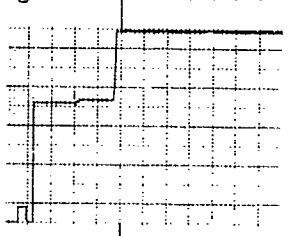
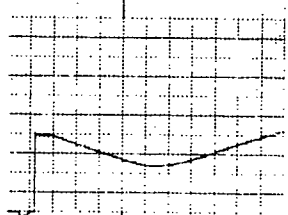
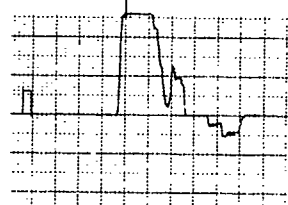
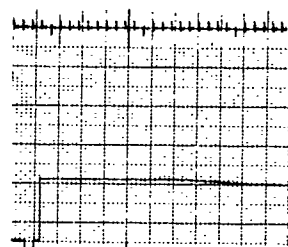


γ
(DEG)



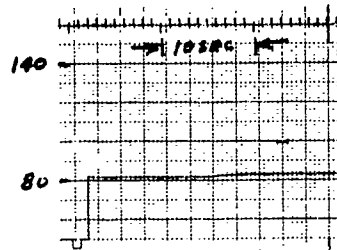
IBFNT GO-AROUND.
C/N = 3.
DECISION HEIGHT
= 300' AGL.

PITCH AND FLAPS UP.
PITCH AUG. ONLY.
FLAP RATE = 5 DEG/SEC.
RUN K.

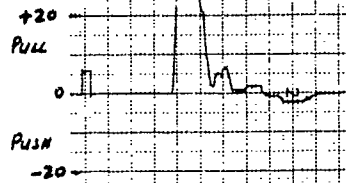


PITCH AND FLAPS UP.
PITCH AUG. ONLY.
FLAP RATE = 5 DEG/SEC.
RUN L.

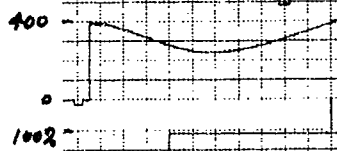
AIRSPPEED
(KTS)



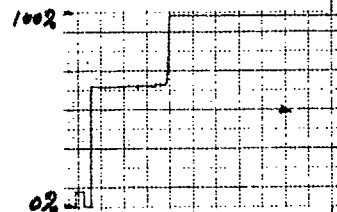
δ STICK
(% FULL TRAVEL)



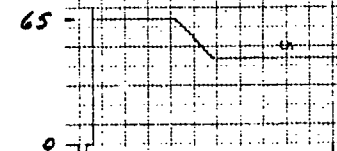
ALTITUDE
(FT AGL)



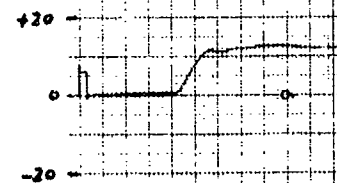
THROTTLE
(% THRUST)



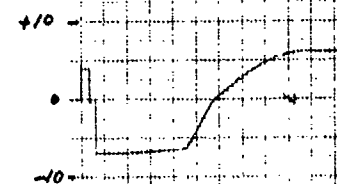
FLAPS
(DEG)



θ
(DEG)

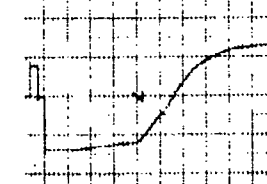
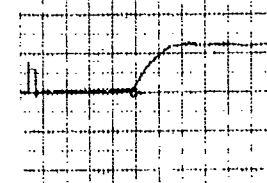
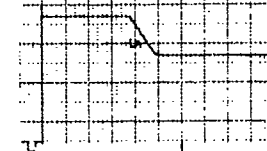
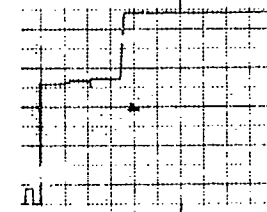
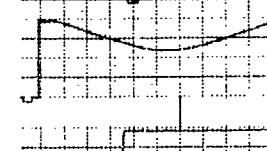
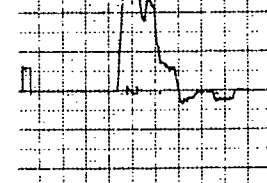
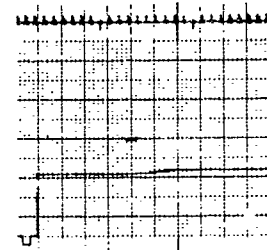


γ
(DEG)



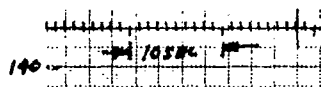
IDENT GO-AROUND.
C/H = 3.
DECISION HEIGHT
= 300' AGL.

PITCH AND FLAPS UP.
PITCH AUG. ONLY.
FLAP RATE = 5 DEG/SEC.
RUN D.

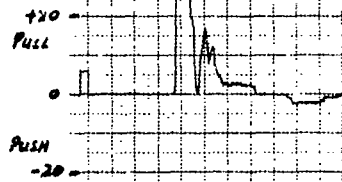


PITCH AND FLAPS UP.
PITCH AUG. ONLY.
FLAP RATE = 7 DEG/SEC
RUN H.

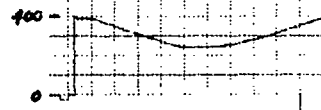
AIRSPEED
(KTS)



δ STICK
(% FULL TRAVEL)



ALTITUDE
(FT. AGL)

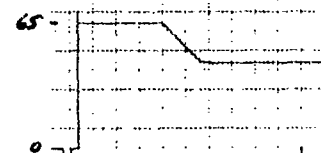


THROTTLE
(% THRUST)

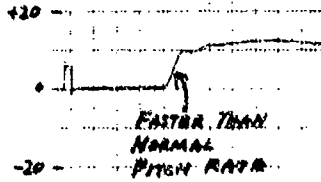


INSTRUMENTS DIVISION

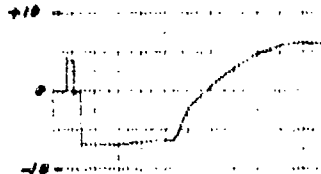
FLAPS
(DEG)



θ
(DEG)



γ
(DEG)



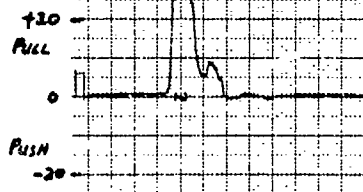
IBF/VT GO-AROUND. PITCH AND FLAPS UP.
C/H = 3. PITCH AUG. ONLY.
DECISION HEIGHT FLAP RATE = 5 DEG/SEC.
= 300' AGL. RUN F.

PITCH THEN FLAPS UP.
FULL AUG. CONTROL.
FLAP RATE = 3 DEG/SEC.
RUN M.

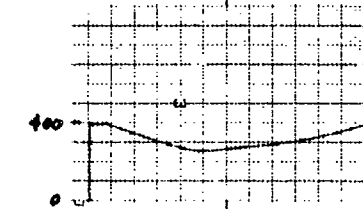
AIRSPED
(KTS)



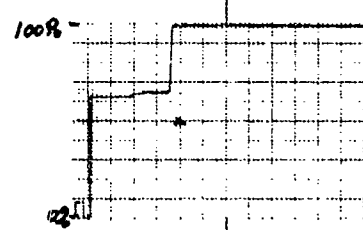
STICK
(% FULL TRAVEL)



ALTITUDE
(FT. AGL)



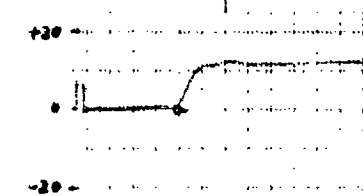
THROTTLE
(% THRUST)



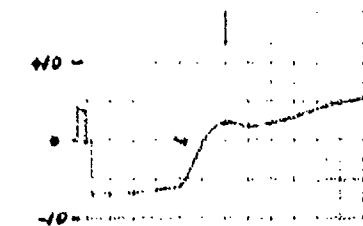
FLAPS
(DEG)



θ
(DEG)



γ
(DEG)



IBF/VT GO-AROUND
L/N = 3
DECISION HEIGHT
= 300' AGL

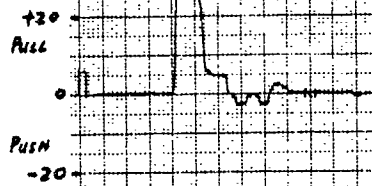
PITCH THEN FLAPS UP.
FULL AUG. CONTROL.
FLAP RATE = 50 DEG/SEC
RUN N.

PITCH THEN FLAPS UP.
FULL AUG. CONTROL.
FLAP RATE = 7 DEG/SEC.
RUN O.

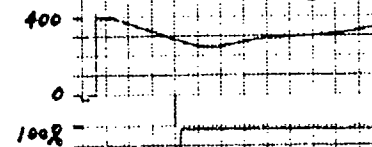
AIRSPED
(KTS)



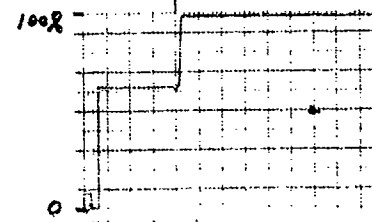
STICK
(% FULL TRAVEL)



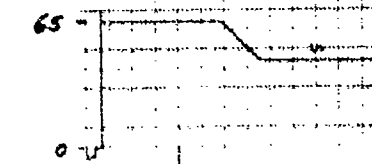
ALTITUDE
(FT. AGL)



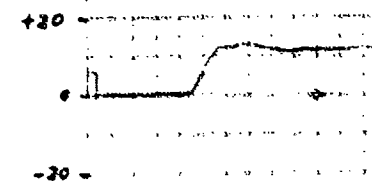
THROTTLE
(% THRUST)



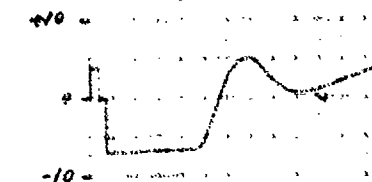
FLAPS
(DEG)



θ
(DEG)

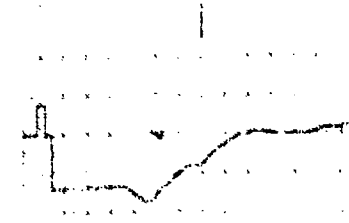
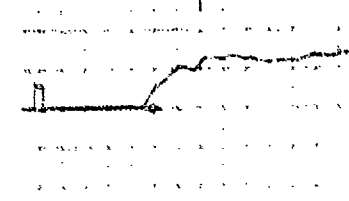
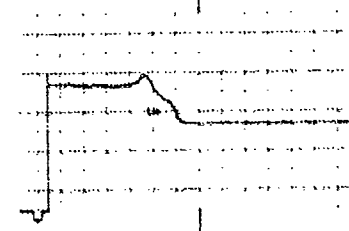
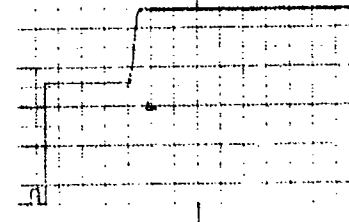
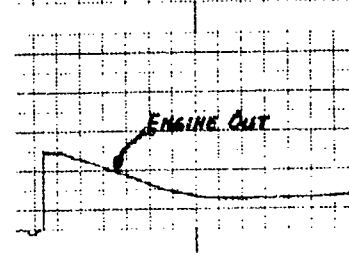
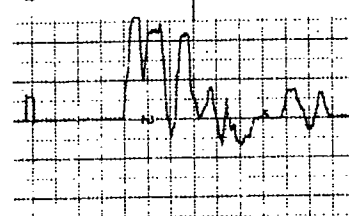
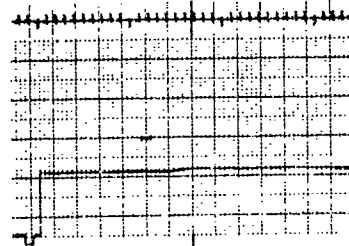


γ
(DEG)



IBF/VT GO-AROUND.
DECISION AGENT
= 300' AGL.

PITCH THEN FLAPS UP.
FULL AUG. CONTROL.
FLAP RATE = 5 DEG/SEC.
RUN P. C/H = 7

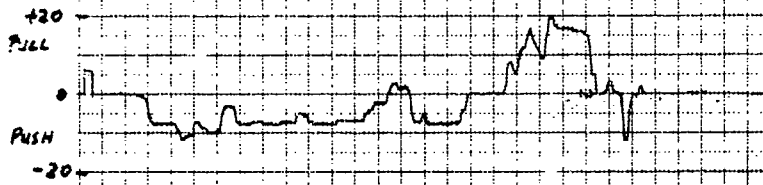


PITCH AND FLAPS UP.
FULL AUG. CONTROL
FLAP RATE = 5 DEG/SEC
RUN G C/H = 4 1/2

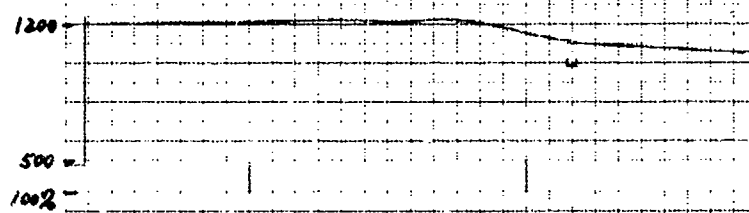
AIRSPED
(KTS)



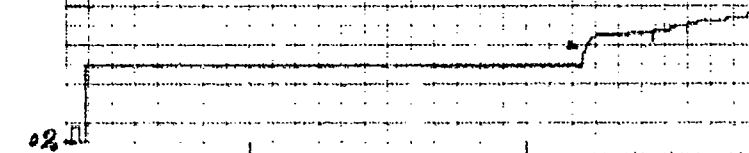
δ STICK
(% FULL TRAVEL)



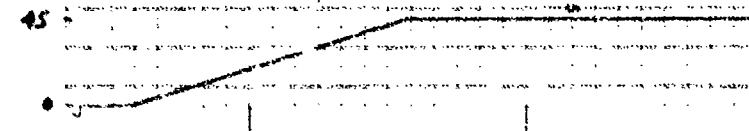
ALTITUDE
(FT. AGL)



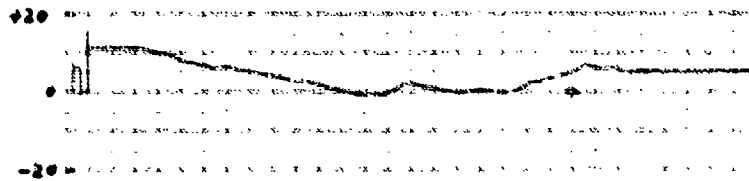
THROTTLE
(% THRUST)



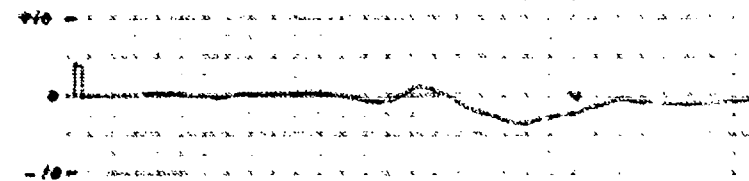
δ FLAP
(DEG)



θ
(DEG)



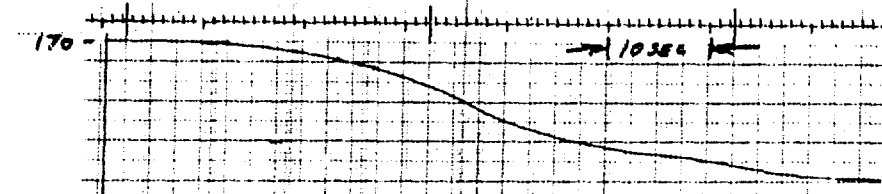
γ
(DEG)



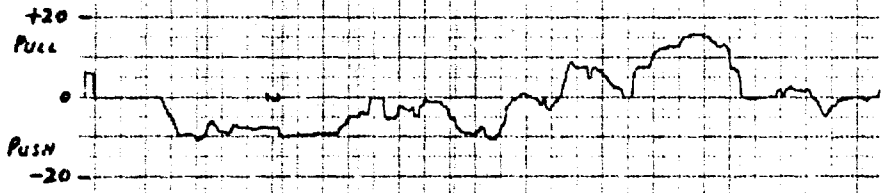
IBF/VT INITIAL TRANSITION.
FLAPS 0 TO 45 DEGREES.
FINAL AIRSPEED = 100 KTS.

FLAP RATE = 1.5 DEG/SEC.
C/H = 6
RUN B

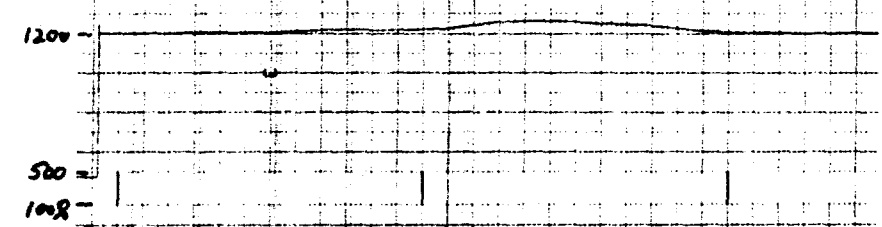
AIR SPEED
(KTS)



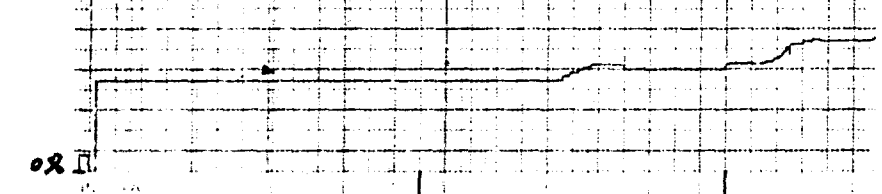
δ STICK
(% FULL TRAVEL)



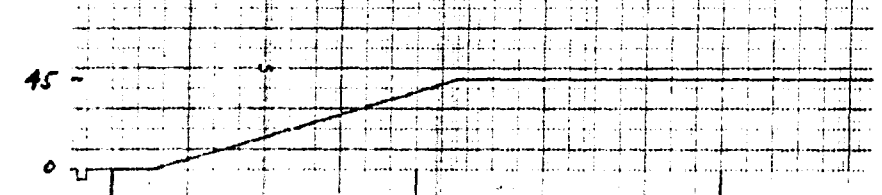
ALTITUDE
(FT AGL)



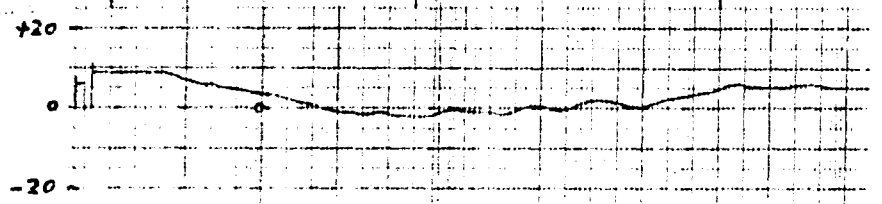
THROTTLE
(% THRUST)



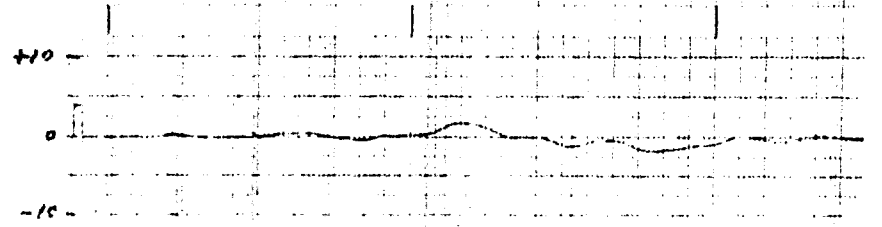
δ FLAP
(DEG)



θ
(DEG)



γ
(DEG)



IRVING ENGINE TRANSITION
FLAPS 0 TO 45 DEGREES
DURING TAKEOFF AT 100 KTS.

FLAP RATE = 45 DEG/SEC
C/M = 0
RUM <

TR. 5

AIRSPEED
(KTS)

δ STICK
(% FULL TRAVEL)

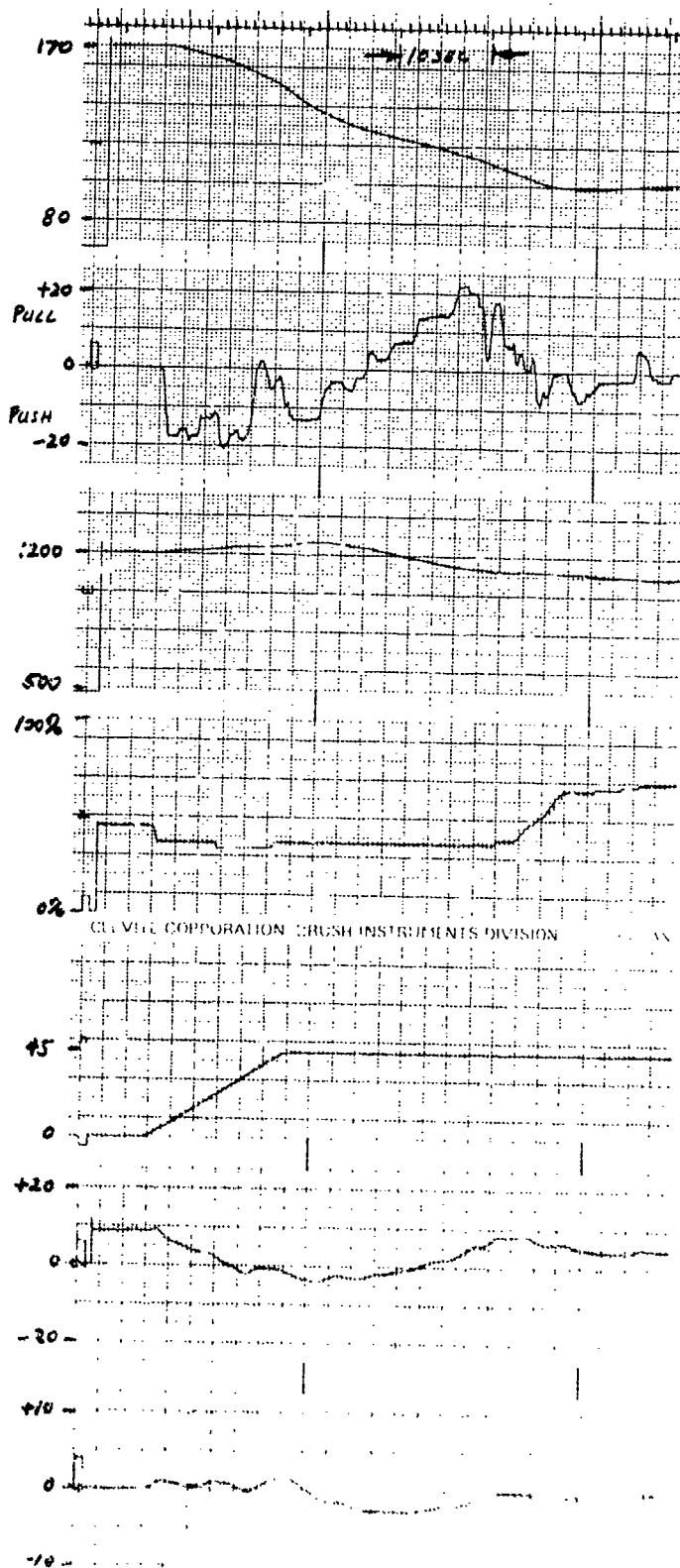
ALTITUDE
(FT. AGL)

THROTTLE
(% THRUST)

δ FLAP
(DEG)

θ
(DEG)

γ
(DEG)



IBS/NT INITIAL TRANSITION
FLAPS 0 TO 45 DEGREES.
FINAL AIRSPEED 100 KTS.

FLAP RATE: 3 DEG/SEC
C/M = 7
RUN E

AIRSPPEED
(KTS)

δ STICK
(% FULL TRAVEL)

ALTITUDE
(FT. AGL)

THROTTLE
(% THRUST)

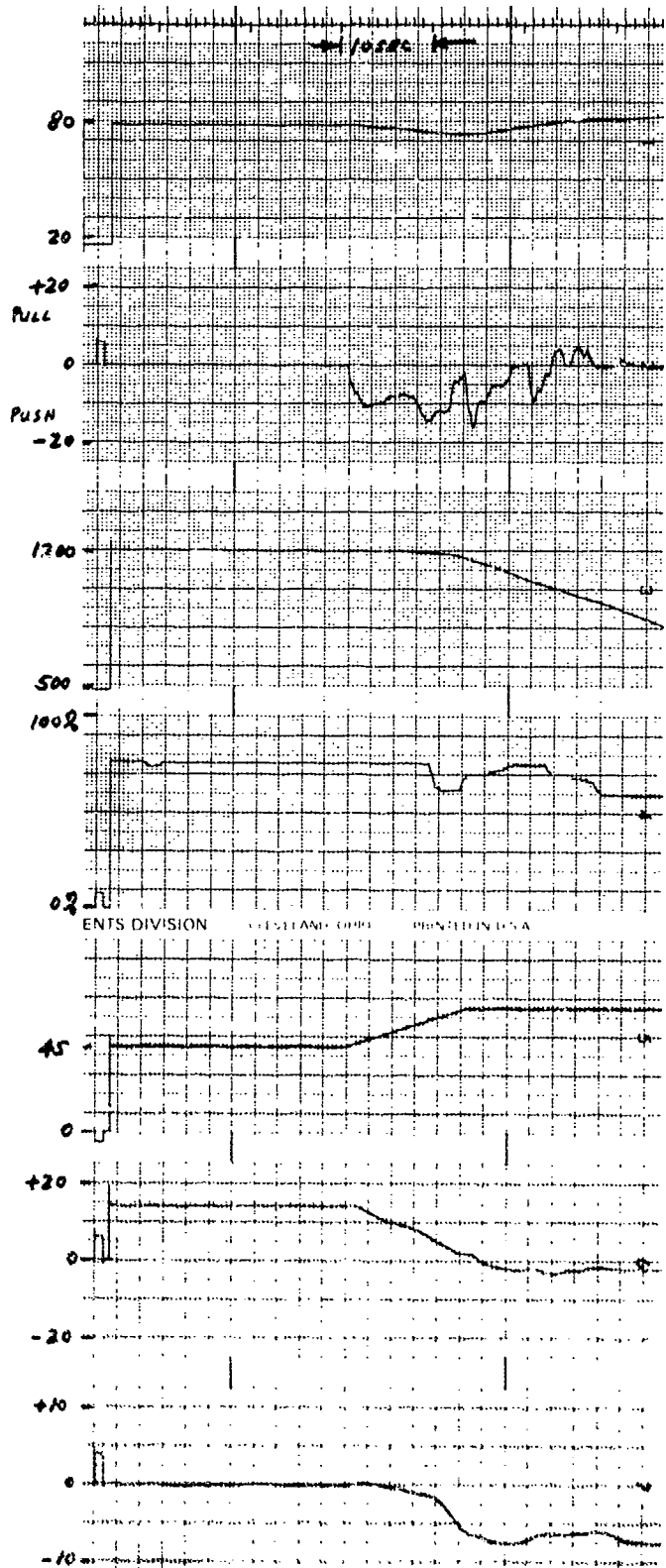
δ FLAP
(DEG)

θ
(DEG)

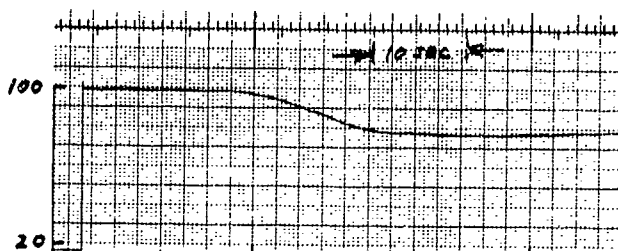
γ
(DEG)

IBF/VT FINAL TRANSITION.
FLAPS 45 TO 65 DEGREES.
FINAL AIRSPEED = 80KTS.

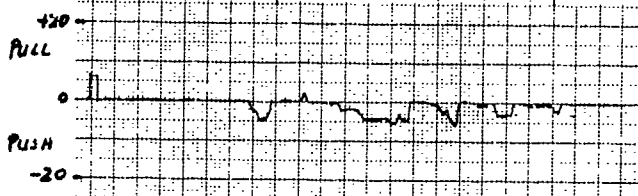
FLAP RATE = 1.5 DEG/SEC.
C/N = 5.
RUN A.



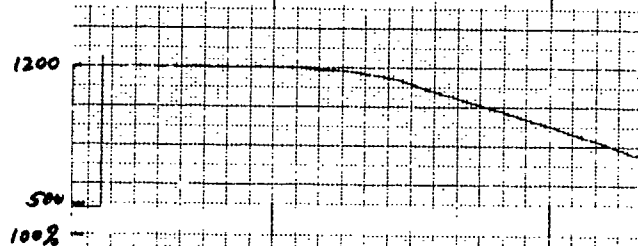
AIRSPPEED
(KTS)



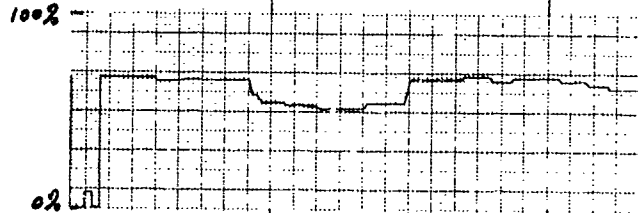
δ_{STICK}
(% FULL TRAVEL)



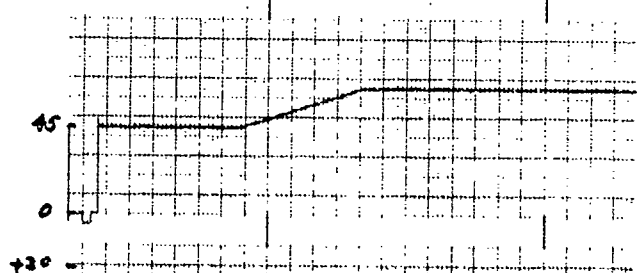
ALTITUDE
(FT. AGL)



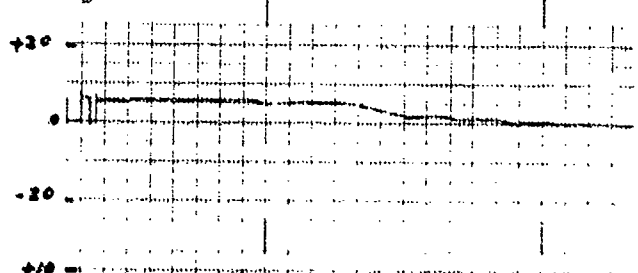
THROTTLE
(% THRUST)



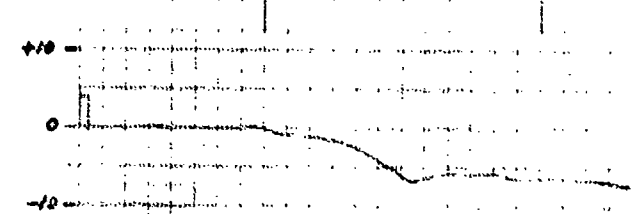
δ_{FLAP}
(DEG)



θ
(DEG)



γ
(DEG)



IBF/VT FINAL TRANSITION
FLAP: 45 TO 65 DEGREES.
FINAL AIRSPEED = 80 KTS

FLAP RATE = 1.5 DEG/SEC.
C/N = 4
RUN C

AIRSPPEED
(KTS)

δ_{STICK}
(% FULL TRAVEL)

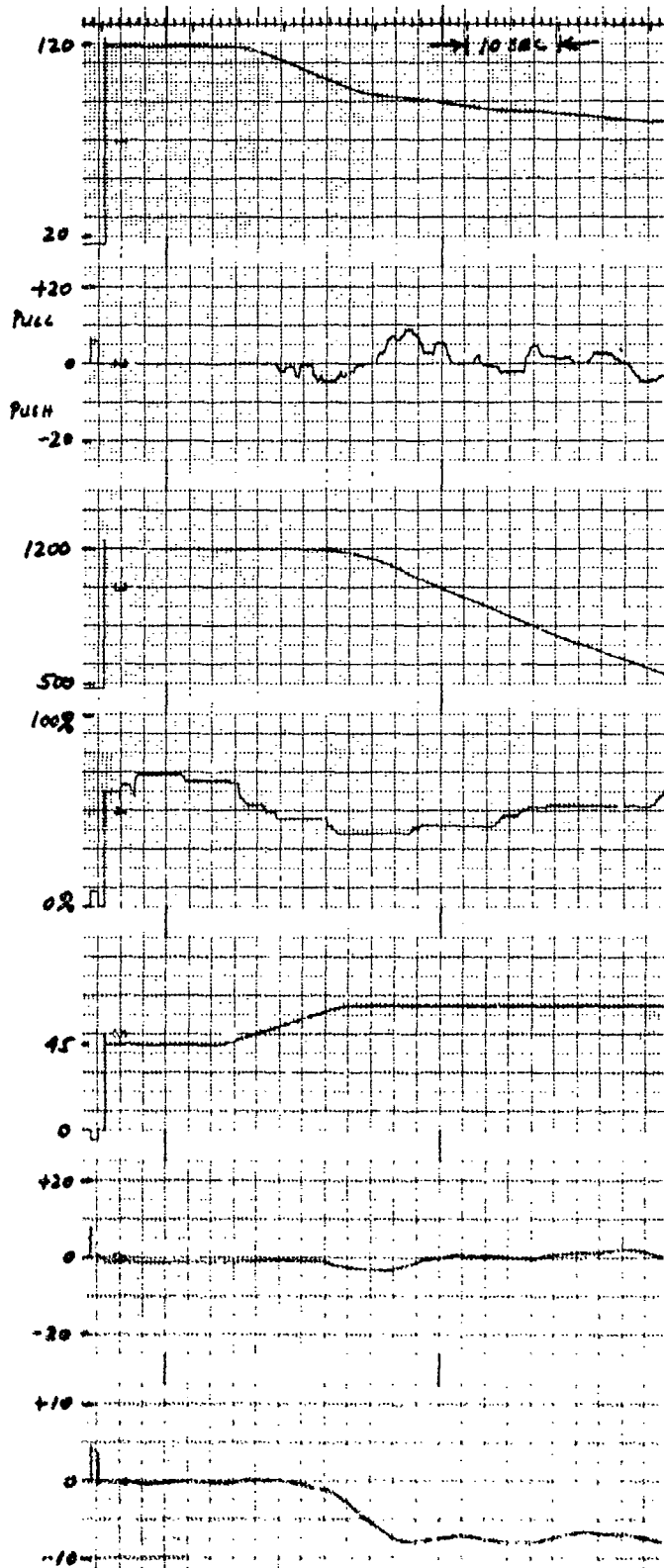
ALTITUDE
(FT. AGL)

THROTTLE
(% THRUST)

δ_{FLAP}
(DEG)

θ
(DEG)

γ
(DEG)



IBF/T FINAL TRANSITION.
FLAPS 45 TO 65 DEGREES.
FINAL AIRSPEED = 80 KTS.

FLAP RATE = 1.5 DEG/SEC.
C/H = 6.
RUN E

AIR SPEED
(KTS)

δ STICK
(% FULL TRAVEL)

ALTITUDE
(FT. AGL)

THROTTLE
(% THRUST)

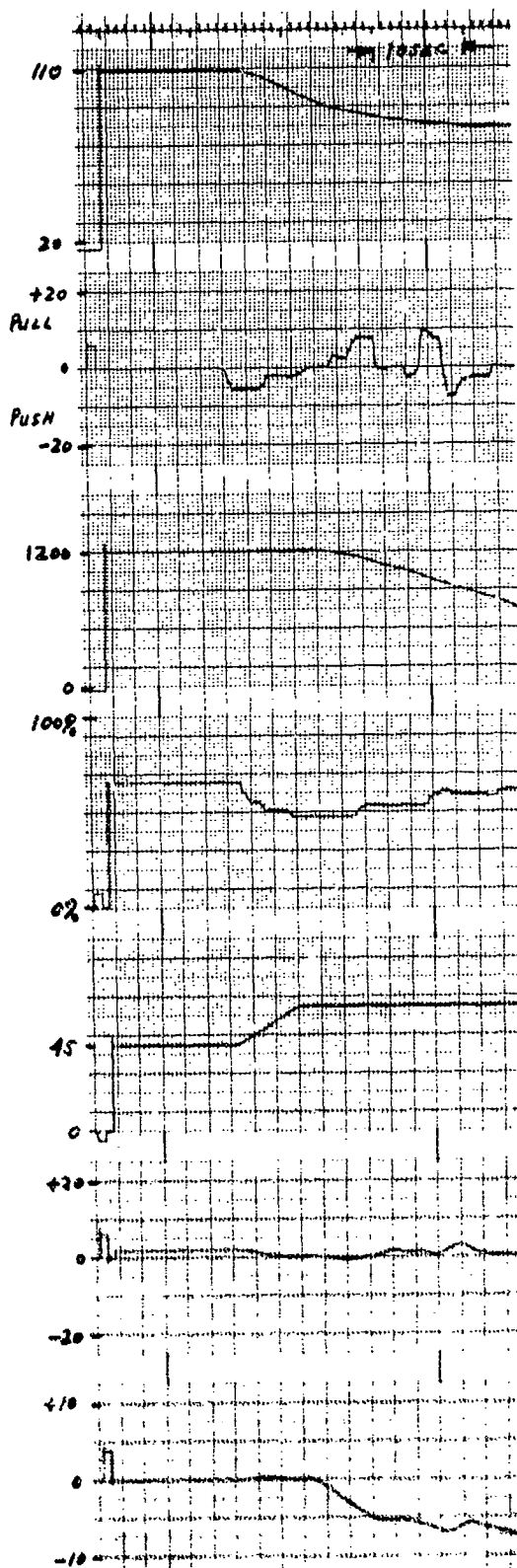
δ FLAP
(DEG)

θ
(DEG)

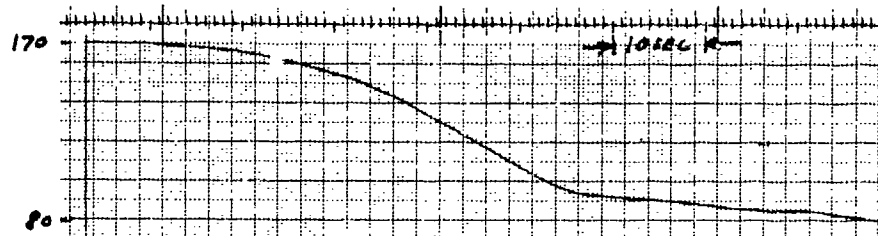
γ
(DEG)

IBF/V7 FINAL TRANSITION.
FLAPS 45 TO 65 DEGREES.
FINAL AIRSPEED = 80 KTS.

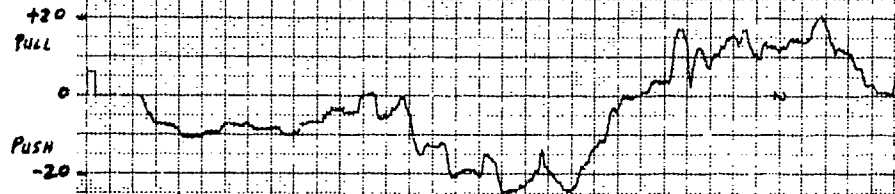
FLAP RATE = 3 DEG/SEC.
C/H = 6.
RUN 6.



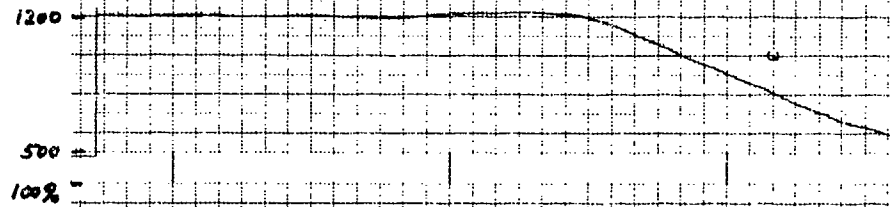
AIR SPEED
(KTS)



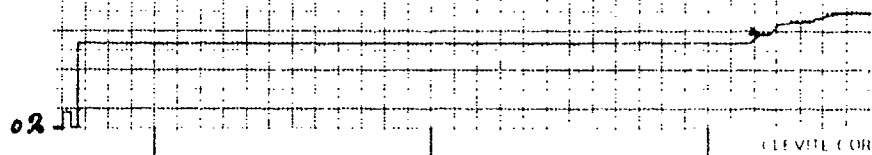
δ_{STICK}
(% FULL TRAVEL)



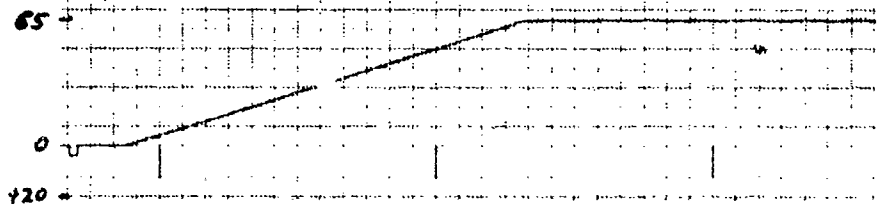
ALTITUDE
(FT. AGL)



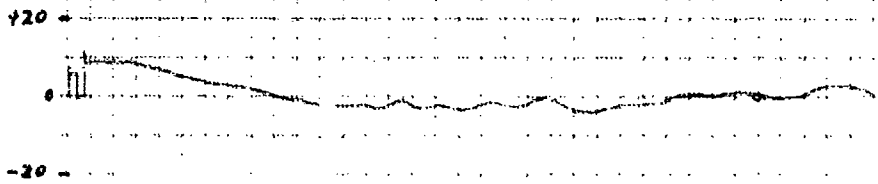
THROTTLE
(% THRUST)



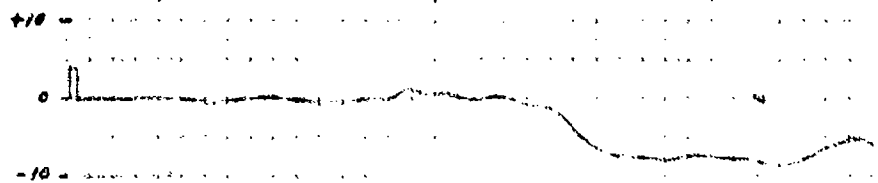
δ_{FLAP}
(DEG)



θ
(DEG)



γ
(DEG)



IBF TOTAL TRANSITION.
FLAPS 0 TO 65 DEGREES
FINAL AIRSPEED = 80 KTS.

FLAP RATE = 1.5 DEG/SEC.
C/N = 8 1/2.
RUN B.

VECTORED THRUST

(VT)

AIRSPEED
(KTS)

δ_{STICK}
(% FULL TRAVEL)

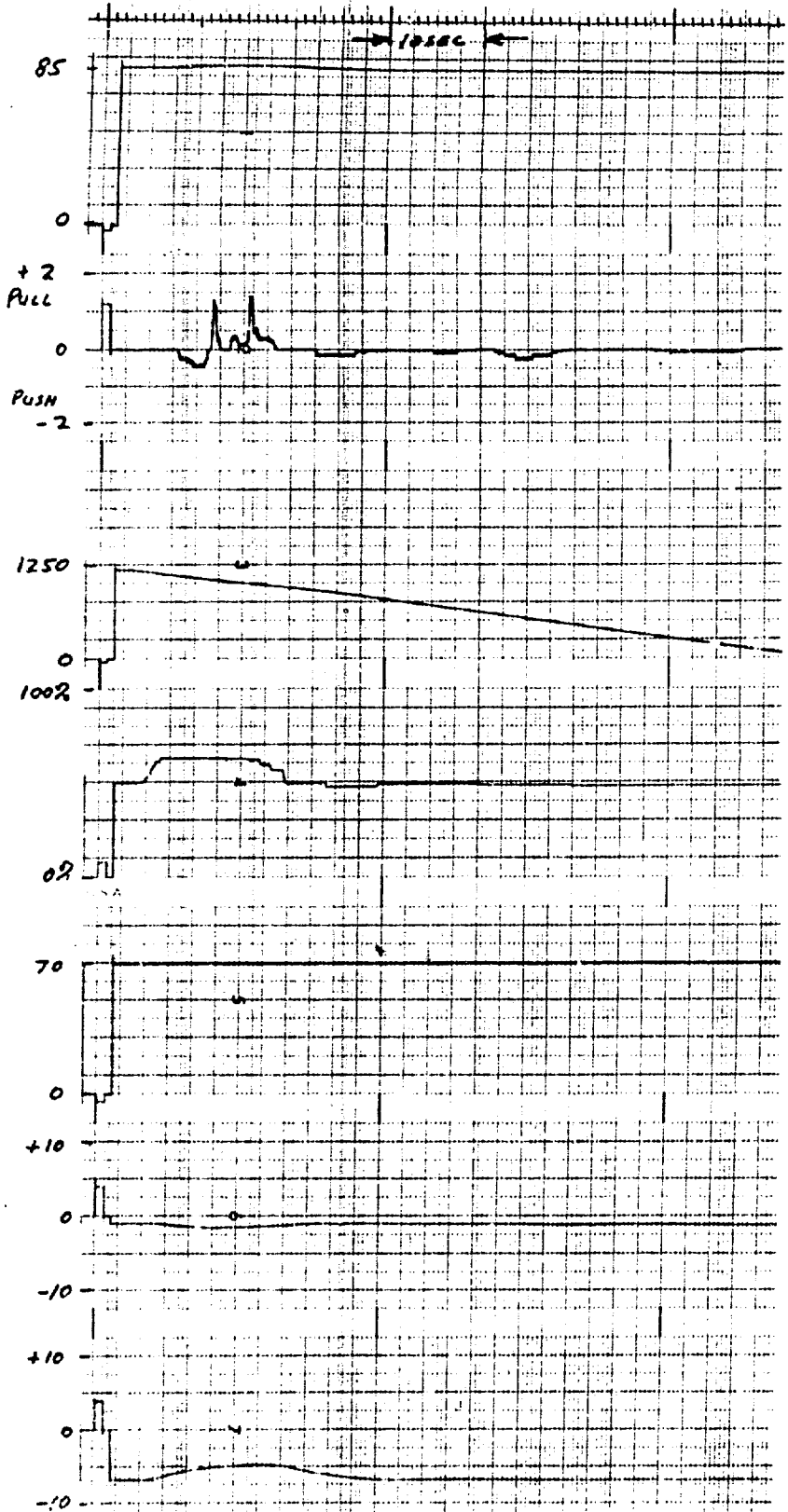
ALTITUDE
(FT AGL)

THROTTLE
(% THRUST)

δ_{FLAP}
(DEG)

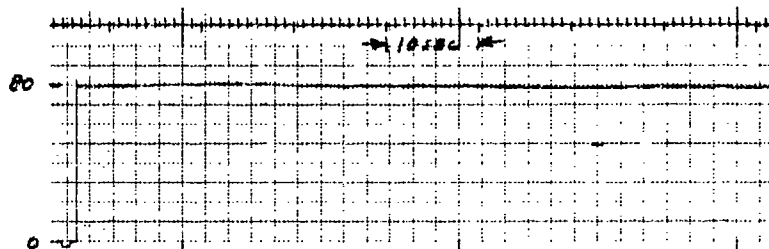
θ
(DEG)

γ
(DEG)

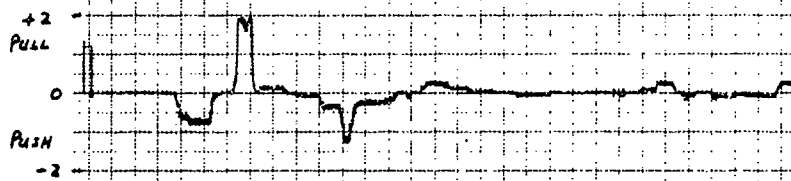


VT APPROACH $C/H = 2\frac{1}{2}$ $\gamma = -7^\circ$ γ CONTROL BY POWER.
RUN A PITCH AUG. ONLY.

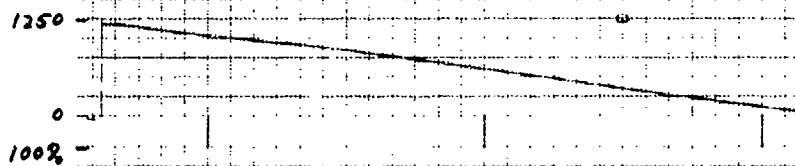
AIRSPPEED
(KTS)



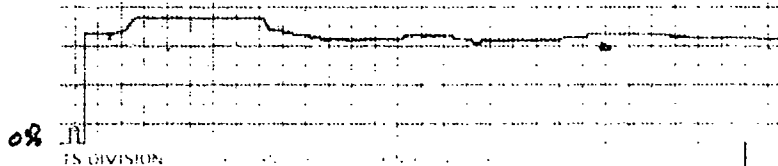
δ STICK
(% FULL TRAVEL)



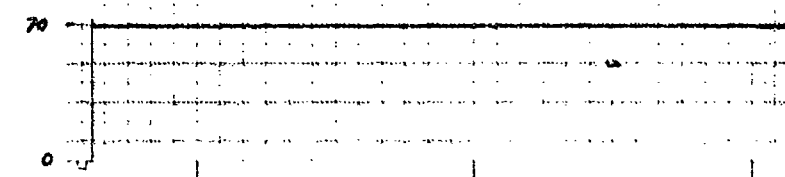
ALTITUDE
(FT. AGL)



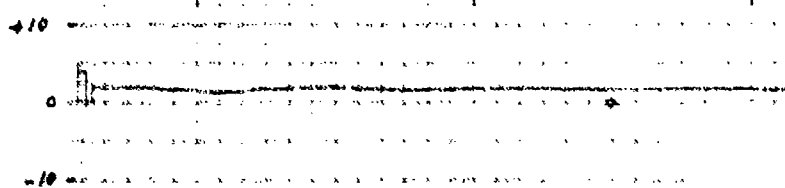
THROTTLE
(% THRUST)



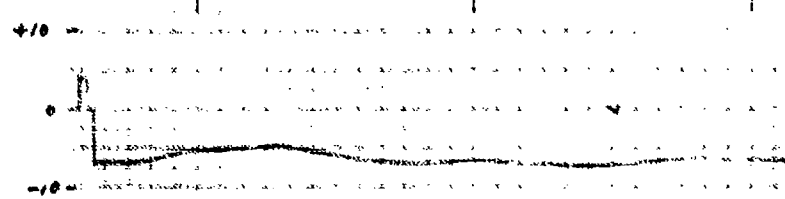
δ FLAP
(DEG)



θ
(DEG)



γ
(DEG)



VT APPROACH. $C/N = 3$. $\gamma = -7^\circ$ γ CONTROL BY POWER.
RUN D. PITCH AUG. ONLY.

AIRSPPEED
(KTS)

δ STICK
(% FULL TRAVEL)

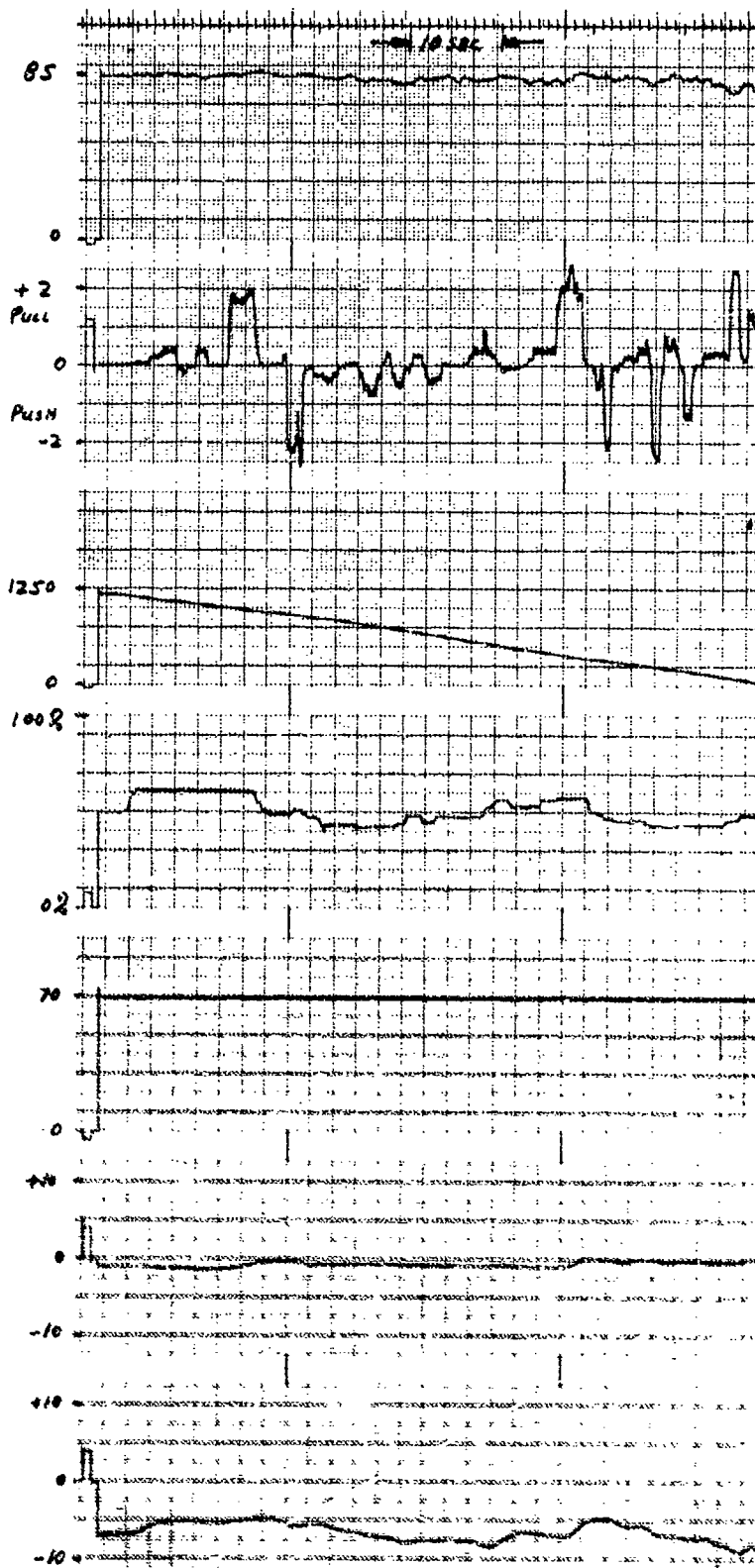
ALTITUDE
(FT. AGL)

THROTTLE
(% THRUST)

δ FLAP
(DEG)

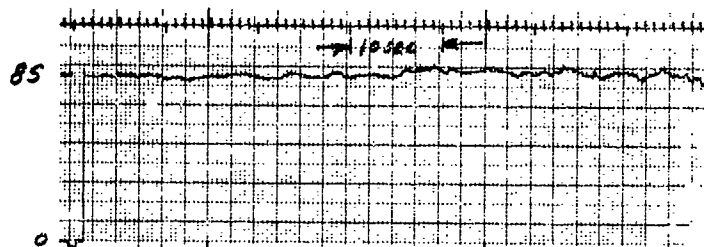
θ
(DEG)

γ
(DEG)



VT APPROACH C/H = 6. $\gamma = -7^\circ$ γ CONTROL BY POWER.
RUN F. GUST MODEL. PITCH AUG. ONLY

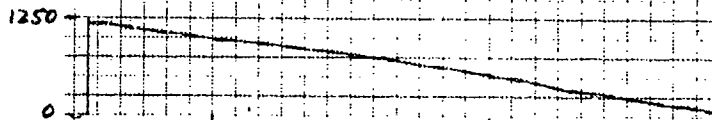
AIRSPED
(KTS)



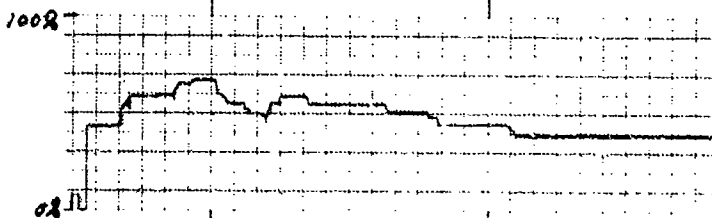
δ STICK
(% FULL TRAVEL)



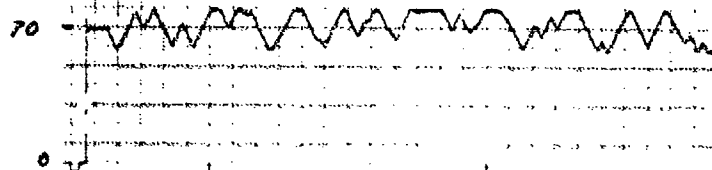
ALTITUDE
(FT. AGL)



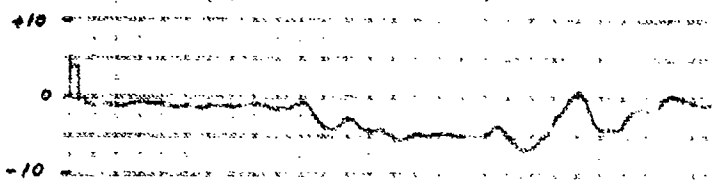
THROTTLE
(% THRUST)



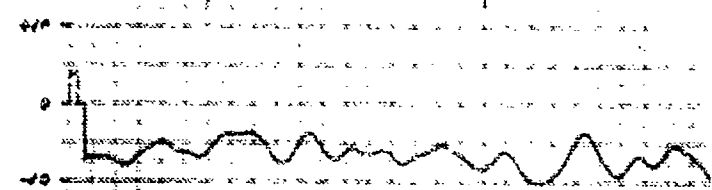
δ FLAP
(DEG)



θ
(DEG)

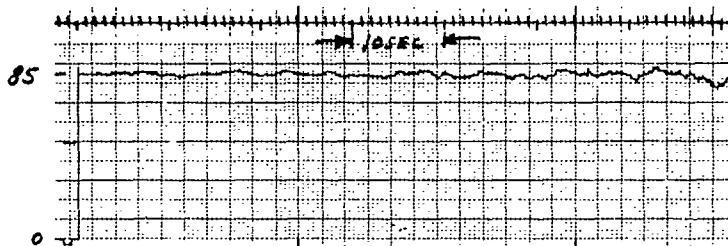


γ
(DEG)



VT APPROACH. $C/H = 9$. $\delta = -7^\circ$. δ CONTROL BY MITCH.
RUN H. GUST MODEL. FULL AUG. CONTROL.

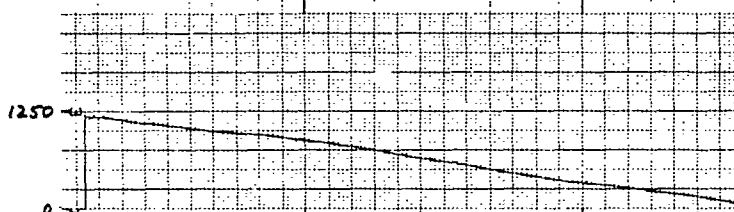
AIRSPEED
(KTS)



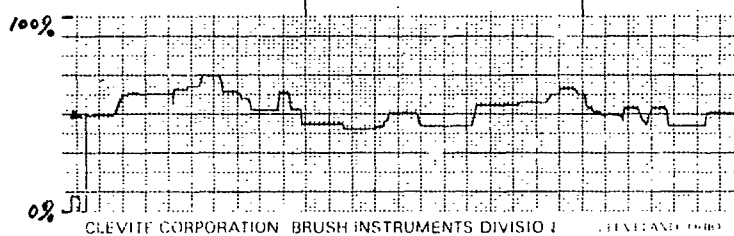
δ STICK
(% FULL TRAVEL)



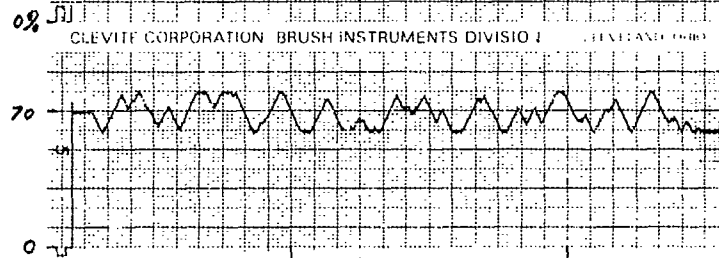
ALTITUDE
(FT. AGL)



THROTTLE
(% THRUST)



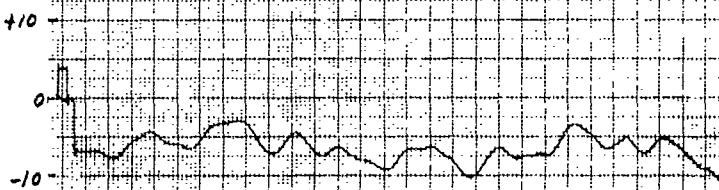
δ FLAP
(DEG)



θ
(DEG)

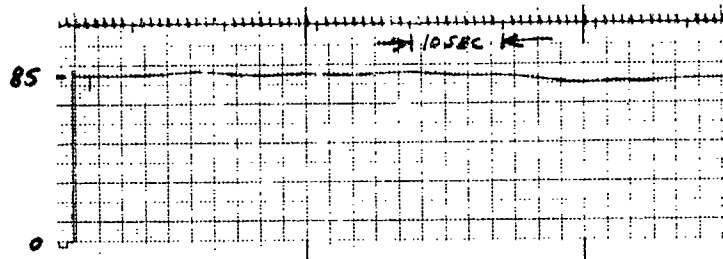


γ
(DEG)

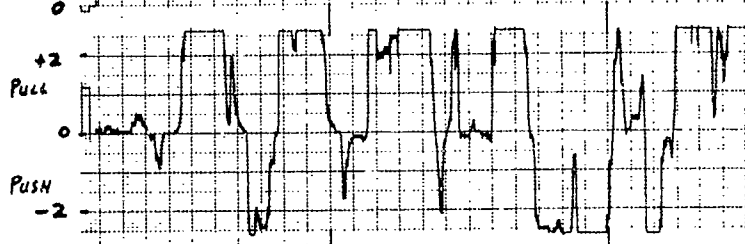


VT APPROACH. $C/H = 8$. $\gamma = -7^\circ$. γ CONTROL BY POWER
RUN I. GUST MODEL. FULL AUG. CONTROL.

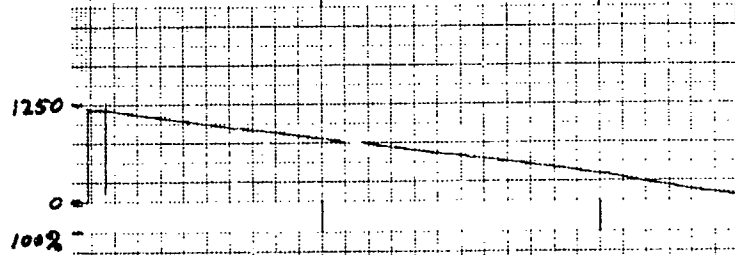
AIRSPEED



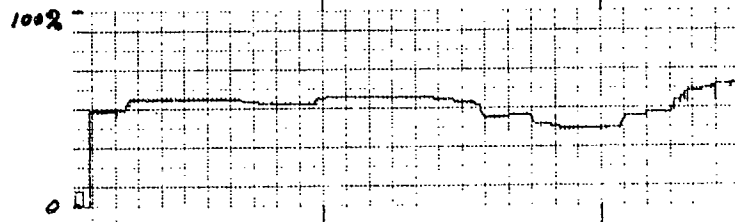
δ_{STICK}
(% FULL TRAVEL)



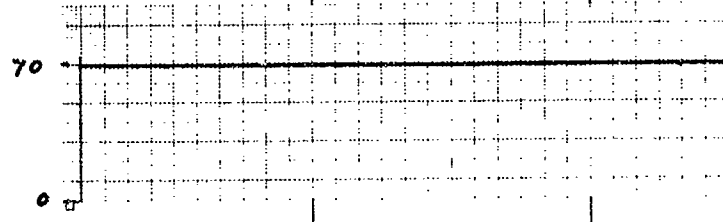
ALTITUDE
(FT. AGL)



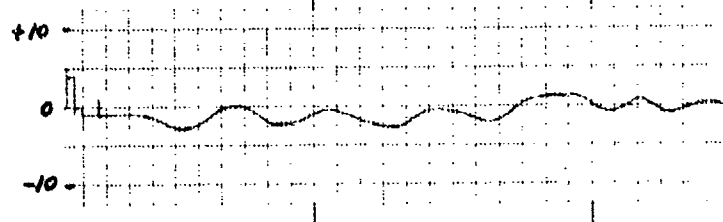
PROTYLE
(% THRUST)



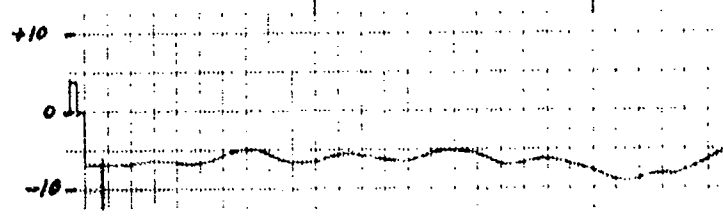
δ_{FLAP}
(DEG)



θ
(DEG)

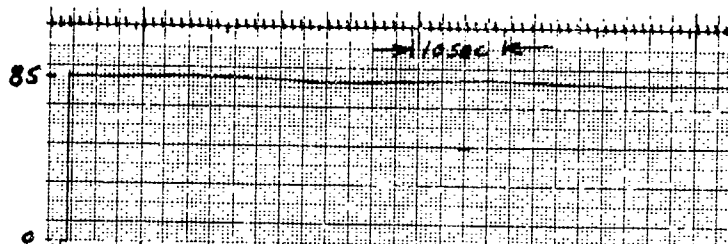


γ
(DEG)

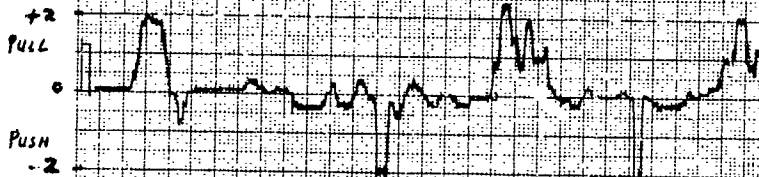


VT APPROACH. $C/H = 9\frac{1}{2}$. $\gamma = -7^\circ$. γ CONTROL BY POWER.
RUN J. BARE AIRFRAME.

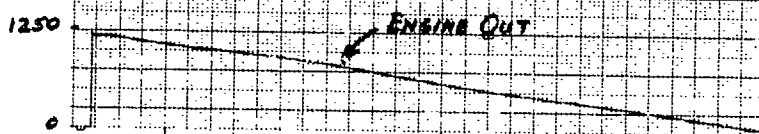
AIRSPPEED
(KTS)



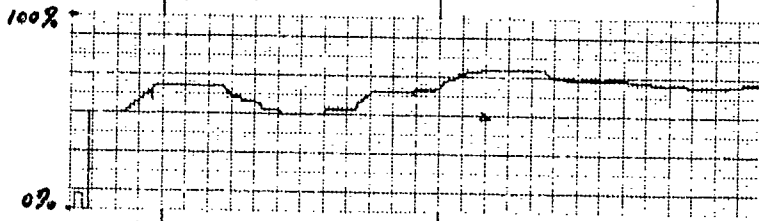
δ STICK
(% FULL TRAVEL)



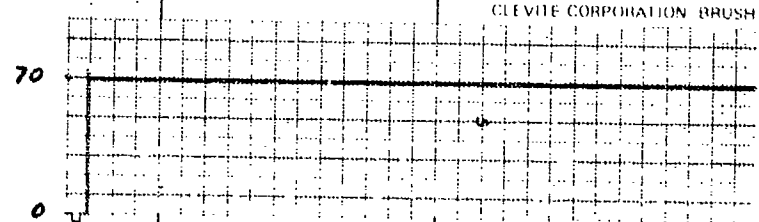
ALTITUDE
(FT. AGL)



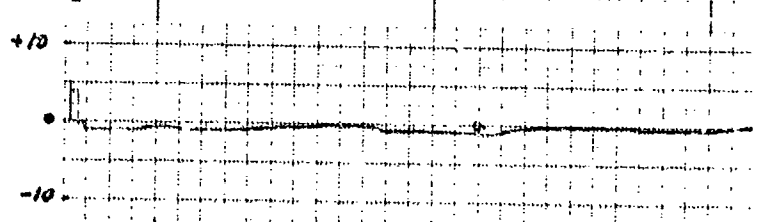
THROTTLE
(% THRUST)



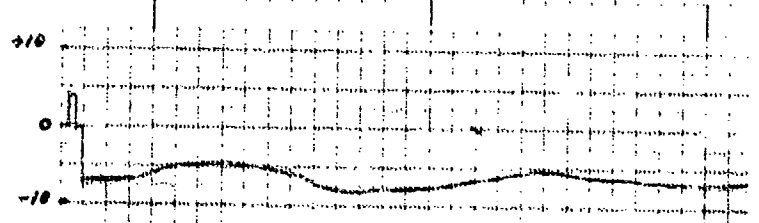
δ FLAP
(DEG)



θ
(DEG)

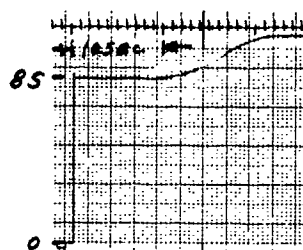


γ
(DEG)

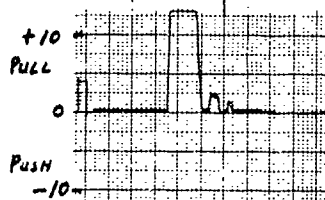


VI APPROACH. C/N = 5. $\gamma = -7^\circ$. γ CONTROL BY POWER.
RUN K. ENGINE OUT. PITCH AUG. ONLY.

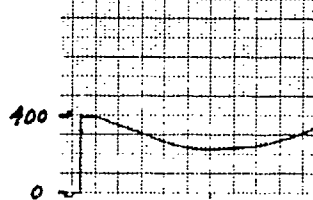
AIRSPEED
(KTS)



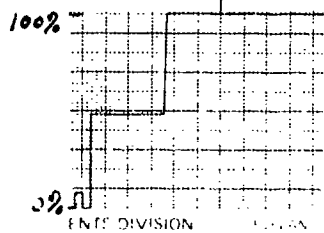
δ STICK
(% FULL TRAVEL)



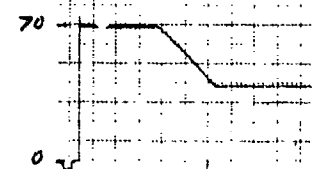
ALTITUDE
(FT. AGL)



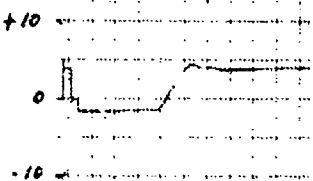
THROTTLE
(% THRUST)



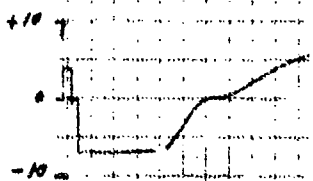
FLAPS
(DEG)



θ
(DEG)

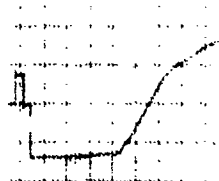
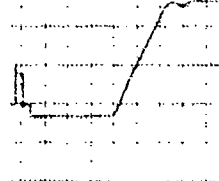
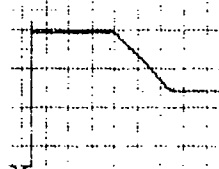
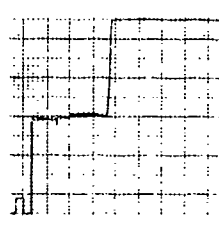
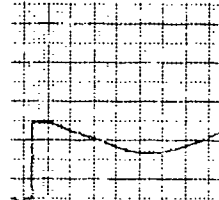
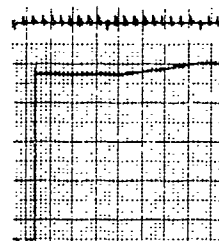


γ
(DEG)



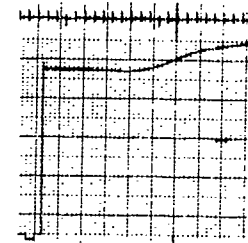
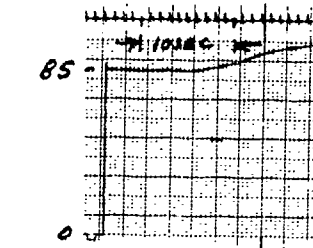
VT GO-AROUND.
C/N = 3.
DECLINATION HEIGHT
= 300' AGL.

PITCH AND FLAPS UP.
PITCH AUG. ONLY.
FLAP RATE = 5 DEG/SEC.
RUN D.

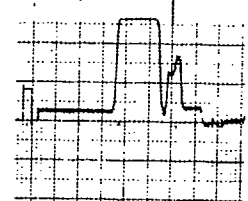
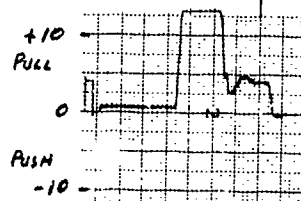


PITCH AND FLAPS UP.
PITCH AUG ONLY.
FLAP RATE = 5 DEG/SEC.
RUN E.

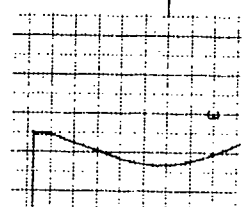
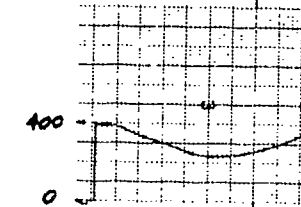
AIRSPEED
(KTS)



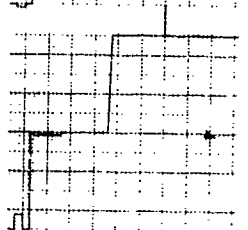
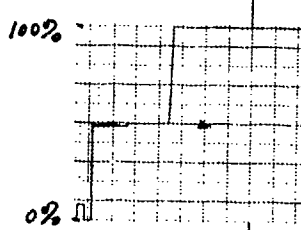
STICK
(% FULL TRAVEL)



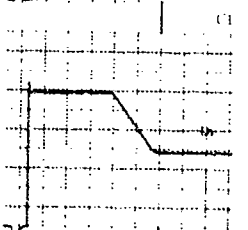
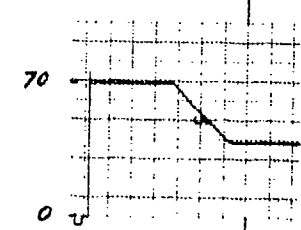
ALTITUDE
(FT. AGL)



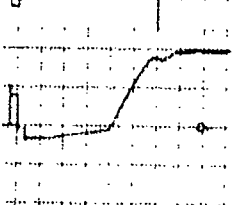
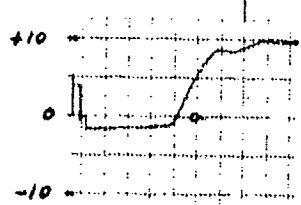
THROTTLE
(% THRUST)



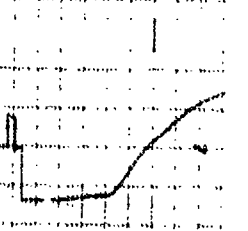
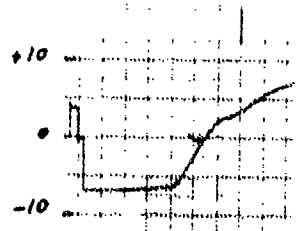
FLAPS
(DEG)



θ
(DEG)



γ
(DEG)



VT GO-AROUND.
C/N = 3.
DECISION HEIGHT
= 300' AGL.

PITCH AND FLAPS UP.
PITCH AUG ONLY.
FLAP RATE = 5 DEG/SEC.
RUN F.

PITCH AND FLAPS UP.
PITCH AUG. ONLY.
FLAP RATE = 7 DEG/SEC.
RUN H.

AIRSPPEED
(KTS)

STICK
(% FULL TRAVEL)

ALTITUDE
(FT. AGL)

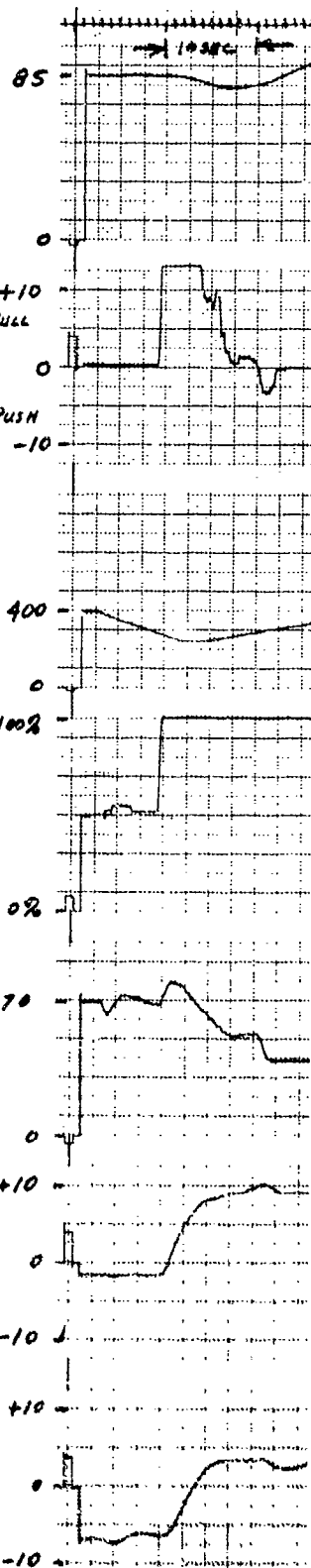
THROTTLE
(% THRUST)

FLAPS
(DEG)

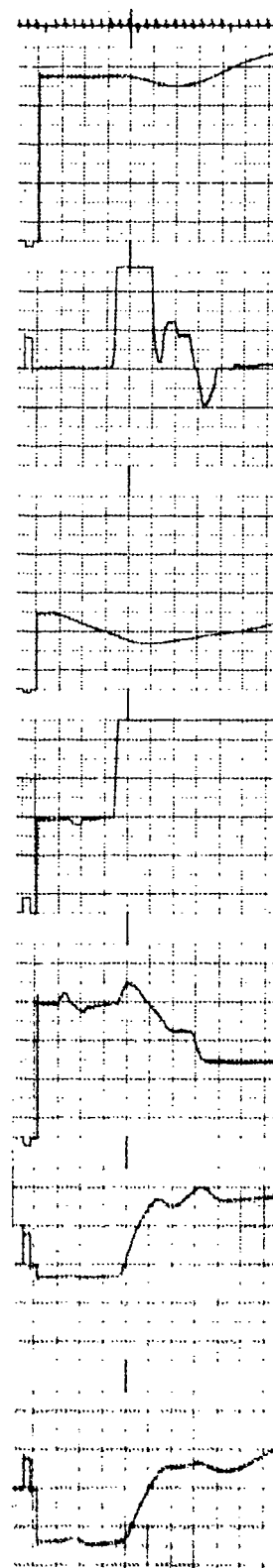
θ
(DEG)

γ
(DEG)

VT GO-AROUND.
C/N = 3.
DECISION HEIGHT
= 300' AGL.

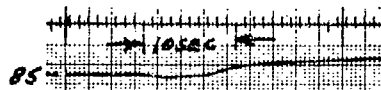


PITCH THEN FLAPS UP.
FULL AUG. CONTROL.
FLAP RATE = 5 DEG/SEC.
RUN K.



PITCH THEN FLAPS UP.
FULL AUG. CONTROL.
FLAP RATE = 7 DEG/SEC.
RUN L.

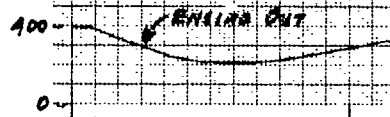
AIRSPPEED
(KTS)



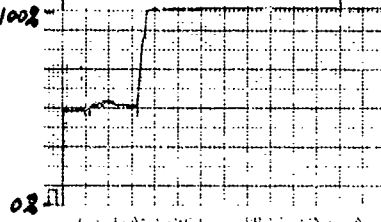
STICK
(% FULL TRAVEL)



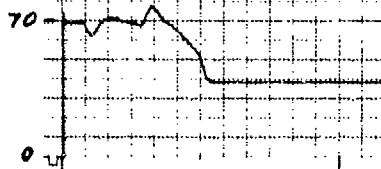
ALTITUDE
(FT. AGL)



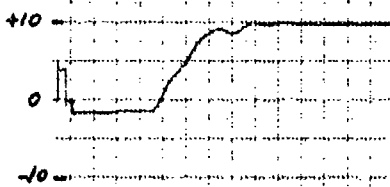
THROTTLE
(% THRUST)



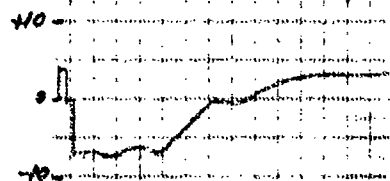
FLAPS
(DEG)



θ
(DEG)

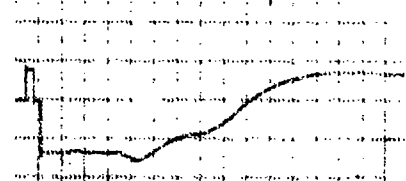
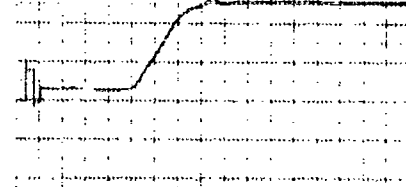
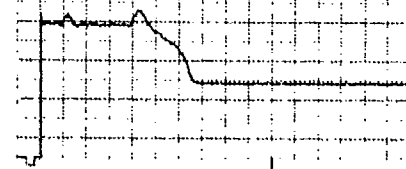
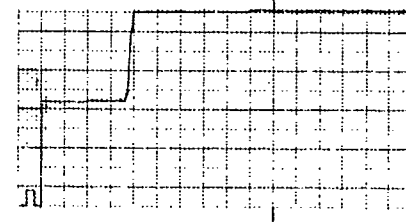
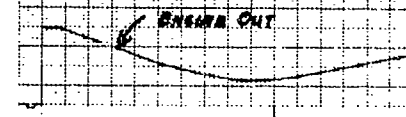
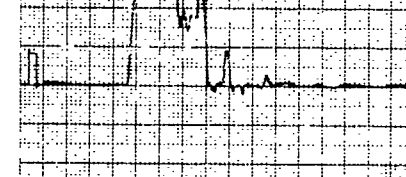
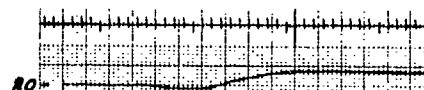


γ
(DEG)



VT GO-AROUND.
L/H = 3.
DECISION HEIGHT
= 301 AGL

PITCH AND FLAPS UP.
FULL AUG. CONTROL.
FLAP RATE = 5 DEG/SEC.
RUN M. ENGINE OUT.



PITCH AND FLAPS UP.
FULL AUG. CONTROL.
FLAP RATE = 5 DEG/SEC.
RUN N. ENGINE OUT.

AIRSPPEED
(KTS)

δ STICK
(% FULL TRAVEL)

ALTITUDE
(FT. AGL)

THROTTLE
(% THRUST)

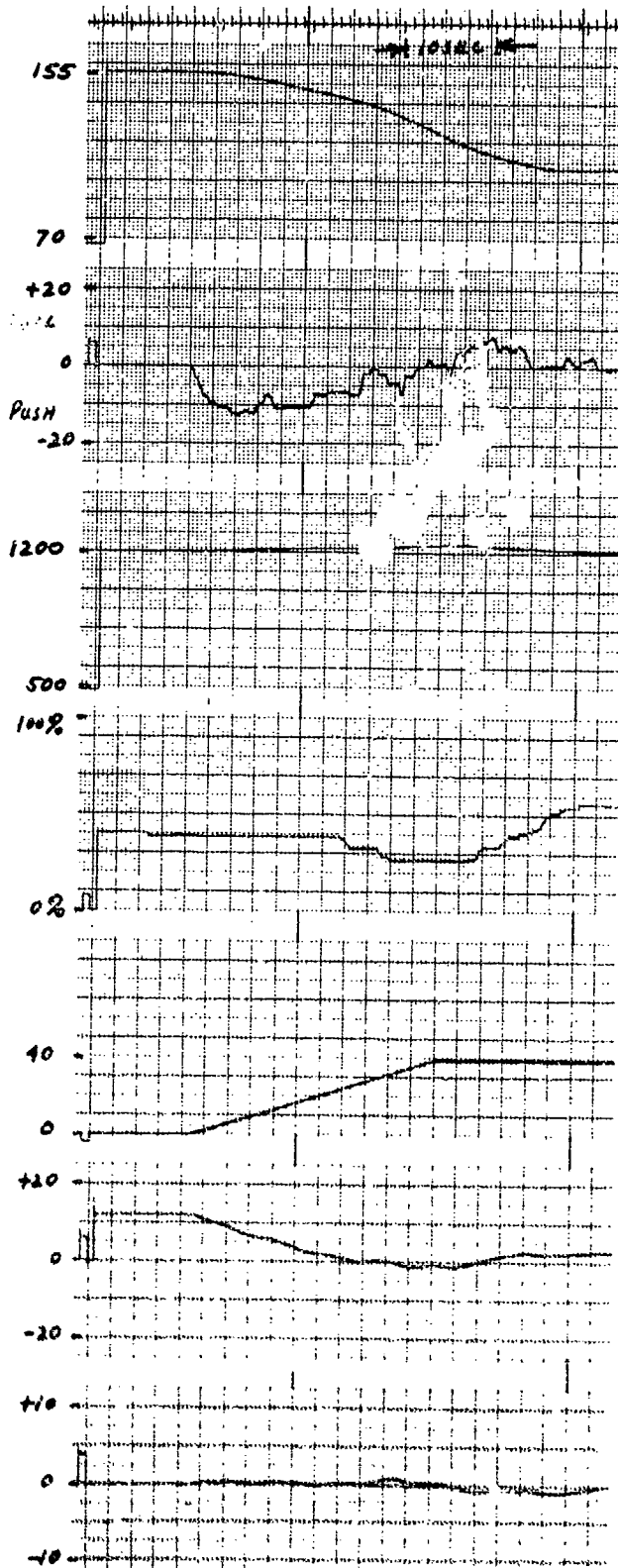
δ FLAP
(DEG)

θ
(DEG)

γ
(DEG)

VT INITIAL TRANSITION.
FLAPS 0 TO 40 DEGREES.
FINAL AIRSPEED = 105 KTS.

FLAP RATE = 1.5 DEG/SEC.
C/N = 4 1/2.
RUN B.



AIRSPPEED
(KTS)

δ_{STICK}
(% FULL TRAVEL)

ALTITUDE
(FT. AGL)

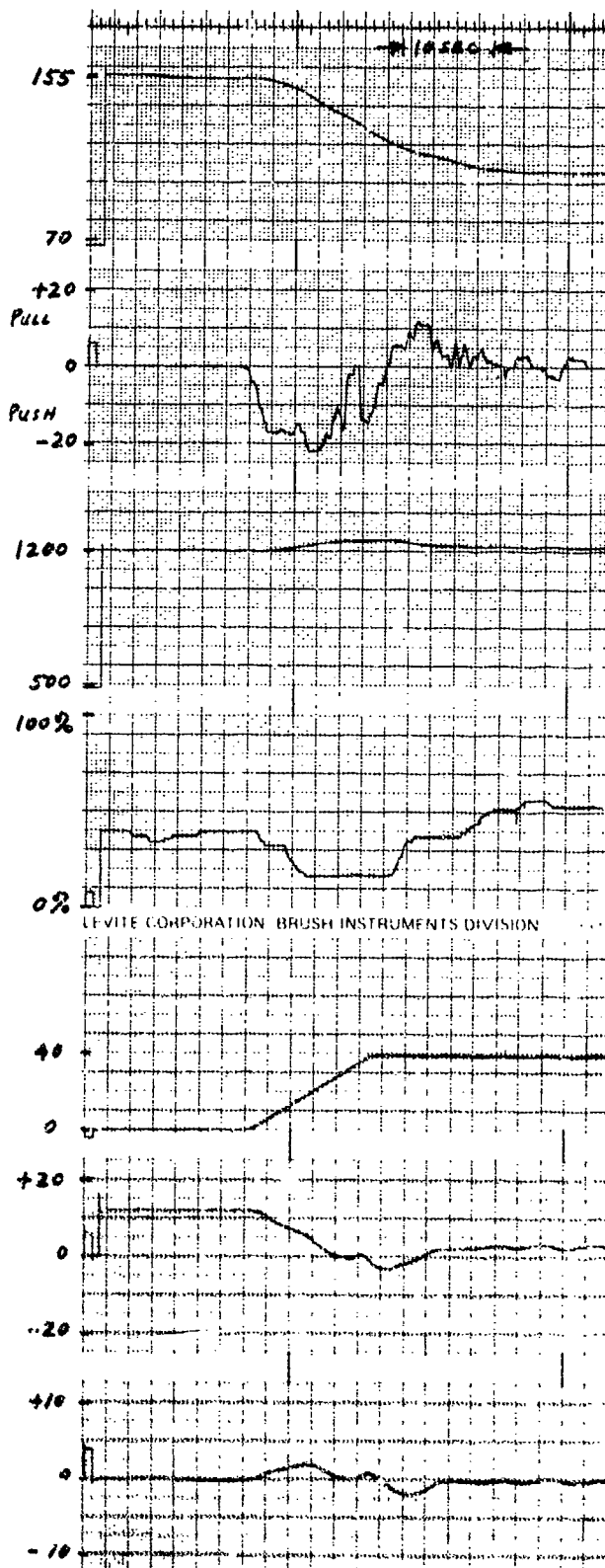
THROTTLE
(% THRUST)

δ_{FLAP}
(DEG)

θ
(DEG)

γ
(DEG)

VT INITIAL TRANSITION.
FLAPS 0 TO 40 DEGREES.
FINAL AIRSPEED = 105 KTS.



FLAP RATE = 3 DEG/SEC.

C/H = 6.

RUN D.

AIRSPPEED
(KTS)

δ STICK
(% FULL TRAVEL)

ALTITUDE
(FT. AGL)

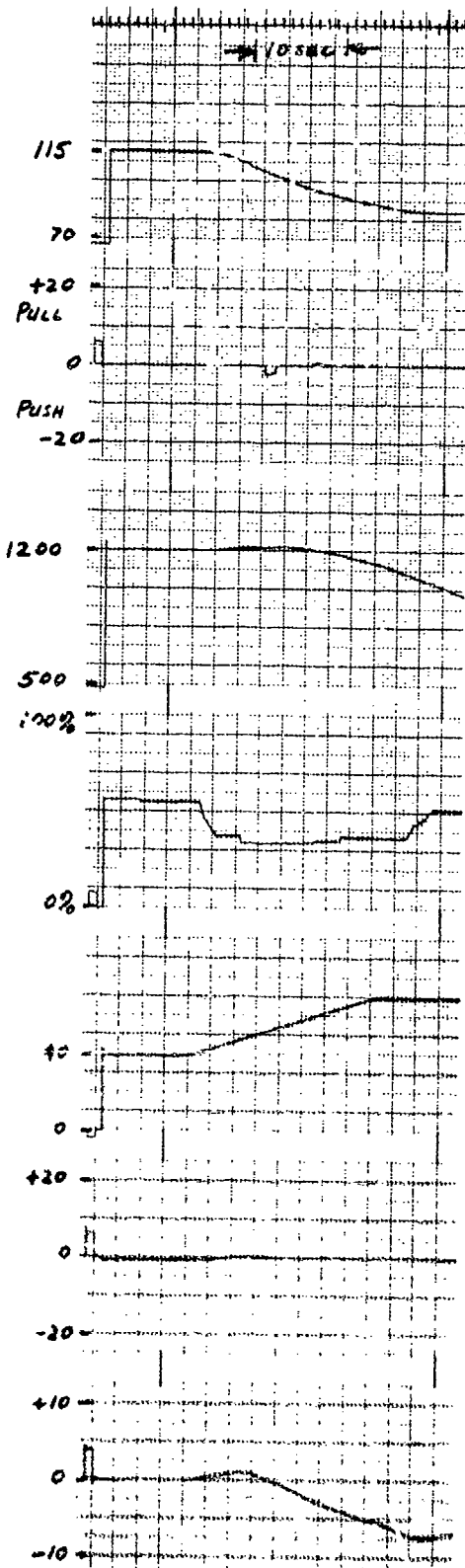
THROTTLE
(% THRUST)

δ FLAP
(DEG)

θ
(DEG)

γ
(DEG)

VT FINAL TRANSITION.
FLAPS 40 TO 70 DEGREES.
FINAL AIRSPEED = 85 KTS.



FLAP RATE = 1.5 DEG/SEC.
C/N = 3 1/2.
RUN M.

AIR SPEED
(KTS)

δ_{STICK}
(% FULL TRAVEL)

ALTITUDE
(FT. ALL)

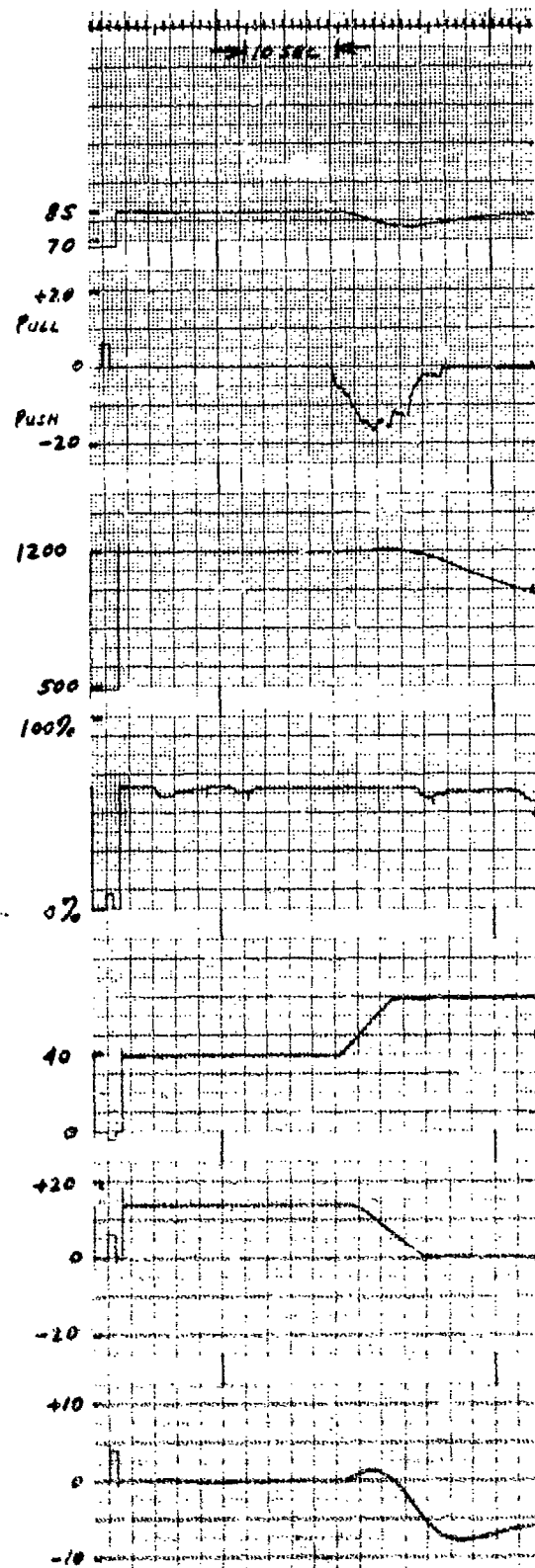
THROTTLE
(% THRUST)

δ_{FLAP}
(DEG)

θ
(DEG)

γ
(DEG)

VT FINAL TRANSITION.
FLAPS 40 TO 70 DEGREES.
FINAL AIRSPEED = 85 KTS.



FLAP RATE = 5 DEG/SEC.
C/N = 5.
RUN A.

AIRSPEED
(KTS)

δ STICK
(% FULL TRAVEL)

ALTITUDE
(FT. AGL)

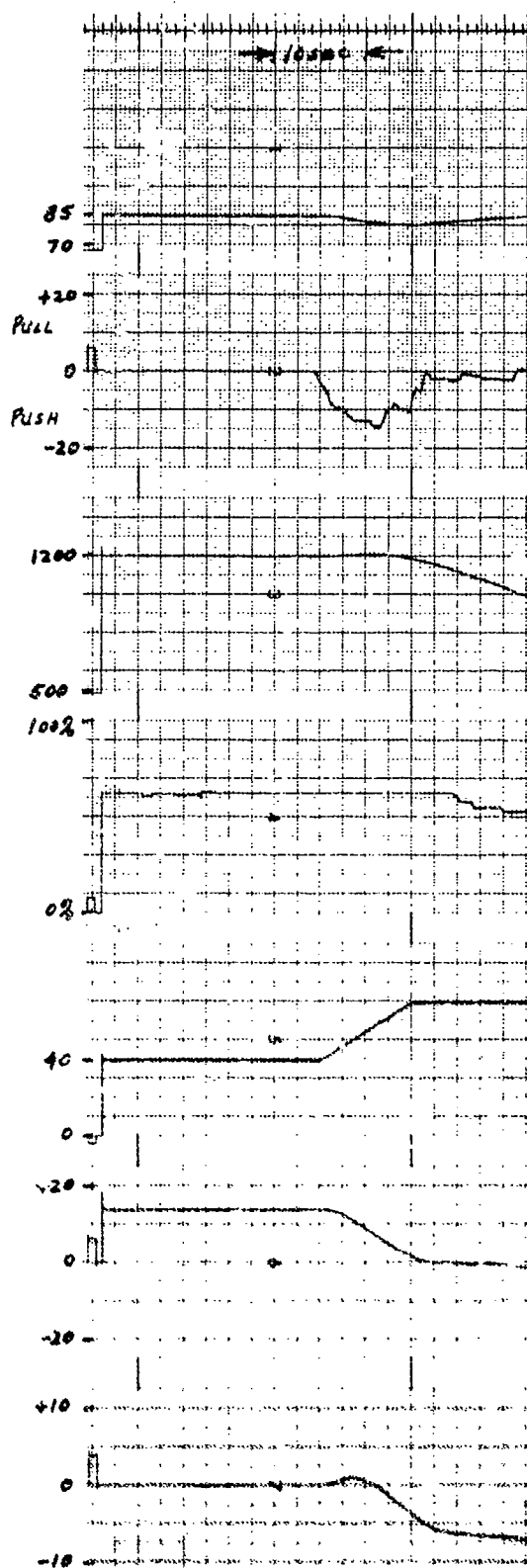
THROTTLE
(% THRUST)

δ FLAP
(DEG)

θ
(DEG)

γ
(DEG)

VT FINAL TRANSITION.
FLAPS 40 TO 70 DEGREES.
FINAL AIRSPEED = 85 KTS.



FLAP RATE = 3 DEG/SEC.
C/N = 3 1/2.
RUN D.

AIRSPPEED
(KTS)

δ_{STICK}
(% FULL TRAVEL)

ALTITUDE
(FT. AGL)

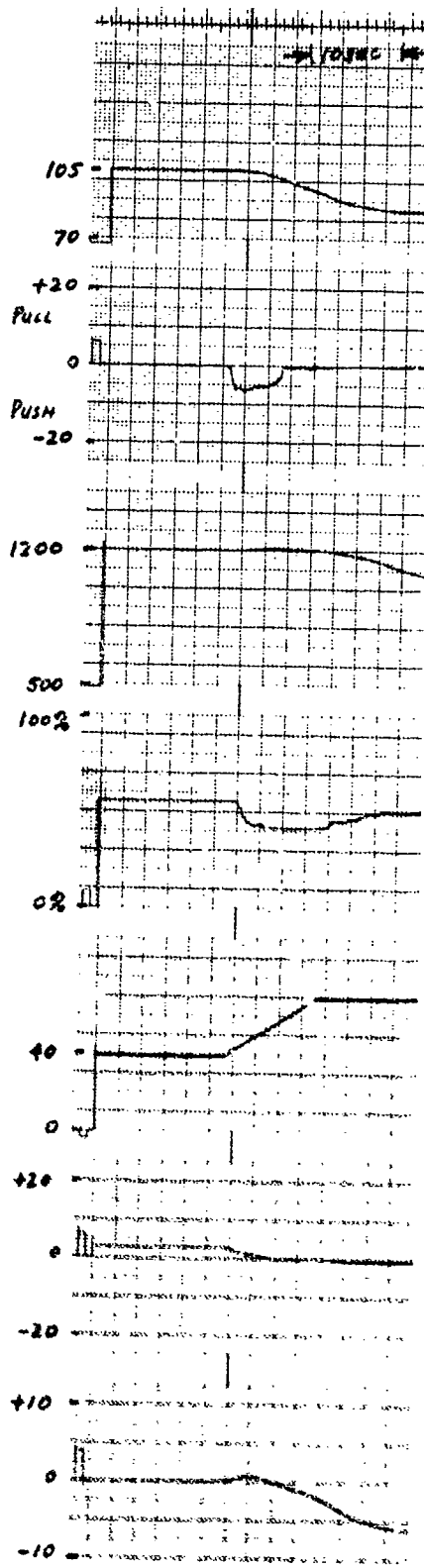
THROTTLE
(% THRUST)

δ_{FLAP}
(DEG)

θ
(DEG)

γ
(DEG)

VT FINAL TRANSITION.
FLAPS 40 TO 70 DEGREES.
FINAL AIRSPEED = 85 KTS.



FLAP RATE = 3 DEG/SEC.

$C/N = 2\frac{1}{2}$.

RUN E.

AIR SPEED
(KTS)

δ STICK
(% FULL TRAVEL)

ALTITUDE
(FT. AGL)

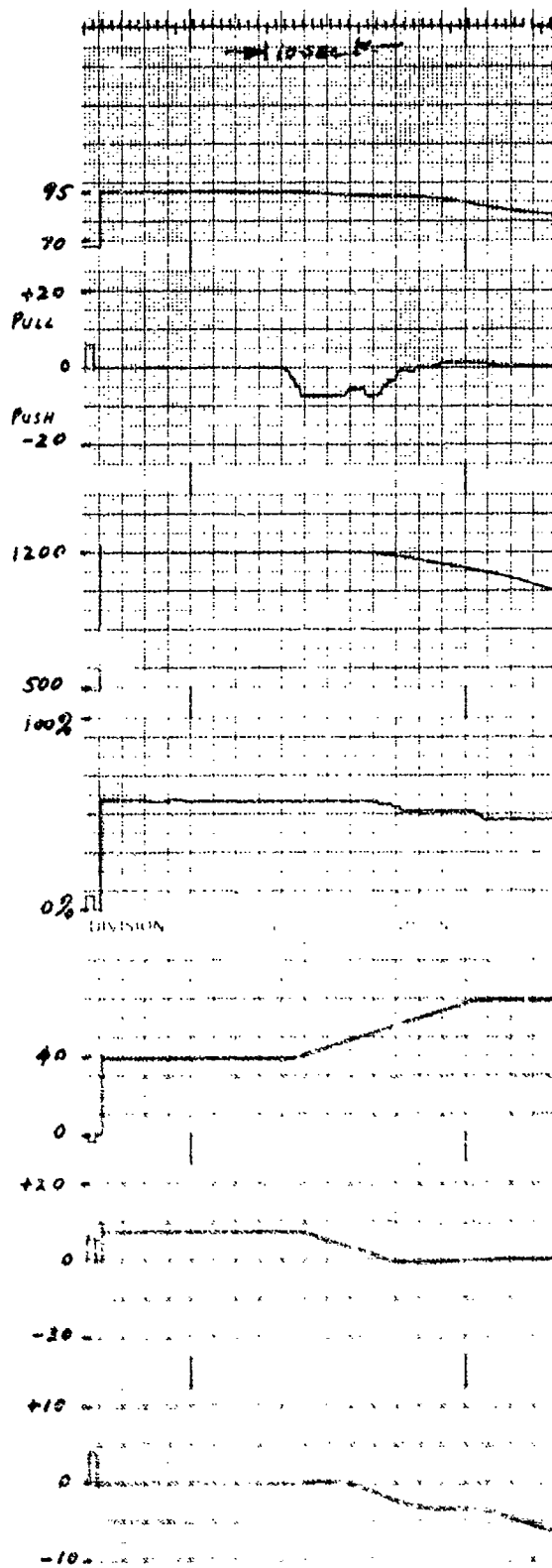
THROTTLE
(% THRUST)

δ FLAP
(DEG)

θ
(DEG)

γ
(DEG)

V.F. FINAL TRANSITION.
FLAPS ADJ TO 70 DEGREES
FINAL AIRSPEED = 85 KTS



FLAP RATE = 1.5 DEG/SEC.

C/N = 7.

RUN 6.

AIRSPPEED
(KTS)

δ_{STICK}
(% FULL TRAVEL)

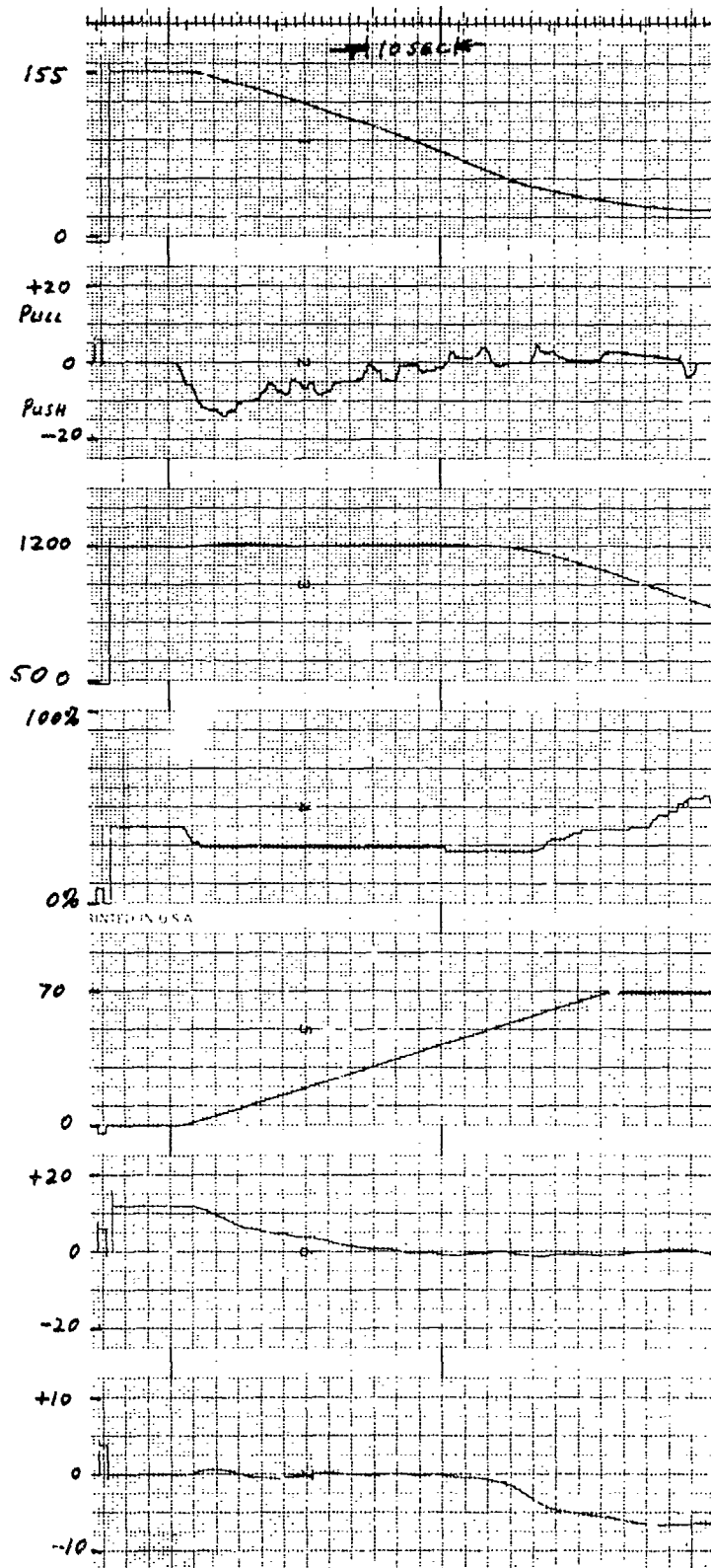
ALTITUDE
(FT. AGL)

THROTTLE
(% THRUST)

δ_{FLAP}
(DEG)

θ
(DEG)

γ
(DEG)



VT TOTAL TRANSITION.
FLAPS 0 TO 70 DEGREES.
FINAL AIRSPEED = 85KTS.

FLAP RATE = 1.5 DEG/SEC.
C/H = 4 1/2.
RUN A.

APPENDIX IV

EVALUATION CRITERIA AND QUESTIONNAIRE FOR
SIOL TACTICAL AIRCRAFT INVESTIGATION (STAI)

APPENDIX IV

EVALUATION CRITERIA AND QUESTIONNAIRE FOR STOL TACTICAL AIRCRAFT INVESTIGATION (STAI)

This questionnaire is designed to extract information from the evaluation pilot during and after the simulation evaluation. It is intended to provoke thoughts for discussion as well as providing rationale and criteria that can aid in arriving at a Cooper/Harper (C/H) pilot rating. It is not an all inclusive probe of the flying qualities of the simulated aircraft, but it felt that the questionnaire can serve as an aid in evaluating handling qualities, aerodynamic coefficients, design synthesis, and desired techniques for flying the aircraft in an operational manner. The questionnaire is intended to provide a descriptive answer more than merely yes or no.

The questionnaire is broken down into three subcategories of the terminal flight phase: transition to the STOL configuration; approach; go-around. Transition is further broken down into a one-configuration change, a two-configuration change, and a general transition questionnaire.

APPROACH

1. Is airspeed better controlled by pitch or by power?
2. Is flight path angle better controlled by pitch or by power?
3. Which of these techniques for flight path control and airspeed control appear better suited for flying STOL approaches?
4. Are there objectionable features of flight path control by one of these techniques which affect performance and control of airspeed?
5. If so, what are they?
6. Are there objectionable features of airspeed control by one of these techniques which affect performance and control of flight path angle?
7. If so, what are they?
8. Can airspeed and glide path corrections be accomplished in a natural precise manner by the desired technique?
9. Is power response satisfactory?
10. Is there an objectionable tendency to suffer power oscillations while trying to stabilize on the glide path?
11. Do power changes create objectionable airspeed changes?
12. Is pitch attitude easily maintained?

13. Do power changes create objectionable pitch changes?
14. Do pitch changes create objectionable airspeed or angle of attack changes?
15. Is Lat-Dir control easily maintained?
16. Are there any objectionable Lat-Dir modes?
17. Do the Lat-Dir time constants appear satisfactory?
18. Does the addition of turbulence create any objectionable characteristics?
19. If so, what are they?
20. Is adequate control of all flight modes available during turbulent conditions?
21. Could landings be safely and repeatably performed from the approach during turbulence using a 60-foot by 2000 feet runway?
22. Is visibility adequate during the approach?
23. Is there uncomfortable feeling of flying nose low during the approach?
24. Does an engine out situation occurring on the approach create a need for an objectionable amount of pilot compensation for control?

25. Can an approach be safely continued to landing assuming an engine out occurs during the approach?
26. Must an approach be abandoned on the occurrence of an engine out for safety of flight purposes?
27. Is there a point in the approach at which neither a continued approach to touchdown nor a go-around can be successfully accomplished upon loss of an engine?
28. If so, where is that point?
29. Are there any objectionable control techniques required for an engine out approach?
30. Is the pitch trimming system satisfactory for normal approaches?
31. Does the augmentation system contribute significantly to control of flight path angle, turn coordination, Lat-Dir modes, Longitudinal modes?
32. If so, which ones?
33. What contribution does the Autospeed mode provide during the approach without turbulence?
34. What contribution does the Autospeed mode provide during approach with turbulence?
35. What contribution does the Approach mode provide during the approach without turbulence?

36. What contribution does the Approach mode provide during the approach with turbulence ?
37. Does the combined usage of Approach & Autospeed modes improve aircraft control significantly without turbulence ?
38. Does the combined usage of Approach & Autospeed modes improve aircraft control significantly with turbulence ?
39. Does the flight technique change when using either or both of the modes as compared to without these modes ?
40. Does the presence of turbulence while using these modes indicate a change in required technique as compared to flying without turbulence ?

GO-AROUND

1. Can a go-around be successfully accomplished without a flap change?
2. Can a go-around be successfully accomplished by raising the flaps all the way up in one step?
3. Is this dependent upon the flap rate?
4. If an intermediate flap selection is used for a successful go-around, can the flap change be accomplished in a safe repeatable fashion?
5. Is this intermediate flap position suitable for flying a subsequent GCA or missed approach pattern?
6. Should the flaps be raised on initiation of the go-around or should the retraction be delayed until after the pitch change if any is accomplished?
7. If the recommendation is for the flaps to be raised upon go-around initiation, is it safe if a delay occurs in flap retraction to the intermediate position?
8. Is the aircraft performance for a potential delay in flap retraction sensitive to such things as flap position, flap rate, pitch attitude change, or pitch rate?
9. If so, which ones?

10. If the flaps are retracted simultaneous with go-around initiation, is the aircraft performance sensitive to such things as flap position, flap rate, pitch attitude change, or pitch rate?
11. If so, which ones?
12. Assuming the go-around is initiated at a 100 foot Decision Height (DH), can the go-around be safely and repeatably be performed in less than 100 feet?
13. Is successful accomplishment of the go-around within 100 feet of altitude loss objectionably dependent upon special techniques or sensitive to variations in technique, pitch rates, pitch attitude changes, or control schemes?
14. If so, which ones?
15. Is there any tendency for the airspeed to droop during the go-around?
16. Does the airspeed appear able to either accelerate or at least hold to the approach value?
17. Does the angle of attack approach any value which makes control a questionable area?
18. Is the airspeed performance objectionably sensitive to flap position, flap rates, pitch rates, pitch attitude changes, techniques, or control schemes?

19. If so, which ones?
20. Is the pitch attitude change easily obtained and held?
21. Is there a tendency for the flight path angle to droop or take an unacceptably long time to establish a climb during the go-around?
22. If so, which one?
23. Is a desired steady increase in flight path angle to an acceptable climb value objectionably sensitive to pitch attitude, pitch rate, flap rate, technique, or control scheme?
24. If so, which ones?
25. Can Lat-Dir control be easily maintained during go-around?
26. Is the attitude necessary for a successful go-around comfortable from a crew/passenger viewpoint?
27. Is visibility at this attitude satisfactory?
28. Does the Autospeed mode enhance or degrade the go-around operation?
29. Does the Approach mode enhance or degrade the go-around operation?

30. Do the pilot initiated automatic flap retraction features provide for safe single pilot operation?

31. Are they required?

INITIAL TRANSITION

1. Is it difficult to maintain constant altitude during the transition?
2. Are special techniques required?
3. Is pitch or is power the primary means of altitude control?
4. Does the primary means of altitude control change during the transition?
5. If yes, is this objectionable or confusing or is it satisfactory?

FINAL TRANSITION

1. Is there any tendency to oscillate with power in achieving trim conditions on the glide path ?
2. Is power response generally satisfactory ?
3. Is pitch control easily maintained during the transition ?
4. Is altitude loss easily controlled when intercepting the glide path during the transition ?
5. Does the aircraft tend to balloon during the transition ?
6. If so, is it objectionable or is it satisfactory ?
7. Does it take an excessive time to acquire the glide path during the transition ?

TOTAL TRANSITION

1. Can the transition to the final STOL configuration from conventional flight be safely conducted in one step?
2. Is it practical and operationally sound to transition in one step at low pattern altitudes?
3. Does the altitude tend to balloon or droop without adverse control compensation?
4. Does the control technique change during the transition in an objectionable or confusing manner?

TRANSITION GENERAL

1. Does airspeed bleed off if necessary in a controllable manner?
2. Can airspeed be accurately controlled or held to any interim value or final target airspeed?
3. What are these problems if any?
4. Are they objectionable or are they satisfactory?
5. Can airspeed be stopped at the desired value without confusing techniques?
6. Are there any pitch stick reversals?
7. Are they objectionable or are they satisfactory?
8. If objectionable, is this because of magnitude, rapidity, or both?
9. Are there any power change reversals?
10. Are they objectionable or are they satisfactory?
11. If objectionable, is this because of magnitude, rapidity, or both?
12. Are there any pitch change reversals?

13. Are they objectionable or are they satisfactory?
14. If objectionable, is this because of magnitude, rapidity, or both?
15. Are there any apparent non-linear gradient changes in either pitch stick force or deflections during pitching moments?
16. Are they objectionable or are they satisfactory?
17. Are there any apparent non-linear gradient changes in either pitch stick force or deflections during airspeed changes?
18. Are they objectionable or are they satisfactory?
19. Is the pitch trimming system adequate throughout the transition?
(Phugoid, Power Effects, Pitch Changes).
20. Are there any Lat-Dir stabilizing problems?
21. Are they objectionable or are they satisfactory?
22. Does this appear to be as a result of poor stick or rudder centering or is it as a result of exciting the Lat-Dir modes?
23. Are the Lat-Dir time constants satisfactory for the Lat-Dir Modes?
24. Is it easy to excite these modes?

25. If so, which ones?
26. Is the damping satisfactory for these modes?
27. Can turns be easily coordinated?
28. Is visibility adequate throughout the transition?
29. Is there any uncomfortable feeling of flying nose down at any time throughout the transition?
30. Does pitch augmentation significantly improve the capability of performing any part or all of the transition?
31. Would an altitude hold mode be desirable or required for the transition phase?

APPENDIX V

TEST AND EVALUATION PLAN FOR THE STAI (EBF)
ON THE MOVING-BASE LARGE AMPLITUDE SIMULATOR

APPENDIX V

TEST AND EVALUATION PLAN FOR THE STAI (EBF) ON THE MOVING-BASE LARGE AMPLITUDE SIMULATOR

This appendix shows the plan for evaluating the EBF version of a medium STOL transport on the moving-base, large amplitude simulator (LAS). Not all of the runs tabulated herein were performed at the moving-base facility. A late review of this plan eliminated some runs which fixed-base studies showed to be of lesser significance to the evaluation objectives. Attempts to relate this plan to the sample data of Appendix III should recognize that some moving-base runs may have been eliminated on engineering judgment and that the included data samples were selected from a much larger number of moving-base evaluation runs.

ABBREVIATIONS AND DEFINITIONS

δF	- Flap position in degrees
$\dot{\delta F}$	- Flap movement rate in degrees/second
$i\delta F$	- Initial flap position in degrees
$f\delta F$	- Final flap position in degrees
A/S	- Airspeed in knots
iA/S	- Initial airspeed in knots
fA/S	- Final airspeed in knots
$\dot{\theta}$	- Pitch rate
	Nom - \approx 4 degrees/second
	Slow - \approx 2 degrees/second
	Fast - \approx 7 degrees/second
$\Delta \theta$	- Pitch attitude change in degrees
Modes	- Control System Configuration
	No - Pitch attitude hold, turn coordination, pitch-lateral-directional damping
	A/S - AUTOSPEED button plus No
	App - APPROACH button plus No
	Both - AUTOSPEED and APPROACH button plus No
	B.A/F - Bare Airframe, without any augmentation or damping
Tech	- Control technique
	Conv - Conventional A/C control of airspeed and flight path angle (γ by pitch - A/S by power)
	STOL - STOL A/C control of airspeed and flight path angle (γ by power - A/S by pitch)

Cond - Conditions of aircraft or external source

- 30 kt - Variable 90-degrees crosswind with initial value of 30 knots
- G - With gust model
- EO -2 sec - With critical engine out - 2-second delay recovery
- Up 40 - Flaps raised simultaneously with go-around to 40 degrees
- Pitch 40 - Flaps raised after $\Delta\theta$ complete to 40 degrees
- Fwd - Most forward C.G. location
- Aft - Most aft C.G. location
- Lt - Lightest aircraft weight
- Hvy - Heaviest aircraft weight

CFB - Convair Fixed-Base Simulator

LAS - Large Amplitude Simulator

* - Record data runs for comparison of Convair fixed-base simulation to LAS

IC - Initial Condition

AGL - Above Ground Level (feet)

INITIAL CONDITIONS

- A. Approach - 12,000 ft from end of runway threshold (X-distance)
Trimmed for -1° flight path angle (γ)
200 ft offset to right of localizer/runway centerline
Heading parallel to runway heading ($\psi = 0^\circ$)
1200 ft AGL
- B. Go-around - 5100 ft from end of runway threshold (X-distance)
Trimmed on -7° flight path angle (γ)
On localizer/runway centerline
Heading parallel to runway heading ($\psi = 0^\circ$)
- C1. Transition (Final) - 16,000 ft from end of runway threshold (X-distance)
Trimmed for 0° flight path angle (γ)
On localizer/runway centerline
Heading parallel to runway heading ($\psi = 0^\circ$)
1200 ft AGL
- C2. Transition (Initial) - 21,000 ft from end of runway threshold (X-distance)
Trimmed for 0° flight path angle (γ)
On localizer/runway centerline
Heading parallel to runway heading ($\psi = 0^\circ$)

C3. Transition - 24,000 ft from end of runway threshold (X-distance)
 (Operational) Trimmed for 0° flight path angle (γ)
 10,000 ft left of localizer/runway centerline
 Heading 90° right of runway heading ($\psi = 90^\circ$)
 2,000 ft AGL

Table V-1. Approach (CFB Data Runs) for Establishment of a Data Base

δF	A/S	Tech	Modes	CFB Run	LAS Run
60	80	STOL	Both	A	A20
60	80	CONV	Both	B	A36
60	80	CONV	No	C	A24
45	80	STOL	No	D	A2
50	80	STOL	No	E	A4
55	80	STOL	No	F	A6
60	80	STOL	No	G	A8
60	80	STOL	A/S	H	A12
60	75	STOL	No	I	A7

Table V-2. Approach (CFB Data Runs) for Establishment of a Data Base

δF	δF	Tech/Cond	$\Delta\theta$		Modes	CFB Run	LAS Run
60	5	Up 40	15	Nom	Both	A	G8
55	5	Up 40	15	Nom	Both	B	G14
55	5	Up 40	10	Nom	No	C	G17
50	5	Up 40	10	Nom	Both	D	G60
55	5	Up 0	10	Nom	Both	E	G4
55	5	Up 40	10	Nom	Both	F	G60
60	5	Up 40	10	Nom	Both	G	G61
55	5	Pitch 40	10	Nom	Both	H	G23
55	3	Pitch 40	10	Nom	Both	I	G62
55	5	Pitch 40	10	Nom	No	J	G25
60	5	Pitch 40	15	Nom	Both	K	G63
55	5	Up 40	5	Nom	Both	L	G64
55	5	Up 40	10	Fast	Both	M	G64
60	5	Up 40	20	Nom	Both	N	G66

Table V-3. Transition (CFB Data Runs) for Establishment of a Data Base

iA/S	fA/S	δF	i δF	f δF	CFB Run	IAS Run
140	115	3	0	40	A	IT2
155	115	3	0	40	B	IT6
170	115	3	0	40	C	IT10
155	115		0	40	D	IT7
155	115	1.5	0	40	E	IT5
80	80	3	40	55	F	FT2
90	80	3	40	55	G	FT6
115	80	3	40	55	H	FT10
125	80	3	40	55	I	FT14
90	80	5	40	55	J	FT7
115	80	5	40	55	K	FT11
115	80	1.5	40	55	L	FT9
155	80	3	0	55	M	TT5

Table V-4. Approach (Moving Base-LAS)

δF	A/S	Tech/Cond	Modes	Run	IC
45	75	STOL	No	A1	A
*45	80	STOL	No	A2	A
50	75	STOL	No	A3	A
*50	80	STOL	No	A4	A
55	75	STOL	No	A5	A
*55	80	STOL	No	A6	A
*60	75	STOL	No	A7	A
*60	80	STOL	No	A8	A
45	80	STOL	A/S	A9	A
50	80	STOL	A/S	A10	A
55	80	STOL	A/S	A11	A
*60	80	STOL	A/S	A12	A
45	80	STOL	App	A13	A
50	80	STOL	App	A14	A
55	80	STOL	App	A15	A
60	80	STOL	App	A16	A
45	80	STOL	Both	A17	A
50	80	STOL	Both	A18	A
55	80	STOL	Both	A19	A
*60	80	STOL	Both	A20	A
45	80	Conv	No	A21	A
50	80	Conv	No	A22	A
55	80 ±	Conv	No	A23	A
*60	80	Conv	No	A24	A
45	80	Conv	A/S	A25	A
50	80	Conv	A/S	A26	A

Table V-4. Approach (Moving Base-LAS), Cont

ΔF	A/S	Tech/Cond	Modes	Run	IC
55	80	Conv	A/S	A27	A
60	80	Conv	A/S	A28	A
45	80	Conv	App	A29	A
50	80	Conv	App	A30	A
55	80	Conv	App	A31	A
60	80	Conv	App	A32	A
45	80	Conv	Both	A33	A
50	80	Conv	Both	A34	A
55	80	Conv	Both	A35	A
*60	80	Conv	Both	A36	A
45	80	STOL/G	No	A37	A
45	80	Conv/G	No	A38	A
45	80	STOL/G	A/S	A39	A
45	80	Conv/G	A/S	A40	A
45	80	STOL/G	App	A41	A
45	80	Conv/G	App	A42	A
45	80	STOL/G	Both	A43	A
45	80	Conv/G	Both	A44	A
55	80	STOL/G	No	A45	A
50	80	Conv/G	No	A46	A
50	80	STOL/G	A/S	A47	A
50	80	Conv/G	A/S	A48	A
50	80	STOL/G	App	A49	A
50	80	Conv/G	App	A50	A
50	80	STOL/G	Both	A51	A
50	80	Conv/G	Both	A52	A
55	80	STOL/G	No	A53	A

Table V-4. Approach (Moving Base-LAS), Cont

δF	A/S	Tech/Cond	Modes	Run	IC
55	80	Conv/G	No	A54	A
55	80	STOL/G	A/S	A55	A
55	80	Conv/G	A/S	A56	A
55	80	STOL/G	App	A57	A
55	80	STOL/G	App	A58	A
55	80	STOL/G	Both	A59	A
55	80	Conv/G	Both	A60	A
60	80	STOL/G	No	A61	A
60	80	Conv/G	No	A62	A
60	80	STOL/G	A/S	A63	A
60	80	Conv/G	A/S	A64	A
60	80	STOL/G	App	A65	A
60	80	Conv/G	App	A66	A
60	80	STOL/G	Both	A67	A
60	80	Conv/G	Both	A68	A
45	80	STOL/EO-2 sec	No	A69	A
45	80	STOL/EO-2 sec	A/S	A70	A
45	80	STOL/EO-2 sec	App	A71	A
45	80	STOL/EO-2 sec	Both	A72	A
50	80	STOL/EO-2 sec	No	A73	A
50	80	STOL/EO-1 sec	No	A73-1	A
50	80	STOL/EO-Min Time	No	A73-2	A
50	80	STOL/EO-2 sec	A/S	A74	A
50	80	STOL/EO-2 sec	App	A75	A
50	80	STOL/EO-2 sec	Both	A76	A
55	80	STOL/EO-2 sec	No	A77	A
55	80	STOL/EO-2 sec	A/S	A79	A
55	80	STOL/EO-2 sec	App	A79	A
55	80	STOL/EO-2 sec	Both	A80	A
60	80	STOL/EO-2 sec	No	A81	A
60	80	STOL/EO-1 sec	No	A81-1	A
60	80	STOL/EO-Min Time	No	A81-2	A

Table V-4. Approach (Moving Base-LAS), Cont

δF	A/S	Tech/Cond	Modes	Run	IC
60	80	STOL/EO-2 sec	A/S	A82	A
60	80	STOL/EO-2 sec	App	A83	A
60	80	STOL/EO-2 sec	Both	A84	A
45	80	STOL	B. A/F	A85	A
50	80	STOL	B. A/F	A86	A
55	80	STOL	B. A/F	A87	A
60	80	STOL	B. A/F	A88	A
45	80	STOL/G	B. A/F	A89	A
50	80	STOL/G	B. A/F	A90	A
55	80	STOL/G	B. A/F	A91	A
60	80	STOL/G	B. A/F	A92	A
45	80	STOL/EO-2 sec	B. A/F	A93	A
45	80	STOL/EO-1 sec	B. A/F	A93-1	A
50	80	STOL/EO-1 sec	B. A/F	A94	A
50	80	STOL/EO-	B. A/F	A94-1	A
55	80	STOL/EO-2 sec	B. A/F	A95	A
60	80	STOL/EO-2 sec	B. A/F	A96	A
45	80	STOL/Fwd	No	A97	A
50	80	STOL/Fwd	No	A98	A
55	80	STOL/Fwd	No	A99	A
60	80	STOL/Fwd	No	A100	A
45	80	STOL/Aft	No	A101	A
50	80	STOL/Aft	No	A102	A
55	80	STOL/Aft	No	A103	A
60	80	STOL/Aft	No	A104	A
45	80	STOL/Aft-Lt	No	A105	A
50	80	STOL/Aft-Lt	No	A106	A
55	80	STOL/Aft-Lt	No	A107	A
60	80	STOL/Aft-Lt	No	A108	A
60	80	STOL/Aft-Lt	B. A/F	A108-1	A
45	80	STOL/Fwd-Hvy	No	A109	A

Table V-4. Approach (Moving Base-LAS). Cont

δF	A/S	Tech/Cond	Modes	Run	IC
50	80	STOL/Fwd-Hvy	No	A110	A
55	80	STOL/Fwd-Hvy	No	A111	A
60	80	STOL/Fwd-Hvy	No	A112	A
60	80	STOL/Fwd-Hvy	B. A/F	A113	A
60	80	Conv/Fwd-Hvy	No	A114	A
60	80	Conv/Fwd-Hvy	B. A/F	A115	A
55	80	STOL/30 kt	No	CW1	A
55	80	Conv/30 kt	No	CW2	A
55	80	STOL/30 kt/G	No	CW3	A
55	80	Conv/30 kt/G	No	CW4	A
55	80	STOL/30 kt	B. A/F	CW5	A
55	80	STOL/30 kt/G	B. A/F	CW6	A

Table V-5. Go-Around (Moving Base-LAS)

δF	$\dot{\delta F}$	Tech/Cond	$\Delta\theta$	$\dot{\theta}$	Modes	Run	IC
60	5	Up 0	15	Nom	Both	G1	B
60	5	Up 35	15	Nom	Both	G2	B
60	5	Up 45	15	Nom	Both	G3	B
*55	5	Up 0	10	Nom	Both	G4	B
55	5	Up 35	10	Nom	Both	G5	B
55	5	Up 45	10	Nom	Both	G6	B
60	5	Up 40	15	Nom	No	G7	B
*60	5	Up 40	15	Nom	Both	G8	B
60	1.5	Up 40	10	Nom	No	G9	B
60	3	Up 40	10	Nom	No	G10	B
60	5	Up 40	10	Nom	No	G11	B
60	7	Up 40	10	Nom	No	G12	B
55	5	Up 40	15	Nom	No	G13	B
*55	5	Up 40	15	Nom	Both	G14	B
55	1.5	Up 40	10	Nom	No	G15	B
55	3	Up 40	10	Nom	No	G16	B
*55	5	Up 40	10	Nom	No	G17	B
55	7	Up 40	10	Nom	No	G18	B
60	5	Up 40	5	Nom	No	G19	B
55	5	Up 40	5	Nom	No	G20	B
60	5	Pitch 40	10	Nom	Both	G21	B
60	7	Pitch 40	10	Nom	Both	G22	B
*55	5	Pitch 40	10	Nom	Both	G23	B
*55	7	Pitch 40	10	Nom	Both	G24	B
*55	5	Pitch 40	10	Nom	No	G25	B
55	7	Pitch 40	10	Nom	No	G26	B

Table V-5. Go-Around (Moving Base-LAS), Cont

$i\delta F$	δF	Tech/Cond	$\Delta\theta$	$\dot{\theta}$	Modes	Run	IC
60	5	Up 40/G	10	Nom	No	G27	B
55	5	Up 40/G	10	Nom	No	G28	B
60	5	Pitch 40/G	10	Nom	Both	G29	B
55	5	Pitch 40/G	10	Nom	Both	G30	B
60	5	Up 40	10	Nom	B. A/F	G31	B
55	5	Up 40	10	Nom	B. A/F	G32	B
60	5	Up 40/EO-2 sec	10	Nom	No	G33	B
60	7	Up 40/EO-2 sec	10	Nom	No	G34	B
55	5	Up 40/EO-2 sec	10	Nom	No	G35	B
55	7	Up 40/EO-2 sec	10	Nom	No	G36	B
50	5	Up 40/EO-2 sec	10	Nom	No	G37	B
50	7	Up 40/EO-2 sec	10	Nom	No	G38	B
60	5	Fwd/Up 40	10	Nom	No	G39	B
60	5	Aft/Up 40	10	Nom	No	G40	B
55	5	Fwd/Up 40	10	Nom	No	G41	B
55	5	Aft/Up 40	10	Nom	No	G42	B
60	5	Fwd-Hvy/Up 40	10	Nom	No	G43	B
60	5	Aft-Lt/Up 40	10	Nom	No	G44	B
55	5	Fwd-Hvy/Up 40	10	Nom	No	G45	B
55	5	Aft/Lt/Up 40	10	Nom	No	G46	B
60	5	Up 40	10	Slow	No	G47	B
60	5	Up 40	10	Fast	No	G48	B
60	5	Fwd-Hvy/Up 40	10	Slow	No	G49	B
60	5	Fwd-Hvy/Up 40	10	Fast	No	G40	B
60	5	Aft-Lt/Up 40	10	Slow	No	G51	B
60	5	Aft/Lt/Up 40	10	Fast	No	G52	B

Table V-5. Go-Around (Moving Base-LAS), Cont

δF	$\dot{\delta} F$	Tech/Cond	$\Delta\theta$	$\dot{\theta}$	Modes	Run	IC
55	5	Up 40	10	Slow	No	G53	B
55	5	Up 40	10	Fast	No	G54	B
55	5	Fwd-Hvy/Up 40	10	Slow	No	G55	B
55	5	Fwd-Hvy/Up 40	10	Fast	No	G56	B
55	5	Aft-Lt/Up 40	10	Slow	No	G57	B
55	5	Aft-Lt/Up 40	10	Fast	No	G58	B
*50	5	Up 40	10	Nom	Both	G59	B
*55	5	Up 40	10	Nom	Both	G60	B
*60	5	Up 40	10	Nom	Both	G61	B
*55	3	Pitch 40	10	Nom	Both	G62	B
*60	5	Pitch 40	15	Nom	Both	G63	B
*55	5	Up 40	5	Nom	Both	G64	B
*55	5	Up 40	10	Fast	Both	G65	B
*60	5	Up 40	20	Nom	Both	G66	B

Table V-6. Transition (Moving Base--LAS)

iA/S	fA/S	δF	Cond	i δF	f δF	Run	IC
80	80	1.5		40	55	FT1	C1
* 80	80	3		40	55	FT2	C1
80	80	5		40	55	FT3	C1
80	80	7		40	55	FT4	C1
90	80	1.5		40	55	FT5	C1
* 90	80	3		40	55	FT6	C1
* 90	80	5		40	55	FT7	C1
90	80	7		40	55	FT8	C1
*115	80	1.5		40	55	FT9	C1
*115	80	3		40	55	FT10	C1
*115	80	5		40	55	FT11	C1
115	80	7		40	55	FT12	C1
125	80	1.5		40	55	FT13	C1
*125	80	3		40	55	FT14	C1
125	80	5		40	55	FT15	C1
125	80	7		40	55	FT16	C1
90	80	1.5	Fwd-Hvy	40	55	FT17	C1
90	80	3	Fwd-Hvy	40	55	FT18	C1
90	80	5	Fwd-Hvy	40	55	FT19	C1
90	80	1.5	Aft-Lt	40	55	FT20	C1
90	80	3	Aft-Lt	40	55	FT21	C1
90	80	5	Aft-Lt	40	55	FT22	C1
115	80	1.5	Fwd-Hvy	40	55	FT23	C1
115	80	3	Fwd-Hvy	40	55	FT24	C1
115	80	5	Fwd-Hvy	40	55	FT25	C1
115	80	1.5	Aft-Lt	40	55	FT26	C1

Table V-6. Transition (Moving Base-LAS), Cont

IA/S	fA/S	δF	Cond	15F	f δF	Run	IC
115	80	3	Aft-Lt	40	55	FT27	C1
115	80	5	Aft-Lt	40	55	FT28	C1
140	115	1.5		0	40	IT1	C2
140	115	3		0	40	IT2	C2
140	115	5		0	40	IT3	C2
140	115	7		0	40	IT4	C2
*155	115	1.5		0	40	IT5	C2
*155	115	3		0	40	IT6	C2
*155	115	5		0	40	IT7	C2
155	115	7		0	40	IT8	C2
170	115	1.5		0	40	IT9	C2
*170	115	3		0	40	IT10	C2
170	115	5		0	40	IT11	C2
170	115	7		0	40	IT12	C2
90	80	1.5	Gust	0	40	IT13	C2
90	80	3	Gust	0	40	IT14	C2
90	80	5	Gust	0	40	IT15	C2
115	80	1.5	Gust	0	40	IT16	C2
115	80	3	Gust	0	40	IT17	C2
115	80	5	Gust	0	40	IT18	C2
155	115	1.5	Gust	0	40	IT19	C2
155	115	3	Gust	0	40	IT20	C2
155	115	5	Gust	0	40	IT21	C2

Table V-6. Transition (Moving Base-LAS), Cont

iA/S	fA/S	δF	Cond	i δF	f δF	Run	IC
140	80	1.5		0	55	TT1	C2
140	80	3		0	55	TT2	C2
140	80	5		0	55	TT3	C2
155	80	1.5		0	55	TT4	C2
155	80	1.5		0	55	TT4-1	C3
*155	80	3		0	55	TT5	C2
155	80	3		0	55	TT5-1	C3
155	80	5		0	55	TT6	C2
170	80	1.5		0	55	TT7	C2
170	80	3		0	55	TT8	C2
170	80	5		0	55	TT9	C2